



FI9800067

LAPPEENRANNAN TEKNILLINEN KORKEAKOULU  
LAPPEENRANTA UNIVERSITY OF TECHNOLOGY

UDK 621.1  
621.039  
621.311.25

TIETEELLISIÄ JULKAISUJA  
RESEARCH PAPERS

43

LT KK - T J - 43

## THIRD INTERNATIONAL SEMINAR ON HORIZONTAL STEAM GENERATORS

LAPPEENRANTA  
1995

29 - 23

R

ISBN 951-763-942-2  
ISSN 0356-8210

# THIRD INTERNATIONAL SEMINAR ON HORIZONTAL STEAM GENERATORS

October 18-20, 1994, Lappeenranta, Finland



## **THIRD INTERNATIONAL SEMINAR ON HORIZONTAL STEAM GENERATORS 18 — 20 October 1994, Lappeenranta, Finland**

### **PREFACE**

Insufficient understanding of realistic thermal hydraulic behaviour of the horizontal steam generators was recognised few years ago when performing safety analyses for VVER reactors. To improve the situation, Finnish nuclear organisations took an initiative to start international cooperation to gather existing experimental and theoretical knowledge of the behaviour of horizontal steam generators under normal operation, transient and accident conditions. Consequently, two International Seminars of Horizontal Steam Generator Modelling were arranged in March 1991 and September 1992 in Lappeenranta, Finland. The seminars concentrated on thermal hydraulic experiments and analytical modelling of the flow behaviour both in the primary side and in the secondary side. The experience from these seminars was most encouraging. New experimental results, comparisons of existing experimental facilities and approaches to calculational modelling were presented. Particularly, the participants experienced the seminars as a useful forum for fruitful discussions.

In the final discussions of the second seminar, a common agreement was that continuation of cooperation would be beneficial, and that the scope of the seminars could be widened to structural and aging issues. A general feeling among the participants was that it might be very beneficial to bring structural and thermal hydraulic experts together in the next seminar, since difficulties in governing the interface of these areas were detected.

The third seminar consisted of six sessions. The topics were thermal hydraulic experiments and analyses, primary collector integrity, management of primary-to-secondary leakage accidents, feedwater collector replacement and discussion of VVER-440 steam generator safety issues. As previously, the organisers were IVO International Ltd, Lappeenranta University of Technology (LTKK) and VTT Energy, but now in collaboration with the International Atomic Energy Agency (IAEA).

Session I demonstrated that the experimental basis of the thermal hydraulic behavior is not yet sufficiently wide. New results were available only from two integral facilities, i.e. Finnish PACTEL and Hungarian PMK. The PACTEL results with a new steam generator are encouraging, and the experiments will continue. The theoretically predicted flow reversal in the lower tube bundle was now clearly found in the PACTEL experiments. The discussion also indicated that the same would be true for the PMK2 experiments.

Dr. S.A. Logvinov of Gidropress discussed the separate effect experiments directed to study the flow distribution in the feedwater distributor of PGV-440. The results help to explain the corrosion-erosion mechanism, which has been found to cause damage to the distributor. Another paper was presented concerning the Czech results of the influence of

the new feedwater distributor on the impurity distribution.

Session II of thermal hydraulic analyses gathered the most papers. The calculational efforts should meet two clearly different objectives. First, the modelling capability of the system codes should be developed to such a level that would satisfy the need to calculate the steam generator behaviour during all conditions, and particularly during transient and accident conditions. Secondly, there is a need for more accurate flow calculations to predict the fluid flow conditions on the steam generator secondary side. To do this, 3-D calculation codes have been developed. Such calculations were deemed to be of a crucial importance for determining thermal hydraulic boundary conditions for the structural evaluations of any proposed design changes. Good examples of such changes are the primary collector replacements and lifetime definitions, and feedwater distributor replacements.

The applications of system codes RELAP5, ATHLET, CATHARE, APROS and DINAMIKA were presented. This work is going on in all the participating countries. The main issues of code application are whether the 1-D nodalization model is sufficient, how detailed nodalization is required, and how to obtain relevant data for validation and assessment. It was pointed out that the most significant resolution of nodalization problems is tailoring according to the application. The safety analyzer should understand well the role and importance of the model from the viewpoint of the specific application. Too detailed models may become unpractically large for the computer capacity. On the other hand, too simple models may give totally wrong picture of the process.

The design calculation codes and models were discussed in six papers. The lack of sufficient experimental data to support the development was again recognized here. Some help to the situation can be expected, since a steam generator data bank is being collected in Russia as presented by Dr. Vasiljeva. In the near future this data bank will be made available, and it should be useful for the model development and validation purposes.

Primary collector integrity was a topic of Session III. The main issues are the thermal loadings of the PGV-4 (VVER-440) primary collector, and the integrity of the tube connection part of the cold primary collector of PGV-1000. Thermal hydraulic conditions as well as plant operations have a strong influence on these integrity issues.

A large leakage accident from the primary-to-secondary side (PRISE) is possible in the horizontal VVER steam generators. The break can be a lift-up of the primary collector cover, or a ductile failure of the collector wall in the area of tubing connections. That is why the large PPRISE accidents (the break area up to 90—100 cm<sup>2</sup>) are defined as a design basis accident for the VVER plants e.g. in Finland. Session IV discussed, how such PRISE accidents can be effectively managed. The analysis task is particularly difficult, since the PRISE management relies to a large degree on successful operator actions. The different management concepts require well established analyses, and preferentially also the simulator support. The probability aspects were discussed based on the quantification results of the Loviisa PSA study.

A very acute problem of the feedwater distributor experiencing severe erosion-corrosion problems in the PGV-4 was the topics of Session V. Two principally different designs exist for replacing the eroded pipe sections. One is developed by Hidropress of Russia, and it

has been installed into six steam generators in the Ukrainian Rovno plant, and into one at Loviisa Unit 2. The design employs the idea of locating the new distributor and of injecting the feedwater through the short nozzles above the tube bundle. The other design has been developed in Czech Republic by Vitkovice. Again the distributor locates above the tube bundle, but the feedwater is injected in the middle of the tube bundle through long nozzles. Such feedwater distribution systems have been installed into sixteen steam generators at Dukovany. A modified version with a mixing chambre has been installed into two steam generators at Bohunice Unit 3. Very active discussion was conducted concerning the practical and theoretical questions.

Final Session VI was organized as a panel discussion. The panelists expressed their opinion concerning the prioritization of the VVER steam generator safety issues. The discussion has been summarized by Dr. Strupczewski, the session chairman, in the last paper of these proceedings.

The continuation of this Seminar was suggested and recommended by a number of participants. Also, the IAEA is willing to continue the support. The Finnish organizers proposed tentatively to have the next seminar in Lappeenranta in summer 1996.

*Harri Tuomisto, IVO IN*  
*Heikki Purhonen, VTT*  
*Timo Haapalehto, LTKK*  
*Andrzej Strupczewski, IAEA*

# THIRD INTERNATIONAL SEMINAR ON HORIZONTAL STEAM GENERATORS

18 - 20 October 1994, Lappeenranta, Finland

## PROGRAMME

Tuesday, 18 October 1994

- 8:30 Registration
- 9:00 Opening of the Seminar  
Prof. Heikki Kalli, LTKK
- 9:15 Aim and Programme of the Seminar  
Dr. Harri Tuomisto, IVO International

### Session I

#### THERMAL-HYDRAULIC EXPERIMENTS OF HORIZONTAL STEAM GENERATORS

*Chair: Dr. N. Trunov, Gidropress, Russia*

*Co-Chair: Prof. H. Kalli, LTKK, Finland*

- 9.30 J. Kouhia, V. Riikonen, H. Purhonen (VTT Energy, Lappeenranta, Finland)  
PACTEL: Experiments on the Behavior of the New Horizontal Steam Generator
- 10.00 Gy. Ézsöl, L. Szabados, I. Trosztel (AEKI/KFKI, Hungary)  
PMK-2 Experiment Study on Steam Generator Behaviour
- 10.30 *Coffee Break*
- 11.00 S.A. Logvinov, V.F. Titov (OKB Gidropress, Russia), M. Nótáros, I. Lenkei  
(Paks NPP, Hungary)  
Thermohydraulics of PGV-4 Water Volume During Damage of the Feedwater  
Collector Nozzles
- 11.30 L. Papp (Vítkovice, Czech Republic)  
Influence of Feedwater and Blowdown Systems on the Mineral Distribution in  
WWER Steam Generators
- 12.00 V. Yrjölä (VTT Energy, Finland)  
Results of Questionnaire for the Needs of Measured Data for the Steady-State  
Calculations

- 12.15 Discussion on Session I  
12.30 *Lunch*

### Session IIa

## THERMAL-HYDRAULIC ANALYSES OF HORIZONTAL STEAM GENERATORS

*Chair: Mr. S. Savolainen, IVO Loviisa, Finland*  
*Co-Chair: Mr. D. Bestion, CEN Grenoble, France*

- 14.00 V.F. Titov, V.M. Zorin, V.I. Gorburov (OKB Hidropress, Russia)  
Mathematical Simulation of Processes in Horizontal Steam Generators and the Program of Calculation of Its Characteristics
- 14.30 M. Protze (Siemens/KWU, Germany)  
RELAP5/MOD2 Post-Test Calculation of a Loss-of-Feedwater Experiment at the PACTEL Test Facility
- 15.00 *Coffee Break*
- 15.30 T. Haapalehto et al (LTKK, Finland)  
Analyses of the PACTEL Loss-of-Feedwater Experiments
- 16.00 Yu. Belyaev (OKB Hidropress, Russia), W. Luther (GRS, Germany), S. Spolitak (RRC-KI, Russia), N. Trunov, I. Tshekin (OKB Hidropress, Russia)  
Modelling Horizontal Steam Generator with ATHLET: Verification of Different Nodalization Schemes and Implementation of Verified Constitutive Equations
- 16.30 O. Ubra (Škoda, Czech Republic), M. Doubek (Czech Technical University)  
Horizontal Steam Generator PGV-1000 Thermal-Hydraulic Analysis
- 17.00 Yu.V. Belyaev, S.I. Zaytsev, G.A. Tarankov (OKB Hidropress, Russia)  
Verification of DINAMIKA-5 Code on Experimental Data of the Water Level Behaviour in PGV-440 Under Dynamic Conditions
- 17.30 Discussion on Session IIa
- 18.00 Social Programme

Wednesday, 19 October 1994

### Session III

#### PRIMARY COLLECTOR INTEGRITY

*Chair: Dr. O. Matal, Energovýzkum, Czech Republic*

*Co-Chair: Mr. Y. Hytönen, IVO International, Finland*

- 9.00 O. Matal, J. Klinga, T. Šimo (Energovýzkum, Brno, Czech Republic)  
Primary Collector Wall Local Temperature Fluctuations in the Area of Water-Steam Phase Boundary
- 9.30 A.G. Ageev, R.V. Vasilieva, B.I. Nigmatulin, G.A. Tarankov (ENIN, EREC, Hidropress, Russia)  
Data Bank of Hydrodynamics, Thermal Tests and Tube Temperature Regimes of PGV-4 and PGV-1000 Natural Steam Generators
- 10.00 *Coffee Break*
- 10.30 C. Lin, A. Strupczewski (IAEA, Vienna)  
Steam Generator Collector Integrity of WWER-1000 Reactors
- 11.00 Discussion on Session III

### Session IV

#### MANAGEMENT OF PRIMARY-TO-SECONDARY LEAKAGE ACCIDENTS

*Chair: Mr. B. Mohsen, IVO International, Finland*

*Co-Chair: Mr. J. Kouhia, VTT Energy, Finland*

- 11.30 E. Balabanov, A. Ivanova (Energoproekt, Sofia, Bulgaria)  
Analyses of Steam Generator Collector Rupture for WWER Using RELAP5 Code
- 12.00 J. Szczurek (IAE, Świerk, Poland)  
RELAP5/MOD2.5 Analyses of SG Primary Collector Head Rupture in VVER-440 Reactor
- 12.30 *Lunch*
- 14.00 B. Mohsen, K. Jänkälä (IVO International)  
Management of Primary-to-Secondary Leaks at Loviisa NPP
- 14.30 M. Protze (Siemens/KWU, Germany)  
PRISE Management Concept
- 15.00 Discussion on Session IV
- 15.30 *Coffee Break*

**Session IIb****THERMAL-HYDRAULIC ANALYSES OF HORIZONTAL STEAM GENERATORS**

*Chair: Mr. T. Haapalehto, LTKK, Finland*  
*Co-Chair: Ms. M. Protze, Siemens, Germany*

- 16.00 P. Matejovič, L. Vranka, E. Václav (VUJE, Slovakia)  
Application of Thermal-Hydraulic Codes in VVER-440 Steam Generator Modelling
- 16.20 V. Melikhov, O. Melikhov, B. Nigmatulin (EREC, Elektrogorsk, Russia)  
Numerical Modelling of Secondary Side Thermal-Hydraulics of Horizontal Steam Generators
- 16.40 I. Karppinen (VTT Energy, Finland)  
Modelling Studies of Horizontal Steam Generator PGV-1000 with CATHARE
- 17.00 I. Ovcharova (Energoproekt, Sofia, Bulgaria)  
Parametric Study for Horizontal SG Modelling
- 17.20 J. Ylijoki (VTT-Energy), C. Palsinajärvi, K. Porkholm (IVO IN, Finland)  
Modelling the Horizontal Steam Generator with APROS
- 17.40 A.G. Ageev, V.F. Titov, B.I. Nigmatulin, G.A. Tarankov (ENIN, Hidropress, EREC, Russia)  
Modernization of PGV-1000 Separator Scheme to Improve an Efficiency and Reliability
- 18.00 P. Král (NRI Řež, Czech Republic)  
RELAP5/MOD3.1 Analysis of Main Steam Header Rupture in VVER-440/213 NPP
- 18.20 Discussion on Session IIb
- 18.45 Social Programme

Thursday, 20 October 1994

**Session V**

**FEEDWATER COLLECTOR REPLACEMENT**

*Chair: Dr. N. Trunov, Hidropress, Russia*

*Co-Chair: Mr. S. Savolainen, IVO Loviisa, Finland*

- 9.00 G.A. Tarankov, N.V. Trunov, V.F. Titov (OKB Hidropress, Russia), V.V. Urbansky (Rovno NPP, Ukraine), I. Lenkei, M. Nótáros (Paks NPP, Hungary)  
Study of Thermohydraulic Characteristics of Upgraded Feedwater Collector in PGV-440 Steam Generator
- 9.30 O. Matal (Energovýzkum, Brno, Czech Republic), K. Gratzl (Vítkovice s. c., Ostrava, Czech Republic) J. Klinga (Energovýzkum, Brno, Czech Republic), J. Tischler, M. Mihálik (Bohunice NPP, Slovakia)  
Advanced Feedwater Distributing System for WWER-440 Steam Generators
- 10.00 *Coffee Break*
- 10.30 S. Savolainen and B. Elsing (IVO, Loviisa NPP, Finland)  
Feedwater Distribution Pipe Replacement at Loviisa NPP
- 11.00 I. Kusák, F. Cikryt (Vítkovice J.S.C., Czech Republic)  
Feed Water Piping in SG 440 MW
- 11.30 Discussion of Session V
- 12.00 *Lunch*

**Session VI**

**VVER STEAM GENERATOR SAFETY ISSUES**

*Chair: Dr. A. Strupczewski, IAEA, Vienna*

*Co-Chair: Mr. J. Mišák, Nuclear Regulatory Authority, Slovak Republic*

- 13.30 Panel Discussion of the Safety Issues of VVER Steam Generators  
-----
- 15.15 Closing Remarks
- 15.30 Adjourn

## THIRD INTERNATIONAL SEMINAR ON HORIZONTAL STEAM GENERATORS

18 - 20 October 1994, Lappeenranta, Finland

### LIST OF PARTICIPANTS

<i>Name</i>	<i>Organisation</i> <i>Address, telephone, telefax</i>
<b>Bulgaria</b>	
Ms. Ivanka Ovcharova	Energoprojekt, Sofia Nuclear Safety&Automation Division, Accident Analysis 51, James Baucher Blvd, 1407 Sofia, Bulgaria Tel. +359-2-62 40 09, fax +359-2-66 89 51
<b>Czech Republic</b>	
Mr. František Cikryt	VÍTKOVICE J.S.C., 600-Power Systems Engineering Head of Project and Design 706-02 Ostrava 6, Czech Republic Tel. +42-69-29 26135, fax +42-69-29 26460
Mr. Svatopluk Česla	VÍTKOVICE J.S.C., Service of NPPs, Director 706-02 Ostrava 6, Czech Republic Tel. +42-69-29 26811, fax +42-69-29 29839
Mr. Pavel Král	Nuclear Research Institute Řež plc Department of Thermal-Hydraulic Analysis 250 68 Řež, Czech Republic Tel. +42-2-66412171 ext. 2447, fax +42-2-66412029
Dr. Oldřich Matal	Energovýzkum Brno Ltd. Božetěchova 17, 612 00 Brno, Czech Republic Tel. +42-5-412 14661, fax +42-5-746058
Dr. Ludovit Papp	VÍTKOVICE J.S.C., Technical Division Institute of Material Engineering, NPP Project Manager Pohraniční 31, 706-02 Ostrava 6, Czech Republic Tel. +42-69-29 23923, fax. +42-69-29 29827
Dr. Olga Ubrá	ŠKODA PRAHA a.s. Milady Horákové 109, 160 41 Praha 6, Czech Republic Tel. +42-2-24396466, fax +42-2-24396434
<b>France</b>	
Mr. Dominique Bestion	Commissariat à l'Energie Atomique (CEA) Centre d'Études Nucléaires de Grenoble (CEN-G) Head of the CATHARE Physical Development Group 17, rue des Martyrs, 38054 Grenoble Cedex 9, France Tel. +33-76 88 36 45, fax +33-76 88 51 77
Mr. Ismo Karppinen	Institut de Protection et de Sûreté Nucléaire, IPSN/DES/SEPRI, BP 6, 92265 Fontenay-aux-Roses, France Tel. +33-1-46 54 71 59, fax.+33-1-47 46 86 76
Mr. Eric Laugier	Institut de Protection et de Sûreté Nucléaire, IPSN Bât. 729, Centre de Caradache 13108 St Paul lez Durance, France Tel. +33-42 25 39 47, fax.+33-42 25 78 60

**Germany**

Mr. Wolfgang Luther  
Gesellschaft für Anlagen- und Reaktorsicherheit (GRS) mbH  
Forschungsgelände, 85748 Garching, Germany  
Tel. +49-89-32004126, fax +49-89-32004 299

Ms. Marion Protze  
Siemens-KWU  
Freyeslebenstr. 1, P.O.Box 3220,  
D-91058 Erlangen, Germany  
Tel.+49-9131-185474, fax +49-9131-184345

**Hungary**

Mr. Mihály Nótáros  
Paks NPP Ltd, Head of Section of Technical Support  
PF 71, H-7030 Paks, Hungary  
Tel. +36-75-318917, fax +36-1-1565579

**Poland**

Dr. Jan Szczurek  
Institute of Atomic Energy, Świerk  
05-400 Otwock, Poland  
Tel. +48-22-330358, fax +48-2-7793 888

**Russia**

Prof. Aleksander Ageev  
EREC Research & Engineering Centre of Nuclear Plants Safety  
Senior Researcher  
Bezmyannaya 6, Electrogorsk, Moscow Region, Russia 142530  
Fax +7-09643-30515

Mr. Iouri V. Beliaev  
OKB Hidropress  
Ordzhonikidze 23, 142103 Podolsk, Moscow Region, Russia  
Tel. +7-095-1379652

Dr. Sergej A. Logvinov  
OKB Hidropress, Head of Department  
Ordzhonikidze 23, 142103 Podolsk, Moscow Region, Russia  
Tel. +7-095-1379652

Dr. Vladimir I. Melikhov  
EREC Research & Engineering Centre of Nuclear Plants Safety  
Senior Researcher  
Bezmyannaya 6, Electrogorsk, Moscow Region, Russia 142530  
Fax +7-09643-30515

Prof. Valentin F. Titov  
OKB Hidropress, Chief Designer, Head of Branch  
Ordzhonikidze 21, 142103 Podolsk, Moscow Region, Russia  
Tel. +7-095-1379652

Dr. Nikolai B. Trunov  
OKB Hidropress  
Ordzhonikidze 23, 142103 Podolsk, Moscow Region, Russia  
Tel. +7-095-1379652

Dr. Rimma V. Vasilieva  
EREC Research & Engineering Centre of Nuclear Plants Safety  
Senior Researcher  
Bezmyannaya 6, Electrogorsk, Moscow Region, Russia 142530  
Fax +7-09643-30515

**Slovakia**

Mr. Peter Matejovič  
VÚJE, Nuclear Power Plant Research Institute  
Okružná 5, 91864 Trnava, Slovakia  
Tel. +42-805-605152, fax +42-805-42403

Mr. Jozef Mišák  
Chairman, Nuclear Regulatory Authority  
Slovak Republic  
Bajkalská 27, P.O. Box 24, 820 07 Bratislava 27, Slovakia  
Tel. +42-7-5221531, fax +42-7-293603

Mr. Milan Mihálik  
Nuclear Power Plant Bohunice  
91931 Jaslovské Bohunice, Slovakia  
Tel. +42-805-21301, fax +42-805-24467

## IAEA

Prof. Andrzej Strupczewski  
International Atomic Energy Agency  
Wagramerstrasse 5, P.O.Box 100, A-1400 Vienna, Austria  
Tel. +43-1-2360-2513, fax +43-1-234564

## Finland

Mr. Juhani Hyvärinen  
Mr. Hannu Ollikkala  
Finnish Centre for Radiation and Nuclear Safety (STUK)  
P.O.Box 14, FIN-00881 Helsinki, Finland  
Tel. +358-0-759881, fax +358-0-75988382

Mr. Yrjö Hytönen  
Mr. Heikki Kantee  
Mr. Kalle Jänkälä  
Mr. Jarmo Korhonen  
Mr. Olli Kymäläinen  
Mr. Bahey Mohsen  
Mr. Christer Palsinajärvi  
Dr. Harri Tuomisto  
IVO International Ltd  
Nuclear Power Plant engineering  
Rajatorpantie 8, P.O.Box 112, FIN-01019 IVO, Finland  
Tel. +358-0-85611, fax +358-0-8561 3403

Mr. Bernhard Elsing  
Mr. Heikki Jokineva  
Mr. Alpo Savikoski  
Mr. Samuli Savolainen  
Imatran Voima Oy, Loviisa NPP  
FIN-07901 Loviisa, Finland  
Tel. +358-15-5501, fax +358-15-5504435

Mr. Jaakko Miettinen  
Mr. Sixten Norrman  
Mr. Thomas Stenius  
Mr. Jukka Ylijoki  
VTT Energy, Nuclear Energy  
P.O.Box 1604, FIN-02044 VTT, Finland  
Tel. +358-0-4561, fax +358-0-456 5000

Mr. Jyrki Kouhia  
Mr. Heikki Purhonen  
Mr. Markku Puustinen  
Mr. Vesa Riikonen  
Dr. Jari Tuunanen  
VTT Energy  
P.O.Box 20, FIN-53851 Lappeenranta, Finland  
Tel. +358-53-62111, fax +358-53-621 2379

Prof. Heikki Kalli  
Mr. József Bánáti  
Mr. Timo Haapalehto  
Ms. Satu Kainulainen  
Ms. Virpi Korteniemi  
Mr. Reijo Munther  
Mr. Pekka Raussi  
Mr. Timo Ritoumumi  
Ms. Christine Sarrette  
Mr. Eero Virtanen  
Lappeenranta University of Technology (LTKK)  
P.O.Box 20, FIN-53851 Lappeenranta, Finland  
Tel. +358-53-62111, fax +358-53-621 2799

## CONTENTS

PREFACE	i
PROGRAMME OF SEMINAR	iii
LIST OF PARTICIPANTS	iv
PACTEL: Experiments on the Behavior of the New Horizontal Steam Generator <i>J. Kouhia, V. Riikonen, H. Purhonen (VTT Energy, Lappeenranta, Finland)</i>	1
PMK-2 Experiment Study on Steam Generator Behaviour <i>Gy. Ézsöl, L. Szabados, I. Trosztel (AEKI/KFKI, Hungary)</i>	10
Thermohydraulics of PGV-4 Water Volume During Damage of the Feedwater Collector Nozzles <i>S.A. Logvinov, V.F. Titov (OKB Hidropress, Russia), M. Nótáros, I. Lenkei (Paks NPP, Hungary)</i>	33
Influence of Feedwater and Blowdown Systems on the Mineral Distribution in WWER Steam Generators <i>L. Papp (Vítkovice, Czech Republic)</i>	49
Results of Questionnaire for the Needs of Measured Data for the Steady-State Calculations <i>V. Yrjölä (VTT Energy, Finland)</i>	56
Mathematical Simulation of Processes in Horizontal Steam Generators and the Program of Calculation of Its Characteristics <i>V.F. Titov, V.M. Zorin, V.I. Gorburov (OKB Hidropress, Russia)</i>	64
RELAP5/MOD2 Post-Test Calculation of a Loss-of-Feedwater Experiment at the PACTEL Test Facility <i>M. Protze (Siemens/KWU, Germany)</i>	71
Analyses of the PACTEL Loss-of-Feedwater Experiments <i>V. Korteniemi, E. Virtanen, T. Haapalehto (LTKK, Fin.), J.Kouhia (VTT Energy, Fin.)</i>	89
Modelling Horizontal Steam Generator with ATHLET: Verification of Different Nodalization Schemes and Implementation of Verified Constitutive Equations <i>Yu. Belyaev (OKB Hidropress, Russia), W. Luther (GRS, Germany), S. Spolitak (RRC-KI, Russia), N. Trunov, I. Tshekin (OKB Hidropress, Russia)</i>	97

Horizontal Steam Generator PGV-1000 Thermal-Hydraulic Analysis <i>O. Ubra (Skoda, Czech Republic), M. Doubek (Czech Technical University)</i>	107
Verification of DINAMIKA-5 Code on Experimental Data of the Water Level Behaviour in PGV-440 Under Dynamic Conditions <i>Yu.V. Belyaev, S.J. Zaytsev, G.A. Tarankov (OKB Gidropress, Russia)</i>	118
Primary Collector Wall Local Temperature Fluctuations in the Area of Water-Steam Phase Boundary <i>O. Matal, J. Klinga, T. Šimo (Energovýzkum, Brno, Czech Republic)</i>	136
Data Bank of Hydrodynamics, Thermal Tests and Tube Temperature Regimes of PGV-4 and PGV-1000 Natural Steam Generators <i>A.G. Ageev, R.V. Vasilieva, B.I. Nigmatulin, G.A. Tarankov (ENIN, EREC, Gidropress, Russia)</i>	143
Steam Generator Collector Integrity of WWER-1000 Reactors <i>C. Lin, A. Strupczewski (IAEA, Vienna)</i>	166
Analyses of Steam Generator Collector Rupture for WWER Using RELAP5 Code <i>E. Balabanov, A. Ivanova (Energoproekt, Sofia, Bulgaria)</i>	187
RELAP5/MOD2.5 Analyses of SG Primary Collector Head Rupture in VVER-440 Reactor <i>J. Szczurek (IAE, Świerk, Poland)</i>	198
Management of Primary-to-Secondary Leaks at Loviisa NPP <i>B. Mohsen, K. Jänkälä (IVO International)</i>	220
Application of Thermal-Hydraulic Codes in VVER-440 Steam Generator Modelling <i>P. Matejovič, L. Vranka, E. Václav (VUJE, Slovakia)</i>	226
Numerical Modelling of Secondary Side Thermal-Hydraulics of Horizontal Steam Generators <i>V. Melikhov, O. Melikhov, B. Nigmatulin (EREC, Elektrogorsk, Russia)</i>	249
Modelling Studies of Horizontal Steam Generator PGV-1000 with CATHARE <i>I. Karppinen (VTT Energy, Finland)</i>	273
Parametric Study for Horizontal SG Modelling <i>I. Ovcharova (Energoproekt, Sofia, Bulgaria)</i>	291
Modelling the Horizontal Steam Generator with APROS <i>J. Ylijoki (VTT-Energy), C. Palsinajärvi, K. Porkholm (IVO IN, Finland)</i>	301
Modernization of PGV-1000 Separator Scheme to Improve Efficiency and Reliability <i>A.G. Ageev, V.F. Titov, B.I. Nigmatulin, G.A. Tarankov (ENIN, Gidropress, EREC, Russia)</i>	311

RELAP5/MOD3.1 Analysis of Main Steam Header Rupture in VVER-440/213 NPP <i>P. Král (NRI Řež, Czech Republic)</i>	326
Study of Thermohydraulic Characteristics of Upgraded Feedwater Collector in PGV-440 Steam Generator <i>G.A. Tarankov, N.V. Trunov, V.F. Titov (OKB Hidrogress, Russia), V.V. Urbansky (Rovno NPP, Ukraine), J. Lenkei, M. Nótáros (Paks NPP, Hungary)</i>	362
Advanced Feedwater Distributing System for WWER-440 Steam Generators <i>O. Matal (Energovýzkum, Brno, Czech Republic), K. Gratzl (Vítkovice s. c., Ostrava, Czech Republic), J. Klinga (Energovýzkum, Brno, Czech Republic), J. Tischler, M. Mihálik (Bohunice NPP, Slovakia)</i>	375
Feedwater Distribution Pipe Replacement at Loviisa NPP <i>S. Savolainen and B. Elsing (IVO, Loviisa NPP, Finland)</i>	385
Feed Water Piping in SG 440 MW <i>I. Kusák, F. Cikryt (Vítkovice J.S.C., Czech Republic)</i>	399
Panel Discussion: Safety Issues of VVER Steam Generators in WWER NPPs	411

# PACTEL: Experiments on the Behaviour of the New Horizontal Steam Generator

J. Kouhia, V. Riikonen, H. Purhonen

*VTT Energy, P.O.Box 20, FIN-53851, Lappeenranta, Finland*

## Abstract

Experiments were performed to study the behaviour of the PACTEL facility, a medium scale integral test loop simulating VVER-440 pressurized water reactors. The study focused on the operation of the new horizontal steam generator model installed in PACTEL. Three experiments were conducted: a small-break test to observe the steam generator behaviour over a range of primary coolant inventories, a hot leg loop seal experiment to study the cyclic behaviour of a loop seal and a loss of secondary side feedwater test to examine the effect of uncovered tubes in the steam generator. A reverse flow was observed in the lower part of the U-tube bundle of the steam generator during natural circulation. The flow reversal point dropped when the tubes uncovered, during secondary inventory reduction.

## 1. Introduction

Limited experimental data is available on the behaviour of horizontal steam generators in different abnormal conditions. An operation of the horizontal steam generator is very different from the vertical U-tube steam generator, which has been studied extensively using various test facilities. Thus more information is needed on the behaviour of the horizontal steam generator for safety analysis of reactor concepts which use this type of steam generators.

Modelling of the horizontal steam generator in a volumetrically scaled test facility is more difficult than modelling of the vertical steam generator. If the same height as in the reference reactor is maintained, then the U-tubes must be wounded or bent in a very different way from the power plant. On the other hand, if the tubes are maintained as U-tubes, then the height of the steam generator must be lowered.

Natural circulation is recognized as an important core cooling mechanism in a nuclear power plants during both regular operations and potential transients. The general behaviour of natural circulation as a function of coolant inventory is of particular interest in a small-break loss-of-coolant accident (SBLOCA) scenario where the core cooling could be required at reduced inventories. A series of tests was conducted using the PACTEL facility to examine the behaviour of the loop flow as a function of primary side coolant inventory. These tests are reported in reference [1]. In an other study, a set of experiments was performed to observe the effect of loss of secondary side feedwater during low core power conditions [2]. Similar tests to these were performed using PACTEL with a new steam generator model. The tests were conducted with one loop, since the other two loops still have the original steam generator model.

This paper describes a series of experiments performed to investigate the

horizontal U-tube steam generator behaviour in natural circulation. A short facility description is given together with the PACTEL steam generator geometry and the measurement instrumentation. The behaviour of the test facility is explained during the SBLOCA experiment. A test was carried out to observe the behaviour of the hot leg loop seal and it is discussed in chapter 4. Finally the effect of decreasing secondary side level has been described.

## 2. Facility description

PACTEL is a volumetrically scaled (1:305), out of pile model of the VVER-440 reactors used in Finland. The facility is an integral test facility and it includes all the main components of the reference reactor. The reactor vessel is simulated by a U-tube construction consisting of separate core and downcomer sections. The core is comprised of 144 electrically heated fuel rod simulators. The geometry and the pitch of the rods is the same as in reference power plant. The maximum total core power is 1 MW, or 22% of scaled nominal power. The maximum primary pressure is 8.0 MPa compared to 12.3 MPa of the reactor.

Component heights and relative elevations correspond to those of the full scale reactor to match the natural circulation pressure heads in the reference system. The hot and cold leg elevations of the power plant have been reproduced. This is particularly important for the loop seals. Unlike other PWRs there is a loop seal in the hot leg in a VVER-440. This is a consequence of the steam generator location, which is almost at the same height as the hot leg connection to the upper plenum. The collector is connected to the hot leg at the bottom of the steam generator, hence a roughly U-shaped pipe

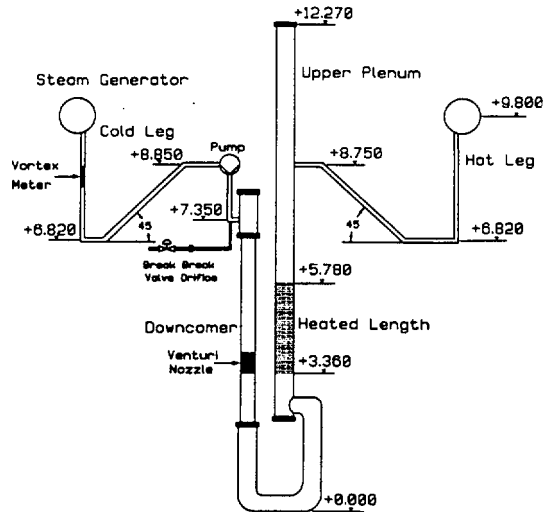


Fig. 1. Geometry of the PACTEL facility.

is needed to complete the connection. The cold leg loop seal is formed by the elevation difference of the inlet and outlet of the reactor coolant pump. Fig. 1 shows the geometry of the loop seals.

### 2.1 Steam generator description

The number of loops has been reduced from six of the reference system to three in PACTEL, thus one PACTEL steam generator model corresponds to two in the power plant. The original steam generator model of PACTEL had full length heat exchanger tubes and the same tube cluster geometry as in the power plant steam generator. This way the tube bundle height was less than 15% of the height of the reference steam generator. The use of this model is limited when for example the internal flow is studied as was pointed out in reference [3].

The new steam generator, which has been installed in one loop, has 118 U-tubes and the length of the tubes (2.8 m) is about third of the full scale steam



generator (9.0 m). The outer diameter of the tubes is 16 mm which corresponds the reference system and the inner diameter is 13 mm (13.2 mm in the power plant). In order to have higher tube bank, the pitch in vertical direction has been increased to 48 mm instead of 24 mm of the reference steam generator. The pitch in the horizontal direction has been maintained.

The shell outer diameter is 1 m. Because of the higher vertical pitch than in the reference system the secondary side is larger than the scaled down secondary volume. This distorts the time scale of secondary side transients. Two compartments has been constructed on each side of the steam generator to decrease the mass of water that is directly involved to the primary to secondary heat transfer process. The compartments are not totally isolated from the rest of the secondary side, but the coolant has number of flow paths in and out of the compartments.

Fig. 2 shows the cross section of the PACTEL steam generator. The instrumented tubes are filled with black colour. An instrumented tube has temperature measurements in the primary and secondary sides in three or four different locations. The thermocouple locations are marked as a,b,c and d in the horizontal cross section drawing. The tube layers are numbered with Roman numbers.

### 3. Small-break test

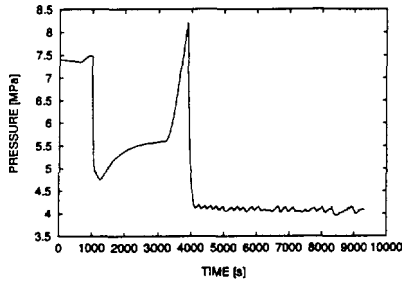
An experiment was performed to study the behaviour of the steam generator over a continuous range of primary side coolant inventories. Only one loop was used in the test. The experiment was started with a steady state operation at the full inventory and forced convection. The primary circulation pump was stopped and the

break was opened in the cold leg at 1000 s. At the same time the pressurizer was isolated from the remainder of the primary system to prevent the coolant flow between the pressurizer and rest of the primary side. The break size was 1 mm or 0.04% of the PACTEL cold leg cross sectional area. The break size corresponds to 0.12% of the scaled down cold leg area of the reference system. The core power during the entire experiment was 70 kW.

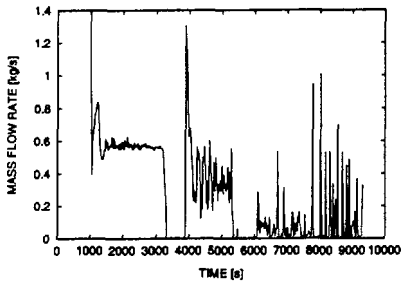
No other actions were taken during the experiment other than maintaining the secondary side level through periodic additions of feedwater. The test was terminated when the cladding temperatures started to rise at the top of the core.

#### 3.1 Overall behaviour of the loop

Fig. 3 shows the measured primary pressure and the downcomer mass flow rate in the experiment SBL-22. After opening the break valve at 1000 s, the primary pressure dropped immediately until the hot leg saturation temperature was reached. The heat transfer from primary to secondary side was due to the single-phase natural circulation. This heat transfer mode continued until 3400 s, when the upper plenum collapsed level reached the hot leg pipe entrance, and the loop flow stagnated. The energy transport from the core to the steam generator was lost, and the primary pressure rose rapidly. The pressure rose and the flow remained stagnant until enough coolant leaked through the break to clear the hot leg loop seal at 3900 s. Similar flow stagnation has been observed in the PMK facility as well [5]. A two-phase mixture flowed to the steam generator and the system pressure started to drop. The loop flow was now two-phase natural circulation and it continued until 5300 s, when boiler condenser mode was established. The mass flow rate was very low in this mode, since



a)



b)

Fig. 3. Behaviour of the primary pressure (a), and the downcomer mass flow rate (b).

condensing is extremely effective way to transport energy from the core to the heat sink. The behaviour of the PACTEL facility during SBLOCA test is explained in more detail in reference [1]. Even if the steam generator model has been changed from the previous natural circulation test series, the overall behaviour of the loop have remained roughly the same. Table 1 summarises the different heat transfer modes.

### 3.2 Behaviour of the steam generator in the small-break test

A more detailed description of the behaviour of the steam generator is given in this chapter. By positive flow direction we mean flow from the hot collector to the cold collector. After the pump has been

Table 1. Heat transfer modes during the small-break LOCA experiment.

time[s]	inventory[%]	mode
1000-3400	100-74	single-phase
3900-5300	67-56	two-phase
5300-9500	56-32	boiler-cond.

stopped the flow reversed in the lowest tube layer (number I), because the density in the cold collector was somewhat higher than in the hot collector. Thus, the pressure was higher at the bottom of the cold collector rather than cold collector [3]. The hot leg temperature rose steadily, when the loop was reaching for new equilibrium. The cold leg temperature remained almost constant, because the secondary side conditions were maintained about the same during the entire test. The rising hot leg temperature dropped even more the hot collector density and the flow reversal was observed in the tubes 19 and 97 at 1500 s (tube layer V). After that the hot leg temperature was still rising, but there was no indication of negative flow in the next instrumented tube layer. Since the flow in the lower part of the U-tube cluster was reversed, the cold coolant was mixed with the hot coolant in the hot collector and the density difference between the collectors did not increase as fast as early in the transient. Fig. 4 shows the situation in the steam generator before the flow stagnation occurred. The upper part of the tube bundle handled most of the heat transfer from primary to secondary.

During the stagnant flow period the temperature distribution in the whole steam generator was almost even and a minor temperature drop was observed due to the heat losses, since there was no

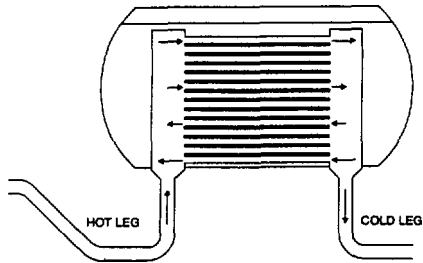


Fig. 4. Flow directions in the steam generator tubes during single-phase flow.

energy transport from the core. When the loop seal cleared and the flow resumed there was liquid in the cold collector and two-phase mixture in the hot collector. This initiated reverse flow in the lower part of the tube cluster. The upper most tubes handled the bulk of the heat transfer. The level in the cold collector started to drop, since the manometric balance of the entire loop was lost (Fig 5). This could be observed as increasing level in the upper plenum. The dropping cold collector level changed the differential pressure over the U-tube bank and the flow turned into the positive direction in layer V, about 100 s after the flow resumed.

It seemed that most of the steam went to the upper most part of the tube cluster. There was clearly liquid flow through the lower part of the tube bank early in the two-phase region. However, this changed when the two-phase flow period advanced further. Towards the end of the two-phase flow stage the differential pressure over the collector changed positive, or the pressure was higher in the hot collector than cold collector. There was no evidence of constant reverse flow in any of the tubes when the elapsed time was 4700 s from the beginning of the experiment. Temperature oscillations were observed in tube 15, which indicated that sometimes the flow direction was negative, however.

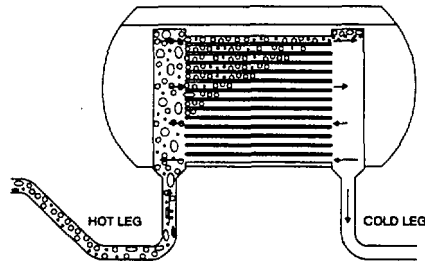


Fig. 5. Behaviour of the steam generator after loop seal clearing in SBL-22.

In the boiler-condenser mode the mass flow rate is very low. Thus, the driving force for the fluid to flow from the hot collector to the cold collector was weak [4]. The cold collector was totally filled by steam, when boiler condenser mode started. The flow from the heat exchange tubes to the cold leg was not continuous, but intermittent flow peaks were observed. These were induced by secondary side pressure fluctuations and the feedwater injection. When the secondary side pressure control valve opened more boiling occurred and more energy was transferred from primary to secondary. Hence, more steam condensed into tubes and liquid flowed to the cold leg. The cold (about 30 °C) feedwater increased the condensation in the tubes as well.

Similar tests with the previous PACTEL steam generator model showed clearly that considerable amount of liquid accumulated into the tubes during the boiler-condenser mode and the retaining water decreased the heat transfer before the tubes emptied to the cold leg. This behaviour was not evident in this experiment. The reason is that the length of the tubes is only third of the tube length of the previous model.

The cold leg loop seal caused flow peaks at the very end of the transient. When the level in the cold leg reached the bottom of

the loop seal, the steam flowed into the inclined part of the cold leg and rose to the pump. A new liquid level was formed and coolant flowed from the cold leg side to the upper plenum to even up the manometric balance of the loop.

#### 4. Loop seal refilling

It has been shown that a loop seal can refill after clearing and the phenomena could be cyclic [1]. The oscillations will be observed if the primary coolant inventory remains the same. This cyclic clearing and refilling of the loop seal was not observed in the small break LOCA case, because when the loop seal cleared the inventory was passed the oscillatory area.

An experiment was performed (LSR-10) with the PACTEL facility to study how the steam flow affects the flow behaviour in the loop seal. In the beginning of the test a steady state was established for 1000 s. The pump was stopped and the pressurizer isolated from the rest of the primary system. The primary coolant inventory was reduced to reach the stagnant flow conditions. The core power was initially set at 1.8 % scaled nominal power, which was low enough to reach

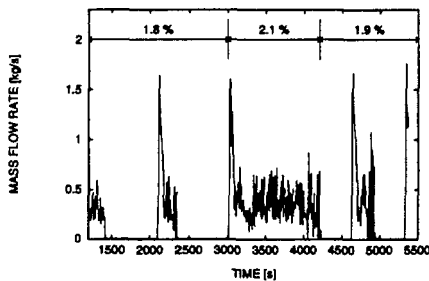


Fig. 6. Loop flow behaviour as a function of time in the experiment LSR-10.

repetitive loop seal filling and clearing. After observing this cyclical behaviour, the core power was increase to 2.1 %. When the loop seal cleared at this power level it remained clear so that a steady two-phase flow was observed. The core power was reduced to 1.9 % which initiated the cyclical clearing and refilling again. Fig. 6 shows the measured loop mass flow rate as a function of time in the experiment LSR-10.

By using the original PACTEL steam generator model the flooding limit was between the core powers of 1.2 and 1.4%. In the experiment LSR-10 the flooding limit was detected with the powers of 1.9-2.1%. The higher limit with the new steam generator model was undoubtedly due to the different geometry where the hot leg is connected to the steam generator primary collector. In the new steam generator there is an increase part between the hot leg and the collector unlike the original model where the hot leg was connected directly to the collector.

The behaviour of the steam generator is very similar to the behaviour in the SBLOCA test in the two-phase region. The redistribution of the coolant, when the loop seal refilled, was not observed in the SBLOCA experiment. As the loop seal filled, the steam in the hot leg, in the collectors and in the steam generator tubes condensated since there was no energy transport from the core any more. There was reverse flow from the cold leg to the steam generator immediately after the flow stagnated. This was observed as an instant drop in the collapsed level of the upper plenum. Each time the clearing of the loop seal occurred the initial conditions were roughly the same.

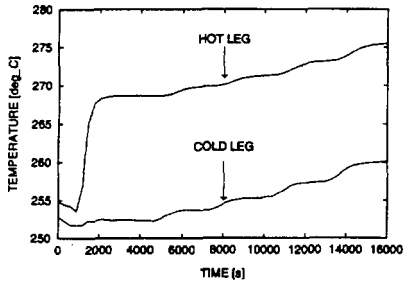


Fig. 7. The hot leg and the cold leg temperature in the loss of feedwater experiment.

### 5. Loss of feedwater experiment

The third type of experiment which was performed to study the characteristics of the PACTEL steam generator model was loss of feedwater test using low core power. The test was started by establishing a steady state with the primary circulating pump running. After 1000 s the pump was switched off and no other actions were taken during the experiment. The primary pressure was maintained through the pressurizer heaters. The experiment was concluded when four heat exchange tube layers were uncovered at about 16,000 s.

A steady single phase flow was reached at about 2000 s. The hot leg temperature was not increasing any more. The

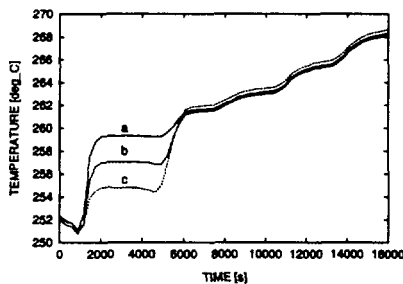


Fig. 8. The primary temperatures in the tube number 28 in LOF-10.

secondary side level was above the top of the tube bundle. A reverse flow was observed at the layers I and V. This was similar behaviour to the SBLOCA test during the single phase natural circulation.

A tube layer uncover was observed as a decrease in the heat transfer of that particular layer. Fig. 8 shows the temperature in the primary side of tube 28. The uncover occurred at 6000 s, which was clearly indicated by the temperature measurements. The primary temperature increased every time a new tube layer uncovered, so there was an indication of uncover of non-instrumented layer as well (Fig. 7).

The temperature difference between the hot and cold collector remained the same during the course of the experiment (Fig. 7). The mass flow rate was nearly constant as well, since the core power was maintained at the initial value of 75 kW. When a tube layer uncovered the upper part of the cold collector was filled with hot coolant and the differential pressure between the collectors changed. In the upper part of the collectors, the differential pressure was very low, since the density was roughly the same in both collectors. In the covered section, the density difference between the two collectors remained

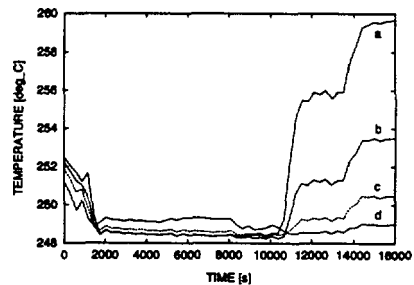


Fig. 9. The primary temperatures in the tube number 19 as a function of time in LOF-10.

almost constant, but the height of this part was decreasing. This lowered the differential pressure between the hot and the cold collector and the flow turned into the positive direction in the layer V at about 10,000 s, as shown in Fig 9. When the flow direction reversed the third tube layer was uncovering.

The secondary side swell level was observed to be about 30 mm higher than the collapsed level. The swell level was determined by comparing the collapsed level to the elevation of a tube layer which was uncovering. Superheated steam was detected in the steam line where the temperature was about 12 °C higher than the saturation temperature in the secondary side.

## 6. Conclusions

A new steam generator model has been constructed for the PACTEL facility in installed to one of the three loops of the facility. This model has higher U-tube bundle as the original PACTEL steam generators.

Three different kind of experiments were performed to study the characteristics of the new steam generator model. In the small-break LOCA experiment the behaviour of the system was studied when the primary inventory was decreasing. A reverse flow was observed in the lower part of the U-tube cluster in this experiment. When the cold collector level dropped the flow turned into the positive direction during two phase natural circulation.

Experiment LSR-10 was conducted to study cyclic behaviour of the hot leg loop seal. A higher steam flow was needed to stop the countercurrent flow from the steam generator to the hot leg, than with

the original PACTEL steam generator model. The reason was detected to be the new geometry how the hot leg is connected to the collector.

In the loss of feedwater test (LOF-10) the internal flow in the U-tube bundle changed during the experiment, because the temperature rose in the cold collector, when the tubes started to uncover. The level swell was observed to be about 30 mm.

## References

- [1] Lomperski S.W., Kouhia J., Natural circulation experiments with a VVER reactor geometry. Nuclear Engineering and Design. 147 (1994) 400-424.
- [2] Tuunanen J., Thermal-hydraulic studies on the safety of VVER-440 type nuclear power plants. Lappeenranta university of technology, research papers 33, 1994, Lappeenranta, Finland.
- [3] Proceedings of second international seminar of horizontal steam generator modelling. Lappeenranta university of technology, research papers 30, 1993, Lappeenranta, Finland. pp. 17 - 57.
- [4] Sonnenburg H.G., Tuomisto H., Analysis of a selected two-phase flow phenomenon in VVER reactors with horizontal steam generators. Nuclear Engineering and Design. 145 (1993) 261-270.
- [5] Bandurski T., G. Ezsöl, L. Maroti, I. Tóth, Modelling of two-phase natural circulation in a WWER-plant: PMK experimental results, Proceedings of the 4th Topical Meeting on Nuclear Reactor Thermal-Hydraulics, Karlsruhe, Germany, Vol. 1 (1989), pp. 478-483.

PMK - 2  
EXPERIMENTAL STUDY ON  
STEAM GENERATOR BEHAVIOUR

by

Gy. Ézsöl, L. Szabados, I. Trosztel

/To be presented at the "Third International Seminar  
on Horizontal Steam Generators",  
18-20 October 1994, Lappeenranta, Finland.)

KFKI Atomic Energy Research Institute  
Budapest, 1994.

## 1. ABSTRACT

The PMK-2 is a full pressure scaled-down model of the Paks Nuclear Power Plant, with a 1:2070 scaling ratio for the volume and power. It has a steam generator model which is a vertical section of the horizontal steam generator. The model has hot and cold collectors similarly to the steam generators of the plant. The heat transfer tubes are horizontal tubes. There are 82 rows of tubes and the elevations, as well as the heat transfer surface distribution is the same as in the plant. The elevation of the feed water supply is similar to that of the plant.

To study the temperature distribution in both the primary and the secondary side several thermocouples are built in, in addition to the overall instrumentation of the loop which has again a high number of measurement channels.

Paper gives a description and results of SPE-4, with special respect to the steam generator behaviour in both steady state and transient conditions. Detailed information is given in Ref. [1].

Axial distribution of coolant and feedwater temperatures are given for the primary and the secondary side of hot and cold collectors and the temperature distribution in the centre of steam generator.

## 2. A SHORT INTRODUCTION TO THE PLANT AND THE FACILITY

Figure 1 shows the scheme of the primary circuit of the Paks Nuclear Power Plant. Two important features of the VVER-440/213 type plants can be seen as: loop seal in the hot leg and the horizontal steam generator. The primary and partly the secondary circuit is modelled by the PMK-2 facility, a scaled down model of the plant. All the important components of the plant are modelled, including the safety systems and the most important protection systems. The full pressure model has a scaling ratio of 1:2070 for the volume and the power, while the elevations are kept 1:1. A flow diagram is presented in Fig. 2.

A schematic drawing of the horizontal steam generator of the plant is given in Fig. 3. The steam generator in the PMK-2 facility is modelled by a vertical section of horizontal steam generator as shown in Fig. 4 and 5. There are 82 rows of heat exchanger tubes with a shape given in the lower part of Fig. 5. The feed water is entering at about the same elevation as in the plant's steam generator, to simulate the secondary side behaviour as correctly as possible.

In order to measure the coolant and feed water temperature distribution, a number of temperature measurements is provided in the steam generator model as presented in Fig. 6.

The instrumentation applied to the measurement is presented in Table 1. Circles in Figs. 4 and 6 refer to item No. of Table 1.

### 3. DESCRIPTION OF THE TEST

The experiment is characterized as follows:

- A  $\varnothing$  3 mm cold leg break, modelling a 7.4% break in the Paks NPP
- Starting from full power
- With injection from three hydroaccumulators (SIT)
- Without injection from high pressure injection system
- The secondary side is isolated after transient initiation
- With injection from LPIS
- With secondary side bleed
- With emergency feed water injection

#### Initial conditions

The initial conditions at  $t = 0$  s are characterized by the data as follows:

##### Primary circuit

- |  |           |
|--|-----------|
| ◦ Pressure in upper plenum                           | 12.33 MPa |
| ◦ Loop flow  | 4.91 kg/s |
| ◦ Core inlet temperature                             | 540.1 K   |
| ◦ Core power   | 665.12 kW |
| ◦ Coolant level in pressurizer,<br>from 0.00 m level | 9.12 m    |
| ◦ SIT-1 pressure                                     | 6.05 MPa  |
| ◦ SIT-2 pressure                                     | 6.04 MPa  |
| ◦ SIT-1 level, from 0.00 m level                     | 9.44 m    |
| ◦ SIT-2 level, from 0.00 m level                     | 9.83 m    |

##### Secondary circuit

- |   |           |
|---|-----------|
| ◦ Pressure in SG  | 4.56 MPa  |
| ◦ Coolant level above bottom of SG<br>secondary side, from 0.00 m level | 8.95 m    |
| ◦ Feed water flow   | 0.35 kg/s |
| ◦ Feed water inlet temperature  | 494.2 K   |

#### Sequence of events

- |   |                  |
|---|------------------|
| ◦ Break valve starts to open                            | 0.0 s            |
| ◦ Secondary side isolation starts<br>(closing time 6 s) | 0.0 s            |
| ◦ Break valve open                                      | 0.1 s            |
| ◦ Transient for power is initiated at                   | 11.15 MPa        |
| ◦ Modelling of the pump coast down is<br>initiated at   | 9.21 MPa         |
| ◦ SIT-1 and SIT-2 actuated at                           | 5.90 MPa         |
| ◦ SIT-1 empty, from 0.00 m level                        | 8.22 m           |
| ◦ SIT-2 empty at a SIT-2 level of<br>from 0.00 m level  | 9.01 m           |
| ◦ Secondary bleed is initiated at                       | 9.21 MPa + 150 s |

- Secondary emergency feed is initiated at 0.93 MPa
- LPIS initiation 1.04 MPa
- Total mass through the break at 1800 s is 154.19 kg
- The test is terminated at 1800 s

#### 4. RESULTS OF MEASUREMENT

Presentation of the measurement results is given in two parts: steady-state and transient behaviour of the steam generator.

##### 4.1 Steady-state conditions

The primary side coolant temperatures at the inlet and outlet of the heat exchanger tubes at different elevations are as follows: TE43, TE44 at the elevation of 8.163 m; TE45, TE46 at the elevation of 7.591 m; TE 47, TE48 at the elevation of 6.385 m. The temperature distributions as a function of elevations are presented in Fig. 7.

It can be seen in the Figure that there is a strong decrease of the coolant temperature even in the hot collector. The temperature difference between the hot and the cold collector is decreasing with the elevation as shown in Fig. 8.

The variation of the feed water temperature as a function of the elevation is shown in Fig. 9. The elevations are the same as in the primary side with three different radial positions: hot collector, middle of SG vessel and cold collector. The effect of the "cold" feed water injection results in a significant sink in the temperatures.

##### 4.2 Transient conditions

To show the overall behaviour of the primary and the secondary side, the pressures are presented in Fig. 10 as a function of the transient time. It can be stated that the secondary pressure governs the primary pressure.

The primary side coolant temperatures, as a function of time are presented in Fig. 11 for heat exchanger tube inlet, and in Fig. 12 for the outlet.

The Figures show the following effects:

- The extensive injection from SITs can be seen in the temperature TE47 only.
- At about 800 s a significant increase in the TE43 and TE44 can be observed. It results from the event that the feed water level in the secondary side drops to the levels of TE43 and TE44.

- At 1380 s the activation of the LPIS injection can clearly be seen, in the time variation of TE44.

The secondary side feed water temperatures are presented in Figs. 13 to 15. It can be seen that there is no significant difference among temperatures at the different radial positions. Temperatures are below the saturation temperature, except for the TE87 and TE84 in the late phase of the transient.

## 5. CONCLUSIONS

The experiment gives data and offer idea for the modelling of the steam generators, especially for the proper choose of the nodalization applied to computer codes. Test results show that the modelling applied up till now can and should be improved to describe the temperature distribution inside the steam generator correctly.

Further experiments are needed to obtain a much more complete data set for code validation purposes.

## Reference

- [1] Simulation of a Beyond Design Basis Accident with Bleed and Feed Preventive Measures.  
IAEA-TECDOC (to be published).

Table 1. Identification of parameters

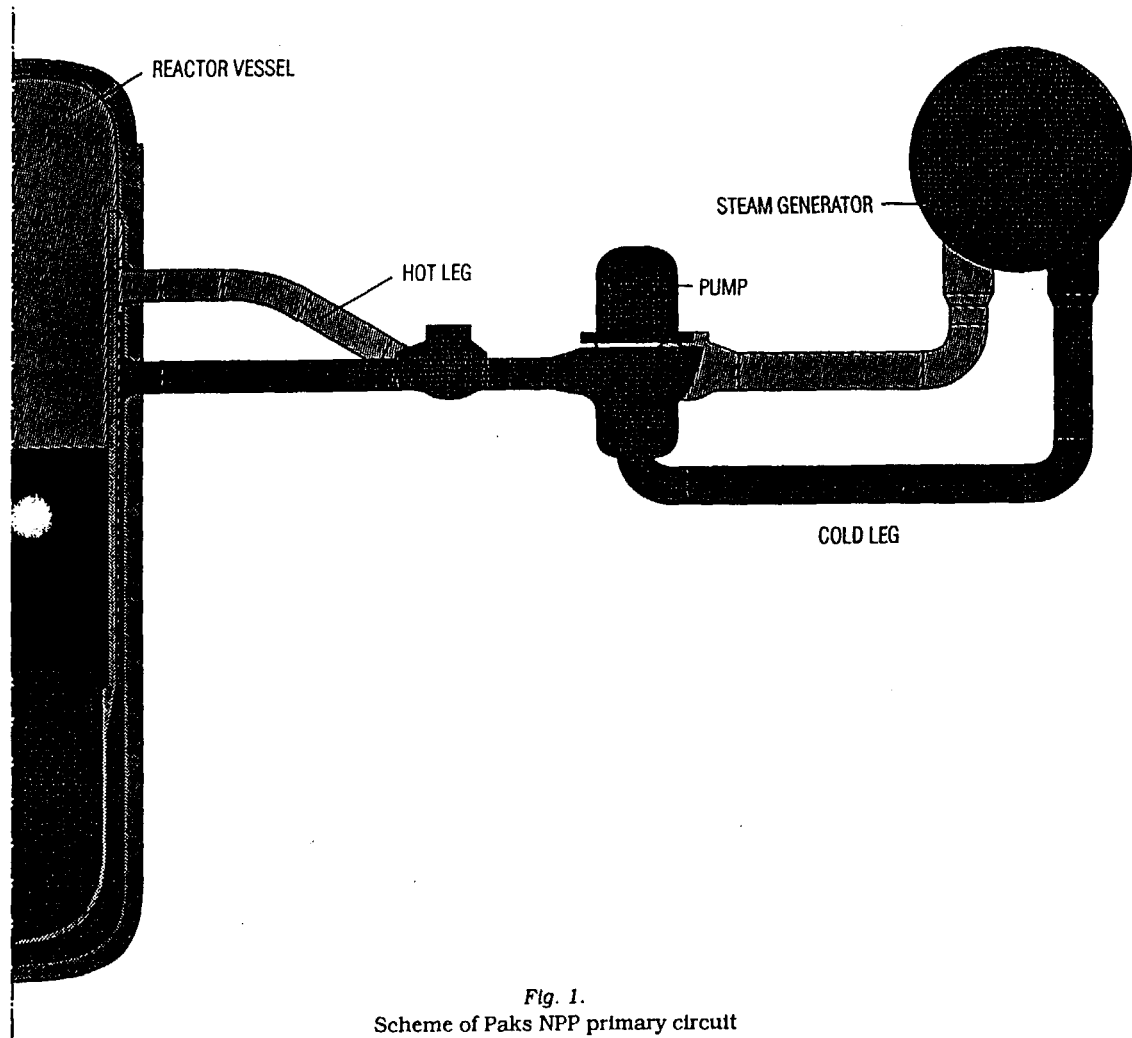
Item No.	Identification	Location and type of measurement	Elevation	Measurement accuracy, less than $\pm$	Unit
1.	TE11	Heater rod surface, thermocouple	1.494 m		
2.	TE12	" "	2.954 m		
3.	TE13	" "	3.464 m		
4.	TE14	" "	3.464 m		
5.	TE15	" "	3.464 m		
6.	TE23	Wall in upper plenum, "	6.225 m		
7.	TE62	Wall in downcomer, "	4.995 m		
8.	TE43	Heat exchanger inlet (1) "	8.163 m		
9.	TE45	" (2) "	7.591 m		
10.	TE47	" (3) "	6.385 m		
11.	TE44	" outlet (1) "	8.163 m		
12.	TE46	" (2) "	7.591 m	2 K	K
13.	TE48	" (3) "	6.385 m		
14.	TE80	Sec. water hot coll. (1) "	8.163 m		
15.	TE82	" (2) "	7.591 m		
16.	TE84	" (3) "	6.385 m		
17.	TE83	" middle (1) "	8.163 m		
18.	TE85	" (2) "	7.591 m		
19.	TE87	" (3) "	6.385 m		
20.	TE86	" cold coll. (1) "	8.163 m		
21.	TE88	" (2) "	7.591 m		
22.	TE89	" (3) "	6.385 m		
23.	TE01	break flow temperature, "	4.825 m		
24.	TE22	Upper plenum temperature, Pt resistance	4.644 m	1 K	K
25.	TE24	" " "	8.375 m	"	K
26.	TE60	Coolant pump inlet, "	3.525 m	"	K

Table 1 (cont.)

Item No.	Identification	Location and type of measurement	Elevation	Measurement accuracy, less than ±	Unit
27.	TE61	Coolant downcomer inlet, Pt resistance	4.520 m	1 K	K
28.	TE63	Coolant at core inlet, "	0.190 m	"	K
29.	TE41	SG primary coolant inlet, "	5.995 m	"	K
30.	TE42	SG primary coolant outlet, "	5.995 m	"	K
31.	PR01	Back pressure behind break simulator	4.825 m		kPa
32.	PR21	Upper plenum	3.754 m	0.05 MPa	MPa
33.	PR71	Pressurizer pressure	10.077 m	0.05 MPa	MPa
34.	PR81	SG secondary	11.212 m	0.02 MPa	MPa
35.	PR91	SIT-1	10.130 m	0.05 MPa	MPa
36.	PR92	SIT-2	10.130 m	0.05 MPa	MPa
37.	DP11	Core	0.190/3.754 m	1 kPa	kPa
38.	DP12	DP between 1 and 8	3.754/6.225 m	1 kPa	kPa
39.	DP13	DP between 1 and 2	5.995/6.225 m	1 kPa	kPa
40.	DP15	DP between 4 and 5	2.725/3.525 m	1 kPa	kPa
41.	DP16	Pump DP between 4 and 5	-0.318/0.382 m	1 kPa	kPa
42.	DP17	Pump DP between 5 and 6	3.525/4.664 m	1 kPa	kPa
43.	DP18	Pump DP between 6 and 7	4.664/0.190 m	1 kPa	kPa
44.	DP41	SG primary	5.995/5.995 m	1 kPa	kPa
45.	LE11	Reactor model	0.190/9.220 m		m
46.	LE21	Upper plenum, part 1, DP	5.504/9.220 m	$4 \times 10^{-2}$ m	m
47.	LE22	Upper plenum, part 2, DP	4.664/5.504 m	$5 \times 10^{-2}$ m	m
48.	LE23	Upper plenum, part 3, DP	3.754/4.664 m	$5 \times 10^{-2}$ m	m
49.	LE31	Hot leg loop seal, DP (reactor side)	4.802/6.080 m	$1.5 \times 10^{-2}$ m	m
50.	LE42	SG hot collector, part 1, DP	7.500/8.445 m	"	m
51.	LE43	SG hot collector, part 2, DP	6.608/7.500 m	"	m
52.	LE44	SG hot collector, part 3, DP	5.995/6.608 m	"	m
53.	LE45	SG primary, hot leg, DP	4.802/8.445 m	$3 \times 10^{-2}$ m	m
54.	LE46	SG primary, cold leg, DP	2.725/8.445 m	$3 \times 10^{-2}$ m	m
55.	LE47	SG cold collector, part 1, DP	7.500/8.445 m	$1.5 \times 10^{-2}$ m	m
56.	LE48	SG cold collector, part 2, DP	6.608/7.500 m	"	m

Table 1 (cont.)

Item No.	Identification	Location and type of measurement	Elevation	Measurement accuracy, less than $\pm$	Unit
57.	LE49	SG cold collector, part 3, DP	5.995/6.608 m	$1.5 \times 10^{-2}$ m	m
58.	LE51	Cold leg part 1, DP	2.725/5.995 m	$3 \times 10^{-2}$ m	m
59.	LE52	Cold leg pressure drop, reactor side	3.525/4.995 m	$1.5 \times 10^{-2}$ m	m
60.	LE60	Downcomer head, DP	4.354/4.995 m	"	m
61.	LE61	Downcomer, DP	0.190/4.995 m	$5 \times 10^{-2}$ m	m
62.	LE71	Pressurizer, DP	7.95/10.077 m	$2 \times 10^{-2}$ m	m
63.	LE72	Pressurizer surge line, DP	6.025/7.950 m	"	m
64.	LE81	SG secondary, DP	6.58/11.212 m	$5 \times 10^{-2}$ m	m
65.	LE91	SIT-1 level, DP	8.13/10.130 m	$2 \times 10^{-2}$ m	m
66.	LE92	SIT-2 level, DP	8.13/10.130 m	"	m
67.	FL51	Core outlet, normal, venturi	5.504 m	0.06 kg/s	kg/s
68.	FL52	Core outlet, low flow, venturi	5.504 m	0.02 kg/s	kg/s
69.	FL53	Cold leg, normal, venturi	4.825 m	0.06 kg/s	kg/s
70.	FL54	Cold leg, low flow, venturi	4.825 m	0.02 kg/s	kg/s
71.	FL01	Break flow, venturi	4.025 m		kg/s
72.	FL81	Feed water flow, venturi	4.990 m	0.02 kg/s	kg/s
73.	MA01	Total mass leaked through break, DP	-	1.0 kg	kg
74.	DE21	Upper plenum, $\gamma$ attenuation	5.700 m	-	-
75.	PW01	Electrical power		3.0 kW	kW
76.	LV21	Local void in upper plenum, void-probe	6.225 m		
77.	LV31	Local void in hot leg loop seal, "	5.400 m		
78.	LV32	" " "	5.400 m		
79.	LV33	" " "	4.802 m		
80.	LV41	" in SG hot collector, "	5.995 m		
81.	LV42	" in SG cold collector, "	5.995 m		
82.	LV51	" in cold leg, "	3.525 m		
83.	LV52	" " "	3.525 m		



*Fig. 1.*  
Scheme of Paks NPP primary circuit

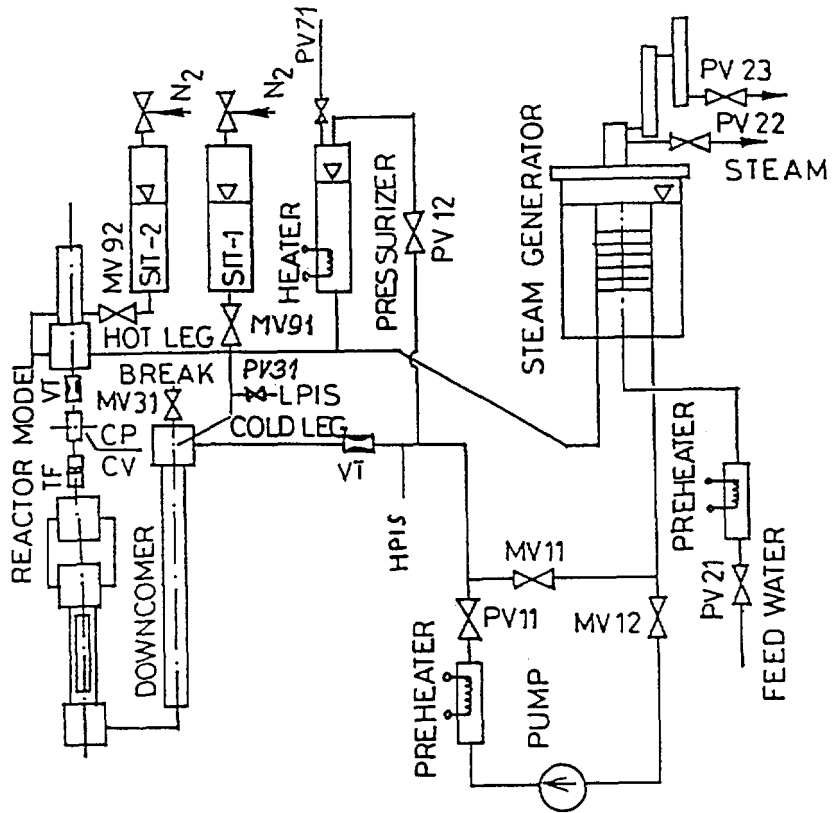
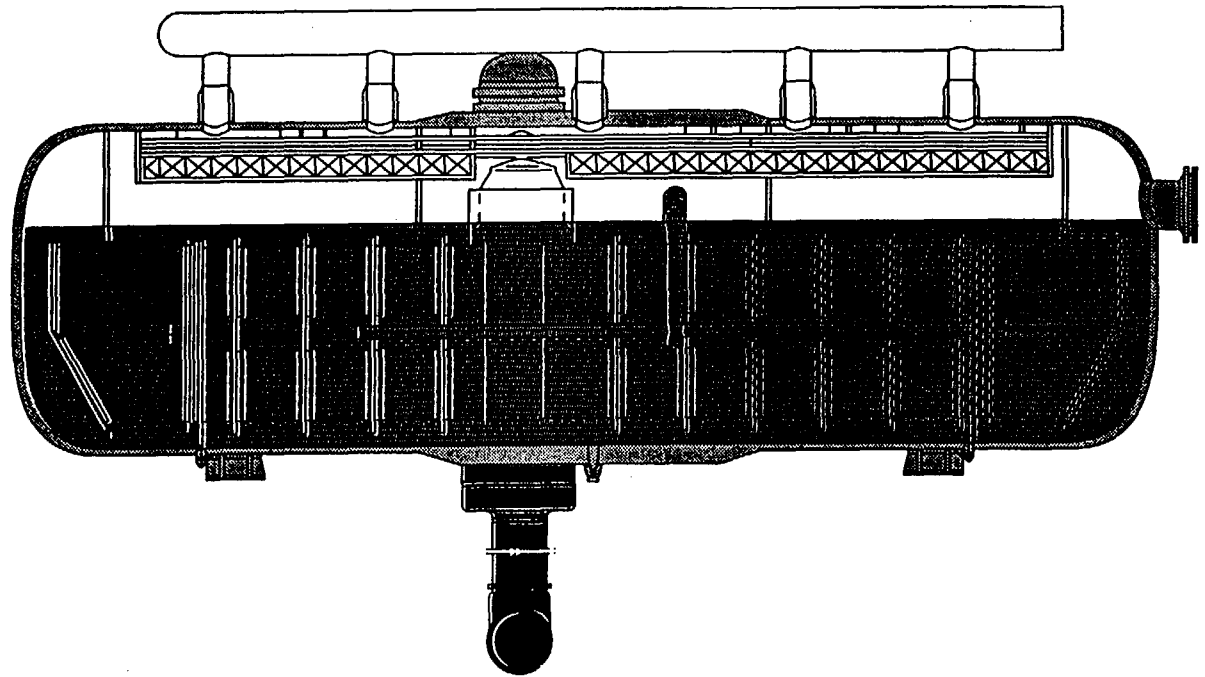


Figure 2. Flow diagram of PMK-2 facility

Abbreviations are:

PV	-	pneumatic control valve
MV	-	motor valve
VT	-	flow measurement device
TF	-	flow measurement device
CP	-	density measurement device
CV	-	density measurement device
SIT-1	-	hydroaccumulators
SIT-2	-	hydroaccumulators
HPIS	-	high pressure injection system
LPIS	-	low pressure injection system



*Fig. 3.*  
Paks NPP Steam Generator



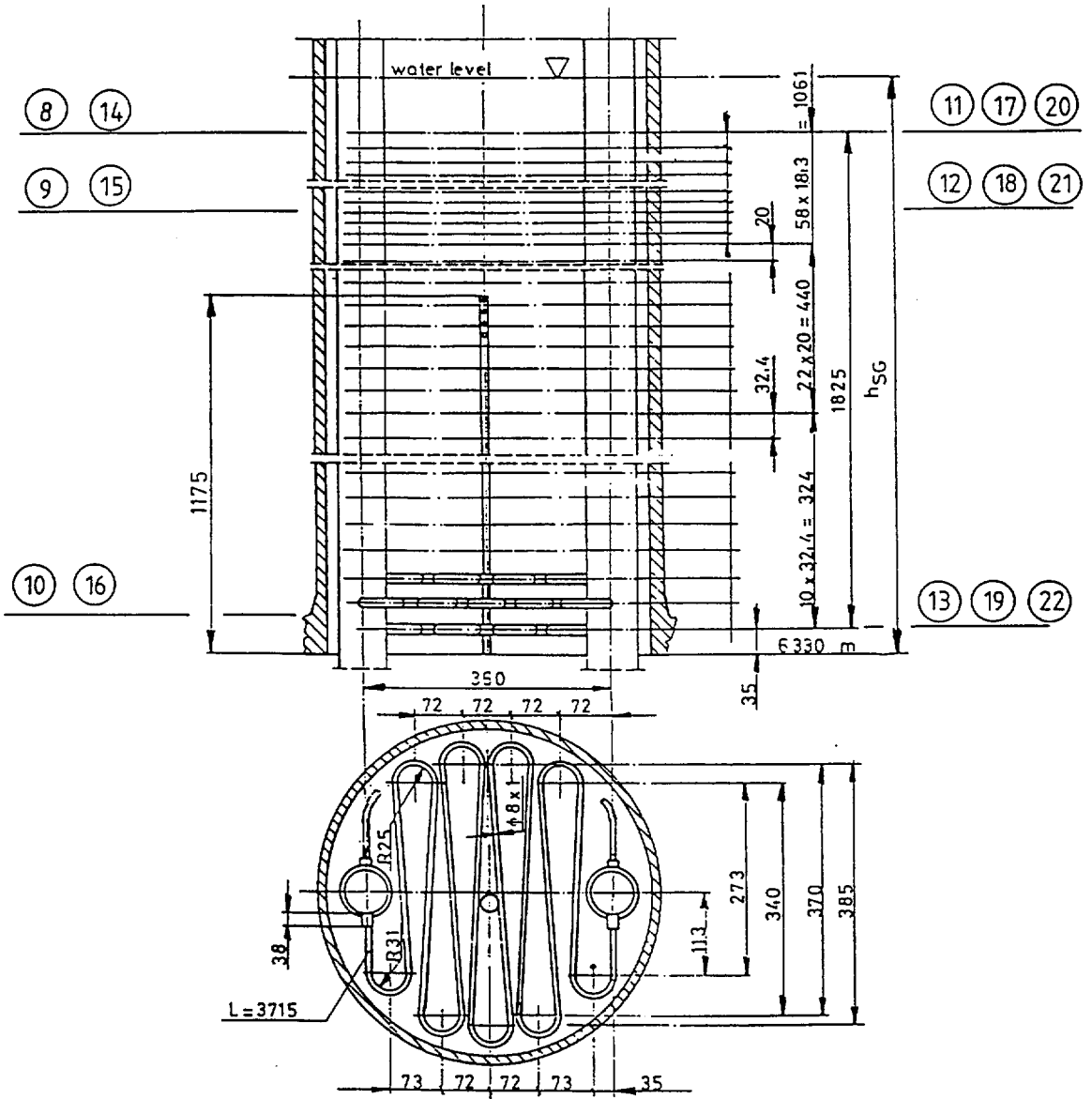


Figure 5.

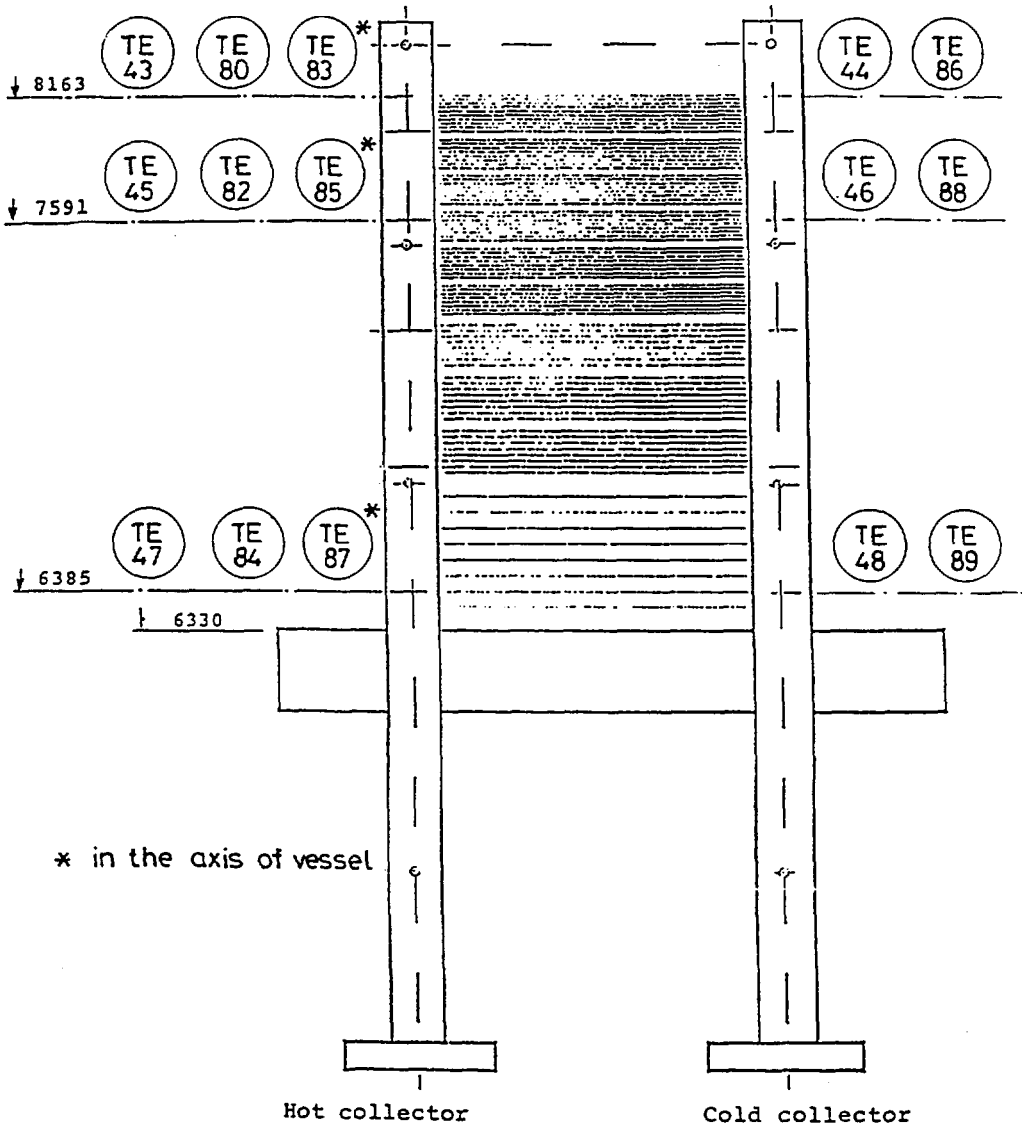


Figure 6.

Temperatures in the secondary side

## IAEA-SPE-4

## CLB LOCA WITH SECONDARY B&amp;F ON PMK-2

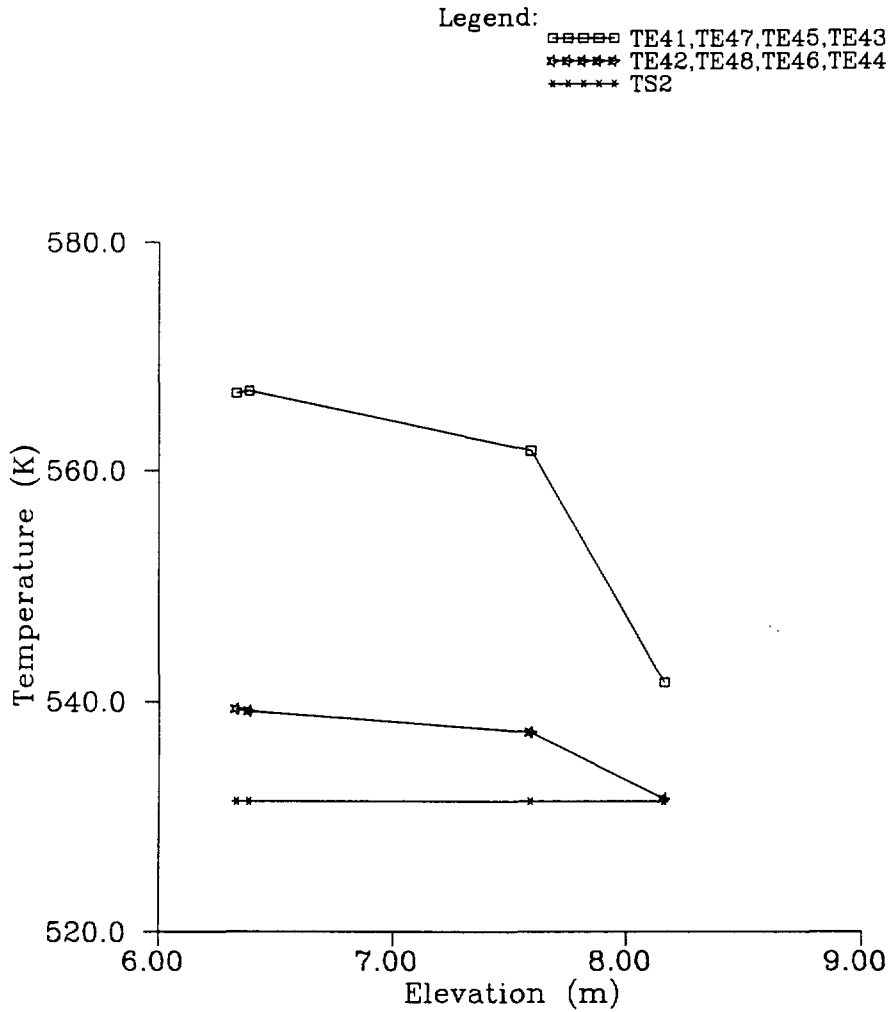


Fig. 7. Heat exchanger in-, outlet temperature in steady state situation and saturated temperature in secondary side

## IAEA-SPE-4

## CLB LOCA WITH SECONDARY B&amp;F ON PMK-2

Legend:

□□□□ DT - prim

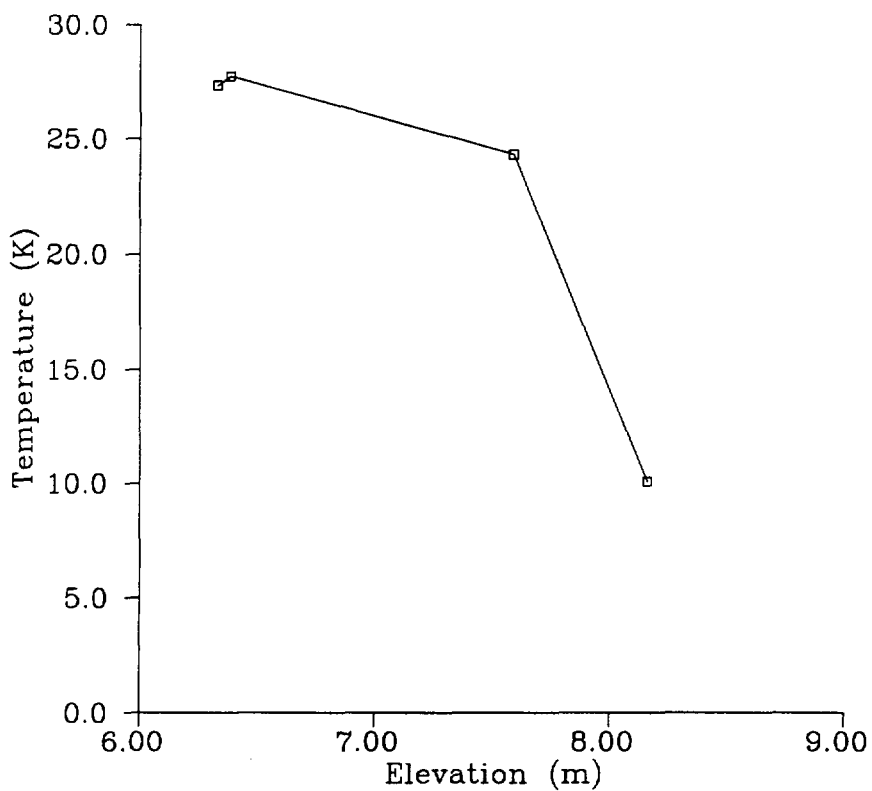


Fig. 8. Heat exchanger primary DT distribution in steady state situation

## IAEA-SPE-4

## CLB LOCA WITH SECONDARY B&amp;F ON PMK-2

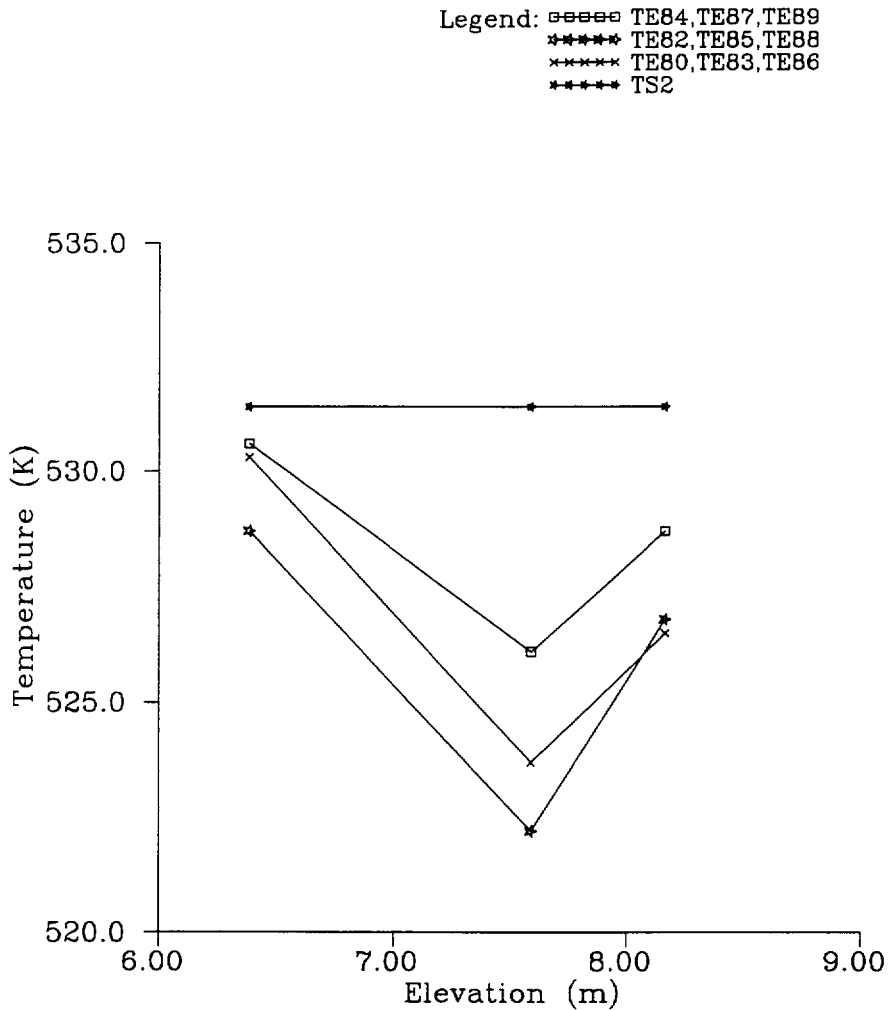


Fig. 9. Steam generator secondary side temperature distribution and saturated temperature in steady state situation

## IAEA-SPE-4

## CLB LOCA WITH SECONDARY B&amp;F ON PMK-2

Legend:

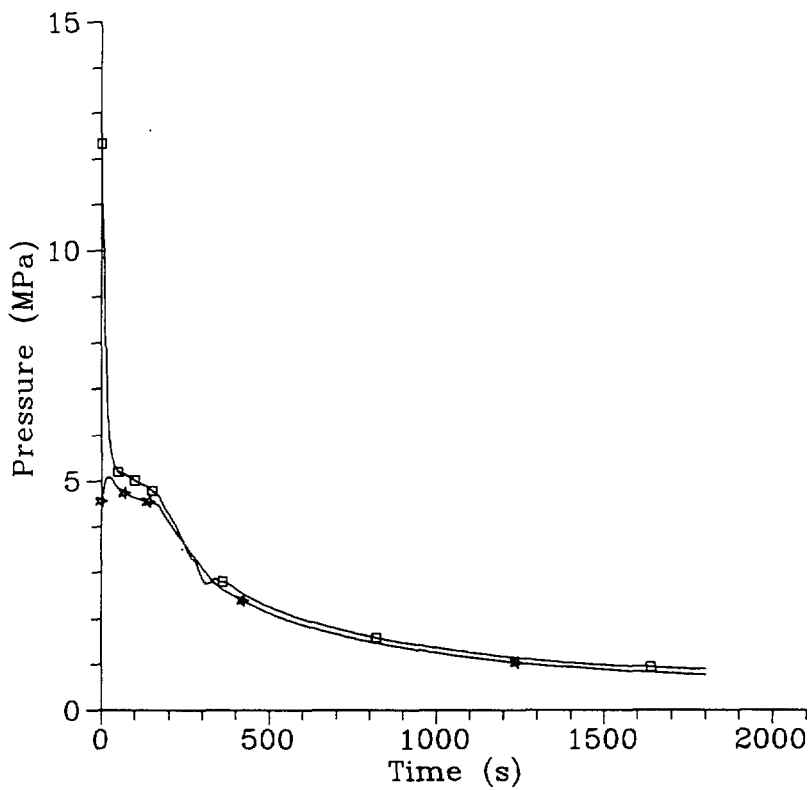
□□□□ PR21  
\*\*\*\*\* PR81

Fig. 10. Pressure in primary and secondary side

## IAEA-SPE-4

## CLB LOCA WITH SECONDARY B&amp;F ON PMK-2

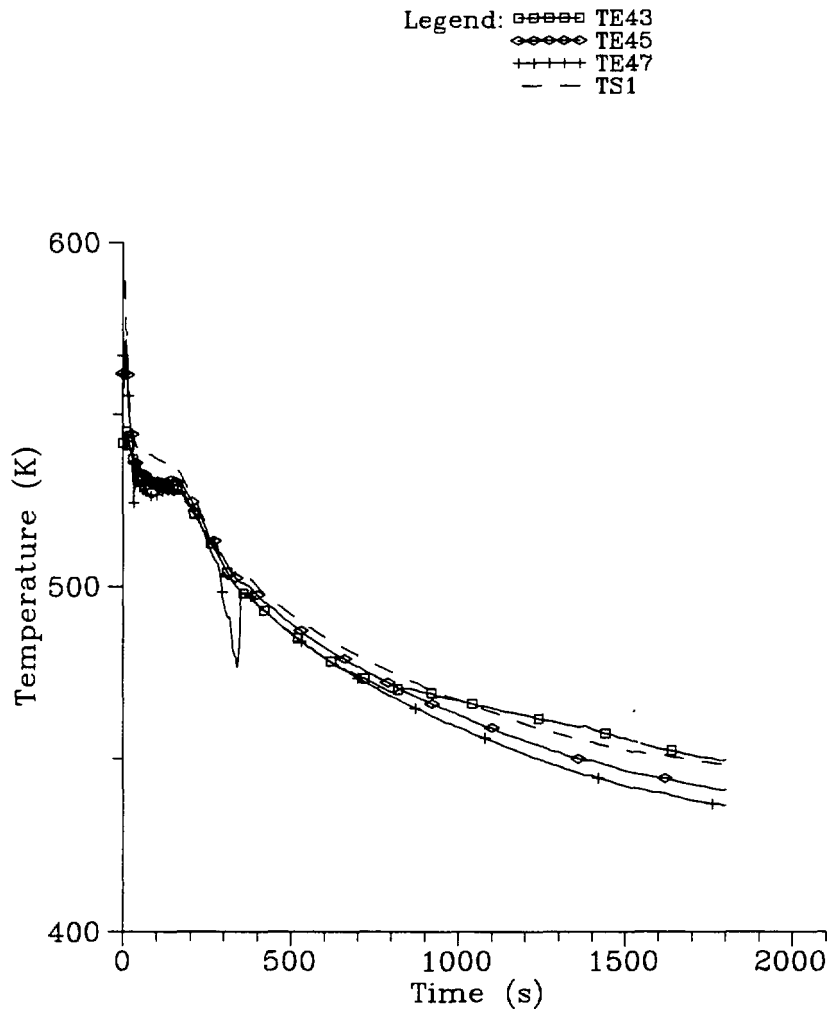


Fig. 11. Heat exchanger inlet temperature

## IAEA-SPE-4

## CLB LOCA WITH SECONDARY B&amp;F ON PMK-2

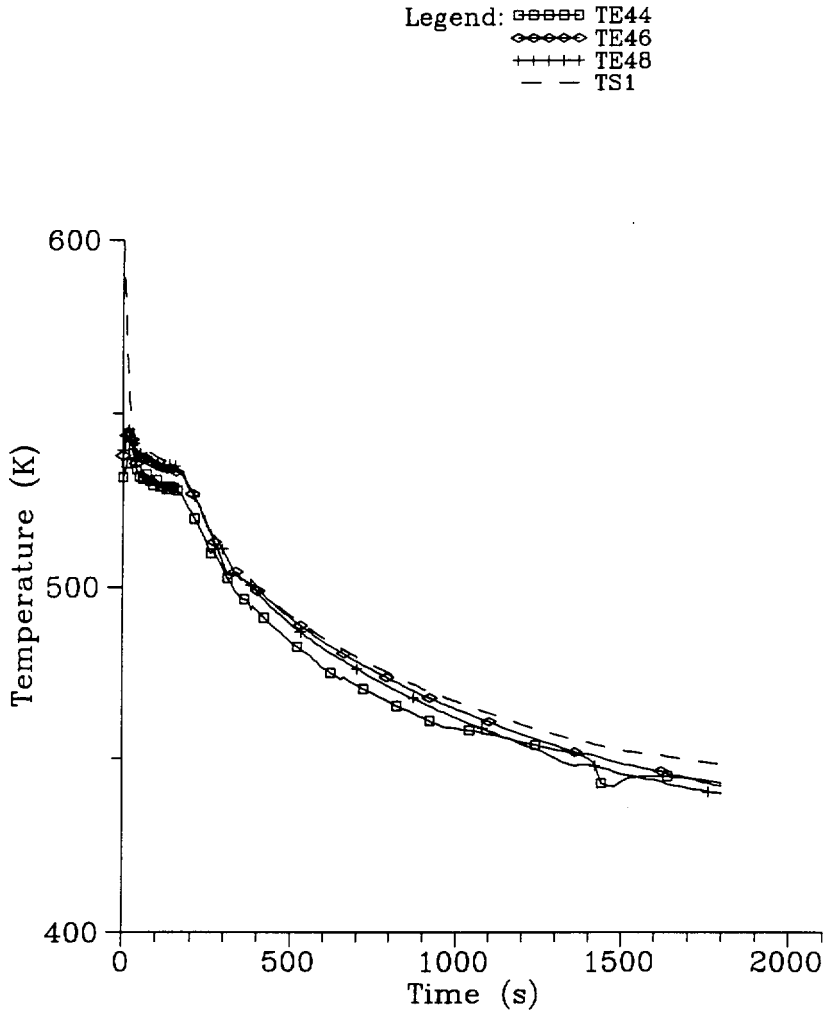


Fig. 12. Heat exchanger outlet temperature

## IAEA-SPE-4

## CLB LOCA WITH SECONDARY B&amp;F ON PMK-2

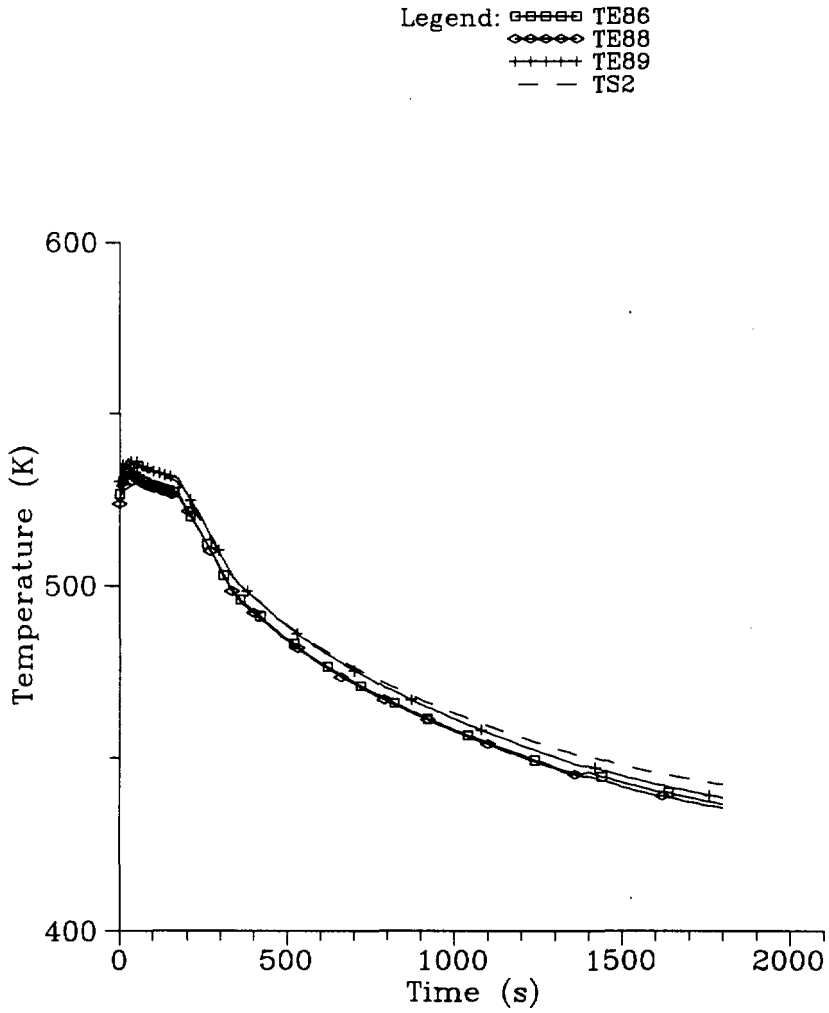


Fig. 13. Sec. water cold coll. temperature

## IAEA-SPE-4

## CLB LOCA WITH SECONDARY B&amp;F ON PMK-2

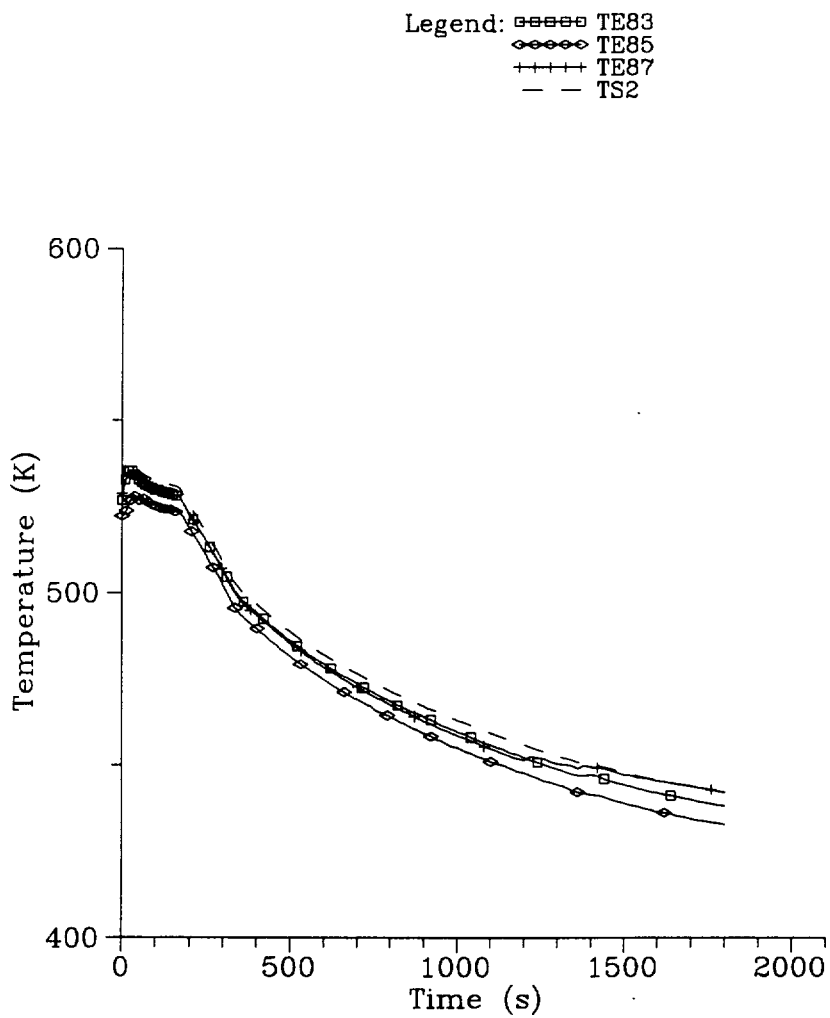


Fig. 14. Sec. water middle temperature

## IAEA-SPE-4

## CLB LOCA WITH SECONDARY B&amp;F ON PMK-2

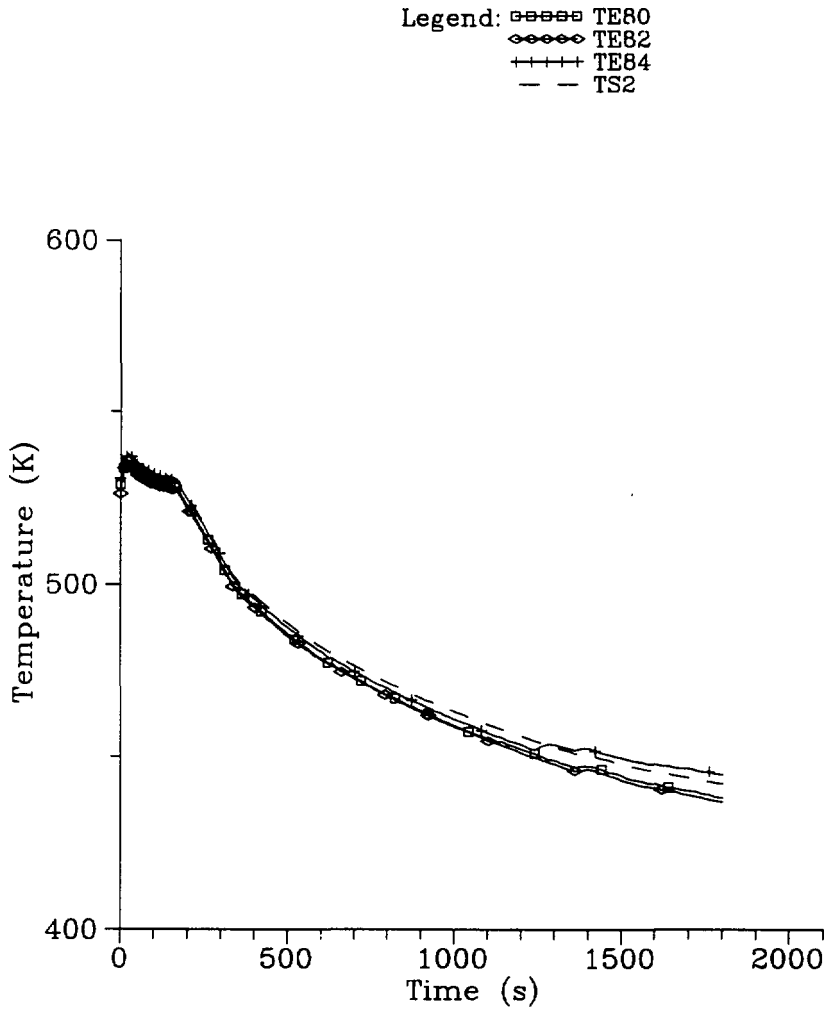


Fig. 15. Sec. water hot. coll. temperature

## **THERMAL-HYDRAULICS OF PGV-4 WATER VOLUME DURING DAMAGE OF THE FEEDWATER COLLECTOR NOZZLES**

S.A.Logvinov, V.F.Titov (OKB Hidropress, Russia)

U Notaros. I.Lenkei (NPP Paks. Hungary)

### **ABSTRACT**

A number of VVER-440 plants has experienced the distributing nozzles of feedwater collector being damaged due to corrosion-erosion wearing. Such phenomenon could result in feedwater redistribution within the SG inventory with undesirable consequences. The collector with damaged nozzles has to be replaced but a certain time is needed for the preparatory works. The main objective of the investigation conducted is to assess if the safe operation of SG is possible before collector replacement. It was shown that the nozzle damage as observed did not result in the dangerous disturbances of thermohydraulics as compared with the conditions existing at the initial period of operation.

### **INTRODUCTION**

A number of VVER-440 plant has experienced damages to the distributing nozzles of feedwater collector within PGV-4 steam generator. These Collectors as well as the nozzles are made of steel 20 beings under a certain conditions sensitive to corrosion-erosion wearing. The picture of nozzle damages was visualized in detail at NPP Paks by means of scanning TV-camera. A degree of their damage is directly related to their locations on the SG collector: the closer to the T-joint they are (i.e. to the feedwater pipeline-to-collector cut-in point) they are the more they are damaged, till complete failure. And on the contrary near collector ends the nozzles have remained completely intact.

The more serious collector damage that can follow the nozzle damage is through-wall damage of T-joint that could greatly affect feedwater distribution inside the SG and lead to the dangerous consequences. Thus, after the nozzle damages were identified the collector should be replaced. Preparation for replacement thereof requires some time during which it is desirable that SG operation would not be stopped. It is possible if we are sure that nozzle damages have not brought to the considerable variations in the water inventory thermohydraulics.

When the nozzle damages were indicated at NPP Paks the question was whether it was possible to keep SG operation till the collector was replaced. To solve this problem the experimental study was conducted in order to reveal the possible variations in the water volume thermohydraulics. Investigation was conducted on two models that simulated both the nozzle original state and various degrees of their-damages. By comparing the results obtained a conclusion has been made concerning variation in operating conditions of the water volume. Model 1 in scale 1:2 simulated the whole feedwater collector with the nozzles. The experiments performed at this model were aimed at:

- determination of feedwater flowrate distribution through the nozzles along the collector axis:
- determination of variation in static pressure inside the collector:
- determination of variation in jet geometry when simulating the nozzle damages.

Model 2 in scale 1:1 simulated the fragment of the boiler water and feedwater mixing zone. The experiments performed at this model were aimed at revealing how mixing pattern varies during nozzle damages. Overcooling of the boiler water washing the heat-exchanging tubes as well as thermal pulsation in the interface layer were of the greatest interest.

## **I. DESCRIPTION OF THE EXPERIMENTAL MODEL AND INVESTIGATION PROCEDURES**

### **1.1. Hydraulic model of the collector**

A sketch of the model made of tube 84x4,5 mm in scale 1:2 is shown in Fig. 1. Collector nozzles

are located in pairs and are joined in six large groups (three from each side) . Five groups have 14 pairs of nozzles each, one - 16. In addition, on the left ("cold") side there are two pairs of nozzles near the T-joint and near the end. On the right side there are two pairs of nozzles only near the T-joint. In all, the model has 92 pairs of nozzles made from tube 14x2 mm. The nozzles are threaded to make replacement easy. The damaged nozzles were simulated as shown in Fig.2. Type "a" nozzle simulated the initial geometry whereas type "b" nozzle with sidewall opening - initial degree of damage, type "c" nozzle the failure when only "tongue" has remained from the nozzle and, at last, type "d" nozzle - completely failed nozzle. Such categorization of the damages was accepted on the basis of results of collector inspection at NPP Paks. In all 6 combinations with nozzles of the indicated types have been tested (see Fig. 3). Model was connected to the hydraulic test rig providing water supply up to 150 m<sup>3</sup>/h with temperature 20-50°C. This flowrate ensured, first, the operating velocities of flows and, second, independence of the dimensionless hydraulic characteristics upon Reynolds number. To make measurement convenient the collector was turned by 90 degree around its axis so that blowdown through the nozzle was directed downwards. Provision was made for possible blowdown both under water level and into atmosphere. In the last case water flowrate through each pair of nozzles was measured by the volumetric method by means of the movable dosing tank. Static pressure distribution along the collector was defined by the piezometers.

## 1.2. Model of mixing region

Fig. 4 shows the SG cross-section and the volume fraction that Was simulated on the fragment model in scale i 1. Mixing region presents itself a horizontal corridor in the lower part of heat-exchanging bundle hot side. Feedwater jets are directed into the corridor. In such a way the direct contact of feedwater and corridor surrounding pipes is avoided.

General view of the model is shown in Fig.5 . It presents itself a box with dimensions 910x1300x245 mm. As far as 1000 mm it is divided by the vertical baffle into two parts. One part serves to accommodate the collector fragment with three pairs of nozzles and the adjacent part of tube bundle. The bundle is divided into two halves between which there is a corridor 96 mm high Each half has 6 rows of tubes along the height. Tubes 16 mm in diameter are located

in the rectangular lattice with 30 mm pitch along the horizontal and 24 mm pitch along the vertical. Below the tube bundle there is an equalizing lattice providing for the uniform flow inlet into the bundle. Herein there is the injection collector for steam-simulating air. Air bubble passing causes additional flow turbulency that facilitates mixing. But unlike steam, air does not provide the mixing region with heat energy that promotes feedwater heating up. Feedwater out of the collector fragment is supplied into the model via three pairs of nozzles being replaceable. Damages to the nozzles are simulated the same as in model 1.

The other part of box is the letdown section through which water is leaving the model.

It is necessary to note that modelling of mixing process is approximate, but the possible shortcomings of modelling in equal degree is typical both for the intact nozzles and damaged ones. Thus when comparing the results obtained the qualitative conclusions as regards the consequences of damaged nozzles are quite objective. Precise quantitative modelling in this particular case is so complicated that it is commensurable with experiments performed right on the SG.

Model as for the boiler water is connected to the loop with pump. After its starting up water is heated up to 70-75°C by Joule heat. Furthermore, feedwater is supplied by a separate pump concurrent with water removal from the loop. Feedwater temperature is equal to 15-20°C, so loop water starts cooling. But during the first minute faster the experiment starts water temperature at the tube bundle inlet remains constant. This time is enough to perform measurements under the stationary conditions.

To assess mixing efficiency the water temperature was measured at the surface of tubes surrounding corridor. In all, there were installed 60 thermocouples facing the corridor. Their readings were registered by the quick-acting data acquisition system IMPACT-3590 of Schlumberger company.

Experiments were performed in the following range of parameters:

- blowdown velocity of nozzle jets - 2 and 4 m/s;
- water velocity in the bundle upstream the corridor
  - 0,1; 0,25 and 0,5m/s;
- initial temperature difference - up to 55°C

In PGV-4 the average jet velocity for the whole SG is equal to 2 m/s, maximum - 4 m/s. Water velocity upstream the corridor is not known precisely but is within the said range,

differences in the saturation temperature and the feedwater temperature is 37°C ( with temperature of the latter being 223°C).

## 2. INVESTIGATION RESULTS

### 2.1. Experiments on the collector hydraulic model

The main investigation results on this model are shown in Fig.6. The upper diagram indicates distribution of the relative flowrates through the nozzles versus their locations on the collector.

Experiment results with all combinations of the nozzles (see Fig.3) are in the shaded region. Curves for each combination are not pointed out because locations thereof are arbitrary with respect to each other and the non-essential components are of no interest. Total relative flowrates in the groups of nozzles O,A,B and C (see Fig.6) for the various combinations are presented in the table below.

Total relative flowrates in the groups of nozzles

Collector side		Combinations investigated (Fig. 3)					
		1	2	3	4	5	6
cold	C	0.208	0.220	0.234	0.238	-	-
	B	0.160	0.181	0.156	0.156	-	-
	A	0.123	0.080	0.102	0.096	-	-
	O	0.008	0.007	0.008	0.008	-	-
hot	O	0.001	0.005	0.007	0.006	0.008	0.008
	A	0.118	0.078	0.089	0.098	0.098	0.093
	B	0.147	0.193	0.175	0.173	0.158	0.163
	C	0.192	0.225	0.229	0.234	0.336	0.237

From table it is seen that the total relative flowrates are in weak dependence upon the degree of nozzle damages, i.e. feedwater distribution along the SG axis varies a little. Jet deviations from the preset direction was not observed. When simulating the damages of types "a" and "d" (see Fig. 2) the accelerated failure of jets was observed that improves mixing.

Minimum flowrate occurs through the nozzles of group O being the closest to T-joint, hereat, this flowrate is extremely unstable in time and sometimes it stops completely. The cause for such phenomena becomes clear when considering static pressure distribution along the collector. Pressure near the T- joint when the nozzles are intact is even negative that could result in the reverse flow of boiling water with steam bubbles. When simulating damages to the nozzles there is no negative pressure but its value is close to zero.

If to compare the pattern of flow distribution through the nozzles And the picture of their dies at NPP PAKS it is possible to make a conclusion that nozzle damages are in inverse relationship to the flowrate: the less is the flowrate the more is the nozzle damage. Such fact being strange at the first sight can be explained by considering the local hydrodynamics at the nozzle inlet. Fig 7. shows the approximate velocity field at the nozzle inlet with two extremes: near the T- joint (A) and far from it (B). In the first case the axial velocity in the collector is maximum (in SG it is; equal to 4,5 m/s). When a part of flow is bypassed to the nozzle the vector-axial velocity near the wall is deviated for a small angle that creates the conditions for direct impact of jets with the nozzle wall in point 1 wherein erosion of the oxide film occurs. The identical process occurs in point 2 wherein the high velocity of jet that impact the wall is provided by the intensive vortex occupying a considerable part of the flow area. High velocities acting along the normal to the surface are not necessarily connected with maximum flowrates through the nozzle. Flowrates near the collector ends are maximum but the nozzles have preserved intact there. Axial velocity at the collector ends is practically equal zero whereas at the nozzle inlet the velocity field is symmetrical. Small vortex at the inlet edge does not create intensive circulation and the normal component of velocity is too small to cause erosion of the oxide layer.

The nozzles located in the vicinity of T- joint could be affected by the other damage mechanism related to cavitation. The latter is possible when saturated water with steam bubbles gets into the nozzle. The both mechanisms of erosion-type failure of the oxide film is also mentioned in /1/.

## 2.2 Experiments to study mixing

This model dealt with comparison of feedwater and boiler water mixing by the above procedure. Water temperature in the mixing corridor was measured by the thermocouples installed on the tubes surrounding the corridor from above and below.

The dimensionless temperatures were derived from the thermocouple readings such as:

$$\Theta = \frac{t_i - t_c}{t_h - t_c},$$

where  $t_i$  - temperature in the given point,  
 $t_c$  - temperature of the cold water (feedwater),  
 $t_h$  - temperature of hot water (boiler water).

If  $\Theta = 0$  then the cold water is not heated up, if  $\Theta \rightarrow 1$  then the complete mixing occurs.

Investigation results with nozzles of type "a", "c" and "d" are shown graphically in Fig.8 in the form of value spreading along the upper boundary of the corridor (towards jet motion).

Data for the lower boundary are not indicated as being more favorable

Experiments were conducted with six combinations of bundle velocity circulation,  $V_o$ , and nozzle velocity (averaged over its cross-section),  $V_n$ . In addition, one experiment was conducted with air injection upstream the bundle. All the experiments were conducted without simulation or the transit. flow inside the collector because tests on the hydraulic model have shown that in all cases the jets out of the nozzles preserve the preset direction.

It is seen from the diagrams that the minimum water temperatures in all the versions tested are equal in practice but coordinates with minimum temperature do not coincide. However, the latter has no influence for assessment of the factors decreasing the tube durability. Thermal pulsations on the tube walls are defined by the liquid temperature difference outside and inside the tube. If with the nozzles damaged it remains unchanged then there is no grounds to consider that the tube appeared to be in the more unfavorable conditions. Maximum amplitude of thermal

pulsations (in this paper) did not exceeded 5% of the initial temperature difference at frequency 0,1-0,2 Hz. Unfortunately there is no identical data available for the real PGV-4. Only water temperature in a separate points of the mixing corridor was measured and appeared to be rather high.

## CONCLUSIONS

1. Damages to the distributing nozzles of feedwater collectors inside PGV-4 at a number of VVER-440 plants have stimulated investigations to be conducted in order to evaluate influence of the damages upon the SG serviceability.

2. Investigation on the hydraulic model of collector has shown that damages to the nozzles does not greatly change feedwater distribution along the SG axis. Distribution of feedwater flowrate along the SG axis is rather non-uniform from the very beginning of operation. Flowrate through the nozzles near the T-joint is minimum and unstable in time with possibility for saturation water with steam bubbles being intaken into the collector. This phenomena could cause the cavitation erosion.

3. Distribution of nozzle damages on the collector and flow distribution through the nozzles witness of the important role of hydrodynamics in the corrosion-erosion processes affecting the nozzle materials.

4. Investigations on the SG fragmented model has shown that nozzle failure does not cause additional cooling of the boiler water near the tubes surrounding the mixing corridor. Operating conditions of the tubes from the viewpoint of thermal effects remain unchanged in practice.

5. Replacement of the collector with damaged nozzles is needed, i.e. corrosion-erosion process exert influence upon the T-joint as well that, eventually, could fail. But SG operation with the damaged nozzles on the collector is allowed provided the collector would be replaced as soon as possible.

**REFERENCES**

1. В. Кастнер, Х. Ноппер, Р. Реснер. Защита трубопроводов от коррозионной эрозии. - "Атомная энергия" , т.75, вып. 4, октябрь 1993, стр. 286-294.

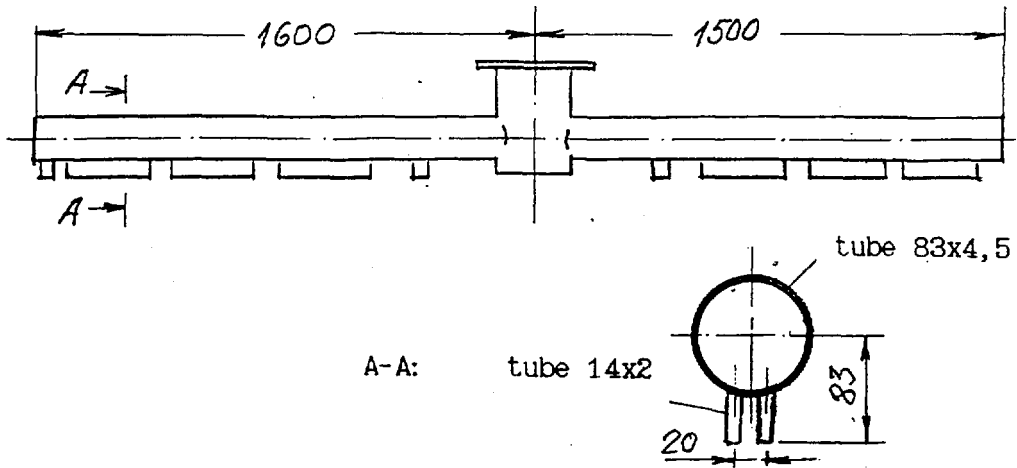


Fig.1. General view of the feedwater collector model

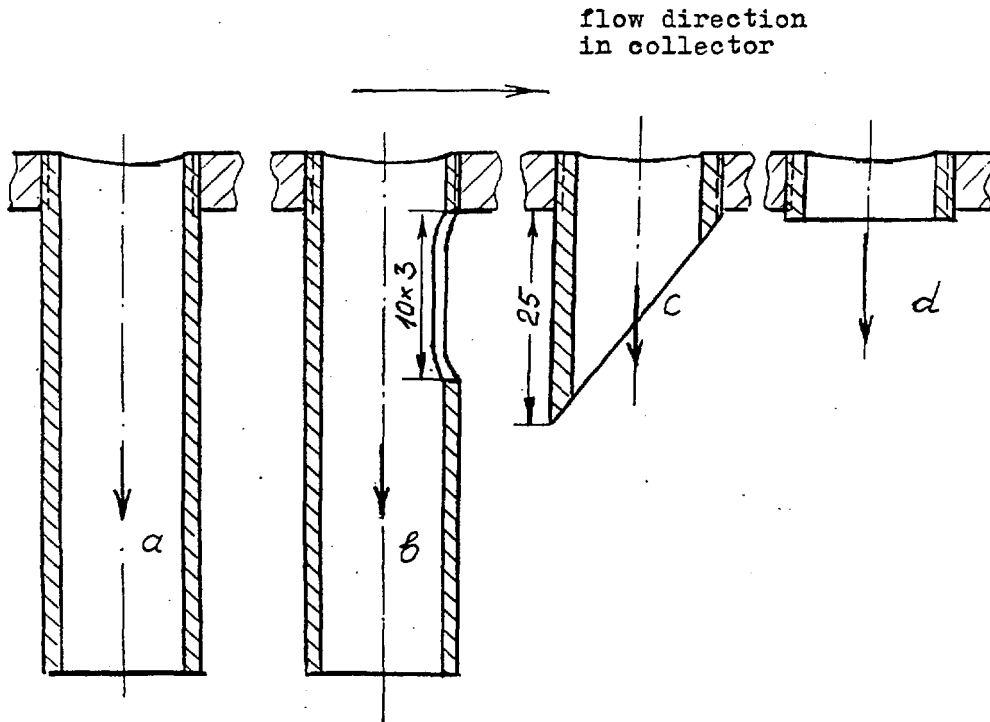


Fig.2. Simulation of the nozzles different damage

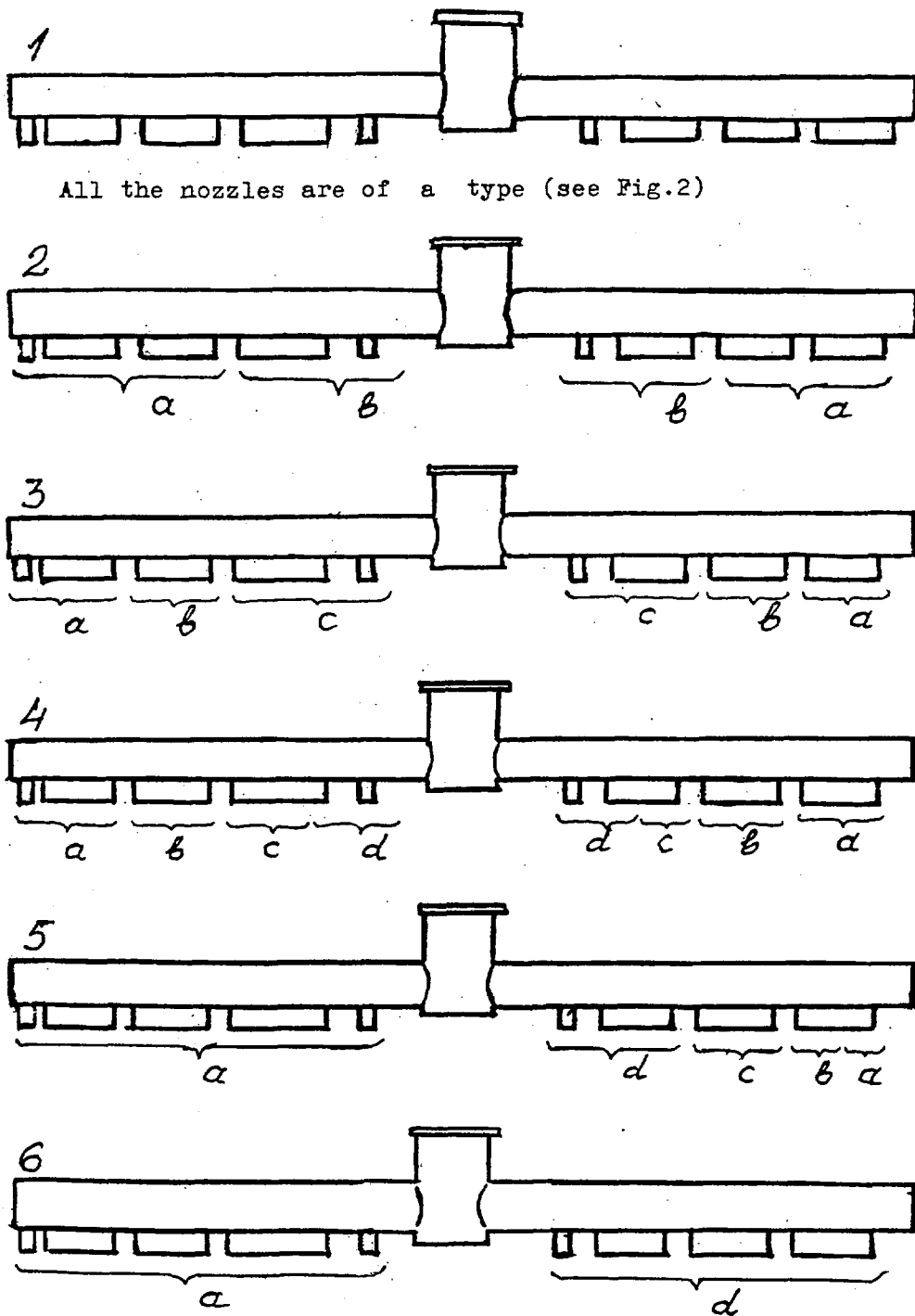


Fig.3. Arrangement of the different type nozzles on the test collector

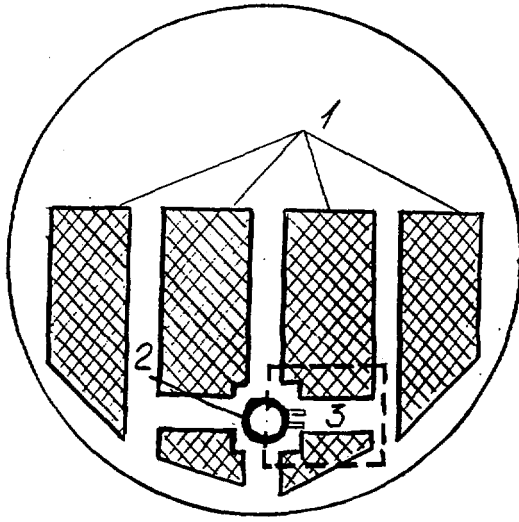


Fig. 4. SG cross-section and region to be investigated

- 1 - tube bundles
- 2 - feedwater collector with nozzles
- 3 - modelled region

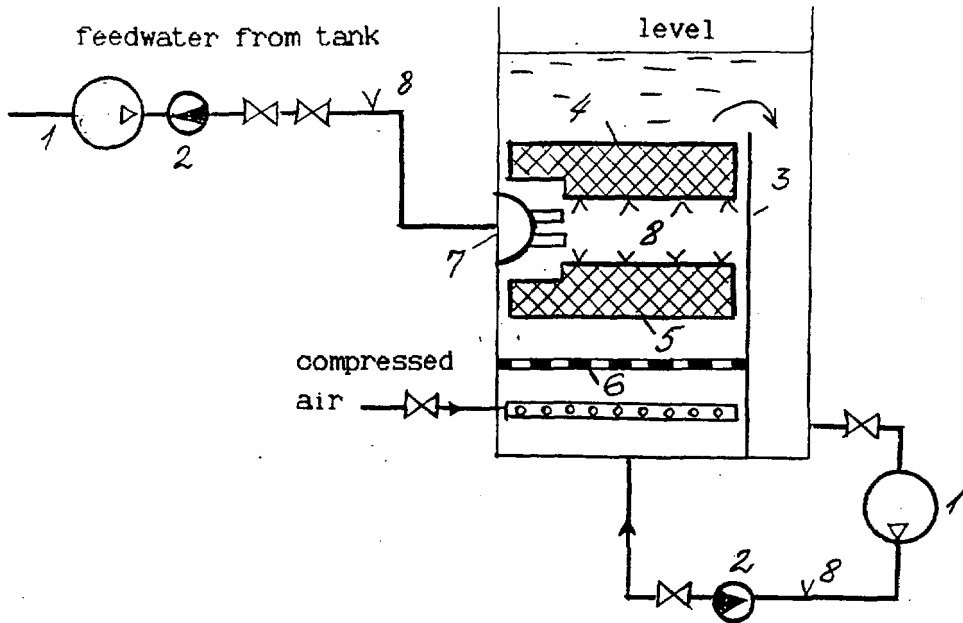


Fig. 5. Test facility for mixing study

- 1 - pump; 2 - flowmeter; 3 - tight wall; 4 - upper tube bundle; 5 - lower tube bundle; 6 - throttling grid;
- 7 - collector with nozzles, 8 - thermocouple

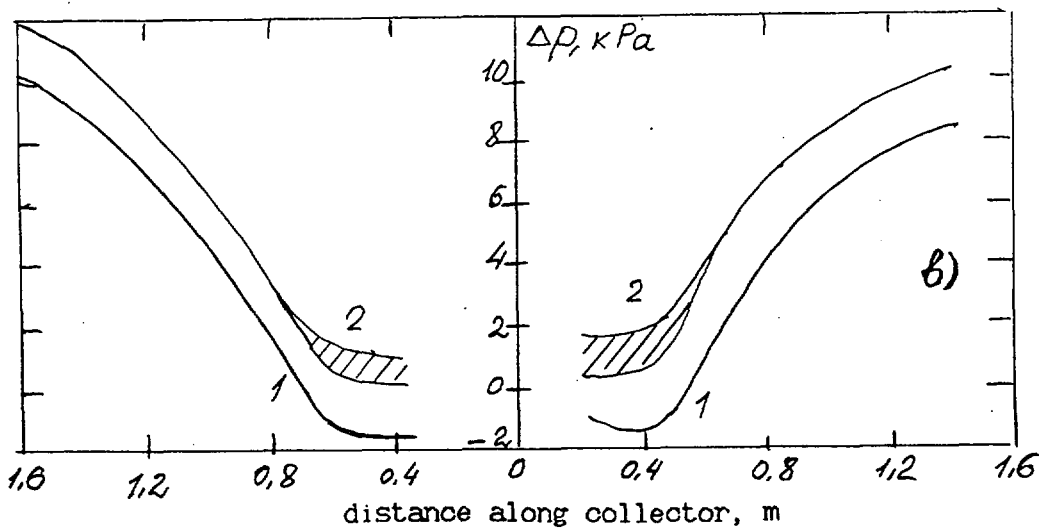
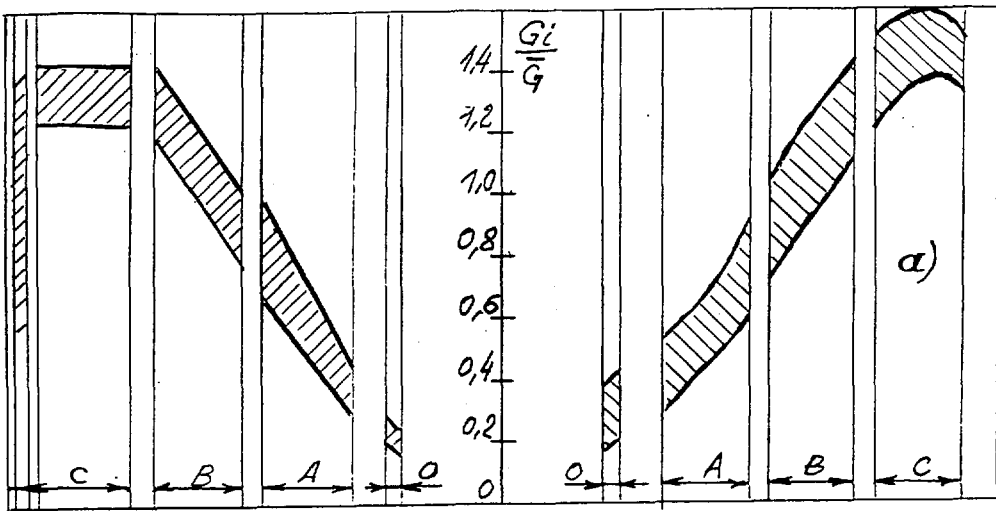
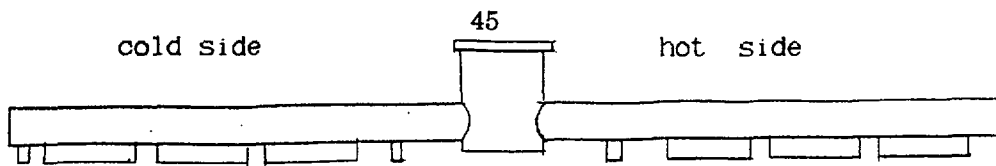


Fig.6. Relative flow rates through nozzles (a)  
 and pressure distribution along collector (b)  
 flow rates: for the all nozzles combinations (see Fig 3)  
 pressures: 1 - for undamaged nozzles  
 2 - for the rest combinations of damaged nozzles

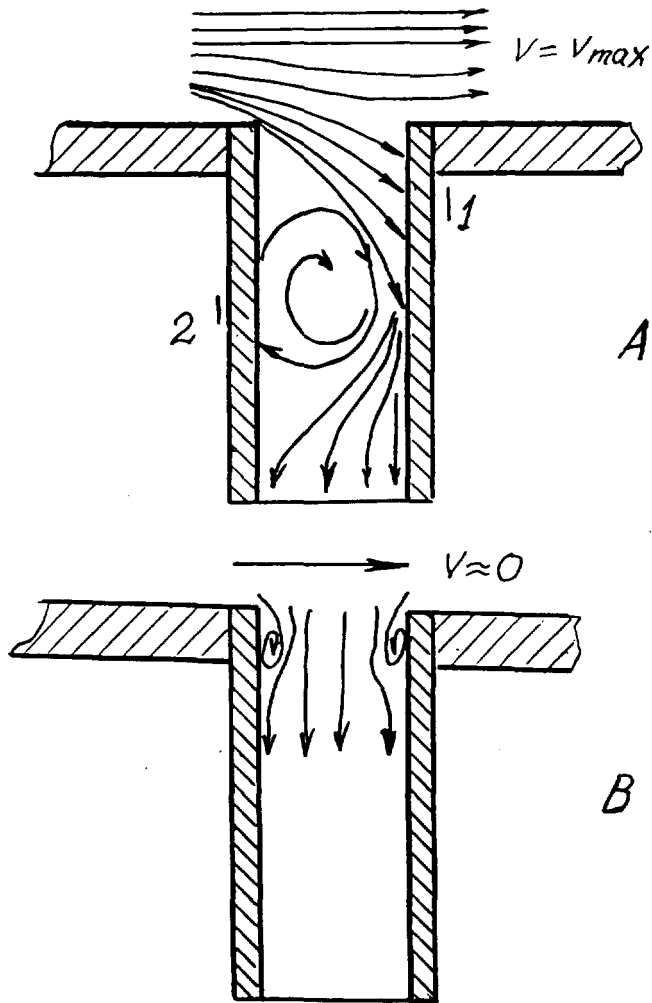


Fig. 7 . Velocities field at the nozzle inlet  
(quantitative picture) for two  
different inlet conditions

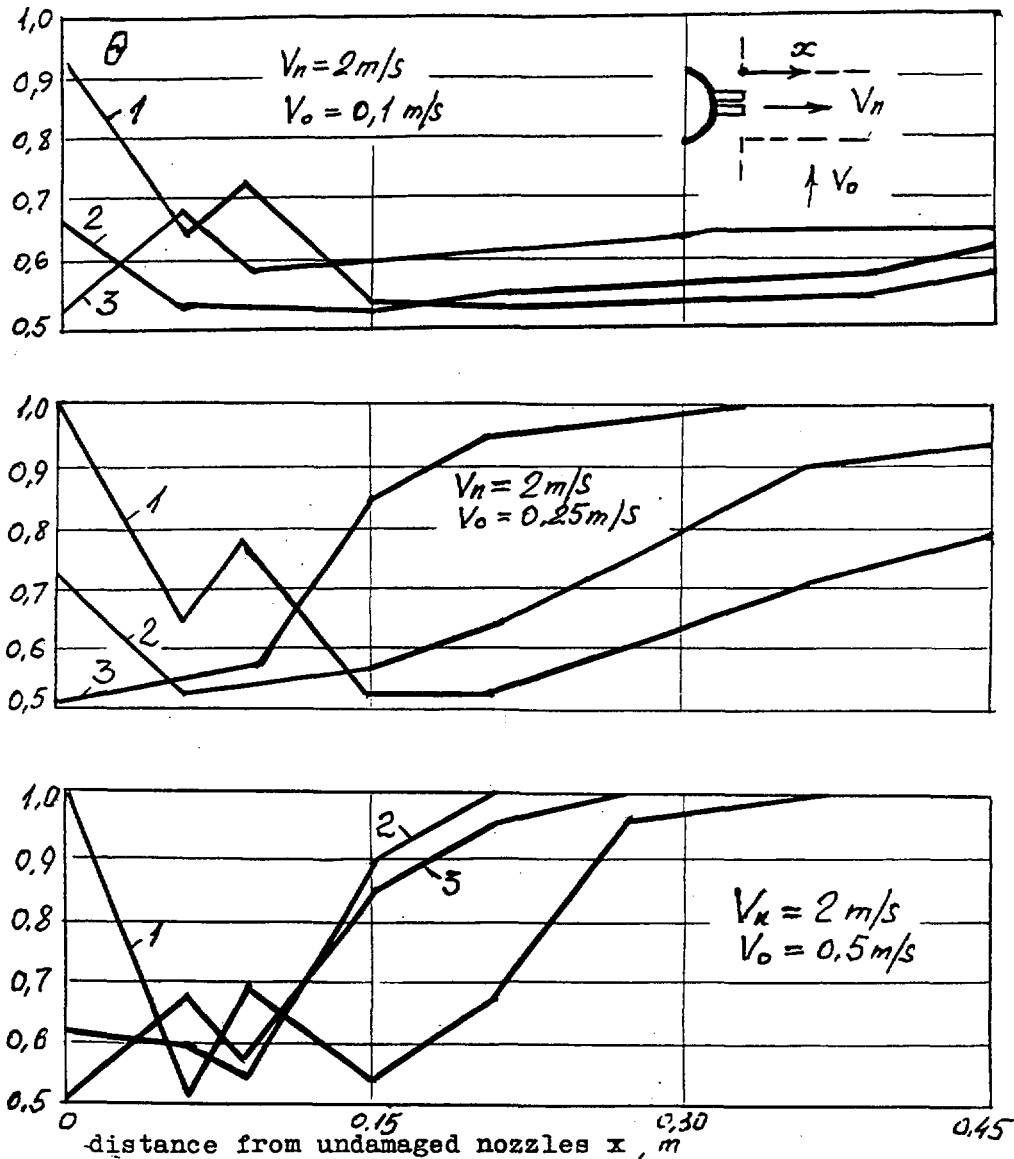


Fig.8. Dimensionless water temperature distribution along jet direction near upper tubes

- 1 - undamaged nozzles, Fig.2a
- 2 - damaged nozzles, Fig.2c
- 3 - damaged nozzles, Fig.2d

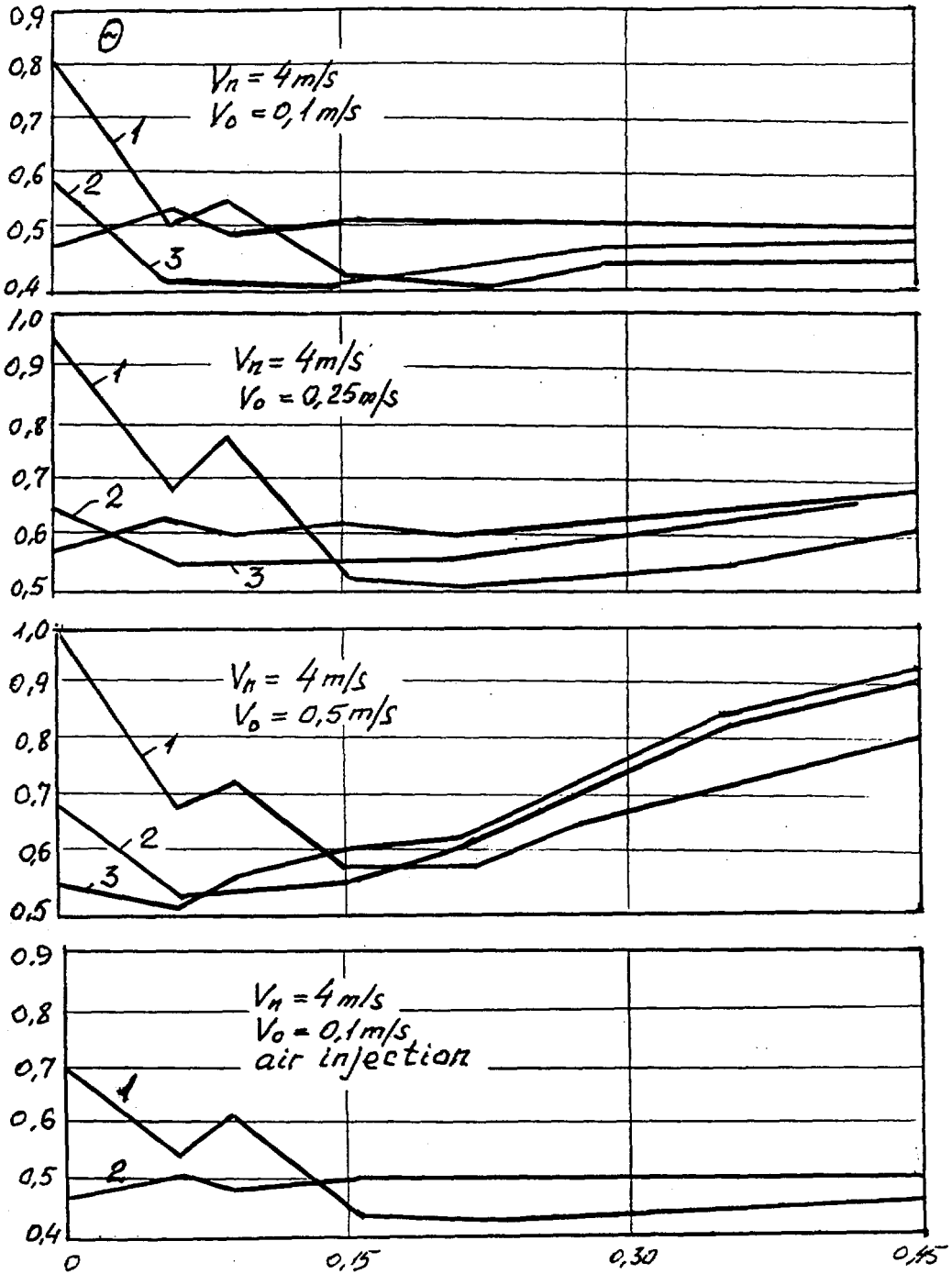


Fig.8. (continued)

# INFLUENCE OF FEEDWATER AND BLOWDOWN SYSTEMS ON THE MINERAL DISTRIBUTION IN WVER STEAM GENERATORS

L. Papp\*

\* Institute of Material Engineering, VITKOVICE R & D,  
Ostrava, Czech Republic

## 1. Introduction

After modification of Dukovany NPP steam generator feedwater system, the increased concentration of minerals was measured in the cold leg of modified steam generator. Some modifications were performed on operating WVER 1000 steam generators with aim to optimize the water chemistry in the collectors area.

Since the distribution of minerals can substantially affect on corrosion processes in steam generators, VITKOVICE, as a producer of WVER steam generators, has focused his attention on the optimizing of these systems.

To predict the mineral distribution on the secondary side of steam generators for considered feedwater/blowdown systems, the simple model of flow distribution in the secondary side of SG was developed.

## 2. Description of the Model

Since the problem of flow distribution in horizontal steam generators is very complex, two-dimensional flow model was used. It means, the mineral distribution in the vertical direction is assumed to be constant.

The horizontal plane of SG was divided into two sections

with mass balance equilibrium. The geometry of each section depends on feedwater distribution in steam generator. In this way, each section can be calculated as an independent part of steam generator. Both sections are divided into  $n$  subsections for which the mass conversation equation is calculated.

### 3. Results of Calculations

The distribution of minerals in modified Dukovany NPP WVER 440 steam generator was calculated. The basic calculation diagram is shown in Fig.1. Based on mass-balance calculation, the steam generator was divided into sections E<sub>1</sub>- E<sub>5</sub> , and, E<sub>6</sub>- E<sub>12</sub>. The calculated distribution of minerals (relative concentrations) for original blowdown system is shown in Fig.2. It is evident that according to measurements, the maximum of mineral concentration is in the area of cold bottom of steam generator.

To optimize the water chemistry, two modifications were analysed:

1. Feedwatre system modification
2. Blowdown system modification

As follow from our calculations, substantial improvement of secondary water chemistry can be achieved using blowdown system modification. Distribution of relative concentrations of minerals for improved blowdown system is shown in Fig.3.

Similar analysis was performed for WVER 1000 steam generators. Based on experimental data published, two important conclusions can be formulated:

1. Feedwater does not penetrate into tube bundle in the collectors area. Upon tube bundle feedwater flow to the steam generator bottoms. This flow distribution affects high mineral concentration in the collector area. On principle, in case of feedwater input upon tube bundle, the mineral concentration in the collector area will be

higher than in certain distance from collectors.

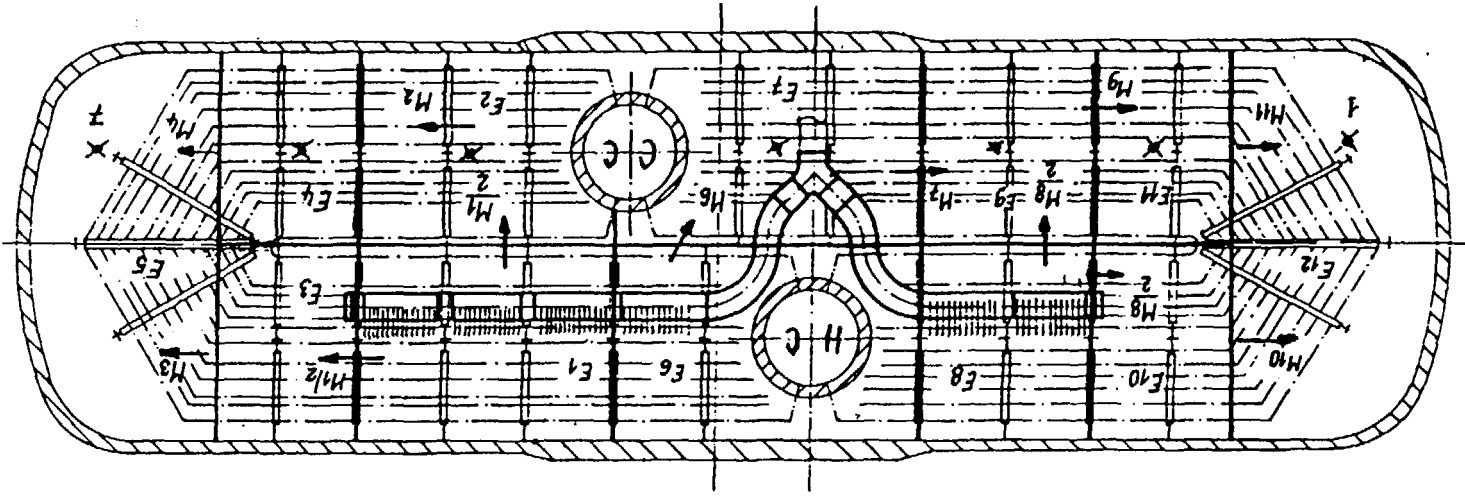
2. Present upper feedwater systems don't perform the basic design target - to uniform the two-phase level loading.

Therefore, the modified WVER 1000 feedwater system with immersed feedwater input was analysed. The calculated distribution of minerals is qualitatively same as the results shown for WVER 440 SG. From our calculations follow that using modified blowdown system - blowdown from ~~cold~~<sup>hot</sup> bottom area - the concentration of minerals decrease in the hot collector area about 100 times, and, in the cold collector area about 40 times.

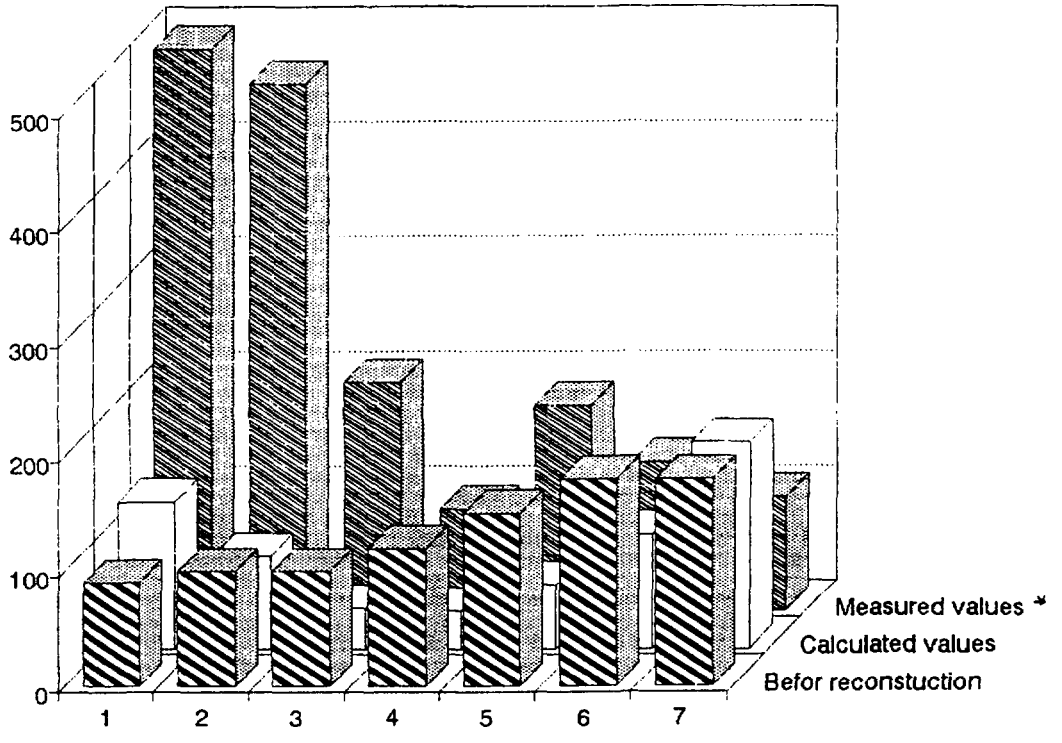
#### 4. Conclusuons

1. In case of given feedwater system, influence of blowdown modifications on the distribution of minerals in a steam generator is minimal. Influence on the magnitude of concentration is substantial.
2. For the given blowdown system, feedwater modifications have a substantial influence on the distribution of minerals in the SG volume.
3. Modifications of blowdown/feedwater systems have to be performed simultaneously.
4. Present WVER SG feedwater/blowdown modifications improve secondary water chemistry in the collector areas, but, don't solve the problem of two-phase level steam-loading. Therefore, the immersed feedwater system should be analysed in detail.

Fig. 1

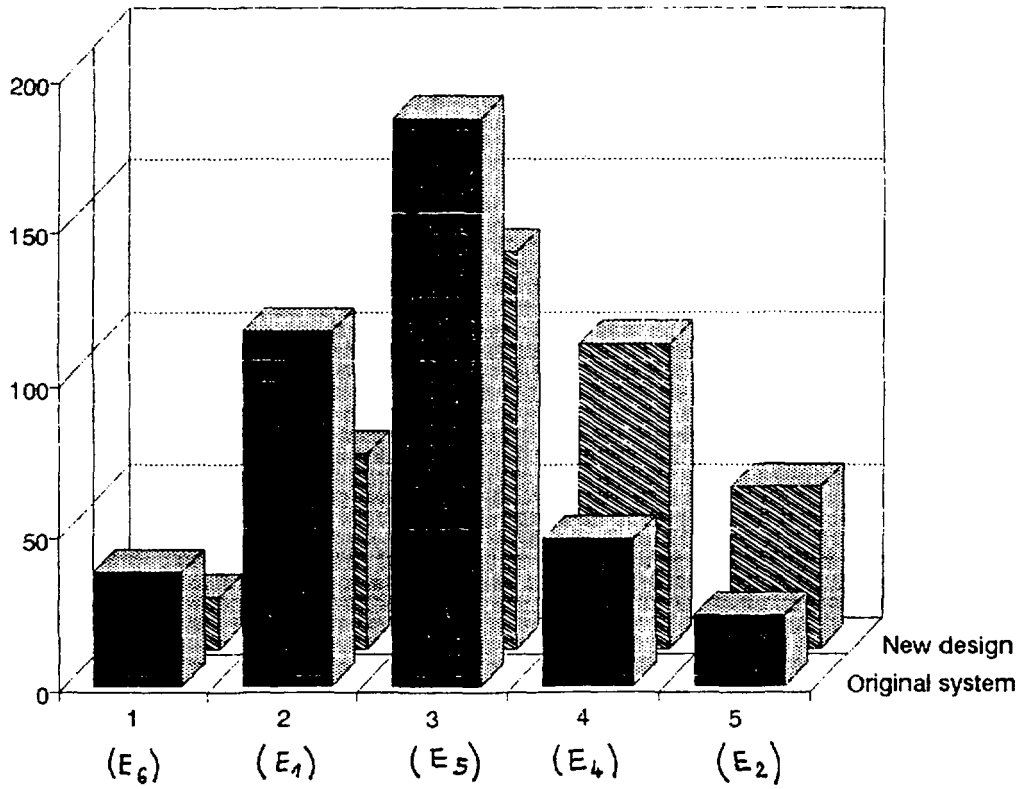


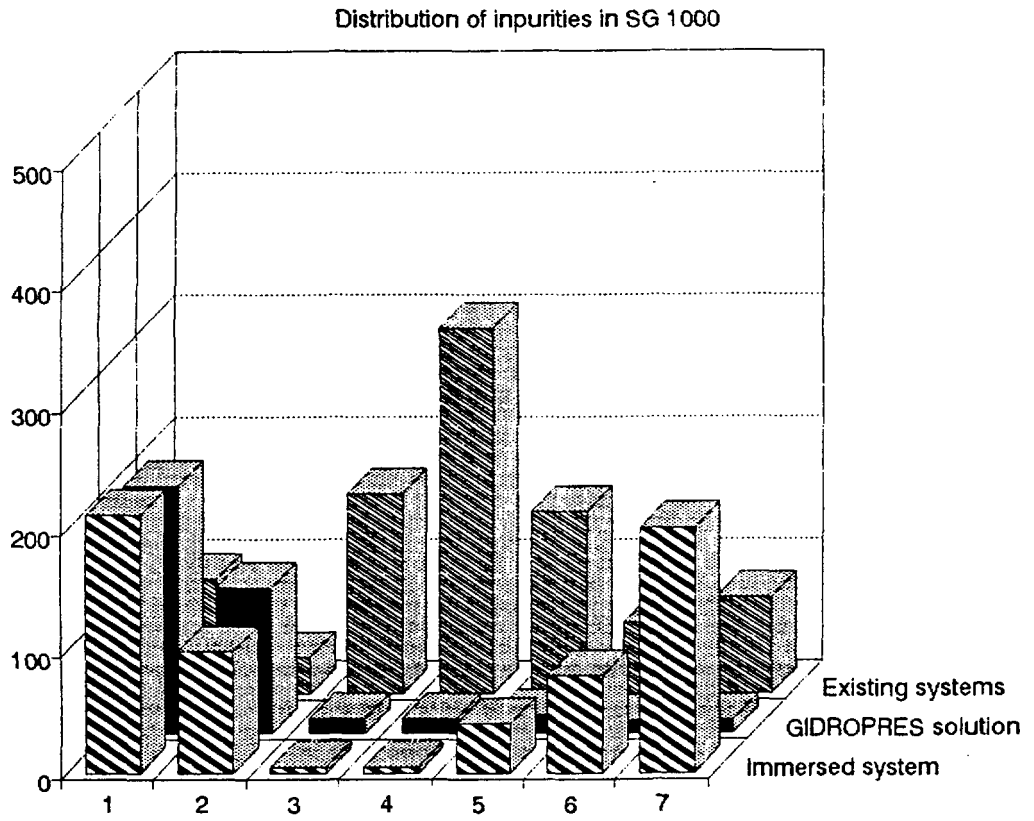
Distribution of impurities  
in SG 440MW



\* Befor final reconstruction

Distribution of impurities  
along the tube length





# **Results of Questionnaire for the Needs of Measured Data for the Steady-State Calculations**

**Vesa Yrjölä  
VTT ENERGY  
P. O. Box 1604  
FIN-02044 VTT  
Finland**

**To be presented at**

**THIRD INTERNATIONAL SEMINAR  
ON  
HORIZONTAL STEAM GENERATORS,  
October 18-20, 1994,  
Lappeenranta, Finland**

The First International Seminar on the Modelling of Horizontal Steam Generators was arranged in March 1991. As a outcome of the seminar, it was agreed to arrange a common calculational exercise to calculate the secondary side flow conditions during normal plant operation. OKB Gidropress of Russia supplied the experimental results for the exercise (Ref. [1]). They included some measured data of the local velocities and void fractions for the steam generators of the VVER-440 and VVER-1000 type reactors. It was a notable improvement for the modeler since earlier primarily the initial boundary conditions were only known.

The results of the common calculational exercise presented in the Second International Seminar in September 1992 were still mainly preliminary and it was felt necessary to continue these efforts. However in the final discussion it was concluded, that the given experimental results were not sufficient for a real code assessment --- still too many quantities have to be guessed. It was pointed out that it is advisable to define a minimum set of necessary data. For this purpose it was decided that VTT should made a query among the participants of the seminar, where they can give their opinion of the essential data. The aim was that the modeler should take into consideration, what is really needed and what are physical constraints of obtaining such data.

Four answer were received to the query. The organizations that submitted data are listed in Table I.

TABLE I

Organization	Designer	Country	Specific to the SG type of
Centre d'Etudes Nucléaires de Grenoble (CENG)	T. Haapalehto <sup>1</sup> D. Bestion	France	general plan
IVO International Ltd (IVO-IN)	C. Palsinajärvi	Finland	VVER-440
Nuclear Research Institute REZ plc (NRI)	M. Kyncl O. Matal <sup>2</sup>	Czech Republic	VVER-1000
Siemens AG	M. Protze	Germany	VVER-440

The answers from IVO and Siemens are specifying most detailed both the type and location of the required instrument, together with the importance of the quantity when solving the problem. Both replies are specific to the VVER-440 type steam generator. The NRI answer is based on the instrumentation plan of the one SG in Temelin NPP and summarizes also

<sup>1</sup> Lappeenranta University of Technology (LTKK)

<sup>2</sup> Energovózkum Ltd

measurements that are more specific for the study of the SG collector safety. It is the only response that was describing VVER-1000 type steam generator. The conclusion of the CENG answer is that the very detailed model of the secondary side is not important until a real 3-dimensional computational fluid dynamic code is applied. Thus CENG mainly appreciate measurements that are needed for the determination of the heat transfer to the secondary side as a boundary condition.

The summary of the results of the query are presented in Tables II through XI and attached figures in the appendix. The importance of the measurement for calculation model is justified as:

- I Minimum data set (= model verification is impossible without this measurement)
- II Great improvement for the reliability of the model.

Tables II through XI cannot be seen as a final conclusion for the required data set, but they include all values that the modelers reported necessary. Some tables may include multiple times the same quantity. It is considered necessary because the modelers either evaluated the importance differently or located them in different positions. Quantities as in Table IV (mass flow rate) and Table V (mixture velocity) may in principle be commensurable variables but they may also be dependent both on the calculation model and on other measured variables or on the type of the measurement. The contents of this summary will hopefully give a firm basis for the discussions in the next SG seminar, and contribute to draw the final conclusions.

#### REFERENCES

- 1. Letter Nr. 26-3/693 (12.12.1991) from Prof. V.F. Titov with supplements of geometrical and initial data for calculation in the secondary volume of PGV-440 and PGV-1000.

TABLE II Temperature measurements

Quantity in the calculation model	Type of measurement in experimental data	Location	Importance	Specific to SG of
Secondary fluid temperature	Thermocouple (Ø 1-2 mm)	From SG bottom to the top of tube bundle in three horizontal zones (see Fig. Siemens-1 in Appendix)	II	VVER-440
Secondary fluid temperature		Temperature profile (if any ?)	I	
Secondary fluid temperature		Horizontal temperature profile in three cross-sections (See Fig. IVO-1 A in Appendix) Vertical shell side downcomer temperature profile in three cross-sections (See Fig. IVO-1 B in Appendix)	I I	VVER-440 VVER-440
Primary water temperature	Resistance thermometer Resistance thermometer	SG inlet SG outlet		VVER-1000 VVER-1000
SG feed water temperature	Resistance thermometer	SG inlet		VVER-1000
SG steam temperature	Resistance thermometer	SG outlet		VVER-1000
Structure surface temperature	Thermocouple	SG collectors walls SG nozzles SG vessel walls	I	VVER-1000 VVER-1000

TABLE III Pressure measurements

Quantity in the calculation model	Type of measurement in experimental data	Location	Importance	Specific to SG of
Secondary pressure	Pressure transducer	Inlet and outlet of SG	I	VVER-440
Primary side pressure	Pressure gauge	Pressurizer Reactor		VVER-1000
Secondary side pressure	Pressure gauge	SG Pipeline		VVER-1000
System pressure		Global parameters	II	
Secondary pressure	High resolution pressure gauge (to determine the exact saturation temp.)	SG secondary steam dome	I	VVER-440

TABLE IV Mass flow rate measurements

Quantity in the calculation model	Type of measurement in experimental data	Location	Importance	Specific
SG secondary side fluid mass flow rate	Turbine flow meters + void fractions + (See also initial data for the calculation by Prof. Titov)	From SG bottom to the top of tube bundle in three horizontal zones (see Fig. Siemens-1 in Appendix)	I	VVER-440
SG feed water mass flow rate	Flow orifice	SG feed water inlet pipe		VVER-1000
SG blow down water mass flow rate	Flow orifice	SG blow down water outlet pipe		VVER-1000
SG feed water mass flow rate		SG feed water inlet line	I	VVER-440
SG steam line mass flow rate		SG steam outlet line	I	VVER-440
SG secondary side fluid mass flow rate		Flow rates into and from tube bundles in three cross-sections (see Fig. IVO-2 in Appendix)	I	VVER-440

TABLE V Mixture velocity measurements

Quantity in the calculation model	Type of measurement in experimental data	Location	Importance	Specific
SG secondary side fluid mixture velocity		Fluid mixture velocities into and from tube bundles in three cross-sections (see Fig. IVO-2 in Appendix)	I	VVER-440
Velocity		Local values	Useless without 3-D code	

TABLE VI Water velocity measurements

Quantity in the calculation model	Type of measurement in experimental data	Location	Importance	Specific
SG secondary side water velocity	Turbine flow meters (See initial data for calculation by Prof. Titov) $W' = W_g (1 - \phi)\eta$	From SG bottom to the top of tube bundle in three horizontal zones (see Fig. Siemens-1 in Appendix)	I	VVER-440
SG secondary side water velocity temperature		Water velocities into and from tube bundles in three cross-sections (see Fig. IVO-2 in Appendix)	II	VVER-440

TABLE VII Steam velocity measurements

Quantity in the calculation model	Type of measurement in experimental data	Location	Importance	Specific
SG secondary side steam velocity	Mini local vortex meter	From SG bottom to the top of tube bundle in three horizontal zones (see Fig. Siemens-1 in Appendix)	II	VVER-440
SG secondary side steam velocity temperature		Steam velocities up from tube bundles in three cross-sections (see Fig. IVO-3 in Appendix)	II	VVER-1000

TABLE VIII Steam void fraction measurements

Quantity in the calculation model	Type of measurement in experimental data	Location	Importance	Specific
SG secondary side steam void fraction	Differential pressure transducer or see initial data for calculation by Prof. Titov	From SG bottom to the top of tube bundle in three horizontal zones (see Fig. Siemens-1 in Appendix)	I	VVER-440
Secondary side steam void fraction	Wire sensors Trace method	Inside SG secondary SG steam outlet pipeline		VVER-1000 VVER-1000
Secondary side steam void fraction		Local values	Useless without 3-D code	
SG secondary side steam void fraction		Three dimensional void profile (see Fig. IVO-4 in Appendix)	I	VVER-440

TABLE XI Level and chemistry measurements

Quantity in the calculation model	Type of measurement in experimental data	Location	Importance	Specific
Collapsed level	Differential pressure transducer EMUS-System (electromagnetic-supersonic measurement)	Secondary side collapsed level in three horizontal zones (see Fig. Siemens-1 in Appendix)	II	VVER-440
Level at secondary side	Condensate chambers and pressure drop Wire sensors Thermocouples	Outside the SG vessel Inside SG Primary collector		VVER-1000 VVER-1000 VVER-1000
Salt concentration in water at secondary side	Sampling lines and chemical analysis	Inside the SG vessel		VVER-1000
Collapsed level	Differential pressure transducer	Over whole SG vessel	I	
Swell level	Heated and unheated thermocouples	Global parameters	II	

Geometrical data  
of WER-440 SC

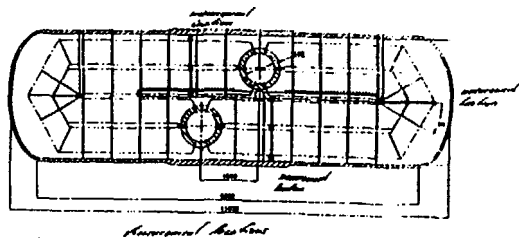
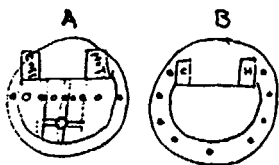


Figure Siemens-1



The measurements of: 3 cross sections for measurement  
- Temperature  
- gas flow rate  
- steam/water/mix. velocity  
should be located, at least in 3 cross sections  
see drawing →

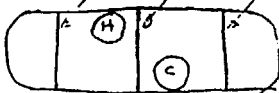
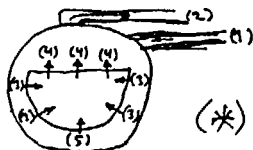


Figure IVO-1



The measurements of: 3 cross sections for measurement  
- Temperature  
- gas flow rate  
- steam/water/mix. velocity  
should be located, at least in 3 cross sections  
see drawing →

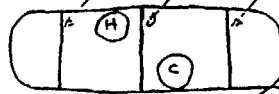
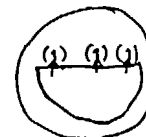


Figure IVO-2



The measurements of: 3 cross sections for measurement  
- Temperature  
- gas flow rate  
- steam/water/mix. velocity  
should be located, at least in 3 cross sections  
see drawing →



Figure IVO-3

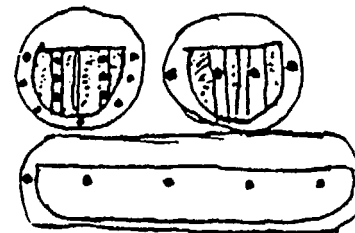


Figure IVO-4

# MATHEMATICAL SIMULATION OF PROCESSES IN HORIZONTAL STEAM GENERATOR AND THE PROGRAM OF CALCULATION OF ITS CHARACTERISTICS

Titov V.F., Zorin V.M., Gorburov V.I.  
(OKB "Gidropress", Moscow Energy Institute, Russia)

For description of hydrodynamical processes in the horizontal steam generator (SG) two-phase volume number of relations is used.

Under conditions of the working medium column hydrostatical equilibrium in the natural circulation (NC) circuit and at the relative steam velocity of  $W_a$  it can be stated:

$$\frac{W''_{01}}{W''_{01} + W'_{01} + W_a} = \frac{W''_{02}}{W''_{02} + W'_{02} + W_a} \quad (1)$$

where  $W'_{01}, W'_{02}$  - liquid phase velocity in channels 1, 2 respectively;  
 $W''_{01}, W''_{02}$  - vapor phase velocity.

If a steam generating unit has several circulation circuits ( $n > 2$ ) having various vapor phase flow rate and when vapor phase velocity depends on height  $Z$  in some fashion, hydrostatical equilibrium condition for channel with number  $i$  can be written as:

$$\varphi_i(Z) = \bar{\varphi}(Z) \quad (2)$$

where  $\bar{\varphi}(Z)$  - average void fraction, calculated using average reduced velocities of vapor and liquid phases.

If average water velocity at the level of bottom tube row of horizontal tube sheet is  $W_0$  and under condition of  $\varphi_i(Z)$  in all channels, the equation for the reduced velocity of liquid will be:

$$W_{0i}(Z) = (W_a + \bar{W}_0) \frac{W''_{0i}(Z)}{W''_0(Z)} - W_{0i}(Z) \frac{\rho''}{\rho'} - W_a \quad (3)$$

From stated equations follows:

1. In cross-section of channel number  $i$  at the height  $Z$  water will move

upward if  $W''_{oi}(Z) > W''_o(Z)$ .

2. Velocity of downward water motion in a NC circuit can not be less than  $-W_a$ .

If there are not any partitions, separating channels, in the circulation circuits can take place horizontal flows of working medium, which represent the flow rate difference between cross-sections  $Z+\Delta Z$  and  $Z$  (ignoring evaporation at height  $\Delta Z$ ).

The velocity of horizontal water flows is

$$W_{hi}(Z) = \frac{\partial}{\partial Z} \left[ A_i(Z) \left( W'_{oi}(Z) - W'_{oi}(Z) \frac{\rho''}{\rho'} \right) \right] \quad (4)$$

Here  $A_i(Z)$  - channel perimeter at height  $Z$  through which the horizontal flows are possible.

Taking into account the pressure loss while working medium vertical movement, hydrostatical equilibrium condition of the circulation circuit channels will be the equality of pressure differential  $\Delta P_i(Z)$  between two horizontal cross-sections. Then instead of condition  $\varphi_i(Z) = \varphi(Z)$  we can write

$$\bar{\varphi}_i(Z) - \frac{\Delta P_i(Z)}{g \Delta Z (\rho' - \rho'')} = const, \quad (5)$$

where  $\bar{\varphi}(Z)$  - average value of void fraction in the channel number  $i$  at the height  $Z$  in the range of  $\Delta Z$ .

For a circuit with two channels, taking into account the pressure loss in vertical flows  $\Delta P_1$  and  $\Delta P_2$  as well as in horizontal flows  $\Delta P_h$ , hydrostatical equilibrium condition can be represented as

$$\varphi_1(Z) - \frac{\Delta P(Z) - \Delta P_2(Z) - \Delta P_{h2l}(Z)}{g \Delta Z (\rho' - \rho'')} = \varphi_2(Z) \quad (6)$$

For calculation of the pressure loss in two-phase flow a homogenous mixture flow model was admitted

$$\Delta P = \frac{\xi}{2} (W_0'' \rho'' + W_0' \rho') |W_0'' + W_0'| \quad (7)$$

On the basis of stated mathematical relations a non-prepared circulation

circuit of the PGV-1000 big tube bank was analyzed (tubes 16x1.5;  $S_1=23$  mm;  $S_2=19$  mm; number of horizontal rows  $n_h = 110$ ; number of tubes in row  $n_{tr} = 30$ ;  $t_s = 278.5$  °C; heat transfer coefficient  $K = 6.0$  kW/m<sup>2</sup>·K.

Under these conditions  $W_a=0.33$  m/s.

Condition (5) subject to (7) at  $Z = S_2$  can be converted to a dimensionless form

$$W_R^2 + W_R \left(1 + 2S + \frac{P-R}{S}\right) + P \left(1 + \frac{1}{S}\right) + S(1+S) = 0, \quad (8)$$

where

$$W_R = \frac{W_0''}{W_a} \frac{\rho' - \rho''}{\rho'}; \quad P = \frac{\xi_c}{\xi_{ts}}; \quad S = \frac{S_c}{S_{ts}}; \quad R = \frac{2 g S_2}{\xi_{ts} W_a^2};$$

$S_c$  and  $S_{ts}$  - downflow channel and tube sheet clearance.

This equation gives the possibility of the downflow channels classification as follows: a big one, where water velocity in any cross-section not reaches  $-W_a$  value; a medium one, where at least in one cross-section water velocity equals  $-W_a$ ; a small (narrow) one, where water velocity equals  $-W_a$  in all cross-sections.

This analysis was realized using a code, which ignores the horizontal flows of vapor phase.

Tube bank has been represented as three circulation channels ( $i=1, 2, 3$ ). 22 horizontal cross-sections has been taken. Equilibrium condition (5) has been used. For each pair of cross-sections were being determined: the steam-water mixture column weight, pressure loss and total pressure difference  $\Delta P_{ij}$ , where  $j= 1, 2, 3, \dots 22$ .

Pressure loss coefficient for one tube row has been taken 0.16. Horizontal water flows were being determined from material balance

$$G_{ij}^{hot} = G_{w,ij} + \Delta G_{sr,ij} - G_{w,ij-1},$$

where  $\Delta G_{sr,ij}$  - steam rating of channel number  $i$  between cross-sections  $j$  and  $(j-1)$ .

Steam rating of channels (steam flow rate along vertical axis is

$$G_{sr} = G_{sr,i(j-1)} + \Delta G_{sr,ij} + G_{sr,ij}^{hot}$$

Analysis of the results obtained on the bases of stated relations allow to make definite inferences:

1. Simulation of the 50 called unprepared NC circuits using the hydrostatical equilibrium conditions is a sufficiently effective tool for the circulation characteristics analysts and can be used for more complicated NC circuits.

2. The downflow channel width significantly effects the hydrodynamical characteristics distribution along the height of circulation circuit.

3. The steam-water mixture escape from tube sheet into the channels as a characteristic property of unprepared NC circuits. Unprepared NC circuits regimes with the hanging up entrainment of water by the steam are usually instable.

4. Taking into account the pressure loss due to horizontal flows of working medium ( $\xi_n \neq 0$ ) do not change the principal pattern of hydrodynamical situation in an unprepared SC circuit. Characteristic property of a horizontal type SG is the horizontal arrangement of heat exchange tubes, along the length of which the heat flow significantly changes due to the coolant temperature alteration. Such SG from this point of view represents a complex unprepared NC circuits which surely can not be considered as a set of sample circuits because the additivity principle may not be applicated here. The complex circuit has to be calculated as a one. Really, water having passed through some section of the downflow channel do not necessarily feeds the neighboring section of steam generating tube bank only. And on the contrary, water, entering the tube bank do not necessarily comes to it by the immediately neighboring Its tube bank channel only.

Structural (geometrical) SG simulation may be based on the consideration of SG as a set of calculating elements, In particular - the rectangular parallelepipeds. The sizes of fitting each other faces of parallelepipeds, located side by side or immediately one over another, may not coincide. For PGV-1000 the water volume cross-section - part of a circle surface - 19 simulated by 240 rectangle elements - 10 elements per each or 24 horizontal layers. These 10 elements represent slice by slice of the SG cross-section the following details: 1) channel between SG casing or submerged perforated sheet (SPS) flange and side tube bank Tube sheet); 2) side tube bank; 3) channel between tube banks; 4) main tube bank; 5) half or the central channel - and further these details in reverse order. Along vertical axis each element, from 1st (lower) to 22nd horizontal layer, correspond to five tube rows of the steam generating tube bands. Elements of 23rd and 24th horizontal layers serve for simulation of processes under and over the SPS. Along the longitudinal axis the SG is divided

on 12 vertical layers of elements. So, the total number of PGV-1000 calculating elements equals to 2880 (12x10x24).

While heat exchange simulation, the coolant temperature and heat transfer coefficient alterations along the heat exchanging tubes were being determined. In this case was used the possibility of the tube wall thermal resistance changing, so that at given coolant temperatures at tube inlet (tube of medium length), the given coolant temperature at tube outlet would be obtained.

While the SG water volume hydrodynamics simulation the condition (5) is assumed, i.e. the equality of pressure differentials between upper and lower faces or all elements, positioned on the same horizontal layer. Pressure loss in vertical flows was calculated according to (7), total horizontal water flows - according to (9).

Calculational algorithm is based on a double iteration loop. Inside of internal iteration loop, at given pressure differential  $\Delta P_k$  in horizontal layer number  $k$ , the vertical water flow  $G_{w,mnk}$  ( $m, n, k$  - the indexes) for each element of this layer are being determined. Inside or external iteration loop such  $\Delta P_k$  value is being set, so that water flow rate  $G_{w,k}$  meet the layer material balance:

$$G_{w,k} = \sum G_{w,mnk}(\Delta P_k)$$

Both iteration loops use dichotomy method. Convergence of iterations was achieved if the accuracy of internal iterations was high ( $\delta P_k \approx 10^{-6}$ ) and that of external iterations was medium ( $\delta G_w \approx 10^{-2}$ ),

Distribution of total horizontal flows through the four faces of or elements was being carried out using a procedure, which consider characteristic properties of the tube sheets, including presence or tube support plates. The horizontal steam flows were not being determined, but were represented by conventional placement or some number of tubes into the neighboring channels without changing the clearances of these channels.

Material balances consider the feed water flow rates, including the coordinates of its distribution and also the steam condensation while feed water warming-up was regarded. For elements over SPS the pining was considered; for elements with coordinates of blow-down, the blow-down water rates were considered. For simulation of processes under SPS, coefficient of irregularity of steam load was used. This coefficient characterizes the relative deviation of the reduced steam velocity (steam load) from mean steam velocity, and can be calculated as

$$K_{mn}^{irr} = \frac{W_{0,nm}'' - \bar{W}_0''}{\bar{W}_0''},$$

where  $m$  and  $n$  are the coordinates of point being calculated. Also the coefficient of levelling was used, which determine the extent of decrease of all irregularity coefficients due to the effect of a levelling device presence (for example SPS), and can be calculated as

$$K_{lev} = 1 - \frac{K_{2,mn}^{irr}}{K_{1,mn}^{irr}},$$

where  $K_1^{irr}$ , and  $K_2^{irr}$  - the coefficients of irregularity before and after levelling effect.

Calculation of moisture quantity going up on SPS was carried out using the moisture mass flow rate in the SPS holes ( $w_{hole} = 1 - \alpha_{hole}$ )

$$w_{hole} = K_{out} \frac{W_{02}'' - W_a}{W_{02}'' + W_a},$$

where  $W_{02}''$  - reduced steam velocity in the SPS holes (after levelling);  $K_{out}$  - coefficient, regarding the moisture quantity going up on SPS (after a number of code runs  $K_{out} = 0.7$  was taken);  $K_{lev} = 0.925$  (when the SPS perforation degree is 0.075);  $\xi_{SPS} = 1.2$  - the coefficient of SPS holes resistance.

According to the used mathematical model or hydrodynamical processes, the general pattern of the SG circulation can be obtained by superposition of three most significant circulation circuits:

- circulation circuit between the hot and cold halves of SG, which take place due to the temperature head decrease along the U-shaped tubes;
- circulation circuit due to presence of free from tubes volumes - downflow channels;
- circulation circuit around the SPS flange.

Figs. 1-3 show the results of the PGV-1000 hydrodynamical characteristics obtained using the created code, which gives the possibility to consider:

- change of primary circuit coolant parameters, thermal resistance of the tubes wall material, parameters of boiling working medium;
- length change or heat exchanging tubes, number of tubes In each row, clearances between tubes and now area of channels;
- design of feed water distribution assembly and its real lay-out inside of SG;
- design of blow-down assembly, i.e. in maximum degree consider the real SG geometry.

A code is also created which calculates hydrodynamical processes in the SG for VVER-440 reactor. In this case the number of horizontal layers is lowered to 11 (upper level simulates the working medium flows over the tubes),

Characteristics of the SG water volume and general pattern of water flows in SG obtained by the calculation meet the results of measurements carried out on real SG satisfactorily.

The code may be used also for determination of water content on SG. Calculation gives that water content on PGV-1000 is - 31 t and in PGV-4 is - 25 t.

## CONCLUSION

On the basis of mathematical models describing the processes in horizontal SG the code has been worked out, which gives the possibility to calculate the hydrodynamical characteristics in any point of water volume. But presently this code simulates the processes in SG in the stationary (or quasi-stationary) mode of operation only. In the same time this code may be used as a next step to the calculations of the SG characteristics in the non-stationary modes of operation.

## RELAP5/ MOD2 post-test calculation of a Loss of Feedwater experiment at the PACTEL test facility

---

**Marion Protze, Siemens/ KWU**

Post-test calculations for verification purposes of the thermal hydraulic code RELAP5/ MOD2 are of fundamental importance for the licensing procedure. The RELAP5/ MOD2 code has a large international assessment base regarding western PWR. VVER-reactors are russian designed PWRs with some specific differences compared with the western PWR's, especially the horizontal steam generators. For that reason some post-test calculations have to be performed to verify the RELAP5/MOD2 code for these VVER-typical phenomena. The impact of the horizontal steam generators on the accident behaviour during transients or pipe ruptures on the secondary side is significant.

The nodalization of the test facility PACTEL was chosen equally to VVER plant nodalization to verify the use of a coarse modelling of the steam generator secondary side for analyses of transients with decreasing water level in the SG secondary side. The calculational results showed a good compliance to the test results, demonstrating the correct use of a coarse nodalization.

To sum up, the RELAP5/ MOD2 results met the test results appropriately thereby the RELAP5/ MOD2 code is validated for analyses of transients with decreasing water level in a horizontal steam generator secondary side.

### 1. Introduction

---

In the scope of the TACIS-91, Item 1.3: Accident Analyses – project and within the project "Completion of the NPP Mochovce" Siemens/ KWU is responsible for the Non-LOCA analyses. Generally, at Siemens/ KWU LOCA and Non-LOCA analyses for the VVER are being performed using the RELAP5/ MOD2

code. For this reason the RELAP5/ MOD2 code is being verified for Non-LOCA analyses for VVER plants.

At the PACTEL facility a test series of "Loss of secondary side feed water" was performed. In the first test "LOF-01" only one primary loop of the PACTEL facility was in operation. This

The main objective of this post-test calculation is the test of the ability of the code to simulate the water level decrease in the horizontal steam generator to such an extent that one or more heat exchange tubes are not longer covered

by water and correspondingly to test the ability of the code to simulate the correct heat transfer from the primary to the secondary side under such conditions.

## **2. Test description**

---

### **2.1. Description of the PACTEL facility**

The PACTEL facility is a volumetrically scaled model of a 6-loop VVER-440 PWR with three separate loops and 144 full length, electrically heated fuel rod simulators arranged in three parallel channels. The fuel rod simulators are heated indirectly. The volume scaling factor is 1:305 and the elevation scaling factor is 1:1. A detailed description of the PACTEL facility can be found in reference [1].

### **2.2. Test description**

The first test in the test series of the "Loss of feedwater" LOF-01 was performed with only one primary loop of the facility in operation. This was realized by closing the primary loop isolation valves in the other two loops. The hot loop isolation valves are located in the loop seal of the hot legs. The loop where the pressurizer is located was isolated, but the connection of the surge line to the hot leg is located between the pressure vessel and the isolation valve.

The test was started at steady-state conditions where the water level in the steam generator secondary side was covering the heat exchange tubes. The heating power was 75 kW corresponding to about 1.7% power in the refe-

rence reactor. The feed water injection to the steam generator secondary side was closed at the beginning of the test. The experiment was continued until the heat transfer to the secondary side ceased and the primary pressure started to rise.

Because of the heat losses the primary pressure decreased slightly. The pressurizer heaters held up the primary pressure and in accordance with the switching off or on of the heaters the pressure varied. All other main primary parameters remained unchanged until the uppermost layer of heat exchanger tubes in steam generator secondary side were no longer covered by water. As the swell level in the steam generator secondary side dropped below the first layer of these tubes (the collapsed water level on the secondary side was about 25 centimeters above the bottom of the steam generator) the heat transfer from the primary to the secondary side was disturbed and this affected the loop flow rate on the primary side. After a while the loop flow rate returned to nearly the original value. This was repeated for the next layers until all the steam generator secondary side heat exchanger tubes became free of water what resulted in an increase of primary temperature. Finally the collapsed water level in the pressure vessel sunk and

the cladding temperatures increased. On this state the test was stopped.

### 3. Calculational results

---

#### 3.1. RELAP5/ MOD2 description

RELAP5/ MOD2 is a light water reactor system transient analysis code that can be used for simulation of a wide variety of PWR system transients of interest in reactor safety. The primary system, secondary system, feedwater train, I&C system, and core neutronics can be simulated. The code models have been designed to permit simulation of postulated accidents ranging from large break LOCA to accidents involving the plant controls and fuel system. Transient conditions can be modelled up to the state of fuel damage. RELAP5/ MOD2 was produced by improving and extending the modeling base that was established with the release of RELAP5/ MOD1 in December 1980. The code has been in a frozen status since April 1985. The modeling approach and instructions for application of the code are documented in a two-volume user manual /2/ and two additional reports /3,4/. In volume 1 of /2/ the basis for the system models and their numerical implementation is described. Volume 2 contains recommendations for the proper use of code models and detailed descriptions of the input data requirements for use of the code. Special models and correlations used in the code are presented in a detailed form in /4/. Furthermore results of developmental assessment problems are documented in /3/. RELAP5/ MOD2 cycle 36 is executing on CDC and CRAY computers. SIEMENS/ KWU currently uses the version RELAP5/MOD2/V251, which is –

with respect to physics – identical to cycle 36 but has been transferred to Apollo 30 and HP 700 Workstations.

#### 3.2. Nodalization scheme

The nodalization of the test facility was chosen to be the same as it is used for plant nodalization to verify the use of a coarse modelling of the steam generator secondary side for analysis of transients with decreasing water level in the steam generator secondary side.

The nodalization scheme of the PACTEL facility is represented by 354 volumes and 358 junctions. All three loops of the facility were modelled separately. The pressurizer-model is connected to loop 2 (pressurizer-loop). For the post-test calculation of the LOF-01 test the nodalization was changed with respect to the one-loop model. The second and third loop were disconnected from the gate valves in the hot and cold legs respectively so that the pressurizer is connected to the hot leg of the second loop and therefore is affected by the primary system.

The core section was divided into four parallel channels. Three of them simulate the fuel rod bundles of the facility and the fourth was used to simulate the bypass flow.

The hot leg described accurately the hot leg loop seal as well as the simulation of the cold leg described the pump seal in an accurate way.

The steam generator secondary side was simulated by three modelled tube layers of heat exchanger tubes each including three real layers of heat exchanger tubes of the test facility. The height of each volume, where the heat transfer takes place, corresponds to the rows of the primary side. The three downward volumes simulate the bypass between the heat exchanger tubes for natural circulation.

The steam generator secondary side was modelled like it is used by plant calculations to show whether this steam generator model for plant analyses is sufficient for Non-LOCA analyses. Because of numerical reasons a very fine model of the steam generator secondary side could lead to effects which do not have an influence on the accident behaviour in reality. For that reason a very fine steam generator secondary side modelling should be avoided.

Heat structures were used to model the heat exchanger tubes, pressurizer heaters, fuel simulators as well as the pipe walls, valves and flanges on the primary and secondary side. The heat losses to the environment and the form loss coefficients were obtained from the characterizing tests of the facility.

The nodalization schemes of the test facility are shown in Figure 1 and 2.

### 3.3. Calculational results

The results of the post-test calculation by using the RELAP5/ MOD2 code showed a very good compliance with the experimental data. This is illustrated in Figures 3 to 15, which show a comparison of the experimental and the calcula-

tional data of the main parameters on primary and secondary sides.

Prior to closing the feedwater supply on the steam generator secondary side the system was at quasi steady state conditions. The only disturbances of steady state were caused by the operation of the pressurizer heaters. Up to 180 sec the heater power is 2 kW. After this time the heater power is switched over to 6 kW. As a result the primary pressure increased up to 7.5 MPa at 350 s when the heater power is reduced again to 2 kW. The pressurizer heaters were operating during all time the experiment.

In exception of the primary pressure all main primary parameters remained unchanged as long as the modelled layers of heat exchanger tubes in the steam generator secondary side were covered by water.

After 3250 sec the first modelled layer in the steam generator was uncovered by water. The heat transfer to the secondary side was disturbed which affected the mass flow rate on the primary side. It decreased for a short time and then returned to the almost original level after approximately 1000 sec. Within the same time the cladding temperature started to increase very slowly. The steam in the steam generator upper part was slightly overheated.

After 5800 sec the level in steam generator secondary side dropped below the second modelled layer. The heat transfer to the secondary side was disturbed to such an extent that the mass flow rate could not return to the original rate after the sharp decrease. Then the temperature in the steam generator primary side increased and later also the primary

pressure increased. The calculation was stopped after 7200 sec.

### **3.4. Comparison of the calculational with the test results**

The decrease of the mass flow rate of the primary coolant after uncovering the modelled layers of the heat exchanger tubes was much higher than after uncovering the layers in the experiment. Because of the coarse nodalization three steam generator heat exchanger tube layers were combined in one modelled layer. For that reason the decrease of the heat transfer to the secondary side and accordingly the decrease of the mass flow rate on the primary side after uncovering the first modelled layer was much higher than in the experiment. By using a fine nodalization the parameter

behaviour on the primary and secondary side showed a higher harmony between the calculational and experimental results after uncovering the heat exchanger layers. But the differences between the results by using the coarse or the fine nodalization are not significant compared to the experimental results so that an use of a fine nodalization of the steam generator secondary side for these accidents would not be useful.

The increase of the primary pressure and temperature and the increase of the cladding temperature in the RELAP calculation was slightly faster due to the higher heat transfer. This is more conservative for the events in which the water level of steam generator secondary side is decreasing (e.g. ATWS, Loss of feedwater supply).

## **4. Conclusion**

---

The nodalization of the test facility was chosen to be the same as it is used for plant nodalization to verify the use of a coarse modelling of the steam generator secondary side for analysis of transients with decreasing water level in the steam generator secondary side. The calculational results showed a good compliance to the test results, demonstrating the correct use of a coarse nodalization.

To sum up, the RELAP5/ MOD2 results met the test results appropriately thereby the RELAP5/ MOD2 code is validated for analyses of transients with decreasing water level in the horizontal steam generator secondary side.

## 5. References

---

- /1/ Purhonen H., Miettinen J.  
PACTEL – Parallel Channel Test Loop  
General Description for ISP  
Technical Research Centre of Finland,  
Nuclear Engineering Laboratory  
Technical report no. 9/91  
Lappeenranta 1991
- /2/ RELAP5/ MOD2 CODE MANUAL,  
Volume 1 und 2  
V.H. Ransom et al.  
NUREG/CR-4312 EGG-2396,  
August 1985
- /3/ RELAP5/ MOD2 CODE MANUAL,  
Volume 3  
Developmental Assessment  
V.H. Ransom et al.  
EGG-TFM-7952, December 1987
- /4/ RELAP5/ MOD2 Models and Correla-  
tions  
R. A. Dimenna et al.  
NUREG/CR-5194 EGG-2531,  
August 1988

## 6. Figures

---

- Fig. 1: Nodalization of ITF PACTEL
- Fig. 2.1.: PACTEL Nodalization of RPV with measurement device location
- Fig. 2.2.: PACTEL, Loop 1
- Fig. 3: Cladding temperature in channel A; upper part
- Fig. 4: Cladding temperature in channel A; upper part
- Fig. 5: DC, core inlet fluid temperature
- Fig. 6: Core outlet, lower plenum fluid temperature
- Fig. 7: Mass flow cold leg 1, 2
- Fig. 8: Mass flow downcomer
- Fig. 9: Pressure in upper plenum, SG sec. side
- Fig. 10: Water level in Steam Generator secondary side
- Fig. 11: Total core power
- Fig. 12: Heat transfer in the steam generator, sec. side
- Fig. 13: Heat transfer coefficients in the SG sec. side in the first, second and third layers
- Fig. 14: SG, prim. side tube 23 fluid temperature A,B,C
- Fig. 15: SG, sec. side tube 26, 23, 11 fluid temperature B



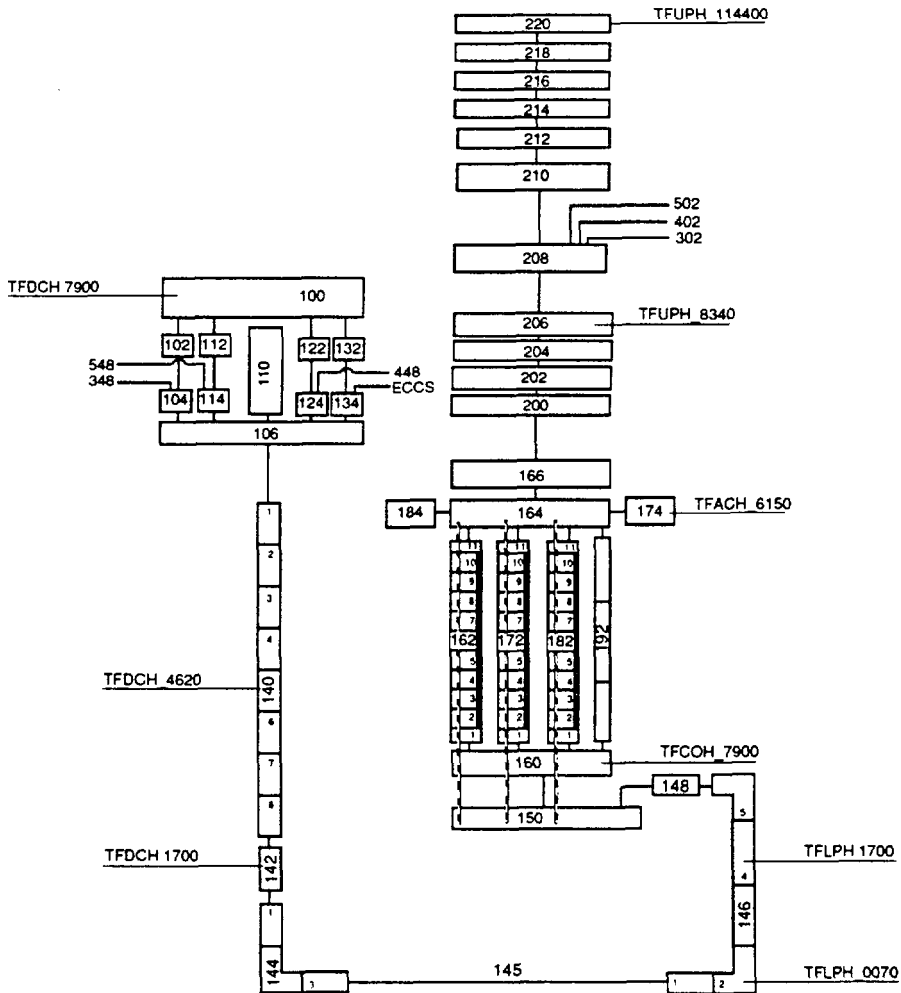


**Fig. 2.1 : PACTEL  
 Nodalization of Reactor Pressure Vessel  
 with measurement device location**

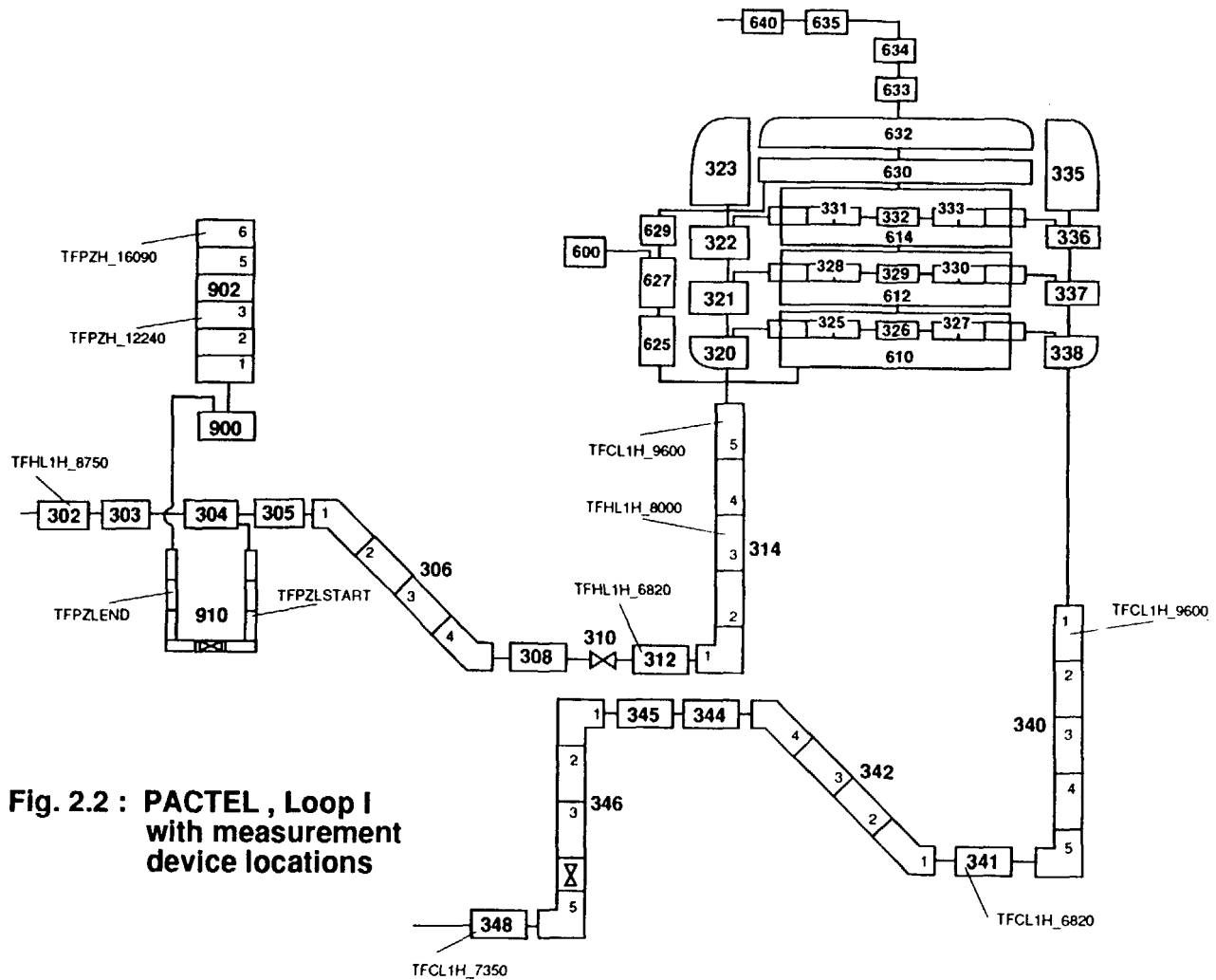
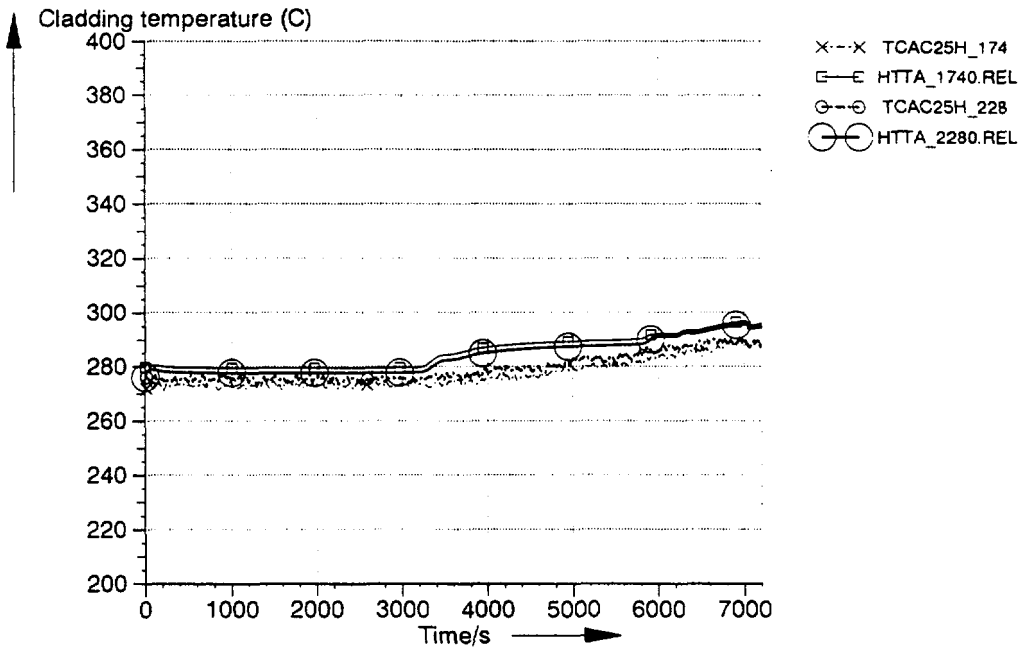
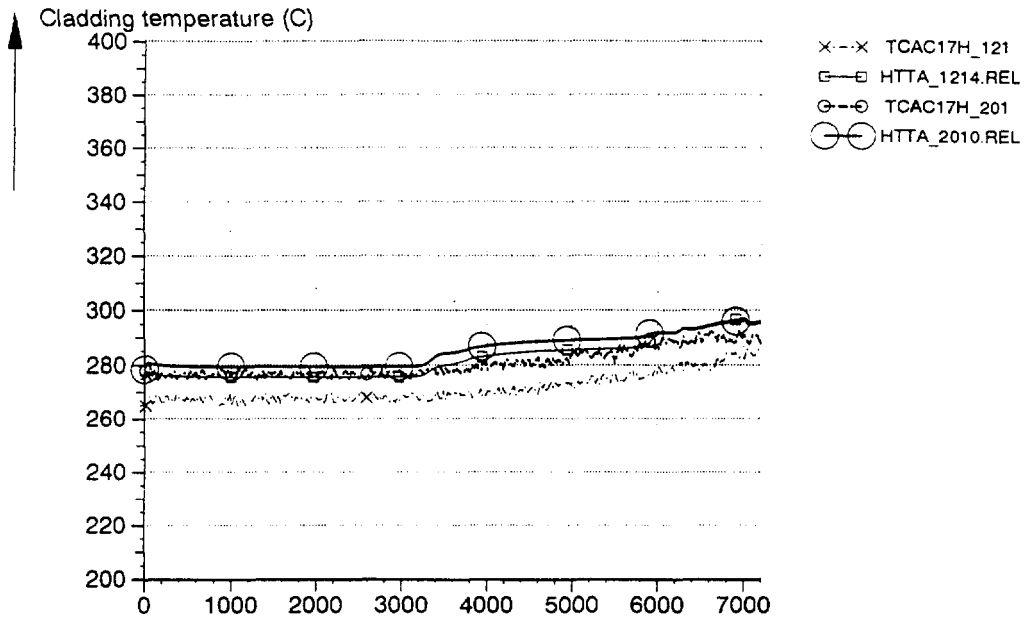


Fig. 2.2 : PACTEL , Loop I with measurement device locations

DOKU-Kennung : 941011.0842.21794

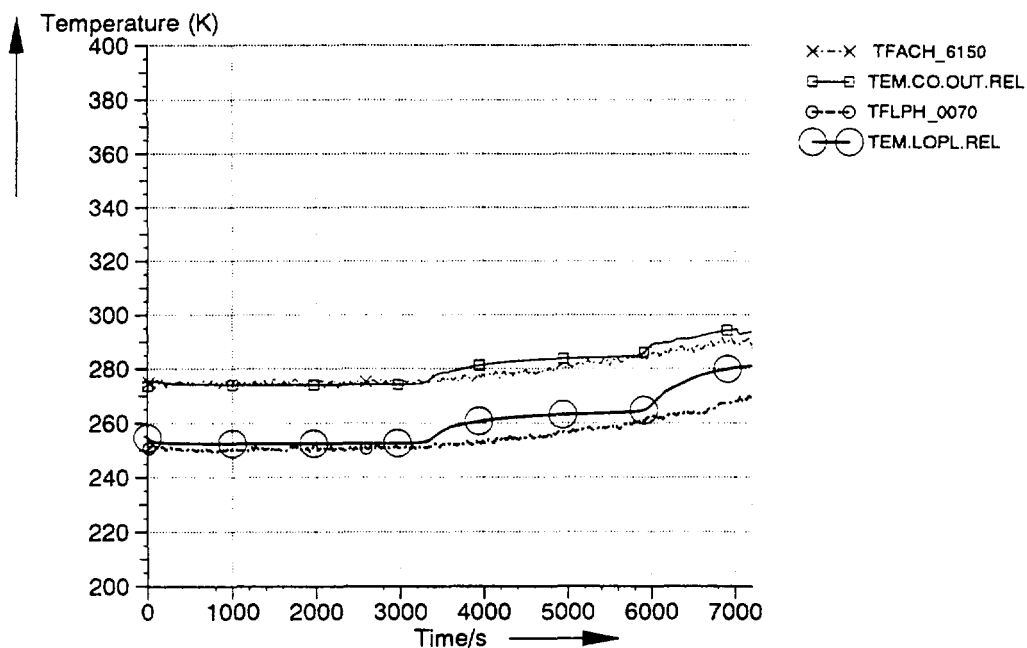
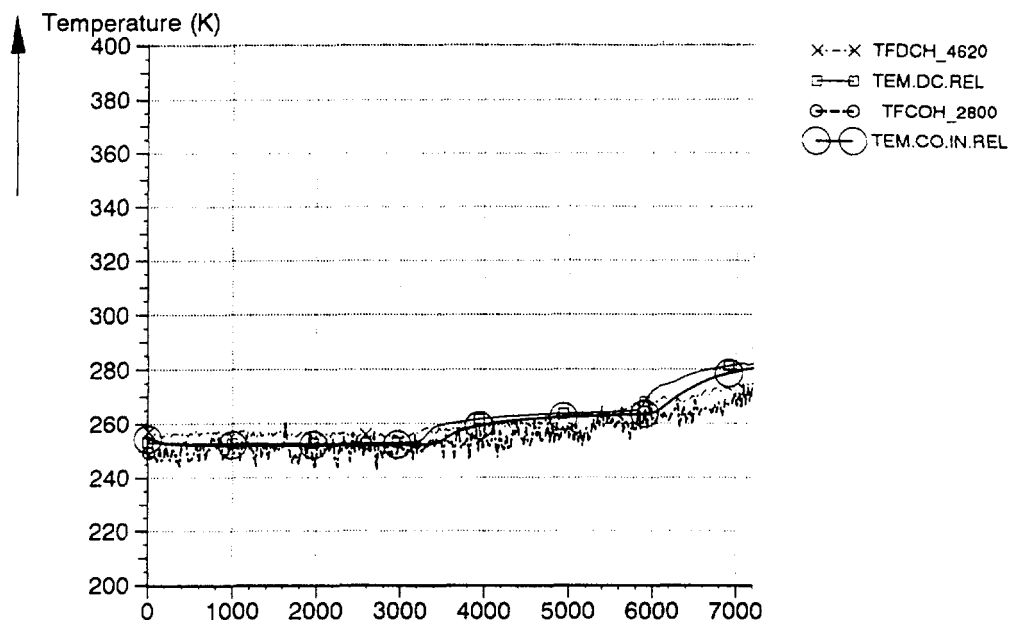


ITF PACTEL; Loss of Feedwater supply LOF01

Fig. 3: Cladding temperature in channel A; upper part

Fig. 4: Cladding temperature in channel A; upper part

DOKU-Kennung : 941011.0842.21794

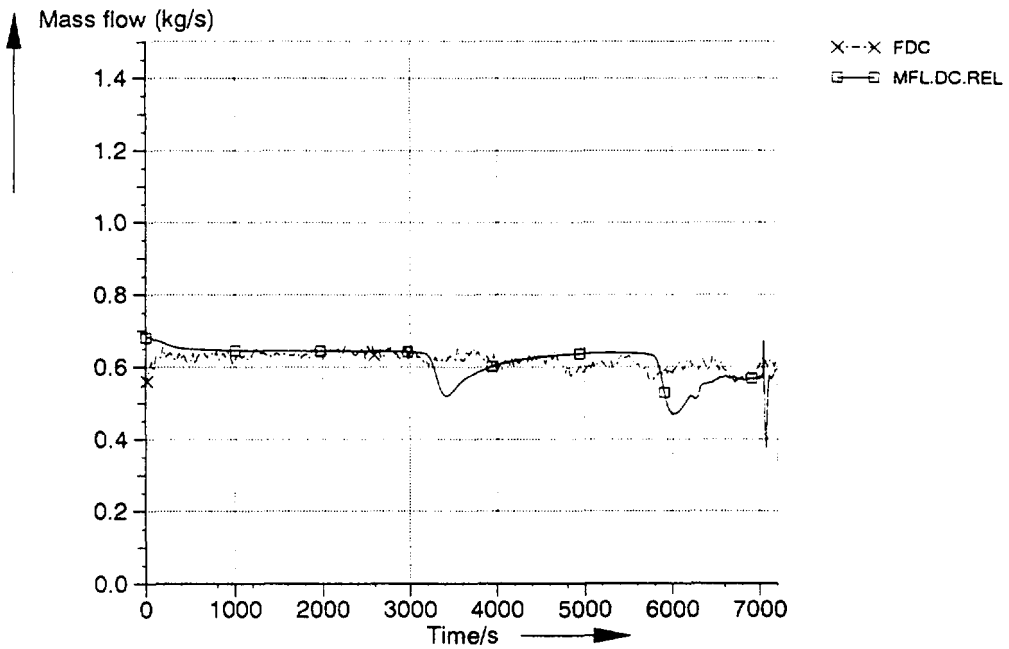
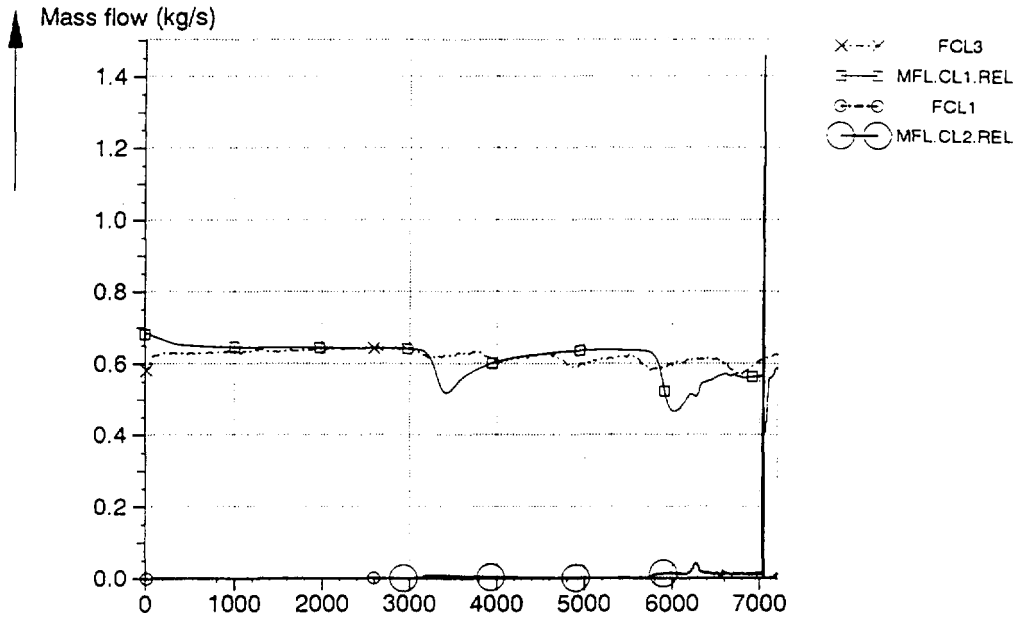


ITF PACTEL; Loss of Feedwater supply LOF01

Fig. 5: DC, core inlet fluid temperature

Fig. 6: Core outlet, lower plenum fluid temperature

DOKU-Kennung : 941011.0842.21794



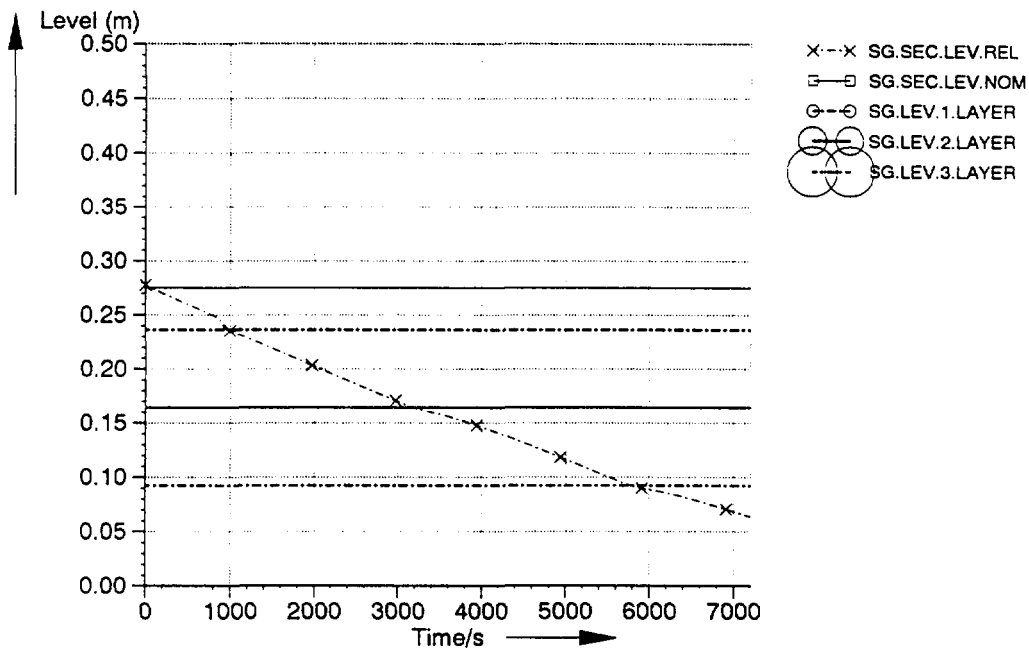
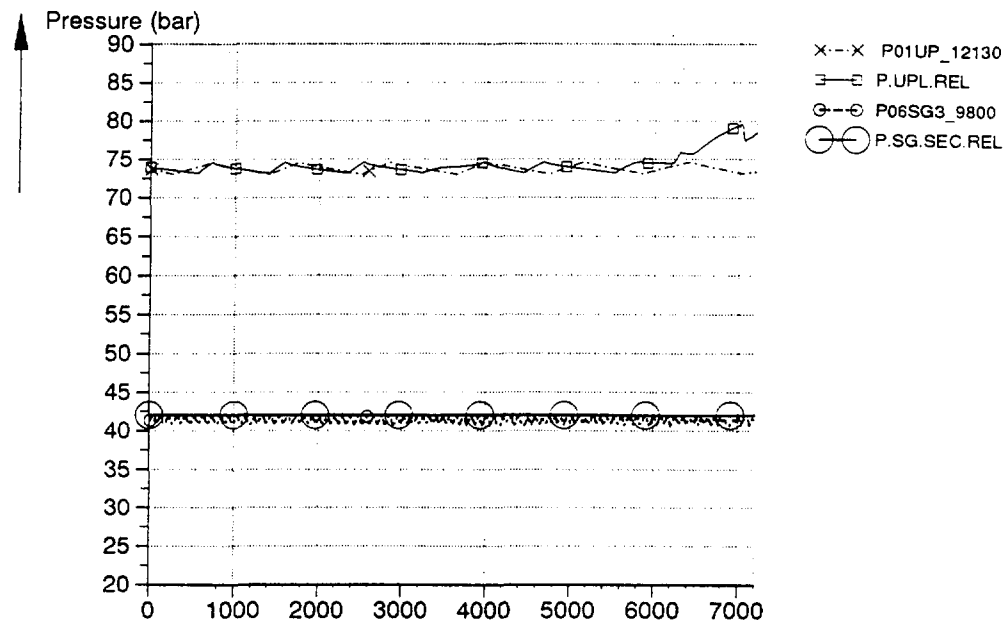
ITF PACTEL; Loss of Feedwater supply LQF01

Fig. 7: Mass flow in cold leg 1, 2

Fig. 8: Mass flow in downcomer

Relap5/2.5 Siemens NDS1 Protze

DOKU-Kennung : 941011.0842.21794



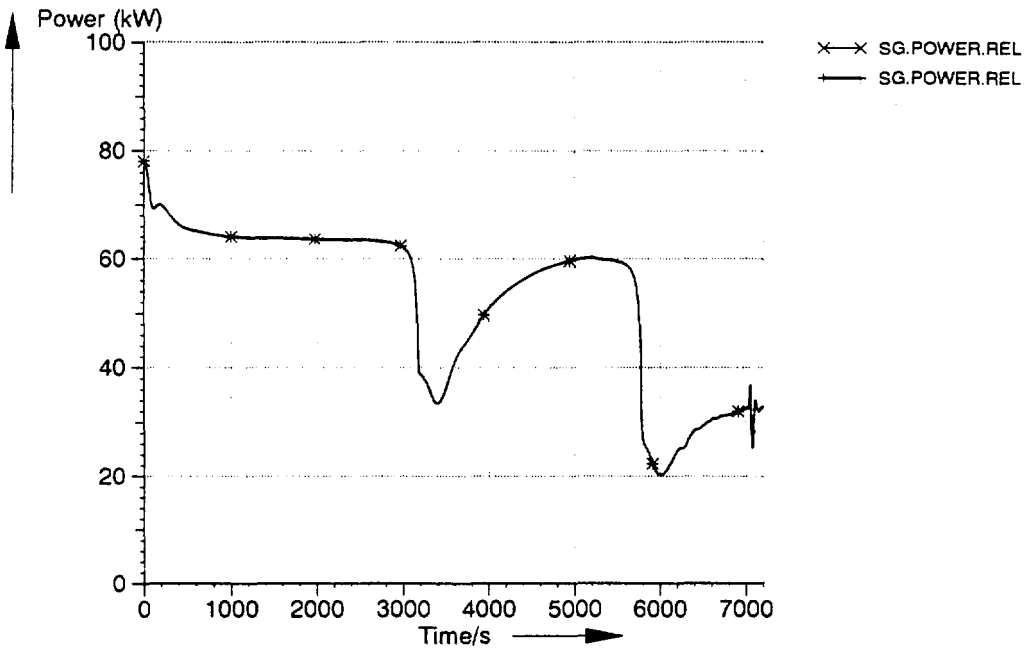
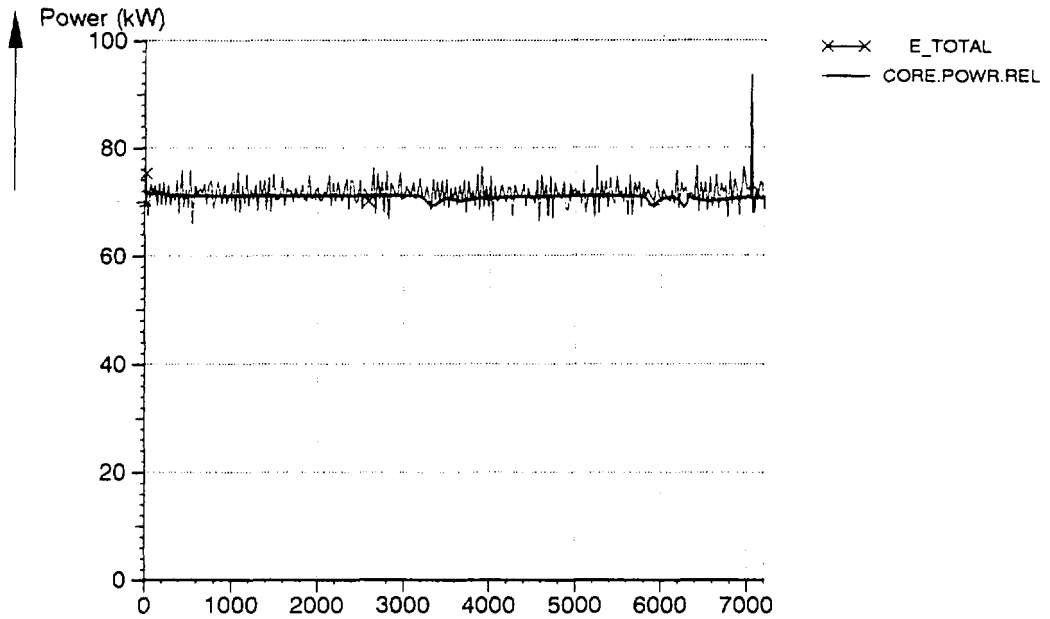
ITF PACTEL; Loss of Feedwater supply LOF01

Fig. 9: Pressure in upper plenum and SG sec. side

Fig. 10: Water level in Steam Generator secondary side

Relap5/2.5 Siemens NDS1 Protze

DOKU-Kennung : 941011.0842.21794



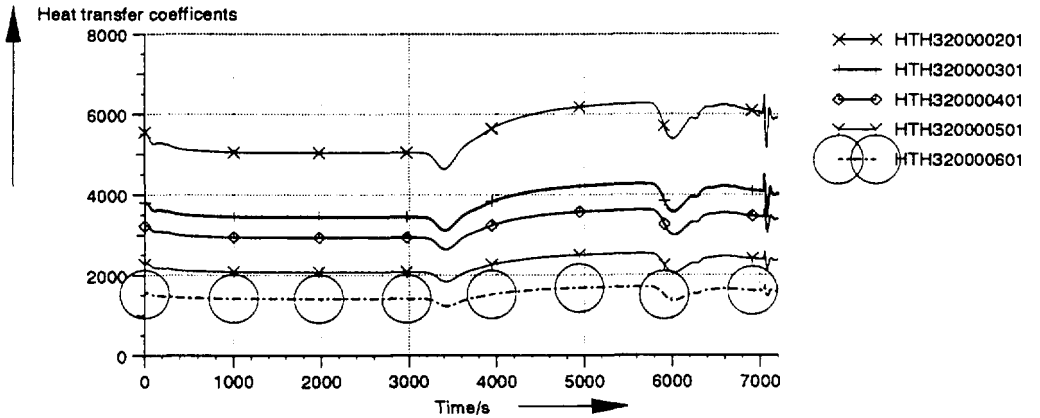
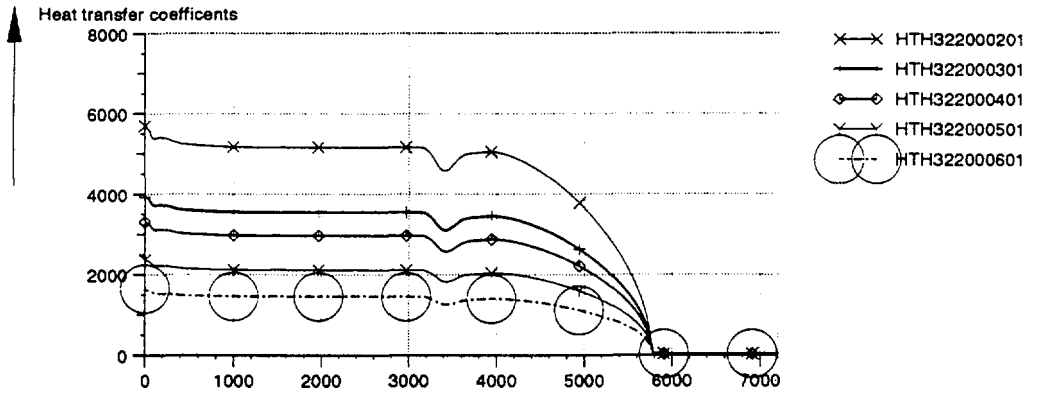
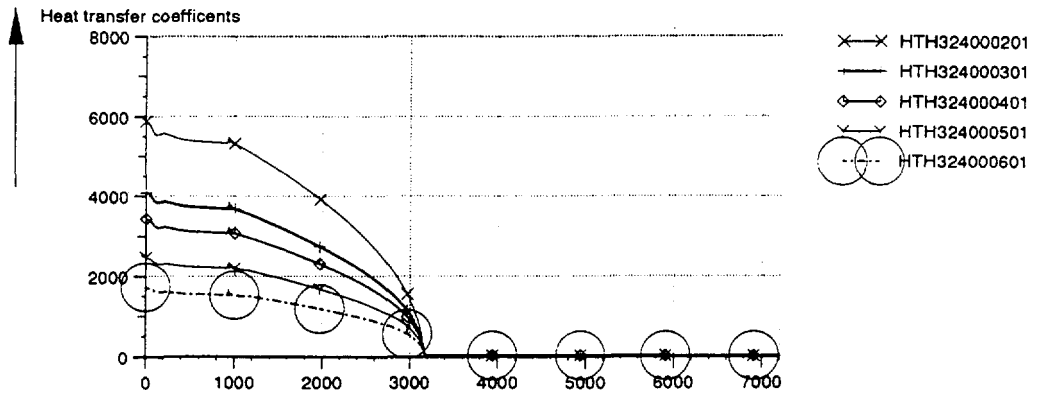
ITF PACTEL; Loss of Feedwater supply LOF01

Fig. 11: Total core power

Fig. 12: Heat transfer in the steam generator, sec. side

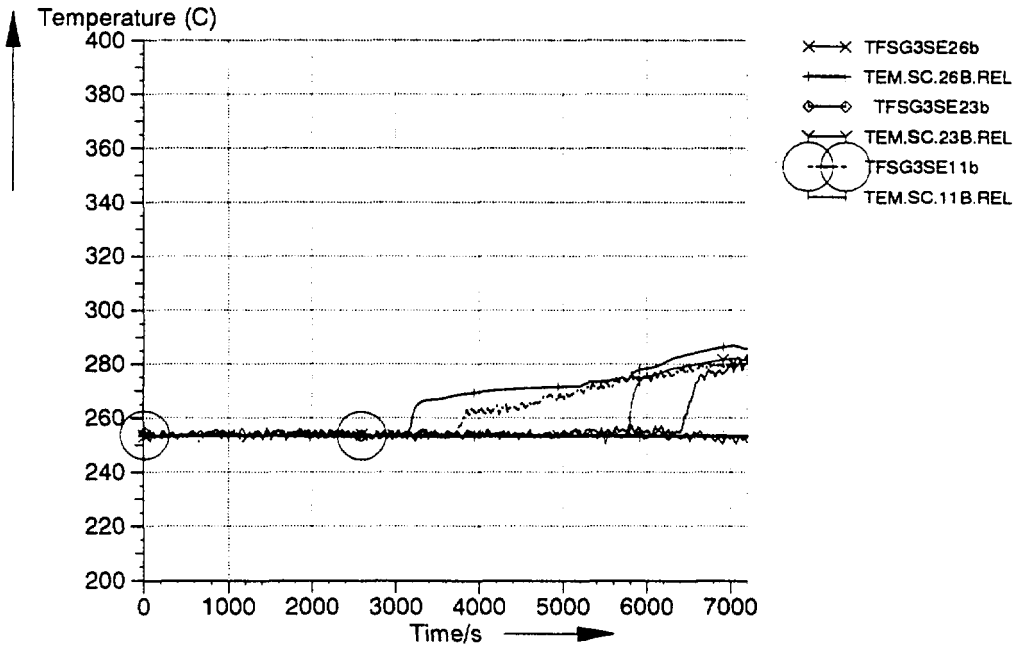
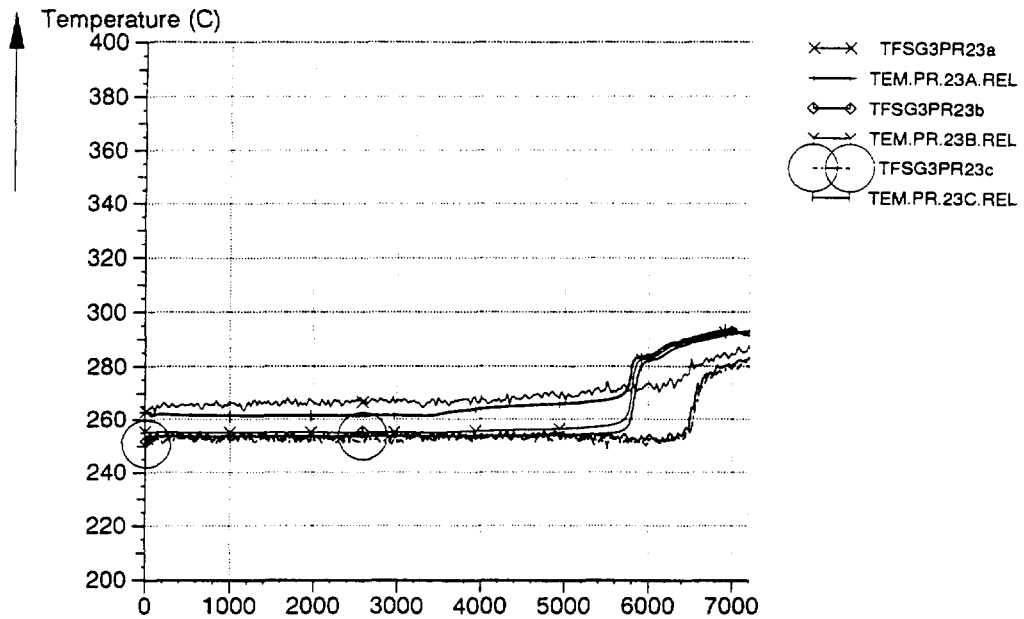
Relap5/2.5 Siemens NDS1 Protze

DOKU-Kennung : 941011.0842.21794



ITF PACTEL; Loss of Feedwater supply LOF01  
Fig. 13: Heat transfer coefficients in SG sec. side  
in the first, second and third layer

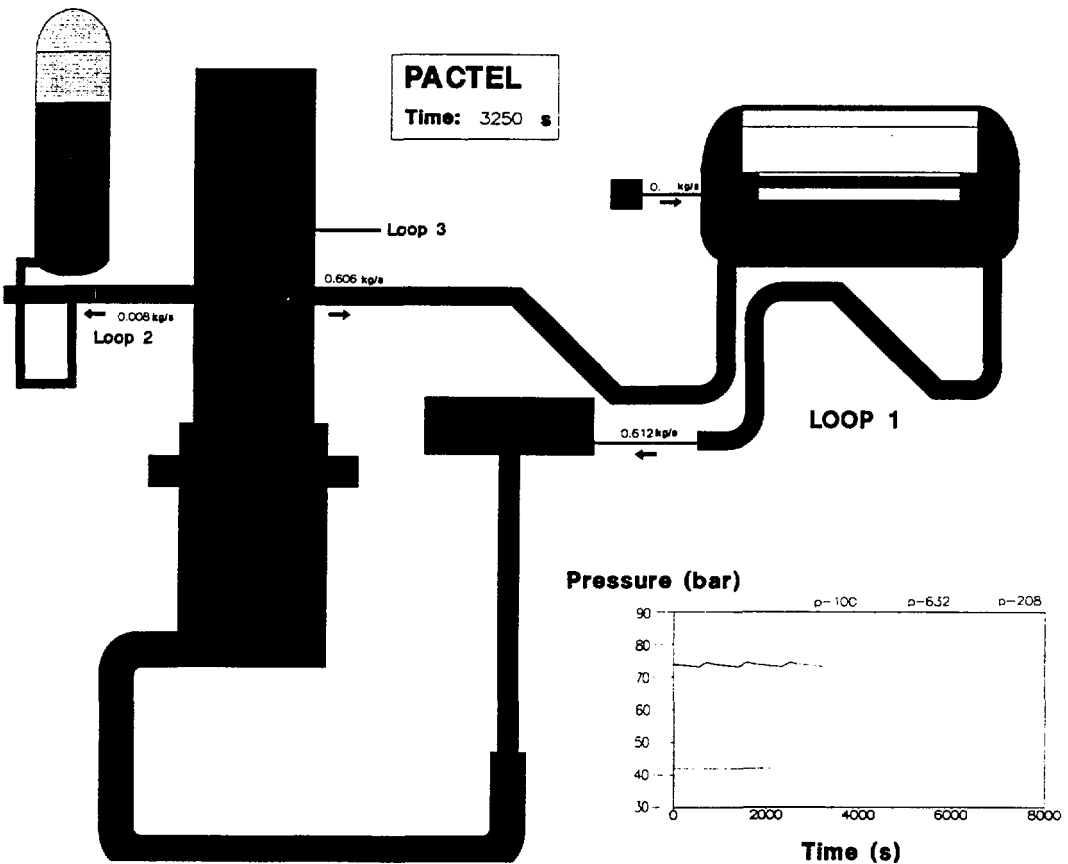
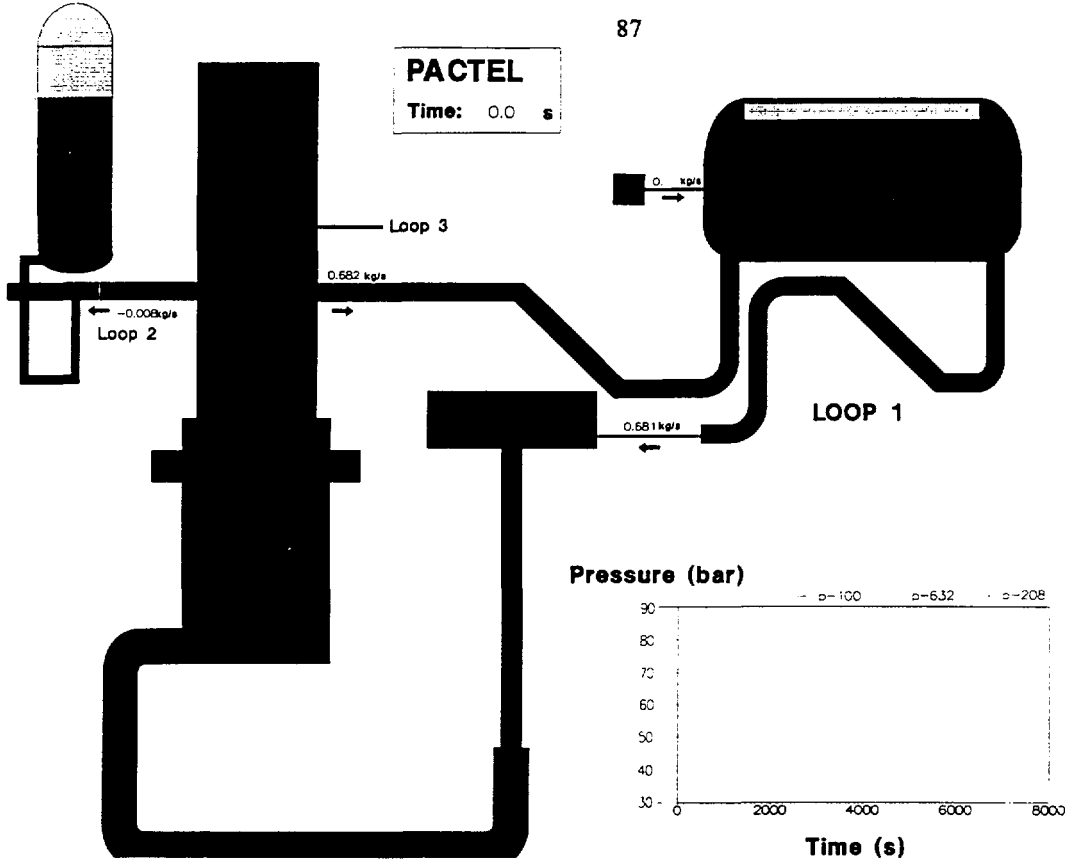
DOKU-Kennung : 941011.0842.21794

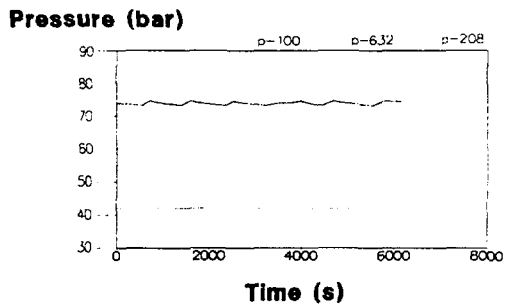
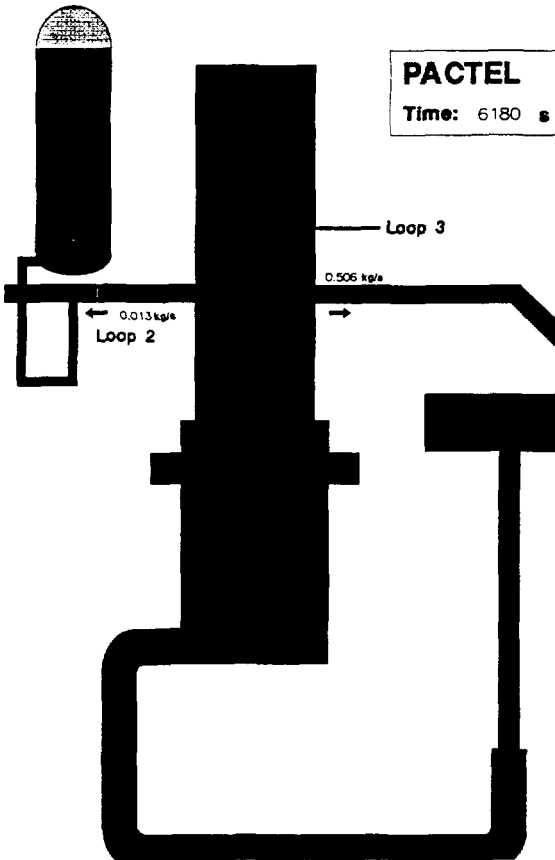
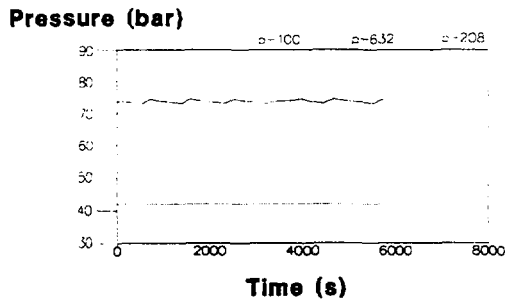
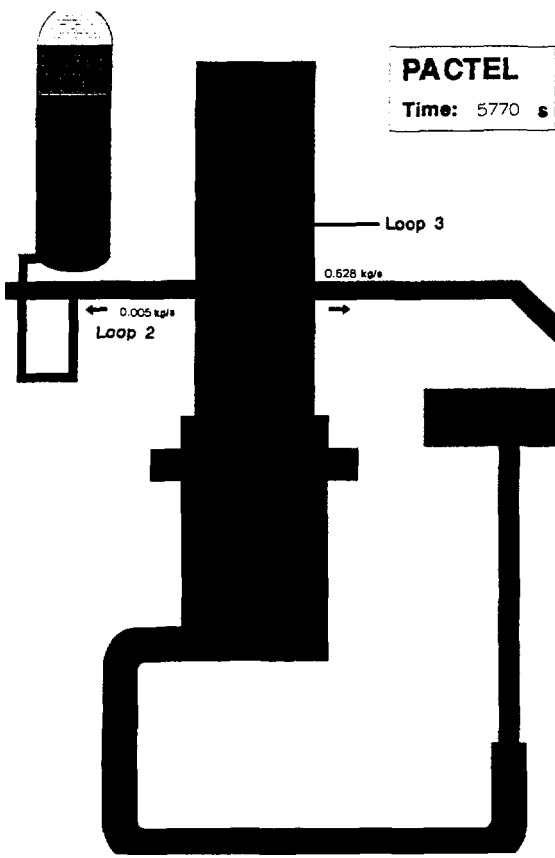


ITF PACTEL; Loss of Feedwater supply LOF01

Fig. 14: SG, prim. side tube 23 fluid temperature A,B,C

Fig. 15: SG, sec. side tube 26, 23, 11 fluid temperature B





## ANALYSIS OF THE PACTEL LOSS-OF-FEEDWATER EXPERIMENTS

V. Korteniemi, E. Virtanen, T. Haapalehto  
Lappeenranta University of Technology  
P.O.Box 20, FIN-53851 Lappeenranta, Finland

J. Kouhia  
VTT Energy, Nuclear Energy  
P.O.Box 20, FIN-53851 Lappeenranta, Finland

## 1. INTRODUCTION

During the last few years western safety organizations have started to perform safety analysis for the Russian design nuclear power plants. These analysis are based on the calculations in which large thermal-hydraulic system codes are used. Normally these codes are validated only for western type pressurized water reactors (PWR) where the lay-out and the geometry of certain components differ drastically from the Russian type pressurized water reactors (VVER). In particular, the steam generators are different; horizontal in VVERs and vertical in PWRs. The horizontal steam generators have two vertical collectors and horizontal U-shaped heat exchange tubes. The behaviour of the horizontal steam generator is very different compared to the vertical steam generator. For example, the loss of feed water transients are slower because the secondary side of a horizontal steam generator contains much more water. During a total station black-out accident a vertical steam generator dries in some tens of minutes but a horizontal steam generator in some hours.

During a normal operation all the heat exchange tubes of a horizontal steam generator are covered with water but in the case of loss of feed water accident the

secondary side water level starts to decrease. When the level falls below highest tube rows the heat transfer from primary to secondary side starts to deteriorate and the primary coolant temperature begins to rise. If the heat transfer decreases more rapidly than the decay heat produced in the core, the primary circuit pressure rises up to the opening pressure of the pressurizer relief valve. The primary coolant leaks out of the system and as a result the reactor core may be damaged.

The western thermal-hydraulic system codes, like RELAP5 and CATHARE2, are developed and validated to model the phenomena in the vertical steam generators. The differences between vertical and horizontal steam generators are so significant that the calculational models developed for the vertical steam generators are not directly applicable for the horizontal steam generators. The PACTEL loss of feed water experiments have been performed to study the overall behaviour of the horizontal steam generators and especially to produce experimental data for code assessment. In this paper the results from APROS, CATHARE2 and RELAP5 calculations of a series of experiments are presented.

## 2. FACILITY DESCRIPTION

PACTEL (Parallel Channel Test Loop) /1/ is a volumetrically scaled (1:305) out of pile model of the Russian design VVER-440 reactors used in Finland. The facility is an integral test facility designed and developed in cooperation of Lappeenranta University of Technology and VTT Energy. PACTEL includes all the main components of the primary circuit of the reference reactor. The reactor vessel is simulated by an U-tube construction consisting of separate core and downcomer sections. The core is comprised of 144 electrically heated fuel rod simulators. The geometry and the pitch of the rods are the same as in the reference reactor. The rods are divided into three roughly triangular shaped parallel channels, which represent the intersection of the corners of three hexagonal VVER rod bundles. The maximum core power is 1 MW, representing 22 % of the scaled nominal power. The maximum primary pressure is 8.0 MPa compared to 12.3 MPa of the reference reactor.

The component heights and the relative elevations correspond to those of the full scale reactor to match the natural

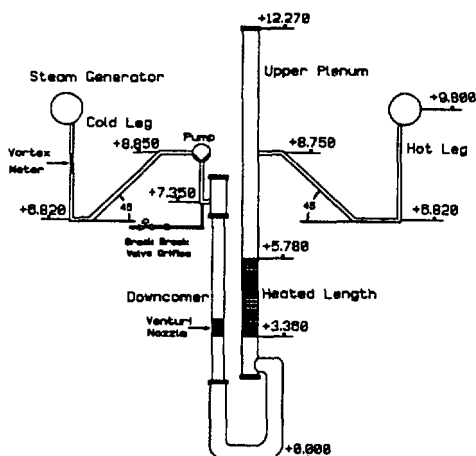


Fig. 1. Geometry of the PACTEL facility.

circulation pressure heads in the reference system. Unlike in PWRs VVER-440 has a loop seal in the hot leg. This is a consequence of the steam generator location, which is almost at the same height as the hot leg connection to the upper plenum. The primary collector of the steam generator is connected to the hot leg at the bottom of the steam generator, hence a roughly U-shaped pipe is needed to complete the connection. The cold leg loop seal is formed by the elevation difference of the inlet and outlet of the reactor coolant pump. The elevations of the PACTEL facility and the geometry of the loop seals are shown in Fig. 1.

### 2.1. Steam generator description

The number of the loops has been reduced from six in the reference system to three in PACTEL, thus one PACTEL steam generator corresponds to two in the power plant. The Full Length Steam Generator (FLSG) of PACTEL has full length heat exchange tubes and the same tube bundle geometry as in the power plant steam generator /2/. The tube bundle height is less than 15 % of the height of the reference steam generator. This fact limits the use of the FLSG, when for example the effects of the decrease of the secondary side level are studied.

The Large Diameter Steam Generator (LDSG), which has been installed in one loop, has vertical primary collectors and horizontal heat exchange tubes (Fig. 2). The 118 U-shaped heat exchange tubes are arranged in 14 layers and 9 vertical columns. The average length of the tubes (2.8 m) is about third of that in the full scale steam generator (9.0 m). The outer diameter of the tubes is 16 mm, which corresponds to the reference system and the inner diameter is 13 mm (in the power plant 13.2 mm). In order to have a higher tube bundle, the pitch in the vertical

direction has been doubled (48 mm) compared to the reference steam generator. The pitch in the horizontal direction has been maintained.

The outer diameter of the shell is 1.0 m (in the power plant 3.34 m). Because of the higher vertical pitch, the secondary side is larger than the scaled down secondary volume. This distorts the time scale of secondary side transients. Two compartments has been constructed on each side of the LDSG to decrease the mass of water, what is directly involved in the primary to secondary heat transfer process. The compartments are not totally isolated from the rest of the secondary side, but the coolant has number of flow paths in and out of the compartments.

The instrumentation of the LDSG contains mainly temperature measurements. The primary and secondary side temperatures are measured in eight tubes in three or four different locations in each tube. The inlet and outlet temperature of the primary coolant, the primary mass flow rate, the mass flow rate of the feed water and the differential pressure on the secondary side are measured as well. The measured collapsed level is based on the differential pressure measurement.

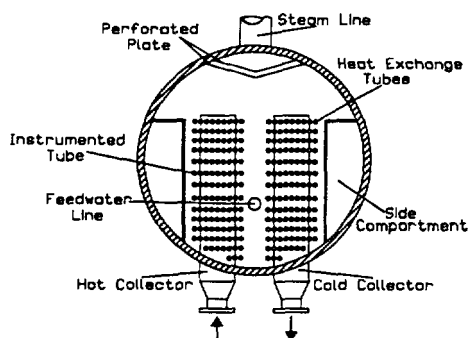


Fig. 2. Vertical cross section of Large Diameter Steam Generator (LDSG) of PACTEL.

### 3. EXPERIMENTS

Three experiments, SG-2, SG-3 and SG-4, were conducted in which the behaviour of the LDSG construction of PACTEL facility was studied. The experiments were like the loss of feed water experiments but instead of reducing the secondary level continuously it was reduced in steps.

In these experiments only one loop with the LDSG was in operation. The primary coolant pump was operating during the whole experiment. Primary and secondary side pressures were different from one experiment to the other (Table 1).

Table 1. Primary and secondary pressures in the experiments.

EXPERIMENT	PRIMARY PRESSURE	SECONDARY PRESSURE
SG-2	3.0 MPa	0.7 MPa
SG-3	1.2 MPa	0.3 MPa
SG-4	7.5 MPa	4.2 MPa

In the beginning of each experiment the core power was set as high as possible and it was kept constant until a steady state was reached. The collapsed level of the secondary side was then reduced stepwise. Feed water injection was stopped and when the secondary level had dropped 50 mm the injection was started again. In Fig. 3 is shown the measured feed water mass flow rate in experiment SG-3. The system was allowed to settle down for 30 minutes between each step. When the secondary side coolant level had dropped below the highest heat exchange tube row the heat transfer from primary to secondary side began to decrease. The temperature in the outlet of the cold collector and also in the inlet of the hot collector began to rise. In order to keep the coolant temperature in the inlet of the hot collector constant the core

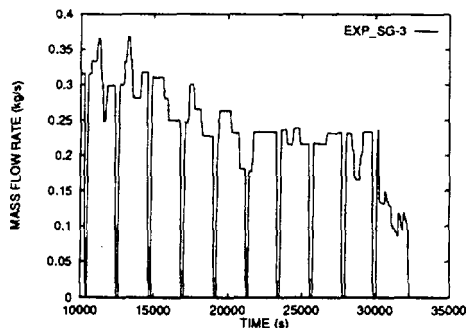


Fig. 3. Measured feed water mass flow rate in experiment SG-3.

power was reduced. Also the feed water mass flow rate was changed to correspond the evaporation rate and to keep the collapsed level constant during the settling down period.

#### 4. CALCULATIONS

##### 4.1. Computer codes used in the calculations

Three computer codes, APROS version 2.11, CATHARE2 V1.3U and RELAP5/MOD3.1, were used in the calculation of the experiments.

APROS (Advanced Process Simulator) code is developed in Finland by VTT and Imatran Voima Oy (IVO) /3/. APROS simulation environment contains database, graphics and physical models for the simulation of nuclear and conventional power plants and chemical processes. The database includes several predefined process components, like tanks, steam generators, pumps and valves, that makes it easier to create a new simulation model. Thermal-hydraulics of APROS include single phase, three- five- and six-equation flow models.

The French thermal-hydraulic code CATHARE is being developed by Electricité de France (EDF), Framatome and the French Atomic Energy Commission

(CEA) /4/. The CATHARE2 code is based on a two-fluid, six-equation model for best-estimate simulation of PWR's loss of coolant accidents and operational transients.

RELAP5 is thermal-hydraulic system code developed at the Idaho National Engineering Laboratory (INEL) for best-estimate transient simulation of light water reactor coolant systems /5/. RELAP5/MOD3.1 is the latest version based on a nonhomogeneous and nonequilibrium (six-equation) model for the two-phase system.

##### 4.2. Nodalization

In the calculations only the steam generator part of the facility was modelled, the rest of the facility was given as a boundary condition. The same nodalization scheme was used for all the computer codes although some code dependent alterations had to be made. The APROS model was constructed using five-equation calculation level modules e.g. nodes and branches. The nodalization scheme for APROS and RELAP5 is shown in Fig. 4. The CATHARE2 nodalization scheme is presented in Fig. 5. The difference between these two models is in the modelling of the secondary side.

In the primary side model for APROS and RELAP5 codes the vertical collectors were modelled with eight nodes each and for CATHARE2 with two volume elements. Heat exchange tubes were lumped into seven pipe components. The lowest pipe component represented three lowest tube rows, the next five components two tube rows each and the highest component modelled the highest tube row. All the pipe components were divided horizontally into five nodes in the APROS and RELAP5 models and into ten nodes in the CATHARE2 model. Hot and cold legs were modelled as boundary conditions, where pressure and temperature are controllable.

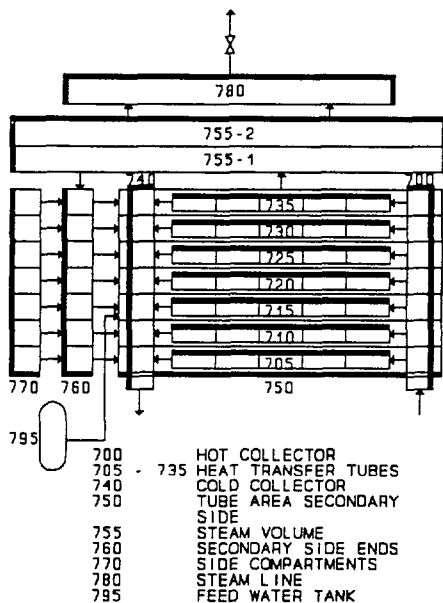


Fig. 4. Nodalization of the steam generator for APROS and RELAP5.

On the secondary side in the APROS and RELAP5 models the heat exchange tube area was modelled with seven nodes and the vapor volume above the heat exchange tubes with two nodes. The steam generator ends as well as the side compartments were modelled with separate components which were connected to each other and to the tube bundle area with cross-flow junctions. This construction allowed vertical internal recirculation typically associated with horizontal steam generators.

In the CATHARE2 nodalization the secondary side was modelled with U-shaped pipe element which was connected from both ends to the volume element modelling the steam dome of the steam generator. Cross-flow between the downcomer part and the riser part was not included. The

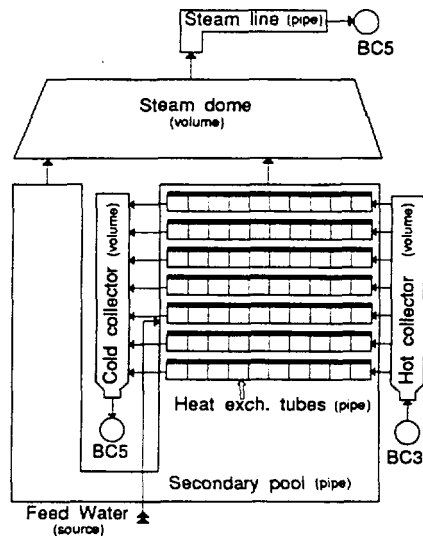


Fig. 5. Nodalization of the steam generator for CATHARE2.

internal recirculation could take place until the swell level dropped below the junction connecting the riser and the steam dome.

In all models feed water was injected into the third lowest node in the heat exchange tube area. The steam line from steam volume was modelled as pipe component. Primary side pressure, coolant mass flow rate, hot leg temperature, secondary side pressure and feed water mass flow rate were given as a boundary condition. The values were obtained from the measurement data of each experiment.

All metal structures except the thin plates between heat exchange tube area and side compartments were modelled. The material properties were obtained from the manufacturers. Heat losses to the environment were taken into account in the simulation. A constant heat transfer coefficient together with a constant environment temperature was used as a boundary condition.

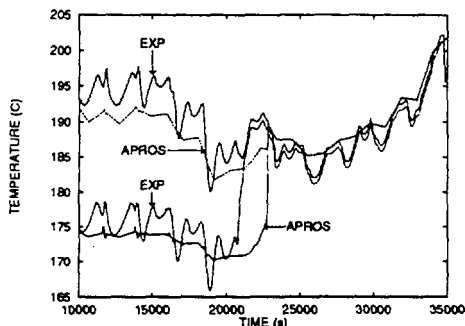


Fig. 6. Primary temperatures in one tube from experiment SG-2 and from APROS calculation.

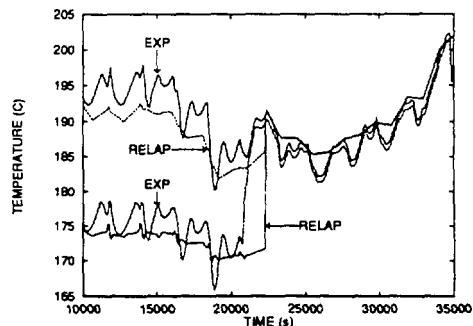


Fig. 8. Primary temperatures in one tube from experiment SG-2 and from RELAP5 calculation.

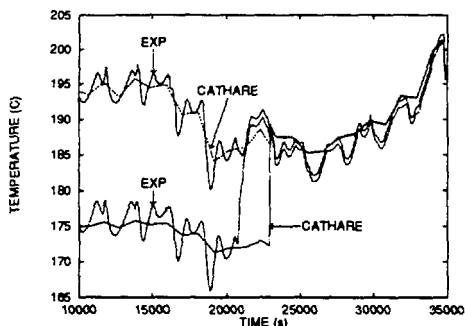


Fig. 7. Primary temperatures in one tube from experiment SG-2 and from CATHARE2 calculation.

#### 4.3. Results of the simulations

The heat transferred from the primary side to the secondary side is a function of the temperature difference between hot and cold collector. Because most of the heat transfer occurs through the heat exchange tubes, the ability of a code to calculate the overall heat transfer can be evaluated by observing the inlet and outlet temperatures of the heat exchange tubes.

In Figs. 6, 7 and 8 are shown the measured primary temperatures from one instrumented heat exchange tube together with the corresponding temperatures

calculated with APROS, CATHARE2 and RELAP5 respectively. The measurement locations were 200 mm from the hot collector and 500 mm from the cold collector and the calculation nodes of APROS and RELAP5 were 279 mm from both collectors. This caused a small difference between the measured and calculated values. Because the heat exchange tubes were divided into ten nodes in the CATHARE2 model, the temperatures shown in Fig. 7 were closer to the measured values. The oscillations in the measured temperatures were not well reproduced because the boundary condition values for the hot leg temperature were based on the averaged measurement data. The uncovering of the tube could clearly be seen around 20500 seconds in the experiment and around 22500 seconds in the RELAP5 calculation. APROS and CATHARE2 calculated the uncovering of the tube to occur a little later. The time difference between experiment and calculation results was caused by the nodalization. In this place two heat exchange tube rows were lumped together and the temperature measurements were located in the upper tube row.

In the experiment steam superheating was observed after the highest heat exchange tubes were uncovered. In Figs. 9,

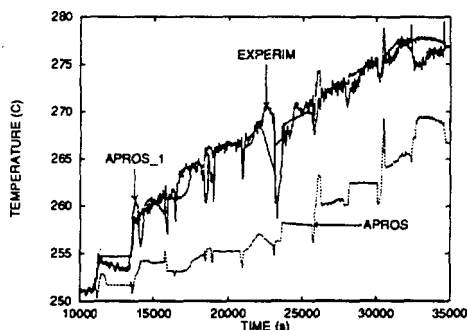


Fig. 9. Secondary temperatures in the highest tube layer from experiment SG-4 and from APROS calculations.

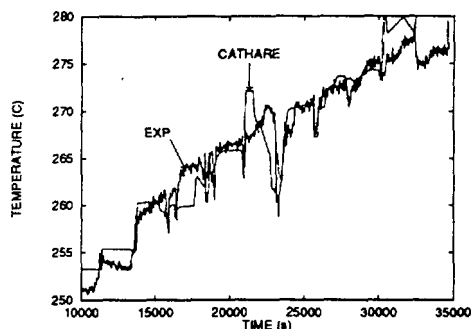


Fig. 10. Secondary temperatures in the highest tube layer from experiment SG-4 and from CATHARE2 calculations.

10 and 11 are shown the measured secondary side temperatures in the highest tube layer together with the temperatures from the APROS, CATHARE2 and RELAP5 calculations respectively. Both APROS and RELAP5 codes underestimated the steam superheating whereas CATHARE2 estimated the steam temperature to be higher. In the APROS calculations it was observed that hydraulic diameter of the secondary nodes had a significant influence on the steam temperature. If the hydraulic diameter is not given for the code when defining a simulation model the code calculates it based on the given flow area of the node. The code calculates the hydraulic diameter  $D_h$  from equation (1) using the flow area  $A_f$  of the node. APROS\_1 in Fig. 9 is the

$$D_h = \sqrt{\frac{4 \cdot A_f}{\pi}} \quad (1)$$

result from the calculation where the code was allowed to calculate the hydraulic diameter itself. As can be seen the calculated steam temperature is nearer the measured values. In the other calculation presented here (APROS in Fig. 9) the hydraulic diameter  $D_h$  was given to the code and it was the same which was used

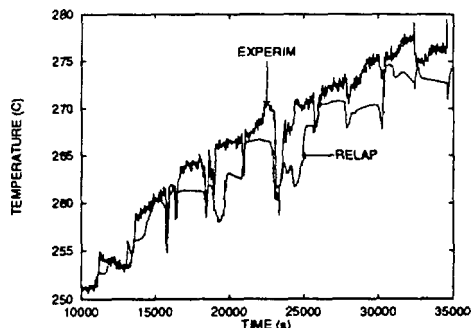


Fig. 11. Secondary temperatures in the highest tube layer from experiment SG-4 and from RELAP5 calculation.

in the RELAP5 calculations. The hydraulic diameter was calculated using equation (2)

$$D_h = \frac{4 \cdot A_f}{P_w} \quad (2)$$

where  $A_f$  is the flow area of the node and  $P_w$  is the wetted perimeter. Here the wetted perimeter was twice the length of the heat exchange tubes which were located in the node. When calculated from equation (1) the hydraulic diameter for a tube bundle area secondary side node was 1.002 m and calculated from equation (2) 50 mm. Even

the difference between measured and calculated steam temperatures in some cases was around 15 K the effect on the overall heat transfer was negligible because the heat transfer to single phase steam was small compared to the heat transfer to steam-water mixture.

## 5. CONCLUSIONS

Three PACTEL loss of feed water experiments has been calculated using the APROS version 2.11, CATHARE2 V1.3U and RELAP5/MOD3.1 computer codes. The main parameter to be compared was the temperature difference between hot and cold collectors, e.g. the total power transferred from primary to secondary side. In all the calculations the results obtained were acceptable. The differences are partly caused by the nodalization. Some differences were caused by the rather rapid changes in the experimental boundary conditions which were not completely reproduced. When the results were compared more in detail some differences were observed. Especially it was observed that APROS and RELAP5 underestimated the secondary side steam temperatures while CATHARE2 calculated them to be somewhat higher. Even the difference between measured and calculated steam temperatures is relatively large it has small effect on the overall heat transfer.

The assessment calculations presented here are not sufficient to validate the codes used but they show that the APROS, CATHARE2 and RELAP5 codes are able to model the overall behaviour of the horizontal steam generators. However, some problems seem to exist on their capabilities to model the phenomena on the secondary side. In order to improve the models some new experiments are needed, because in the experiments performed the boundary conditions were too complex. Also some parameters were not measured, like steam

flow rate and heat exchange tube surface temperatures, limiting the usefulness of the experiments for the comparison.

## REFERENCES

- /1/ Raussi, P., Munther, R., Kalli, H., Kouhia, J., Puustinen, M., "Experimental VVER Safety Studies in Finland", Trans. of ENC'94, Int. Nuclear Congress, Lyon, France, October 2-6, 1994.
- /2/ Purhonen, H., Miettinen, J., "PACTEL - Parallel Channel Test Loop, General Description for ISP-33", Proceedings of ISP-33, First Workshop, 18-19 February, Lappeenranta, Finland, 1992.
- /3/ Porkholm, K., Hänninen, M., Puska, E. K., Ylijoki, J., "APROS Code for the Analysis of Nuclear Power Plant Thermal-Hydraulic Transients", Eight Proceedings of Nuclear Thermal-Hydraulics, ANS Winter Meeting, Chicago, Illinois, November 15-20, 1992.
- /4/ Barre, F., Bernard, M., "The CATHARE Code Strategy and Assessment", Nuclear Engineering and Design, Vol. 124 (1990), pp. 257-284.
- /5/ Carlson, K. E., Riemke, R. A., Rouhani, S. Z., Shumway, R. W., Weaver, W. L., "RELAP5/MOD3 CODE MANUAL, Volume 1: Code structure, System Models and Solution Methods", EG&G Idaho, Inc., Idaho Falls, Idaho, USA, June 1990.
- /6/ Virtanen, E., "Computer Code Analysis of Steam Generator in Thermal-Hydraulic Test Facility Simulating Nuclear Power Plant", Master thesis, Lappeenranta University of Technology, Lappeenranta, Finland, 1995 (in Finnish).

**Third International Seminar  
on  
Horizontal Steam Generators**

**18 - 20 October, 1994 in Lappenranta, Finland**

---

**Modelling Horizontal Steam Generator with ATHLET;  
Verification of different nodalization schemes and  
implementation of verified constitutive equations**

Contributing authors:

J.Beliaev	OKB-GIDROPRESS
W.Luther	GRS Garching
S.Spolitak	RNC-KI
N.Trunov	OKB-GIDROPRESS
I.Tschekin	OKB-GIDROPRESS

## **Abstract**

Currently the ATHLET - Code is widely applied for modelling of several Power Plants of VVER type with horizontal steam generators. A main drawback of all these applications is the insufficient verification of the models for the steam generator. This paper presents different nodalisation schemes for the secondary side of the steam generator, the results of stationary calculations, and preliminary comparisons to experimental data. The consideration of circulation in the water inventory of the secondary side is proved to be necessary.

## **Introduction**

The thermo-hydraulic code ATHLET is verified for the typical components in PWR plants and corresponding test facilities. Therefore most of the components in a VVER 440 type power plant can be sufficiently accurate modelled by ATHLET. As a main different component the horizontal steam generator has been found. Particularly the secondary side of the steam generator was treated in the past in a fairly simple manner. Most of applications used one simple vertical pipe for this part of the steam generator. This was essentially justified in the lack of proper experimental values.

This paper presents different nodalization schemes for the secondary side of the steam generator, the results of steady state calculations and preliminary comparisons to experimental data. A help in better modelling of the real physical phenomena on the secondary side of the horizontal steam generator for the actual used programs and datasets is the main concern of this work.

## Specific physical phenomena of VVER 440 type steam generator

The modelling of the secondary side of the horizontal steam generator requires the consideration of some specific physical phenomena:

- strong differences in the spatial distribution of void fraction, steam generation rate and other thermo-hydraulic parameters on the secondary side
- several circulation flows inside and around the tube bundle

The best way to describe the above named phenomena would be the application of a special 3D - model. Such models of the steam generator are actual not available for use in transient safety calculations. Thus a special method of modelling 3-dimensional flow by one-dimensional components was selected. A limited multi-dimensional capability can be achieved by the "multi-channel method". This method is popular largely due to its simplicity compared to original multi-dimensional methods. The 3-dimensional structure of the flow is represented by parallel one-dimensional lumped parameter control volumes with cross connections between corresponding control volumes. The extension of this network depends on how good the approximation should be.

### Nodalization schemes

Due to the demands of the processes to be modelled it seems appropriate to choose different levels of nodalization. Furthermore the comparison of different nodalization schemes provides an answer to the question - how accurate is accurate enough. Therefore models with different nodalizations for the following processes were developed:

- steady state of the steam generator (for the analysis of the distribution of void fraction, the thermal power in the tube bundle, the circulation velocity, the recirculation rate)
- transient processes in the steam generator causing a decrease of water level (Analysis of the change in the heat transfer, estimation of remaining water etc.)
- selected transient processes during different accidents (including a leak from the primary to the secondary side of the steam generator)

The primary side of all these models consists of 4 horizontal pipes modelling the flow of primary coolant water through the tube bundle. The elements of the primary side are shown in Fig.1. For the secondary side 3 different models have been developed. The basic variant consists of a volume below the tube bundle and a volume above the bundle which represents that part of the secondary side containing only steam. The tube bundle itself and a part above the bundle is represented by three vertical pipes divided into 8 volumes. One pipe models in each case the hot and the cold part of the bundle, the third pipe models the lateral volumes and the channels in the middle of the tube bundle. This pipe stands for the volumes of the secondary side without tube bundle (downcomer). All of these pipes are connected with the volumes above and below the tube bundle. The feedwater is injected directly in the hot part of bundle. The hot and the cold pipes are connected with the downcomer pipe by means of cross connections. These cross connections model a horizontal connection between volumes at the same height on the condition that the two vertical pipes have the same nodalization. ATHLET handles the cross connection as one object and provides in this way the user a comfortable possibility to create multi-dimensional hydraulic networks.

The two advanced schemes differ from this basic variant through a more sophisticated representation of the downcomer of the secondary side. In a first step this part is divided in three channels. Two channels for the right and left edge of the vessel (corresponding to the cold and hot collector sides). One channel is used for the middle of the bundle and the two lateral channels near the hot and the cold bundle. The most advanced model divides this channel into 3 channels. Two channels model the slots aside the hot and cold part of tube bundle and the vessel. One channel is applied for the middle of the bundle. The

modelled channels are illustrated in Fig.2. Each area in this figure is modelled by means of a pipe divided into 8 volumes. The cross connections between the heated pipes and the downcomers are illustrated in Fig.3. This figure is simplified by presenting of only 3 cross connections instead of 8. Fig.4 shows the result of the ATHLET Input Graphic for the most advanced variant. The cross connections are not shown in this figure.

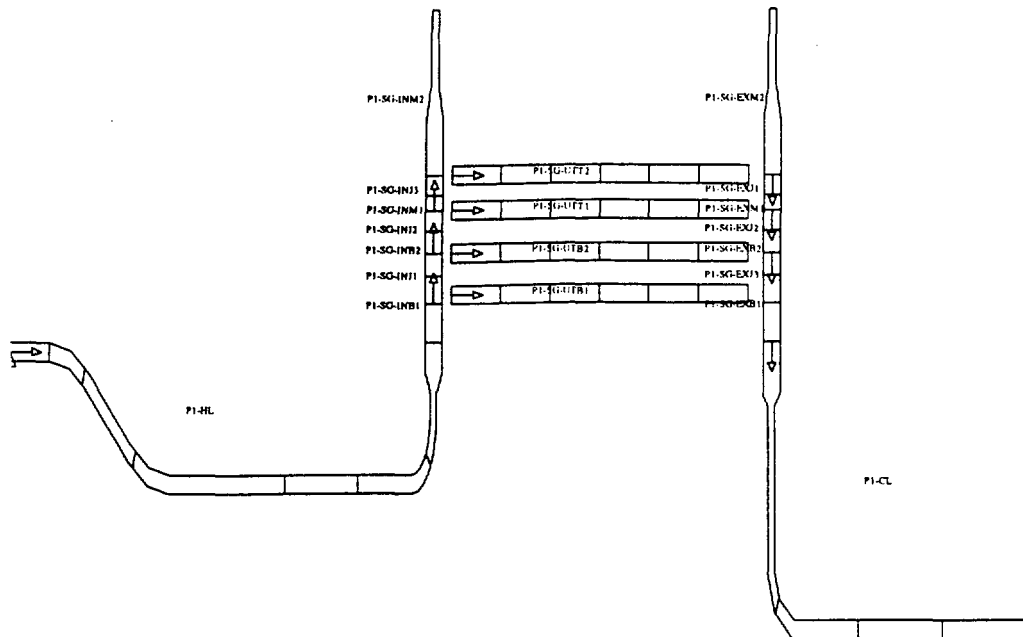


Fig.1 ATHLET Input Graphics for the primary side

### Steamgenerator VVER 440

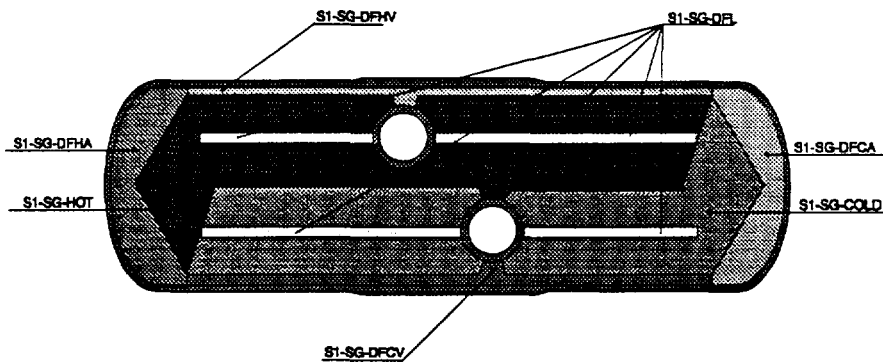


Fig.2: Modelled channels

### Nodalization of the Secondary Side using PIPES and CROSSCONNECTIONS

Simplified scheme - usually 8 crossconnectors have been used

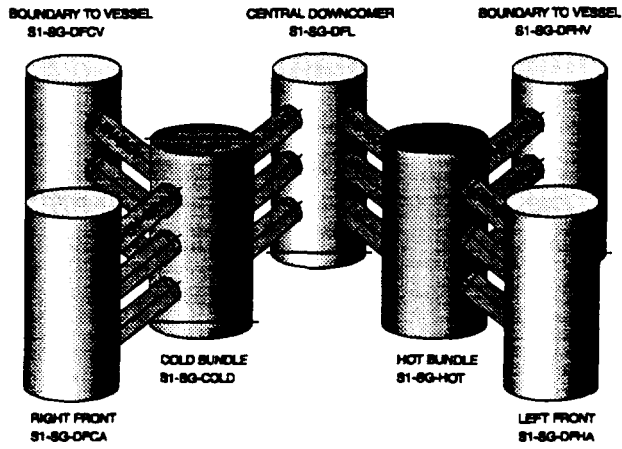


Fig. 3: Advanced model with 5 downcomers

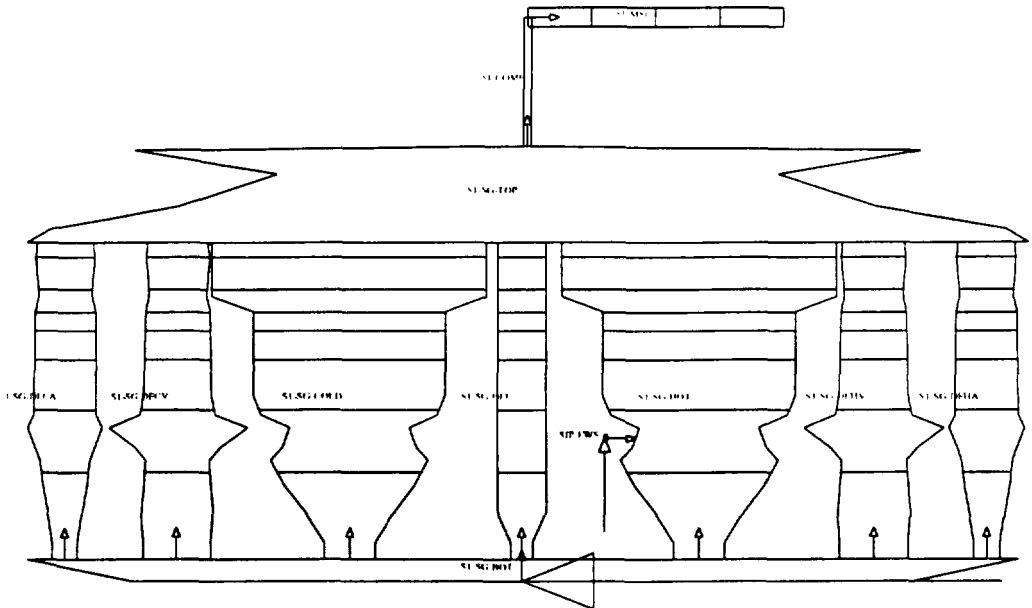


Figure.4: ATHLET Input Graphic of secondary side for advanced model

## Results of steady state calculations

Two different steady state conditions for the steam generator have been calculated using the three different nodalization schemes presented above. The boundary conditions for the two different power levels are shown in Table 1.

Power	104%	90%
<b>Primary side</b>		
Pressure (MPa)	12.23	12.23
Mass flow rate (kg/s)	1.535	1.539
Temperature (°C)	296.4	291.7
<b>Secondary side</b>		
Pressure (MPa)	4.61	4.61
Feedwater mass flow rate (kg/s)	122.2	105.6
Feedwater temperature (°C)	218	215

Tab.1: Boundary conditions for steady state calculations

Table 2 and 3 show some results of the steady state calculations. The circulation mass flows from hot and cold channels to the downcomer channel in the middle of steam generator are illustrated in Fig.5.

	S1-SG-HOT	S1-SG-COLD	S1-SG-DFL
NODE 1	0.36	0.19	0.13
NODE 2	0.41	0.32	0.17
NODE 3	0.48	0.33	0.18
NODE 4	0.47	0.33	0.18
NODE 5	0.55	0.35	0.19
NODE 6	0.30	0.20	0.26
NODE 7	0.84	0.85	0.84
NODE 8	1.00	1.00	1.00

Tab.2: Distribution of void fraction for a power of 104%  
(5 downcomers)

	S1-SG-HOT	S1-SG-COLD	S1-SG-DFL
NODE 1	25.3	9.3	0.23
NODE 2	12.0	9.74	0.06
NODE 3	26.1	9.74	0.02
NODE 4	3.9	1.53	0.00
NODE 5	21.7	8.20	0.02
NODE 6	0.8	0.2	0.01
NODE 7	0.05	0.01	0.0
NODE 8	0.0	0.0	0.0

Tab. 3: Steam generation rate (kg/s) for a power of 104%  
(5 downcomers)

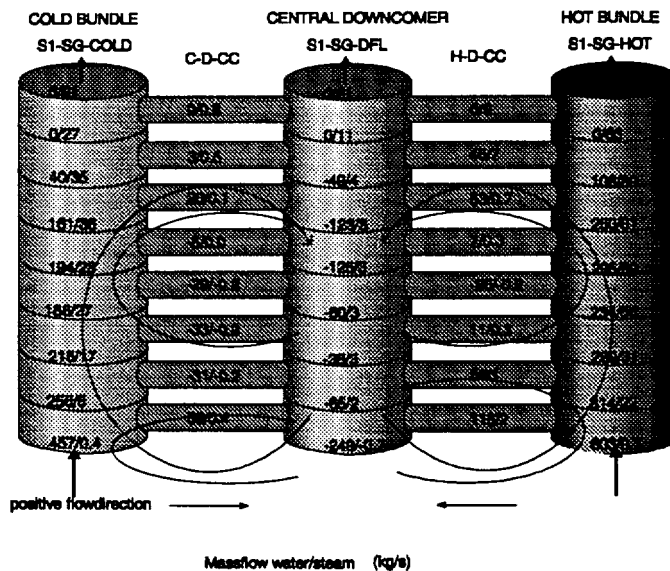


Fig.5: Circulation mass flows for 104% power (5 downcomers)

The calculated heat transfer coefficients have been compared to the calculation results of the programs "DYNAMIKA" and "PGW" (The results of these programs have been verified with statistics methods from 24 different steam generators in 6 power plants). The results of this comparison can be summarized as follows:

- The general heat transfer coefficients (relation between temperature difference primary and secondary side, heat transfer area and transferred power) differ not more than 2%. This is in the range of measurement accuracy. Simple models with one pipe at the secondary side provided strong differences for these values.
- The heat transfer coefficients along the tube bundle on the primary side agree sufficiently.
- The heat transfer coefficients on the secondary side agree well at the beginning of the tube bundle but differ about 50% - 60% at the end of the bundle.

Parameter	VVER 440	1 downcomer	3 downcomers	5 downcomers
<b>Primary side</b>				
Outlet temperature (°C)	266.8	266.2	266.1	266.1
<b>Secondary side</b>				
Mixture level aside of SG vessel at hot collector side (from bottom of SG vessel) (m)	2.105	2.123	1.987	2.026
Collapsed level aside of SG vessel at hot collector side (from bottom of SG vessel) (m)	1.85 <sup>+0.1*</sup>	1.936	1.821	1.865
Void fraction above the top of the hot bundle (+110 - +700mm)	0.32 - 1.0 **	0.31 - 1.0	0.305 - 1.0	0.3 - 1.0
Void fraction above the top of the cold bundle (+120 - +450mm)	0.05 - 1.0 **	0.25 - 1.0	0.192 - 1.0	0.2 - 1.0
Void fraction above the top of the bundle aside of SG vessel at hot collector side (+125 - +450mm)	0.17 - 0.98 **	-	0.121 - 0.99	0.112 - 0.99
Void fraction in downcomers(-700mm under the top of the bundle)	0.13 - 0.38 ***	0.09 ****	0.11 ****	0.09 - 0.18 ***
Steam massflow rate, kg/s	125	129.4	129.5	129.5
Water mass, 10 <sup>+3</sup> *kg	30 - 35	30	30	30

- \* - estimated error of level meter
- \*\* - corresponding to coordinates
- \*\*\* - left value accordingly the channel between vessel and cold tube bundle  
right value accordingly the channel between hot and cold bundle
- \*\*\*\* - averaged value

Tab. 4: Comparison between some measurements and calculations for three developed schemes (104% power)

Parameter	VVER 440	1 downcomer	3 downcomers	5 downcomers
<b>Primary side</b>				
Outlet temperature (°C)	265.9	265.2	265.2	265.2
<b>Secondary side</b>				
Mixture level aside of SG vessel at hot collector side (from bottom of SG vessel) (m)	2.100	2.123	2.011	2.058
Collapsed level aside of SG vessel at hot collector side (from bottom of SG vessel) (m)	1.850 <sup>+0.1*</sup>	1.967	1.860	1.912
Void fraction above the top of the hot bundle (+110 - +700mm)	0.23-1.0 <sup>**</sup>	0.29-1.0	0.29-1.0	0.282-1.0
Void fraction above the top of the cold bundle (+120 - +450mm)	0.02-1.0 <sup>**</sup>	0.23-1.0	0.22-1.0	0.11-1.0
Void fraction above the top of the bundle aside of SG vessel at hot collector side (+125 - +450mm)	0.14-1.0 <sup>**</sup>	-	0.112-1.0	0.11-1.0
Void fraction in downcomers (-700mm under the top of the bundle)	0.2-0.4 <sup>***</sup>	0.08 <sup>****</sup>	0.095 <sup>****</sup>	0.09-0.15 <sup>****</sup>
Steam massflow rate, kg/s	111.1	111.8	111.9	112
Water mass, 10 <sup>+3</sup> *kg	30-35	31	31	31

- \* - estimated error of level meter
- \*\* - corresponding to coordinates
- \*\*\* - left value accordingly the channel between vessel and cold tube bundle  
right value accordingly the channel between hot and cold bundle
- \*\*\*\* - averaged value

Tabl. 5: Comparison between some measurements and calculations for three developed schemes (90% power)

Furthermore measured values in different working power plants for the velocity of circulation mass flow, recirculation ratio, void fraction, levels and temperatures of water were qualitative compared to the results of the ATHLET calculation.

- The calculated circulation directions agree sufficiently in all models.
- The circulation ratio and accordingly the velocities of the circulation mass flow rates in the basic variant with only one downcomers are too low. The advanced models provide a good agreement for this values
- The distribution of void fraction agrees well in all models.
- The basic variant provides too small values for the void fraction in the downcomers.
- Water in all points is in saturation state. That is in a good agreement with measurement results.

The results of comparisons between some calculated values and averaged values from measurement are shown in table 4 and 5. The comparison of the measured values with the calculated values is difficult. These difficulties results mainly from the need to create averaged values from the measured local values. Here is one additional reason for the higher level of nodalization. The comparisons given above should be seen in that way as temporary results. A comprehensive description of the measurements is given in /1/.

## Correlations

Additionally to the work done in the field of nodalization schemes the implementation of special correlations in ATHLET for the crossflow situation on the secondary side of VVER steam generators is prepared. Two essential correlations will be implemented:

- pressure losses for vertical and horizontal flow in the tube bundle
- drift flux correlations for vertical 2 phase flow in the bundle

The correlations for pressure losses are described in /2,3/. They are based on experimental values from different facilities and power plants and must not be changed for implementation in ATHLET. The drift flux parameters have to be created from measured void fractions /2/. This void fraction as a function of the volumetric steam quality can be transformed into the usual drift flux parameters ( $c_0$  and  $V_{vj}$ ).

## Conclusions

The applied multi-channel method allows a proper modelling of the physical phenomena in the secondary side of the steam generator. The choice of separate channels for the mass flow in the hot and cold part of the bundle and in different downcomers has a profound effect on the accuracy of the model. In practice, the application of sophisticated models for the secondary side of the (often more than one) steam generator is limited because the time it takes to perform its calculation grows very quickly as more pipes are used. Concrete recommendations for the level of nodalization necessary for a given transients can actually not be given. The planned dynamic calculations on base of experimental data will be a basis for further improvements in this field.

**References**

- /1/ Schekin I., Trunov N., Beljajev Ju.  
Preliminary materials on the results of experimental data acquisition of horizontal steam generators for VVER-440/213 type reactors. Report, OKB GIDROPRESS, November, 1993
- /2/ Kolbasnikov A., et al.  
Investigation of the hydrodynamics of steam-water mixtures between heat conductor surfaces of a tube bundle to improve steam generators in VVER power plants. Elektricheskie Stanzii, No.8, 1991
- /3/ Kozlov Ju., Kolbasnikov A.  
The calculation of pressure losses for two-phase flow on heat transfer surfaces of the steam generators of nuclear power plants. Energomashinostrojenie, No.9, 1989

# HORIZONTAL STEAM GENERATOR PGV-1000 THERMAL-HYDRAULIC ANALYSIS

Olga Ubra  
SKODA Company  
Prague, Czech Republic

Michael Doubek  
TH Comp Hradec Kralove  
Postgraduate student  
Czech Technical University  
Prague, Czech Republic

## ABSTRACT

*A computer program for the steady state thermal-hydraulic analysis of horizontal steam generator PGV-1000 is presented. The program provides the capability to analyze steam generator PGV-1000 primary side flow and temperature distribution, primary side pressure drops, heat transfer between the primary and secondary sides and multidimensional heat flux distribution. A special attention is paid to the thermal-hydraulics of the secondary side. The code predicts 3-D distribution of the void fraction at the secondary side, mass redistribution under the submerged perforated sheet and the steam generator level profile. By means of developed computer program a detailed thermal-hydraulic study of the PGV-1000 has been carried out. A wide range of calculations has been performed and a set of important steam generator characteristics has been obtained. Some of them are presented in the paper.*

## 1. INTRODUCTION

Thermal-hydraulic behavior of a horizontal steam generator is in comparison with a vertical one different and more complicated, especially on the secondary side. To better understand the horizontal steam generator thermal-hydraulics a three-dimensional computer program for the steam generator PGV-1000 steady state analysis has been developed.

The developed computer program is capable to analyze :

1. Steam generator primary side hydraulics ,
  - primary side flow distribution in tube bundles ,
  - velocity distribution in collectors ,
  - pressure drop distribution on the primary side and the total primary side pressure drop.
2. Heat exchanger behavior ,
  - heat transfer for various situations in the tube and shell side (low level and

- the effect of tube bundle uncover is taken into account),
  - multidimensional heat flux distribution, total heat flux transferred through heat exchanger tubes (steam generator heat power),
  - primary side fluid temperature distribution - temperature profile along the tubes,
  - outlet mixed mean temperature of the primary side fluid,
  - steam outlet temperature and the temperature of the steam-water mixture at the shell side,
  - steam generator tube temperature profile.
3. Steam generator secondary side thermal-hydraulics and thermodynamics,
- average circulation rate for the cases with the level above the top of the tube bundles ;
  - 3-D void fraction distribution in the shell side,
  - steam and water volumes under the level, steam generator water mass inventory,
  - mass redistribution under the perforated sheet (for the cases with level above the perforated sheet),
  - minimal thickness of the steam layer under the perforated sheet (for the cases with the level above the top tube bundles),
  - secondary side pressure (for the plant operation in Mode that maintains a constant mean coolant temperature in the primary system),
  - steam flow rate,
  - secondary side pressure drops between the perforated sheet and outlet of the steam collector, the total secondary side pressure drop.

The nodalization which has been used and the physical methods applied to calculations will be shortly described.

A detailed thermal-hydraulic and thermodynamic study of the horizontal steam generator PGV-1000 for the Czech nuclear power plant Temelin has been carried out with the developed computer program. A wide range of calculations has been performed and a set of important steam generator characteristics has been obtained. Selected results will be presented.

## 2. A COMPUTER PROGRAM FOR THE THERMAL-HYDRAULIC ANALYSIS OF THE STEAM GENERATOR PGV-1000

For the mathematical simulation the steam generator is divided into three main regions.

1. The area between the bottom of the steam generator and upper tubes of the heat exchanger (the top of the tube bundles).

This region is subdivided in horizontal and vertical directions as it is shown in Fig.1 and Fig.2. The heat exchanger is divided into two bundle groups - inner and outer. Both bundle groups and their corresponding secondary volumes are subdivided in

the vertical direction into layers, the inner group into four layers and the outer one into three layers. Every tube is divided into eleven nodes in the axial tube direction.

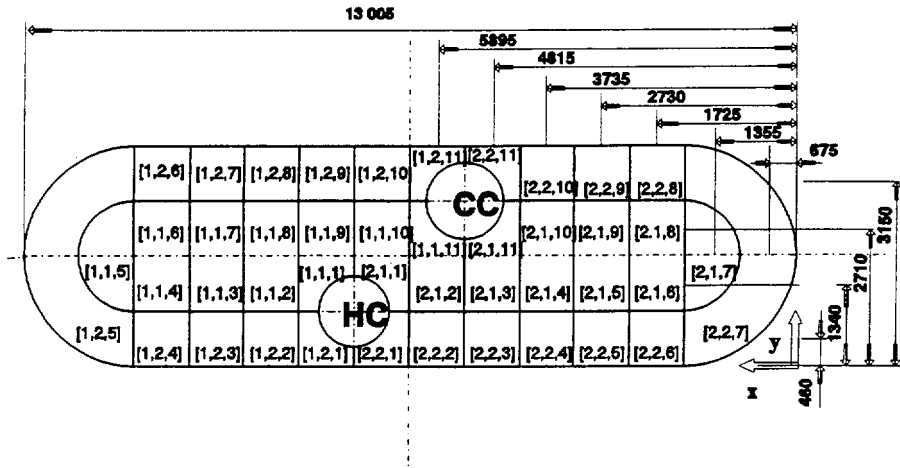


Figure 1: Tube Bundle Nodalization [horizontal direction]

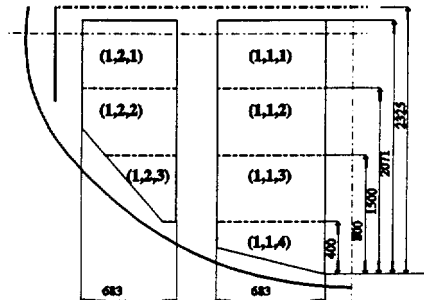
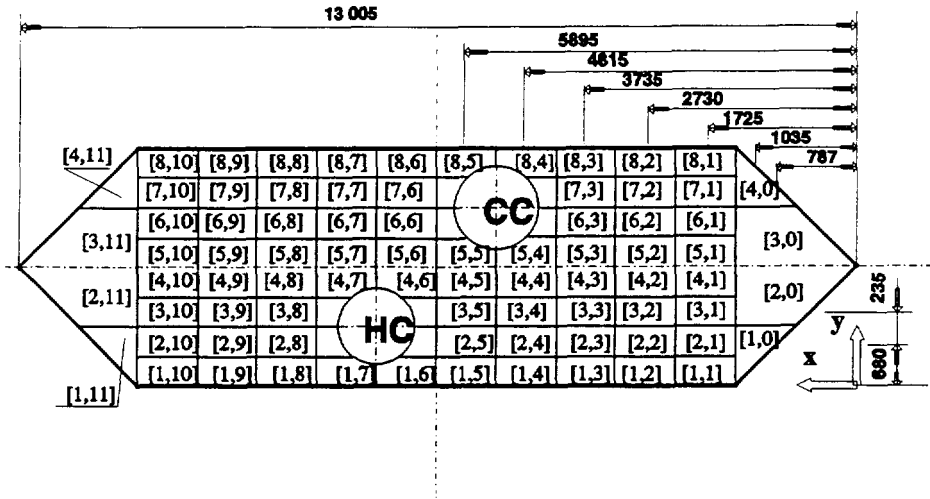


Figure 2: Tube Bundles Nodalization [vertical direction]

2. The region between the top of the tube bundles and the steam generator level. The nodalization of this area is derived from the division of the submerged perforated sheet shown in the Fig.3. Note that, all key phenomena in this area, especially the equal distribution of generated steam depends on the design and location of the perforated sheet.
3. The steam region between steam generator level and the outlet of the steam collector - steam dome with moisture separator and steam line.  
The model representation of this region is very simple. For steady state only the pressure losses across the louvers moisture separator system and across the short



**Figure 3: Perforated Sheet Division**

steam lines connecting the steam dome with the steam collector are calculated. The proper operation of the moisture separators is checked.

### 2.1 Simulation Methods

A computer program for steady state calculations of steam generator primary side hydraulics yields :

- primary flow distribution in the tubes,
- pressure drop distribution along the steam generator primary side.

For the calculation of primary side flow distribution the heat exchanger is divided into groups of tubes as is shown in Fig.2. Average flow velocity is evaluated for each group. The primary results of the calculation are the velocity distribution in the header and the flow velocities in the tubes. Model representation of the primary side pressure drops takes into account pressure drops in the inlet and outlet tubes connecting the steam generator with the hot and cold legs of the circulation loops, in both collectors and in the heat exchanger tubes.

The nodalization of the heat exchanger tube bundles for steady state thermal analysis corresponds to that shown Fig.1,2. The iterative method of calculation is based on thermal balance. The calculation is performed for every node separately and a global thermal balance is checked. The main result is the heat flux distribution in the steam generator shell side. The global heat flux is the essential parameter for the assessment of secondary side pressure and steam output. The program takes into consideration two

possibilities - the steam generator is above the top of tube bundles and the steam generator level is under the top of tube bundles with some tube uncovered.

A computer program for steady state thermal hydraulic analysis of the steam generator secondary side provides the capability to determine the average circulation rate for the cases with the level above the top of the tube bundles, void fraction distribution in the region between the steam generator bottom and upper rows of heat exchanger bundles, mass redistribution in the area between the upper part of the tube bundles and the submerged perforated sheet, and the steam generator level profile.

To determine the average value of the circulation rate a simple flow diagram is assumed. Two phase mixture rises up through the area in tube bundles, above the tube bundles steam and water are separated. The water flows back in the downcomer and in the free space between the tube bundles. The average value of the circulation rate is determined through the iteration method based on the pressure balance in the upflow section with heat exchanger tubes and in downflow section, free of tubes. The applied method builds on the theory of industrial steam boilers with natural circulation [1].

For the assessment of void fraction distribution the region between steam generator bottom and upper tube rows of heat exchanger is divided in vertical direction into layers of equal height of 50 mm. The heat flux into an arbitrary volume is obtained from the heat exchanger calculation. The feedwater distribution is taken into account. The calculation of the void fraction begins in the bottom of the steam generator and proceeds step by step over the layers to the top of the region. Two different methods have been developed for this calculation. The first method is based on the circulation rate assessment and it is applied to cases where the average level is above the top tube bundles. The second method is based on the theory of free bubbles rising through liquid by buoyancy [2] and it is used for all cases with the level under the top of tube bundles. The second method of void fraction assessment does not take into consideration the circulation of the fluid. In the comparison with the first one the second method gives slightly conservative results in the direction of higher void fraction, especially in the close vicinity of the hot collector.

For the cases with the level above the top tube bundle, the effect of perforated sheet is simulated. Hydrodynamic processes in the region between upper rows of the tube bundles and submerged perforated sheet depend on perforated sheet design, especially on the degree of the perforation and on the height of the perforated sheet rim. The goal of the simulation is to assess the steam flow rate from more loaded zones to the less loaded regions and to determine the thickness of the steam layer in different locations below the perforated sheet. The nodalization of this region corresponds to the perforated sheet division, which is shown in Fig.3. The iterative method which is used for mass redistribution assessment is based on different hydrostatic pressure in neighboring elements.

For the determination of the local value of steam generator level height and for assessment of the steam generator level profile two different method are used, one for the cases with the level above perforated sheet and the second one, for the level under the perforated sheet.

For the determination of the shape of mixture level above the perforated sheet, the steam-water mixture zone above perforated sheet should be analyzed. The nodalization is derived from the perforated sheet division. In every node, the void fraction, water volume and finally the height of the mixture level are calculated.

The determination of the level profile in the area between the steam generator bottom and perforated sheet is based only on the calculation of void fraction.

The complete mathematical model for the steam generator PGV-1000 thermal-hydraulic study is formulated in [3].

### 3. VERIFICATION AND APPLICATIONS

Only a limited verification of the model could be performed. Some results of void fraction calculations were compared with experimental data obtained by Russian organization Gidropress and published in [4], [5]. The comparisons have shown relatively good agreement. When more experimental data are available, more conclusive verification will be materialized.

About one hundred calculations have been performed and a great amount of interesting information has been obtained. The special attention has been paid to the secondary side analysis, primarily to the mixture level profile, 3-D void fraction distribution and to the distribution of the heat flux transferred to the secondary medium under different operation conditions.

Some important steam generator characteristic parameters have been investigated, e.g.

- 3-D distribution of the void fraction as a function of load at constant pressure and as a function of pressure at constant load;
- the steam generator level profile as a function of load and a function of pressure;
- the average void fraction as a function of steam generator load at constant pressure;
- the average level as a function of load for constant pressure and as a function of pressure for constant load;
- secondary side water and steam volumes and masses as functions of load at constant pressure;

For illustration some results of calculations are given in Fig.4 to 16. The vapor volume  $V''$  and the water volume  $V'$  under the steam generator level as functions of the heat power  $Q$  are shown in Fig.4,5. It is evident from Fig.4 that the vapor volume  $V''$  is proportional to  $Q$  for a given (fixed) pressure  $p$ . The increase is higher for low pressure than for high pressure. The water volume  $V'$  in Fig.5 decreases proportionally with increasing  $Q$ .

The vapor volume  $V''$  and the water volume  $V'$  as functions of pressure are shown in Fig.6,7. It can be observed from Fig.6. that the vapor volume  $V''$  decreases with increasing pressure  $p$  for a given (fixed) heat power  $Q$ . The decrease is higher for higher

heat power. The water volume  $V'$  in Fig.7. increases with increasing of pressure. The vapor volume - heat power relationship is twice stronger than the relationship between the vapor volume and pressure. In these calculations primary fluid volumetric flow rate, primary pressure, feed water flow rate and temperature and the steam generator level correspond to the nominal operating conditions.

The heat flux profiles and the tube temperature profiles for the tube bundles [1,1,1], [1,1,3] and [1,1,4] under three different secondary side pressures and reduced level (1.9m) are shown in Figures 8 through 10. The void fraction profiles in vertical direction in the elements close to the hot and cold collectors [1,1,1], [1,1,5], [1,1,7], [1,1,11], [1,2,3] and [1,2,10] obtained for the same input data are presented in Fig.11,12,13. The notation of the tube bundles corresponds to Fig.1. The void fraction profiles for the different thermal power and nominal steam generator level (2.55m) are shown in Fig.14,15,16.

## 5. SUMMARY

The presented work is a contribution to the investigation of the horizontal steam generator behavior. The developed computer program provides the capability to determine overall behavior of the steam generator in steady state under various load and pressure conditions and to provide more detailed information about multidimensional two-phase flow in the steam generator shell side. This includes void fractions, circulation flow rates, the dynamics of the swelled level, heat transfer with reduced levels etc. The detailed knowledge of these parameters can provide information needed for the efficient nodalization of the horizontal steam generator in large nuclear industry safety analysis codes.

## 6. REFERENCE

- [L1] Lokshin, V.A.-Peterson, D.F.-Svarc, A.L.: *Gidravliceskij Rozcot Kotelnych Agregatov (Normativnyj Method)* - Energia, Moskva, 1978. (in Russian)
- [L2] Avdeev, A.A.-Avdeeva, A.A.: *Kipeniye zhidkosti pri sbrose davleniya*, Teploenergetika 1980/8. (in Russian)
- [L3] Doubek, M.-Ubra, O.-Zuna, Z.: *Steam Generator PGV 1000, Steady State. Research Report Z-490*, CTU, Dept. of Thermal and Nuclear Power Plants, Prague, 1994.
- [L4] *International Seminar of Horizontal Steam Generator Modelling Vol.I, Vol.II* - Lapperranta 1991, Proceedings, Lapperranta University of Technology, Finland.
- [L5] Vasiljeva, A.G.-Dmitrijev, A.I.: *Issledovanie gidrodinamiki Parogeneratora PGV 1000*. Energomasinostrojenie, 1987. (in Russian)

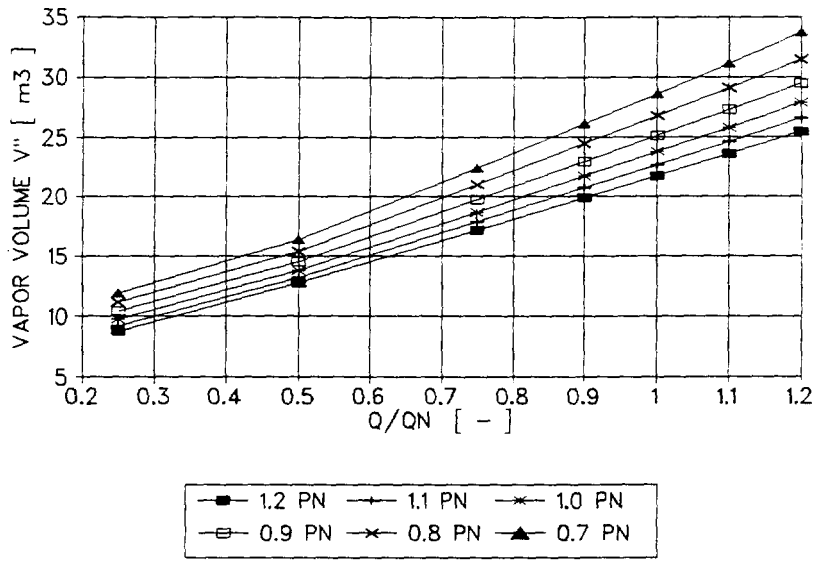


Figure 4

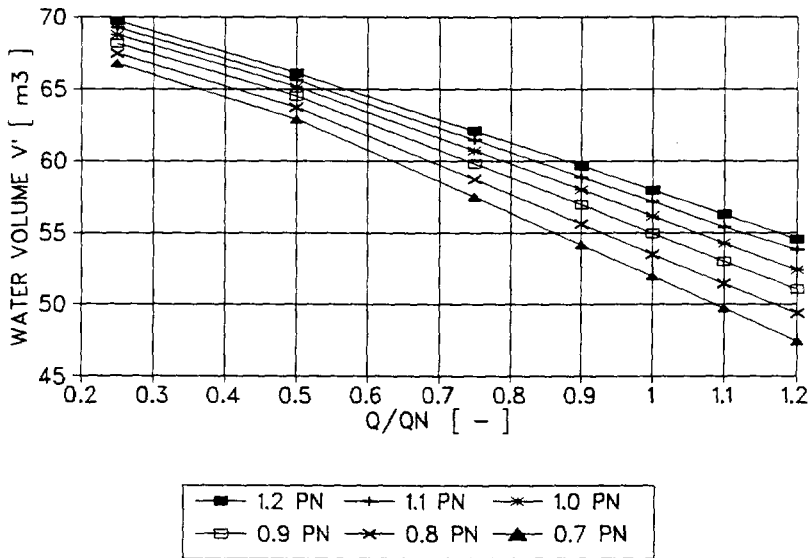


Figure 5

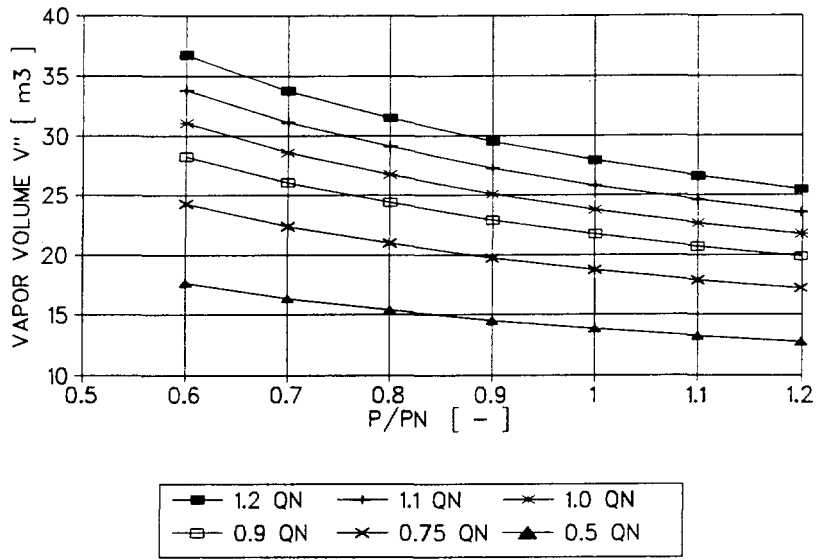


Figure 6

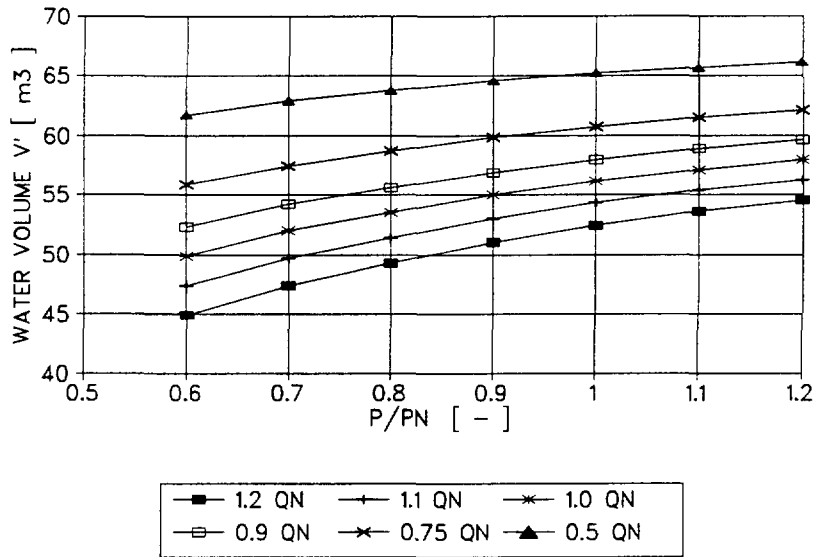


Figure 7

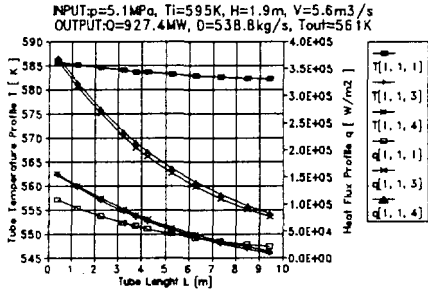


Figure 8

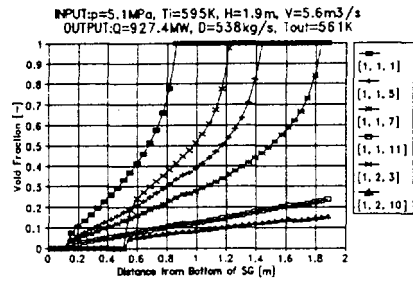


Figure 9

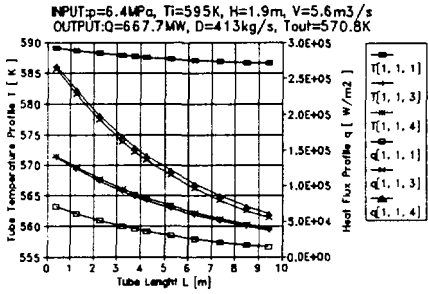


Figure 10

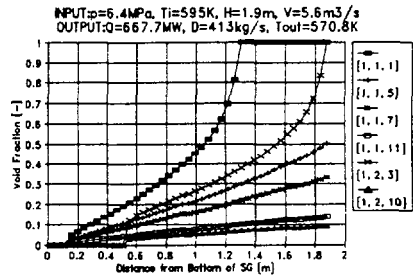


Figure 11

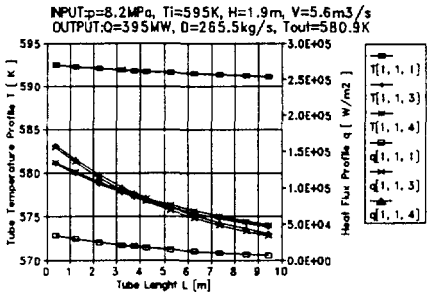


Figure 12

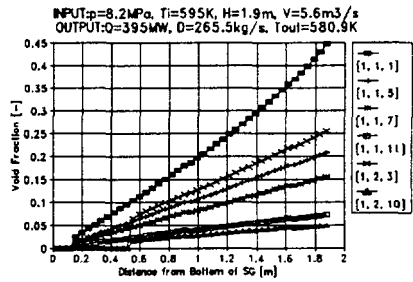


Figure 13

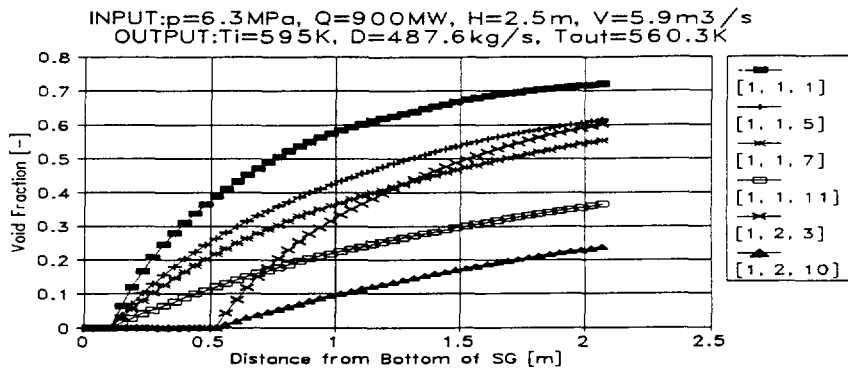


Figure 14

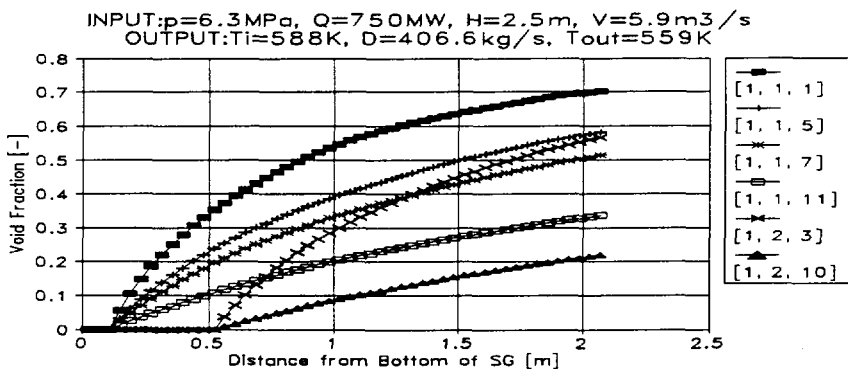


Figure 15

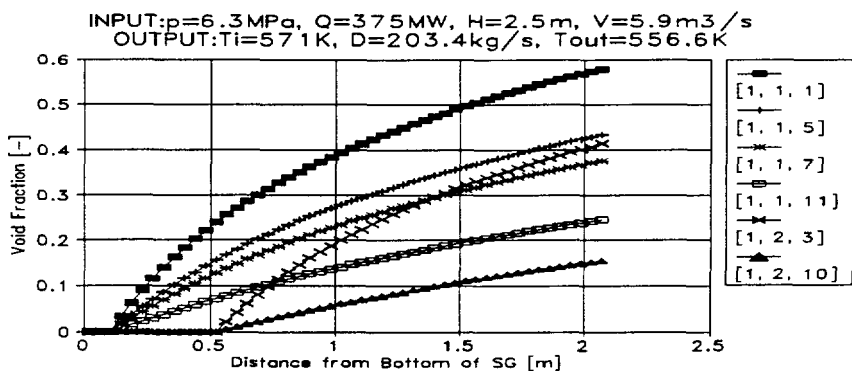


Figure 16

MINISTRY OF RUSSIAN FEDERATION OF ATOMIC ENERGY

OKB "GIDROPRESS"

VERIFICATION OF DINAMIKA-5 CODE ON EXPERIMENTAL DATA OF  
WATER LEVEL BEHAVIOUR IN PGV-440 UNDER DYNAMIC CONDITIONS

Beljaev Yu.V., Zaitsev S.I., Tarankov G.A.

ABSTRACT

Comparison of the results of calculational analysis with experimental data on water level behaviour in horizontal steam generator (PGV-440) under the conditions with cessation of feedwater supply is presented in the report.

Calculational analysis is performed using DIMANIKA-5 code, experimental data are obtained at Kola NPP-4.

III International seminar on simulation  
of horizontal steam generators,  
Lappeenranta, Finland, October, 1994

Experimental data obtained at operating NPP units with VVER are basic for verification of calculational codes used for substantiation of operation and reliability of this type units equipment.

Special examinations of SG mass and physical level behaviour under various operational steady-state and dynamic conditions were conducted. The main objective of these examinations was the analysis and evaluation of measurement (monitoring) systems operation, keeping and control of water level under various operating conditions. Though most obtained data can and shall be used for calculational codes verification.

Calculational analysis of the dynamic conditions with cessation of feedwater supply into one loop SG and this loop RCP connection and disconnection was performed as one of the stages of DINAMIKA code verification. These conditions are typical of significant level variation and RCP connection and disconnection give peculiar features in the process course.

Performed analysis results and their comparison with the experiment are presented in the report.

The conditions scenario.

The conditions scenario and experimental data on time dependant parameter variation are assumed as per report /1/.

Under initial conditions when the reactor worked at nominal power, all protections and lockings were put into operation, the main feedwater controller worked under the conditions "D". The conditions onset is associated with SG-2 feedwater line valves closing at 240 s. Water level started to decrease sharply and at 305 s when water level was decreased by 400 mm of nominal the operator disconnected RCP-2. After RCP-2 disconnection the rate of the level decreasing was lowered and further decreasing was due to SG water evaporation under the conditions of loop operation with stable counter current. Water level decrease to the level of 900 mm as per a large level gauge and then actions on SG-2 level recovering were started.

Unit power was decreased to 80% after RCP-2 disconnection.

As it was stated in report /1/ SG-2 steam generation after RCP run-out was settled at the level 22-30% N that causes doubts and requires further discussion.

Before RCP connection SG-2 level was increased to 1800 mm as per the large level gauge. RCP was connected at 3725 s; feedwater controller was changed into automatic conditions simultaneously.

SG mass water level was measured with standard level gauges with the range 4000 mm (large) and 630 mm (small). There are 2 large level gauges and 5 small ones in each SG. Indications of two large level gauges (RP-182, RP-188) and 2 small ones (RP-194, RP-208) are presented in the report).

Code, calculational diagram and algorithm.

Calculational analysis of the conditions specified was performed using code DINAMIKA-5 brief description of which including also horizontal steam generator model is given in /2/.

Six actual unit loops were simulated by fore calculational loops the first three of which have "weight" 1 are united by steam using one semi-header; the fourth calculational loop with "weight" 3 operates into the second semi-header. Each of calculational loops was divided into 13 sections along the length 5 of which being along SG tubing. Reactor chambers are in the first calculational space, the core was simulated using three parallel channels divided into 7 sections along the height.

Calculational analysis of the given conditions was practically identical to the conditions scenario but for two moments. It was stated in the report /1/ that after the level was decreased to 900 mm the actions on level recovering were performed. However any information concerning the way it was performed is not presented. Thus feed water flowrate was predicted preceding from the curve of level variation. And besides it was assumed that turbine controllers operated under the conditions of pressure maintenance also due to absence of information about their work.

Excitation actions were carried out in the second loop.

## Discussion of results

As many-year experience proved computation of the experiments performed at actual NPP units meets difficulties. As a rule the experiments are aimed at concrete objectives thus the most significant attention is paid to recording of that parameters which are pertinent with these objectives. Thus it is rather often that the parameters important from the viewpoint of calculations are absent in the experiment reports according to different reasons.

Identical difficulties were not excluded during performing of the present calculation. Some of them were mentioned above. And besides the information on primary parameter variation and especially over loop N 2 (flowrates, temperature values) didn't allow to perform the more detailed analysis of the results obtained.

The main results of the calculational analysis and their comparison with the experimental data are presented in Figs.1-12.

The curves presented show that satisfactory agreement of experimental and calculational results over the whole parameter range excluding SG 2 steam flowrate which is 22-30% N according to the experiment is observed. At the same time SG-2 relative thermal power is about 7-8% of nominal that is more in compliance with the calculation results.

Quantification of SG 2 steam generation value proceeding from the primary parameters (flowrate and temperature differential) also produces the value not more than 10 %. It may be assumed that measurement accurateness is decreased at insignificant values of steam flowrate.

One more significant disagreement of calculational and experimental results is observed in SG 2 thermal power variation during the period from 300 to 450 s. In this case it is difficult to explain thermal power increase (to 130% of nominal at 390-th s, see Fig. 10) when counter current has already been settled in the second loop. SG 2 power could increase only during the period when feedwater supply was stopped, but the pump still was in operation. The most probably the mistake was made during experimental data treatment.

#### Conclusion.

Proceeding from the analysis performed it may be stated that code DINAMIKA-5 simulates SG processes over integral parameters satisfactorily as from the quality so quantity points of view. Unfortunately absence of data on primary circuit didn't allow to perform the most complete analysis. More complex and precise approach to data acquisition and treatment may be recommended for experiments planning and conduction as well as for reports performing.

#### REFERENCES

1. Преварительные материалы по результатам сбора и обобщения экспериментальных данных по горизонтальным парогенераторам реакторных установок с ВВЭР-440/213. ОКБ "Гидропресс", 1993.
2. Beljaev Yu.V. et al. Calculation of conditions with drop of the level over PGV-1000 secondary side using DINAMIKA-5 code. International seminar of horizontal steam generator modelling. Lappeenranta, Finland, September, 1992.

Kota NPP-4. CESSATION OF FEEDWATER SUPPLY INTO SG 2

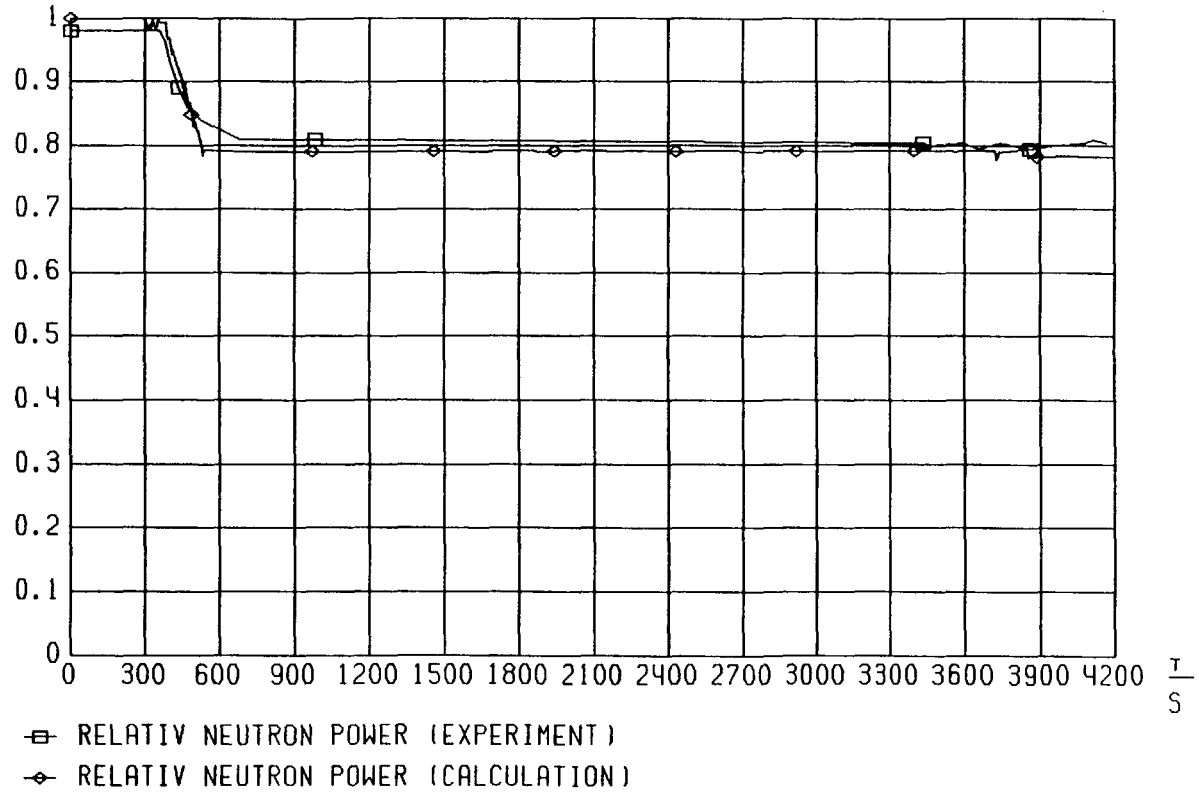


Fig. 1

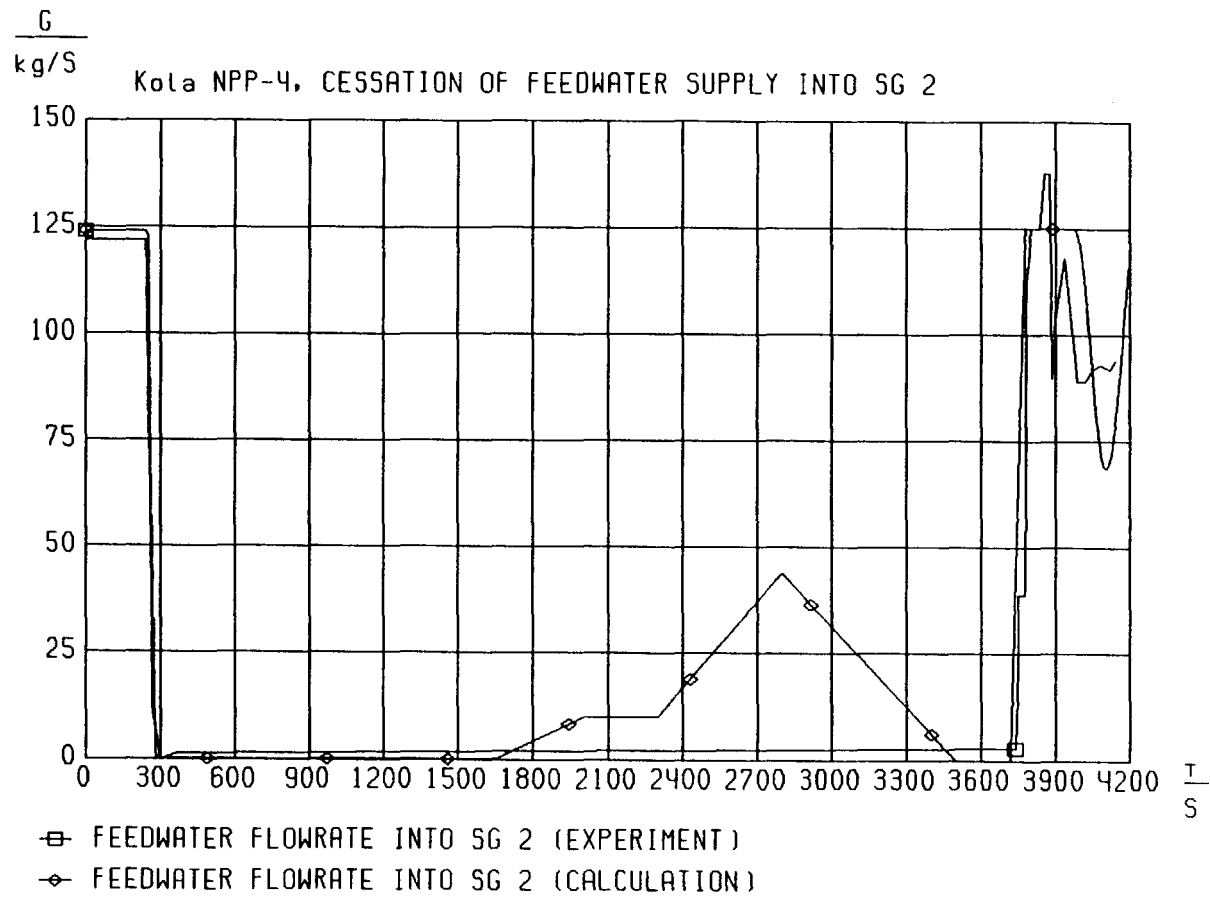


Fig. 2

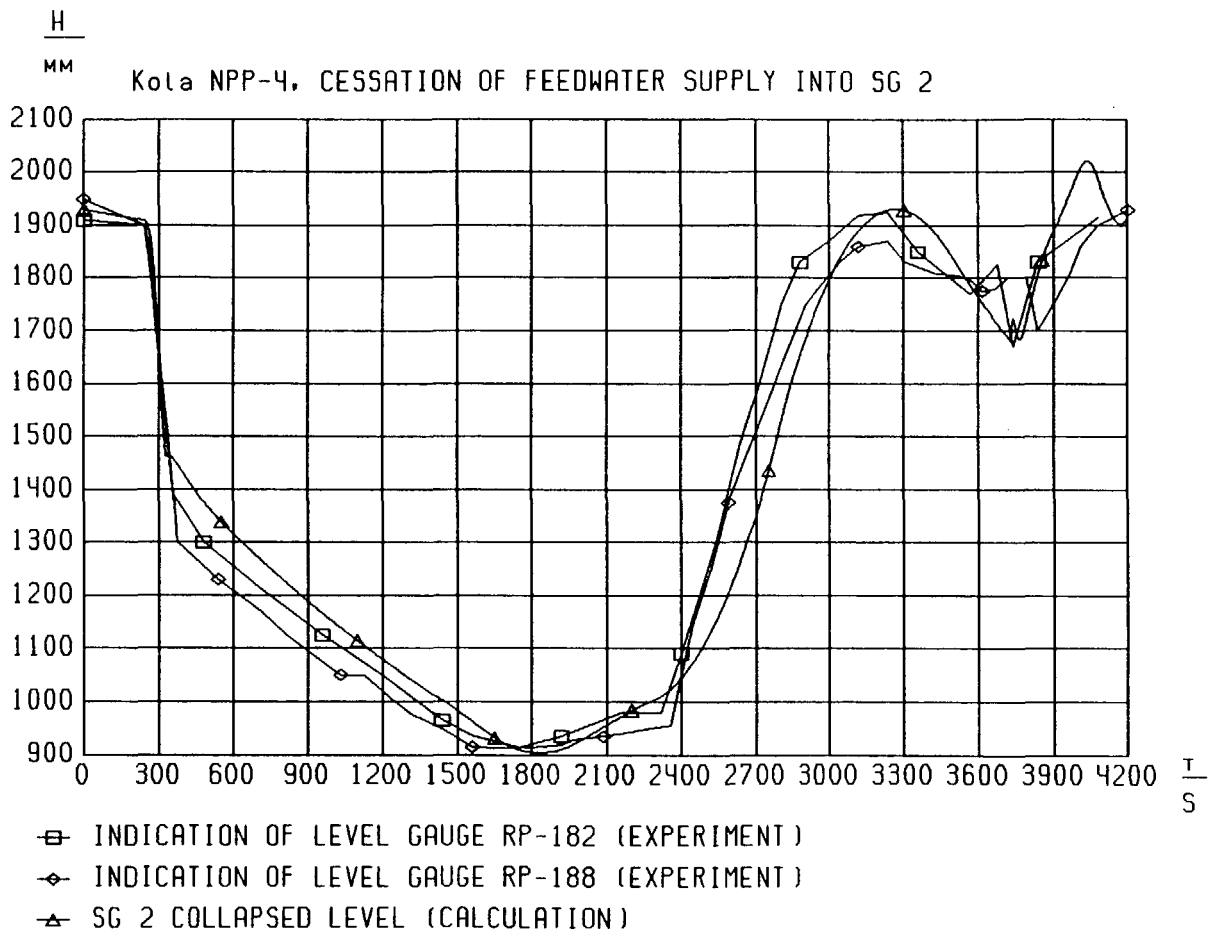


Fig. 3

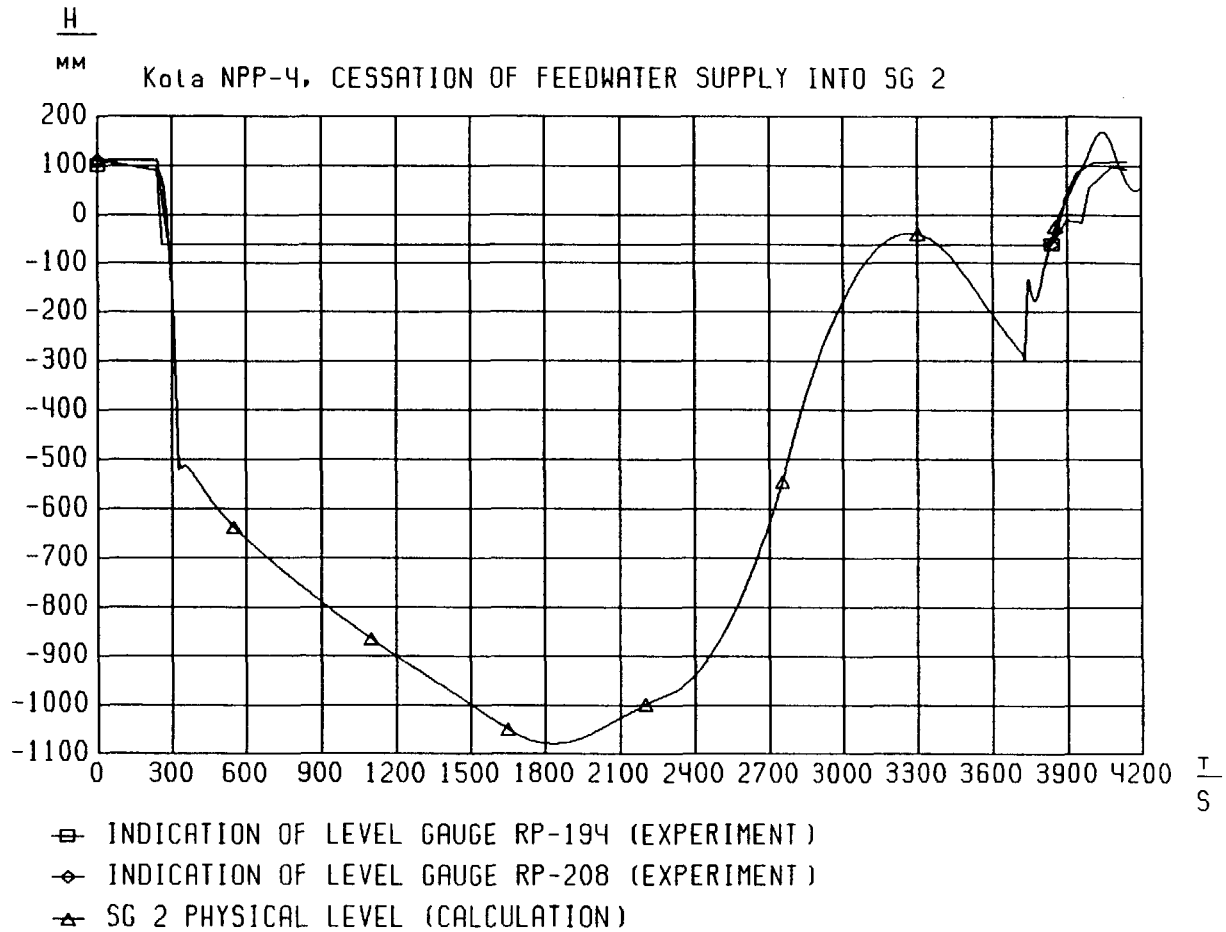


Fig. 4

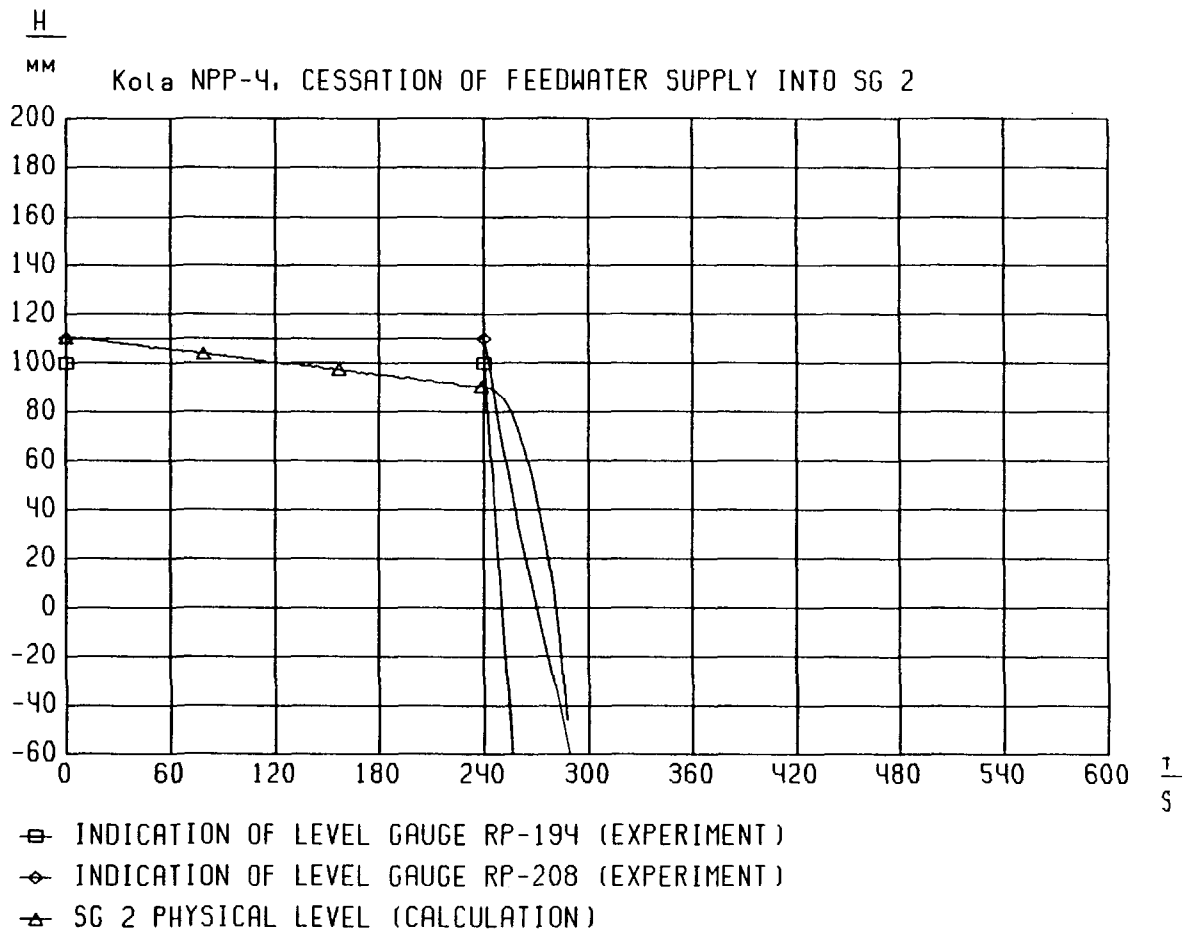


Fig. 5

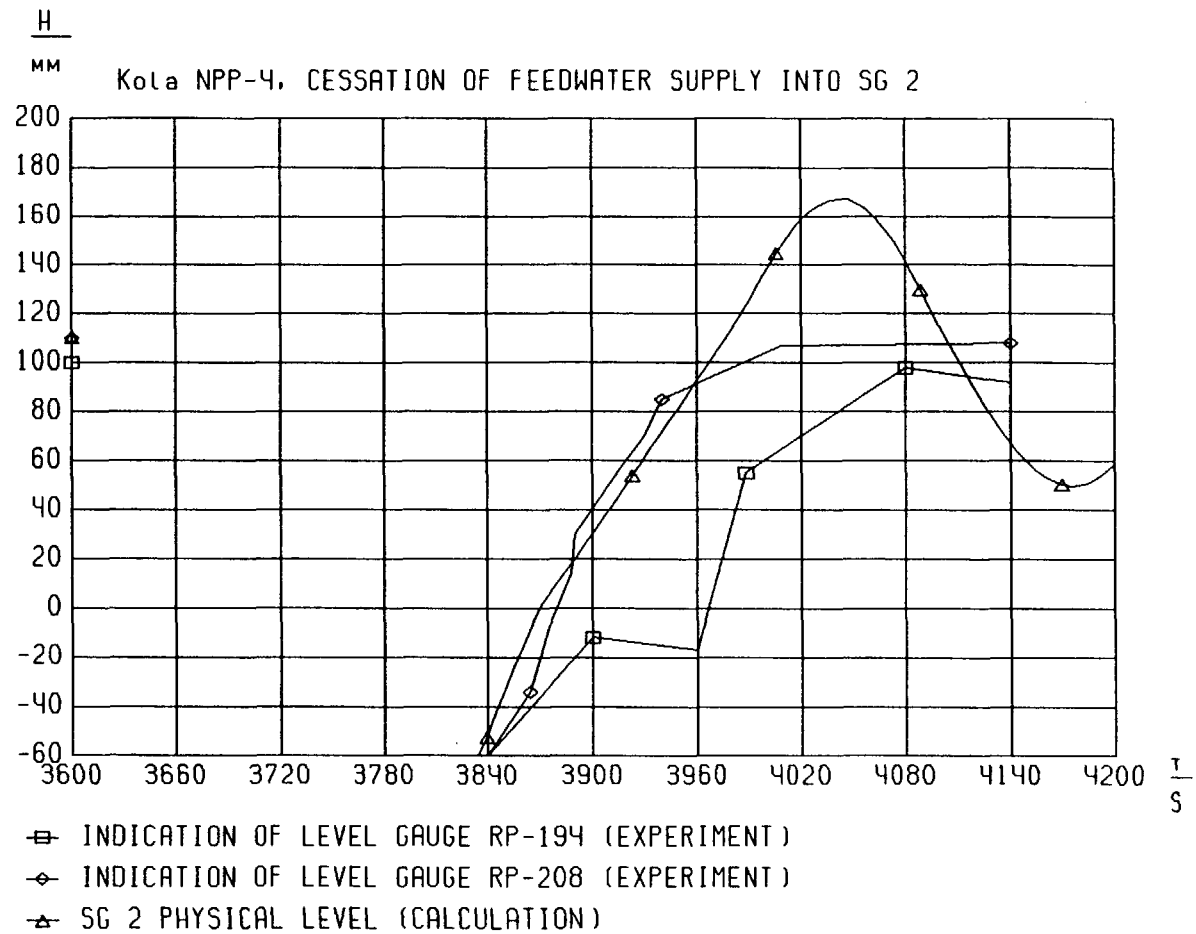


Fig. 6

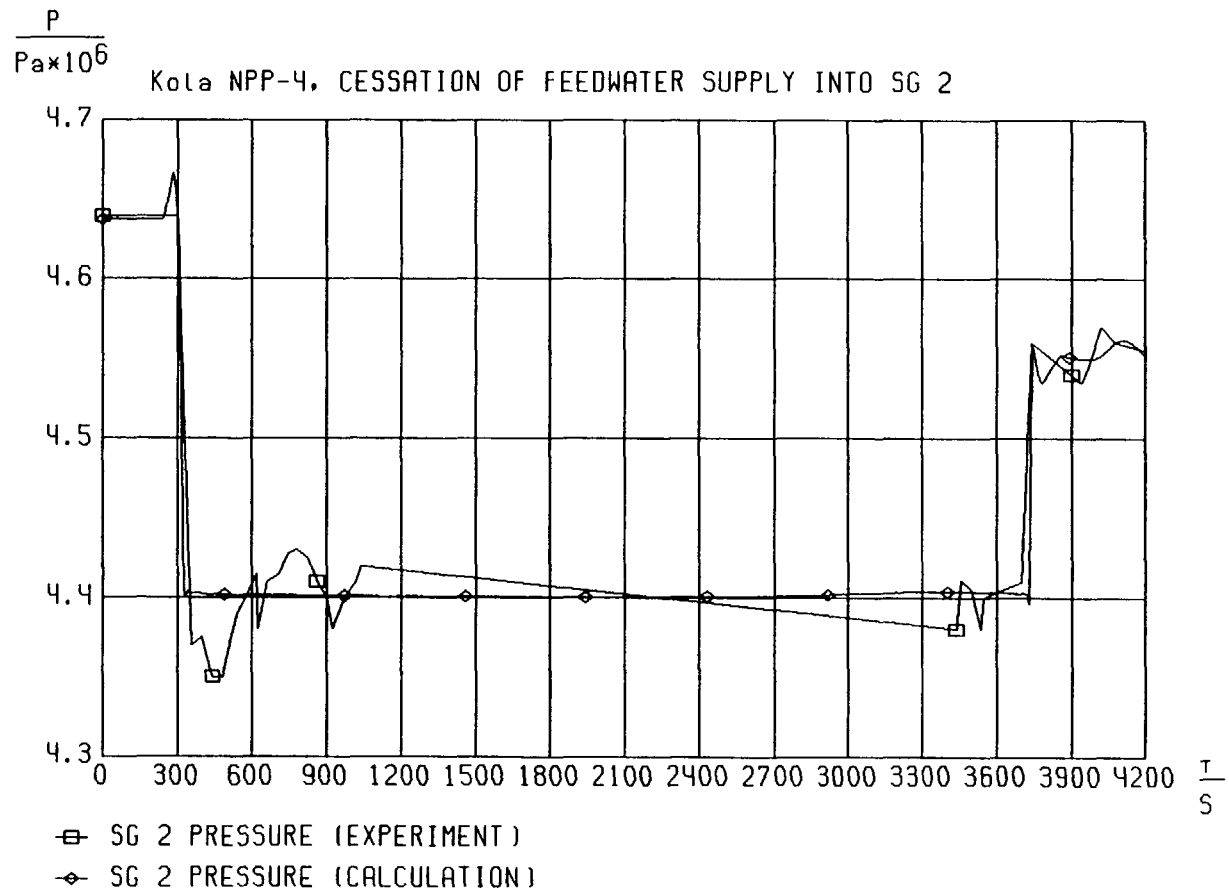


Fig. 7

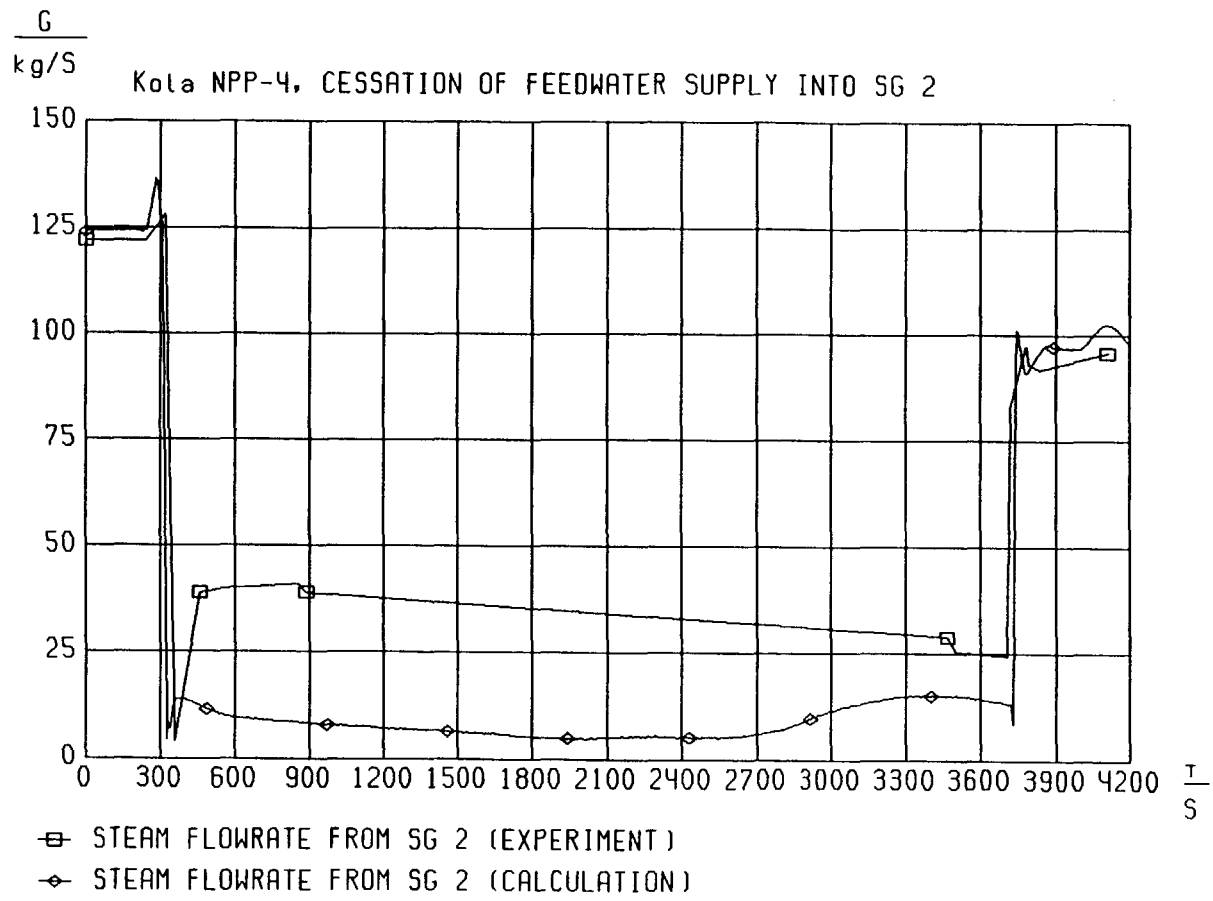


Fig. 8

KoLa NPP-4, CESSATION OF FEEDWATER SUPPLY INTO SG 2

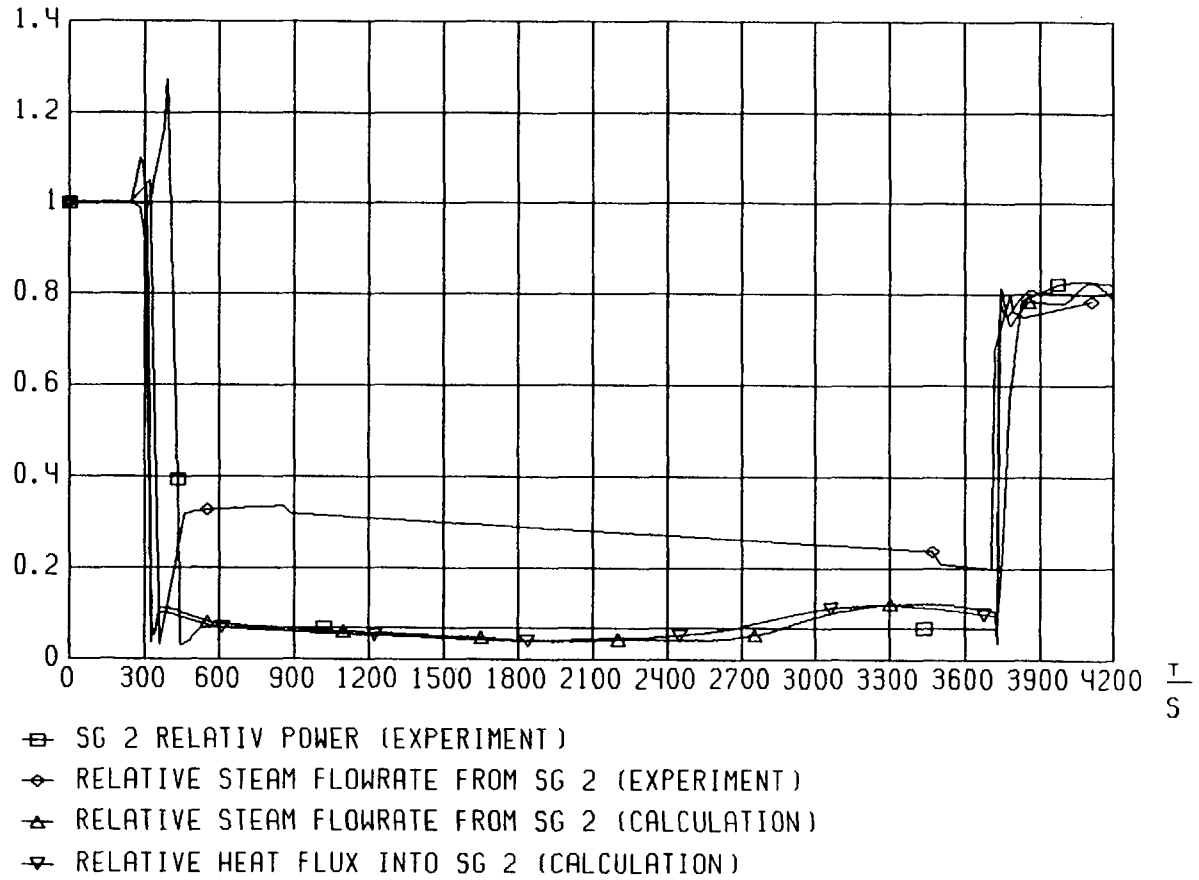
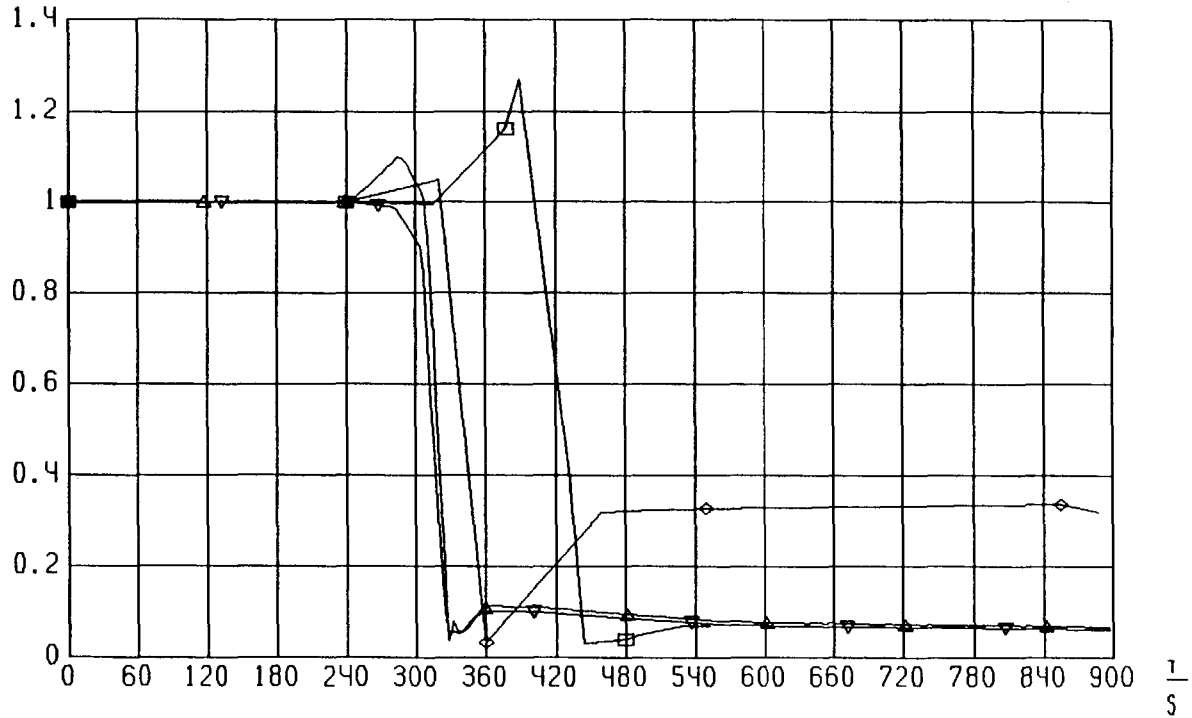


Fig. 9

Kota NPP-4, CESSATION OF FEEDWATER SUPPLY INTO SG 2



- ▣ SG 2 RELATIV POWER (EXPERIMENT)
- ◇ RELATIVE STEAM FLOWRATE FROM SG 2 (EXPERIMENT)
- ▲ RELATIVE STEAM FLOWRATE FROM SG 2 (CALCULATION)
- ▽ RELATIVE HEAT FLUX INTO SG 2 (CALCULATION)

Fig. 10

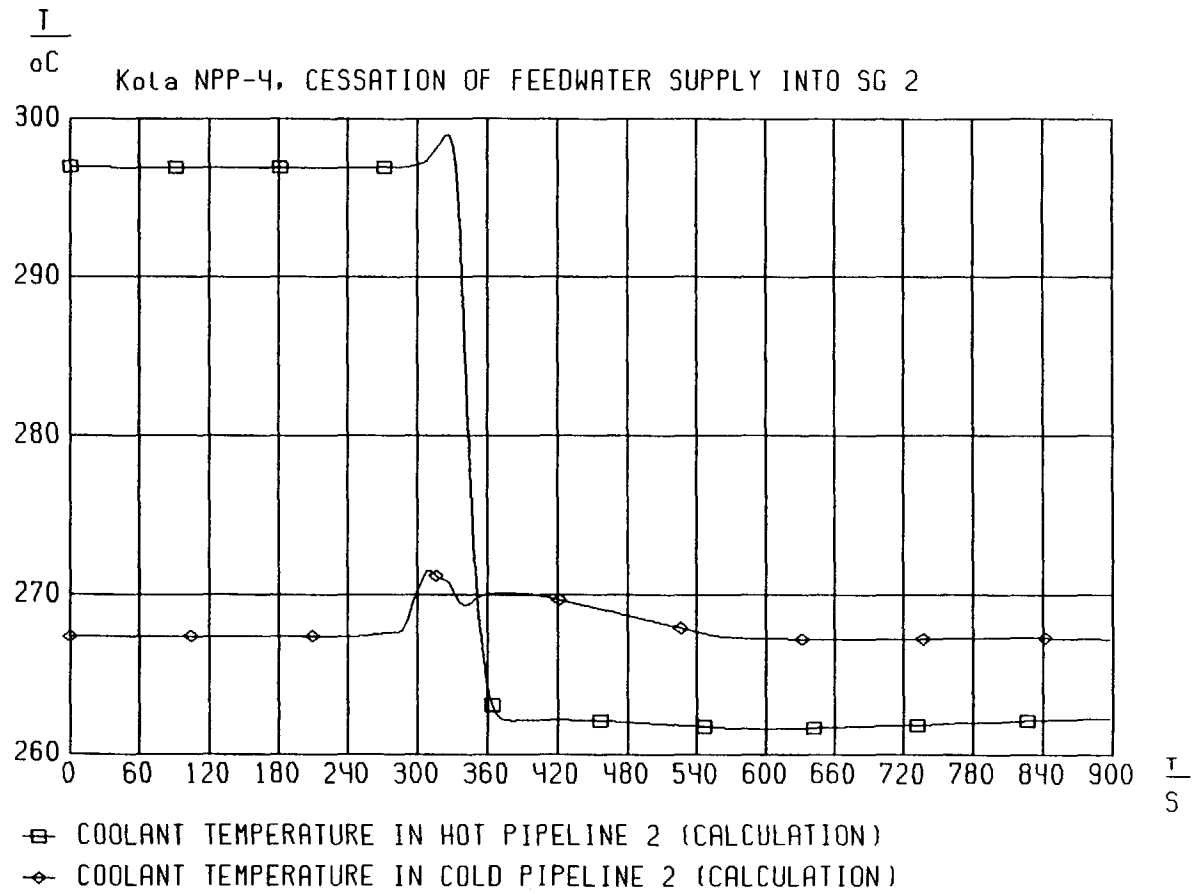


Fig. 11

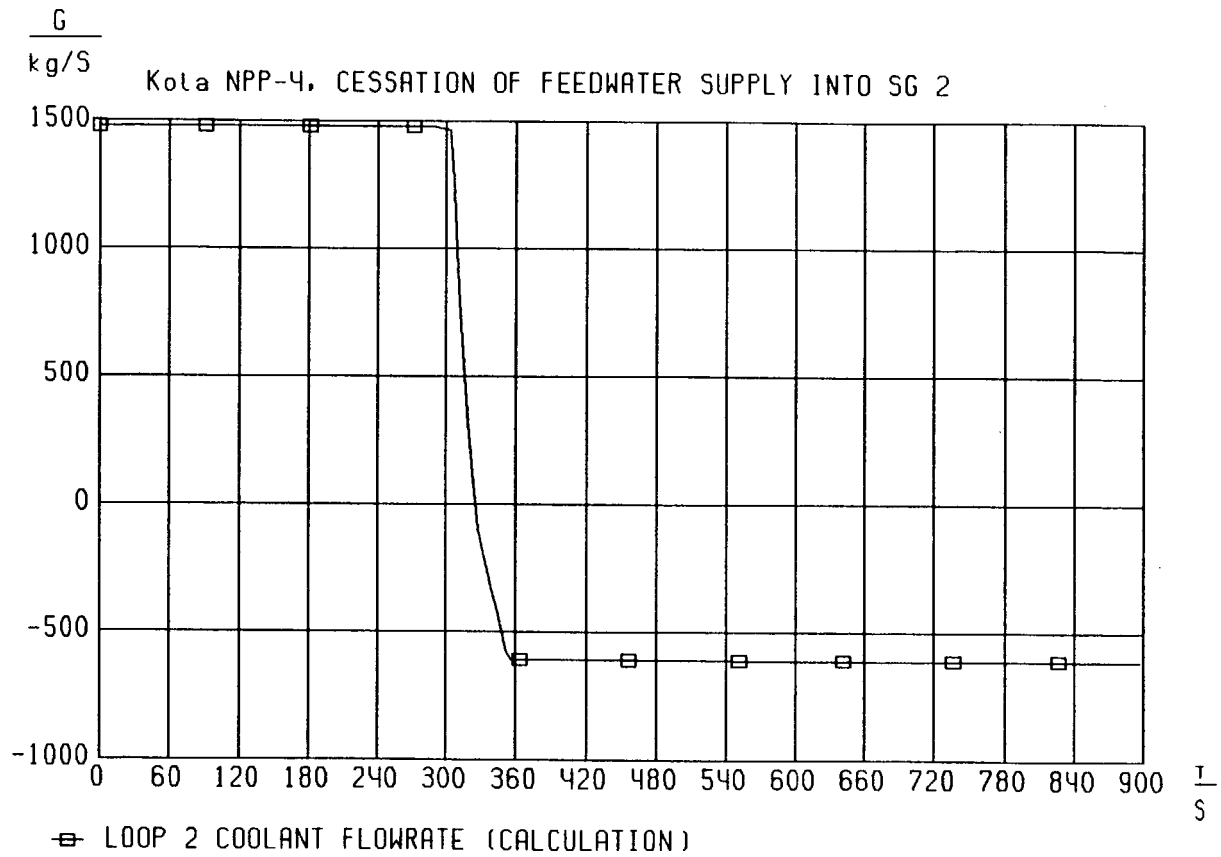


Fig. 12

# PRIMARY COLLECTOR WALL LOCAL TEMPERATURE FLUCTUATIONS IN THE AREA OF WATER - STEAM PHASE BOUNDARY

Oldřich Matal, Jozef Klinga, Tomáš Šimo, Energovýzkum Ltd,  
Brno, Czech republik

Prepared for "Third International Seminar on Horizontal Steam  
Generators, 18 - 20 October 1994, Lappeenranta, Finland

## Abstract

A limited number of temperature sensors could be installed at the primary collector surface in the area of water - steam phase boundary.

The surface temperatures as well WVER 440 Steam generator process data were measured and stored for a long time and off-line evaluated.

Selected results are presented in the paper.

## 1. INTRODUCTION

Behaviour of the primary collector of a WVER 440 steam generator was studied during a time period of three fuel campaigns, Ref [1]. The primary collector was equipped by a number of sensors. A group of thermocouples was installed at the outer collector surface in the area of water-steam phase boundary. This thermocouples TK1, TK2, TK3 etc are schematically shown in Fig 1. The sensors hardcables penetrated the high pressure boundary of the steam generator in an extra designed penetration located in the bottom of the collector secondary cover.

The sensor signal were measured and stored by a measurement system of the type EMS-93, which was developed, manufactured and installed by Energovýzkum Ltd.

## 2. SELECTED RESULTS

The position of water-steam phase boundary as well as the magnitude of temperature fluctuations vary with the steam generator (SG) power level. This expected results are shown in Fig 2 and Fig 3 respectively. The SG thermal power level of 104,2 MW corresponds to the left part and of 229,2 MW to the right part of both diagrams.

A typical amplitude spectrum obtained from thermocouple signals attached to the primary collector surface is in Fig 4. The frequencies of significant temperature fluctuations are below 0,25 Hz.

The random signal of the thermocouple attached to the primary collector surface can be classified in to classes using rainflow counting method, Ref [2]. Each class is characterized by a magnitude of the temperature amplitude.

Number of temperature cycles is counted in each class and for an average temperature. A typical result is demonstrated in Fig 5. The total number of local temperature cycles at the primary collector surface in this case was 63 in the class 1, 107

in the class 2, 96 in the class 3 etc counted in the time interval of 24 hours.

### 3. CONCLUSIONS

The total number of local temperature cycles counted at the primary collector outer surface in the area of water-steam phase boundary is at least of  $10^5$  in an year.

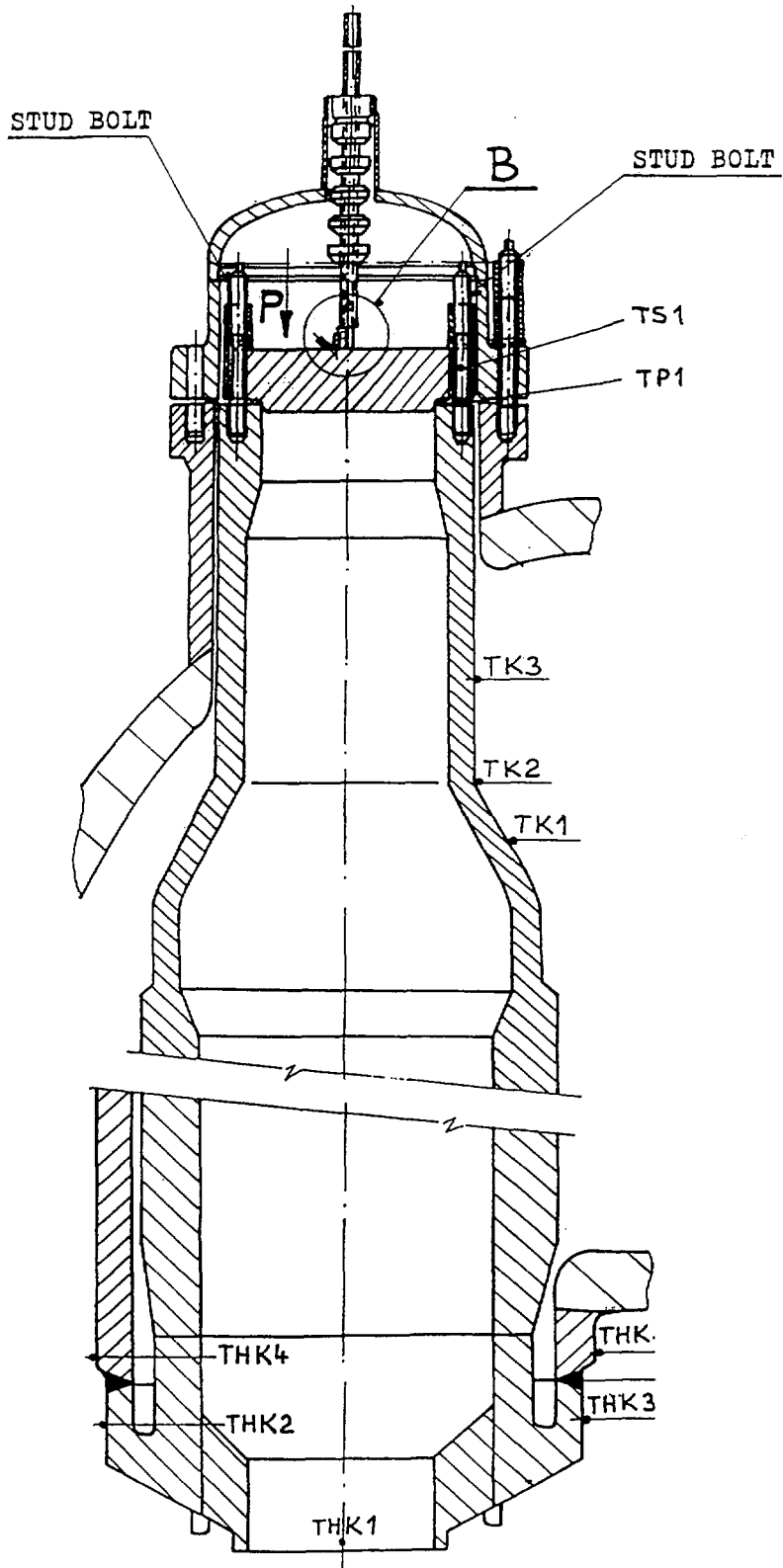
Significant local temperature fluctuations measured in this area are below 0,25 Hz.

The water-steam phase boundary around the inlet primary collector reaches the moisture separation system partially when the WVER 440 SG is operating at the nominal power level.

### 4. REFERENCES

- [1] Matal, O., Šimo, T., Holý, F., Vejvoda, S. :  
Operational Monitoring of Temperatures and State of Stress of Primary Collectors, Their Stud Bolts and Cover and Temperatures of Steam Generator's Pressure Vessel at the Nuclear Power Unit WVER 440, Proceedings of the 7th International Conference on Pressure Vessel Technology, 31 to 5 June 1992, Düsseldorf, FRG
- [1] Downing, D. :  
Simple rainflow counting algorithm, Int. J. Fatigue, January 1982, p.31-40.

Fig 1: SCHEMATIC DIAGRAM OF SENSOR LOCATIONS AT THE PRIMARY COLLECTOR



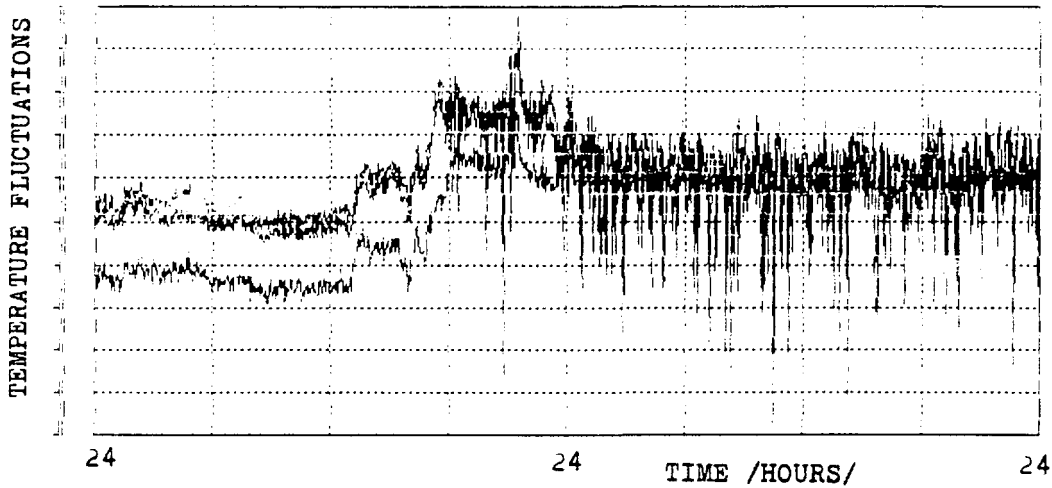


Fig 2: TYPICAL TEMPERATURE FLUCTUATIONS AT THE CONICAL SURFACE OF A SG 440 PRIMARY COLLECTOR

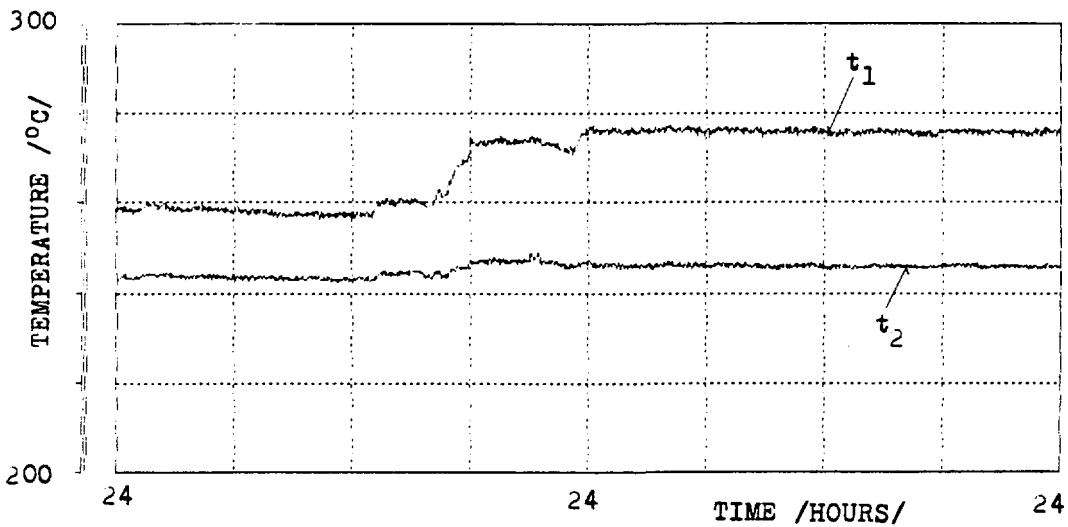


Fig 3: TEMPERATURE AT THE WATER INLET COLLECTOR SURFACE ( $t_1$ ) AND WATER OUTLET COLLECTOR SURFACE ( $t_2$ ) VERSUS TIME

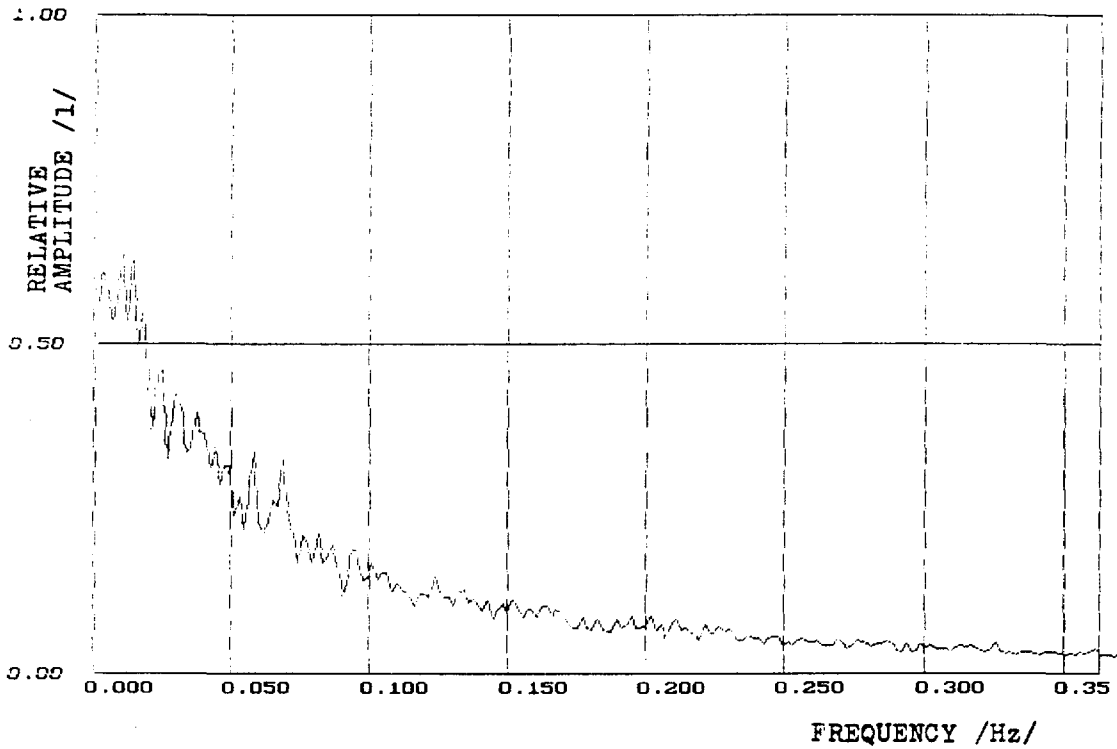


Fig 4: AMPLITUDE SPECTRUM TYPICALLY OBTAINED FROM TEMPERATURE SENSOR SIGNALS

AVERAGE TEMPERATURE	AMPLITUDE CLASSES					
	1	2	3	4	5	6
[ °C]						
260	0	0	0	0	0	0
262	1	2	0	0	0	0
264	6	9	3	5	8	0
266	27	64	78	35	18	6
268	29	31	15	1	0	0
270	0	1	0	0	0	0
272	0	0	0	0	0	0
Total	63	107	96	41	26	6

Fig.5 Rain flow counting of temperature cycles at the primary collector conical surface in the time period of 24 hours



**Electrogorsk Research & Engineering Centre  
of Nuclear Plants Safety**

---

Bezymyannaya 6  
Moscow region  
Russia, 142530

phone: +7 (09643) 3-05-21  
fax: +7 (09643) 3-05-15

**Data Bank  
On Hydrodynamics, Thermal Tests And Tube  
Temperature Regimes of PGV-4 & PGV-1000  
Natural Steam Generators**

*Prof. A.G.Ageev , Dr. R.V.Vasileva, Prof. B.I.Nigmatulin,  
Prof. V.F.Titov, Dr. G.N. Tarankov*

*(EREC, OKB "Hydropress")*

## CONTENTS

1. Introduction
2. Data Bank Volume
3. Data Bank Structure
4. Content of The Data Bank Part Ready For Use
5. Conclusions



## 1. INTRODUCTION

The data bank was prepared by EREC, OKB "Hydropress" using results of static and dynamic tests of PGV-4 and PGV-1000 natural steam generators cared out at Kolskaya, Novo-Voronezhskaya, Ugno-Ukrainskaya, Balakov-skaya and Hmelnitskaya NPP within period of 1974-1993. It is destined for making calculation codes verification.



## 2. DATA BANK VOLUME

The data bank consists of 8 volumes.

**Volume 1.** Experimental data bank on the hydrodynamics of Novo-Voronezhskaya NPP third unit PGV-4 steam generator.

**Volume 2.** Data bank on the hydrodynamics of Novo-Voronezhskaya NPP fifth unit PGV-1000 steam generator.

**Volume 3.** Data bank on the hydrodynamics of Balakovskaya NPP first unit PGV-1000 steam generator.

**Volume 4.** Data bank on the thermal tests and tube temperature regimes of Yuzhno-Ukrainskaya NPP first unit PGV-1000 steam generator.



**Volume 5.** Data bank on the dynamic regimes of PGV-4 steam generator, (will be ready in November 1994).

**Volume 6.** Data bank on the dynamic regimes of PGV-1000 steam generator, (will be ready in January 1995).

**Volume 7.** Data bank on the separation tests of PGV-1000 steam generator, (will be ready in February 1995).

**Volume 8.** Data bank on the salt distribution in the water volume of PGV-1000 steam generator, (will be ready in May 1995).



### 3. DATA BANK STRUCTURE

The data bank contains:

- measurement scheme;
- measuring appliances;
- regime parameters measurement rang;
- method of experiment execution;
- method of experimental data processing;
- graphical interpretation and experimental data tabels.



**Volume I. Experimental data bank on the hydrodynamics of Novo-Voronezhskaya NPP third unit PGV-4 steam generator.**

1. Inside-vessel measurement system: six void fraction hydrostatic measuring transducers, six turbine flow-meters for flow velocity determining (fig.1, 2, 3).

2. Regime parameters measuring range: steam generator loading is 50- 100% of power (225-480 t/h), feed water temperature is 135-215°C, level changing is from -200 to +200mm according to the level-meter of the general control board.



3. That was investigated 28 regimes and 670 experimental points were obtained.

4. Velocity definition accuracy is  $\pm 0.05\text{m/c}$ , void fraction definition complex accuracy class is 1,6.

5. Information: experimental data on the void fractions, flow velocities, circulation divisibility, circulating water flow distribution; velocity local oscillations were pointed out under the levels lower than the project ones.



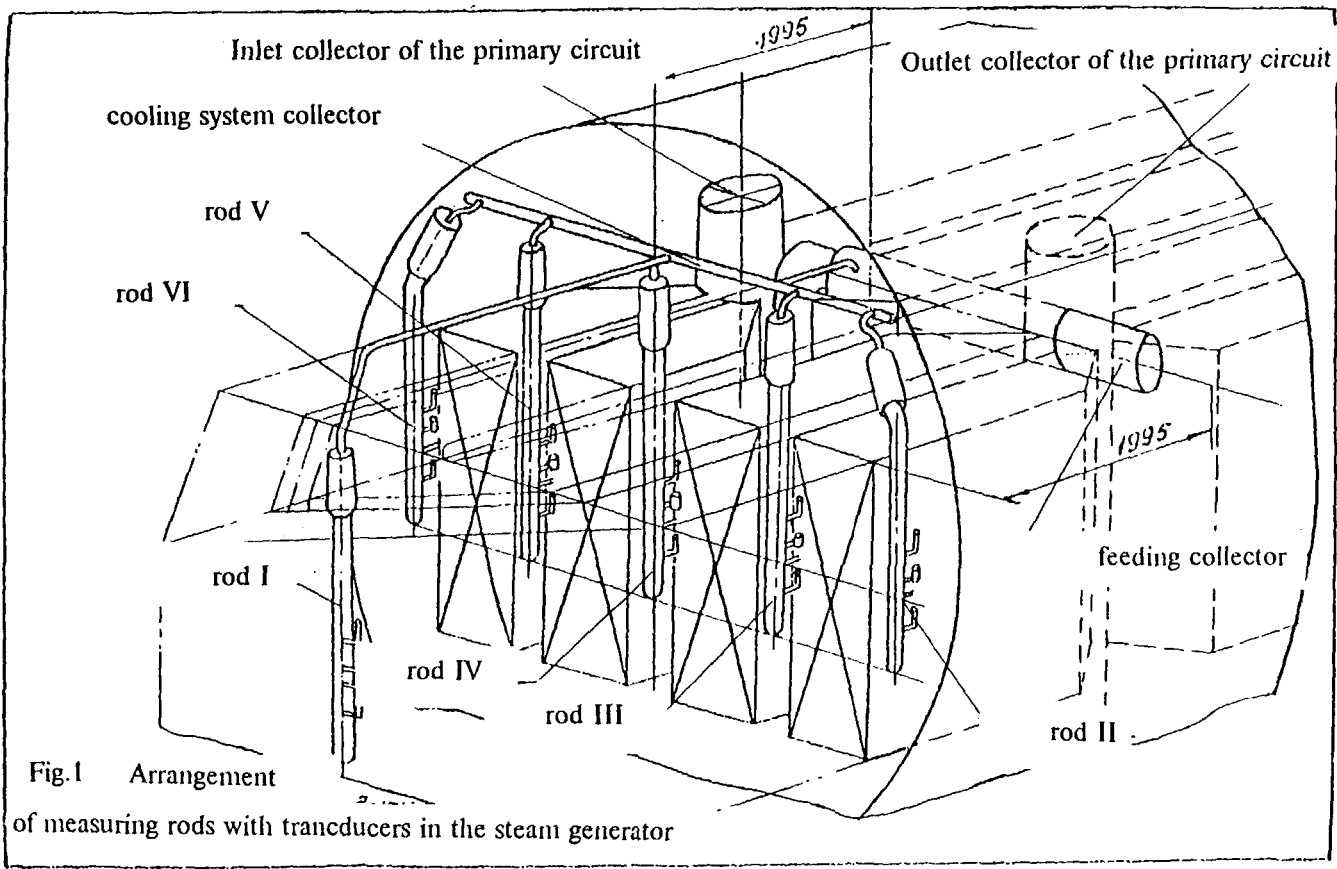
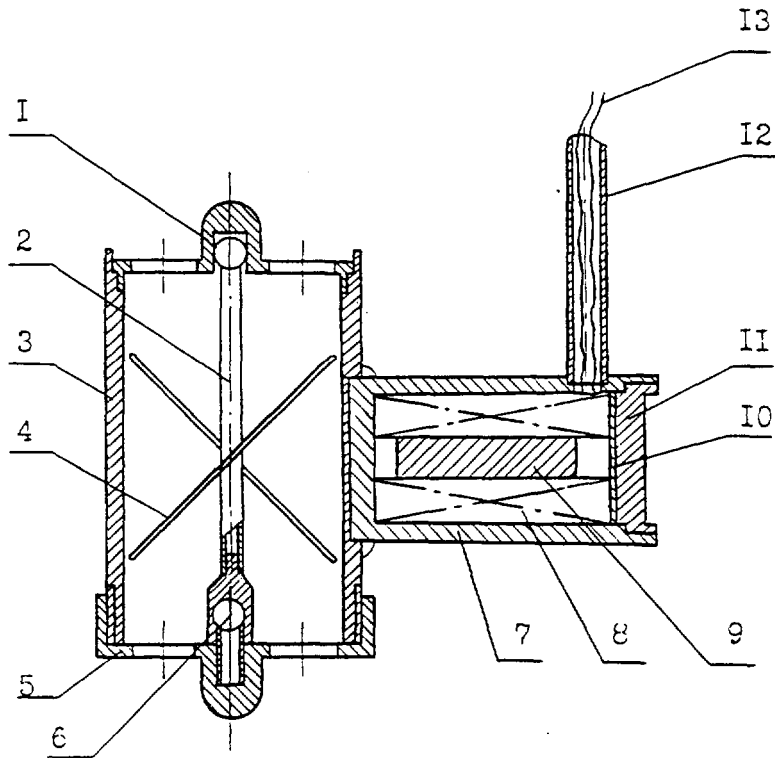


Fig.1 Arrangement of measuring rods with transducers in the steam generator

## The assembled turbine flow-meter



- 1 - top crosspiece, 2 - blade wheel, 3 - flow-meter carcass, 4 - blade,  
 5 - bottom crosspiece, 6 - blade wheel bottom carrier, 7 - induction coil frame,  
 8 - induction coil, 9 - constant magnet, 10 - heat-insulating gasket (technological),  
 11 - seal, 12 - tube for the coil conductors outlet ( $d=6 \times 1$ ), 13 - POG-conductor

Fig.2

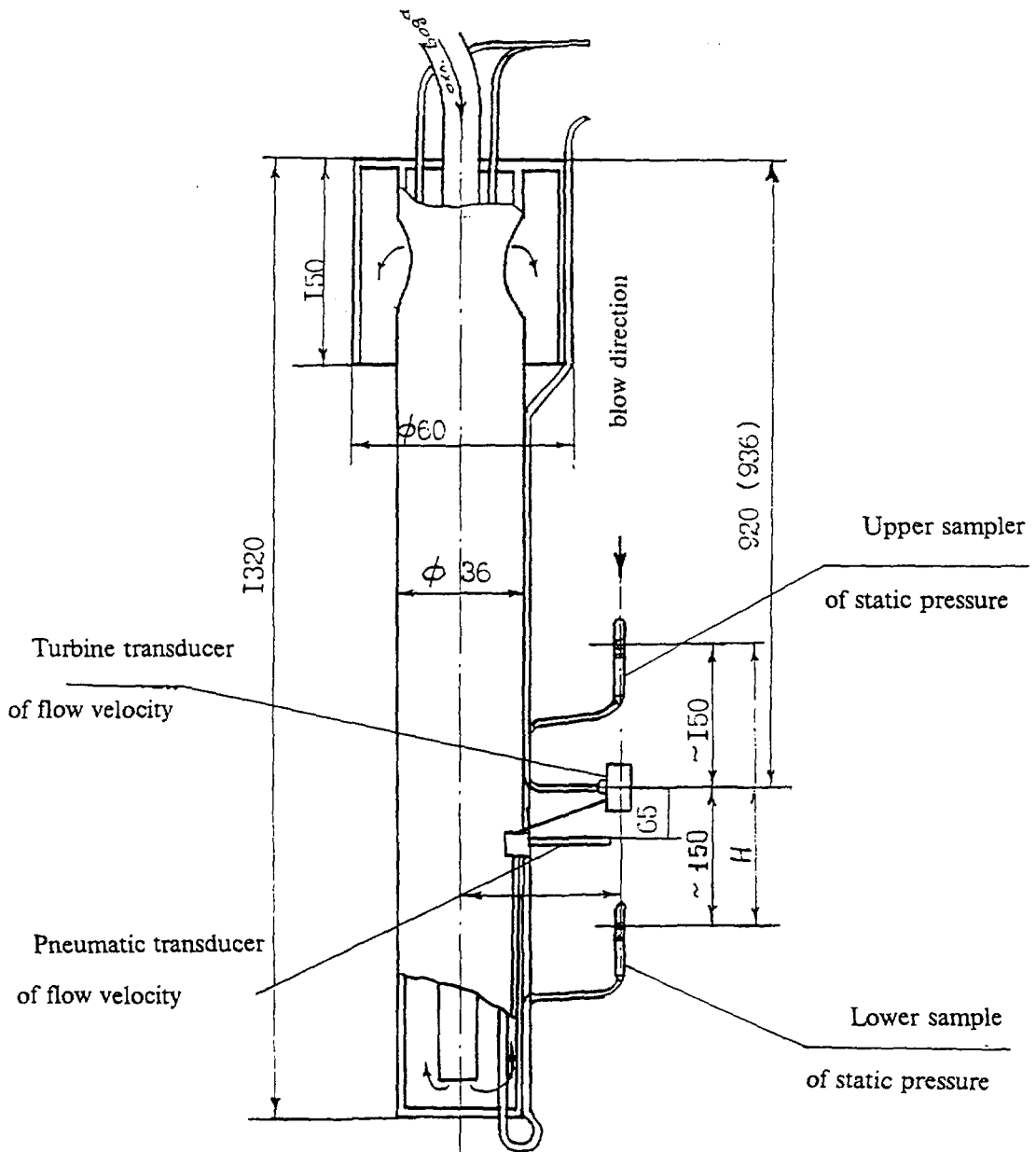


Fig.3 Measuring rod

## **Volume 2. Data bank on the hydrodynamics of Novo-Voronezhskaya NPP fifth unit PGV-1000 steam generator.**

1. Inside vessel measurement system: 18 void fraction hydrostatic measuring transducers, 5 turbine flow-meters for flow velocity and direction determining (fig. 4, 5).

2. Regime parameters measuring range: power change interval is 23-100%, steam load 340 - 1470 t/h, mass level changing is from -300 to +300mm according to the level-meter of the general control board.

3. That was investigated 344 regimes and 4980 experimental points were obtained.

4. Velocity definition accuracy is  $\pm 0.05$  m/c, void fraction definition complex accuracy class is 1,6.



5. Construction peculiarities: the submerged perforated plate embraces the heat exchanging bundle, the investigations were made for two submerged perforated plate modifications with relative living section of 3.7% and 6.1%.

6. Information: experimental data on the void fractions, flow velocities and types, local values of circulation divisibility, submerged perforated plate hydraulic resistance and related water flow through its holes.

Under power of 90-100% there was a not calculated throw of steam-water mixture ( $\varphi=0.8$ ) into the steam volume from the gap between the edge of submerged perforated plate and the vessel at the hot part of the bundle with the velocity of 1m/c.





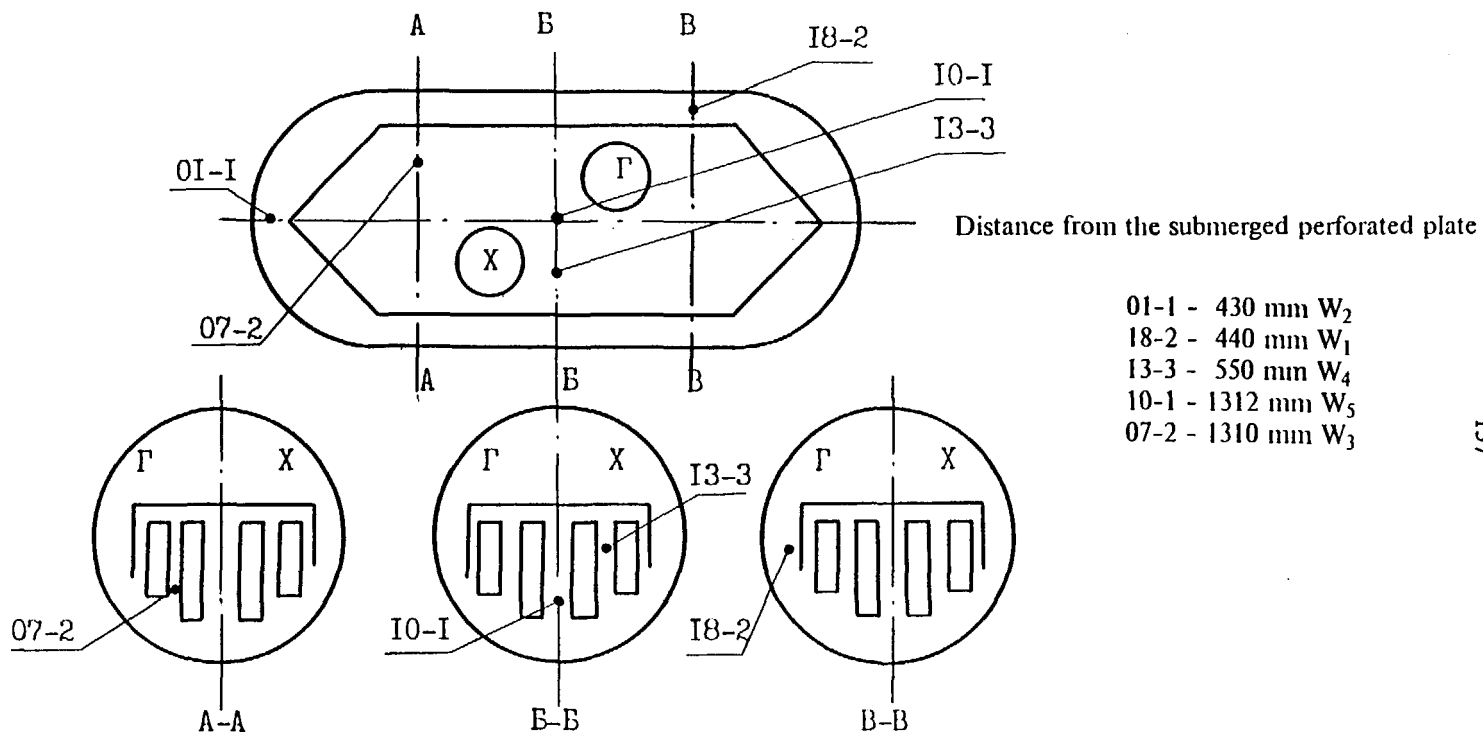


Fig. 5 Installation scheme of the turbine flow-meters in the steam generator

**Volume 3. Data bank on the hydrodynamics of Balakovskaya NPP first unit PGV-1000 steam generator.**

1. Inside vessel measurement system: 11 void fraction hydrostatic measuring transducers, 5 turbine flow-meters for flow velocity determining.

2. Regime parameters measuring range: power change interval is till 100%, steam load up to 1470 t/h, mass level changing is from 2.3 to 2.6m according to the level-meter of the general control board, feed water temperature changing is from 160°C to 217°C.

3. That was investigated 43 regimes and 1750 experimental points were obtained.

4. Velocity definition accuracy is  $\pm 0.05$ m/c, void fraction definition complex accuracy class is 1.6.



5. Construction peculiarities of the modified submerged perforated plate: the submerged perforated plate embraces the heat exchanging bundle, relative living section is 7.3%, the gap between the vessel and the edge at the hot side is covered with plates having the perforation of 8%.

6. Information: experimental data on the void fractions, flow velocities and types, submerged perforated plate hydraulic resistance. The additional plates installation practically didn't made any influence to the water volume hydrodynamics.

The steam-water mixture throw was liquidated.



Installation scheme of the hydrostatic transducers in SG-4

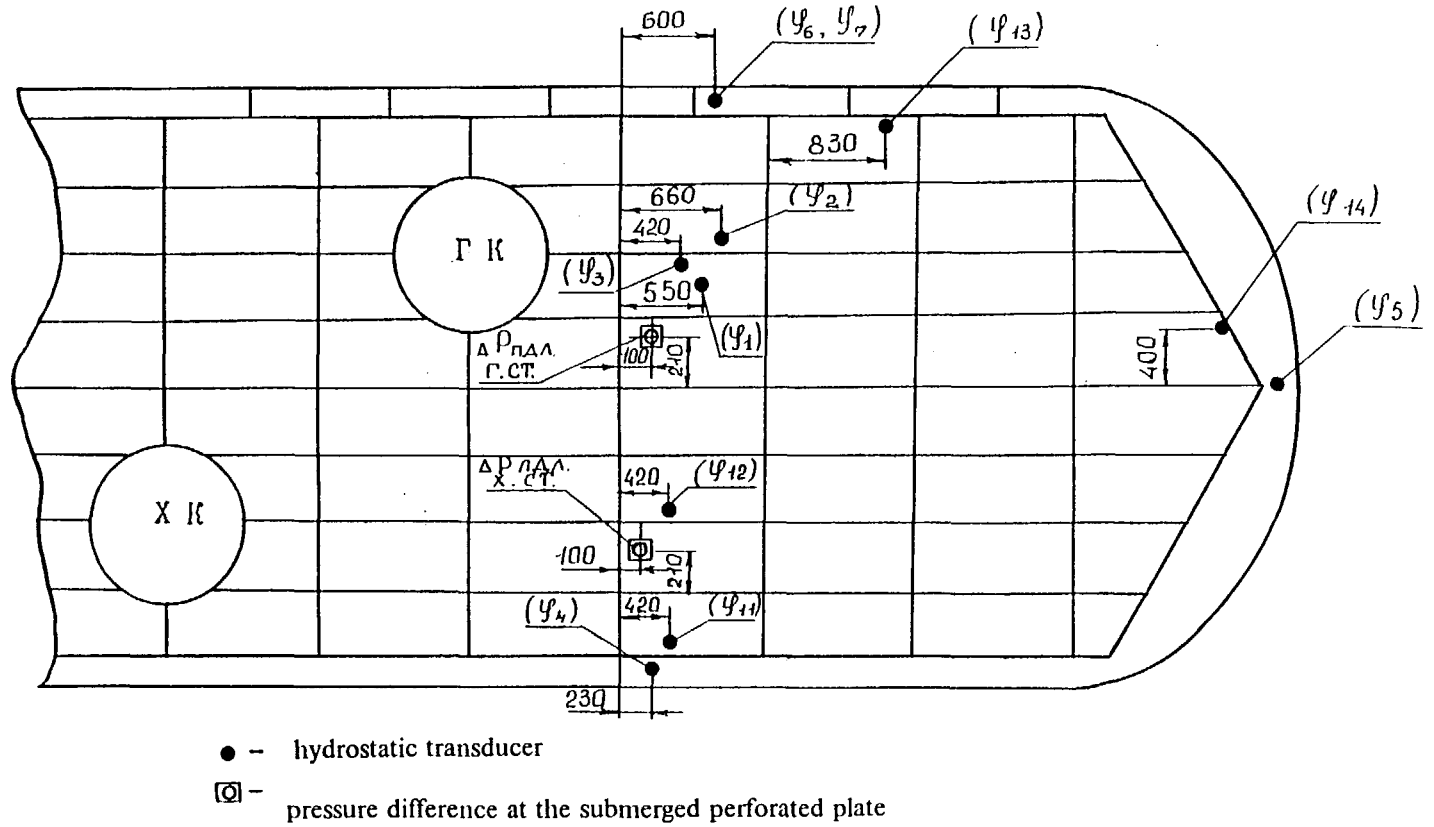


Fig. 6

Tranducer arrangement coordinates in PGV-1000 of YU NPP, NV NPP and Balakovskaya NPP

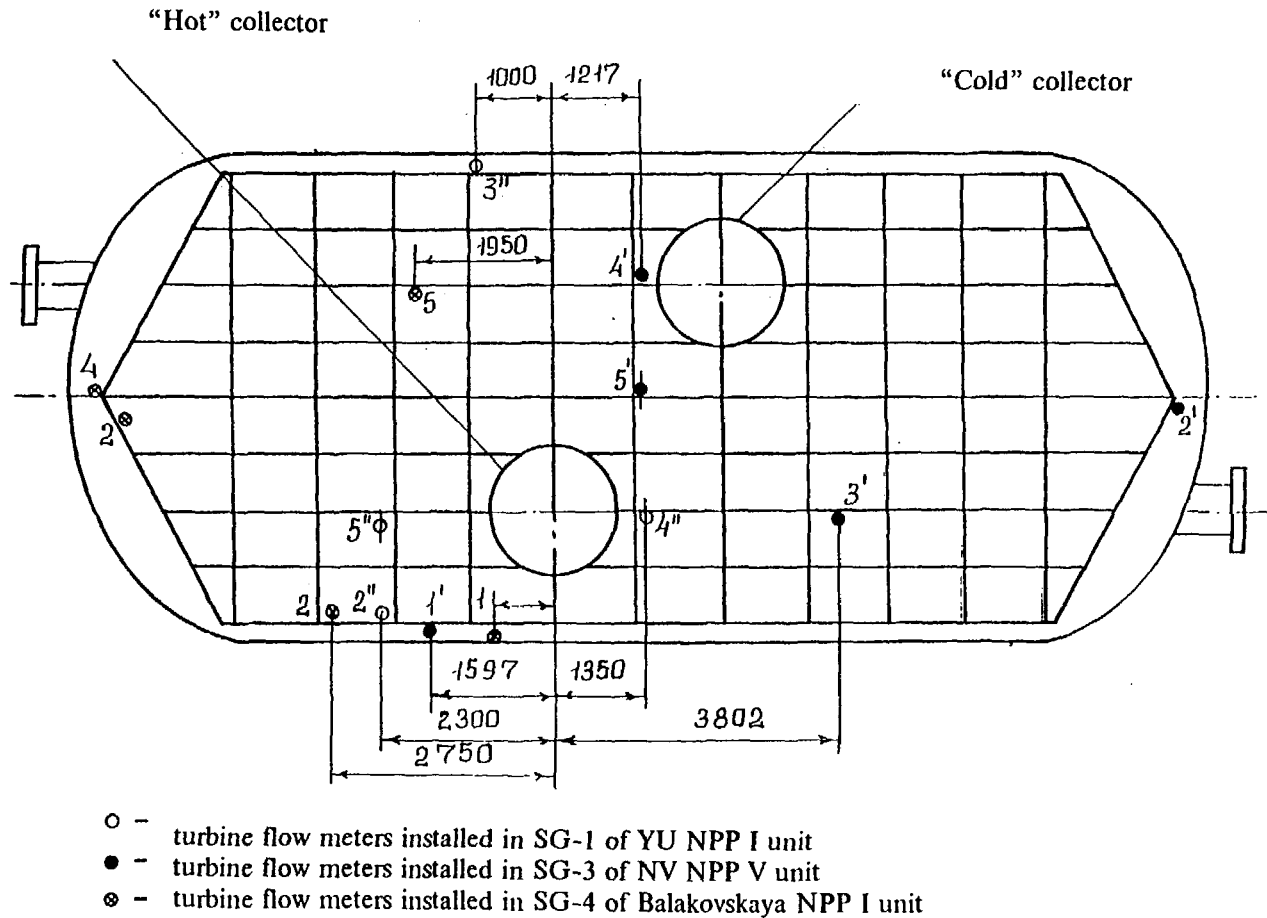


Fig.7

**Volume 4. Data bank on the thermal tests and tube temperature regimes of Yuzhno-Ukrainskaya NPP first unit PGV-1000 steam generator.**

1. Measurement system: under heat exchanging tubes thermometring there are 21 microthermocouples at the 095 and 112 serpentine tubes in the top and third upper tube row (fig.8), standard measuring devices under the heat tests conducting.

2. Regime parameters measuring range: power change interval is 4-102%, steam load up to 1500 t/h, feed water temperature changing is from 155°C to 222°C, mass level changing is from -250 to +40mm according to the level-meter of the general control board.

3. That was investigated 213 regimes and 2310 experimental points were obtained.



4. KSP-4 potentiometer accuracy class is 0.5, PP-63 potentiometer accuracy class is 0.05.

5. Information: experimental data on the heat exchange effectiveness, stable temperature regime of 095 serpentine tube within all the range of regime parameters changing, temperature pulsation decreasing with the power rise in the top row of 112 serpentine tube in all the sections.



Arrangement scheme of the microthermocouples on the serpentine tubes of the PG-1 bundle

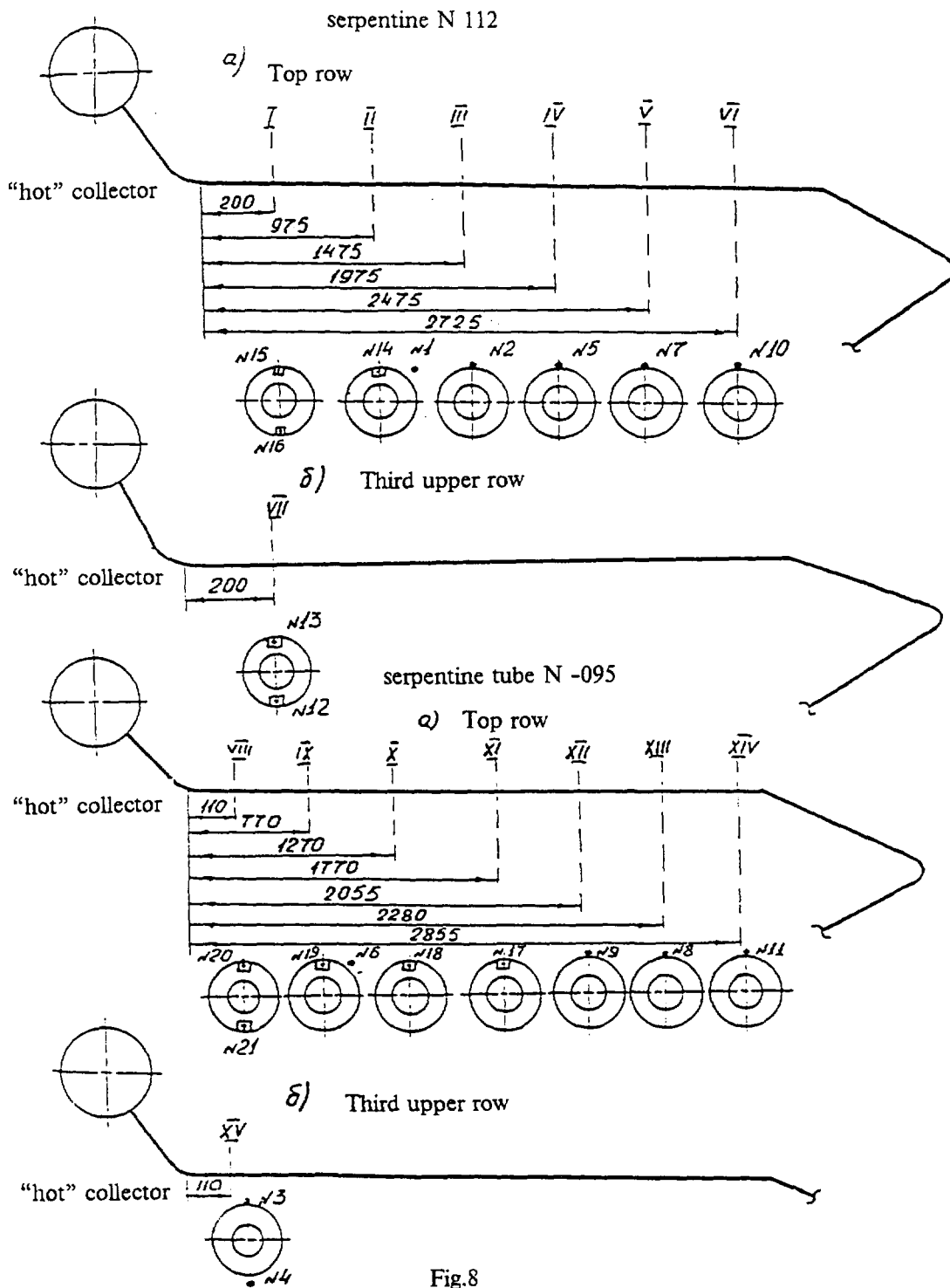


Fig.8

## CONCLUSIONS

At the present time 630 regimes investigation results are presented in the bank, 9700 experimental points are obtained. In the whole finished form in the bank that have been collected a maximum information volume on the tests of CIS-states natural steam generators of VVER-440 and VVER-1000 reactors.

---

**THIRD INTERNATIONAL SEMINAR  
ON  
HORIZONTAL STEAM GENERATORS**

**18-20 October 1994, Lappeenranta, Finland**

**STEAM GENERATOR COLLECTOR INTEGRITY OF  
WWER-1000 REACTORS**

**IAEA EXTRABUDGETARY PROGRAMME  
ON THE SAFETY OF WWER NPPs**

Chengge Lin, A. Strupczewski  
International Atomic Energy Agency

IAEA, Vienna, October 1994

**CONTENTS**

1. INTRODUCTION
2. SAFETY CONCERN
3. STATUS
4. CAUSE ANALYSIS FOR COLLECTOR CRACKS
  - 4.1. FRACTURE MORPHOLOGY
  - 4.2. FAILURE CAUSE ANALYSIS
    - 4.2.1. Aspects related to material
    - 4.2.2. Aspects related to design
    - 4.2.3. Aspects related to fabrication
    - 4.2.4. Aspects related to operation
5. DAMAGE MECHANISM AND RESULTING RECOMMENDATIONS
  - 5.1. DAMAGE MECHANISM
  - 5.2. RECOMMENDATIONS RESULTING FROM DAMAGE MECHANISM
    - 5.2.1. Material related aspects
    - 5.2.2. Design related aspects
    - 5.2.3. Fabrication related aspects
      - 5.2.3.1. Fabrication technology
      - 5.2.3.2. Residual stresses
    - 5.2.4. Operation related aspects
  - 5.3. ENGINEERING JUDGEMENT OF CRACKED COLLECTORS
6. MEASURES
  - 6.1. REVIEW OF EXISTING MEASURES
    - 6.1.1. Backfitting measures for SG collectors with explosive expansion
    - 6.1.2. SG feedwater and blowdown modifications
    - 6.1.3. Inspection and measurements
    - 6.1.4. Cracked collector repair at the plant
  - 6.2. SUGGESTIONS OF MEASURES ON EXISTING SGS
    - 6.2.1. SGs under operation
  - 6.2.2. Steam generators with old design before operation
  - 6.3. NEW DESIGN: SHORT TERM MODIFICATIONS
7. GENERAL CONCLUSIONS AND RECOMMENDATIONS
8. ACKNOWLEDGEMENTS

## 1. INTRODUCTION

At the Consultants' Meeting on 'The Safety of WWER-1000 Model 320 Nuclear Power Plants' organized by the IAEA within the framework of its Extrabudgetary Programme on the Safety of WWER-1000 NPPs, which was held in Vienna, 1-5 June 1992, the problem of WWER-1000 steam generator integrity was identified as an important issue of safety concern.

Considering the safety importance of this issue, a Consultants' Meeting on 'The Steam Generator Integrity of WWER-1000 Nuclear Power Plants' was convened in Vienna in May 1993, attended by 15 international experts in the area to compile information on the steam generator operating experience, deficiencies and corrective measures implemented and planned. In order to also include information from the main designer OKB Hidropress and to finalize the meeting report the IAEA convened a second meeting on the issue on 23-27 November 1993.

The present paper summarizes the information and conclusions from those meetings.

## 2. SAFETY CONCERNS

The first WWER-1000 NPP was put into operation in 1980 and there are currently 19 units operating (November 1993) with 76 PGV-1000 (PGV-1000M) steam generators. The accumulated operational experience is more than 70 reactor-years. In addition, construction of some units was frozen and over 30 PGV-1000M steam generators are being stored by the manufacturer.

The PGV-1000 is a horizontal steam generator, the design of which is based in principle on the 'smaller' WWER's steam generator design with some modifications. In particular the material of the collectors was changed, austenitic stainless steel 08Kh18N10T was replaced by low alloy steel 10GNMFA with higher mechanical (tensile) properties. In contrast to their smaller predecessors, the PGV-1000 steam generators suffered from problems, in particular cracking in the cold collectors. In the period 1986-1991 a number of steam generators had to be replaced due to the cracking problem. Consequently, efforts were initiated to identify the causes of the degradation and it was concluded that a combination of material aspects, design and operation loads are responsible for the damage. Based on the findings available, corrective measures were proposed and implemented at the plants as well as to the design of the steam generators manufactured for the plants under construction.

It is considered that SG collector ruptures are accidents of high safety significance for two main reasons:

- The radioactive primary coolant may be discharged to the environment via the main steam atmosphere dump valves (BRU-A), in the event of a valve sticking open. Worst case calculations show that about 200 t primary coolant/SG water/ECCS water mixture will be released to the environment. Assuming the primary coolant activity during operation ( $I^{131}$ :  $1.2 \times 10^{-4}$  Ci/kg,  $\Sigma I$ :  $3.8 \times 10^{-4}$  Ci/kg) the individual thyroid doses for shift personnel will be lower than 4 mSv. For the critical population group off-site (children below the age of 8) the thyroid doses will not exceed 0.5 msv which can be judged as level 3 according to the INES scale.
- The long term cooling of the core is questionable in case of loss of primary coolant water via BRU-A. The main steam atmospheric dump valves may not close after longer water-steam discharge and there are no isolation valves in front of them.

### 3. STATUS

As of November 1993, 19 units of the WWER-1000 type (7 units in Russia, 10 in Ukraine and 2 in Bulgaria) with a total operating experience of more than 70 years are in operation with 76 SGs of the PGV-1000 (1000M) type.

In the period from late 1986 to 1991 cracks have been revealed in the ligaments between tube holes on the cold collector in 24 SGs at 6 NPPs. Operating time before detection of this damage has varied between 7000-60 000 hours for the affected SGs.

So far cracks have been detected only in the cold collector. However, "indications" have also been reported for the hot collector.

The use of an explosive process to expand the tubes ends into the collector body is a feature common to all SGs which have exhibited collector ligament cracking. The steel used, in all cases where cracking was experienced, emanates from the open melting process. Since beginning of 1988 only steel processed by electroslag remelting has been used for the manufacturing of collectors.

According to the destructive examinations performed on replaced SG collectors, 3 types of collector ligament cracks can be defined (see Fig. 1):

- Satellite cracks of the length up to 1 mm,
- Planetary cracks of the length up to the full thickness of ligament, and
- Arterial cracks, of the length up to 1000 mm.

The crack propagation rate is presently not fully explored. What is known is that by eddy current examination the existence of planetary and arterial cracks can be determined. The maximum crack propagation rate observed until now accounts for six ligaments within one operating cycle. The shape of a large crack bridging several ligaments is said to have a conical form as opposed to the normally accepted elliptical form. The critical crack length has been estimated to be more than 1000 mm.

Since 1989, a lot of modifications have been introduced in the steam generators or in the condition of their operation. They can be summarized as follows:

- Additional mechanical rolling to eliminate the crevices between tubes and collector (not implemented on SGs in operation).
- Release of the collector heads by removal of material in the contact area.
- Low-temperature stress relieving heat treatment (LTHT) of collector material in the perforated zone.
- Chemical cleaning of the SGs' heat transfer area (Kozloduy NPP Unit 5)
- Modification of feedwater distribution and blowdown systems.
- Modification (provisional) of the feed and blowdown water chemistry specifications, (Table VI).

- Introduction of collector ligaments integrity monitoring by means of eddy current examination during the outages. Presently an average of 15% of the tube holes of operating steam generators are subject to annual inspection.
- For SGs under fabrication the explosive expansion process is replaced by hydraulic expansion.

#### 4. CAUSE ANALYSIS FOR COLLECTOR CRACKS

##### 4.2.1. Aspects related to material

The steel 10GN2MFA was permitted as a structural material for NPP equipment by former USSR organization Gosatomnadzor in 1974, after validation tests meeting Gosatomnadzor's rules.

Starting from 1987 several explanations of causes and mechanisms of collector damage have been proposed: corrosion cracking at low-rate strains; plasticity degradation due to technological procedures (drilling, explosive expansion, strain ageing, hydrogen embrittlement, and damage accumulation at quasi-static strain owing to low-temperature creep in corrosive operating medium. Extensive metallurgical investigations of steel 10GN2MFA has been carried out, including the studies of samples taken from damaged SG collectors at NPP. The following results were obtained:

- Plastic degradation of the surface layer in the hole occurs due to hole drilling and explosive expansion and results in specimen cyclic life reduction during in-water tests; preliminary conditioning at different temperatures affects the cyclic life; results of cyclic strength tests of ligament metal specimens in water showed that after conditioning at 'cold' collector temperature for 1000 cycles a net of cracks appeared but after conditioning at the 'hot' collector temperature for 10 000 cycles the specimens did not suffer cracking.
- strain ageing is characterized as transition temperature increase by 30-60°C and impact toughness reduction at 'cold' collector temperature by 40%;
- stepwise drop of characteristic reduction of area appeared in a typical CERT-test (constant strain rate test) with original (non-degraded) material at the temperature of 270°C, that is close to the 'cold' collector temperature (Fig. 2);
- steel 10GN2MFA tends to slow strain corrosion cracking in water at 230-290°C and strain rates of  $10^{-6}$  -  $10^{-7}$  s<sup>-1</sup>. In the temperature region of 230-320°C the correlation  $F = f(t)$  is minimum at 250-270°C.
- when the unexpanded zones within the tube holes in specimens taken from damaged SG collectors were examined, multiple corrosion cracking of practically all holes was detected in 'cold' collectors as the most stressed locations over the 'wedge' and on the central axis where the stresses were substantially lower. In the 'hot' collector holes, a significantly lower number of hole edge defects like corrosion pits or pitting with severely corroded tips were detected.
- it is found that both the drilling and explosive expansion cause a degradation (about twice) in local plasticity and a significant ( $\approx$  40%) increase in surface hardness;

- it is found out that the collector metal in the ligaments is subject to residual stresses; they are quite significant, equalling up to 30 kg/mm<sup>2</sup>.
- open-melted collector metal has local impurity concentrations, including manganese sulfide which have deleterious effects during hydrogen cracking as well as during anode cracking;
- correlation of data on hydrogen ion concentration (pH index) with time before cracking demonstrated increased liability to cracking of steel 10GN2MFA at low pH values. The higher sensitivity of this steel to SG water chemistry and its deviations, indicates the governing role of water chemistry in case of unsatisfactory operation of water supply path, fresh water leakage, ion-exchanging resin intrusion etc. (Fig. 3);
- it is revealed that effects of hydrogen diffusion lead to substantial decreases of strength and plasticity (by 3-4 times);
- for steel 10GN2MFA loaded beyond the yield point, that is, being actually in the plasticity region, the process of low temperature creep is of great importance for the slow quasi-static strain. The investigation is continuing.

The new data obtained lead to the conclusion that the steel 10GN2MFA, at the temperatures at which the 'cold' collector operates, has unfavourable properties previously unknown. These were not revealed during the 'standard qualification' testing prior to the decision to use this material. The properties discussed appear only under a combination of process history of the metal, manufacturing (residual) and operating loads and of water chemistry. Together with investigations of other trends the studies of steel 10GN2MFA have shown that a mechanism of SG 'cold' collector ligament damage was not known before in the Russian SG fabrication industry. The damage occurs under the conditions of slow strain related to low-temperature creep is dependent on metal local strength and plasticity resulting from interaction of high residual stresses and operating load stress fields in secondary circuit and on the water chemistry. The effects revealed show themselves in a narrow range of combinations of non-linear effects of damaging factors close to the 'cold' collector operating conditions.

The damage mechanism seems to be to some extent comparable to 'strain induced cracking' (SICC), observed in low carbon steel piping of boiling water reactors in western countries; there, of course, the oxygen content plays a significant additional role. In WWER reactors with expected low oxygen level, a low pH value might play a similar role. The preconditions for this 'strain induced cracking' are the simultaneous occurrence of low alloy steel, low strain rates with stresses being sufficient to cause plastic deformations, high oxygen content and temperatures between approximately 150 and 300°C. In all cases failures are connected with additional loadings (e.g. pipe-whip restraints which inhibit strain, welding flaws leading to notch effects) or stress concentrations in connection with pitting.

The SICC is judged to be determined by an anodic solving process and re-passivation at the crack tip (Fig. 4, 5). Unalloyed and low alloy steels in high-temperature water form a protective coating (magnetite), which is resistant to global and local corrosion under normal BWR and PWR conditions. This coating has only a low ductility (because of its oxide structure) and breaks at strain values far below the yield strength of the base material. It is thought that the crack initiation process begins by the breaking of the magnetite protective layer as a result of slow strain changes during operation. Corrosion attack can then occur (pitting accelerated by locally higher conductivity and the electro-chemical effect of copper) providing further stress concentration. Crack propagation during

cold shutdown occurs, probably during cold shutdown by low frequency mechanical loading (e.g. during startup). This is exacerbated by oxygenated high temperature water.

The effect is accelerated in case of existing MnS-inclusions.

#### **4.2.2 Aspects related to design**

The SG PGV-1000 design is based on SG experience for WWER 440 reactors. The collector structure of both SCs is in principle the same, with similar non-symmetrical perforation zone. The explosive technology has also been used in the SGs of WWER 440, the main difference being in the material used.

PGV-1000 strength calculations for operational conditions were performed according to the valid normative requirements and meet them for the whole spectrum of design conditions. The loads due to operational conditions (not considering the manufacturing residual stresses) meet the requirements of standards for strength over all the design service life.

On the basis of design analysis, as a measure to improve the collectors SSS, a flattening of the wedge profile was proposed and realized on those SGs where it was possible, with a reduction in the stress concentration coefficient of about 15%. Perforation asymmetry relative to vertical axis through the wedge peak was removed. As shown lately, these measures have not proved effective against SSS.

#### **4.2.3. Aspects related to fabrication**

Measurements taken before and after expansion showed that for the processes used the sequence of explosive tube expansion did not significantly affect the collector SSS.

Calculating analysis was carried out using the data of collector strain during explosive expansion. The results showed that for the collector loose state the conventional-elastic process stress level in the 'wedge' area is about the yield strength of steel 10GN2MFA and for the collector 'contact' state it may reach a value of two times as high.

Comparison of residual manufacturing stresses with the stress level resulting from the operational loads allows the conclusion to be drawn that the main factor of the stress state in the collector damaged area is the tube explosive expansion.

Starting from 1990 the explosive expansion was abandoned and replaced by a hydraulic one for the SG under fabrication.

In summary, the negative factors leading to collector loading by high residual stresses and partial loss of plasticity in the course of fabrication have been identified and also measures to improve collector reliability and life prolongation (collector loosening, tubes additional expansion, low-temperature heat treatment, replacement of explosive expansion for hydraulic one, ligament integrity monitoring) have been taken.

#### **4.2.4. Aspects related to operation**

The 'hot' collector was free of temperature inequality and fluctuations. The distribution of soluble impurities in SG water volume was studied. The investigations showed that distribution of soluble impurities cannot be the governing cause of 'cold' collector damages as the area of maximum impurity concentration is not around the 'cold' collector, but between 'hot' collector and 'hot' SG edge, where they are 2-2.5 times as high.

It has been shown elsewhere that at low strain rates ( $6.8 \times 10^{-7} \text{ s}^{-1}$ ) the corrosion cracking resistance of steel 10GN2MFA melted in open hearth furnace noticeably depends upon medium pH, chlorides and oxygen content. A decrease in pH value (transition to acid region), and an increase in the chloride and oxygen content reduces the steel 10GN2MFA corrosion cracking resistance.

The susceptibility of steel 10GN2MFA to hydrogen embrittlement has been studied. The hydrogen content of the metal was found to increase when in contact with water at the operational conditions of temperature and pressure. The degree of increase depends upon water pH value, e.g. if pH = 4.5 and holding-up = 1000 hours, the hydrogen content exceeds its initial concentration by 1.5-1.8 times. It is observed that the hydrogen content increases with holding-up duration. At the initial pH value = 9.0, no hydrogen concentration increase is observed. Hydrogenated specimen tests demonstrated that reduction of area (tensile test) drops from 51% to 9.3% with hydrogen content increase from 0.34 cm<sup>3</sup>/100 g to 3.53 cm<sup>3</sup>/100 g. Thus the tests show that collector integrity depends upon the water chemistry. Administrative and technical decisions on the water chemistry problem have been taken.

## 5. DAMAGE MECHANISM AND RESULTING RECOMMENDATIONS

### 5.1. DAMAGE MECHANISM

Collector damage is a complex multi-influence phenomenon. The fact is revealed in its peculiarities; only cold collectors are damaged, indicating localization of flaws, collector ligament rupture morphology, and the damage mechanism itself.

Operational temperature is of major importance for explanation of cold collector damage. Precisely at the cold collector operational temperature (280-290°C) the medium is especially aggressive and causes the metal plasticity degradation under the conditions of slow strain observed especially for 10GN2FMA steel melted in open-hearth furnace which has the highest sensitivity to stress corrosion cracking.

The cold collector degrades only under the combined effect of high-level stresses (the resultant of manufacturing and operational stresses leading to low temperature creep and slow plastic strain) and of the corrosive medium. The corrosive effect increases significantly with plastic strain and with the reduction of pH in the structural gap between the tube and the collector wall at cold collector temperature.

This fact leads to the basic conclusion that the general damage mechanism is an 'environmentally assisted cracking' (EAC);

### 5.2. RECOMMENDATIONS RESULTING FROM DAMAGE MECHANISM

### 5.2.1. Material related aspects

- Low alloy steels are not susceptible to EAC under defined pure water conditions.
- But in water, containing high level of oxygen or low pH value and at low strain rates or constant loading, low alloy steels are sensitive to damage.
- Damage process is accelerated by presence of MnS-inclusions in general.
- To reduce or eliminate the occurrence of intergranular cracking during subcritical crack growth by EAC mechanism, it is necessary to maintain very low level of microsegregating elements, e.g. phosphorus.

#### Recommendations:

1. Steel making technologies reducing sulphur and sulphide inclusions content should be applied.
2. Secondary metallurgical methods (vacuum metallurgy, electroslag remelting etc.) are suitable to improve considerably the toughness level of the steel.
3. The possibility of applying other structural steels to collectors or to its perforated area can also be considered. The special aspects of a bimetallic weld in such an outstanding location (inside the SG) has to be considered very carefully.
4. The qualification programme of steel shall include a check of corrosion and mechanical strength at low strain rates and corrosive medium attack.

### 5.2.2. Design related aspects

- Design of collector is characterized by the presence of non-perforated zones (V and path configuration) which result in stress concentration during fabrication and operation. Gidropress experts calculated this stress concentration factor increased by 15% as compared with that in the area of uniform perforation.
- Thickness of ligament obtained in design from the strength calculation does not fully conform to the explosive loading during the tube expanding process. But Gidropress experts considered thickness of ligaments meets the requirements of standards and amounts to more than 9 mm from the secondary side.
- The design of the cold and hot collectors is identical. Absence of hot collector cracks indicates that the design geometry is not the major factor affecting initiation and propagation of the cracks on the cold collectors.
- In order to avoid over-expansion of tube during explosive expansion the design provides a non-expanded area at the secondary side. This leads to a crevice in which local deleterious chemical conditions can exist.
- According to experiences gained in WWER 440 SGs and also in 1000 SGs the feedwater supply designs do not ensure homogenous water chemistry around the collector.

**Recommendations:**

1. The perforated area geometry should be improved by avoiding the non-perforated path and by 'smoothing' the 'wedge' profile..
2. Crevices between tubes and ligaments should be minimized for example by supplementary rolling expansion for new SG collectors.
3. Verification by suitable calculation models and full scale measurements for above mentioned recommendations are necessary.

**5.2.3. Fabrication related aspects**

The manufacturing procedures and technological processes should be optimized for a specific design, but in the given case the tube expansion technology is mismatched with the collector structural design.

*5.2.3.1. Fabrication technology*

- Proper use of drilling technology and equipment results in compressive stress state on the hole surface, protecting the hole from the beginning of stress related corrosion attack.

Achievement of the compressive stress state needs adjusted qualification of the process, the equipment and quality assured performance.

- It is necessary to consider the effect of cladding and tube to collector welding on the stress state.
- For the SGs of WWER-1000 reactor, two technologies of tube expansion have been used; these are explosive tube expansion (for most SGs in operation) and hydraulic tube expansion.

The explosive technology according to the existing requirements has the following consequences:

- (i) The average level of the perforated area plastic strain measured in direct way is  $\sim 0,5\%$ , but a strain value of 3-5% may exist locally which leads to strain ageing phenomenon at operation temperature;
- (ii) macroscopic deformation of the collector (average strain in the collector perforated area as a whole is  $\sim 0,5\%$ ) this effect can be reduced by modification of the sequence of explosive expansion process in the whole collector;
- (iii) high residual tensile stresses especially in the area of ligament corresponding to the transition of expanded to non-expanded part of the tube.

According to stress investigations, residual stresses of manufacturing origin exceeding yield strength are localized in the non-perforated parts (V-configuration and non-perforated path).

In contrast to that the hydraulic tube expansion technology as applied in Vřtkovice results in only partial plastic deformation of the ligament, low residual stresses in the non-perforated zones and compressive stresses on the internal surface of holes.

**Recommendations:**

1. Increasing service life of the collectors requires to lower the residual stresses in ligaments resulting from fabrication.
2. In presently manufactured but not yet operated SGs where the tubes were expanded explosively, stress relieving is needed, e.g. by low temperature heat treatment and supplementary expansion of non-expanded parts of tubes; the methods and equipment used for these processes will need to be proved, and the impact of LTHT (tube sensitization risk) shall also be analysed.
3. In case of SGs which are in operation the recommended step after preliminary non-destructive testing is to apply localized short term heat treatment which will both reduce the residual stress and improve the material properties. Also this procedure needs full size model qualification and calculation and measurements of stresses as well. At OKB Gidropress such investigations have been performed.
4. Additional rolling on collectors of SGs in operation has disadvantages of not forming fully consistent metallic bond between tube and hole and of the risk of excessive strains in the tube due to possible over-rolling. Conclusions in respect of this approach cannot be drawn until inspection results are available following longer in-service experience.
5. At present status of knowledge the closing of crevices is not recommended without verification that the crevices are completely cleaned from oxides and salts. If the results of verification are positive, the cleaning should be combined with subsequent additional rolling.

**5.2.3.2. Residual stresses**

- The hydraulic tube expansion can improve the stress state in ligaments and the whole body of the collector because only partial plastic deformation of ligaments occurs which results in compressive residual stresses on the hole surface and in relatively low tensile stress at the elastic-plastic boundary.

**5.2.4. Operation related aspects**

- The water chemistry contributes substantially to the initiation and propagation of cracks in affected collectors.
- Deviations from proper water chemistry were observed. Existence of Cu in water from condenser and tubes accelerated the corrosion process. Absence of continuously monitoring techniques of required sensitivity for water chemistry makes the timely corrections of deviations impossible.
3. Startup and shutdown regimes should be optimized in order to avoid high thermal and stress gradients in the SG collectors. In addition, the conservation of the steam generators during the outages should also be considered. In some Member States, wet lay-up chemistry has

been fairly well standardized in terms of pH control (> 9.8 with ammonia) and hydrazine concentration (> 75-150 or 200 ppb). During restart, the auxiliary feedwater should be dosed with ammonia and hydrazine to maintain a minimum pH around 8.8-9.0 and a hydrazine content which is at least 3 times the dissolved oxygen concentration.

## 6. MEASURES

### 6.1. REVIEW OF EXISTING MEASURES

Measures which have been already taken on WWER-1000 SGs are reviewed in this section. After a short description, each measure is analysed with recommendation given in section 6.2.

#### 6.1.1. Backfitting measures for SG collectors with explosive expansion

- Thermal heat treatment (about 450°C) of cold and hot collectors was performed before or after plant startup.
- Complementary mechanical rolling of crevice area of cold and hot collectors was performed before steam generator commissioning for twenty steam generators.
- Restoring clearance between collectors (cold and hot) and SG vessel flange was performed for all steam generators in operation.

#### Analysis:

- *A thermal heat treatment is needed to release the residual stresses in the collector.*
- *The experience of 2 years operation of about 1.5 million connection of tube and collectors showed that there is no indication for loss of tightness between tube and collector bore, if LTHT is performed without subsequent rolling.*
- *Technology of the subsequent mechanical rolling of crevice area shall not lead to over-rolling (beyond secondary side) which can induce high residual stresses in the tube. This rolling can modify the microstructure of the stainless steel tube, thus the technology for detection of potential cracks shall take it into account.*
- *After plant startup, mechanical rolling (or any other expansion process) of the crevice area requires thorough precleaning of the crevice.*

#### 6.1.2. SG feedwater and blowdown modifications

The modifications taken in feedwater and blowdown systems of operating plants involve:

- (i) feedwater redistribution mainly in hot side,  
no more feedwater injection in (new) continuous blowdown area,
- (ii) additional vertical partition plate near the cold end of SG,

- (iii) additional blowdown piping for total continuous blowdown rate under the water level in the compartment between partition plate and cold end,
- (iv) existing blowdown areas reserved for periodical blowdown only, and
- (v) associated increase of blowdown rate.

Analysis:

- *The whole set of modifications lowers mineral concentrations in the SG secondary side: factor = 50 in hot side, factor = 2 to 3 near cold collector. Only exception: the new compartment area where continuous blowdown is done.*
- *The modifications improve the continuous blowdown efficiency by extracting water from the high mineral concentration area (compartment created between partition plate and SG cold end).*
- *Continuous blowdown flowrate has to be set as high as acceptable in order to comply with the applicable secondary water specifications.*

### 6.1.3. Inspection and measurements

Each SG is subject to inspection at manufacturers. Eddy current examination of cold and hot collector ligaments has been carried out annually since 1988 during maintenance outages and also during unscheduled outages when the causes of SG water radioactivity increase were sought.

Analysis:

- *A pre-service examination of both hot and cold collectors is a necessary element for further comparison with in-service examination results.*

### 6.1.4. Cracked collector repair at the plant

The repair consists of the drilling tubes out in those holes in which the cracks in ligaments have been revealed during inspection; subsequently these holes are plugged by thin-walled blank flanges across practically the whole thickness of collector. The repair duration is not very long (about one day for one hole). In case of a large number of cracked ligaments in the same area, this repair technique cannot be applied and the SG has to be replaced.

Analysis:

- *Up to date, the operating experience of such a repair is one year, which is not sufficient to conclude, even if no crack has been detected during collector inspection at refuelling outage. A qualification programme for repair techniques is necessary.*

## 6.2. SUGGESTIONS OF MEASURES ON EXISTING SGS

Measures are proposed for SGs under operation (section 6.2.1.) and SGs with old design before operation (section 6.2.2.).

### 6.2.1. SGs under operation

Recommendations related to detection, inspection, feedwater and blowdown modifications, plant operation conditions, repair and mitigation of accident are made for SGs under operation.

Recommendations:

#### *Inspection of collectors*

1. 100% inspection of cold collectors by automated eddy current technique is recommended for detection of collector ligament cracks. Priority has to be given to the discontinuity areas (e.g. 'V' area).  
All ligaments are to be inspected in cold collectors every four years except the discontinuity areas which are to be inspected every year.  
The discontinuity areas of hot collectors are also to be inspected with a four year periodicity. This periodicity could be relaxed after the first four year period.
2. For heat treated collectors without subsequent rolling, random inspections of tube-to-collector tightness are recommended in order to decide whether additional expansion of all tubes is needed in the explosive expansion area.

#### *On-site crack detection*

3. It is recommended to develop, qualify and implement a plant detection system in all plants, in order to detect crack propagation during operation of collectors (acoustic emission system could apply). Priority is to be given to the cold collectors when installing these systems.

#### *Steam Generator feedwater and blowdown modifications*

4. Present SG modifications (see section 6.1.2) can still be optimized by predictive calculations and on-site verifications (e.g. 2 compartments, one at each end). The modifications should be extended to all operating (or new) SGs.

#### *Plant operating conditions*

5. Secondary water chemistry specifications  
Specifications should be strictly complied with, during operation for feedwater and blowdown water. Corrective actions should be described. It is recommended that these specifications should meet, in the future, international standards for PWR plants (EPRI Guidelines) after adaptation to the stainless steel tube material. In order to comply with the specific secondary water chemistry an "on-line monitoring" system is also recommended.
6. Condenser tubing leaktightness  
It shall be checked as required in order to achieve satisfactory secondary water chemistry.

7. Chemical cleaning in SG secondary side should be recommended after investigation of the damage mechanism is completed and inspection results are available.

*Collector repair*

8. The basic principle of the existing method being kept, the repairing process shall be qualified, and if necessary modified, after representative full-scale tests.
9. A criterion, based on economical and safety considerations, shall be defined in order to decide on repairing or replacement.

*Mitigation of large crack leakage accident*

10. The development of specific operating procedures is recommended, by analyzing from a safety point of view the operator actions which permit to minimize activity releases after such primary to secondary leakage, including safe shutdown.
11. Once the specific operating procedures are approved, training of operator staff is recommended in order to lower human error risk in case of such accident.

**6.2.2. Steam generators with old design before operation**

Recommendations related to stress relieving, crevice closure, inspection and feedwater-blowdown modifications are made for SGs with old design before operation.

Recommendations:

*Residual stress relieving and crevice closure*

1. In case of non-heat-treated SGs, it is recommended that both hot and cold collectors be heat-treated at optimized temperature, i.e. sufficient to significantly decrease residual stresses and not too high in order to prevent tube SCC sensitizing. Consequently, the tube-to-collector tightness shall be checked. If leak tightness is not achieved, a supplementary expansion is to be performed in the explosive area.
2. A supplementary expansion can also help close the crevice near to the secondary side. A particular attention shall be paid to the end of expansion: it shall be close to secondary side but not beyond (2 to 3 mm).
3. In case of heat treated collectors with subsequent mechanical rolling, the tube-to-collector tightness shall be checked.

*Collector ligament inspection*

4. 100% inspection of cold collector by automated eddy current technique is recommended.

*SG Feedwater and blowdown modifications*

5. Once optimized, the SG modifications shall be applied to SGs in the shop before commissioning.

### 6.3. NEW DESIGN: SHORT TERM MODIFICATIONS

#### Recommendations:

##### *Material choice*

1. Two solutions have to be studied in parallel
  - collector made of stainless steel (perforated zone), and
  - collector made of improved low alloy steel.
2. The present low alloy steel material shall be improved (see item "Material related aspects" in section 5.).

##### *Drilling process*

3. It is recommended to use a qualified drilling technology which avoids bore wall defects and results in compressive stress on the bore surface.

##### *Expansion process*

4. The explosive expansion process shall be avoided. The hydraulic process is recommended for the full thickness of collector wall. The expansion shall be recorded.
5. The minimum ligament thickness and the hydraulic expansion pressure shall be optimized to prevent ligament plastification and to ensure tube-to-collector close attachment.

##### *SG thermal hydraulics*

6. The flow distribution in the secondary side (water volume) shall be optimized (calculations) and verified (tests) in order to minimize mineral concentration in collector areas. The feedwater operation should not lead to water level fluctuations during normal operations.

## 7. GENERAL CONCLUSIONS AND RECOMMENDATIONS

1. 24 operating SGs (PGV-1000M) have developed cracks in primary collectors, in the period from 1986 till 1991. Cracking took place after 7000 - 60000 hrs (much less than planned lifetime) of operation. All the cracking occurred at or near the V-configuration of the perforated zone and non-perforated path. According to the available information, this phenomenon occurred on the cold collectors of the SGs. In two cases indications have been reported for hot collectors.
2. The SG collector cracking is a matter of safety concern. It may cause leakage from primary to secondary water/steam system, and may even have a potential for collector break if the measures were not undertaken. The observed maximum crack length from the secondary side

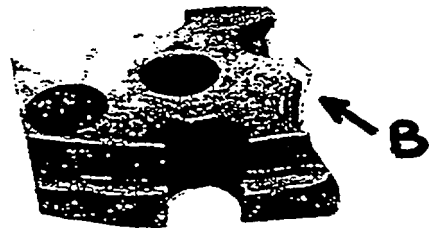
is about 1000 mm, and the critical crack length for this type of crack would be expected more. A collector break may result in two main consequences: i) release of radioactive primary coolant via secondary atmospheric dump valves to the environment, and therefore ii) loss of reactor core water inventory for long-term core cooling.

3. The causes of collector cracking analysed are identified as environmentally assisted cracking (EAC) at temperatures of about 280°C. But the damage mechanism needs to be quantified according to factors of impact related to material, environment and stresses in order to specify the countermeasures and to precise the recommendations given in this report. A co-ordinated programme to address the damage mechanism and the predictive model in more detail should be established.
4. The cracking phenomenon seems to be clarified so far, and countermeasures are judged to be effective to address the problem. This is especially important also for development of advanced SG-types.
5. Some existing measures taken for WWER-1000 SGs were reviewed. The stress-relieving heat treatment as well as the loosening of the header by machining is needed to release the stresses in the collector. Experience has shown no indication of losing tightness between tube and collector. A complementary mechanical rolling of crevice area is not recommended for SGs in operation because it may lead to over-rolling with respect to the deposits in the crevices; in case of SGs not yet in operation an additional mechanical rolling after LTHT is expected to have a positive effect. The feedwater and blowdown system modifications improve the blowdown efficiency and lower the mineral concentrations in the SG secondary side. The existing non-destructive examination reduces the risk of large crack and leakage during operation, but further development is needed and testing volume on cold collectors need to be intensified within an outage. Up-to-date, the operating experience with repaired collector is only one year.
6. New measures related to detection, inspection, repair, material, manufacturing processes, stress-relieving, accident mitigation and especially operation conditions (water chemistry) were suggested for WWER-1000 SGs under operation and SGs with old design before operation. Some short term modifications are also recommended for new SG design.
7. It should be demonstrated that the measures adopted are sufficient to prevent a catastrophic break of the collectors with very low probability of occurrence.
8. A safety analysis on the WWER-1000 SG collector break accident for longer time scenarios should be made in order to assess the radiological consequence and to develop proper mitigation measures.

Specific emergency operating procedures and operating staff training should be prepared to minimize the adverse consequences.

## 8. ACKNOWLEDGEMENTS

The results presented in this paper were reached through the joint efforts of the IAEA consultants who participated in two IAEA meetings on the subject and used experimental results obtained mainly by OKB Hidropress (Russian Federation), Vitkovice (Czech Republic), the NPP operators in Kozloduv and Zaporozhe NPPs, with valuable contributions of western organizations which studied the problems of SGs in WWER 1000 reactors, mainly Intercontrole ( France), and Siemens ( Germany). The IAEA staff involved in the preparation of the IAEA report on SG collector integrity of WWER 1000 reactors ( WWER-RD-057), included the leader of the Extrabudgetary Programme on Safety of WWER NPPs, Mr. L. Lederman and the staff members, Mr. Mr. R.Havel, J.Hohn, and C.Lin.



TYPICAL PLANETARY COLLECTOR CRACK ON PULLED COLLECTOR SAMPLE

TYPICAL PLANETARY (B) AND ARTERIAL (A) COLLECTOR CRACKS ON PULLED COLLECTOR SAMPLE

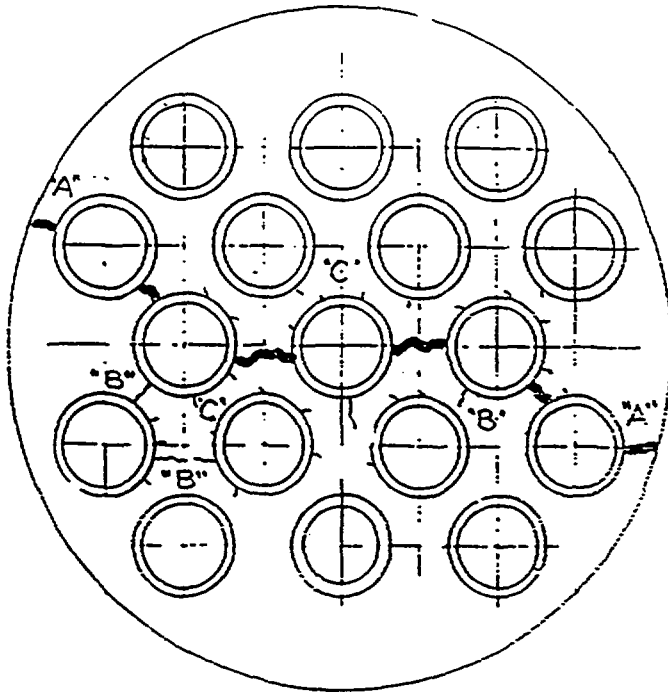


FIG. 1. Schematic presentation of typical collector cracks: arterial cracks (A), planetary cracks (B) and satellite cracks (C).

Reduction of area

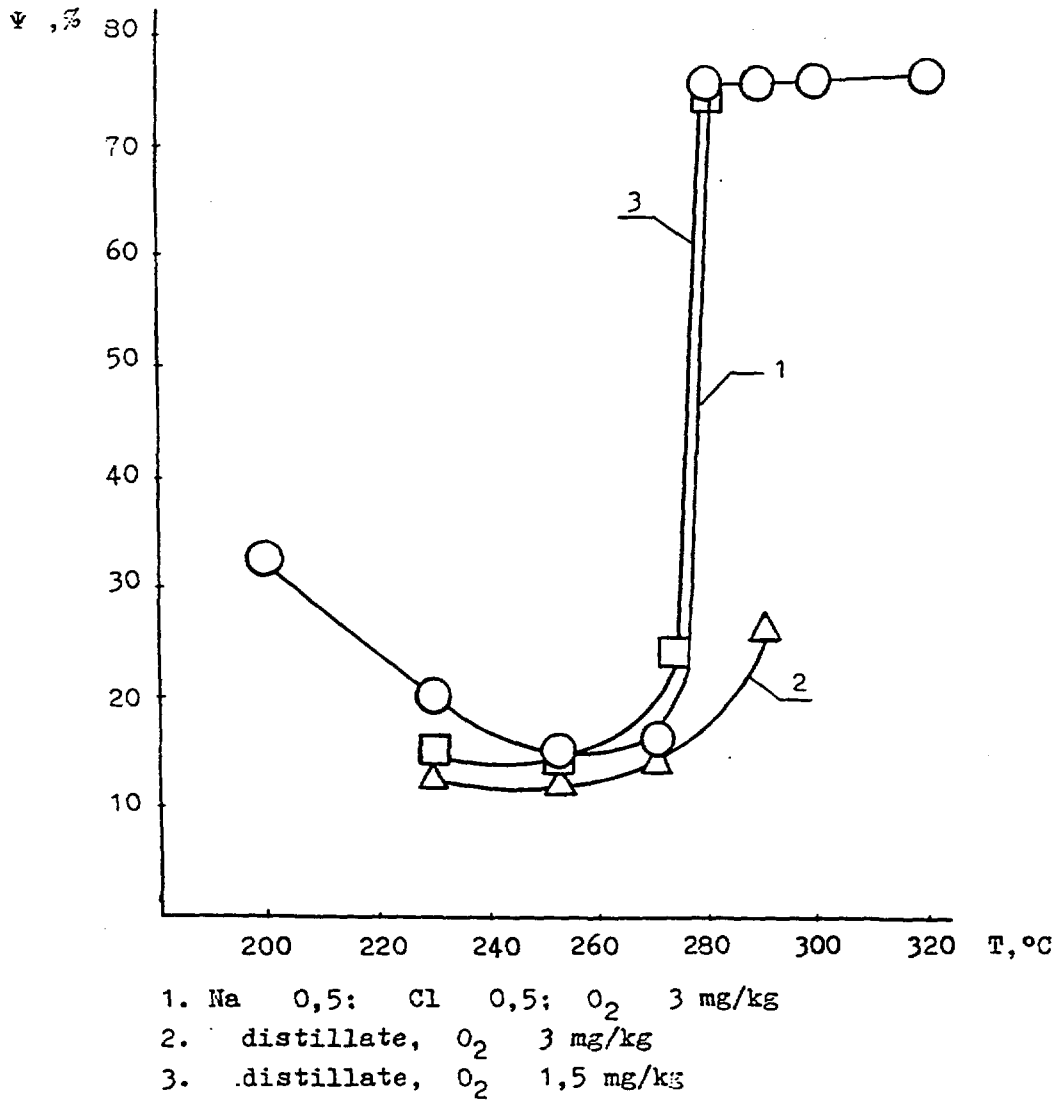


FIG. 2. Influence of ambient temperature on steel 10GNM2MFA brittle fracture resistance during tests in high-parameter water under slow strain tension load

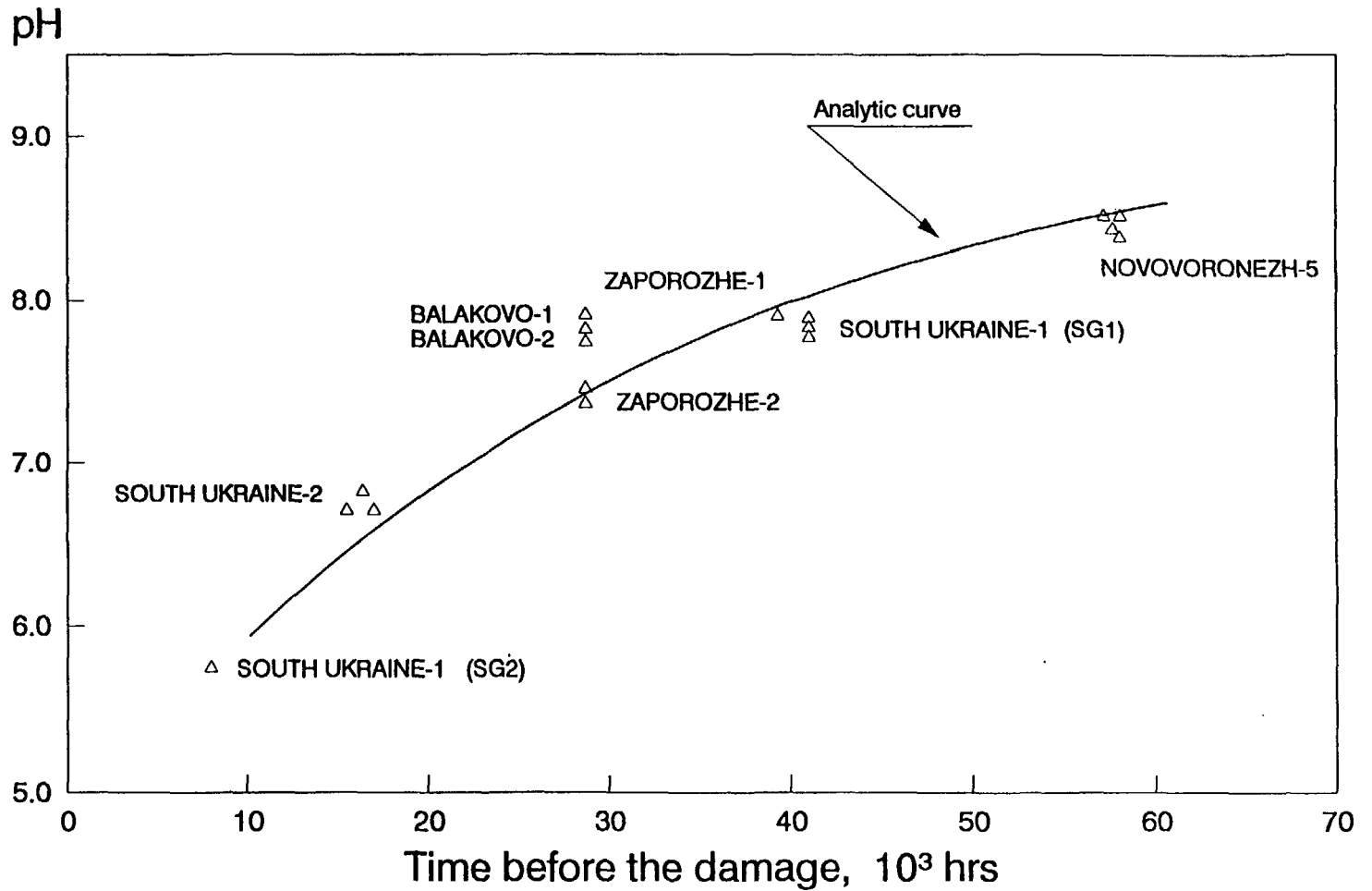
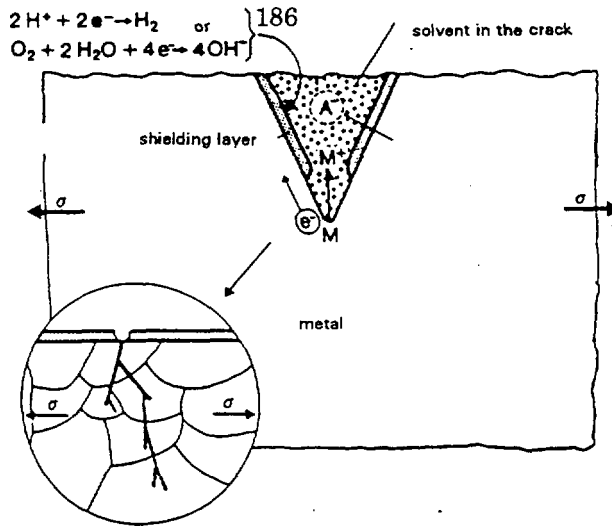


FIG.3



SICC is determined by anodic solving process and the kinetic of repassivation at the crack tip. Cracking is transgranular. Especially near MnS-inclusions an influence of hydrogen can be observed.

FIG. 4. Strain-induced corrosion cracking (SICC)

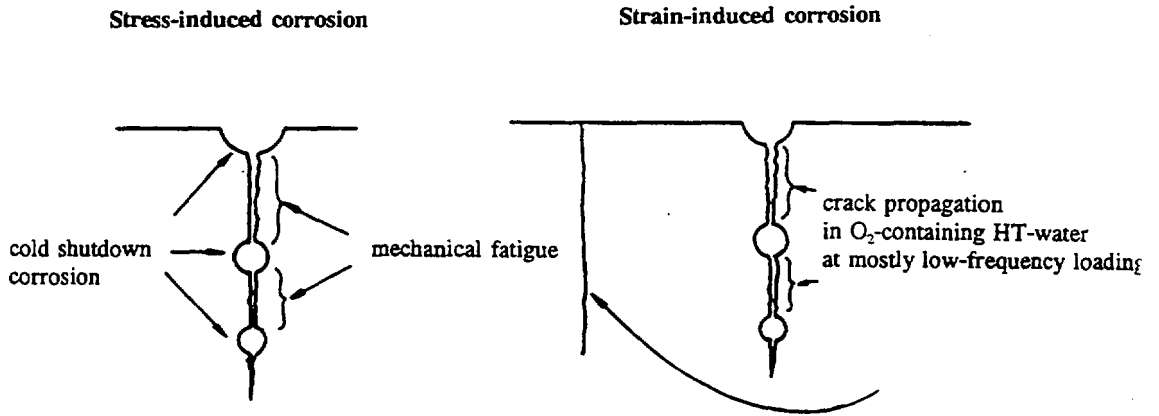


FIG. 5. Schematic description of crack corrosion types

**THIRD INTERNATIONAL SEMINAR ON HORIZONTAL STEAM  
GENERATORS**

**18-20 October 1994, Lappeenranta, Finland**

**ANALYSES OF STEAM GENERATOR COLLECTOR RUPTURE FOR WWER-1000  
USING RELAP5 CODE**

**E. Balabanov, A. Ivanova  
ENERGOPROEKT, Sofia, Bulgaria**

**ABSTRACT**

The paper presents some of the results of analyses of an accident with a LOCA from the primary to the secondary side in the steam generator of a WWER-1000/320 unit. The objective of the analyses is to estimate the release of primary coolant to the atmosphere, to point out the necessity of a well defined operator strategy for this type of accident as well as to evaluate the possibility to diagnose the accident and to minimize the radiological impact on the environment.

The analyses related to leakages from the primary to the secondary side of the steam generator presented in this report have been performed during this year for the purposes of PSA Level 1 of the units with WWER-1000/320 at Kozloduy NPP and some of them have been used as input for emergency drills at these units. Here is an attempt to summarize the results with respect to the functions defining the safety status of the units, namely:

- Decay heat removal from the core
- Heat removal from the primary circuit
- Heat removal from the secondary circuit
- Containing of the radioactive materials

The analyses have been performed on a Pentium computer under DOS, using the RELAP5/RMA code version, which is an analogue of RELAP5/2.5. The model of the unit was developed in Energoproekt, based on a qualified Data Base of the units and tested against plant data for steady state and some transients. The model of the reactor is with two parallel channels representing the average core and the hot assembly and a third channel, representing the core bypass. The main circulation loop with the affected steam generator is modeled separately and the other three are lumped together.

The model of the steam generator is created so that to be able to take into account:

- Decrease of the heat transfer area in case of a decrease of the level in the steam generator
- Internal circulation and flow distribution in the steam generator shell
- Vapour void fraction distribution in the secondary side, especially in the tube bundle region

The basic discretization scheme of the steam generator is given in Fig. 1. The same figure represents the steady state conditions in the steam generator, reached after a stabilization period of 100 s. This model will be proposed to be used in the framework of the IAEA project RER/9/020 "Safety assessment of WWER-1000/320".

According to the design documentation of the steam generator PGV-1000M, the primary collector cover is fixed to place by a set of bolts and is enclosed in a manifold, which is part of the SG shell. The design pressure of the manifold is the same as that of the primary circuit. In case of partial or complete rupture of the bolts, the primary collector cover will be lifted, opening a break from the primary collector to the top part of the SG shell. In this case the limiting flow area of the break is the cross section of the annulus between the outside of the primary collector and the inside of the secondary side manifold. The width of this annulus is approximately 3 mm and the resulting break area is 78.54 cm<sup>2</sup>, which corresponds to an equivalent diameter of 100 mm. The average length of the annulus is about 20 mm.

In order to obtain more adequate modeling of the thermalhydraulic parameters in the vicinity of the break, some modifications were introduced to the scheme presented in Fig.1 as follows:

- The upper volume of the broken hot collector is split into 5 volumes, with a geometry corresponding to the actual geometry of the component. The fourth of these, the "break volume", is 0.2 m long and contains the break at its outlet. The fifth volume is above the break. This finer discretization is selected in order to be able to follow the water level in the collector.
- The break is modeled as a trip valve connecting the break volume to the outlet of the top volume representing the secondary side. The smooth area change option was used for the valve and the pressure loss coefficients were determined taking into account the flow area changes (1.5 in both directions). Analyses were performed using both best-estimate and conservative values for the flow discharge coefficients at the break. The results presented here are with the conservative values of 1.0 both for subcooled and for saturation conditions. The conservative approach in this case is used in order to obtain maximum pressure in the affected steam line, creating the possibility for reaching the setpoint for opening of the safety valve(s).

The selection of the initial and boundary conditions for the analyses is aimed at the creation of the most unfavorable set of resulting parameters with respect to the listed above safety functions.

The heat removal from the core is a function of the reactor power and the coolant flow rate. The characterizing parameters are the DNB, the subcooling of the coolant at the core exit and the maximum cladding temperature. The factors which influence unfavourably these parameters are the peaking factors, the loss of forced circulation due to the tripping of the reactor coolant pumps, the maximum time delays for the actuation and the minimum configuration of the safety systems. The earlier closing of the turbine stop valves decreases the heat removal from the primary circuit and respectively from the core.

The heat removal from the primary circuit is a function of the coolant flow rate, the status of the steam generators tube bundles and on the availability of the routes for heat removal from the secondary side. The earlier tripping of the reactor coolant pumps, the unavailability of the turbine bypass system (BRU-K) and the earlier turbine trip have a negative effect on this function.

The radioactivity release to the atmosphere is a function of the break flow rate and on the availability of BRU-K. The higher primary pressure, at other identical conditions, increases the break flow. In this sense the availability of three trains of the ECCS would have a negative effect on the total coolant release to the atmosphere.

The parameters, which are important for the determining of the source term, are the break flow rate, the break enthalpy and the integrated release of primary coolant to the environment. The time and duration of the release is of primary importance with respect of the estimation of the possibilities for operator intervention and of the development of an operator strategy for the accident mitigation. It is also a parameter which is used by the plant emergency planning programme.

These considerations were taken into account in the selection of the scenarios to be analysed, namely:

- The accident is initiated at power operation of the plant. Taking into account the inaccuracies and uncertainties of the power measurement, the initial reactor power is 102% of the nominal. The coolant flow is assumed to be nominal. After reactor trip the decay heat was determined using the ANS-79-1 curve, increased by 20%. The RCP coast down is calculated using the four-quadrant characteristics of the pumps.
- The efficiency of scram is without the efficiency of the part-length rod bank and assuming that the most efficient control rod fails to drop into the core. The time delay for signal processing is assumed to be 1.4 s and the time for control rod insertion into the core is the maximum allowed (4 s).
- The electrical heaters in the pressurizer are assumed to be available until the loss of power supply, if the level in the pressurizer is high enough for their operation. The heaters operation partially compensates for the pressure decrease resulting from the loss of coolant, thus increasing the break flow rate.
- The loss of external grid (if any) is a consequence of the turbine trip. The result is a tripping of the reactor coolant pumps and the loss of BRU-K. The tripping of the reactor coolant pumps leads to decreased core flow rate and respectively to higher energy release through the break.
- The operators do not make any attempt to apply an emergency procedure during the first 30 min of accident.

The configuration of ECCS has a contradictive effect on the accident development. The minimum configuration creates more severe conditions for the core, while the maximum configuration pressurizes the primary circuit and increases the break flow. For this reason the two boundary cases of one train of ECCS and three trains of ECCS were analysed.

The system for protection of the secondary circuit from overpressurization is represented by one steam dump to atmosphere system (BRU-A) and two SG safety valves for each steam generator. The fresh steam lines up to these valves are modeled with their actual dimensions and both the BRU-A and the safety valves operate according to the pressure in their vicinity.

The setpoints and dump capacities of the valves corresponds to the plant data of Kozloduy NPP and are as follows:

**BRU-A:**

Opening pressure	7.16 MPa(73 kgf/cm <sup>2</sup> )
Closing pressure	6.276 MPa (64 kgf/cm <sup>2</sup> )
Controlled pressure	6.67 MPa (68 kgf/cm <sup>2</sup> )
Time for full opening/closing	15 s
Capacity of a fully open BRU-A at steam line pressure 6.7 MPa	900 t/h

**SG safety valves:**

	Opening pressure	Closing pressure
First SG SV	8.2 MPa (84 kgf/cm <sup>2</sup> )	6.86 MPa (70 kgf/cm <sup>2</sup> )
Second SG SV	8.4 MPa (86 kgf/cm <sup>2</sup> )	6.86 MPa (70 kgf/cm <sup>2</sup> )
Time for full opening:	1 s	
Capacity of one SV:	800 t/h	

As the cases when BRU-K remains available would lead to minor releases and due to the fact that the basic results with respect to accident mitigation are applicable to these cases, here only the results with ultimate loss of BRU-K due to loss of external grid are included. The two limiting cases with one train of ECCS and with three trains of ECCS available are presented as cases A and B respectively. This availability applies also to the emergency feed water system. Table 1 gives the timing of events for cases A and B respectively.

The development of the accident is typical for small LOCA from the primary circuit. The initial phase is characterised by a rapid decrease of the primary pressure and pressurizer level. The decrease of the primary pressure leads to the generation of a signal for reactor scram after a few seconds. The reactor scram is followed by turbine trip and opening of BRU-A. Later into the transient the primary pressure is determined by the secondary pressure. Depending on the ECCS configuration, after a certain period of time the leak is compensated. A peculiarity of this accident is that the affected steam generator becomes part of the primary circuit and the coolant lost through the break is released directly to the atmosphere as a result of the operation of the system for protection of the secondary circuit from overpressurization. According to the operational logic of BRU-A the leak may be interrupted for a certain period of time. As a result the mass balance of the primary circuit is restored faster, the pressure in the primary circuit begins to increase and, in case of lack of a well defined operator strategy, a second opening of BRU-A occurs, resuming the primary leak to the atmosphere. The BRU-A flow after the second opening will depend on the ECCS injection rate, thus the further cooling of the primary circuit will be by a "feed and bleed" process, but the coolant lost from the primary circuit will not be returned to the big safety injection tank. So the duration of this way of cooling will be limited by the capacity of the big Boron tank and after its depletion the unit will be left without any means for cooling. This once more confirms the importance of the operator strategy for primary to secondary leaks.

The status of the functions defining safety and important for the accident under consideration is:

**Decay heat removal from the core**

The heat generated in the core is removed due to the steady natural circulation established in the primary circuit after the tripping of RCP. The more severe case in this aspect is case A, for which the maximum void fraction in the core is reached 600 s into the transient and remains below 23% in the average core and 45% for the hot assembly. The maximum cladding temperature remains below its initial value throughout the transient.

**Heat removal from the primary circuit**

The heat generated in the core and transferred to the primary coolant is removed both through the break and through the tube bundles of the intact steam generators. After the 250 s of transient the primary pressure is a function of the secondary pressure for both cases A and B. The cooldown of the primary circuit in case B is enhanced by the intensive injection of cold water by the three trains of ECCS. In the initial phase

of the accident the energy removed through the break reaches 900 MW. Later, with the depressurization of the primary circuit and the decrease of the break flow rate, this value is reduced below 250 MW. In case B, after the second opening of BRU-A of the affected SG, the heat removed through the break stabilizes at about 125 MW.

#### **Heat removal from the secondary circuit**

The heat transferred from the primary circuit both by the tube bundles and directly input through the break is successfully removed from the secondary side due to the operation of BRU-A. It has to be mentioned, that if the opening setpoint, opening velocity and capacity of the BRU-A and the opening setpoint of the first safety valve of the SG are different from those listed above (corresponding to the Technical specifications), it may be expected that the BRU-A will not be capable to remove the excess heat from the affected steam generator and the first safety valve will also be opened.

#### **Containing of the radioactive materials**

The release of primary coolant activity outside the hermetic containment is a direct consequence of the type of accident. Some of the coolant input to the affected steam generator will be released to the atmosphere and/or to the condenser. Before the turbine trip some of the primary coolant will be transferred to the turbine.

Due to the fact that the first opening of BRU-A is expected very early into the transient (14-15 s), it is obvious that the radioactivity release to the atmosphere can not be avoided completely.

The second opening of BRU-A is a function of the operating trains of the high pressure injection system. It is reached during the first half hour of transient (at 670 s) only in the case of three trains of ECCS operating. In case of lack of failures of the ECCS system the liquid void fraction in the corresponding steam line of the affected steam generator rapidly increases after the 300 s (after the first closing of BRU-A). So, in case of a second opening, it is highly probable that the BRU-A will fail to close because it is not qualified for a two-phase flow. Table 2 presents the release from the affected BRU-A to the atmosphere at the 15-th and at the 30-th min of the transient.

It is clear that the minimum configuration of ECCS gives a higher release during the first minutes and provides more time for the operators until a second opening. The maximum configuration of ECCS leads to a smaller release during the initial phase and to an earlier second opening. The maximum configuration will also lead to an earlier depletion of the safety injection tanks. These considerations show the importance of the application of a well defined operator strategy aimed at:

- Prevention of the filling of the steam lines with liquid water.
- Prevention of a second opening of BRU-A of the affected steam generator
- Ensuring the possibility for boration of the primary circuit and of a boron concentration higher than the target concentration for cold shutdown, having in mind that during the cooldown process there will be reverse flow through the break from the broken SG to the primary circuit
- Prevention of the depletion of the ECCS tanks

The first condition for the application of a proper emergency procedure is the quality and quantity of the information allowing the operators to recognise the situation, that is, the symptoms of the accident. As it was mentioned above, the accident has the features of a small LOCA from the primary circuit. During the initial phase the coolant flow from the primary to the secondary circuit is up to 630 kg/s. Due to the loss of coolant, the primary pressure decreases by some 0.1 MPa/s, generating a signal for reactor scram due to low primary pressure at power above 75% of the nominal. At the same time a rapid decrease of the pressurizer level is observed, forbidding the operation of the pressurizer heaters. The depressurization of the primary circuit due to subcooled blowdown leads to a decrease of the subcooling in the hot legs of the primary circuit below 10 K and to the generation of a plant protection signal, causing the isolation of the containment as well as to the actuation of the ASSS programme. After the isolation of the containment the reactor coolant pumps will be tripped due to the isolation of their supporting systems. The pressure in the affected steam generator starts to increase and at the time of scram is 0.15 MPa above the nominal. The pressure in the

intact steam generators is not influenced. The break flow rate being high, the feed water controller is not able to maintain the level in the affected steam generator. So, the symptoms of the accident can be defined as:

**(1) Symptoms of the primary circuit:**

- Decrease of the primary pressure and pressurizer level
- Reactor scram due to the low primary pressure signal
- Generation of a plant protection signal due to a decrease of the subcooling in the hot legs below 10 K. Tripping of the reactor coolant pumps after the isolation of the containment resulting from this signal.
- Decrease of the subcooling in the hot legs, causing the generation of a plant protection signal and the isolation of the containment.

**(2) Symptoms of the secondary circuit:**

- Increased pressure and level in the affected steam generator.
- Disbalance between feed water flow and steam flow in the affected steam generator. The main and emergency feed water lines are isolated automatically. The affected SG starts filling with water.
- Increased radioactivity in the steam line of the affected SG and in the turbine ejectors.
- Increased activity of the SG let-down water.

**(3) Symptoms of the containment**

- The parameters of the confinement are not changed.
- The confinement is isolated due to a signal for primary LOCA (subcooling in the hot legs < 10 K)

These symptoms are well expressed and allow the recognition of the accident and the affected steam generator.

The first two of the objectives of an operator strategy can be achieved by organized cool down of the unit below the setpoint of BRU-A opening through the BRU-K or the BRU-A of the intact loops. In addition the electrical supply of the BRU-A of the affected SG should be disconnected. The cooldown of the primary circuit will interrupt the flow through the break to the affected steam generator and, respectively the filling of the fresh steam part with liquid water. After the pressure in the primary circuit is reduced sufficiently, the affected steam generator should be isolated from the rest of the fresh steam part by closing the fast acting isolation valves.

The third objective is more complex and needs a more sophisticated approach. The operation of the high pressure injection system would increase the boron concentration in the primary circuit. The necessary boration for cold shutdown is usually achieved by the normal make-up/let-down system, which is automatically isolated due to the plant protection signal. So the operators should take the necessary measures to reconnect the system and then continue the boration until the boron concentration is higher than the specified value.

The achievement of the last objective depends on the possibility to avoid a second opening of BRU-A as well as on the reducing of the part of the secondary side which is directly connected to the primary side by closing of the fast acting isolation valve of the faulted SG.

The results of the analyses show that the radiological consequences of an accident with a primary collector break in the steam generator can not be avoided completely but can be considerably limited by the application of a well defined operator strategy. The information and means for applying of such a strategy is available on the WWER-1000/320 units.

TABLE 1: Timing of events

No	Event	Time (s)	
		Case A	Case B
1.	SG collector cover opening	0.0	0.0
2.	Reactor scram due to primary pressure < 150 kgf/cm <sup>2</sup> and reactor power > 75%. 1.5 s for signal processing is included	10.2	10.2
3.	Turbine trip 1.5 s after reactor scram signal	11.75	11.75
4.	Tripping of main feed water pumps together with turbine trip	11.75	11.75
5.	Loss of external grid together with turbine trip - generation of a signal for DG start - tripping of the reactor coolant pumps	11.75	11.75
6.	BRU-A of the affected SG starts opening due to high pressure	14.0	14.0
7.	BRU-A of the intact SGs start opening due to high pressure	15.0	15.0
8.	Maximum pressure in the affected SG reached (8.0 MPa)	20.0	20.0
9.	Generation of a plant protection signal due to subcooling in any of the hot legs < 10 K. Actuation of the ASSS programme	35.5	35.5
10.	Start of high pressure injection to the primary circuit (10 s delay for the pump(s) start and valves repositioning)	45.5	45.5
11.	Saturated conditions in the hot legs	120.0	120.0
12.	Start of emergency feed water injection to the intact SGs	160.0	160.0
13.	Pressurizer empty	200.0	200.0
14.	Liquid void fraction through the BRU-A of the affected loop >40%	1450.0	350.0
15.	Closing of BRU-A of the intact SGs	350.0	160.0
16.	Maximum void fraction in the core reached	600.0	180.0
17.	Positive mass balance of the primary circuit	800.0	200.0
18.	Tanks of the high pressure injection pumps are empty. Switching to the big Boron solution tank	400.0	400.0
19.	The pressure in the affected SG is equal to the primary pressure	900.0	250.0
20.	Closing of BRU-A of the affected SG	950.0	250.0
21.	Repeated operation of BRU-A of the affected SG: - opening - closing - opening - closing	- - - -	670.0 1020.0 1080.0 -
22.	Coolant temperature above the core decreases below the saturation temperature	1400.0	200.0
23.	End of the calculation	1800.0	1800.0

TABLE 2: Integrated release from BRU-A of the affected SG to the atmosphere

	During the first 15 min	During the first 30 min
Case A (1 HPIS train)	50.5 t	50.5 t
Case B (3 HPIS trains)	27.0 t	83.0 t

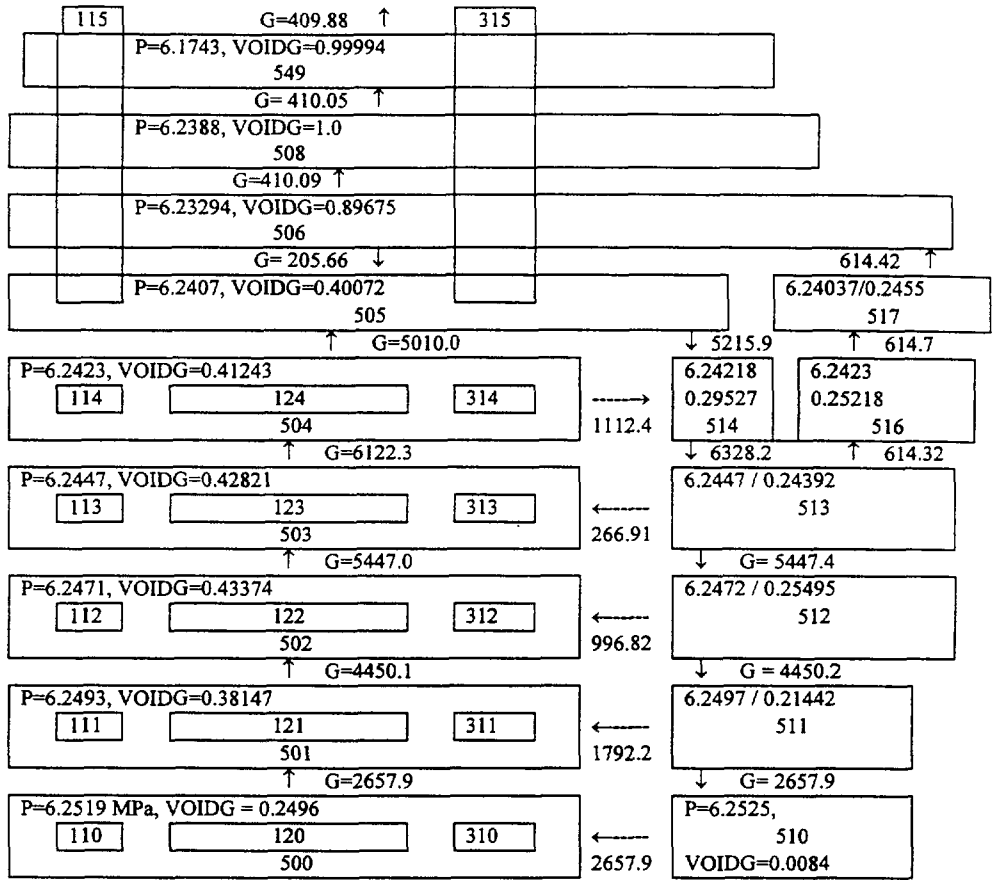


FIG. 1. Discretization scheme and steady state conditions in the steam generator

WWER1000/320: SG collector rupture

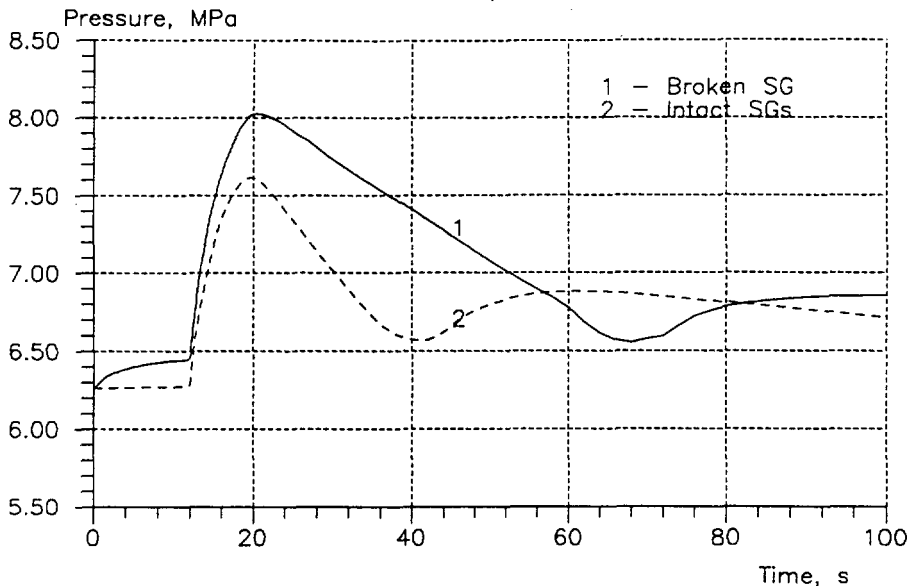


FIG.2. Pressure in the steam generators during the initial phase of the accident

WWER1000/320: SG collector rupture

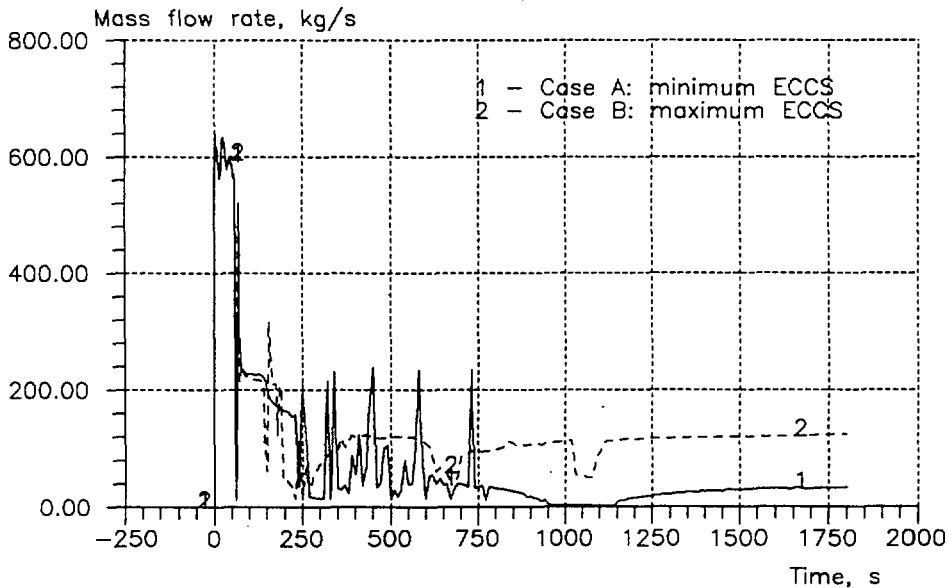


FIG.3. Break flow rate

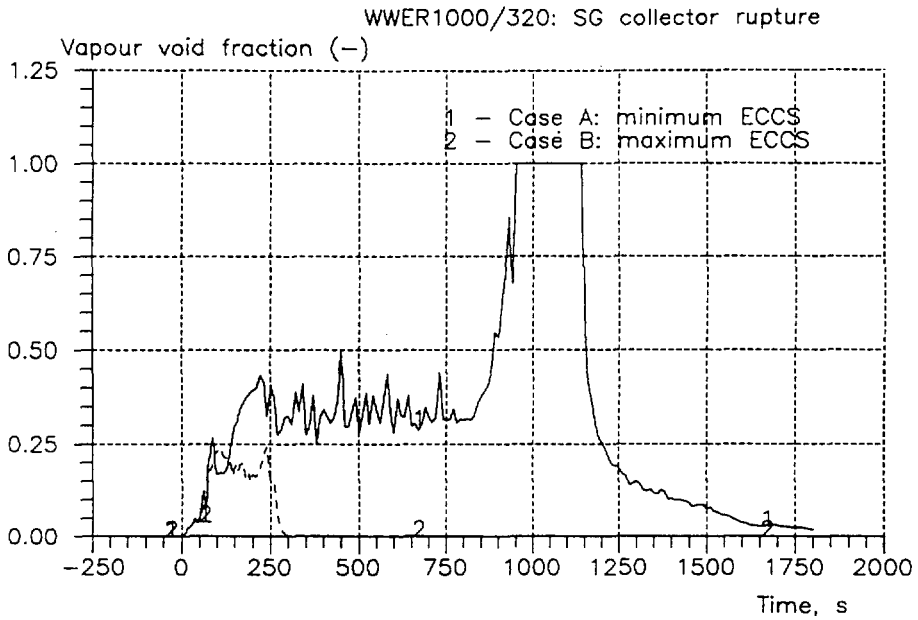


FIG. 4. Vapour void fraction through the break

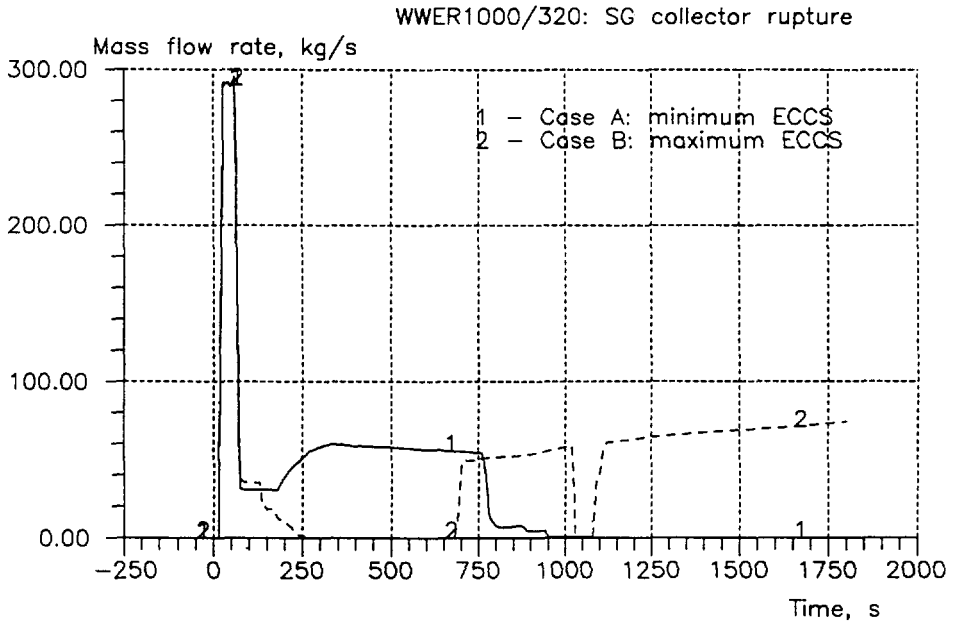


FIG. 5. Mass flow rate through the BRU-A of the broken SG

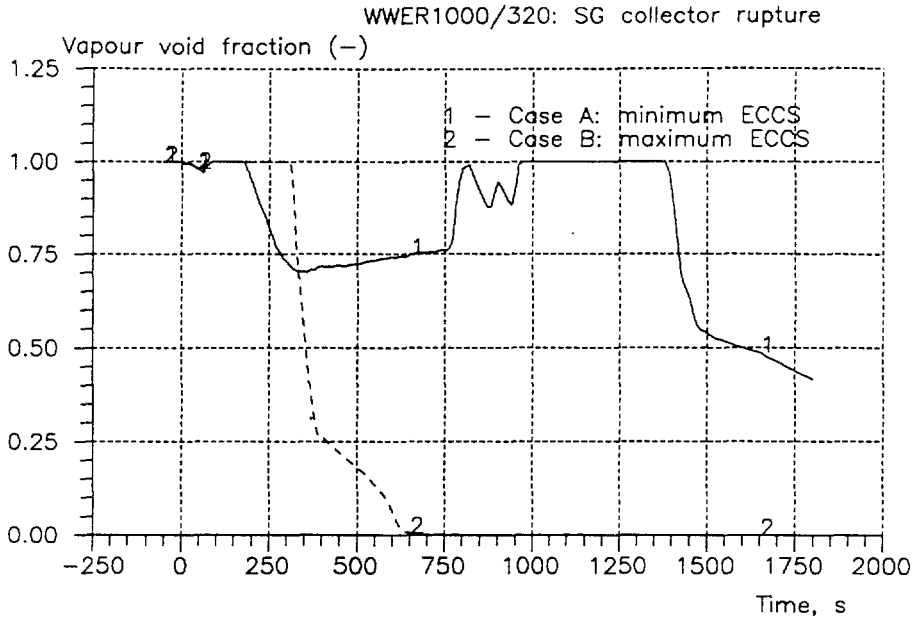


FIG. 6. Vapour void fraction at BRU-A of the broken SG

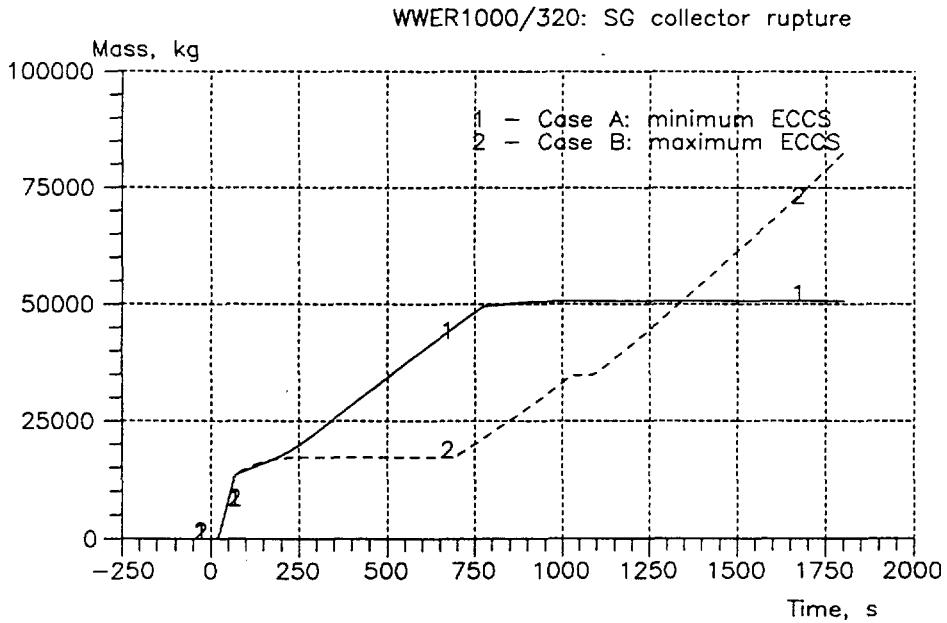


FIG. 7. Total mass released through BRU-A of the broken SG

THIRD INTERNATIONAL SEMINAR  
ON  
HORIZONTAL STEAM GENERATORS  
LAPPEENRANTA, FINLAND, 18 - 20 OCTOBER 1994

RELAP5/MOD2.5 ANALYSES OF SG PRIMARY  
COLLECTOR HEAD RUPTURE IN  
WWER-440 REACTOR

J. Szczurek  
Institute of Atomic Energy  
Świerk, Poland

Oktober, 1994

## 1. INTRODUCTION

The SG primary collector head rupture at the WWER plant with horizontal steam generators belongs to a particularly important class of loss of coolant accidents because:

- It has a relative high probability of occurrence;
- It presents a significant risk that dose limits will be exceeded, specially if the affected steam generator safety valve fails to close after opening;
- The contribution of primary to secondary leakage (PRISE) sequences to the core melt frequency is significant. The core damage frequency resulting from PRISE sequences was evaluated for Loviisa NPP as equal to 38 % of the total core damage frequency [1];
- There is some risk of pressurized thermal shock to the pressure vessel;
- It requires that the operator takes the optimum decisions under conditions of limited knowledge about the status of the plant and implements extra safety measures to bring the unit to a safe state.

The paper presents the results of the analyses of SG manifold cover rupture performed with RELAP5/MOD2.5 (version provided by RMA, Albuquerque, for PC PPS). The calculations presented below are based on RELAP5 input deck for WWER-440/213 Bohunice NPP, developed within the framework of IAEA TC Project RER/9/004.

The presented analyses are directed toward determining the maximum amount of reactor coolant discharged into the secondary coolant system and the maximum amount of contaminated coolant release to the atmosphere.

In all cases considered in the analysis, maximum ECCS injection capacity is assumed. The paper includes only the cases without any operator actions within the time period covered by the analyses. In particular, the primary loop isolation valves are not used for isolating the broken steam generator.

Two scenarios are analysed: with and without the SG safety valve stuck open. The affected steam generator safety valve will stick to open position when water starts to flow through the valve.

For the scenario with the steam generator safety valve stuck open, two cases with different break flow discharge coefficients are considered.

The results obtained in the analyses provide information about the primary coolant releases to the secondary circuit and further. This information can be used for evaluation of the radiological consequences of the accident.

Some conclusions are formulated with respect to timing of the accident and to potential accident mitigation measures.

## **2. INPUT MODEL, INITIAL AND BOUNDARY CONDITIONS**

The actual 6-loop system is modelled by three loops, one of which is the single broken loop with the pressurizer and the other two lumped loops represent two and three loops, respectively (Fig.1). This is a compromise between the efforts to describe the asymmetrical conditions in the loops and a reasonable size of the input deck.

The steam generator model applied in the project is based on the approach developed in Technical Research Center of Finland (VTT) [2].

The SG secondary side arrangement takes into consideration the tube bundle water regions (160-162), the volume including the water level above tubings (181), the steam dome (184,186) and the internal downcomer. The side volumes between the heat exchanger tubes and boiler walls are added to allow recirculation in the model. These downcomer volumes also enable circulation inside the tube bundle and in the side regions. The junctions between the tube bundle volumes and side volumes are crossflow type.

The model of steam lines including the main steam header and turbine is shown in Fig.2. Six steam lines of the natural plant connecting secondary side of steam generators with the main steam header are modeled by 4 SG lines, two single and two double lines. Steam lines from SG secondary side of triple loop are represented by one single and one double steam line. The model of common steam lines is arranged into two symmetrical and identical parts related to TG1 and TG2.

With respect to the expected processes during SG manifold cover rupture, the original model of the steam lines and of the SG collector were modified as follows:

- The steam line between steam generator and isolation valve is modelled in detail to be able to calculate pressure behaviour

in the affected steam generator correctly and to estimate the liquid void fraction in the vicinity of SG safety valve;

- The upper part of the broken collector (115), above the tube bundle region, is split into several components, with the objective to calculate the proper vapour void fraction in the break node;
- The break is modelled by single break valve connecting the upper node of the hot collector volume (115) with an additional "breakable" volume.

The initiating event for accident analysis is a rupture of SG manifold cover of hot collector. The limiting break size is the flow area of the annulus between the primary collector upper end and the manifold of the SG vessel. The path is a 4 mm wide annular gap having length of 15 mm. An equivalent break diameter of 107 mm is chosen as representative in the existing configuration.

For opening of 107 mm diameter hole, the primary to secondary leakage is expected to be conservatively overestimated [3], since the pressure loss in the narrow gap is not taken into account. In the paper, it is attempted to solve the modeling problem with the break mass flow through the selection of the break flow discharge coefficients.

In the basic conservative cases (with and without the SG safety valve stuck open) default values of the coefficients (1.0, 1.0) are used. For more realistic description of the break mass flow, the case with the SG safety valve stuck open is recalculated assuming lower values of these coefficients (both equal to 0.65).

Performed analyses are conservative with respect to radioactivity release. Main assumptions and conditions used in the analyses are as follows:

- No operator actions are considered within the time period covered by the calculations (including no isolation of the affected SG from the both primary and secondary side);
- Maximum availability of ECCS is assumed (3 trains of HPIS, 3 trains of LPIS and 4 hydroaccumulators);
- Core power: 104% , decay heat generation: ANS-79-1 + 20%;
- Primary coolant flow rate: 1.03 of nominal.
- Off-site power is lost together with turbine trip;

- Primary pressure and primary inventory controllers operate as designed;

### 3. RESULTS OF ANALYSES

#### 3.1 Scenario without SV stuck open

The flow discharge coefficients at the break are assumed 1.0.

The timing of events is given in Table 1. The main parameters are presented in Figs 3 -10 for the simulated transient up to 2000 s.

The initial phase of transient is characterized by fast depressurization of the primary circuit and rapid increasing of the affected SG water level (the initial break mass flow rate is about 680 kg/s).

At first, turbine trip signal appears at 11 s due to high SG level. Then scram and other protection system trips signals are generated.

The first opening of BRU-A and SV-1 of each steam generator occurs very early into the transient. During the period of the affected SG safety valve operation the liquid void fraction through this valve reaches 35%. This is a good reason to assume a failure of the valve to close, because it is not qualified for two-phase discharge.

After some 200 s into the transient the primary pressure is controlled by the secondary side. This leads to a decrease of the break mass flow rate to about 100 kg/s. The assumed capacity of HPIS trains is enough to compensate the break flow.

The minimum liquid level in pressure vessel is about 2.6 m above the top of the core and the peak cladding temperature follows the coolant temperature throughout the calculated transient.

The most important items with respect to limiting of the release of primary coolant to the atmosphere are as follow:

- Opening of BRU-a and SG SV. The first discharge to the atmosphere from the safety valve of the affected steam generator is limited to the first 182 s. During this time the total release from the secondary side to the environment is about 29.5 t. Up to 2000 s into the transient a second pressurization of the secondary side is not expected and the

pressure remains below the setpoint for opening of any safety and relief valve.

- Water flow in steam lines. The affected steam generator is full of water at 350 s of transient, and a few seconds later the water level reaches the highest part of the corresponding steam line. Reverse flow to the intact steam generators is observed after about 1400 s of transient. This leads to the refilling of all steam generators. At the end of the transient calculation the primary and secondary pressures have stopped to decrease and repressurization of the whole system is expected. The total coolant flow from the primary to the secondary side during 2000 s is 245 t.

### 3.2 Scenario with SV stuck open

#### CASE 1: Break discharge coefficients equal to 1.

The initial phase of the transient repeats the sequence of events in the case described in Section 3.1. The calculations are performed for 3000 s into the transient. The main characteristics of the accident after the failure of the safety valve to close are:

- The break flow rate and the HPIS injection stabilize at about 100 kg/s. The flow through the faulty safety valve is oscillating about this value, depending on its void fraction.
- The heat generated in the core is efficiently removed due to single phase natural circulation established in the primary circuit. At the end of calculations the coolant temperature in the upper plenum is more than 80 K below the saturation temperature. The heat is removed from the system by a "feed and bleed", the feed being from the emergency tanks of ECCS.
- The total primary coolant discharge to the secondary side during the simulated time is approximately 430 t. The total ECCS injections is 446 t. The hydroaccumulators are emptied at 2150 s into the transient. The total amount of coolant discharged to the environment is 413 t.
- The total amount of water injected by the three trains of HPIS is 310 t. This means that by the end of the calculated time all 3 HPIS tanks are empty and HPIS are injecting Boron solution from the LPIS tanks. Assuming the stabilized break and HPIS flow rate (100 kg/s), the LPIS tanks will be completely exhausted within 7600 s. If LPIS is also switched on this time will be decreased. The exhausting of all ECCS leads to a severe accident sequence.

Some of the results, mostly related to the coolant release and ECCS injection, are presented in Figs 11-14. At the end of the calculation the primary pressure is about 1.2 MPa.

Break discharge coefficients equal to 0.65.

The calculations were performed up to 4250 s into the transient time. Selected thermal-hydraulic parameters are shown in graphical form in Figs. 15-20. Results of calculations for the both cases with SG SV stuck open are summarized in Table 2.

At the beginning of the transient break mass flow is much lower than in the previous case with discharge coefficients equal to 1. Maximum break mass flow rate is 440 kg/s instead 680 kg/s in Case 1 (Figs 16 and 7, respectively).

Primary and secondary pressure behaviour during the whole calculated period is presented in Fig. 15. At the initial phase of the transient, resulting from a lower break mass flow rate primary pressure decreases less rapidly than in the previous case. As a consequence, the accident is progressing with slightly different timing.

The turbine trip signal and other protection system trips signals are generated about 5 s later than in Case 1 (Table 2). The similar delay is observed as concern first opening of BRU-A and SG SVs. The broken SG is full of water at 122 s (at 94 s for Case 1).

No dryout or overheating of fuel rods is predicted during the transient. In the secondary side two BRU-A and the first SG safety valves are able to limit the pressure. The second SG safety valves remain closed.

At the end of the simulation period primary pressure about 1.0 MPa remaining below the LPS operational limit.

The important conclusion follows from the second part of the Table 2. in which some integrated mass flows and inventories are compared. The data are summarized at 1800 s into the transient, when the operator is usually assumed to begin to act. For both assumed values of the break discharge coefficients, it was obtained the very similar results related to the total amount of coolant discharged to the environment, the total amount of coolant released through the break as well as the integrated HPIS inflow.

#### 4. CONCLUSIONS

- \* Due to the early opening of SG safety valve complete prevention of the release of primary coolant to the environment is not possible.

There is significant risk that SG SV would stick to open position due to water flow through it and the dose limits might be exceeded.

Amount of coolant released to the atmosphere during the first 30 minutes (after this time the operator is assumed to begin to act) is equal about 242 t in the case of SG SV stuck open;

- \* Due to the early liquid flow in the steam lines, only the automatic actions related to the isolation of the affected steam generator on the secondary side might prevent water flow beyond the main steam line isolation valve.

The estimated time margin is 400 s;

- \* The accident scenarios considered in the analyses, if not mitigated by appropriate operator actions, would lead to core damage.

Depletion of HPS and LPS tank would occur at about 7600 s. (extrapolation of results based on Fig.20);

- \* During ECCS injection phase, there is not any core overheating danger.

The minimum liquid level in pressure vessel is 2.6 above the core and the peak cladding temperature followed the coolant temperature.

#### 5. POTENTIAL ACCIDENT MANAGEMENT MEASURES

The following potential mitigation measures may be considered for the initial phase of the transient:

- A . Measures directed to increasing capabilities of ECCS;

- B. Measures directed to decreasing total leakage from primary to secondary circuit;
- C. Measures directed to decreasing the release of contaminated primary coolant into the environment.

Several practical measures have been identified in each of the a/m areas. They address the plant conditions, when primary broken loop is not performed due to hardware failure.

- \* Refilling of the ECCS BWS tanks from emergency boration tanks. This measure will increase time margin for starting cooling-down process and improve conditions for proper behaviour of the operator; - Measure related to A,
- \* Preventing pressurization of the RCS by switching-off those ECCS pumps which are not necessarily needed to cool the core; - Measure related to B,
- \* Depressurization of the RCS by primary feed and bleed, using Pressurizer Relief Valves (PORVs); - Measure related to B,
- \* Isolation of the broken SG on the secondary side and simultaneous cooling-down of the system by the use of other intact SGs; - Measure related to B and C.

#### **REFERENCES:**

- [1] B.Mohsen and J.Vaurio: PSA as a Safety Improvement Tool for Loviisa NPS, Proceedings of the International Conference on Probabilistic Safety Assessment and Management, February 4-7,1991, Beverly Hills, California;
- [2] I.Karppinen: Modelling of Horizontal Steam Generator, Technical Research Centre of Finland, PO Box 169, SF-00181 Helsinki;
- [3] H.Kantee, H.Tuomisto: Large Primary-to-Secondary Leakage Accident in Loviisa VVER-440 Reactor, IVO International LTD. Vantaa, Finland:

**TABLE 1. TIMING OF EVENTS**  
**Primary SG Collector Rupture without SG SV stuck open**

E V E N T	Time, s
Break opening	0.
* Turbine trip due to SG level 200 mm above nominal * Loss of power in conjunction with turbine trip * Scram due to tripping of the last turbine trip * Pump coastdown starts * Tripping of main FW pumps	11.
* ASSS signal generated 2 s after loss of power * DG started	13.
BRU-A starts opening due to high pressure in MSH ( $P_{MSH} > 5.3$ MPa)	14.
ESFAS signal due to primary pressure < 10.8 MPa and PRZ level 2.7 mm below nominal	15.
Opening of SV1 at affected SG ( $P > 5.6$ MPa)	17.
DG ready (10s after ASSS signal)	23.
HPIS injection begins	38.
Pressurizer empty	70.
Closing of the safety valves of the intact SGs	78.
Accumulator injection starts	94.
BRU-A closed	120.
Closing of SV at the affected SG. Liquid void fraction at valve 35%	182.
Broken SG is full of water	350.
Liquid level reaches the highest elevation of the steam line of the broke SG	370.
Liquid void fraction in MSH > 40%	580.
Beginning of filling of intact SGs through the steam lines (revers flow in steam line)	1350.
End of calculation	2000.

**TABLE 2. TIMING OF EVENTS**  
**Primary SG Collector Rupture With SG SV Stuck Open**

E V E N T	Time, s	
	A*	B**
Break opening	0.	0.
* Turbine trip * Loss of power * Reactor scram	11.	15.
BRU-A starts opening due to high pressure in MSH ( $P_{MSH} > 5.3$ MPa)	14.	19.
ESFAS signal due to primary pressure < 10.8 MPa and PRZ level 2.7 mm below nominal	15.	23.
Opening of SV1 at affected SG ( $P > 5.6$ MPa)	17.	22.
HPIS injection begins	38.	41.
Pressurizer empty	70.	102.
Accumulator injection starts	94.	122.
BRU-A closed	120.	72.
Broken SG is full of water	350.	450.
Accumulators emptied	2150.	2200.
End of calculations	3000.	4250.
<b>INTEGRATED FLOW and MASS INVENTORY at 1800 s into the transient</b>	Tons	
	A*	B**
Mass released through the break	74.	270.8
Integrated ECCS inflow	296.	268.
Total amount of coolant discharged to the environment	242.	241.6
Integrated HPIS inflow	172.7	170.1
Total coolant mass in reactor vessel	90.7	82.4
Liquid mass in the broken SG	63.8	63.8

A\* Case A: break discharge coefficients equal to 1.0

B\*\* Case B: break discharge coefficients equal to 0.65

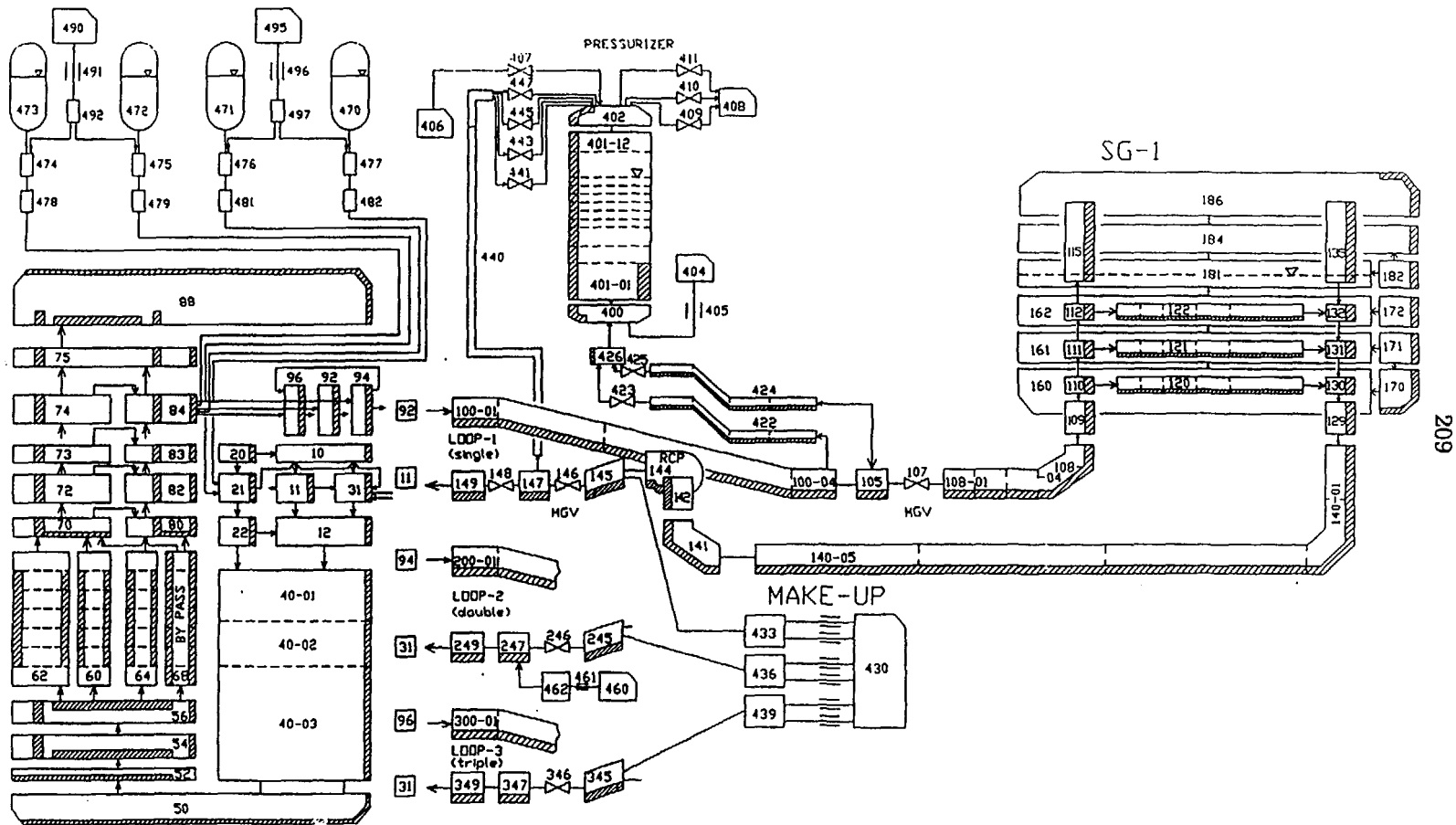


Fig.1 Nodalization scheme of the primary side of WWER 440/213:  
3-loops model

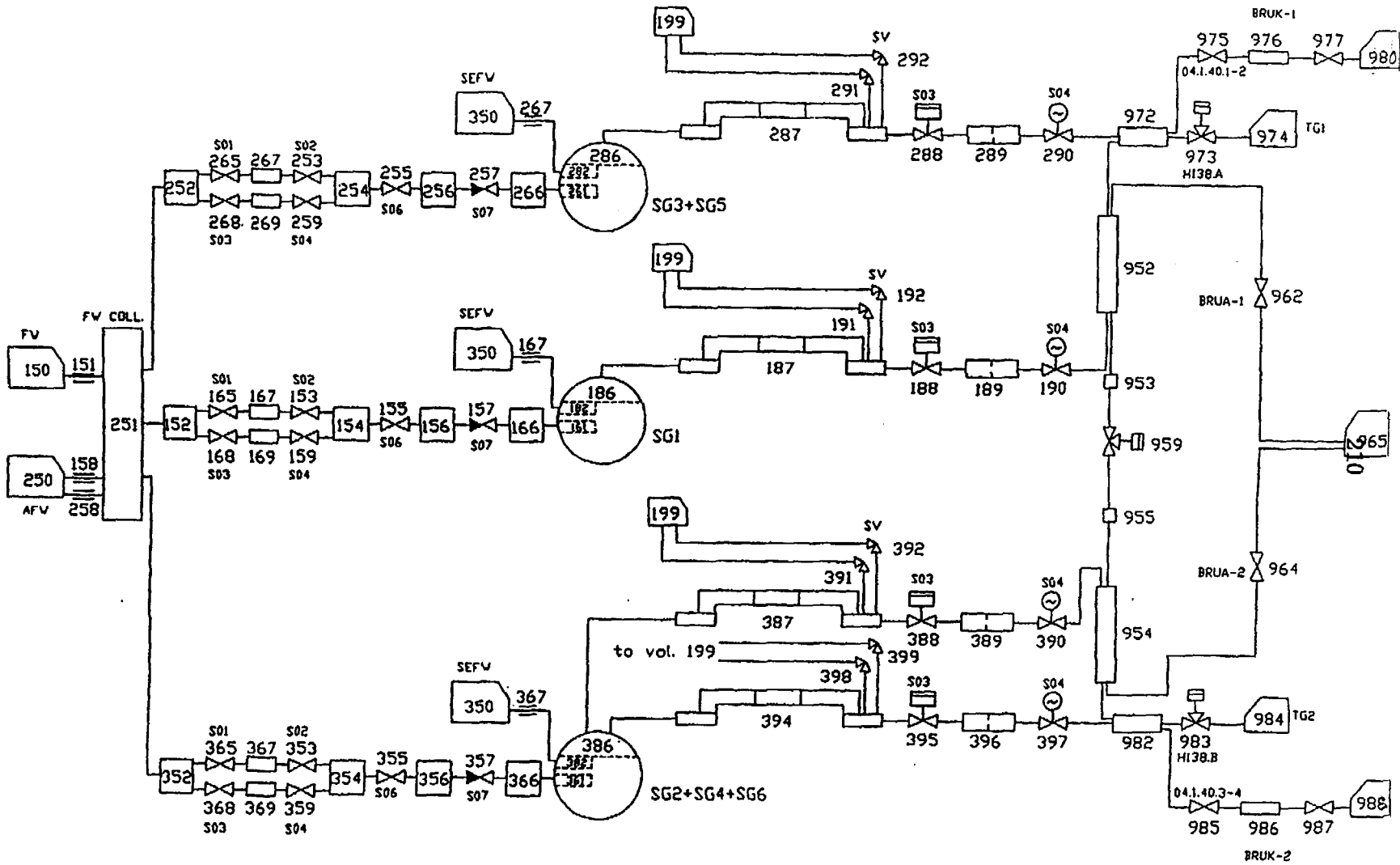


Fig.2 Nodalization scheme of the secondary side of WWR-440/213

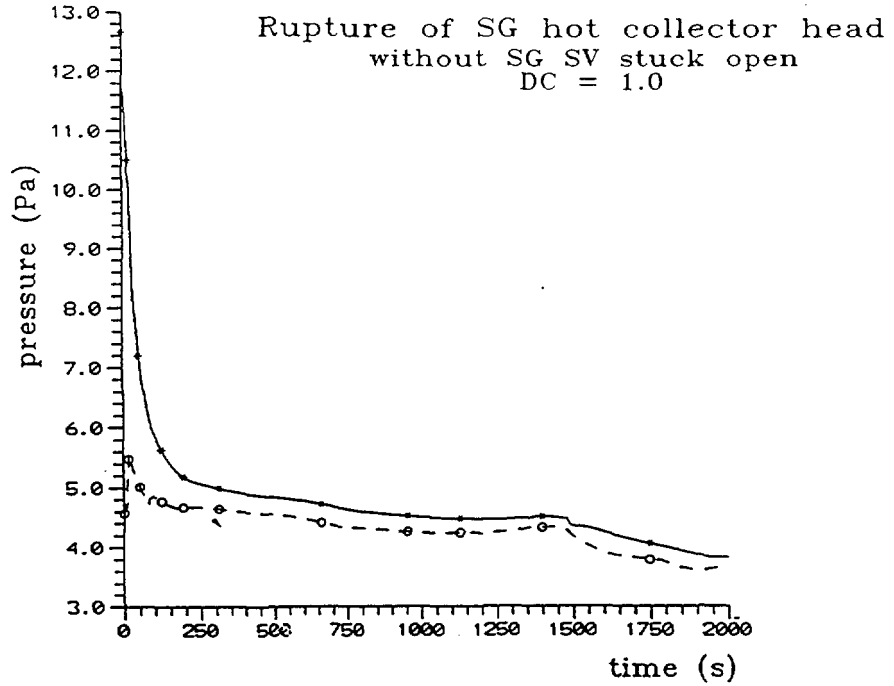


FIG. 3 Primary and secondary pressure

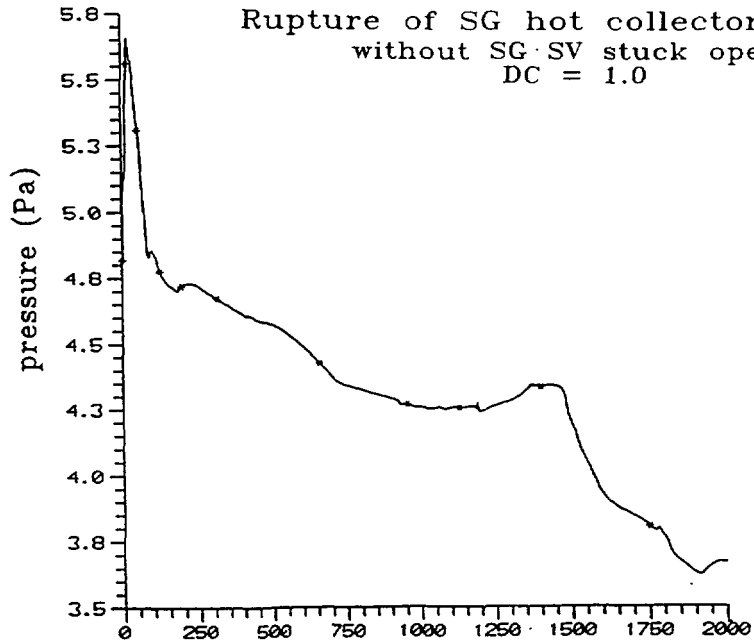


FIG. 4 Pressure in the affected SG

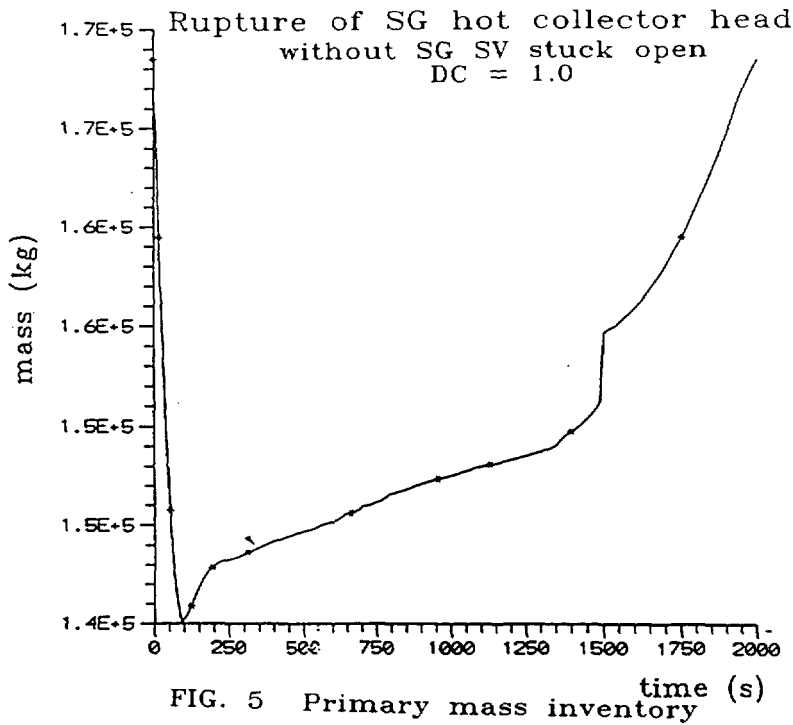


FIG. 5 Primary mass inventory

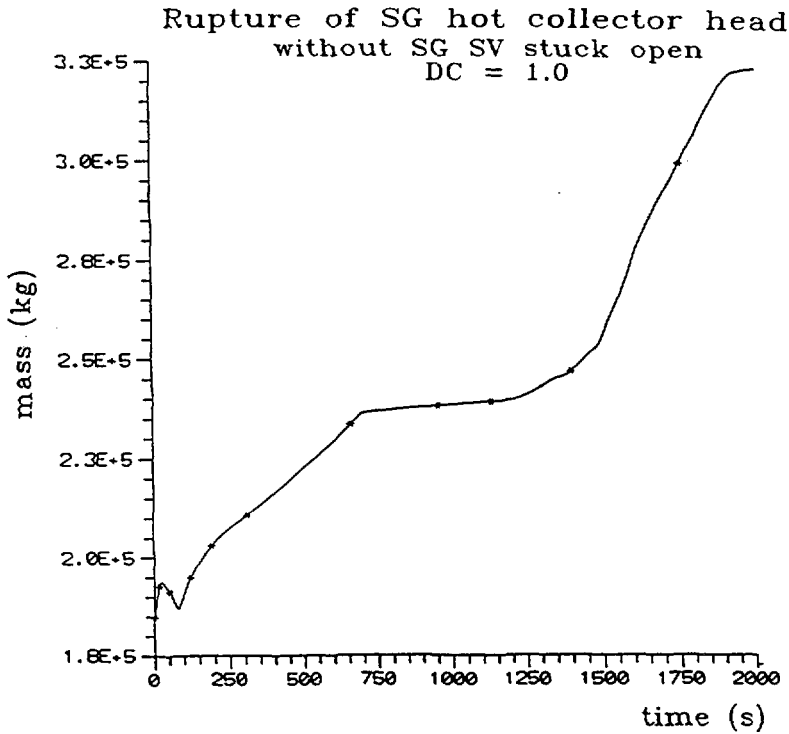


FIG. 6 Coolant mass in the steam generators

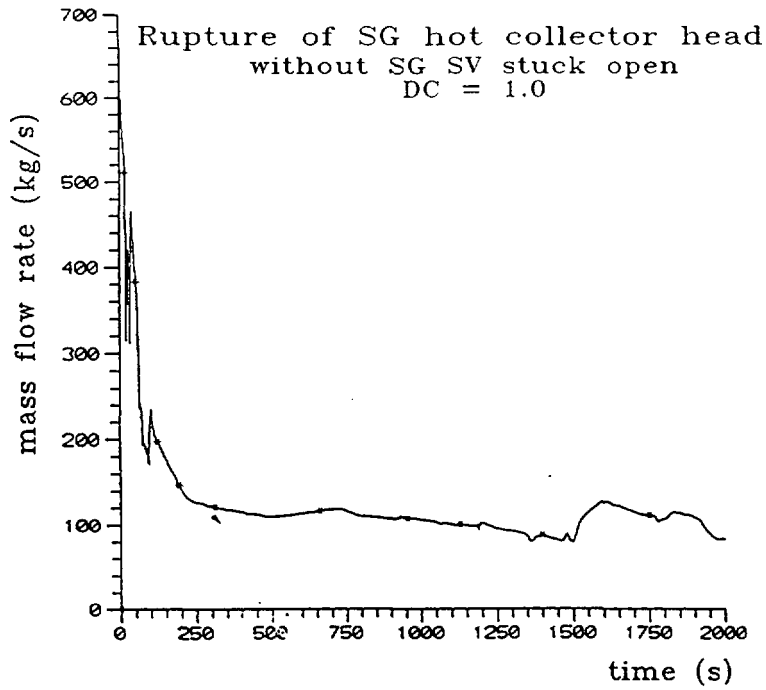


FIG. 7 Break flow rate

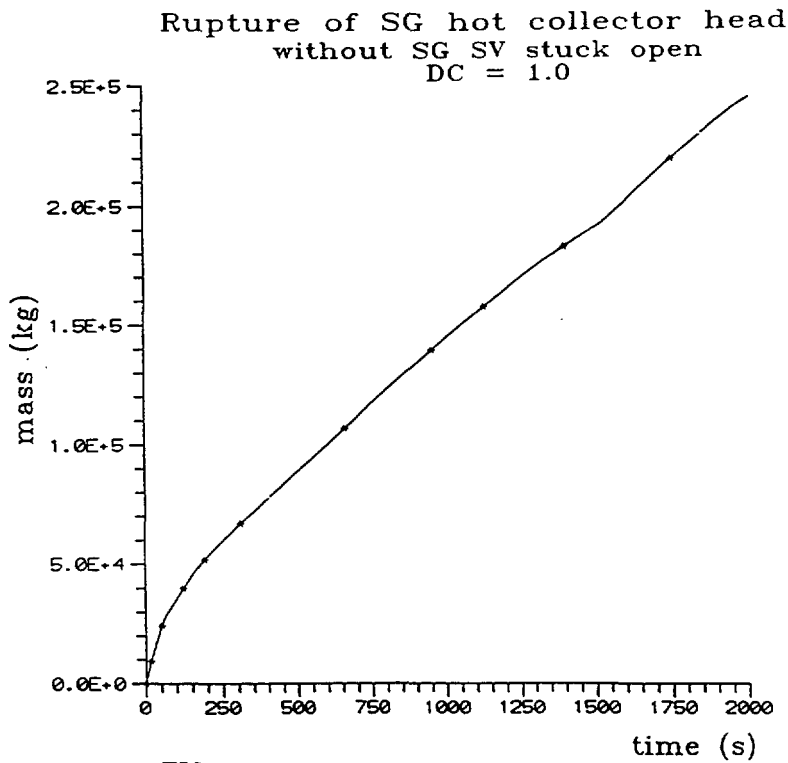


FIG. 8 Integrated break flow

Rupture of SG hot collector head  
without SG SV stuck open  
DC = 1.0

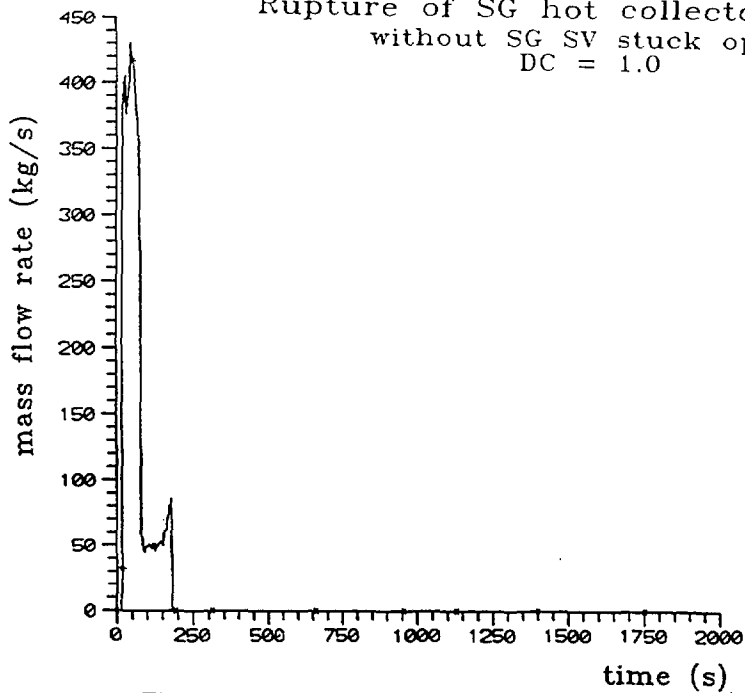


FIG. 9 Total mass outflow to the atmosphere

Rupture of SG hot collector head  
without SG SV stuck open  
DC = 1.0

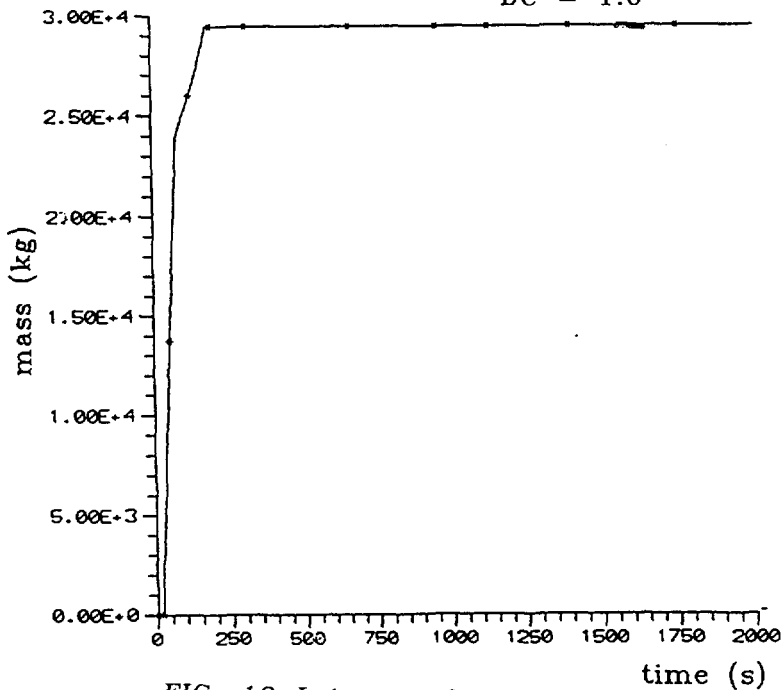


FIG. 10 Integrated coolant release from sec. side

Rupture of SG hot collector head  
with SG SV stuck open  
CD = 1.0

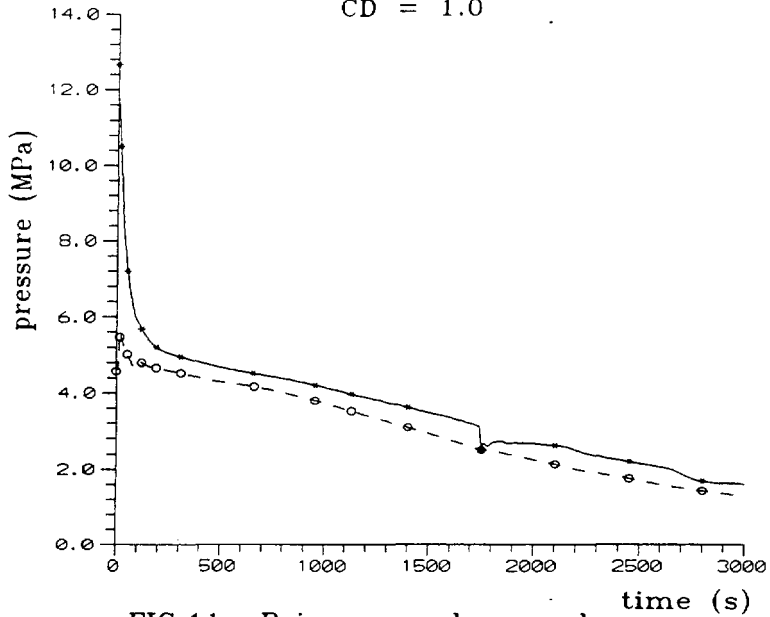


FIG.11 Primary and secondary pressure

Rupture of SG hot collector head  
with SG SV stuck open  
DC = 1.0

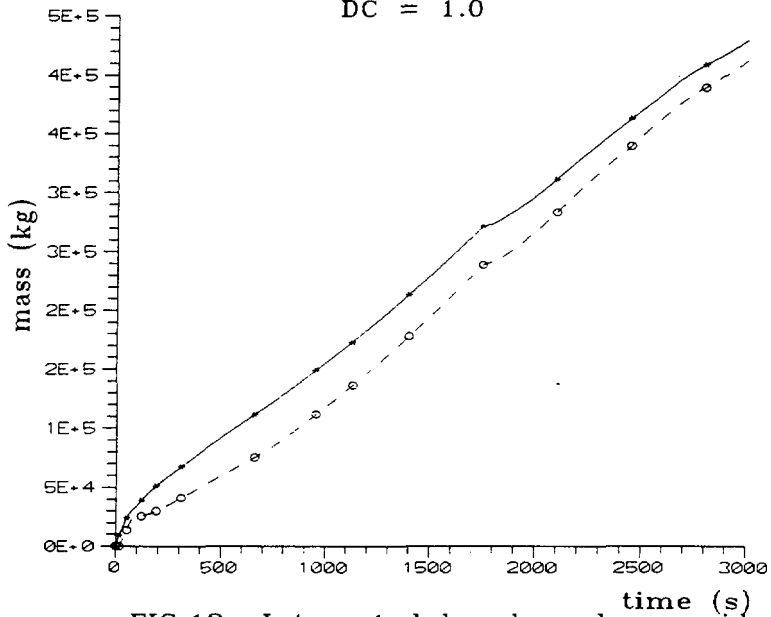


FIG.12 Integrated break and sec. side outflow

Rupture of SG hot collector head  
with SG SV stuck open  
DC = 1.0

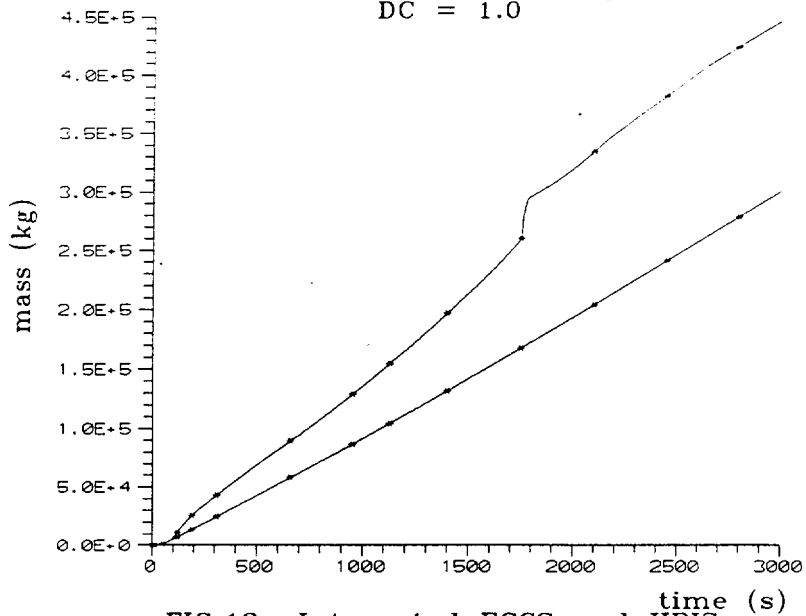


FIG.13 Integrated ECCS and HPIS mass flow

Rupture of SG hot collector head  
with SG SV stuck open  
DC = 1.0

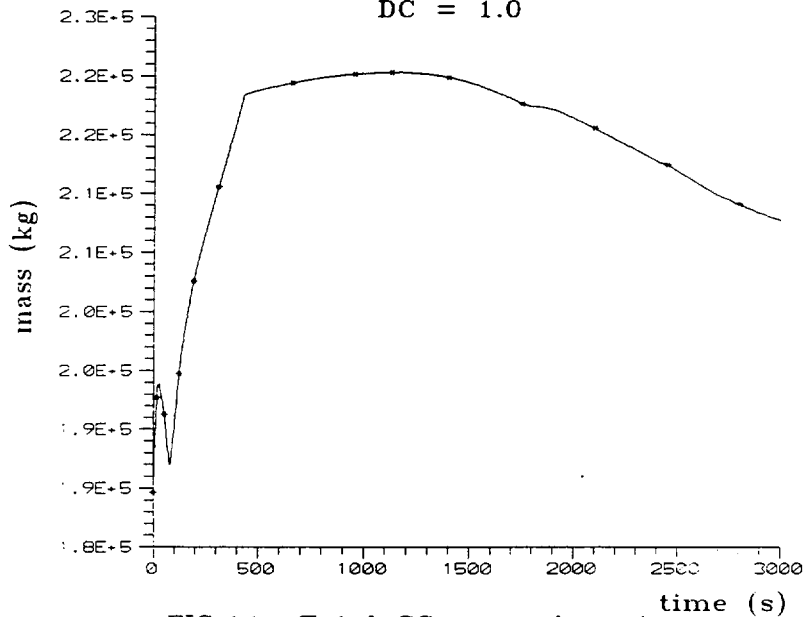


FIG.14 Total SG mass inventory

Rupture of SG hot collector head  
with SG SV stuck open  
CD = 0.65

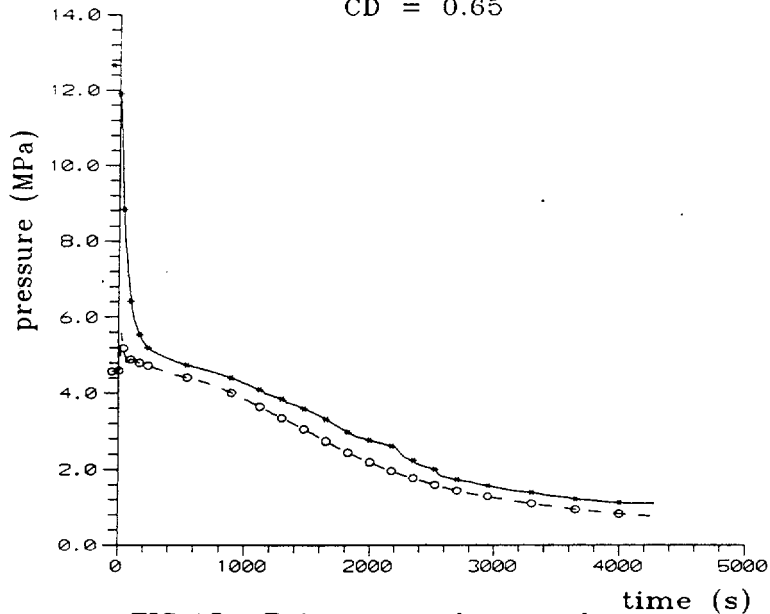


FIG.15 Primary and secondary pressure

Rupture of SG hot collector head  
with SG SV stuck open  
CD = 0.65

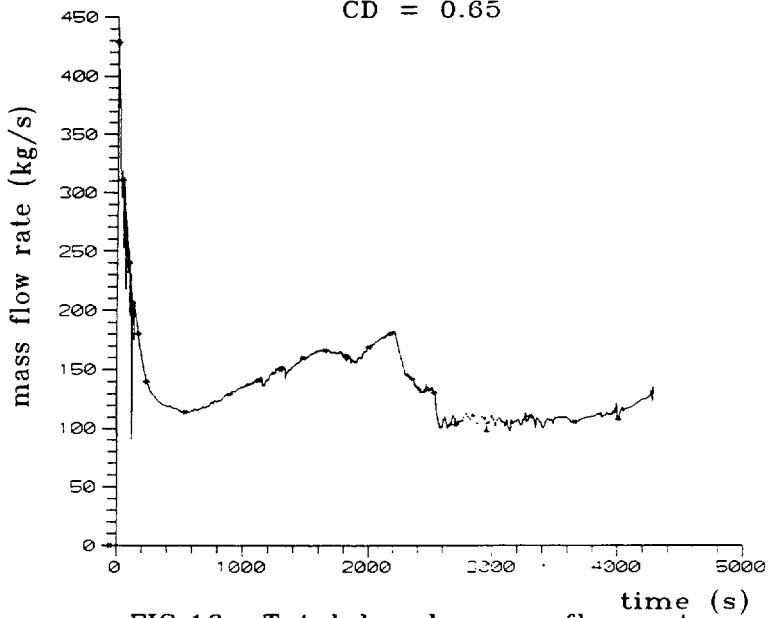


FIG.16 Total break mass flow rate

Rupture of SG hot collector head  
with SG SV stuck open  
CD = 0.65

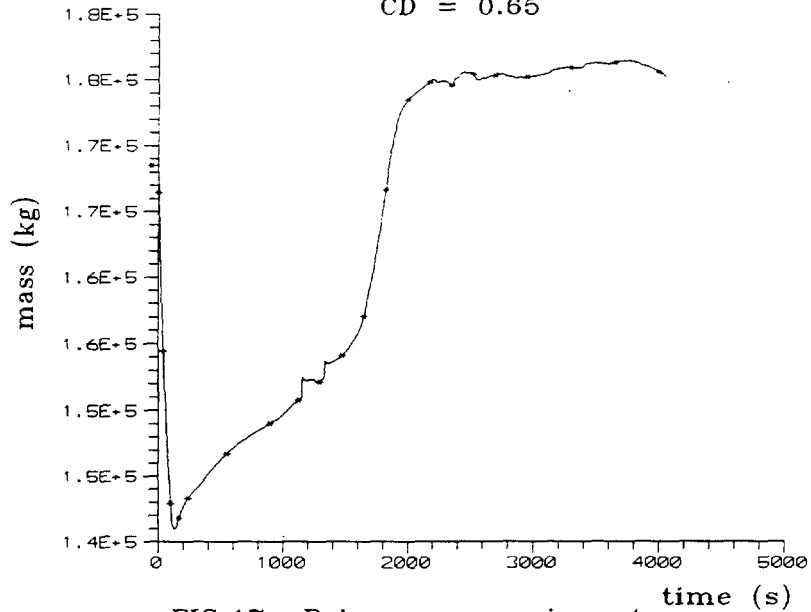


FIG.17 Primary mass inventory

Rupture of SG hot collector head  
with SG SV stuck open  
DC = 0.65

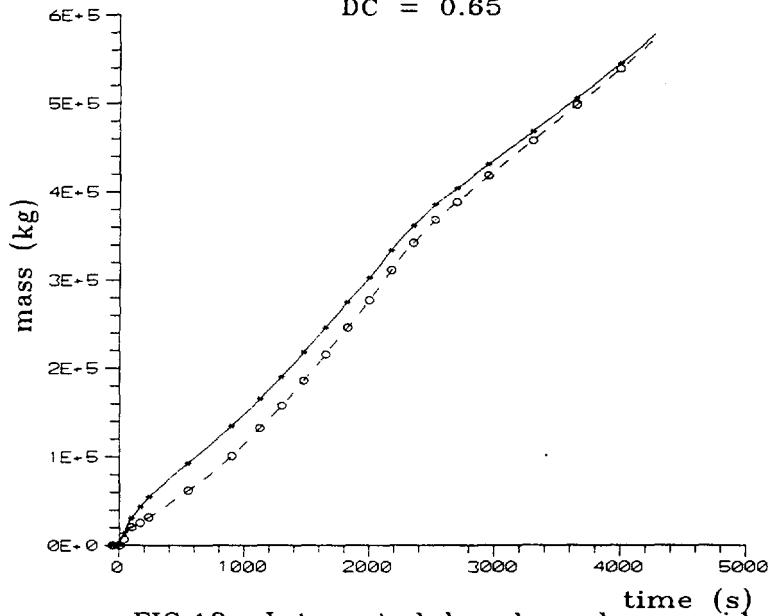


FIG.18 Integrated break and sec. side outflow

Rupture of SG hot collector head  
with SG SV stuck open  
DC = 0.65

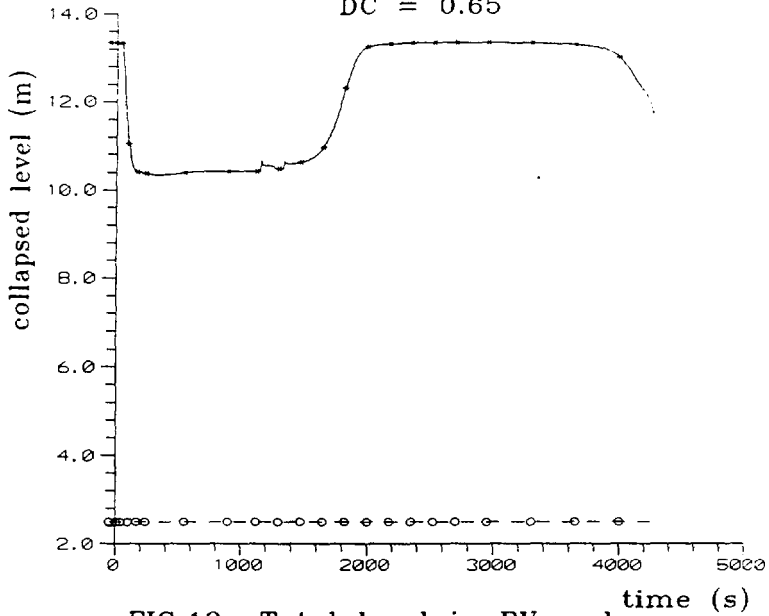


FIG.19 Total level in RV and core

Rupture of SG hot collector head  
with SG SV stuck open  
DC = 0.65

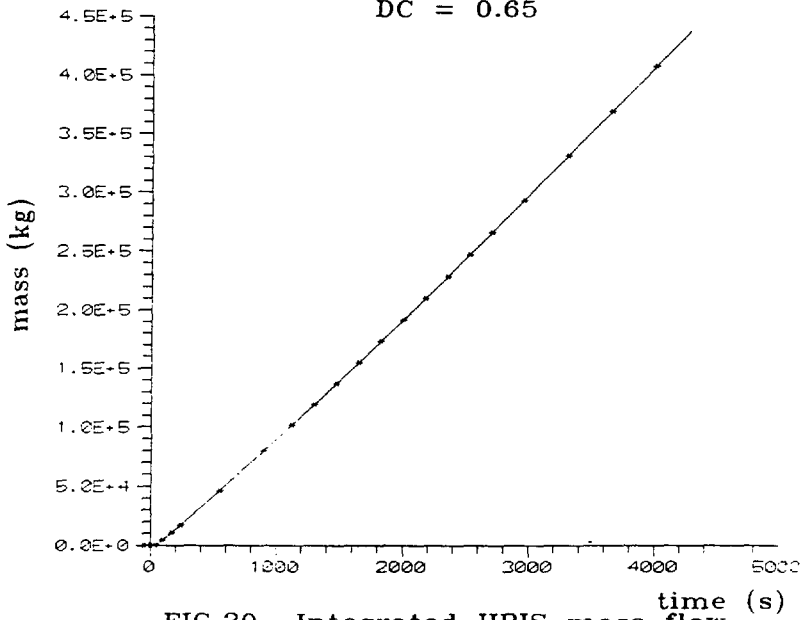


FIG.20 Integrated HPIS mass flow

220

# MANAGEMENT OF PRIMARY-TO-SECONDARY LEAKS AT LOVIISA NUCLEAR POWER PLANT

B. Mohnsen, K. Jänkälä  
IVO International LTD, Vantaa, Finland

## 1 INTRODUCTION

The Loviisa Nuclear Power Plant consisting of two VVER-440 type pressurized water reactor units has been in commercial operation since the late 1970's. The performance of the plant has been excellent and load factors have been continually among the highest in the world.

Specific features for VVER-440 reactors are six primary loops with horizontal steam generators and main gate valves. The structure of the horizontal steam generators construction may cause a large primary to secondary leak in case of a break in the cover of the primary collector. An accident where two primary collector covers opened totally and two covers opened partly took place in Rovno, Ukraine January 1982.

Primary to secondary leaks are one of the main contributors to the core melt frequency in VVER reactors according to the Loviisa 1 Probabilistic Safety Assessment. The high core damage contribution has set requirements for the development of effective means to cope with all sizes of primary to secondary leaks in the steam generator. A concept for all leak sizes has been developed for Loviisa 1 and 2. The solution includes four main areas which are a new steam generator leakage monitoring system based on Nitrogen-16 measurement, an upgraded pressurizer spray system, an increased emergency cooling water reserve and an automated isolation of the defected steam generator.

## 2 DESCRIPTION OF THE BACKFITTING MEASURES

### 2.1 The problem of primary to secondary leaks

The management of primary to secondary leaks in VVER reactors is originally based on isolation of the leaking steam generator from the primary and the secondary side. However, the manual operation of the main gate and other associated valves is unreliable and therefore the isolation from primary side is not certain. In larger leaks, also a possible steam line break as the result of waterhammer may affect the isolation from the secondary side. The steam line isolation has to occur immediately and reliably in order to ensure the integrity of main steam line.

In the case of failed isolation of the leaking steam generator, the primary pressure has to be reduced to that of the leaking steam generator. On the other hand, the primary pressure is increased by the emergency coolant injected into the primary circuit to compensate for the leak. The primary pressure can be reduced by fast cooling from secondary side and by spraying the pressurizer. This sets requirements to the reliability of the pressurizer spray system.

Non-qualified steam generator safety valves would ultimately stick open after cycling to pass two phase medium. Therefore the time needed for the depressurization of the primary circuit may be long and the adequacy of the emergency cooling water reserves become questionable.

The main problems in managing primary to secondary leaks in VVER reactors are isolation of the steam generator, cooling the primary circuit, the adequacy of the emergency cooling water and detection of leaking steam generator. On the basis of these considerations improvements in the management of primary to secondary leaks at Loviisa NPP are directed against those deficiencies. A schematic picture of the backfitting is illustrated in the figure 1.

## **2.2 Steam generator leakage monitoring**

The most effective way to prevent severe consequences of primary to secondary leaks is the early detection of a leak. Every main steam line at Loviisa NPP units 1 and 2 will be equipped with activity measurement which is based on Nitrogen-16 isotope. This enables the leak detection even in case of no leaking fuel elements as well as the observation of the leak development. The activity measurement is informative and is not used for any automatic action.

## **2.3 Isolation of the steam lines**

One target of the backfitting is to improve the isolation of the leaking steam generator to avoid severe consequences caused by a potential waterhammer in the steam line when the steam generator is filled with water. Two redundant isolation signals close the main isolation valve and the block valve in the steam line. The main feed water line of the defected steam generator is also isolated by the signal in order to avoid potential subcooled water entering to the steam line. According to the studies carried out the integrity of a main steam line is very much dependent on the degree of subcooling.

## **2.4 Depressurization of the primary circuit**

In the case of failed isolation of the leaking steam generator by means of the main gate valves and a stuck open safety valve of the steam generator the operator has to equalize the primary and secondary pressures to stop the leak in order to reduce radioactive releases. In Loviisa the upgrading of the pressurizer spraying is based on the emergency spray system that includes two redundant emergency lines connected to the high pressure emergency cooling system. The spray water is feeded with high pressure pumps into the pressurizer. These redundant lines are connected together close to the pressurizer. The system is taken into operation by the operator. The spray mass flow into the pressurizer is controlled by the operator.

## **2.5 Reserve of emergency cooling water**

Assuming a stuck open safety valve in the leaking steam generator, the stopping of the primary to secondary leak may turn out to be of a long duration. As long as there is a pressure difference between the primary and the secondary side the leak continues and the existing emergency cooling water storage of 1000 m<sup>3</sup> may be insufficient. To ensure the adequacy of emergency cooling water the plant will be provided with a new emergency water storage of 1000 m<sup>3</sup> which is common for both units. This new borated water reservoir will be connected to the existing emergency cooling water tank. This new water storage is taken into operation manually by the operator. The water tanks operate as communicating vessels and no active components are needed.

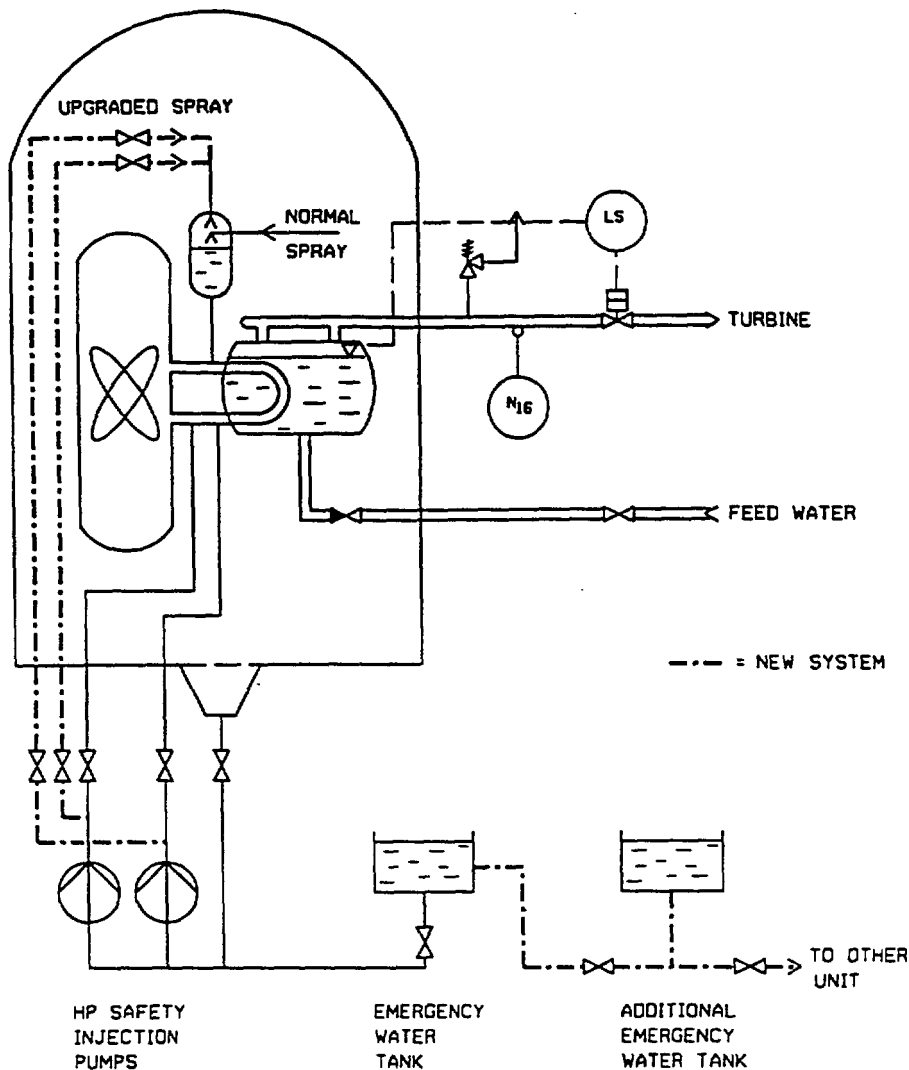


Figure 1. Emergency pressurizer spray system and emergency cooling water storage

### 3 CONSIDERATIONS OF THE BACKFITTING MEASURES

#### 3.1 Choice of backfitting solution

The choice of the backfitting solution is based on the results of the Loviisa 1 PSA and a preliminary study of primary to secondary leaks carried out in the year 1990. When evaluating different alternatives to cope with primary to secondary leaks the main interest was given on how to control plant process in order to stop the leak before the steam generator is filled by water avoiding the opening of the safety valve in the steam generator. It was found out that in small primary to secondary leaks the stopping of safety injection is an useful action in reducing the primary pressure.

In middle size leaks like the rupture of five tubes it is necessary to reduce the primary pressure also by other means. Spraying the pressurizer reduces the pressure effectively but simultaneous cooling of the primary circuit by blowing the steam through the intact steam generators is necessary in order to keep the boiling margin in the primary circuit. In larger leaks i.e collector breaks the filling of the steam generator is very fast and the operator has no chance to avoid the opening of the safety valve of the leaking steam generator. In order to manage larger leaks it was found necessary to increase the emergency cooling water storage. In management of primary to secondary leaks of all sizes a reliable and sensitive steam generator leak monitoring is essential.

### **3.2 Benefits gained**

It is estimated that by the planned plant modifications the core damage frequency due to primary to secondary leaks will be reduced by about 99 % from today's level. A significant reduction also in the contribution to containment by-pass sequences is gained.

Operators' means to cope with primary to secondary leaks of all sizes can be improved significantly by the backfitting. The knowledge of the plant behaviour during primary to secondary leaks has increased. The full size training simulator has been utilized effectively in analysing the feasibility of the backfitting as well as in training the operators to manage primary to secondary leaks.

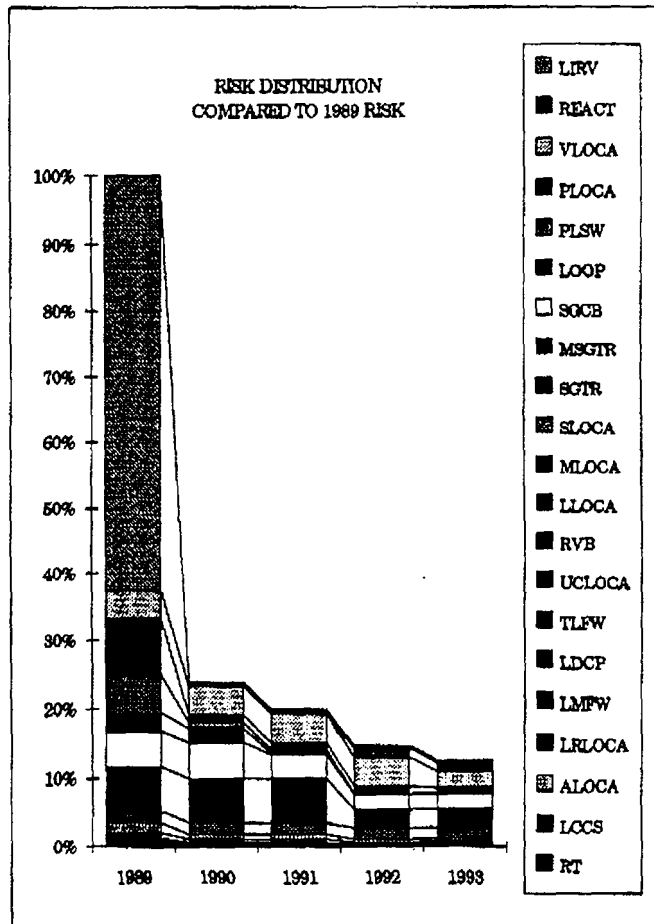
### **3.3 Time-table of commission**

The backfitting will be implemented gradually during the annual shutdowns of the Loviisa plant. The activity measurement of the steam lines and the automatic isolation signal of the leaking steam generator from the high water level in the steam generator will be installed in 1994 to both units and also the modification of the pressurizer spraying will be installed to unit 2 this year. The whole backfitting will be implemented by the end of 1996.

## **4 CONCLUSIONS**

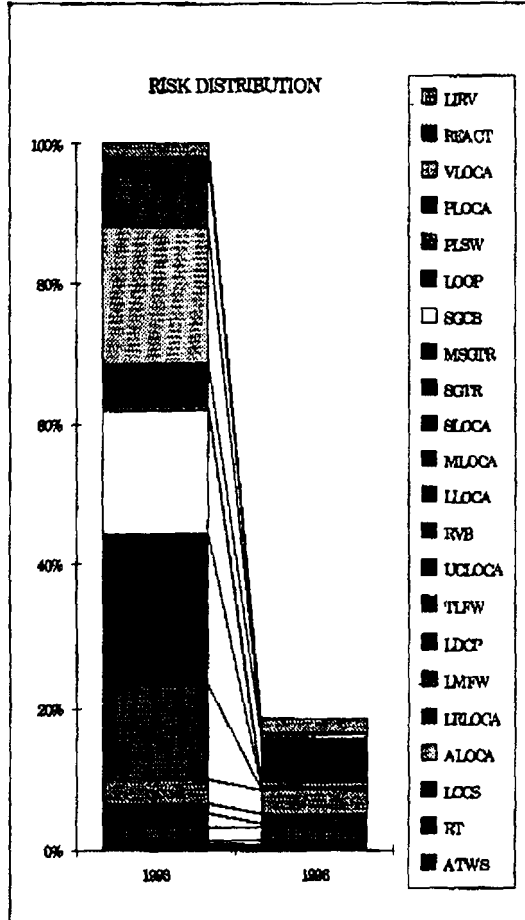
Based on the results of the Loviisa 1 Probabilistic Safety Assessment, measures to reduce the core damage risk of primary to secondary leaks were found necessary. The chosen solution is based on a rapid depressurization of the primary circuit and a simultaneous cooling from the secondary circuit. The sufficiency of emergency cooling water is guaranteed by increasing the capacity of the emergency water tank. The system will be commissioned in 1996.

By these modifications the core damage risk due to primary to secondary leaks and their contribution to containment by-pass sequences is reduced to acceptable level. The management of the primary to secondary leaks at Loviisa NPP will be improved significantly by providing effective means to diagnose and depressurize the primary circuit as well as means for residual heat removal and cooling of the reactor to the cold shutdown state.



LIRV	Loss of Instrumentation Room Ventilation	LLOCA	Large Leakage
REACT	Reactivity accident	RVB	Reactor Vessel Break
VLOCA	Outside Containment Leakage	UCLOCA	Upper Containment Leakage
PLOCA	Medium Pressurizer Leakage	TLEW	Total Loss of Feed Water
PLSW	Partial Loss of Service Water	LDCP	Loss of DC Power
LOOP	Loss of Offsite Power	LMFW	Loss of Main Feed Water
SGCB	Steam Generator Collector Break	LRLOCA	Large RCP-motor Room Leakage
MSGTR	Multiple Steam Generator Tube Rupture	ALOCA	Large Accumulator-line Leakage
SGTR	Steam Generator Tube Rupture	LCCS	Loss of Component Cooling System
SLOCA	Small Leakage	RT	Reactor Trip
MLOCA	Medium Leakage	ATWS	Anticipated Transient Without Scram

Fig. 1. Risk distribution compared to 1989 risk.



LIRV	Loss of Instrumentation Room Ventilation	LLOCA	Large Leakage
REACT	Reactivity accident	RVB	Reactor Vessel Break
VLOCA	Outside Containment Leakage	UCLOCA	Upper Containment Leakage
PLOCA	Medium Pressurizer Leakage	TLFW	Total Loss of Feed Water
PLSW	Partial Loss of Service Water	LDCP	Loss of DC Power
LOOP	Loss of Offsite Power	LMFW	Loss of Main Feed Water
SGCB	Steam Generator Collector Break	I.RLOCA	Large RCP-motor Room Leakage
MSGTR	Multiple Steam Generator Tube Rupture	ALOCA	Large Accumulator-line Leakage
SGTR	Steam Generator Tube Rupture	LCCS	Loss of Component Cooling System
SLOCA	Small Leakage	RT	Reactor Trip
MLOCA	Medium Leakage	ATWS	Anticipated Transient Without Scram

Fig. 2. Risk reduction from today to year 1996.

# APPLICATION OF THE THERMAL-HYDRAULIC CODES IN VVER-440 STEAM GENERATORS MODELLING

P. Matejovič, Ľ. Vranka, E. Václav

Nuclear Power Plant Research Institute (VÚJE)

S L O V A K I A



## 1. Introduction

In last years great effort was concentrated to the development of the best estimate thermal hydraulic codes. However, in application of these codes to the VVER reactors arise some specific problems, mainly due to the following reasons :

- i) these codes are normally validated for PWR of western concept
- ii) due to geometric differences it is sometimes difficult to apply these codes to VVER design

Most of the above mentioned troubles is associated with the modelling of horizontal steam generators. In this contribution, an application of the CATHARE2 V1.3U and RELAP5/MOD3.0 in VVER-440 SGs modelling is presented. Performances obtained using

both codes during the nominal regimes are described and compared. Finally, separate test with water level decreasing on the secondary side is performed with the aim to investigate heat transfer degradation from primary to secondary.

## 2. Nodalization scheme

The nodalization scheme of the horizontal SGs is largely depending on both, the type of the transient to be simulated and computer code used. Each code has its own available modules, which predestine the structure of the nodalization scheme. Usually, each SG model is possible to "tune" to simulate reasonable SG behaviour in nominal conditions. However, when deviate from nominal conditions, validity of these models become more or less limited. This is usually the case of various transients and accidents, which may be associated with water level changes on the secondary side or transition from single to two-phase regimes in the primary side. In the following, two similar CATHARE and RELAP nodalization schemes are described. These models were developed with the aim to cope with above mentioned transients.

### 2.1. Nodalization of the primary

Nodalization of the primary is quite straightforward for both above mentioned codes.

#### **CATHARE :**

Generally accepted scheme is formed by :

- two identical *VOLUME* modules, simulating hot and cold collectors;
- several horizontal *AXIAL* modules, modelling the chosen number of layers; each layer contains corresponding number of the SG heat exchange tubes.

**RELAP :**

The RELAP nodalization scheme usually consists of :

- several *BRANCH* elements modelling hot and cold collectors;
- several horizontal *PIPE* modules, describing the SG heat exchange tubes; these elements are connected to the corresponding *BRANCHes* via two *CROSS-FLOW* junctions.

It is possible to state, that due to sophisticated *VOLUME* modules available in *CATHARE*, this code seems to be more convenient for the primary collectors modelling.

Obviously, such nodalizations are able to simulate stepwise degradation of the SG heat transfer properties in the case when the primary swell level in the collectors descends below the elevation (resp. below the height of influence for *CATHARE* code) of the horizontal junction of given *AXIAL*, resp. *PIPE* module.

Some questions may arise during two-phase natural circulation under boiling-condensation mode, when the saturated steam produced in the core condensates in SG tubes. According to the results of the ISP-33, in such a case due to kapillarity effect is the water amount in SG tubes predicted by the codes underestimated. Thermal-hydraulic codes like *CATHARE2* and *RELAP5* namely are not taking into account this phenomenon. In real SG the heat exchange tubes are slightly inclined (about 1/3°) towards both collectors. This inclination is usually not considered in nodalization schemes what may artificially increase water amount predicted in SG tubes and this way mitigate the above mentioned deficiency.

## 2.2. Nodalization of the secondary

Due to 3-D flow pattern the nodalization of the secondary side is much more artificial. Only limited tools are available in both codes for this purpose.

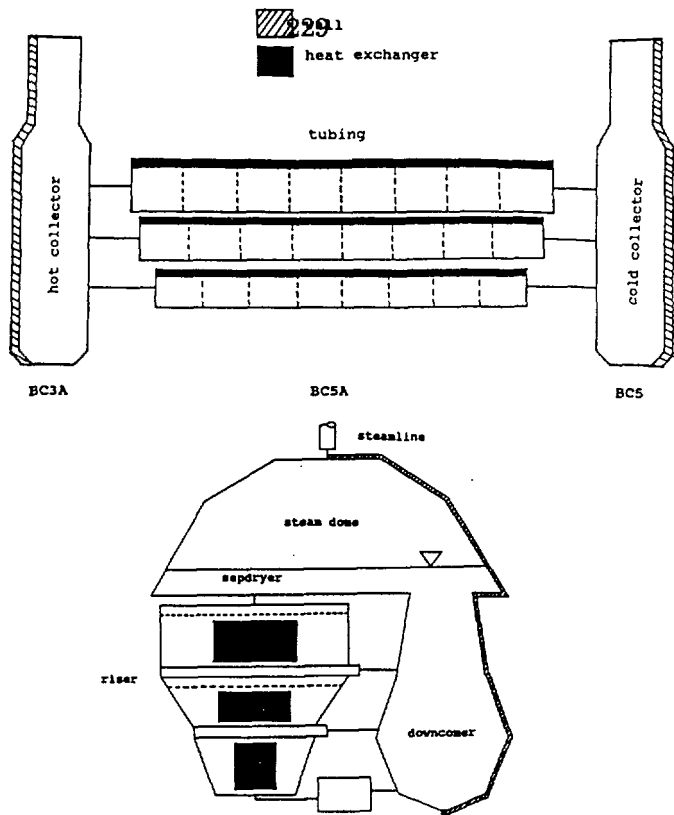


Fig.1. CATHARE nodalization scheme of the steam generator

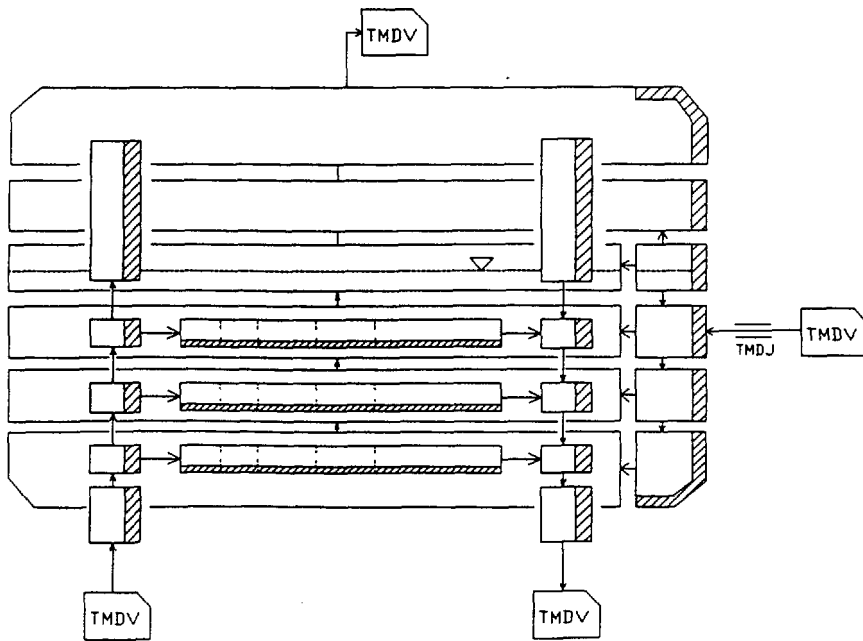


Fig.2. RELAP5 nodalization scheme of the steam generator

**CATHARE :**

Main limitation is, that in CATHARE the heat between two circuits can be exchanged via EXCHANGERS only between AXIAL elements on both, primary and secondary side. This is convenient for vertical SG, where the riser and primary tubing are parallel. However, in the case of the horizontal SG the riser and tubing are orthogonal and consequently, only one cell of the secondary AXIAL element (representing SG riser) may be used for each considered layer of SG tubes. 1-D heat conduction is calculated in the tube wall and is implicitly coupled to the fluid thermal-hydraulics on one side and nearly implicitly or explicitly coupled to the fluid thermal-hydraulics on the other side [4].

Several various schemes ranging from point to recirculation model are currently available. They are described in [1] and therefore only briefly mentioned here. The terminology from [1] is used here.

*Once-through model.* The advantage of this model is its simplicity. However, the conditions on the secondary side are not realistic because the velocities are about one order lower than in real SG. This model is usable when the dominant heat transfer mode is nucleate boiling. Otherwise, the heat transfer coefficients may be underestimated.

*Downcomer model.* This model partly solves problem of recirculation during normal operation. The recirculation continues as long as the swell level is higher than the elevation of the junction between the riser and steam dome volume. When the swell level drops below this junction the circulation stops. This is the situation after reactor scram, when secondary water level collapses. In this case due to cold FW or EFW injection and due to heat flux reverse from secondary to primary (during LOCAs) an unphysical thermal stratification may be established on the secondary side.

*Recirculation model with cross-flow junctions between downcomer and riser* was proposed in [1] to overcome limitations of the downcomer model. Its main disadvantage is the complexity.

However, this model seems to be the most versatile and was therefore chosen as a basis for nodalization in this paper.

Three main regions can be distinguished on the secondary side of SG :

- the riser (heat exchange zone corresponding to coolant volume between tubing);
- downcomer (space between SG shell and tubing where the downward flow occurs);
- steam dome (volume over tubing; here also the separator is placed).

In accordance with the nodalization of the primary side, the riser is divided into three parts modelled by three *AXIAL* elements. Two additional *TEES* were introduced to enable the cross-flow circulation between riser and downcomer. One *VOLUME* modul is used to describe both, SG steam dome and downcomer. *SEPPRYER* option may be used for the junction between SG riser and steam dome.

#### **RELAP :**

Thanks to *BRANCH* modules and *CROSS-FLOW* junctions in *RELAP5* code it is possible to describe similar recirculation model much easier. The final nodalization scheme consists only of 8 *BRANCH* elements. Furthermore, due to explicit character of the code there are no restriction for heat transfer modelling from primary to secondary. Besides SG tubing it is therefore possible to model also heat transfer through the walls of both collectors.

### 3. Steady-state performances

Values presented in Tables 1 and 2 were obtained using the nodalization scheme with nominal boundary conditions according to Fig.1,2. The obtained steady-state values are compared with reference ones in Table 1 and 2.

Table 1 : Steady-state parameters on the SG primary side

V a r i a b l e	Jaslovské Bohunice V-2	CATHARE with SEPDYER	CATHARE without SEPDYER	RELAP
power from primary to secondary [MW]	-	231.8	231.8	231.8
SG inlet temperature [°C]	297.3	297.3*	297.3*	297.3*
SG outlet temperature [°C]	267.8	267.55	267.55	267.9
temperature drop in SG [°C]	29.5	29.75	29.75	29.4
coolant flow at SG outlet [m <sup>3</sup> /s]	1.94	1.94*	1.94*	1.94*
pressure at the SG outlet [MPa]	12.235	12.235*	12.235*	12.23
fouling [%]	-	15.5	15.6	-

Table 2 : Steady-state parameters on the SG secondary side

V a r i a b l e	Jaslovské Bohunice V-2	CATHARE with SEPDYER	CATHARE without SEPDYER	RELAP
SG pressure-steam dome[MPa]	4.61	4.61*	4.61*	4.61*
mixture water level [m]	2.25-2.8	2.1#	2.4#	-
collapsed water level in downcomer [m]	1.8-2.0	2.1	1.8	1.85
water mass in SG [10 <sup>3</sup> kg]	33-38	33.7	31.0	34.0
feedwater temperature [°C]	221.0	221.0*	221.0*	221.0*
steam mass flow from SG[kg]	125.5	125.48	125.48	125.45
recirculation ratio [-]	10 (?)	9.3**	10.6**	7.4**

where :

\* values imposed by boundary condition

# values imposed by regulation

\*\* values imposed by singularity head losses coefficients

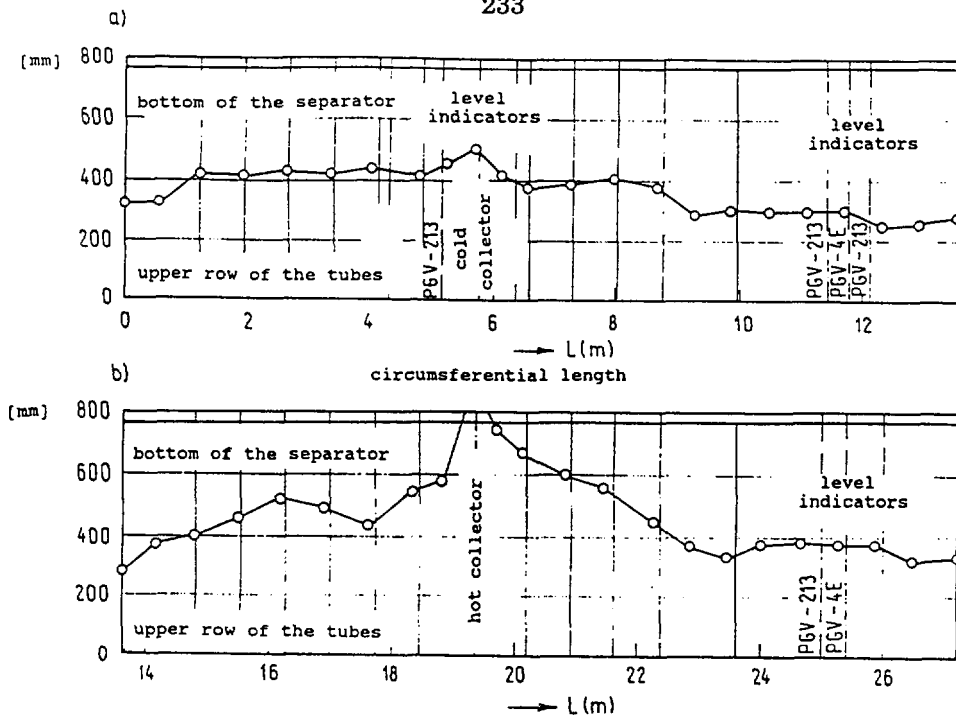


Fig.3. Water level in steam generator according to [5]

The values obtained seem to be close enough to the reference ones. Using above mentioned boundary conditions, the power exchanged, the feed water and steam flow rates are not imposed but correctly predicted by both codes.

In addition to the collapsed water level in SG downcomer CATHARE is able to model also two-phase water level, which is not considered by RELAP. Of course, the mixture level is predicted correctly only using the mode without *SEPDRYER*. In this case due to higher flow velocities on the secondary it is also necessary to use nearly three-times lower head losses coefficients compared to the model with *SEPDRYER* to get the same circulation ratio.

Even in the case without *SEPDRYER* option the water entrainment from steam dome into steam line was very low, only about  $3.2 \cdot 10^{-3}$  kg/s. Very good quality of the natural separation on the secondary water level was also reached using RELAP code.

The steady-state performance with the steam generators and some aspects of the nodalization used are briefly pointed out in the form of the following remarks.

*REMARK 1. Secondary water level*

SG secondary water level is of complicated shape with maximum in the vicinity of the hot collector. Its experimentally measured shape according to the mineral trace on the inner surface of SG shell [5] is illustrated in Fig.3. Using the CATHARE code, one can never get at the same time both, proper SG "average" water level and water mass when using *SEPDRYER* option for junction between upper part of the riser and steam dome. In this case the regulation set point for secondary water level 2.1 m was therefore chosen so to keep proper water amount during nominal operational conditions. In the case without *SEPDRYER* the regulation set point for secondary water level 2.4 m was chosen to keep proper average swell level and the SG water, illustrated in Figs.4,5.

*REMARK 2. Void fraction distribution & heat transfer*

There is not available full experimental map of the void fraction distribution on the secondary side. According to [1] the void fraction 700 mm below the upper row is about 30-40%. The values of the void fraction distribution and heat transfer modes in the SG riser predicted by both CATHARE models are illustrated in Figs.3,4. The values achieved with model without *SEPDRYER* seems to be quite realistic whereas those ones obtained with the second model are rather underpredicted. In both cases, due to subcooled FW injection is the water temperature in the downcomer about 3-4°C below its saturation value. Similar parameters are achieved using RELAP code (Fig.6).

*REMARK 3. Circulation flow pattern*

In all presented models, similar flow pattern with main stream in the lowest junction is naturally established when using similar head losses coefficients for all horizontal cross-flow junctions between SG downcomer and riser.

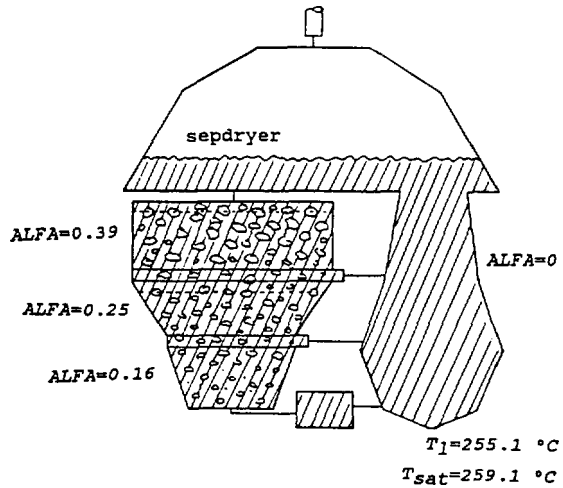
## VOID FRACTION DISTRIBUTION &amp; HEAT TRANSFER MODE

nucleate boiling (IND=5)

$$T_{sat}(p) < T_l < T_w$$

liquid heat-up &  
nucleate boiling (IND=3)

$$T_l < T_{sat}(p) < T_w$$



where:  $T_{sat}(p)$  is saturation temperature  
 $T_l$  is liquid temperature  
 $T_w$  is wall temperature

## CIRCULATION FLOW PATTERN

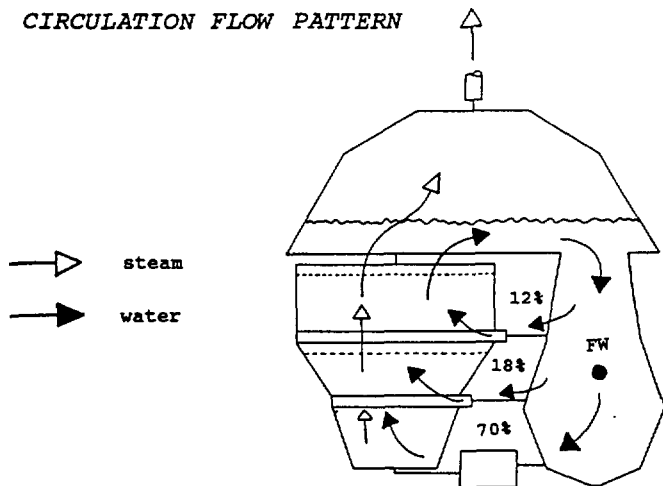
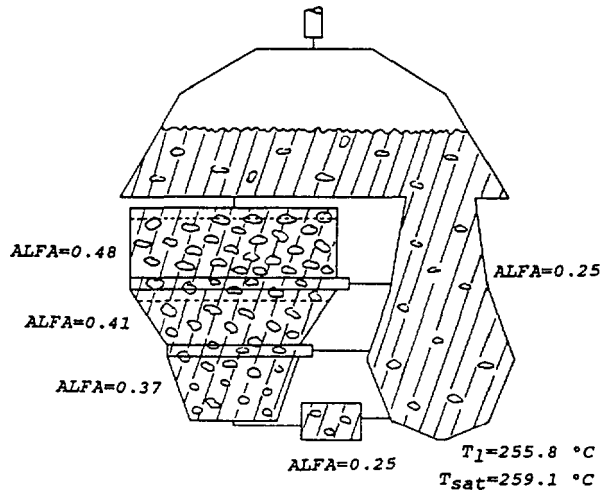


Fig.4 .Basic steady-state values on the SG secondary side,  
case with SEPDRYER option

## VOID FRACTION DISTRIBUTION &amp; HEAT TRANSFER MODE

nucleate boiling (IND=5)

$$T_{sat}(p) < T_l < T_w$$



where:  $T_{sat}(p)$  is saturation temperature  
 $T_l$  is liquid temperature  
 $T_w$  is wall temperature

## CIRCULATION FLOW PATTERN

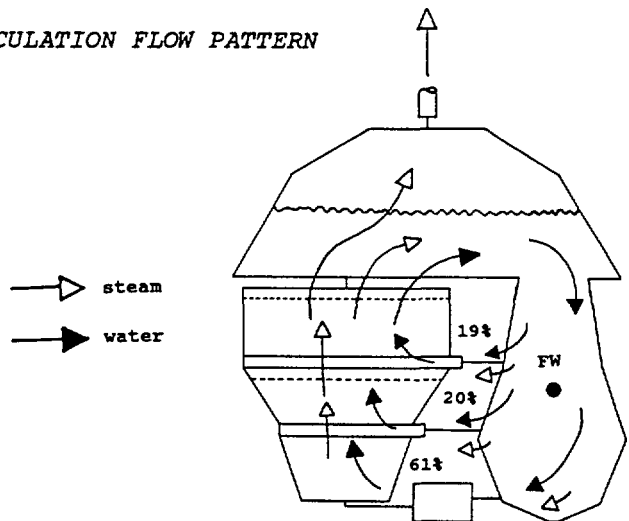


Fig.5 .Basic steady-state values on the SG secondary side,  
 case without SEPDRYER option

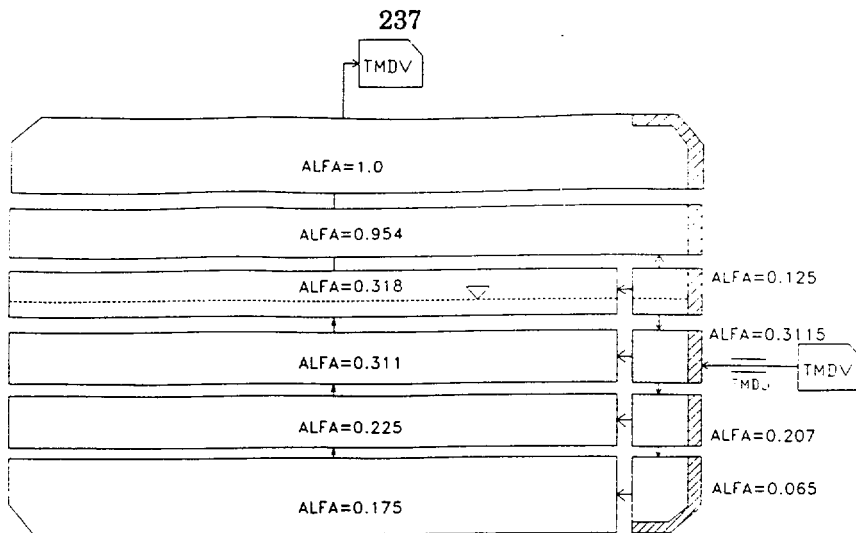


Fig.6. Void fraction distribution, RELAP model

## 4. Secondary water level decreasing transients

### 4.1. Boundary and initial conditions

Only the steam generator with appropriate boundary conditions was modelled.

#### *BOUNDARY CONDITIONS :*

- primary:*
- inlet to the hot collector - *BC3A* for CATHARE and *TMDV* for RELAP code  
(prescribed nominal parameters-imposed condition);
  - outlet from the cold collector - *BC5* or *TMDV*  
(pressure is imposed equal to the value obtained in the steady-state calculation).
- secondary:*
- outlet from the steam generator - *BC5A* or *TMDV*  
(constant pressure equal to the value on the SG outlet is imposed);
  - FW *SOURCE* or *TMDJ* in SG downcomer with  $T_1 = 221^\circ\text{C}$  and mass flow rate prescribed according to scenario used.

The nominal values according to Table 1 were kept during the transient on the primary (mass flow rate, pressure and inlet temperature) and according to Table 2 on the secondary side (pressure).

*INITIAL CONDITIONS :*

Nominal conditions according to Tables 1,2 were considered on the beginning of the transient.

4.2. Scenario

The following transient was considered. At the time  $t=0$  s constant discrepancy between steam and feedwater mass flow is introduced. This discrepancy leads to continual decreasing of the water amount and water level on the secondary side of the SG. During this transient individual rows of the heat exchange tubes should uncover gradually. The transient is described by the following simple differential equation :

$$d [SGMASS(t)]/dt = Q_{FW}(t) - Q_{tot}(t) = const < 0$$

where :  $SGMASS$  is total water mass in SG [kg]  
 $Q_{FW}$  is feedwater mass flow [kg/s]  
 $Q_{tot}$  is total mass flow into steam line [kg/s]

$$Q_{tot} = Q_{steam} + Q_{liquid}$$

Solution of this equation is linear decreasing of  $SGMASS(t)$  in time  $t$ . Possible water entrainment from steam dome into steam line  $Q_{liquid}$  is taken into account. The following rate of decreasing was chosen with the aim to perform a quasi-static transient :  $const = -20$  kg/s. During CATHARE calculation in each computational step of the transient the new value of mass flow rate was defined (*WRITE* directive) for FW source according to the actual total mass flow in the outlet of the secondary side of SG :

$$\begin{aligned}
 Q_{FW}(t) &= Q_{tot}(t) - 20 & \text{if } Q_{tot}(t) > 20 \\
 Q_{FW}(t) &= 0 & \text{if } Q_{tot}(t) < 20
 \end{aligned}$$

In RELAP calculation, the same effect was simply reached using the *TMDJ* with prescribed FW mass flow rate. The calculation was stopped when the SG secondary was nearly empty and the heat transfer from primary to secondary was negligible.

#### 4.3. Results

According to the enclosed figures, in all cases the global behaviour is qualitatively acceptable. Degradation of the SG heat transfer properties occurs in three separate steps what corresponds to the number of modelled heat exchangers. Consequently, there can be seen gradual rise of the primary temperature in SG outlet. At the end of the transient, primary outlet temperature is nearly equal to the inlet one.

At the beginning of the transient, when the initial discrepancy between FW flow and steam production is introduced, the liquid in the SG downcomer become less subcooled than in the nominal conditions and, consequently, slightly increased steam production can be seen. At the end, when the heat transfer from wall to steam is established, the temperature of the steam starts to rise above saturation value.

#### *CATHARE calculation :*

In both used models, the natural phase separation on the secondary water level is efficient enough as long as the swell level is above the junction between riser and steam dome. When the swell level approach to and later drops below this junction, diffusion of liquid into upper subvolume increases significantly. This leads to abnormal water entrainment into the steam line. No special measures with the aim to optimize artificially the flow rate distribution coefficients for were performed this function .

The following heat transfer regimes can be observed during the transient :

IND = 3; 5 forced convection + nucl.boiling; nucl.boiling

IND = 96 transition boiling (6) + natural convection (40)  
+ radiation (50)

IND = 99 post CHF transfer (9) + natural convection (40)  
+ radiation (50); post CHF reached through dry-out  
criterion ( $ALFA > 0.99999$ ).

*RELAP calculation :*

In this case, the transient is more straightforward. The heat transfer degradation occurs in three regular steps and the water entrainment into steam line is negligible. Comparing to the previous case, main differences are due to slightly different description of the volume-height dependence.

The following modes were observed during the transient :

Mode 3;4 nucl.boiling (subcooled or saturated water)  
Mode 6 transition boiling  
Mode 7,8 film boiling  
Mode 9 single phase gas

## 5. Conclusions

Performances with the CATHARE2 V1.3U and RELAP5/MOD3.0 application to the VVER-440 SG modelling during nominal conditions and during transient with secondary water lowering were described. Similar recirculation model was chosen for both codes. In the CATHARE calculation, no special measures were taken with the aim to optimize artificially flow rate distribution coefficients for the junction between SG riser and steam dome.

Contrary to RELAP code, the CATHARE code is able to predict reasonable the secondary swell level in nominal conditions. Both codes are able to model properly natural phase separation on the SG water level.

During the water level decreasing transient both codes are modelling stepwise degradation of the SG heat transfer properties. The number of "steps" is equal to the number of heat exchangers, which are considered in the nodalization scheme. When the secondary swell level drops below the upper row of the SG tubes, the water entrainment into steam line predicted by CATHARE is much higher than this one predicted by RELAP. In this case namely efficiency of the phase separation depends on the hight of the swell level.

## Abbreviations, Acronyms

BC	- Boundary condition
CCFL	- Counter-Current Flow Limitation
CHF	- Critical Heat Flux
EFW	- Emergency Feed Water
FW	- Feed Water
ISP	- International Standard Problem
LOCA	- Loss of Coolant Accident
SG	- Steam Generator
TMDJ	- Time-Dependent Junction
TMDV	- Time-Dependent Volume

## Nomenclature

ALFA	- void fraction
h	- height of water level
p	- pressure
Q	- mass flow rate
$T_1$	- liquid temperature
$T_{sat}$	- saturation temperature
$T_w$	- wall temperature

## 6. References

- [1] T. Haapalehto, D. Bestion : Horizontal steam generator modelling with CATHARE; Validation of several nodalization schemes on plant data, Second International Seminar of the Horizontal Steam Generator Modelling, Lappeenranta Finland, 1993.
- [2] H. Purhonen, J. Miettinen : OECD/NEA/CSNI International Standard Problem No.33 (ISP-33); PACTEL Natural Circulation Stepwise Coolant Inventory Reduction Experiment. Preliminary Comparison Report, Lappeenranta, Finland, April 1993.
- [3] I.Dor : CATHARE2 V1.3. Description of the volume module. Volume M2, STR/LML/EM/94-248, Grenoble, France, August 1994.
- [4] E.Bestion : General description of CATHARE2 V1.3, STR/LML/EM/94-265, Grenoble, France, September 1994.
- [5] F.Urban, L.Zboray : Performance with level indicators of VVER-440 units, Bezpečnost Jaderné Energie (Safety of Nuclear Energy) 1(39), 1993.
- [6] RELAP5/MOD3 code manual, Volume I, Part 1.

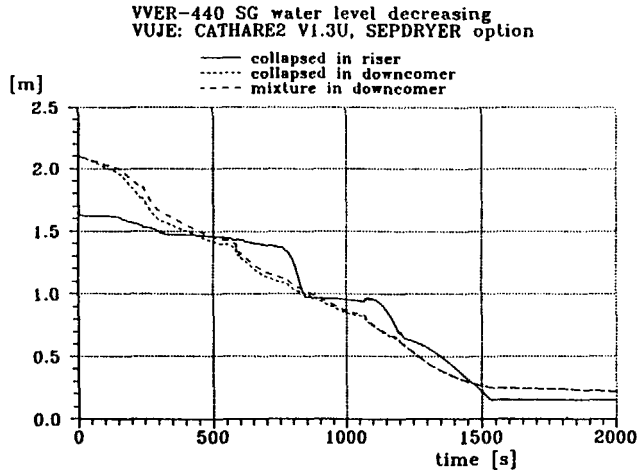


Fig.1. Secondary level in riser and downcomer (collapsed & mixture)

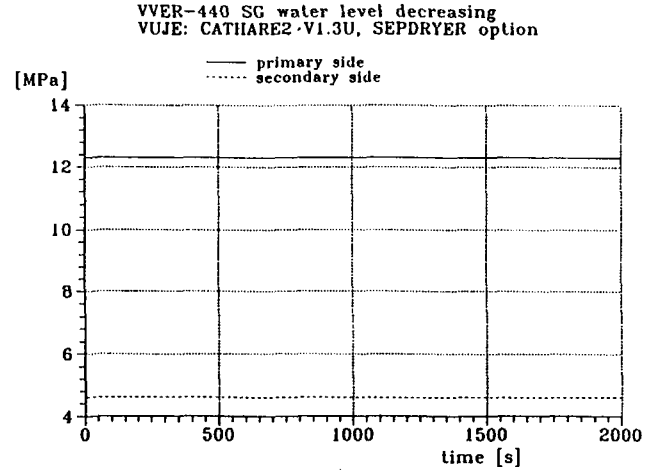


Fig.3. Primary and secondary pressure

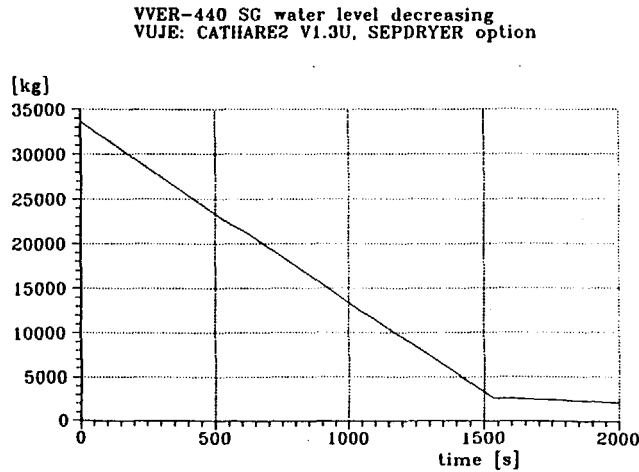


Fig.2. Secondary liquid mass

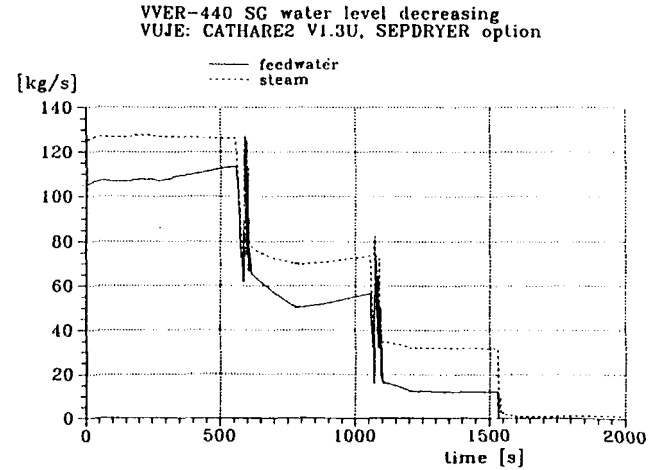


Fig.4. Feedwater and steam mass flow rate

VVER-440 SG water level decreasing  
 VUJE: CATHARE2 V1.3U, SEPDRYER option

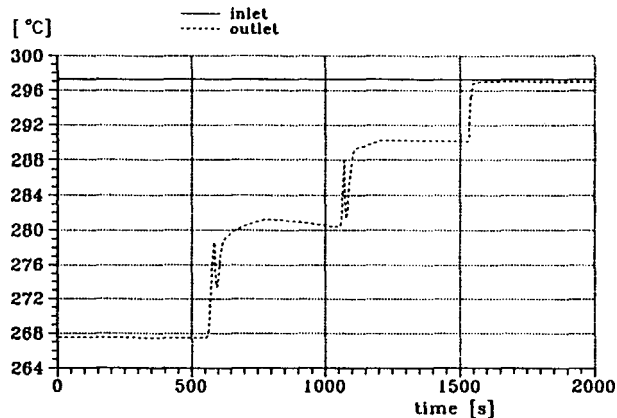


Fig.5. Temperature in SG primary inlet and outlet

VVER-440 SG water level decreasing  
 VUJE: CATHARE2, V1.3U, SEPDRYER option

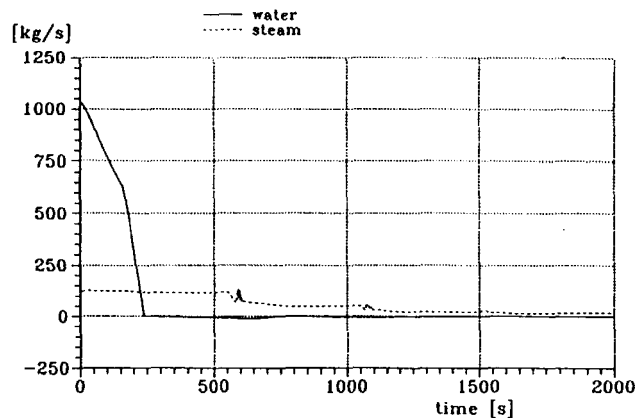


Fig.7. Liquid and steam mass flow rate at the outlet

VVER-440 SG water level decreasing  
 VUJE: CATHARE2 V1.3U, SEPDRYER option

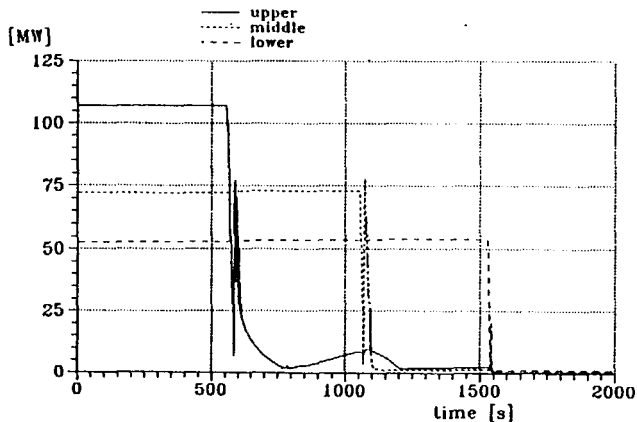


Fig.6. Power exchanged in the upper, middle and lower layer

VVER-440 SG water level decreasing  
 VUJE: CATHARE2 V1.3U, SEPDRYER option

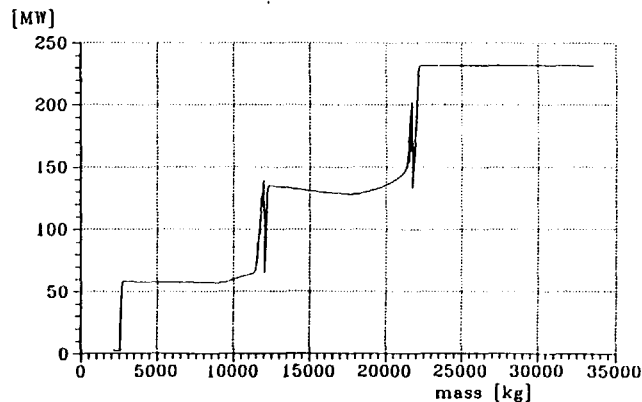


Fig.8. Total exchanged power versus secondary coolant mass in SG

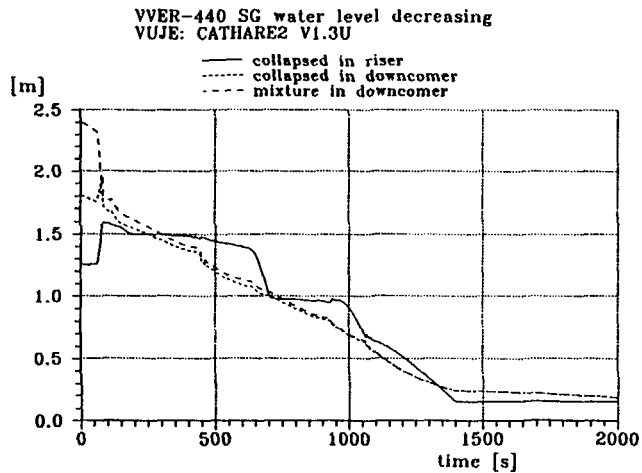


Fig.1. Secondary level in riser and downcomer (collapsed & mixture)

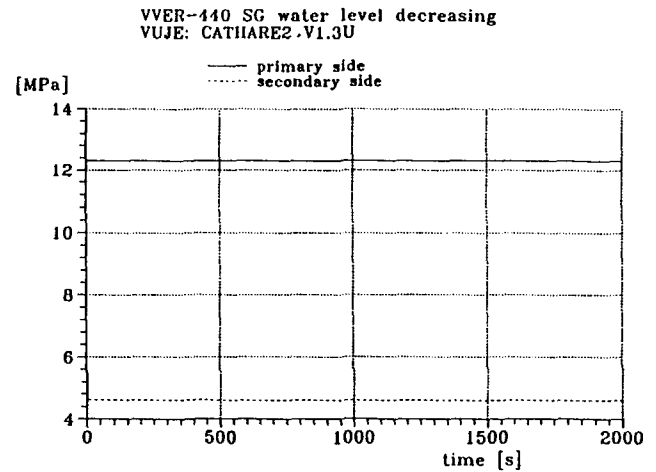


Fig.3. Primary and secondary pressure

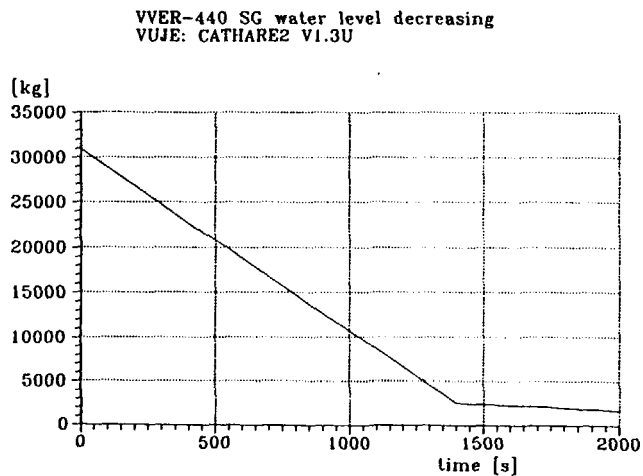


Fig.2. Secondary liquid mass

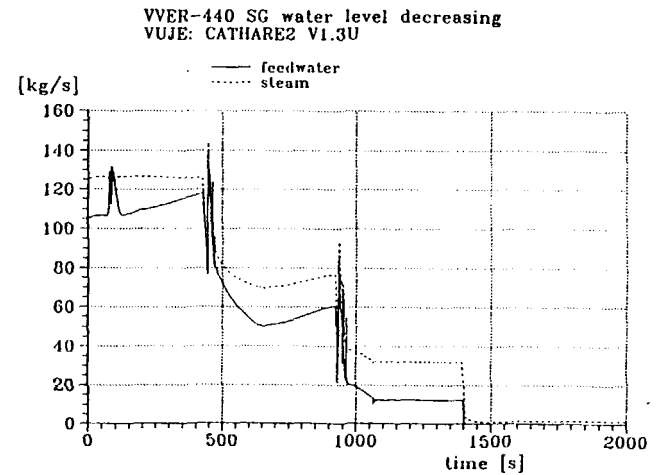


Fig.4. Feedwater and steam mass flow rate

VVER-440 SG water level decreasing  
 VUJE: CATHARE2 V1.3U

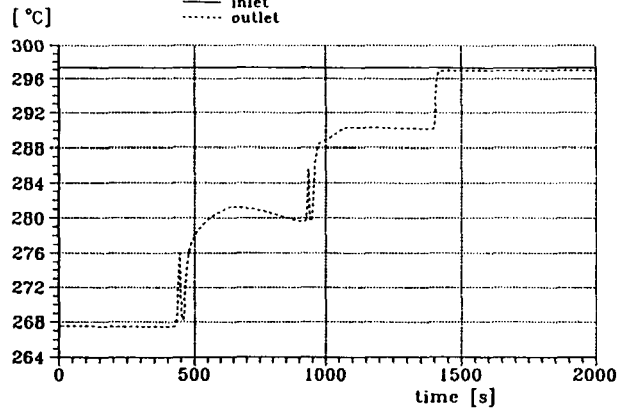


Fig.5. Temperature in SG primary inlet and outlet

VVER-440 SG water level decreasing  
 VUJE: CATHARE2 V1.3U

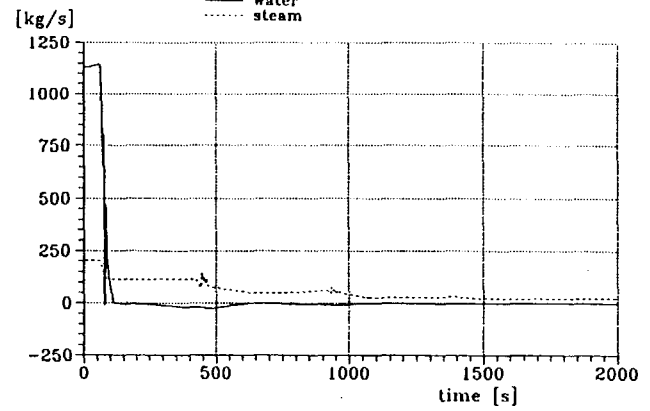


Fig.7. Liquid and steam mass flow rate at the outlet

VVER-440 SG water level decreasing  
 VUJE: CATHARE2 V1.3U

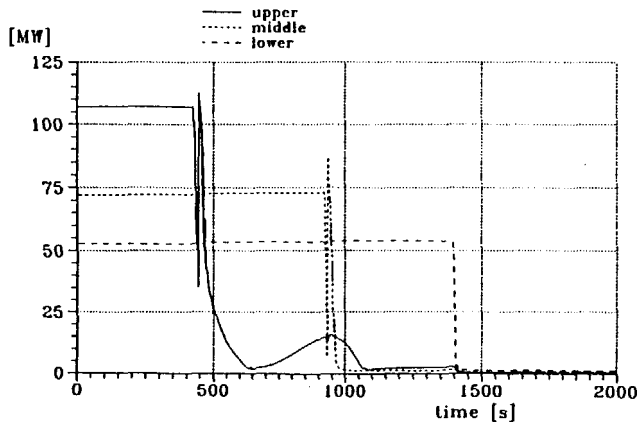


Fig.6. Power exchanged in the upper, middle and lower layer

VVER-440 SG water level decreasing  
 VUJE: CATHARE2 V1.3U

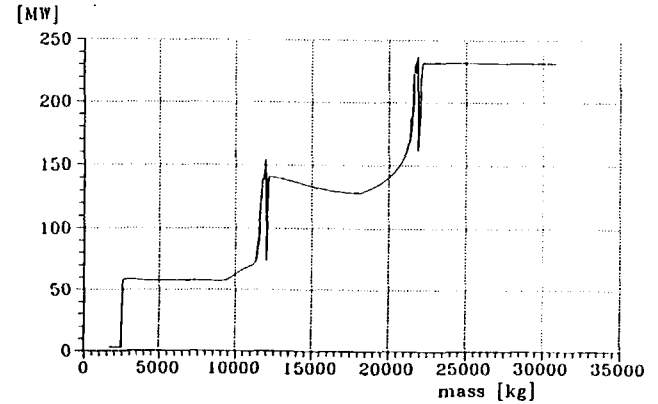


Fig.8. Total exchanged power versus secondary coolant mass in SG

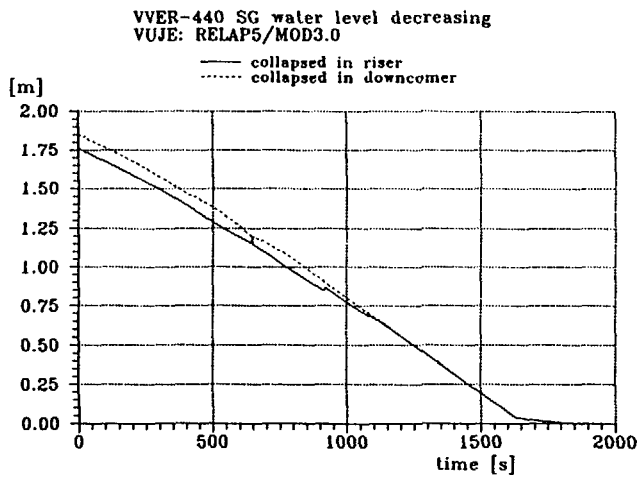


Fig.1. Secondary level in riser and downcomer (collapsed & mixture)

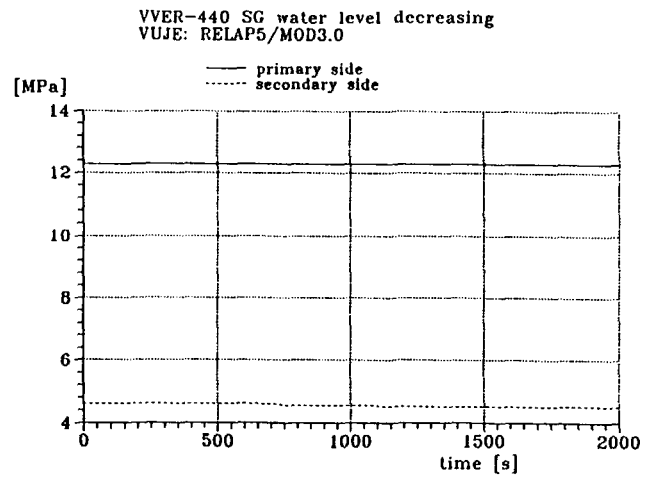


Fig.3. Primary and secondary pressure

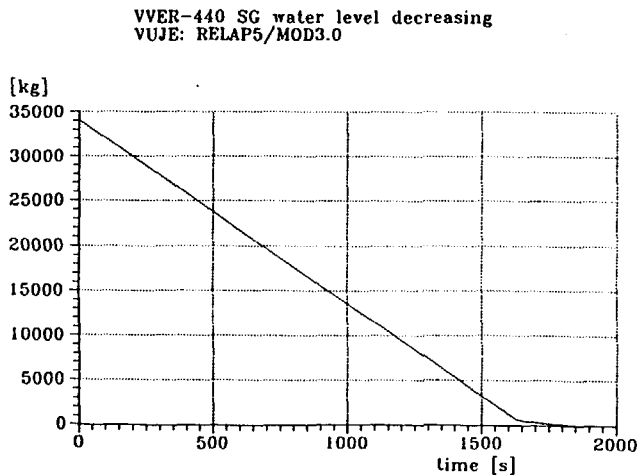


Fig.2. Secondary liquid mass

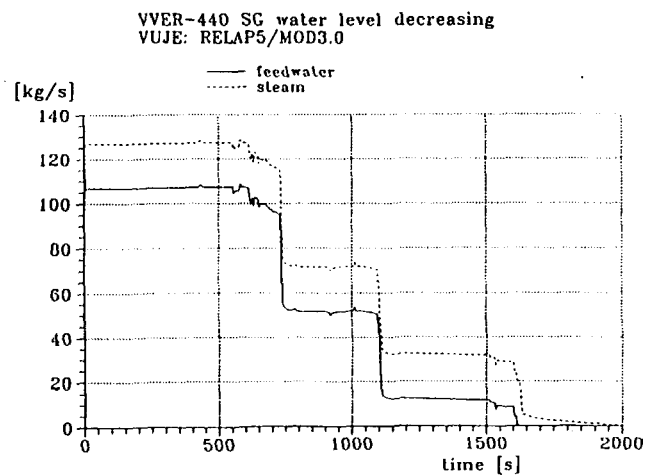


Fig.4. Feedwater and steam mass flow rate

VVER-440 SG water level decreasing  
 VUJE: RELAP5/MOD3.0

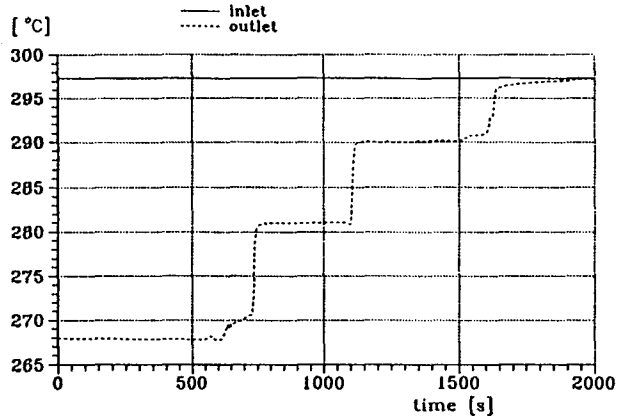


Fig.5. Temperature in SG primary inlet and outlet

VVER-440 SG water level decreasing  
 VUJE: RELAP5/MOD3.0

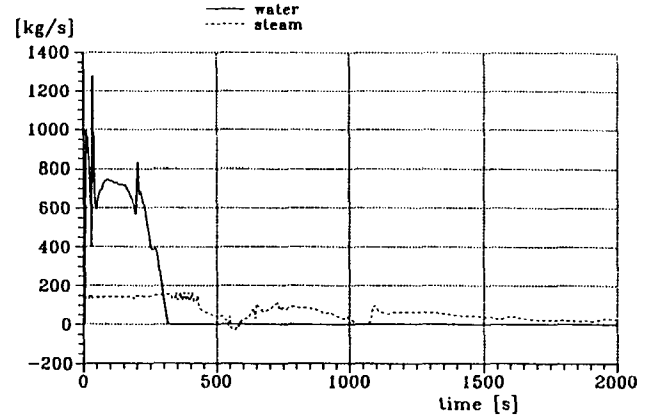


Fig.7. Liquid and steam mass flow rate at the outlet

VVER-440 SG water level decreasing  
 VUJE: RELAP5/MOD3.0

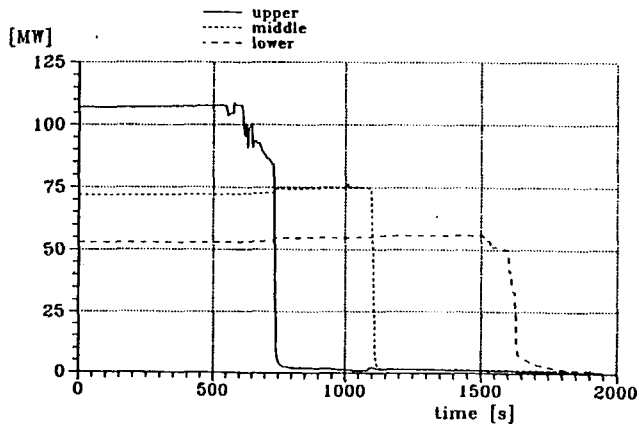


Fig.6. Power exchanged in the upper, middle and lower layer

VVER-440 SG water level decreasing  
 VUJE: RELAP5/MOD3.0

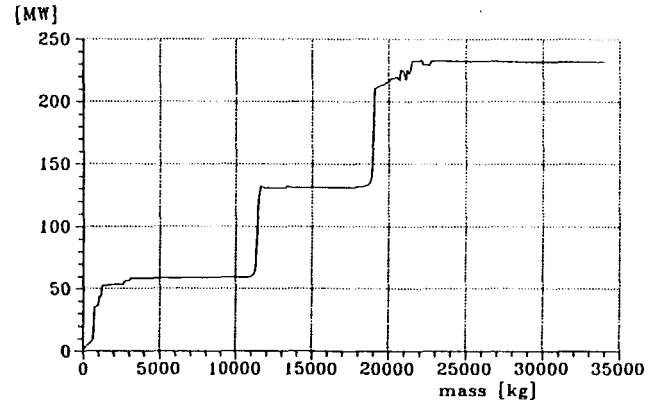


Fig.8. Total exchanged power versus secondary coolant mass in SG

**NUMERICAL MODELING OF SECONDARY  
SIDE THERMOHYDRAULICS  
OF HORIZONTAL STEAM GENERATOR**

**V.I.Melikhov, O.I.Melikhov and B.I.Nigmatulin**

Research & Engineering Centre of LWR Nuclear Plants Safety

Bezmyannaya 6, Electrogorsk,

Moscow Region, Russia 142530

**ABSTRACT**

The mathematical model of the transient three-dimensional secondary side thermal hydraulics of the horizontal steam generator has been developed. The calculations of the steam generator PGV-1000 and PGV-4 nominal regimes and comparison of numerical and experimental results have been carried out.

**INTRODUCTION**

The VVER reactors differ significantly in design compared to reactors of western design. One of these specific design features is a horizontal steam generator, which can be considered as the most important difference to western design.

The steam generator of the VVER-reactors is equipped with horizontal U-tubes. These U-shaped tubes are mounted between vertical inlet and outlet collectors. The hot and cold collectors are positioned in a short distance relative to the horizontal extensions of the U-tubes. A nonuniform heat transfer inducing a nonuniform mass flow distribution on secondary side results from that. The feed-water injection is located above the hot side tubes in order to diminish the level close the hot collector. The general view of the horizontal steam generator PGV-1000 is in the Figure 1.

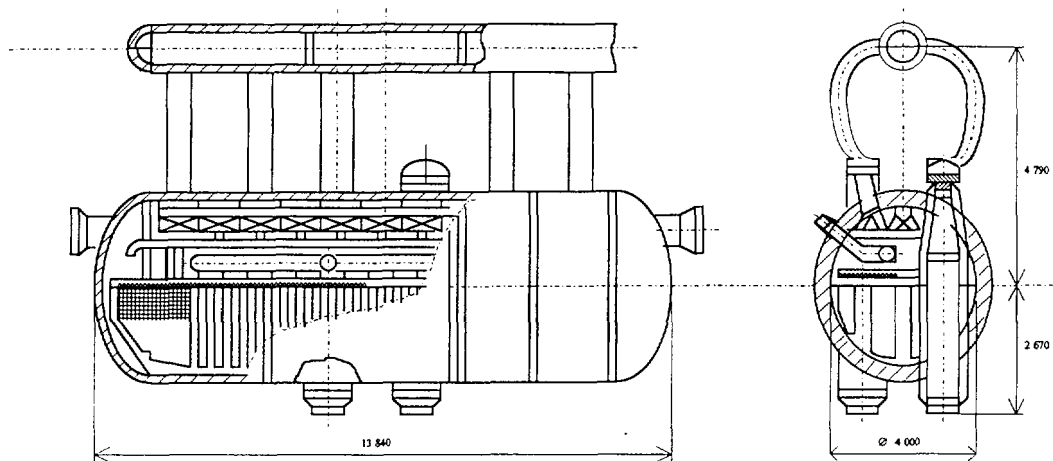


Figure 1. Steam Generator PGV-1000

The development of steam generator PGV-1000 mathematical model is needed for horizontal SG behavior in normal and off-normal operating conditions, investigation of SG response to wide range of thermalhydraulics, geometrical and operation conditions.

The most general model to describe transient thermalhydraulic processes in the steam generator is based on nonsteady three-dimensional multiphase mechanics equations. Mass, momentum and energy conservation laws are formulated for each phase and constitutive relations for different flow regimes are used.

In this paper we present description of mathematical model of horizontal steam generator, numerical method and calculation results.

## **MATHEMATICAL MODEL OF HORIZONTAL STEAM GENERATOR**

The main aim of our investigation is a calculation of thermal-hydraulic processes in the secondary side of SG. For modeling of these processes it is necessary to determine a

heat transfer from tubes of primary side to saturated steam-water two-phase mixture. Therefore, at the beginning we consider the modeling of primary side.

### Primary Side

For determination heat transfer to the secondary side it is necessary to know a temperature distribution of coolant in the tubes having different lengths. The heat exchanger is divided into groups of tubes as it is shown in Figure 2 and the average fluid temperature is evaluated for each group.

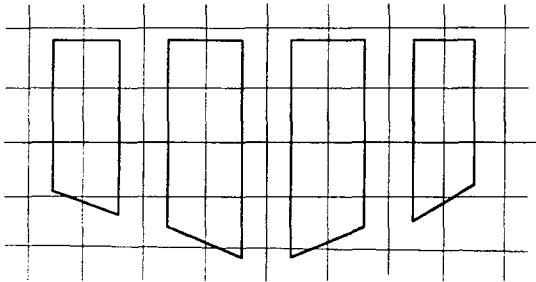


Figure 2. Cross-section of the steam generator.

The temperature distribution along tubes is described by equation of energy

$$\rho c_p \left( \frac{\partial T_I}{\partial t} + w \frac{\partial T_I}{\partial \zeta} \right) = -k (T_I - T_{II}) \frac{S}{V} \quad (1)$$

Here  $\rho$  - coolant density,  $c_p$  - heat capacity,  $T_I, T_{II}$  - temperature in the I and II sides, respectively,  $w$  - coolant velocity,  $S, V$  - surface and volume of tube cell,  $k$  - overall heat transfer coefficient.

Overall heat transfer coefficient is

$$k = \left[ \frac{1}{\alpha_1} + R_w + \frac{1}{\alpha_2} \right]^{-1}$$

$\alpha_1, \alpha_2$  - heat transfer coefficient

$R_w$  - wall thermal resistance.

Heat transfer coefficient for water flow in the tube is defined by Mikheev formula

$$\alpha_1 = 0,021 \cdot (\lambda/d) \text{Re}^{0.8} \cdot \text{Pr}^{0.43}, \quad \frac{\text{W}}{\text{m}^2 \cdot \text{K}}$$

$\lambda$  - water conductivity,  $d$  - tube diameter

$$\text{Re} = \frac{w d_{cp} \cdot \rho}{\mu} - \text{Reynolds number}$$

$$\text{Pr} = \frac{\mu \cdot c_p}{\lambda} - \text{Prandtle number}$$

Heat transfer coefficient from tube surface to saturated mixture is

$$\alpha_2 = 4,32 \cdot (p^{0.14} + 1,28 \cdot 10^{-2} \cdot p^2) q^{0.7}, \quad \frac{\text{W}}{\text{m}^2 \cdot \text{K}}$$

$p$  - pressure, MPa

$q$  - heat flux,  $\text{W}/\text{m}^2$

Wall thermal resistance  $R_w$  is determined by integral condition of energy balance.

After integrating equation (1) with a boundary condition at the inlet  $T_l = T_{in}$ , we receive coolant temperature distribution along tubes of primary sides.

### Secondary Side

The non-steady three-dimensional equations of mass, momentum and energy conservation and constitutive relations are formulated for the water (phase 1) and steam (phase 2). Tubes of primary side in the SG are taken into account by consideration of volume fraction of third phase (tubes). It is used the set of equations of motion for slow flows

### The conservation equation of momentum

Water:

$$\alpha_1 \rho_1^0 \frac{d_1 \bar{U}_1}{dt} = -\alpha_1 \nabla p + \alpha_1 \rho_1^0 \bar{g} + \bar{F}_{21} + \bar{F}_{31} - \Gamma(\bar{U}_{1i} - \bar{U}_1) + M_1(\bar{V}_1 - \bar{U}_1) \quad (2)$$

Steam:

$$\alpha_2 \rho_2^0 \frac{d_2 \bar{U}_2}{dt} = -\alpha_2 \nabla p + \alpha_2 \rho_2^0 \bar{g} - \bar{F}_{21} + \bar{F}_{32} + \Gamma(\bar{U}_{2i} - \bar{U}_2) \quad (3)$$

### Generalized equation of incompressibility

$$\begin{aligned} \operatorname{div}(\alpha_1 \bar{U}_1) + \operatorname{div}(\alpha_2 \bar{U}_2) &= \frac{dP_0}{dt} (\alpha_1 A_1 + \alpha_2 A_2) + \\ &+ \frac{-\Gamma + M_1}{\rho_1^0} + \frac{\Gamma}{\rho_2^0} - B_1 [q_{i1} - \Gamma(i_{s1} - i_1) + q_{31} + M_1(H_1 - i_1)] - \\ &- B_2 [q_{i2} + \Gamma(i_{s2} - i_2)] \end{aligned} \quad (4)$$

where

$$A_1 = \frac{1}{\rho_1^{02}} \left\{ \rho_1^0 \left( \frac{\partial \rho_1^0}{\partial P_0} \right)_i + \left( \frac{\partial \rho_1^0}{\partial i_1} \right)_p \right\}, \quad B_1 = \frac{1}{\rho_1^{02}} \left( \frac{\partial \rho_1^0}{\partial i_1} \right)_p$$

$$A_2 = \frac{1}{\rho_2^{02}} \left\{ \rho_2^0 \left( \frac{\partial \rho_2^0}{\partial P_0} \right)_i + \left( \frac{\partial \rho_2^0}{\partial i_2} \right)_p \right\}, \quad B_2 = \frac{1}{\rho_2^{02}} \left( \frac{\partial \rho_2^0}{\partial i_2} \right)_p$$

**Energy conservation equations**

Water:

$$\alpha_1 \rho_1^0 \frac{d_1 i_1}{dt} = \alpha_1 \frac{dP_0}{dt} + q_{i1} - \Gamma (i_{s1} - i_1) + q_{31} + M_1 (H_1 - i_1) \quad (5)$$

Steam:

$$\alpha_2 \rho_2^0 \frac{d_2 i_2}{dt} = \alpha_2 \frac{dP_0}{dt} + q_{i2} + \Gamma (i_{s2} - i_2) + q_{32} \quad (6)$$

**Equations for determination of volumetric fractions**

$$\frac{\partial \alpha_2}{\partial t} + \text{div}(\alpha_2 \bar{U}_2) = \alpha_2 A_2 \frac{dP_0}{dt} + \frac{\Gamma}{\rho_2^0} - B_2 [q_{i2} + \Gamma (i_{s2} - i_2) q_{32}] \quad (7)$$

$$\alpha_1 + \alpha_2 + \alpha_3 = 1 \quad (8)$$

**Equation for average pressure**

$$\begin{aligned} \frac{dP_0}{dt} = & \left[ \int_s (\alpha_1 \bar{V}_1 + \alpha_2 \bar{V}_2) d\bar{s} - \int_v \left( \frac{-\Gamma + M_1}{\rho_2^0} + \frac{\Gamma}{\rho_2^0} \right) dv + \right. \\ & \left. + \int_v \{ B_1 [q_{i1} - \Gamma (i_{s1} - i_1) + q_{31} + M_1 (H_1 - i_1)] + \right. \\ & \left. + B_2 [q_{i2} + \Gamma (i_{s2} - i_2)] \} dv \right] / \int_v (\alpha_1 A_1 + \alpha_2 A_2) dv \quad (9) \end{aligned}$$

**Equations of state for steam-water mixture**

$$\rho_1^0 = \rho_1^0 (P_0, i_1), \quad \rho_2^0 = \rho_2^0 (P_0, i_2) \quad (10)$$

The indexes 1, 2, 3 refer to water, steam and tubes respectively,  $M_1$  - mass rate of source,  $\bar{V}_1$  - velocity of feed water,  $H_1$  - enthalpy of feed water.

## Constitutive Laws

### Interfacial momentum coupling

#### Steam-Water

In this paper we use correlations given in [1].

It is assumed that steam-water flow regimes are defined by the value of the void fraction  $\phi = \alpha_2 / (\alpha_1 + \alpha_2)$ :  $\phi \leq 0,3$  (Bubbly),  $0,3 < \alpha < 0,7$  (Churn-Turbulent) and  $\alpha \geq 0,7$  (Droplet).

The exchange laws are used available for two-phase systems after making suitable modifications to account for, as a first approximation, the effect of a third phase. In calculating interfacial momentum exchange, one needs to know the projected area concentration of the dispersed phase. Also, in calculating interfacial heat exchange, one needs to know the interfacial area concentration. In a two-phase system, these area concentrations can be estimated from the length scale and the volume fraction of the dispersed phase. However, the presence of a third phase reduces the area concentration as the third phase must also share the same area. Therefore, area concentration is modified by a factor  $\Phi_{ij} = \alpha_j / (\alpha_j + \alpha_k)$ ; representing the effect of the phase  $k$  on the area concentration of phase  $i$  for its interaction with phase  $j$ . Note that with this definition  $\Phi_{ij}$  lies between 0 and 1.

The interfacial momentum coupling is primarily due to drag. The drag force is based on [2]. Specifically,

$$\bar{F}_{ij} = \frac{3}{4} \alpha_i \Phi_{ij} \rho_j \frac{C_{Dij}}{l_j} |\bar{U}_i - \bar{U}_j| (\bar{U}_i - \bar{U}_j)$$

where suffices  $i$  and  $j$  refer to dispersed and continuous phases, respectively. The drag coefficient for churn flow ( $0,3 < \varphi < 0,7$ ) is defined by

$$i = 2 \quad j = 1, C_{Dij} = \frac{8}{3}(1 - \varphi)^2 \quad \text{and} \quad l_i = 4 \left\{ \frac{g\Delta\rho}{\sigma} \right\}^{-1/2}$$

For dispersed flow ( $\alpha_i < 0,3$ ) we have

$$C_{Dij} = \frac{2}{3} l_i \left\{ \frac{g\Delta\rho}{\sigma} \right\}^{1/2} \left\{ \frac{1 + 17.67(f_i(\varphi))^{6/7}}{18.67f_i(\varphi)} \right\}^2$$

where

$$i = 2, \quad j = 1, \quad \varphi \leq 0.3 \quad f_i(\varphi) = (1 - \varphi)^{1.5}$$

$$i = 1, \quad j = 2, \quad \varphi > 0.7 \quad f_i(\varphi) = \varphi^3$$

and  $l_i$  is obtained from

$$\frac{\rho_i |\bar{U}_1 - \bar{U}_2| l_i}{\sigma} = We_{cr} \quad \begin{cases} 8 & \text{for } i = 2 \\ 12 & \text{for } i = 1 \end{cases}$$

### (Steam-Water)-Tubes

The hydraulic resistances assessment of two-phase steam-water flow through heat exchanger tubes is based on the homogeneous model of steam-water mixture.

The pressure losses  $\Delta p_H$  are defined by

$$\Delta p_H = \Delta p_{HO} \left[ 1 + x \left( \frac{\rho_1^0}{\rho_2^0} - 1 \right) \right]$$

Here  $\Delta p_{HO}$  - hydraulic resistance of one-phase medium with circulation velocity  $w_o$  and water density at the saturation temperature,  $x$  - quality. Circulation velocity  $w_o$  is velocity of water under condition

$$\rho_1^0 w_o = \rho_m w_m$$

For longitudinal flow  $\Delta p_{HO}$  is

$$\Delta p_{HO} = \zeta \frac{\rho_l^0 w_0^2}{2}$$

$$\zeta = \frac{64}{Re}, \quad Re < 4 \cdot 10^3$$

$$\zeta = (1.82 \lg Re - 1.64)^{-2}, \quad Re = 4 \cdot 10^3 \div 10^{12}$$

For transverse flow  $\Delta p_{HO}$  is

$$\Delta p_{HO} = \zeta_{\pi} \rho_l^0 \frac{w_0^2}{2}$$

Flow resistance coefficient is

$$\zeta_{\pi} = (4 + 6.6z_2) Re^{-0.28}$$

where  $z_2$  - row number along flow direction.

We assume that hydraulic resistances act only on liquid phase

$$\bar{F}_{31} = \frac{\Delta p_H}{h} \bar{f}, \quad \bar{F}_{32} = 0$$

where  $h$  - size of numerical cell,  $\bar{f}$  - unit vector.

### Interfacial Heat Transfer and Phase Change

It is assumed that steam and water are under saturation condition. The phase change between liquid and gas are calculated such as to maintain local thermodynamic equilibrium.

Let calculated value of water enthalpy  $\bar{i}_1 > i_{1S}$ , then phase change rate is

$$\Gamma = \frac{\alpha_1 \rho_l^0}{\tau} \frac{i_{1S} - \bar{i}_1}{\bar{i}_1 - i_{2S}}$$

where  $\tau$  - time step.

This model couples very nicely with the numerical method. The relaxation time for thermodynamic equilibrium equals the time step ( $\tau \approx 10^{-2} c$ ).

### Numerical Method

We developed original method to solve equations describing small Mach flows of two-phase mixture in the secondary side of steam generator.

Let in some time  $t^n = n \cdot \tau$  where  $\tau$ - time step,  $n$ - number of steps, we know fields of all physical parameters. Then unknown functions for time  $t^{n+1} = (n+1)\tau$  are determined in following order: 1) from Eqs. (5), (6), (7), (8) we determine values  $i_1^{n+1}, i_2^{n+1}, \alpha_1^{n+1}, \alpha_2^{n+1}$ ; 2) calculate  $P_0^{n+1}$  from (9) and  $\rho_1^{0n+1}, \rho_2^{0n+1}$  from (10); 3) from solution of equations (2), (3)  $\bar{U}_1^{n+1}$  and  $\bar{U}_2^{n+1}$  are found, accounting (4).

Let's consider each step of calculations in details.

1) Solving equation (5), the calculation of boiling process is considered as a separate step. On the first fractional step ( $n \rightarrow n + \frac{1}{2}$ ) only convection influence is taken into account. We use explicit scheme of calculation:

$$\alpha_1^n \rho_1^{0n} \frac{i_1^{n+1/2} - i_1^n}{\tau} = - (\bar{U}_1^n \cdot \nabla) i_1^n$$

Supply of feed water, heat transfer from tubes and average pressure change are taken into account on the second fractional step.

$$\alpha_1^n \rho_1^{0n} \frac{\tilde{i}_1^{n+1} - i_1^{n+1/2}}{\tau} = \alpha_1^n \left( \frac{dP_0}{dt} \right)^n + q_{31} + M_1 (H_1 - \tilde{i}_1^{n+1})$$

The calculation on this step are realized by implicit scheme to remove limitations of time step due to source terms.

Then, if value  $\tilde{i}_1^{n+1}$  exceeds enthalpy of saturation water, we believe that  $i_1^{n+1} = i_{1S}$ , and steam generation rate is calculated as

$$\Gamma = \frac{\alpha_1^n \rho_1^{o n} i_{1S} - \tilde{i}_1^{n+1}}{\tau \tilde{i}_1^{n+1} - i_{2S}}$$

Volumetric steam fraction are determined from equation (7), using simple explicit scheme

$$\frac{\alpha_2^{n+1} - \alpha_2^n}{\tau} = -\operatorname{div}(\alpha_2^n \bar{U}_2^n) + \alpha_2^n A_2 \left( \frac{dP_o}{dt} \right)^n + \frac{\Gamma}{\rho_2^{o n}} - B_2 \cdot \Gamma (i_{S2} - i_2)$$

It is assumed, that

$$q_{i2} = q_{32} = 0$$

From (8) we determine a volume fraction of water

$$\alpha_1^{n+1} = 1 - \alpha_2^{n+1} - \alpha_3$$

2) Solving by (9), (10) we can find  $P_o^{n+1}$ ,  $\rho_1^{o n+1}$ ,  $\rho_2^{o n+1}$ .

3) First of all it is considered influence of convection, pressure gradient and sources, which defined by letter S. Calculations are implemented explicitly.

$$\frac{\bar{U}_1^{n+1/2} - \bar{U}_1^n}{\tau} = -(\bar{U}_1^n \cdot \nabla) \bar{U}_1^n - \frac{1}{\rho_1^{o n+1}} \nabla p^{n+1} + S_1 \quad (11)$$

$$\frac{\bar{U}_2^{n+1/2} - \bar{U}_2^n}{\tau} = -(\bar{U}_2^n \cdot \nabla) \bar{U}_2^n - \frac{1}{\rho_2^{o n+1}} \nabla p^{n+1} + S_2 \quad (12)$$

Obtained values  $\bar{U}_1^{n+1/2}$ ,  $\bar{U}_2^{n+1/2}$  are not satisfied to generalized incompressible condition.

So on the second step a velocity correction is made.

$$\frac{\alpha_1^{n+1} \bar{U}_1^{n+1} - \alpha_1^{n+1} \bar{U}_1^{n+1/2}}{\tau} = -\frac{\alpha_1^{n+1}}{\rho_1^{o n+1}} \nabla (\delta p^{n+1})$$

$$\frac{\alpha_2^{n+1} \bar{U}_2^{n+1} - \alpha_2^{n+1} \bar{U}_2^{n+1/2}}{\tau} = -\frac{\alpha_2^{n+1}}{\rho_2^{o n+1}} \nabla (\delta p^{n+1})$$

where  $\delta p^{n+1} = p^{n+1} - p^n$ .

Summing up these equations and using the divergence operation we have gotten the Poisson equation for correction of pressure.

$$\nabla \left\{ \left( \frac{\alpha_1^{n+1}}{\rho_1^{\circ n+1}} + \frac{\alpha_2^{n+1}}{\rho_2^{\circ n+1}} \right) \nabla (\delta p^{n+1}) \right\} = -\frac{1}{\tau} \left\{ \operatorname{div} (\alpha_1^{n+1} \bar{U}_1^{n+1}) + \right. \\ \left. + \operatorname{div} (\alpha_2^{n+1} \bar{U}_2^{n+1}) - \operatorname{div} (\alpha_1^{n+1} \bar{U}_1^{n+1/2}) - \operatorname{div} (\alpha_2^{n+1} \bar{U}_2^{n+1/2}) \right\}$$

Using the equation (4) to define  $\operatorname{div} (\alpha_1^{n+1} \bar{U}_1^{n+1})$  and  $\operatorname{div} (\alpha_2^{n+1} \bar{U}_2^{n+1})$ , we obtain

$$\nabla \left\{ \left( \frac{\alpha_1^{n+1}}{\rho_1^{\circ n+1}} + \frac{\alpha_2^{n+1}}{\rho_2^{\circ n+1}} \right) \nabla (\delta p^{n+1}) \right\} = -\frac{1}{\tau} \left\{ \left( \frac{dP_o}{dt} \right)^{n+1} (\alpha_1^{n+1} A_2 + \alpha_2^{n+1} A_2) + \right. \\ \left. + \frac{-\Gamma + M_1}{\rho_1^{\circ n+1}} + \frac{\Gamma}{\rho_2^{\circ n+1}} - B_1 [q_{i1} - \Gamma (i_{S1} - i_1^{n+1})] + q_{31} + \right. \\ \left. + M_1 (H_1 - i_1^{n+1}) \right] - B_2 [q_{i2} + \Gamma (i_{S2} - i_2^{n+1})] \left. \right\} \quad (13)$$

Integration of this Poisson equation has been done with iterative method of Gauss-Zeidel.

After determination  $\delta p^{n+1}$  a final velocity values are calculated.

$$\frac{\bar{U}_1^{n+1} - \bar{U}_1^{n+1/2}}{\tau} = -\frac{1}{\rho_1^{\circ n+1}} \nabla (\delta p^{n+1}) \quad (14)$$

$$\frac{\bar{U}_2^{n+1} - \bar{U}_2^{n+1/2}}{\tau} = -\frac{1}{\rho_2^{\circ n+1}} \nabla (\delta p^{n+1}) \quad (15)$$

It should be noticed, that this velocity field will satisfy the general condition of incompressibility (4).

Approximation of differential equations was made on the MAC-grid. All computational domain was divided on the cells so, that velocities were determined in the center of edges, and all other values - in the center of cell. The "upwind" differences were used for approximation of convective terms.

The significant moment is that in proposed scheme there is no limit on time step, connected with sonic effects. So calculations can be made with the time step, determined by physical process. Thus the application of explicit approximation in this numerical method is valid.

## RESULTS OF NUMERICAL SIMULATION OF STEAM GENERATOR THERMOHYDRAULICS

Computer code STEG-01 (STEam Generator, 1 version) has been developed on the base of the mathematical model, described in the third section. Nominal regimes of operation of horizontal steam generator PGV-1000 (VVER-1000) and PGV-4 (VVER-440) have been calculated by code STEG-01. Our results predict general flow patterns and the distributions of parameters of steam-water mixture in SG.

### Modelling of PGV-1000

Our calculations gave following picture of two-phase flow in the SG. Between tubes steam-water mixture moves generally up. In the "pure" volume flow has down direction. Under tubes in the central region of SG mixture moves from hot collector to cold one and in the periphery part mixture moves to sides of SG. Water moves down near side surfaces and enters down part of SG (under tubes). Numerical picture of water circulation is similar to experimental one [3].

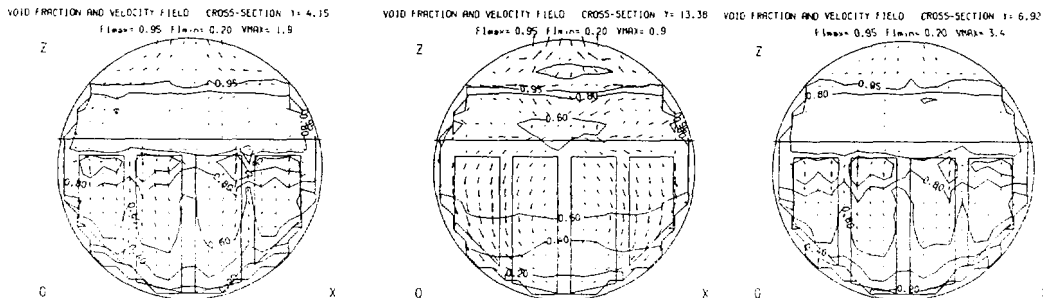


Figure 3. Steam-water velocity and void fraction distribution.

Specific details of steam-water flow in SG are shown on the Fig.3, 4, 5. Steam-water mixture velocity fields and void fraction fields are demonstrated on these figures. Fig.3 shows pictures in 3 cross section of SG:  $y = 4.15$  m ( $y$ -coordinate begins at hot side of SG),  $y = 6.92$ ,  $y = 13.38$  m. Mixture velocity is defined as

$$\bar{V} = \frac{\alpha_1 \bar{U}_1 + \alpha_2 \bar{U}_2}{\alpha_1 + \alpha_2} \quad (16)$$

Hydrodynamic pictures in the horizontal sections between submerged perforated sheets and tubes (a), and in the down part of the SG (b) are shown in the Fig.4.

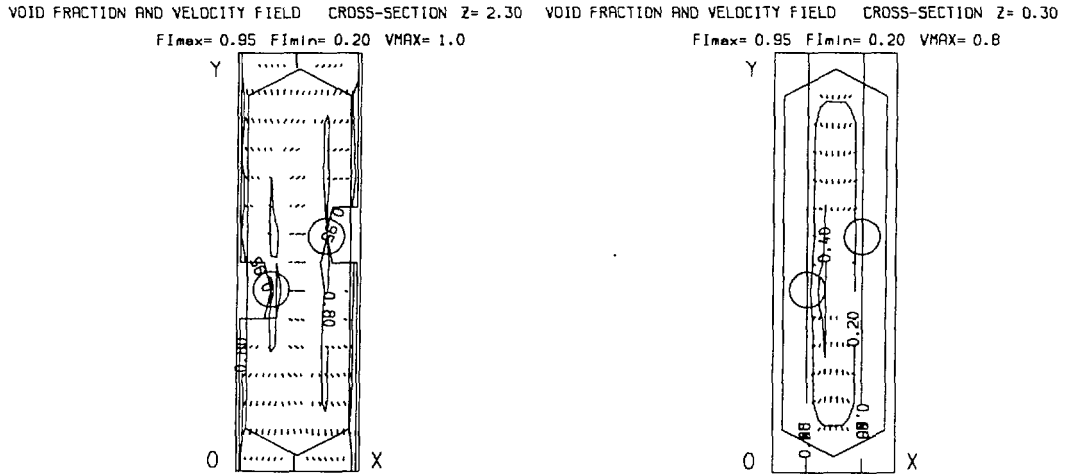


Figure 4.

Hydrodynamic picture in the vertical section of SG is shown on the Fig.5.

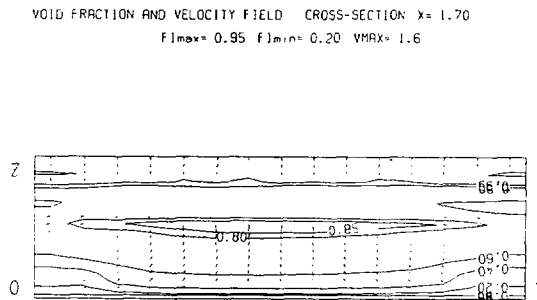


Figure 5.

## Verification of the code STEG-01

Experimental results, obtained at the fifth unit of Novovoronezh NPP VVER-1000 were used to verify the code STEG-01. Investigated SG PGV-1000 [4] was equipped by gauges of velocity and void fraction. Arrangement of gauges is shown on the Fig.6.

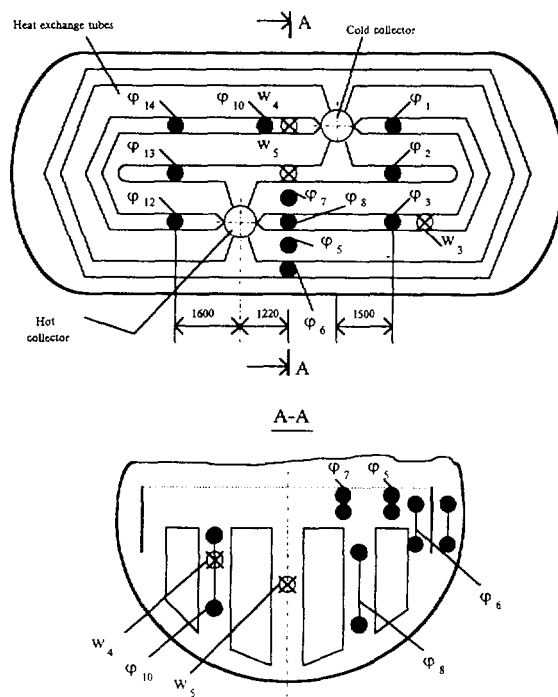


Figure 6. Arrangement of gauges.

A comparison of experimental and numerical data on steam-water mixture velocities is given in the Table 1.

Table 1

Velocity	Experiment	Calculation
$w_3$	0,35	0,45
$w_4$	0,7	0,60
$w_5$	0,3	0,38

There is a satisfied agreement between experimental and calculated results.

A comparison of numerical and experimental void fraction values is given in the Table 2.

Table2

Void fraction	Experiment	Calculation
$\varphi_1$	0,3	0,55
$\varphi_2$	0,45	0,63
$\varphi_3$	0,45	0,54
$\varphi_5$	1,0	0,84
$\varphi_6$	0,7	0,77
$\varphi_7$	1,0	0,89
$\varphi_8$	0,55	0,55
$\varphi_{10}$	0,47	0,56
$\varphi_{12}$	0,52	0,51
$\varphi_{13}$	0,5	0,63
$\varphi_{14}$	0,55	0,54

Also we verified our numerical results against experimental data [5]. Tables 3 and 4 provide a comparison results.

Table 3

Velocity	Experiment	Calculation
$w_3$	0.3	0.42
$w_4$	0.55	0.60
$w_5$	0.3	0.2

Table 4

Void fraction	Experiment	Calculation
$\varphi_3$	(0.2)-0.4	0.50
$\varphi_4$	0.4	0.47
$\varphi_5$	(0.4)	0.52

It was interesting to compare results of our model with another models. Figures 7 and 8 show void fraction distributions along height near hot collector calculated by STEG-01 and mathematical model [6]. It is a good comparison of results.

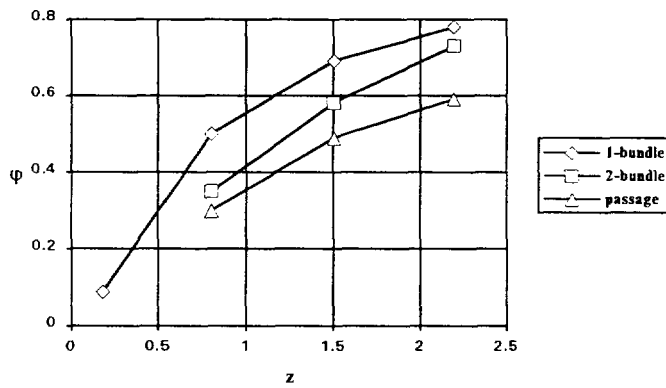


Figure 7. Distribution of void fraction along height [6].

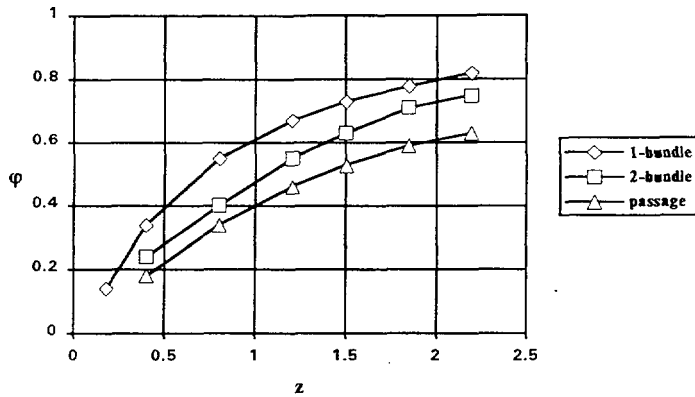


Figure 8. Distribution of void fraction along height (STEG-01).

### Modelling of PGV-4

Nominal operation regime of steam generator PGV-4 has also been calculated by code STEG-01.

Numerical simulation predicts the picture of natural circulation in the steam generator (Fig. 9). Steam-water mixture moves up in the tube bundles and moves down in the downcomer passages.

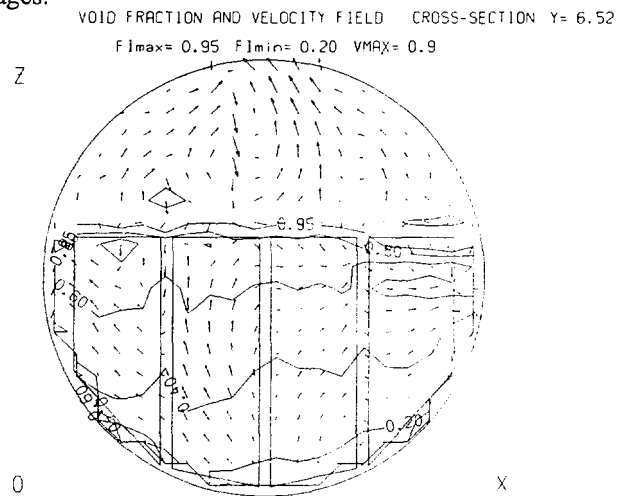


Figure 9. Velocity and void fraction distribution in the SG cross-section.

Calculation results were compared with experimental data obtained at 3rd Unit of Novovoronezh NPP. Five gauges were located in downcomer passages of the bundle from hot side to cold side. Comparison of results are presented in Table 5.

Table 5

Velocity	Experiment	Calculation
$w_1$	-	0.24
$w_2$	-	0.2
$w_3$	0.5	0.3
$w_4$	0.5	0.3
$w_5$	-	0.26

Table 6

Void fraction	Experiment	Calculation
$\varphi_1$	0.25	0.30
$\varphi_2$	0.30	0.32
$\varphi_3$	0.38	0.35
$\varphi_4$	0.38	0.37
$\varphi_5$	0.27	0.24

Void fraction transducers, used in the experiments measured only average values in the some regions. This circumstance introduces some difficulties in the comparison. Nevertheless we consider the results of first verification of STEG-01 as good and hope that after some modifications of mathematical model we obtain better coincidence.

## CONCLUSION

In this paper we have presented the computer code STEG-01 to investigate thermohydraulics of the horizontal steam generator. The mathematical model of

has been developed; calculations of nominal regimes of steam generator operation have been implemented and compared with experimental results.

The code STEG can be considered as structure module describing horizontal SG ,and potentially can be incorporated into the codes , like RELAP or TRAC, improving mathematical models of codes.

Another description is to use the code STEG for detailed calculations of nominal regime of horizontal SG and also different advanced modifications of PGV-1000.

In the next version of code STEG we are going to take into account the presence of internal structures in the SG's vessel more detailed. First of all, it concerns the models of submerged perforated sheet. Also , the calculation of salt concentration ;circulating in the secondary side of SG and depositing on the tubes and collectors, will be incorporated in the program.

Code verification on experimental data will be continued , connected with research to select the best correlation for two-phase flow description.

Full description of the STEG-01 is given in [7].

## REFERENCES

1. Medehekar S., Amarasooriya W.H., Theofanous T.G. *Integrated analysis of steam explosions*. NURETH-4, 1989, Vol. 1, pp.319-326.
2. Ishii M., Zuber N. *Drag coefficient and relative velocity in bubbly, droplet or particulate flows*. *AIChE JI.*, 1979, Vol. 25, pp. 843-855.
3. Titov V.F., Kozlov Yu.V. et al. *Water circulation in the steam generator PGV-1000*. *Teploenergetika*, 1991, N7, pp. 54-58. (In Russian).
4. Ageev A.G., Vasilyeva R.V. et al. *Investigation of hydrodynamics of steam generator PGV-1000*. *Electriccheskie stancii*, 1987, N6, pp.19-23. (In Russian).
5. Trunov N.B. *Enhansment of relilbility and improvement of construction for horizontal steam generators*. Ph.D., 1991 (In Russian).

6. Gorburov V.I., Zorin V.M. *Computer modelling of water hydrodynamics of steam generator PGV-1000*. Teploenergetika, 1994, N5, pp.22-29. (In Russian).

7. Melikhov V.I., Melikhov O.I. *Mathematical modeling of horizontal steam generator*. Preprint 13-03, 1994, Electrogorsk. (In Russian).

**APPENDIX: A DERIVATION OF GOVERNING EQUATIONS  
FOR SLOW FLOWS**

For simplicity of presentation we consider derivation of simplified equations in the case of one-phase compressible flow.

The Euler equations are

$$\frac{\partial \rho}{\partial t} + \operatorname{div}(\rho \bar{U}) = 0$$

$$\frac{\partial \rho \bar{U}}{\partial t} + \nabla(\rho \bar{U} \bar{U}) = -\nabla P + \rho \bar{F}$$

$$\frac{\partial \rho i}{\partial t} + \operatorname{div}(\rho \bar{U} i) = \frac{dP}{dt} + q$$

$$\rho = \rho(P, i)$$

Here  $\rho$  - density,  $\bar{u}$  - velocity,  $P$  - pressure,  $i$  - enthalpy,  $\bar{F}$  - external acceleration,  $q$  - heat source.

Now pressure is expanded as  $P = P_o(t) + p(r, t)$ , where  $P_o(t)$  - average pressure,  $p$  - dynamical pressure ( $p \ll P_o$ ).

We nondimensionalize variables as follows: density, velocity, average pressure and external acceleration are nondimensionalized by  $\rho_*$ ,  $V_*$ ,  $P_*$  and  $F_*$  which are typical quantities of the problem. The dynamical pressure, enthalpy and heat source are nondimensionalized by  $\rho_* V_*^2$ ,  $P_*/\rho_*$  and  $P_* V_*/L$ ,  $L$ - typical length. The scale of time is  $L/V_*$ .

In terms of the nondimensional variables the set of equations becomes

$$\frac{\partial \rho}{\partial t} + \operatorname{div}(\rho \bar{U}) = 0$$

$$\frac{\partial \rho \bar{U}}{\partial t} + \nabla(\rho \bar{U} \bar{U}) = -\nabla p + \frac{\rho \bar{F}}{Fr}$$

$$\frac{\partial \rho i}{\partial t} + \text{div}(\rho \bar{U} i) = \frac{dP_o}{dt} + \frac{1}{Eu} \frac{dp}{dt} + q$$

$$\rho = \rho(P, (P_o + p/Eu), iP, / \rho,)$$

$$\text{Here } Eu = \frac{P_*}{\rho_* V_*^2} - \text{Euler number,}$$

$$Fr = \frac{V_*^2}{F_* L} - \text{Froude number.}$$

In the case of slow flow ( $Eu^{-1} \rightarrow 0$ ) the set of equations becomes

$$\frac{\partial \rho}{\partial t} + \text{div}(\rho \bar{U}) = 0$$

$$\frac{\partial \rho \bar{U}}{\partial t} + \nabla(\rho \bar{U} \bar{U}) = -\nabla p + \frac{\rho \bar{F}}{Fr}$$

$$\frac{\partial \rho i}{\partial t} + \text{div}(\rho \bar{U} i) = \frac{dP_o}{dt} + q$$

$$\rho = \rho(P, P_o, iP, / \rho, i) = \rho(P_o, i)$$

This set of equations describes slow flow of one-phase medium without requiring a simultaneous description of acoustic oscillations arising from the elastic properties of the fluid. Such model equations include the important features of buoyant flows without requiring excessive computer time necessary to determine high-frequency sound waves when numerically integrated. In this sense the equations "filter out" the sound waves.

With assistance of this approach it is easy to derive the governing equations for slow flows in the case of two-phase steam-water mixture.

**Modelling studies of horizontal steam generator PGV-1000 with CATHARE**

I. KARPPINEN

VTT, Finland. Attached in CEA/IPSN/ Département d'évaluation de sûreté, Fontenay-aux-Roses, FRANCE

Abstract

To perform thermal-hydraulic studies applied to nuclear power plants equipped with VVER, a program of qualification and assessment of the CATHARE computer code is in progress at the Institute of Protection and Nuclear Safety (IPSN).

In this paper studies of modelling horizontal steam generator of VVER-1000 with the CATHARE computer code are presented. Steady state results are compared with measured data from the fifth unit of Novovoronezh nuclear power plant.

## 1. Introduction

In France several institutes are using CATHARE code to analyse LOCAs and transients in VVER plants. A lot of efforts have been addressed to modelling VVER plants. In the CATHARE Users Club meeting in Marsh 1994 several different approaches for modelling horizontal steam generator were presented. One of the conclusions of the meeting was that the modelling of the horizontal steam generator was not yet established and the final solution in modelling with the CATHARE code was not yet found. In this paper a use ability of a simple once-through model in simulating the steam generator of VVER-1000 plant is discussed and a more detailed recirculation model is presented.

## 2. The basic model

The basic CATHARE nodalization used at IPSN/DES at a moment is derived from the nodalization used to model the vertical French steam generators. The advantage of this model is simplicity and well known behaviour in different transients. The downcomer area of this model is reduced to get the correct water inventory. The junction between the axial element, describing the tube bundle, and the volume element is a special separator junction. This junction puts all the steam flow to the upper sub volume and all the liquid flows to the lower sub volume. The result of this is there is no voidage in the downcomer. The model is adjusted to give reasonable results in steady state conditions [1,10].

## 3. Once-through model

Once-through model was created as a simplest model with a heat exchanger divided in horizontal layers. Furthermore this kind of model has produced quite good results in simulating the steam generator of VVER-440 [2,3]

The steam generator model consists of one axial (pipe) element describing the lower part below the perforated plate. The tube bundle and the "downcomer" regions are lumped together. The upper part is modelled with a volume element. The main dimensions of the model are shown in picture (Fig. 2).

This model violates some recommendations of CATHARE. To keep a "proper" momentum balance, it is required to have a constant section in the first and in the last mesh of an axial element and the length ratio of two adjacent nodes should be less than 1.2 ( 1.5 in practice ). Following these recommendations would have lead to quite large number of nodes and the heat exchanger should have been divided in more than three horizontal layers. The idea was to keep the model as simple as possible. Furthermore the violation of these recommendations should not have a large effect on the results because velocities are small and acceleration will not play an important role on the conditions in SG secondary side. Interfacial friction and gravity are more important.

The behaviour of this model was not realistic. The reduction of the feed water flow did not have effect to the water level in the volume element above the perforated plate. Moreover the model was not stable. During the steady state calculation the liquid was almost stagnant, but time to time a small liquid flow existed and a change in the direction of liquid flow caused changes on the other parameters too. To solve these problems we have to look to the calculation of interfacial friction in CATHARE.

### 3.1 Interfacial friction

Interfacial friction in an axial element and in a junction between an axial element and a volume element is calculated from a formula [4]:

$$\tau_i = A \times \rho \times DV_2 \times k(\alpha)$$

where:

- $A$  is a friction coefficient
- $\rho$  is a volumetric mass
- $DV_2$  is the square of a velocity difference
- $k(\alpha)$  is a numerical smoothing function

The numerical smoothing function is calculated as follows:

$$k(\alpha) = 1 + \frac{10^{-7}}{\alpha^3} + \frac{3 \times 10^{-15} \times P}{(1 - \alpha)^3}$$

The function  $k(\alpha)$  strongly couples the phases when one of them tends to disappear, this was necessary for numerical reasons.

This coupling of steam and liquid phase seems to lead in liquid hold up in ones through steam generator model. Void fraction in the last node of the axial element is almost 1.0, which leads to high interfacial friction. The liquid velocity in the junction between the axial and the volume elements is all the time upward which prevents liquid to flow down.

The result of this liquid hold up was, that reduction of feed water did not had any effect on the water level in the volume above the perforated level. The void fraction in the tube bundle was increasing, but the steam flow through the perforated plate kept the water level in the volume constant. To overcome this unphysical feature we have to add a second flow path to allow the circulation or the interfacial friction has to be modified.

### 3.2 The CCFL-model

In CATHARE 2, v1.3u, there is a new optional model for CCFL, which replaces the normal interfacial friction calculation in specified junctions. The general CCFL model used allows the user to select the Wallis, Kutateladze, Bankoff and Tien forms of flooding equations with a specific definition of the parameters:  $M_n$ ,  $C_n$  and  $\varepsilon$  [7].

$$J_g^{*1/2} B_o^{\varepsilon/4} + M_n \cdot J_f^{*1/2} \cdot B_o^{\varepsilon/4} = C_n$$

Where  $J_i^*$  is the Wallis number, which represents the ratio of inertia force to hydrodynamic force:

$$J_i^* = J_i \left( \frac{\rho_l}{g \cdot \Delta \rho \cdot d} \right)^{1/2} \quad i = g, f$$

The Bond number,  $B_o$ , can be seen as a dimensionless tube diameter  $D^*$  :

$$D^* = d \left[ \frac{g(\rho_l - \rho_g)}{\sigma} \right]^{1/2}$$

where  $\rho$  is density,  $\sigma$  is surface tension,  $g$  is the gravitational acceleration.  $J_j$  is the superficial velocity.

Because of some problems in the CCFL model the latest version, containing updates 1 to 21, was used. The results were much better with the CCFL model. The behaviour was at least qualitatively reasonable. The void fraction and temperature profiles and internal flows are presented in the figure 2. The CCFL parameters used are:

$S_{real}/S_{model}$	1.0	ratio of the real flow area and the flow area in the model
$d$	0.02 m	dimension used in the Bond number
$M_n$	0.7	
$C_n$	1.5	
$\varepsilon$	1.0	= weight factor between Wallis ( $\varepsilon = 0$ ) and Kutazeladze or Tien ( $\varepsilon = 1$ ) form of the flooding equation

However, in this ones through model the tube bundle and the "downcomer" areas are lumped together and it can not simulate the internal circulation. Furthermore the feed water is provided in the tube bundle unlike in the real steam generator.

#### 4. Recirculation model

The aim in this model was to get realistic void fraction profile in both "downcomer" and tube bundle areas and to simulate the observed internal circulation (Fig. 3). The same type of nodalization has been successfully used at VTT with RELAP5 code. The feed water area above the tube bundle and below the perforated plate is described in the CATHARE nodalization with a wide volume element SG1VBP, the height of which is only 260 mm (Fig. 4). Downward from it is an axial element SG1IDC, which represents the "downcomers" between the tube bundles. The small volume element SG1DCV1 is needed to connect the "downcomer" elements. The "downcomer" is divided in three elements to simulate void fraction profile also in this part of the SG. The elements SG1DCT1 and SG1DCT2 are "tee" components to allow cross flows. In CATHARE users manual, volumes are recommended for connecting a horizontal junction to a vertical flow. In fact volumes were used in a first attempt. But a volume element was not suitable for this particular case, because there is not a fixed elevation for the junction. The cross flow junction simulates not only a single pipe, but the flow exists on the whole height of the node. In a volume element there is always a water level and the properties of out going flow depend weather the junction is above or below the water level. In our case it is more suitable to take node average properties for out going flow and use "tee" component.

The riser part is modelled with three axial elements (SG1BOT, SG1RM, SG1RH) and two tee elements (SG1RT1, SG1RT2) for cross flows. In this model the tube bundle is divided only in three layers. To simulate the heat transfer degradation, when water level is decreasing more layers might be required. The general recommendation of the length ratio of adjacent nodes in

CATHARE is not obtained in this model. Because of a low velocity it was not considered to have a large impact on the results. In CATHARE, the heat exchangers can be connected only in axial elements and the number of the nodes, connected in the same heat exchanger, has to be the same or lower in the secondary side than in the primary side. In an axial element there has to be at least two nodes. Because of these limitations there are nodes in the riser without heat exchangers. The length of these nodes is kept quite short not to create too long discontinuations in steam generation.

The area above the perforated plate is modelled with a volume element SG1VAP. The volume element of CATHARE is very convenient for this purpose, because it will allow to calculate the swell level. The flow area through the perforated plate is  $2.5 \text{ m}^2$ , which gives about 7% perforation. The downcomer between the vertical extension of the perforated plate and the vessel wall is described with an axial element SG1DCTOP. The ends of the vessel are included in this element. The top part of the SG with the steam drier and the drainage tubes are simulated with the volume element SG1SEP. The upstream junction SG1SEPJ is a special separator junction. This junction divides the incoming flow so, that all the steam goes to the upper and the water to the lower sub volume. In steady state the separator is not necessary because there is no liquid flow through the separator, but it might be needed in some transients.

## 5. Flow resistance of the tube bundle

The pressure loss of the tube bundle can be calculated from an experimental formula. One suitable is created by the Russian scientists, Mocan and Revsina [8].

$$\zeta = \left[ \left( 4.6 - 2.7 \frac{S_1 - d_e}{S_2 - d_e} \right) \left( 2 - \frac{S_1}{d_e} \right) + 3.2 \right] \times \text{Re}^{-0.27} (z + 1)$$

where:

$\zeta$	pressure loss coefficient
$S_1$ and $S_2$	are distances between the tubes, $S_1 = 23 \text{ mm}$ , $S_2 = 22.2 \text{ mm}$
$d_e$	is the outside diameter of the tube = $16 \text{ mm}$
$\text{Re}$	Reynolds number
$z$	number of the rows in the tube bundle

If we assume that the average liquid velocity inside the tube bundle is  $0.4 \text{ m/s}$ , we will get  $\text{Re} \approx 51000$  for liquid flow. With the average steam velocity  $0.8 \text{ m/s}$  the Reynolds number for the steam flow is  $22000$ . So the equation of Mocan and Revsina will give for single phase liquid

$$\zeta_l = 0.22 (z + 1)$$

and for single phase steam

$$\zeta_v = 0.27 (z + 1)$$

To define the singular pressure loss coefficients for CATHARE, we can take the average of the coefficients calculated for liquid and steam.

$$\zeta = 0.25 (z + 1)$$

Because the CATHARE code will calculate automatically the wall friction from the hydraulic diameter (perimeter) of the element, we have to reduce this friction from the pressure loss of the tube bundle to get the additional pressure loss of the tube bundle (singular pressure loss coefficients). The wall friction of a channel can be taken from the Moody curves. The wall friction model of CATHARE is equivalent of the Moody curve for a smooth pipe, when  $1200 \leq Re \leq 480000$ . For higher Reynolds numbers the wall roughness is taken in account by limiting the wall friction factor to 0.012 [4]. For the liquid flow ( $Re = 51000$ ) the Moody curves will give  $\lambda_l = 0.021$  and for the steam flow ( $Re = 22000$ )  $\lambda_v = 0.025$ . To get a pressure loss coefficient equivalent to the one defined for the tube bundle we can use an average friction coefficient for liquid and steam  $\lambda = 0.023$ .

$$\zeta_{\text{Moody}} = \lambda l / D_h$$

where:

$$\begin{aligned} \zeta_{\text{Moody}} &= \text{pressure loss coefficient calculate from wall friction} \\ l &= \text{the height of the tube bundle} \\ D_h &= \text{hydraulic diameter} \end{aligned}$$

In our models the tube bundle is divided in three nodes. As an example of the singular pressure loss coefficients we can take the centre node. The height of the node is 603 mm, the hydraulic diameter is 17.4 mm [9] and there is 32 rows of heat exchanger tubes.

$$\zeta = 0.25 (32 + 1) = 8.25$$

$$\zeta_{\text{Moody}} = 0.023 * 603 / 17.4 = 0.8$$

$$\zeta_{\text{singular}} = 8.25 - 0.8 \approx 7.5$$

In the horizontal junctions, SG1XJ1 and SG1XJ2, the average penetration length was assumed to be 1/3 of the width of the tube bundle. So it was assumed that in this distance the mean flow turns to vertical direction. The pressure loss coefficients are calculated as follows,

$$\zeta = 0.25 (z + 1) = 0.25 * 11 = 2.75$$

The wall friction is not reduced in this case because of the relatively short lengths defined for the horizontal junctions.

## 6. Plant measurements

A set of tests were made at the fifth unit of Novovoronezh NPP VVER-1000 [5]. The void fractions were defined by measuring the hydrostatic pressure difference. This method gives the average value of void fraction between the pressure taps. The measuring devices were located between the tube bundles. The elevation of the lower pressure taps varied from 1072 mm to 1092 mm and the higher tap was 2072 - 2097 mm from the bottom of the SG. So the range was 1000 - 1008 mm. In the "downcomer area", between the vessel wall and the vertical extraction of the perforated plate and in the end of the vessel the range for the measurement was 705 mm. The velocities were measured as well between the tube bundles using turbine sensors.

In reference [5] the void fractions and velocities are presented from 7 test (Fig. 5, 6). The tests were made with full power, varying the water level. The location of the most of the measurements were the same than in reference [6](Fig. 7). The void fractions in the channel inside the cold bundle ( $\phi_1$ ,  $\phi_{14}$ ) did not depend on the water level. In the channel inside the hot bundle the void fractions were reducing in two passages, A-A ( $\phi_3$ ) and C-C ( $\phi_{12}$ ), but increasing in passage B-B ( $\phi_8$ ) with increasing water level. In the "centre downcomer" ( $\phi_{13}$ ) and in the end of the vessel ( $\phi_{16}$ ,  $\phi_{18}$ ) the void fractions were lower with higher water level.

In reference [6] we can find some additional data. Void fractions close to the vessel wall are also measured (Fig. 7, 8). These tests were made with different power levels. Generally the void fractions are decreasing linearly with reducing power. However, the effect of reducing power to the void fractions in vertical channels inside the tube bundles is a bit surprising. At nominal power the void fraction  $\phi_1$  is lower than  $\phi_8$ ,  $\phi_{10}$ ,  $\phi_{12}$  and  $\phi_{14}$ ; but at low power it is higher (the same can be observed for  $\phi_3$ , but not so clearly). This might be explained with different forms of circulation and feed water distribution at low power. At high power the high steam upward flow in hot bundle, above which the feed water is injected, might push a larger portion of the cold feed water towards the cold collector and further downwards to the channel inside the cold bundle. This is justified with the fact that at nominal power 3/4 of the steam is generated in the hot bundle [6]. At lower power even higher portion of the steam might be generated close to the hot collector. So the void fraction and velocity profiles may strongly depend on the power,  $w_3$  (Fig. 8).

In both of these references [5] and [6] the measurements have been made in the same power plant and the location and numbering seem to be the same in the most of the measurements. However there are some discrepancies in the data. In the reference [6] the void fractions between the hot and cold tube bundle,  $\phi_2$  and  $\phi_{13}$ , are at nominal power about 0.45. The water level in these measurements was +70 - +100 mm from the perforated plate. The nominal water level is about 100 mm above the perforated plate. In reference [5] the same void fractions are 0.18 and 0.15. In the latter measurements the highest water level was +40 mm, but the void fraction was reducing when water level was increasing. Moreover the void fraction in the downcomer inside the cold bundle, close to the cold collector,  $\phi_1$ , which seem to be measured from the same place is in reference [5] 0.5 and 0.3 in reference [6]. The reason for these differences were not possible to found from the test reports.

## 7. Comparison of the calculations with the measurements

### 7.1 Water inventory

The water inventory in the secondary side is one of the most important parameters of the SG models. The water inventory of the basic model is a bit higher than the estimated water inventory in the actual steam generator, but the reliability of the estimation is not known.

	basic model	ones through model	recirculation model	actual PGV-1000 [1]
liq. mass	46 t	39.4 t	42 t	40 - 42 t

### 7.2 Void fractions

Comparison of the SG models, presented here, with the plant measurements is not a simple task. In the real plant the void fractions inside the tube bundle are probably not the same close to cold and hot collector, because of different heat fluxes. 3/4 of the steam is produced in the hot bundle [6]. This can not be taken in to account in a model which have only one average channel in axial direction. Furthermore the "downcomer" channels in the real steam generator have different void fractions. One can distinguish different vertical channels inside the hot and cold bundle, between the bundles and between the vertical extension of the perforated plate and the tube bundles. All these channels are lumped together in the model.

The comparison of the void fractions can be made only in the downcomer areas and above the tube bundle, because there is no data available inside the tube bundles. That is why the ones through model is not compared with the measurements. The measured void fractions in the downcomer areas are average values between the elevation 1080 and 2080 mm. The void fractions  $\phi_2$  and  $\phi_{13}$  in reference [5], which differ a lot from [6] are not taken in to account in this comparison. From reference [5] the measurements with water level + 40 mm above the perforated plate was chosen, because it was the closest to the nominal level + 100 mm, and from reference [6] the data is taken at nominal power.

The measured void fraction in the downcomers, inside the tube bundle, varied from 0.41 to 0.56. The average value at corresponding elevation in recirculation model, in nodes SG1IDC, SG1DCV1, SG1DCT1 and SG1DCT2, is 0.41 (Fig. 4). It has to be noted, that nodes SG1DCV1, SG1DCT1 and SG1DCT2 contains also the ends of the SG vessel, where the void fraction is lower.

The measured void fraction between the tube bundle and the vertical extension of the perforated plate, close to the hot collector, ( $\phi_6$  [6]) is about 0.7. This one is probably the highest void fraction in the downcomer area. The corresponding void fraction in the model is 0.59, but in the model all the downcomers below the perforated plate are simulated with the same axial element.

The void fractions between the vertical extension of the perforated plate and the vessel wall, in reference [6],  $\phi_4$  and  $\phi_{15}$  are about 0.75, close to the hot collector, and 0.35, on the cold side. The void fraction in the comparative element, SG1DCTOP, is 0.33, but the ends of the vessel, where the void fraction is lower,  $\phi_{16}$ ,  $\phi_{17}$  and  $\phi_{18}$ , are taken in account in this same axial element.

Below the perforated plate the measured void fractions  $\phi_5$  and  $\phi_7$  are close to 1. The exact value for  $\phi_7$  [5] is 0.98. The corresponding calculated void fraction in the upper sub volume of SG1VBP is 0.98.

There is a discontinuation in the void fraction profile in the riser part. One reason for this anomaly is that heat exchange from the primary side is connected only on one node of each axial element and not on the tee elements SG1RT1 and SG1RT2. As already explained in the description of the nodalization, this is due to the structure of CATHARE code. An other explanation are the horizontal cross flow junctions. Sub cooled water is flowing into the lower tee element SG1RT1 and reduces void fraction. From the upper tee element SG1RT2 steam is flowing out and results in a reduction of void fraction. It might be possible to reduce the discontinuation in steam generation by reducing the lengths of the nodes without heat

exchangers. In the CATHARE code one can use a very fine meshing, because the code is fully implicit and the time step is not limited by the Courant conditions.

### 7.3 Velocities

The measurements with water level + 40 mm above the perforated plate was chosen, because it was the closest to the nominal level + 100 mm. The level of water had a smaller effect on the velocities, than the power (Fig. 8)

In the gap between the vessel wall and the vertical plate the measured steam velocity, close to the hot collector,  $w_1$ , is 1.2 m/s [5] (upwards). In this area there is a lot of steam flowing upwards, but as well some steam coming down with the downward liquid flow [6]. This results to the high void fraction which was observed in this region. Calculated steam velocity is 0.5 m/s upward and liquid velocity is 0.1 m/s downward. Again these are average velocities in the hole gap and will take in account the cold side and the ends of the vessel, too. The measured velocities in the end of the vessel,  $w_2$ , are 0.07 and 0.03 m/s.

In all the downcomers the flow, in the measurements, was downward without oscillations and the measured velocities are quite precise [6]. The measured velocities in the upper part of the downcomer, close to the cold collector,  $w_4$ , is 0.65 m/s for the liquid and 0 for the steam. The calculated liquid velocity in the average downcomer at about the same elevation is 1.2 m/s and steam velocity is 0.6 m/s. In the lower part of the downcomer, inside the hot bundle, the measured velocity,  $w_3$ , is 0.31 m/s. This is probably liquid velocity, because the void fraction in this location is quite low. The corresponding calculated velocity is 0.4 m/s.

## 8. Conclusions

The presented recirculation model of the horizontal steam generator PGV-1000 reproduces reasonably well the internal water and steam circulation and void fraction profile in steady state conditions. Even the simple once-through model will predict a correct water inventory and heat transfer. However, the comparison with measured data is quite difficult, because the measurements in down comers gave local values in horizontal plane but only average values of void fraction in vertical direction. In the calculation it is vice versa. The model gives void fraction profile in vertical direction but only average value in horizontal plane.

The behaviour in different transients should still be verified. Especially to simulate the transient, where water level will decrease, it might be necessary to divide the tube bundle in more than three horizontal layers. The present model will give a stepwise reduction of heat transfer.

## 9. References

- 1 G. Huchet: Modelling of the VVER 1000 steam generator with CATHARE II - V.1.3, note technique /SEAC/93/137
- 2 T. Haapalehto, D. Bestion: International seminar of modelling horizontal steam generator.
- 3 L. Sabotinov, E. Laugier: Pre-test and post-test sensitivity study of PACTEL (ISP-33), CATHARE calculations. 17th CUC Meeting, 10-11 February 1993.
- 4 D. Bestion: Dossier descriptif CATHARE M14 - Description generale des lois physiques du module de base (revision 5), Juin, 1990.
- 5 Thermal and hydraulics characteristics of water volume of PGV-4 and PGV-1000 horizontal steam generators under transient and stationary conditions, bank of data, Research & Engineering Centre of Nuclear Plant Safety, Electrogorsk, Russia, 1994, to be published
- 6 Electrical Stations, Moscow, No:6, 1987
- 7 R. Freitas: Description and qualification of the counter-current flow limitation model of the CATHARE code, volume Q 13-1, STR/LML/EM/93-185.
- 8 I.E. Idel'cik: Memento des pertes de charge, coefficients de pertes de charge singulieres et de pertes de charge par frottement, 1969
- 9 A. Sartmadjiev, A. Ivanova: Specification of a reference plant with VVER-1000 for computer safety analyses modelling purposes, IAEA Workshop, Tarnava, CSSR, 1988.
- 10 L. Sabotinov, I. Karppinen, A. Amri: CATHARE VVER-1000 input data deck for Rovno NPP calculations, Improvement and validation, to be published



## SG ones through model

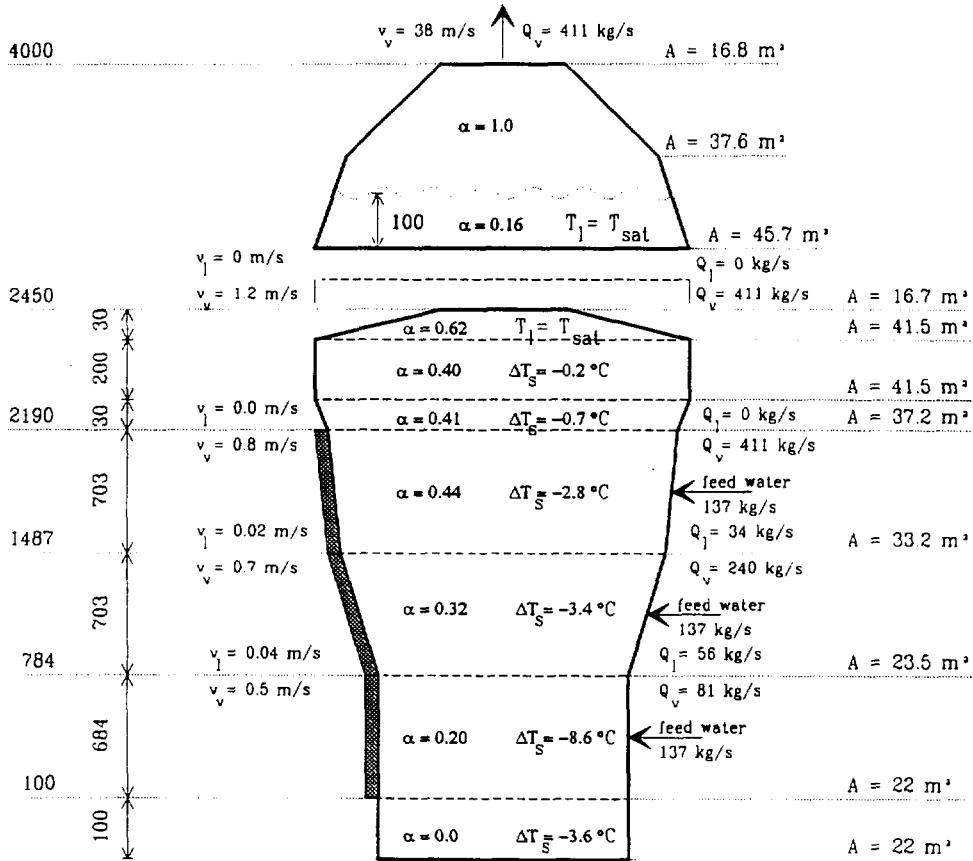
version 12  
3.10.94

Figure 2. Once-through model for VVER-1000 steam generator

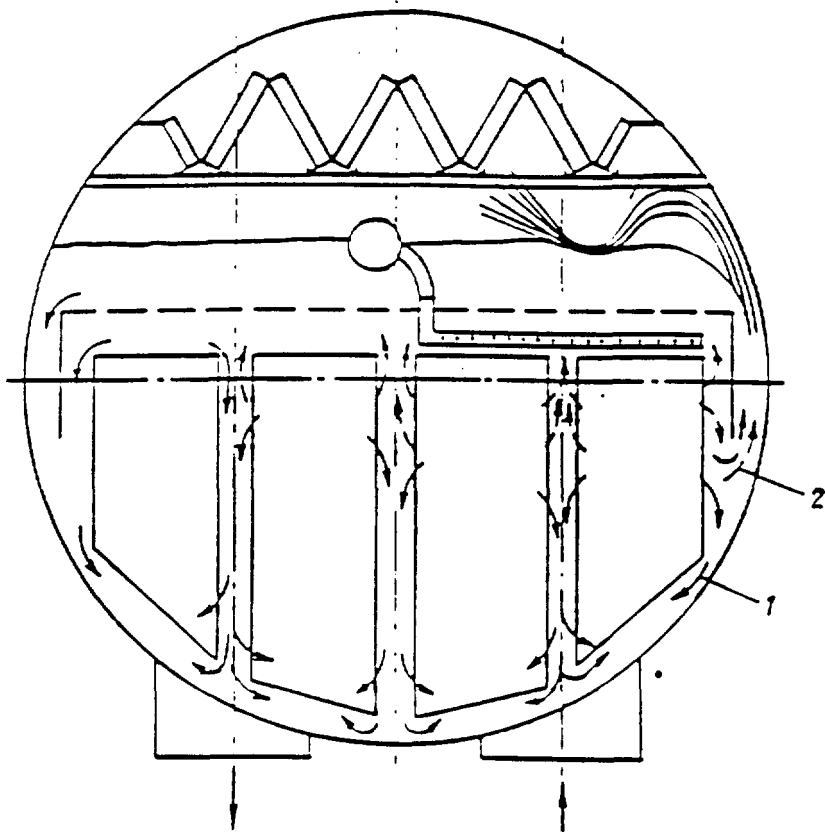


Figure 3. Observed internal flows in VVER-1000 steam generator [Teploenergetiga No: 7, 1990]



Figure 5. Measured void fractions [5]

VOID FRACTION DATA																			Table 1		
NN	Data	Steam flow rate G'' T/H	Power N, %	Mass level, H mm	$\varphi_1$	$\varphi_2$	$\varphi_3$	$\varphi_5$	$\varphi_6$	$\varphi_7$	$\varphi_8$	$\varphi_{10}$	$\varphi_{12}$	$\varphi_{13}$	$\varphi_{14}$	$\varphi_{16}$	$\varphi_{17}$	$\varphi_{18}$	AP <sub>SPS</sub>  100%		
					downcomer passage A-A			under SPS			downcomer passage B-B		downcomer passage C-C			beard-vessel					
					cold	cent	hot				hot	cold	hot	cent	cold	hot	cent	cold			
1	2	3	4	5	6	7	8	9	10	11	12	13	14	15	16	17	18	19	21		
1	19.02.82 18 <sup>10</sup> - 19 <sup>30</sup>	1570	100	-202	0,50	0,2	0,50	-	1,0	1,0	0,45	-	0,62	0,31	0,58	0,48	0,36	0,31	117		
2	19.02.82 20 <sup>30</sup> - 21 <sup>40</sup>	1570	100	-139	0,50	0,2	0,49	-	1,0	1,0	0,46	-	0,60	0,30	0,58	0,44	0,37	0,24	129		
3	19.02.82 22 <sup>30</sup> - 23 <sup>20</sup>	1570	100	-98	0,50	0,19	0,47	-	1,0	1,0	0,46	-	0,59	0,29	0,56	0,41	0,38	0,20	136		
4	20.02.82 0 <sup>10</sup> - 1 <sup>00</sup>	1570	100	-50	0,50	0,19	0,46	-	1,0	0,98	0,47	-	0,57	0,28	0,55	0,39	0,39	0,16	145		
5	20.02.82 3 <sup>10</sup> - 3 <sup>40</sup>	1540	100	-19	0,50	0,18	0,44	-	1,0	0,98	0,48	-	0,56	0,14	0,56	0,38	0,40	0,17	146		
6	20.02.82 4 <sup>20</sup> - 4 <sup>50</sup>	1565	100	+40	0,50	0,18	0,42	-	1,0	0,98	0,48	-	0,54	0,15	0,56	0,21	0,38	0,18	158		
7	20.02.82 5 <sup>20</sup> - 6 <sup>00</sup>	1550	100	+35	0,50	0,18	0,41	-	1,0	0,98	0,50	-	0,55	0,14	0,56	0,25	0,35	0,17	153		
8	18.02.82 10 <sup>00</sup> - 11 <sup>00</sup>	770	50	-82	-	-	-	-	-	-	-	-	-	-	-	-	-	-	-		
9	18.02.82 12 <sup>00</sup> - 12 <sup>40</sup>	1220	79	-70	-	-	-	-	-	-	-	-	-	-	-	-	-	-	136		
10	11.02.82 9 <sup>00</sup> - 9 <sup>30</sup>	1550	100	-160	-	-	-	-	-	-	-	-	-	-	-	-	-	-	152		
11	12.02.82 10 <sup>15</sup> - 11 <sup>00</sup>	1570	100	-160	-	-	-	-	-	-	-	-	-	-	-	-	-	-	162		

Table 2

NN	Velocity data		Steam flow rate	Power	Mass level	$W_1$ , m/s		$W_2$ , m/s		$W_3$ , m/s	$W_4$ , m/s		$W_5$ , m/s	$W_2$ , m/s max	$G'$ , T/h	$G''/G'$
	Data	time				$W_1''$	$W_1'$	$W_2'$	$W_2''$		$W_4'$	$W_4''$				
1		2	3	4	5	6	7	8	9	10	11	12	13	14	15	16
1		19.02.82 18 <sup>h</sup> - 19 <sup>h</sup>	1570	100	-202	1,00	0	0,038	0,13	0,28	0,47	0	-	0,345	356	0,227
2		19.02.82	1570	100	-139	1,03	0	0,054	0,02	0,31	0,38	0	-	0,155	505	0,321
3		20 <sup>h</sup> - 21 <sup>h</sup> 19.02.82 22 <sup>h</sup> - 23 <sup>h</sup>	1570	100	-98	0,99	0	0,055	0,03	0,30	0,54	0	-	0,235	515	0,328
4		20.02.82	1570	100	-50	1,24	0	0,070	0,00	0,26	0,75	0	-	0,240	655	0,417
5		0 <sup>h</sup> - 1 <sup>h</sup> 20.02.82	1540	100	-19	1,06	0	0,065	0,02	0,35	0,53	0	-	0,300	610	0,390
6		3 <sup>h</sup> - 4 <sup>h</sup> 20.02.82 4 <sup>h</sup> - 5 <sup>h</sup>	1565	100	+40	1,22	0	0,073	0,03	0,31	0,65	0	-	0,320	685	0,438
7		20.02.82	1550	100	+35	1,09	0	0,062	0,03	0,26	0,39	0	-	0,240	580	0,375
8		5 <sup>h</sup> - 6 <sup>h</sup> 18.02.82	770	50	-82	0,23	0,04	0,32	0,03	0,38	0,08	0,04	-	-	3000	3,90
9		11 <sup>h</sup> - 12 <sup>h</sup> 18.02.82	1220	79	-70	0,64	0	0,09	0,00	0,66	0,27	0	-	-	845	0,69
10		12 <sup>h</sup> - 13 <sup>h</sup> 11.02.82	1550	100	-160	-	-	0,01	0,15	0,29	-	-	0,29	-	-	-
11		9 <sup>h</sup> - 10 <sup>h</sup> 12.02.82 10 <sup>h</sup> - 11 <sup>h</sup>	1570	100	-160	-	-	0	0,18	-	-	-	0,29	-	-	-

Figure 6. Measured velocities [5]

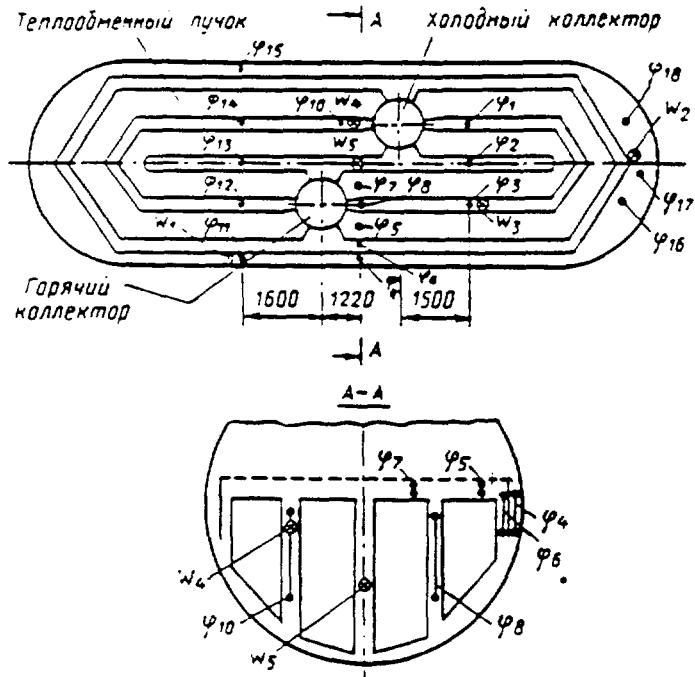


Рис. 1. Схема расположения датчиков паросодержания и скорости потока в парогенераторе ПГВ-1000

Датчик	Расстояние, мм	
	между отборами	от погруженно-го штыя
$\omega_1, \omega_2, \omega_4$	—	450
$\omega_3, \omega_6$	—	1300
$\varphi_1, \varphi_2, \varphi_3, \varphi_8, \varphi_{10}, \varphi_{11}, \varphi_{12}, \varphi_{14}$	1000	350
$\varphi_4, \varphi_{11}, \varphi_{13}, \varphi_{16}, \varphi_{17}, \varphi_{18}$	700	70
$\varphi_5, \varphi_7$	200	35

Figure 7. Location of measurements [6]

Figure 8. Measured void fractions in a function of power and measured velocities in a function of power and level [6]

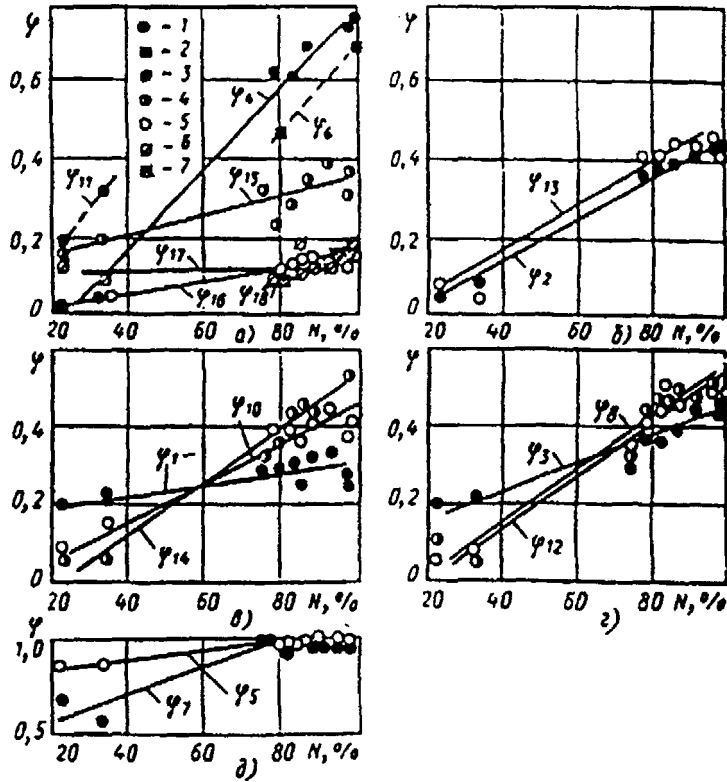


Рис. 2. Графики зависимости паросодержания в различных зонах парогенератора от его мощности при положении массового уровня воды на 70—100 мм выше погруженного щита:  
 а — в зазорах между закранный и корпусом парогенератора, закранный и пучком; 1 —  $\varphi_4$ ; 2 —  $\varphi_6$ ; 3 —  $\varphi_{11}$ ; 4 —  $\varphi_{16}$ ; 5 —  $\varphi_{18}$ ;  
 б —  $\varphi_{17}$ ; 7 —  $\varphi_{18}$ ; в — в центральном коридоре; г — в «холодном» коридоре; з — в «горячем» коридоре; д — под погруженным щитом

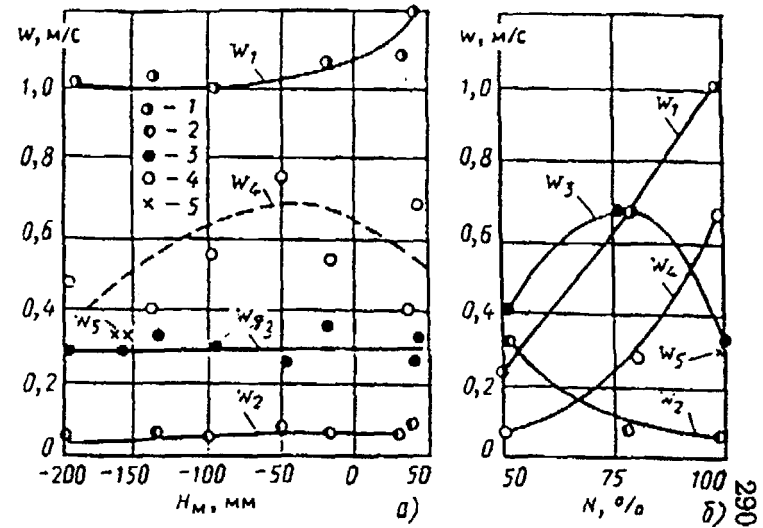


Рис. 3. Графики зависимости средней скорости потока в различных зонах парогенератора от положения массового уровня при номинальной мощности парогенератора (а) и от мощности парогенератора при положении массового уровня на 50—100 мм ниже погруженного щита (б):  
 1 —  $w_1$ ; 2 —  $w_2$ ; 3 —  $w_3$ ; 4 —  $w_4$ ; 5 —  $w_5$

**THIRD INTERNATIONAL SEMINAR ON HORIZONTAL STEAM  
GENERATORS**

18 - 20 October 1994, Lappeenranta, Finland

**PARAMETRIC STUDY FOR HORIZONTAL STEAM GENERATOR  
MODELLING**

I.Ovtcharova, ENERGOPROEKT, Sofia, Bulgaria

**ABSTRACT**

In this paper are presented some of the calculated results of horizontal steam generator PGV - 440 modelling with RELAP5/Mod3. Two nodalization schemes have been used with different components in the steam dome. An study of parameters variation on the steam generator work and calculated results is made in cases with separator and branch.

Steam generators (SG) are essential part of NPP and they play very important role in different nuclear safety analyses. This is connected with the role, SG plays in NPP - connection between primary and secondary sides, boundary against radiation products release, heat removal system in all operating conditions, etc.

Nodalization scheme is of meaning during transient calculation. In case with primary to secondary side leakage simple nodalization works well, but in transients with loss of steam generator inventory, such as steam line break, loss of feed water, secondary safety valves stuck open etc., detail steam generator modelling is necessary.

Recently, there are a great number of useful works dedicated to horizontal steam generator modelling /especially in Proc. of 1 and 2 Int.Seminars of Horizontal Steam Generator Modelling/. During modelling work a lot of problem usually arise, especially in case of horizontal steam generator, because of the real three dimensional heat exchange and hydrodynamics conditions in SG and available one dimensional codes for accident analysis like RELAP5. In the same time very limited number of experimental studies does not make possible to compare the results from modelling process and develop better SG models. This lack of measured data during transient simulation is very important.

It is important to be pointed out that in dependence on nodalization schemes different parameters can affect to SG behaviour. In order to show that some parametric studies were carried out with RELAP5/MOD3. This kind of knowledge could be useful for improving steam generator modelling work .

For this study different kind of steam generator models were developed. Two of them, SG with separator and with branch volumes in the SG top, have been chosen for comparing in steady state of the nominal conditions.

The model with separator volume was chosen because in RELAP5 separator is developed as a special component and in PWR SG modelling it is used preferable. In real SG for WWER design separator fitting is present too. But at the same time in horizontal steam generator with boiling in enough big volume and large flow area above tube bundle the velocities are too low and separator might be not necessary in modelling.

Both models are similar in geometry (for the purpose of comparing). First model /Fig.1./, with separator, consist of three tube bundle volumes - 600, 601 and 602 on the secondary side, small volume above the tube bundle - 603, volume 604 is a separator with parameters VOVER and VUNDER (variable in the study), four downcomer volumes - 605, 606, 607 and 608, volume 609 is bypass volume for liquid fall back. Tube bundle volumes are connected with downcomer volumes by cross flow junctions, volume 604 is connected with bypass volume by cross flow junction and with steam collector (volume 611) by single junction. From the primary side nodalization is made in way that U - tube bundle is simulated by pipes 221, 222, 223 (each one consists of five nodes), hot collector volumes - 211, 212, 213, 214, 215 and cold collector volumes - 225, 226, 227, 228, 229. Junctions between collector volumes and U - tubes are of cross flow type. For the scheme with branch instead of separator volume 609 is joined to volume 604 (branch), volume 605 is joined to volume 603 and liquid fall back to the top of downcomer is given by junction between volumes 603 and 606 /Fig.2./. Feed water injection in both cases is delivered to volume 602 (in the middle of the bundle).

### MODEL WITH SEPARATOR

Reference case is calculated for 500 seconds and most typical results are presented here for comparing with next cases. After about 140 seconds all control parameters are stable till the end of calculation:

Parameter	Value
voidg600010000	0.30174
voidg601010000	0.36096
voidg602010000	0.33475
voidg603010000	0.22636
voidg604010000	0.61548
sglevdcom	2.919 m
sglevtube	1.889 m
sgmass	33004 kg
tempg602010000	529.65 K
tempg604010000	529.66 K
mflow604010000	124.9 kg/sec

For the same case mass flow and liquid and vapour velocities in junctions between tube bundle volumes and downcomer volumes are:

Junction between volumes	Liquid velocity m/sec	Vapour velocity m/sec	Mass flow kg/sec
605 - 603	-0.038	-0.0799	-47.29
606 - 602	-0.134	2.01	-215.09
607 - 601	0.76	0.81	1658.1
608 - 600	1.35	1.709	2466.0

Downcomer mass flows and velocities are:

Junction between volumes	Liquid velocity m/sec	Vapour velocity m/sec	Mass flow kg/sec	Recirculation rate
609 - 605	2.4436	2.84	3857.7	about 31
605 - 606	0.8889	0.4599	3905.0	about 31
606 - 607	1.3371	0.9999	4120.6	about 33
607 - 608	0.605	0.4436	2462.9	about 20

Results are reasonable. Steam generator level according to the downcomer volumes is higher because of separator parameters VOVER and VUNDER (respectively 0.05 and 0.2), keeping vapour away from downcomer volumes, especially in the top downcomer volume liquid fall back volume (voidg in 605 and 609 is almost zero). Vapour will not be carried under to the downcomer until the separator liquid fraction falls below VUNDER. Vapour distribution in the tube bundle volumes is close to the results from some experimental work and papers /1, 2/. Vapour void fraction is lower in volume 603 above the tube bundle, but no heat structure is related to this volume. Calculated steam generator mass is about 33 t and this value is close to the estimated in IVO Ltd, Finland /3 /.

The most important parameters in RELAP5/MOD3 for separator component are VOVER and VUNDER /4 /. VOVER specifies vapour outlet and VUNDER specifies liquid fall back. By choosing proper values for those parameters it is possible to adjust operating mixture level in the downcomer region. It looks that those parameters "govern" operation of steam generator with separator component. Default values according to the RELAP5 Manual are

VOVER = 0.5 and VUNDER = 0.15. That means that when void fraction in separator volume is above the value of VOVER perfect separation is assumed and pure vapour is fluxed out; when VOVER is equal to 1.0, vapour outlet junction behaves as a normal one and when VOVER is small, the vapour outflow corresponds to an ideal separator. When the volume liquid void fraction is greater than the value of VUNDER - pure liquid outflows / 4/.

Some results of calculations with variable values for VOVER and VUNDER are given below:

VOVER variation (VUNDER = 0.2 in all cases)

vover	flow604 kg/sec	sgmass kg	sglevdc m	sglevtube m	voidg 604	voidg 602	voidg 605
0.15	124.89	33004	2.719	1.889	0.61548	0.33475	0.01393
0.3	124.9	33004	2.719	1.889	0.61548	0.33475	0.01393
0.5	124.9	33004	2.719	1.889	0.61548	0.33475	0.01393
0.75	125.12	31455	2.7428	1.7767	0.73978	0.32466	0.00000
0.9	125.69	27669	1.7937	1.6745	0.88827	0.32790	0.49238
1.0	124.44	25620	1.6601	1.5552	0.98593	0.32122	0.52356

It is obviously from this table that VOVER increase till some time does not affect the results, but after that point such increase changes in significant extent SG parameters. Mass flows in junctions are quite different and smaller and for big VOVER voidg distribution is better in the tube bundle volumes, but too high in downcomer volumes, especially in the top of the SG and as a sequence of that calculated level from downcomer volumes is too close to this one, obtained from tube bundle volumes.

VUNDER variation (VOVER = 0.05 in all cases)

vover	flow604 kg/sec	sgmass kg	sglevdc m	sglevtube m	voidg 604	voidg 602	voidg 605
0.02	124.9	33004	2.719	1.889	0.61548	0.33475	0.01393
0.05	124.9	33004	2.719	1.889	0.61548	0.33475	0.01393
0.1	124.9	33004	2.719	1.889	0.61548	0.33475	0.01393
0.15	125.9	33004	2.719	1.889	0.61548	0.33475	0.01393
0.3	125.89	33004	2.719	1.889	0.61548	0.33475	0.01393
0.45	125.42	32978	2.0543	2.0073	0.56464	0.33525	0.45639
0.6	125.42	32978	2.0543	2.0073	0.56464	0.33525	0.45639

The influence of VUNDER is not so strong like in case with VOVER variation. Default values (or smaller) give better results than higher values. Use of higher values results in unstable hydraulics.

Flow energy loss coefficients in cross flow junctions are of parameters, estimated by the user and their values influence steam generator recirculation rate and inventory. Variation of those loss coefficients give next tends:

Junct.	Loss coef.	Mass flow, kg/sec	Sglevdc m	Sglevtube m	Mass, kg	Voidg 602	Voidg 604
606-602	2.0	-726.15	2.0385	2.016	32979	0.34031	0.54754
607-601	2.0	-1667.8					
608-600	2.0	1336.2					
606-602	5.0	-613.13	2.0426	2.0132	32978	0.33359	0.56481
607-601	5.0	-1444.0					
608-600	2.5	1053.2					
606-602	6.25	-117.12	2.7177	1.8915	33005	0.33466	0.61584
607-601	6.25	1390.3					
608-600	3.125	2676.3					
606-602	7.5	-84.858	2.7383	1.888	33005	0.33425	0.62317
607-601	7.5	1414.8					
608-600	3.75	2669.0					
606-602	10.0	-53.971	2.7844	1.8798	33005	0.33331	0.63990
607-601	10.0	1467.4					
608-600	5.0	2691.8					

In order to obtain good hydraulics in SG it is necessary to chose input proper energy loss coefficients. From those data it is possible to observe how energy loss coefficient rise affect mass flow in the SG and other parameters. For chosen geometry higher losses result better mass flow in the SG and stable circulation. In general lower loss coefficients will increase recirculation flow.

Secondary side pressure in the steam line (as one of the boundary conditions, given by TDPVOL) is one of the input parameters for SG modelling and next table illustrate how it affects SG work:

P <sub>sec.side</sub> Pa	T <sub>out</sub> K	Voidg602	Voidg604	Sglevdc m	Sglevtube m	Sgmass kg
44.4+5	538.05	0.33248	0.61643	2.722	1.8927	33038
44.2+5	537.83	0.33475	0.61548	2.719	1.889	33004

By increasing SG secondary side pressure in the steam line it is possible to reach lower vapour fraction in the tube bundle and as a consequence of that - reduced heat transfer between primary and secondary sides (SG cold collector temperature increase) and higher inventory in the SG. With secondary side pressure increase calculated pressures in the tube bundle volumes became higher too. Calculated SG levels are also with higher values. Circulation flow remains in the same order.

Calculation with variation in vertical stratification model on/off shows that in case of using separator component in SG modelling, it does not affect the results at all (the situation is different in the case of using branch instead of separator).

Interphase friction correlations choice affect the results. In case of pipe interphase friction model calculated vapour void fractions in the tube bundle are lower than in case of using bundle interphase friction model:

Interph. fric.mod.	Voidg600	Voidg601	Voidg602	Voidg603	Voidg604	Sglevtube
pipe int.	0.28176	0.33195	0.33152	0.22341	0.67044	1.8741
bundle	0.30174	0.36097	0.33475	0.22636	0.61548	1.8893

### MODEL WITH BRANCH

In the model with branch component in the steam dome instead of separator some difference in calculated results was observed. SG inventory is with about 5 t lower, vapour void fraction is higher (except in volume 600), levels - lower, secondary side pressures - lower (as a result of those tends in pressure and void fractions SG inventory and levels are lower). In this case steady state conditions were obtained very quickly. Main results from this calculation are:

Parameter	Value
voidg600010000	0.28981
voidg601010000	0.34938
voidg602010000	0.37035
voidg603010000	0.42381
voidg604010000	0.98628
sglevdcom	1.63367 m
sglevtube	1.48055m
sgmass	28393.2kg
tempg602010000	529.66 K
tempg604010000	529.66 K
mflow604010000	125.67 kg/sec

Vapour void fraction distribution is better and increasing up to the output of the SG. Velocities and mass flow in the crossflow junctions between downcomer volumes and tube bundle volumes are:

Junction between volumes	Liquid velocity m/sec	Vapour velocity m/sec	Mass flow kg/sec
606 - 602	0.028	-0.54241	26.196
607 - 601	0.08912	0.0474	-175.79
608 - 600	0.47062	0.4594	903.45

Results from downcomer mass flow calculation are given in the next table:

Junction between volumes	Liquid velocity m/sec	Vapour velocity m/sec	Mass flow kg/sec	Recirculation rate
603 - 606	0.36616	-0.333	931.17	about 7
606 - 607	0.27869	-0.0104	838.7	about 7
607 - 608	0.25274	0.0686	911.44	about 7

Recirculation rate is 4 - 5 times smaller in the model with branch component.  
Loss coefficients variation leads to similar behaviour of calculated quantities:

Junct.	Loss coef.	Mass flow, kg/sec	Sglevdc m	Sglevtube m	Mass, kg	Voidg 602	Voidg 604
606-602	4.0	-34.575	1.5861	1.471	28124	0.3751	0.9892
607-601	5.0	74.956					
608-600	2.5	1162.9					
606-602	8.0	-102.53	1.6594	1.4884	28719	0.38011	0.98549
607-601	10.0	18.806					
608-600	5.0	823.03					
606-602	12.0	13.428	1.701	1.489	28935	0.37445	0.98848
607-601	15.0	147.18					
608-600	7.5	762.35					
606-602	16.0	48.088	1.726	1.495	29097	0.37165	0.9874
607-601	20.0	47.553					
608-600	10.0	669.12					

With variation in vertical stratification model on similar results to those in work /1/ results were obtained. SG is with very unstable hydraulics, pressures in the volumes, void fractions, temperatures change every time step. Vapour void fraction in volume 603 is from 0.1 to 0.04, in 604 - between 0.97 and 0.99. The problem with mass flow calculation is analogical. The conclusions from those results is that vertical stratification model should be turned off in case of nodalization with branches.

## CONCLUSIONS

SG modelling work is too complicated. Here was presented only part of eventual parametric study. It is difficult to draw strong conclusions and make any recommendations, based on such results, because specific geometry during nodalization is also very important.

## ACKNOWLEDGEMENT

During my fellowship from IAEA at IVO INT LTD, Safety and fuel office, as a part of my study I tried to understand SG modelling problem and work. Thanks to IAEA for financial support and to IVO for guidance.

## REFERENCES

1. Ismo Karppinen, Modelling of horizontal steam generator with RELAP5/Mod 2 and 3, Int. Seminar on Horizontal Steam Generator Modelling, Lappenranta, Finland, March, 1991.
2. Initial data for calculation of natural circulation in the secondary volume of PGV - 440 and PGV - 1000, Private communication between Dr.H.Tuomisto and Prof.V.F.Titov, December, 1991.

3. Harri Tuomisto, Secondary side water inventory in the Loviisa steam generators, Int. Seminar on Horizontal Steam Generator Modelling, Lappenranta, Finland, March, 1991.
4. RELAP5/MOD3 Code Manual: System Models and Numerical Methods

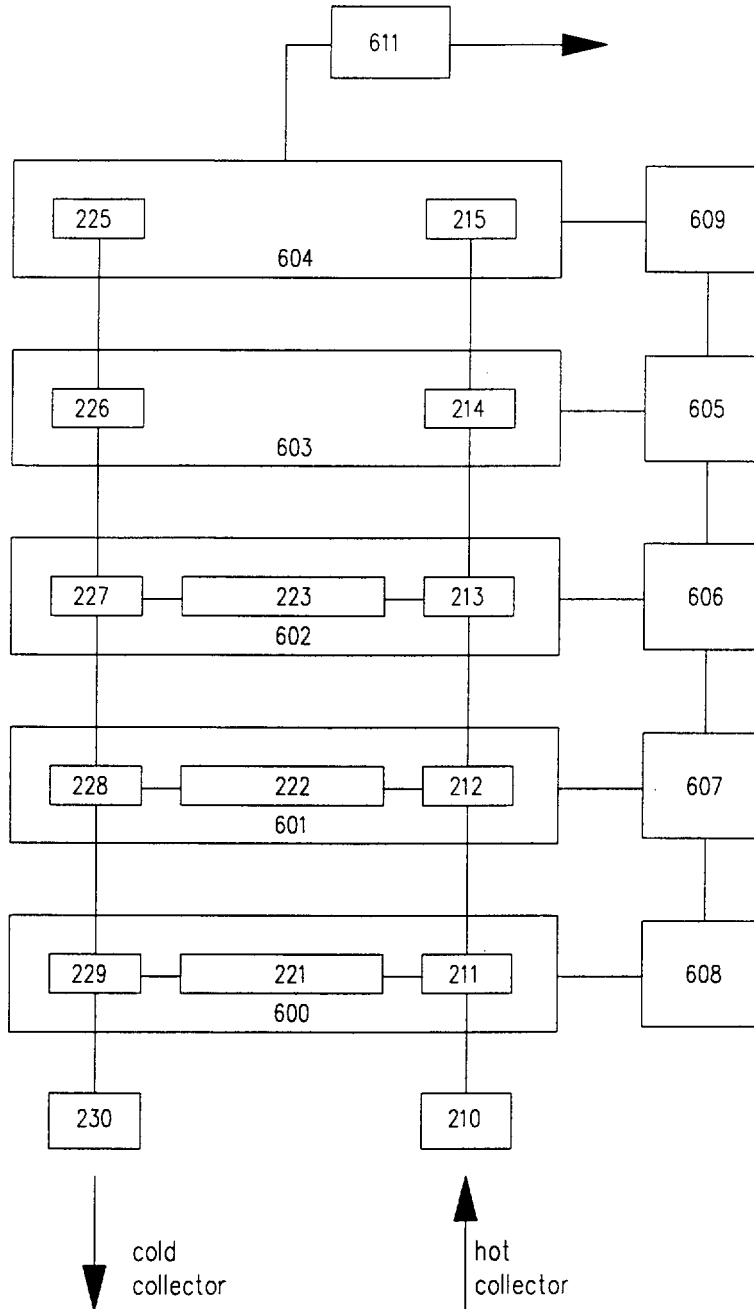


Fig.1 SG with separator

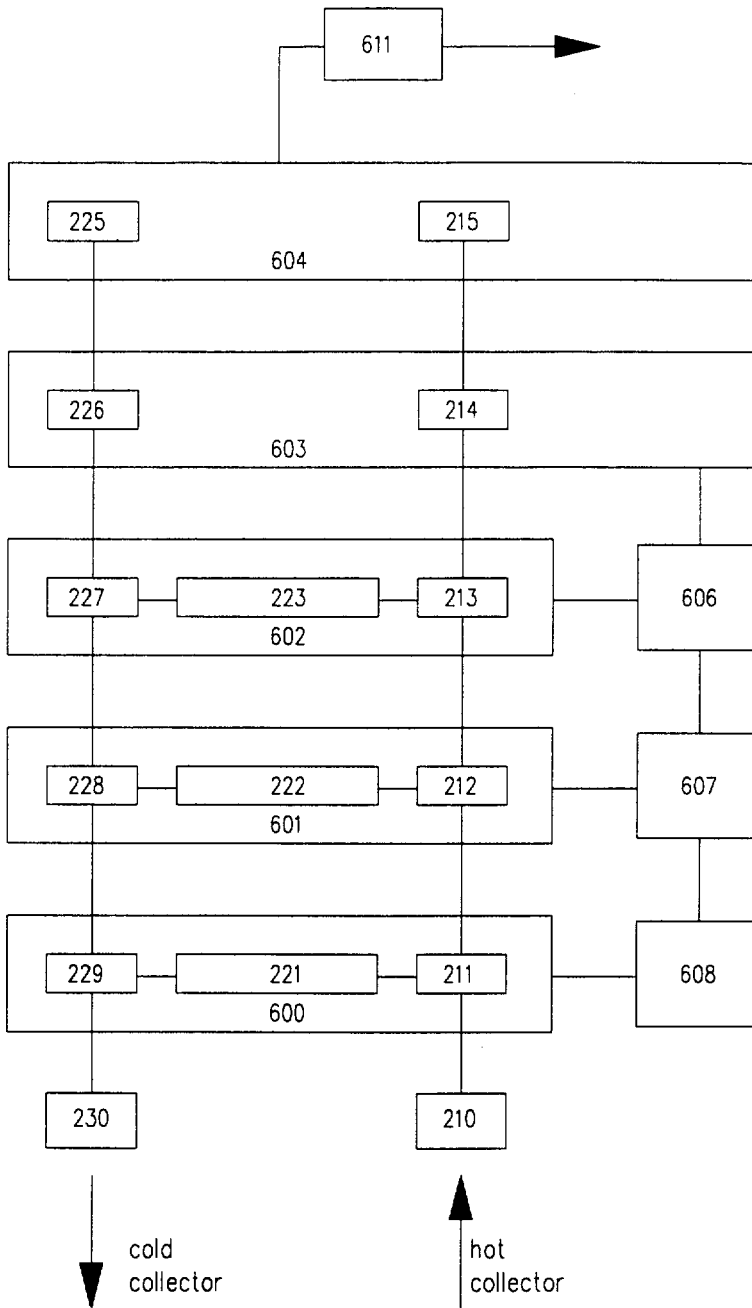


Fig.2 SG with branch

**MODELLING THE HORIZONTAL  
STEAM GENERATOR WITH APROS**

Jukka Ylijoki, VTT Energy, Finland  
Christer Palsinajärvi, IVO International Ltd, Finland  
Kari Porkholm, IVO International Ltd, Finland

**ABSTRACT**

In this paper the capability of the five- and six-equation models of the simulation code APROS to simulate the behaviour of the horizontal steam generator is discussed. Different nodalizations are used in the modelling and the results of the stationary state runs are compared. Exactly the same nodalizations have been created for the five- and six-equation models.

The main simulation results studied in this paper are void fraction and mass flow distributions in the secondary side of the steam generator. It was found that quite a large number of simulation volumes is required to simulate the distributions with a reasonable accuracy. The simulation results of the different models are presented and their validity is discussed.

## 1. Introduction

The APROS simulation environment has been developed by IVO International Ltd and Technical Research Centre of Finland (VTT) since 1986. APROS provides tools, solution algorithms and generic components for use in different simulation systems for design, analysis and training purposes. One of its main nuclear applications is the Loviisa Nuclear Power Plant Analyzer.

A great variety of physical models is available in APROS. For thermal hydraulics this means that one-dimensional three-, five- and six-equation flow models can be used. One-dimensional solution of the heat conduction in the heat structures can be used together with all thermal hydraulic models. Each thermal hydraulic model has its own heat transfer correlation package. The heat conduction model includes material property data for many common materials and new materials can be added easily without code modifications. The five- and six-equation models were used in this study.

The five-equation model is based on the conservation equations of mass and energy for gas and liquid phases and a conservation equation of momentum for the mixture of the phases. The pressures, volume flows and the enthalpies of the two phases are solved from the equations. A separate drift-flux model is used to solve the velocities of the phases. The equations are coupled with friction and heat transfer correlations.

The six-equation model is based on the conservation equations of mass, energy and momentum for the two phases. The equations are closed with empirical correlations describing different two-phase phenomena (wall friction, interfacial friction, interfacial heat transfer and wall heat transfer). Pressures, volume fractions, enthalpies and velocities of each phase are solved from the discretized equations using an iterative procedure.

The thermal hydraulic models of APROS have been extensively tested against separate effects tests and plant data. As an example the 5-equation model of APROS has been applied for the modelling of the horizontal steam generator of the Loviisa Nuclear Power Plant. Different nodalizations have been used in the primary and secondary sides of the model. Simulation results of the stationary state run have been compared with the results of RELAP5/MOD2 calculations and with the experimental plant data [1].

## 2. Simulation Model

Three quite detailed simulation models of the Loviisa Nuclear Power Plant have been created by APROS [2]. The secondary side of the plant is described with the homogeneous thermal hydraulic model in each simulation model. The primary side of the plant and also the secondary side of the steam generators are described with either the homogeneous model, five-equation model or six-equation model. The simulation models where five- and six-equation models are used are the basic models of the calculations presented in this paper. One steam generator has been modelled with different nodalizations. The other steam generators and the rest of the model have the same definitions in every calculation.

The process components of APROS create a set of calculation modules and define their connections according to the definitions of the component. Different nodalizations can easily be created by modifying a few of the parameters of the process component. A process component to describe a horizontal steam generator is available in APROS. Pressures, enthalpies, mass flows and loss coefficients are defined separately for the primary and secondary sides. Also geometric data (volumes, flow areas, length and radius of the tubes and hydraulic diameters) and the water level of the secondary side are given. The process component generates nodes (calculation volumes) and branches (defining flows between nodes) according to the definitions. Also heat structure nodes and branches and heat transfer modules are created for the simulation of heat flows. The user defines the number of nodes to be generated in the collectors, primary side tubes, heater, dome and downcomer respectively.

The steam generators in the basic model consist of two nodes for each collector and three nodes describing the tubes. The secondary side is modelled by one heater (tube bundle) node, one downcomer node and two dome nodes (see figure 1). There is one heat structure connected to each tube node. The heat structure is divided into two heat structure nodes in the radial direction. The inner heat structure node is connected to the tube node with a heat transfer module. There are also heat transfer modules between the outer nodes of all heat structures and the heater node. The model is named the 1-node model according to the number of nodes in the heater.

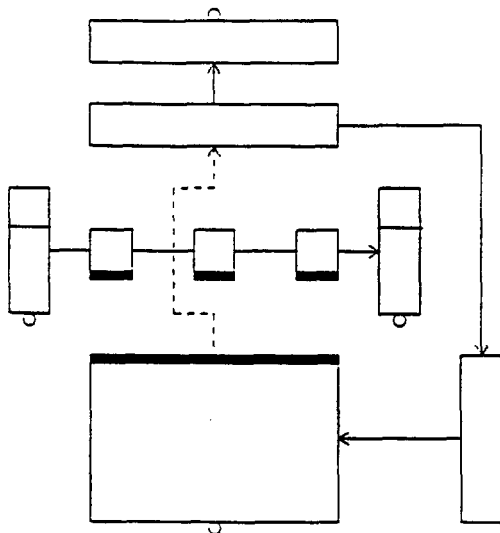


Figure 1. APROS 1-node model of horizontal steam generator

In the 5-node model the primary side tubes, heater and downcomer of the steam generator are each divided into five layers of equal height (figure 2). Also the dome has been divided into five nodes. Heat structures are defined between each tube node and the heater node on the same level. Branches are created between the heater nodes, between the downcomer nodes and also between the heater and downcomer nodes on the same level (cross flow branches). The process component creates nodes of equal size on each level. Because the shape of the real steam generator is not uniform and the tubes are not distributed evenly, the volumes, flow areas and heat transfer areas of the generated calculation modules have been modified after the definition of the process component. This had to be done in order to give more realistic data for the nodes and branches of different levels. Also the cross flow loss coefficients are defined separately for each level according to reference /3/.

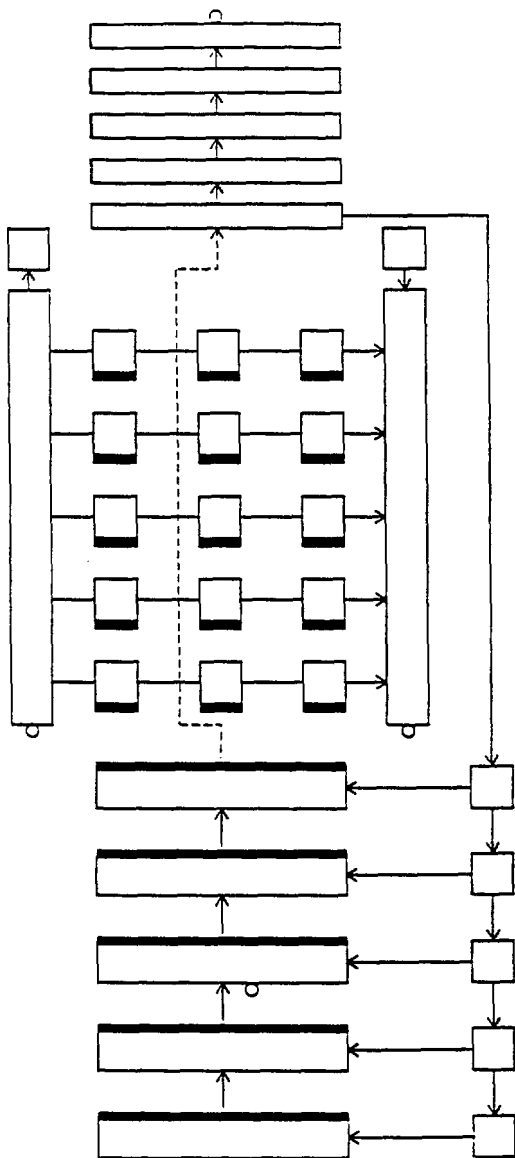


Figure 2. APROS 5-node model of horizontal steam generator

In the 15-node model (figure 3), also the heater is divided horizontally into three nodes. Thus there is an equal number of nodes in the tubes and in the heater. Heat structures are created between the tube and heater nodes of corresponding location. The downcomer is divided into two parts that are connected to the boundary nodes of the heater with cross flow branches. To simplify the model the downcomer nodes are not directly connected to the central heater nodes and the volumes of the downcomers in the ends of the steam generator have been added to the two generated downcomers. The volumes, flow areas, heat transfer areas and cross flow loss coefficients have been defined by the user for each level in the model.

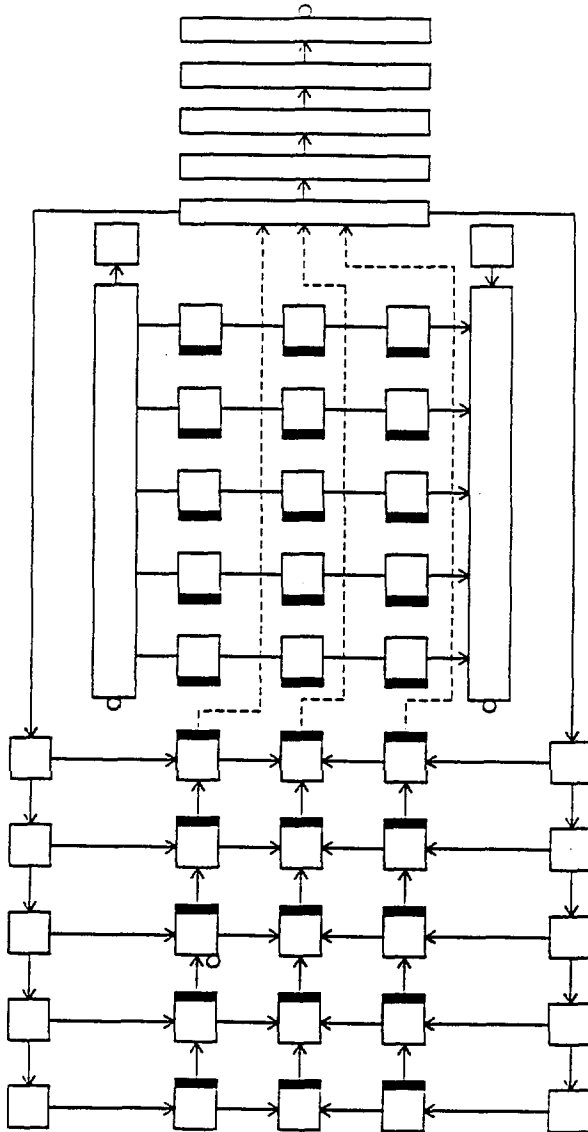


Figure 3. APROS 15-node model of horizontal steam generator

## 3. Simulation Results

The calculated stationary state void fraction and mass flow distributions in the secondary side of the steam generator are presented in this chapter. The results calculated by RELAP5/MOD2 /3/ are shown as a reference. In order to compare APROS and RELAP5 an identical nodalization would have to be defined for both codes. The void fraction measurement is from Novovoronezhskaja unit 3 Nuclear Power Plant /4/.

Table 1. Calculated and measured void fractions in the heater and dome (5-equation model)

Average elevation (m)	1-node	5-node	15-node			RELAP5	Measured
			hot	mid	cold	5-node	
3.0		1.00	1.00				-
2.9	1.00					1.00	-
2.7		1.00	1.00				-
2.5		1.00	1.00				-
2.3	0.78	0.83	0.94			0.88	-
2.1		0.13	0.35				-
1.8		0.25	0.24	0.20	0.02	0.33	-
1.4		0.19	0.19	0.18	0.26	0.34	0.3-0.4
1.0	0.19	0.14	0.14	0.12	0.03	0.30	-
0.6		0.11	0.11	0.10	0.08	0.24	-
0.2		0.04	0.04	0.04	0.01	0.14	-

Table 2. Calculated and measured void fractions in the heater and dome (6-equation model)

Average elevation (m)	1-node	5-node	15-node			RELAP5	Measured
			hot	mid	cold	5-node	
3.0		1.00	1.00				-
2.9	1.00					1.00	-
2.7		1.00	1.00				-
2.5		1.00	1.00				-
2.3	0.82	0.87	0.83			0.88	-
2.1		0.12	0.13				-
1.8		0.27	0.30	0.25	0.21	0.33	-
1.4		0.19	0.22	0.19	0.14	0.34	0.3-0.4
1.0	0.21	0.14	0.17	0.15	0.11	0.30	-
0.6		0.13	0.16	0.13	0.08	0.24	-
0.2		0.07	0.09	0.09	0.04	0.14	-

Table 3. Calculated void fractions in the downcomer (5-equation model)

Average elevation (m)	1-node	5-node	15-node		RELAP5
			hot	cold	5-node
1.8		0.06	0.01	0.04	0.38
1.4		0.06	0.03	0.02	0.27
1.0	0.02	0.07	0.04	0.03	0.22
0.6		0.04	0.05	0.03	0.14
0.2		0.00	0.00	0.00	0.04

Table 4. Calculated void fractions in the downcomer (6-equation model)

Average elevation (m)	1-node	5-node	15-node		RELAP5
			hot	cold	5-node
1.8		0.04	0.07	0.04	0.38
1.4		0.04	0.07	0.05	0.27
1.0	0.00	0.04	0.07	0.05	0.22
0.6		0.05	0.07	0.05	0.14
0.2		0.02	0.03	0.03	0.04

The calculated void fractions in the heater (tables 1 and 2) are a little lower than the measured values. The void fraction distributions (tables 1-4) are similar in the different nodalizations of both thermohydraulic models. In the 15-node version of five-equation model the distribution is disturbed by the large downward flow of water in the cold collector side of the heater and steam is packed in the node of the second highest level.

Table 5. Calculated downward mass flows (kg/s) in the downcomer (5-equation model)

Elevation (m)	5-node	15-node		RELAP5
		hot	cold	5-node
2.0	6040	3110	2530	1840
1.6	6730	3440	3010	2840
1.2	5980	3020	2780	3470
0.8	4780	2350	2160	3200
0.4	3190	1530	1430	2070

Table 6. Calculated downward mass flows (kg/s) in the downcomer (6-equation model)

Elevation (m)	5-node	15-node		RELAP5
		hot	cold	5-node
2.0	4610	2300	2100	1840
1.6	5380	2630	2440	2840
1.2	5200	2470	2370	3470
0.8	4150	1940	1950	3200
0.4	2500	1120	1230	2070

Table 7. Calculated mass flows (kg/s) from downcomer to heater (5-equation model)

Elevation (m)	5-node	15-node		RELAP5
		hot	cold	5-node
1.8	-660	-340	-480	-1000
1.4	790	420	230	-630
1.0	1220	660	630	270
0.6	1590	820	730	1130
0.2	3190	1530	1430	2070

Table 8. Calculated mass flows (kg/s) from downcomer to heater (6-equation model)

Elevation (m)	5-node	15-node		RELAP5
		hot	cold	5-node
1.8	-770	-320	-330	-1000
1.4	180	150	70	-630
1.0	1040	530	420	270
0.6	1660	820	710	1130
0.2	2500	1120	1230	2070

The flow patterns calculated by the five- and six-equation models are quite similar (tables 5-8). The six-equation model simulates a higher recirculation mass flow than the five-equation model. The real circulation mass flows of the steam generator are not known and thus no additional loss coefficients have been defined in order to adjust the calculation results. The amount of the circulation depends on the phase separation effect. The lower the average void fraction in the downcomer is, the higher the circulation becomes. Slight changes in the nodalization and in the calculation of velocity differences had a large effect on the circulation and the void fraction distribution in the downcomer.

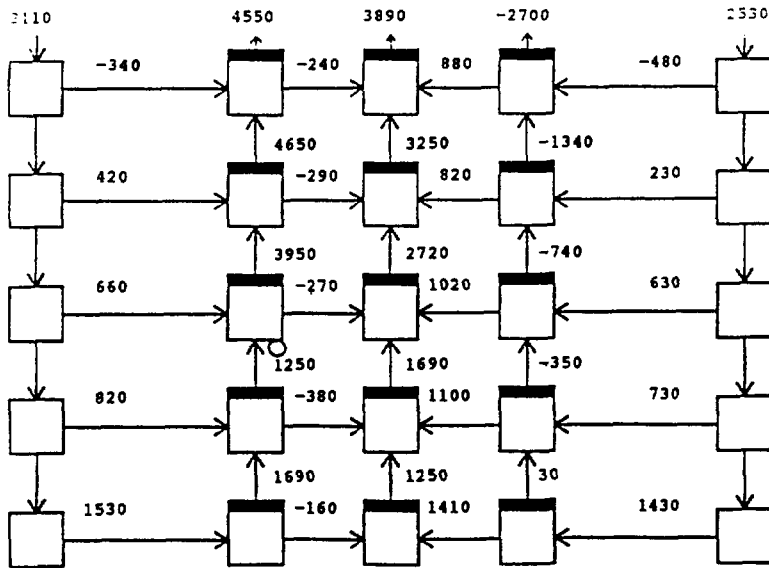


Figure 4. Mass flows (kg/s) calculated by the 15-node model (5-equation model): positive flow is in the direction of the arrow

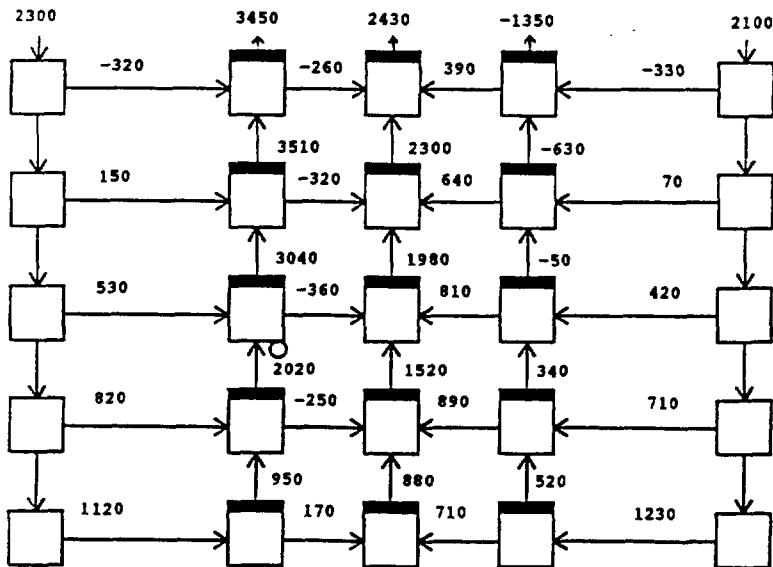


Figure 5. Mass flows (kg/s) calculated by the 15-node model (6-equation model): positive flow is in the direction of the arrow

The 15-node model predicts a flow pattern in which there are some downward flows in the cold collector side of the heater and circulation between the cold collector side and the downcomer occurs. These circulations are caused by different steam generation rates in different parts of the heater.

#### 4. Future Plans

The flow pattern of the steam generator is so complicated that a three-dimensional model is required to account for all the effects. Such a model containing more than 200 calculation nodes will be created in the future. In order to adjust the model properly, it is very important to get also three-dimensional measurement data from a steam generator.

#### 5. Conclusion

It is easy to define different, also quite complicated nodalizations of the horizontal steam generator using the generic process component of APROS. Three different nodalizations have been created by APROS for the five- and six-equation models. The calculated void fraction and mass flow distributions are qualitatively reasonable. The results calculated by the five- and six-equation models differ only a little. In order to take into account all the flow phenomena of the steam generator, a three-dimensional model would be required.

#### References

1. C. Palsinajärvi, Modelling the Horizontal Steam Generator with APROS Simulation Code, Second International Seminar of Horizontal Steam Generator Modelling, 29 - 30 September, 1992, Lappeenranta, Finland.
2. Porkholm, K. et al., Loviisa Nuclear Power Plant Analyzer, Imatran Voima Oy, Research Reports IVO-A-11/92, 1992.
3. I. Karppinen, Modelling of Horizontal Steam Generator with RELAP5/MOD2 and MOD3, International Seminar of Horizontal Steam Generator Modelling, March 11-13, 1991, Lappeenranta, Finland.
4. Initial data for calculations of natural circulation in the secondary volume of PGV-440 and PGV-1000, Private communication by letter between Dr H. Tuomisto and Prof. V.F. Titov, December 1991.



**Electrogorsk Research & Engineering Centre  
of Nuclear Plants Safety**

---

Bezmyannaya 6  
Moscow region  
Russia, 142530

phone: +7 (09643) 3-05-21  
fax: +7 (09643) 3-05-15

**Moderinzation of SGV-1000 separator scheme  
to improve an efficiency and reliability**

*Prof. A.G.Ageev , Prof. V.F.Titov, Prof. B.I.Nigmatulin,  
Dr. G.N. Tarankov*

*(EREC, OKB "Hydropress")*

## CONTENTS

### Introduction

1. The results of production tests of head SGH-1000
2. Fast decisions concerning modernization of separate scheme
3. The features of existing measurement system of level in SG
4. Modernization of separate scheme
5. Proposals for improvement of level measurement and water store in SG by the 4-meter level meters
6. Measures to improve a quality of automatic control of level

### Conclusions



## INTRODUCTION

In PGV-1000 type the separator scheme with sinked under level a hole sheet (SHS) with rim of 730 mm and chevron separator in the upper part of steam volume (Fig. 1) is used.



## **1. RESULTS OF PRODUCTION TESTS OF HEAD PGV-1000**

- off design release of steam-water mixture from clearance between the vessel and the rim at the hot side of SG is detected;
- moisture content is over-design under power of 80-85 %.



## 2. FAST DECISIONS CONCERNING MODERNIZATION OF SEPARATOR SCHEME

- reflecting visor before limiting block of shutters at a hot collector side (Fig. 1) is installed;
- interior cross section of SHS; is increased;

Under it:

- nominal power of block is realized;
- steam-water mixture release was not
- in steam volume appeared reflected steam flow;
- steam capacity reserve not excesses 8-10 %;
- due to hydraulic unequivalent of circulation loops under nominal power of block, some SG work under the bound of capacity of the separate scheme.



### 3. THE FEATURES OF EXISTING MEASUREMENT SYSTEM OF LEVEL IN SG

- allowable range of level change under SHS is limited, operation within this range is impossible;
- SG operation is under indirect parameter level in clearance between SG vessel and SHS rim;
- level measurement system with the 4-meter level meter on the hot and cold ends not show a real water store because of difference in ends void fraction that limited by rims and the main SG volume;
- accepted the level measurement system causes to the change of the 4-meter level meter indication during transient and upset modes, not connected with the water store change.



## **4. MODERNIZATION OF THE SEPARATE SCHEME**

### **4.1. Overlapnthe clearance between SG vessel and SHS from the hot side. The proposal is verified at the NPP Balakovo first block.**

Under it:

- the steam-water release is voided;
- the work of a steam volume is normalized;
- void fraction in a water volume at the hot side of bundle is decreased;



**4.2. Replacement chevron separator with ceiling hole screen (Fig.2). The proposal is verified at NPP Balakovo 4 block.**

Under it:

- steam moisture content at the SG outlet is decreased up to 0.01-0.02%;
- allowable range of level change in SG is increased;
- designed margins in steam capacity is increased from 1.1 to 1.4 times.
- audit conditions, maintenance and of SG upper part is improved.



**4.3. The use of SHS with sluggish packings. The proposal is verified in SG with chevron separator (Fig.3) at Hmelnitskaja NPP a block.**

Packing system that supplies steam from under SHS to steam volume allows:

- to extend the allowable range of level change above SHS up to 300 mm if the shutters up to 500 mm is expelled.
- to extend the design margins in steam capacity from 1.1 to 2.0 time;
- under of shutters (Fig.4) to change over SG operating at level above SHS having a direct influence on turbine plant safety.



## **5. PROPOSALS FOR IMPROVEMENT OF LEVEL MEASUREMENT AND WATER STORE IN SG BY THE 4-METER LEVEL METERS**

- pressure taps with the special pressure tap transducer from the SG cylinder part where is a main water store;

## **6. MEASURES TO IMPROVE A QUALITY OF LEVEL AUTOMATIC CONTROL**

- direct free from transit-time effects measurement of steam flow maintaining high accuracy and decrease of level control transit-time effects in transient and upset modes.



## CONCLUSIONS

Programm of modernization of separate scheme for PGV-1000 is recommended for installation verified at a real NPP SG-s.

Programm realization allows:

- moisture content steam decrease;
- increase margins of steam capacity;
- change over SG operating in connection with level above SHS, that directly determines turbine plant safety.

Measures to improve the measurement system and level water control are proposed.



**Steam generator with state separative scheme with submerged perforated plate and jalousie separator**

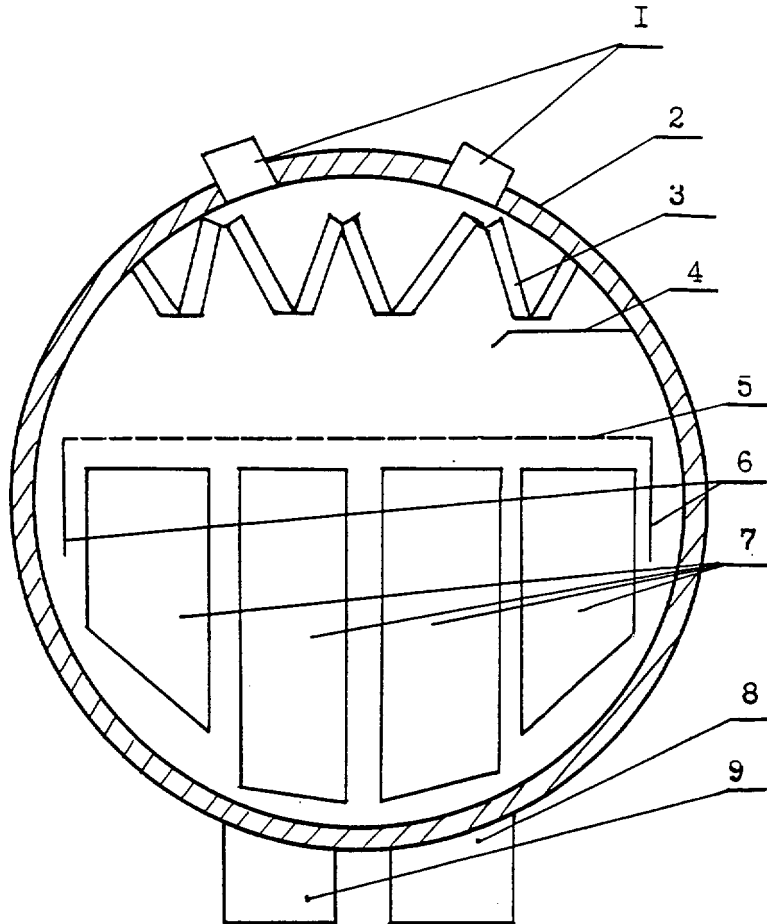


**Fig.1.**

- |                                 |  |
|---------------------------------|--|
| 1 - steam discharge pipes;      | 6 - edges of submerged perforated plate; |
| 2 - vessel;                     | 7 - heat-transfer beam packets;          |
| 3 - jalousie separator;         | 8 - hot collector;                       |
| 4 - repelling shield;           | 9 - cold collector.                      |
| 5 - submerged perforated plate; |  |





**Steam generator with submerged perforated plate  
with un bubbling packings.**

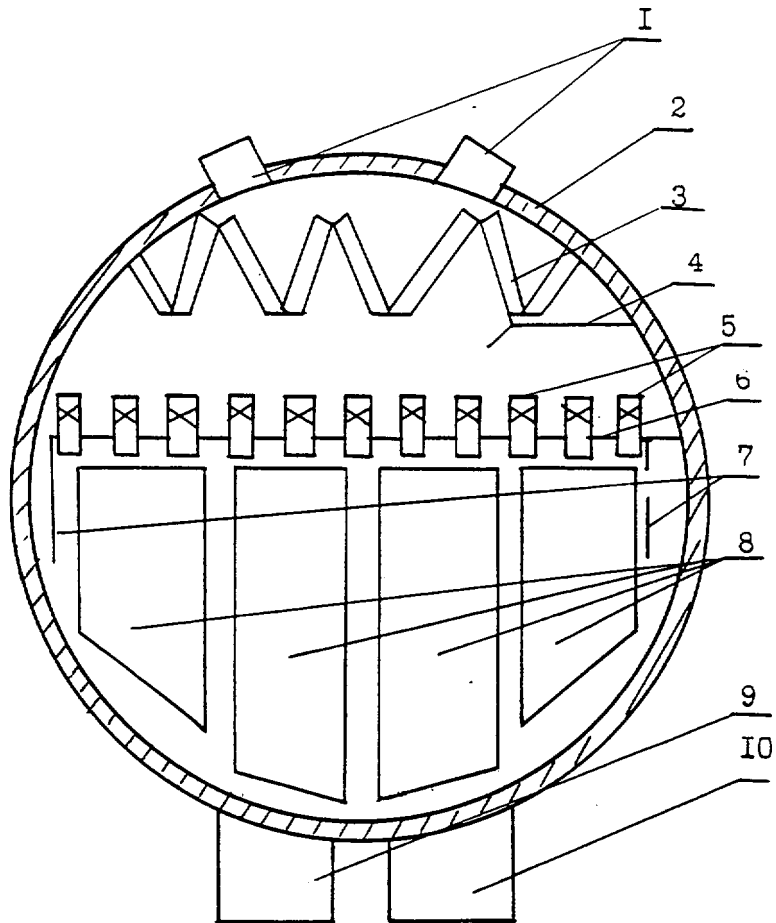


**Fig.3.**

- |                                 |  |
|---------------------------------|--|
| 1 - steam discharge pipes;      | 6 - edges of the submerged perforated plate; |
| 2 - vessel;                     | 7 - heat-trasfer beam packets;               |
| 3 - jalousie separator;         | 8 - hot collector;                           |
| 4 - repelling shield;           | 9 - cold collector.                          |
| 5 - submerged perforated plate; |  |



**Steam generator with submerged perforated plate with unbubbling packings and the steam reception shield; the gap between the vessel and the edge on the hot side is overlapped.**

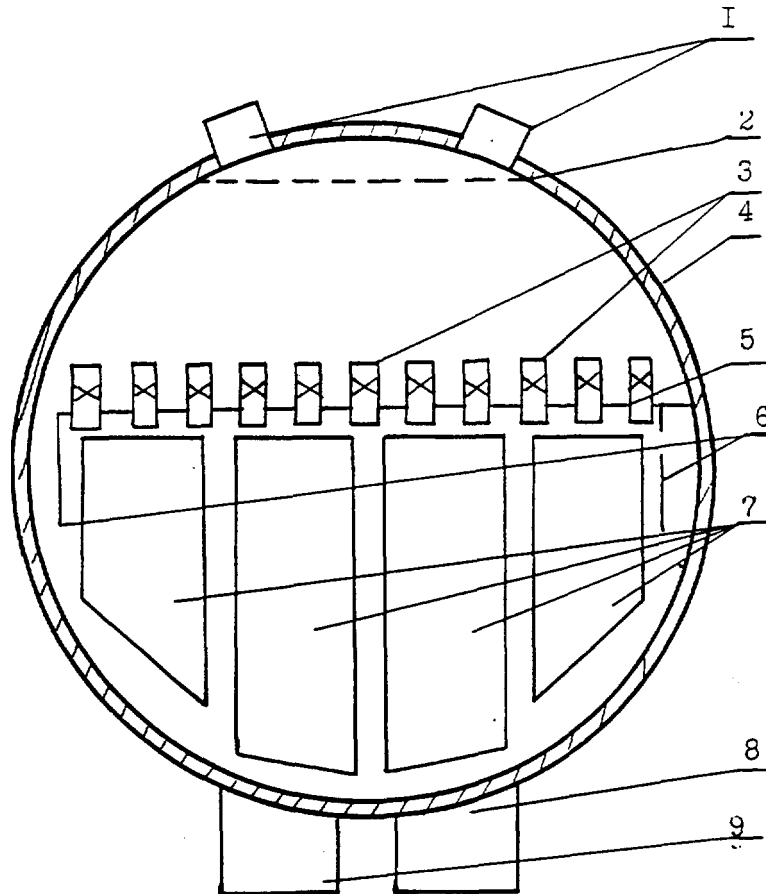


**Fig.4.**

- |                                 |  |
|---------------------------------|--|
| 1 - steam discharge pipes;      | 6 - edges of the submerged perforated plate; |
| 2 - steam reception shield;     | 7 - heat-transfer beam packets;              |
| 3 - unbubbling packing;         | 8 - hot collector;                           |
| 4 - vessel;                     | 9 - cold collector.                          |
| 5 - submerged perforated plate; |  |



ÚJV 10293 T

Prepared for  
Third International Seminar on  
Horizontal Steam Generators

RELAP5/MOD3.1 Analysis  
of Main Steam Header Rupture  
in VVER-440/213 NPP

---

Pavel KRÁL

Nuclear Research Institute  
Řež, Czech Republic

October 1994

## Abstract

The presented paper is focused on two main topics. Firstly we describe the applied modelling of PGV-4 steam generator for RELAP5 code. The results of steady-state calculation under reference conditions are compared against measured data. The problem of longitudinal subdivision of SG tubes is analysed and evaluated.

Secondly, we present a best-estimate analysis of main steam header (MSH) rupture accident in VVER-440/213 NPP. The low reliability of initiation of ESFAS signal "MSH Rupture" leads in this accident to big loss of secondary coolant, full depressurization of main steam system, extremely fast cool-down of both secondary and primary system, opening of PRZ SV-bypass valve with later liquid outflow, potential reaching of secondary criticality by failure of HPIS, etc.

## Abstrakt

Prezentovanou prací lze rozdělit do dvou hlavních částí. Za prvé je to problematika modelování parogenerátoru PGV-4 pro výpočetní program RELAP5. Výsledky výpočtu stacionárního stavu při referenčních okrajových podmínkách jsou porovnány vůči měřeným datům. Je rovněž diskutován vliv podélného dělení modelovaných trubiček PG na dosahované výsledky.

V druhé části práce popisujeme analýzu (realistického typu) havárie s roztržením hlavního parního kolektoru (HPK) na jaderné elektrárně s VVER-440/213 provedené s pomocí programu RELAP5/MOD3.1. Nespolehlivá inicializace havarijního signálu Systému zajištění bezpečnosti "Roztržení HPK" vede v tomto případě k velké ztrátě sekundárního chladiva, plnému odtlakování sekundárního systému (mimo systému napájecí vody), prudkému vychlazení sekundárního i primárního okruhu, zapracování obtokového ventilu PV KO na předeřhivací trase do BN, pozdějšímu úplnému zaplnění kompenzátoru objemu, nebezpečí dosažení sekundární kritičnosti při nenajetí VTČ apod.

## Contents

1. Introduction
2. Input model of VVER-440/213 for RELAP5
  - 2.1 Main characteristics of input model
  - 2.2 Steam generator modelling
3. Steady state calculation with reference boundary conditions
4. Longitudinal nodalization of SG tubing
  - 4.1 Different general modelling attitudes
  - 4.2 Different number of inner volumes
5. Analysis of main steam header rupture accident
  - 5.1 Defining of initiating event
  - 5.2 Initial conditions
  - 5.3 Boundary conditions
  - 5.4 Timing of main events
  - 5.5 Discussion of system behaviour
  - 5.6 Steam generator behavior

## 6. Conclusions

## Nomenclature

## References

- Appendix A: Results of MSH rupture in VVER-440/213 analysis  
- course of main parameters

## Figures

- Fig.1 Nodalization of primary system  
 Fig.2 Nodalization of steam lines system  
 Fig.3 Nodalization of FV system  
 Fig.4 Main parameters of SG-1 under reference steady-state conditions  
 Fig.5 Main parameters of SG-2 at 2.5 sec of the accident  
 Fig.A-01 + Fig.A-12 ... see Appendix A

## Tables

- Tab.1 Steady state (300 s) run results  
 Tab.2 Comparison of 3 different SG tubing longitudinal nodalization  
 Tab.3 Influence of number of inner volumes on the heat transfer prediction (by constant lengths subdivision)

## 1. Introduction

The postulated accident with full or partial rupture of MSH was in original Soviet design of VVER-440/213 "covered" by ESFAS accident signal "MSH Rupture" (based on time derivation of pressure in MSH - see a brief description in Chap.5.5).

The latest analyses performed by advanced thermal hydraulic codes (RELAP5/MOD2 and MOD2.5) in Czech Republic and in Slovakia revealed that this actuation scheme is unreliable and that an ESFAS modification is necessary.

The purpose of the work presented in this paper is to recalculate our older analysis with the latest released version of RELAP5 computer code (R5/M3.1), to share our findings about ESFAS reliability with other VVER specialists, and to study in greater detail the performance of applied SG modelling under both steady state and transient conditions.

## 2. Input model of VVER-440/213 for RELAP5

The input deck used for performing of presented analysis is an input model of Dukovany NPP with VVER-440/213 (the 1.unit). The input deck originates in an "international" input deck of Jaslovske Bohunice NPP prepared under IAEA regional program "Safety Assessment of VVER-440/213". In 1993 the model was substantially enlarged and modified according to specifications of NPP Dukovany (1.unit). Later on we continued in improvements and modifications of the model according to new accident and transient types, that were analysed.

With respect to the seminar orientation, we describe the input model in a very brief way. In more detail we will then discuss the modelling of steam generator.

### 2.1 Main characteristics of input model

The nodalization scheme of the input model is presented in Fig.1 (primary system), Fig.2 (steam lines), and Fig.3 (FW system).

#### Main characteristics of nodalization:

- 3 modelled loops (6 real loops lumped to 1 single, 1 double, and 1 triple loop)
- 4 hydraulic channels in core region (hot assembly, average central core, average peripheral core, bypass)
- reactor UP and DC modelled in multi-channel way
- "3-layers" SG nodalization (for more detail see below)
- detailed description of steam lines and MSH
- detailed description of FW system (from FW tanks to SGs)

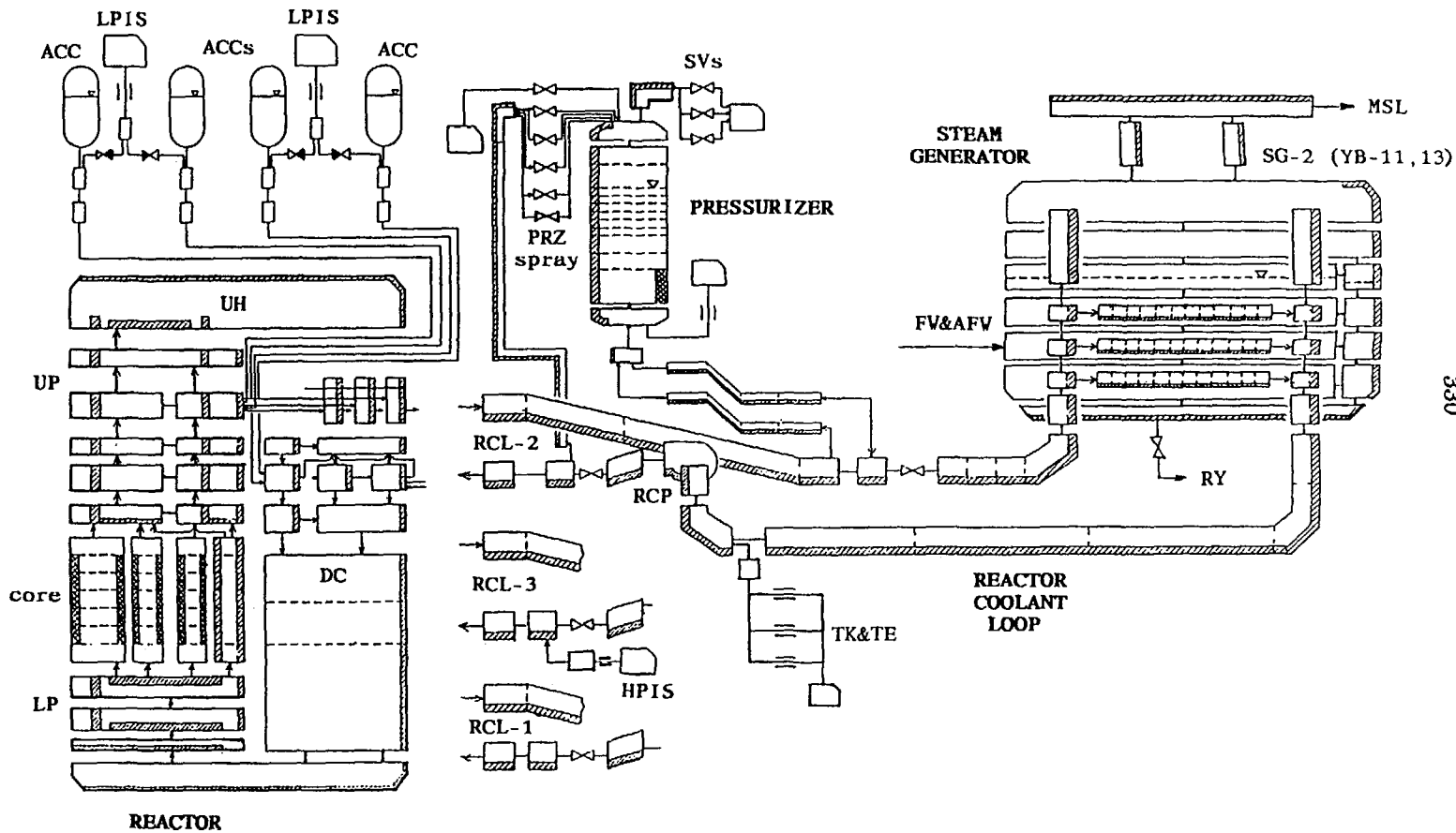


Fig.1 Nodalization of primary system

Main modelled operational control systems:

- reactor power control system "ARM-5S" (regimes "S" and "N")
- reactor power limiting system "ROM" (simplified)
- PRZ heaters and spraying
- primary make-up (TK) and let-down (TE)
- turbine control system "TVER" (simplified)
- "BRU-C" steam bypass valves to main condenser
- FW controllers (for main and bypass FW control valves)

Main modelled safety systems:

- reactor trip signals AZ-1,2,3,4
- following ESFAS signals:
  - "Small Break"
  - "Intermediate Break"
  - "Large Break"
  - "MSH Rupture"
  - "Loss of Feedwater"
- all TSPG (Technological Protection of Steam Generator) signals:
  - "MSL Rupture"
  - "MSH Rupture"
- all LPSG (Local Protection of Steam Generator) signals:
  - high SG level "+75 mm"
  - high SG level "+100 mm"
  - low SG level "-140 mm"
- safety valves at PRZ and SGs
- atmospheric dump valves "BRU-A"
- ECCS (HPIS, ACCs, and LPIS trains)

The steady state parameters are listed in Chap.3 (SG parameters under reference boundary conditions) and in Chap.5.2. (entire system parameters under typical Dukovany NPP full-power conditions).

**2.2 Steam generator modelling**

The nodalization of the steam generator in our input model is a compromise between an attempt to allow simulation of all expectable TH phenomena on one side and the limited CPU-time, man-power and code limitations on the other side.

The primary side of each steam generator is in all three basic region (inlet header, tube bundle, and outlet header) vertically subdivided to enable simulation of headers level movement (->prediction of history of void fraction of fluid entering SG tubes), simulation of reverse flow in bottom tubes layer under natural circulation conditions and other phenomena.

The tube bundle and the relevant section of primary headers are modelled in three layers with "half-cross-flow" junctions between headers' branches and tubing pipes. This division is pretty rough and for some types of transients would be insufficient.

Longitudinal subdivision of each tubing layer (pipe component) is done in "constant lengths" way to 12 internal volumes. More information about this decision and a comparison to other ways of longitudinal subdivision can be found in Chap.4.

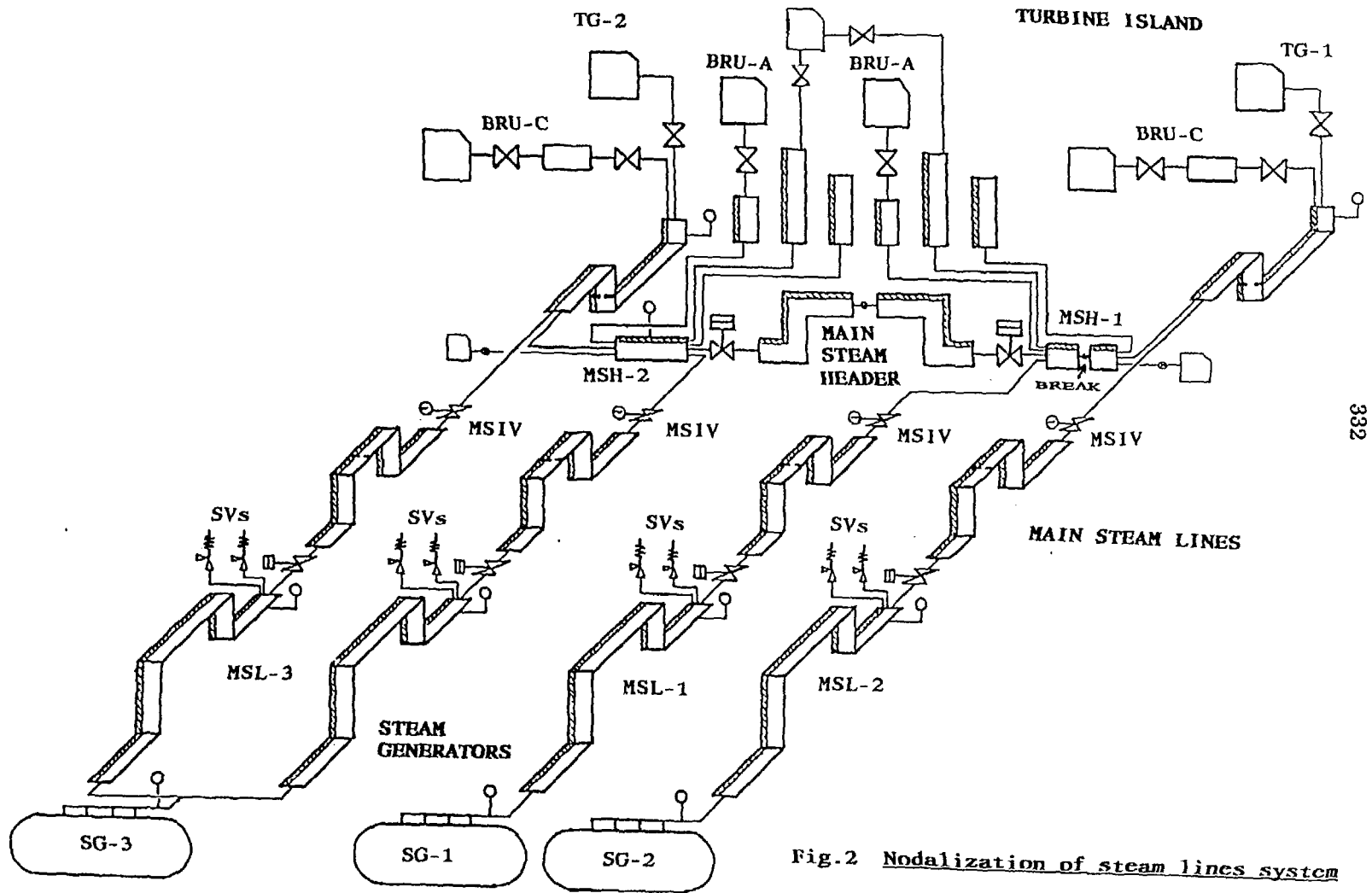


Fig.2 Nodalization of steam lines system

The secondary side of the SG nodalization can be divided into 6 basic regions:

- tube bundle region ... 3 volumes
- side (downcomer) region ... 3 volumes
- non-heated bottom dead volume ... 1 volume
- volumes at nominal mix.level elevation ... 2 volumes
- "steam dome" volumes ... 2 volumes
- steam outlet collector volumes ... 3 volumes

The tube bundle (TB) region was vertically subdivided with respect to primary side nodalization to 3 volumes (allowing to certain extent prediction of wetted part of SG tubing secondary surface, etc.). The downcomer region was subdivided in the same way, enabling internal SG recirculation.

The junctions between TB and DC volumes were originally (MOD2.5) of cross-flow type, but after input model transfer to MOD3 code versions we got horizontal stratification (HST) flow regime at these junctions resulting in too high phases slip and low recirculation. This problem was partially eliminated by redefining of these junctions as normal junctions connecting bottom sides of appropriate volumes.

As for the special RELAP5 options and another modelling decisions made during preparation of SG secondary side input data, we went in following way:

- vertical stratification flow regime was deactivated in TB and DC volumes
- normal interphase friction model was used in all control volumes (including TB volumes)
- local loss factors were specified by help of Ref.4
- cross-flow junctions were at secondary side used between "level" volumes, and between vertical and horizontal pipes of outlet collector (half "to volume" cross-flow junction)
- in vol-186 (see Fig.4) we specified a small hydraulic diameter corresponding to SG separator geometry
- we did not use any artificial bending down of SG tubing to enable condensate cumulation on primary side of SG (e.g. in SBLOCA) - the phenomena detected during ISP-33 PACTEL experiment
- we did not use any artificial increase of tubing material conductivity or an enlargement of tubing surface.

The feedwater collector is connected to middle tube bundle volume (accord. to real FW collector location and its outlet holes orientation). For case of "reflooding" of secondary surface of SG tubing, we use an auxiliary set of valves between last volume of FW train and particular SG tube bundle volumes (to exceed problems arising from discrete and too rough vertical nodalization of tube bundle region). We model as well the continual SG drainage from the bottom volume.

As for another nodalizations of PGV-4 prepared and used in NRI, there was a "six-layer" nodalization of SG used for ATVS analysis in the end of 1993 [Ref.3]. Next more detailed nodalization of VVER horizontal SG prepared in the NRI was presented at previous seminar (Mr.Kyncl's contribution). A next expected impulse for more detail way of modelling of horizontal SG will be the release of "3-D" RELAP version or installation of other "3-D" code in NRI.

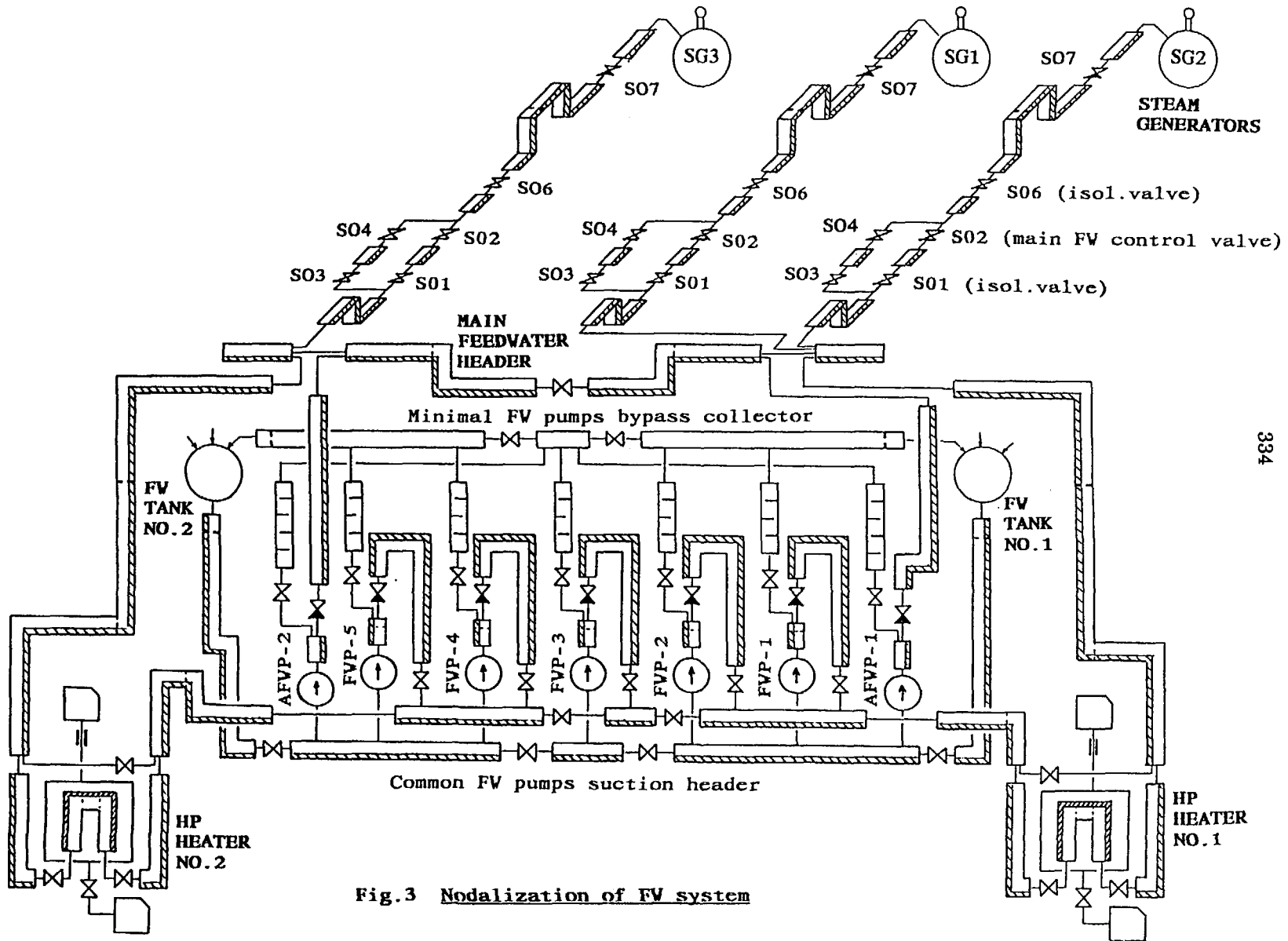


Fig.3 Nodalization of FW system

### 3. Steady state calculation with reference boundary conditions

Because the typical steady state conditions used in our analysis (according to Dukovany NPP) are a bit different from the boundary conditions used by the participants of previous seminars, we included this chapter focused only on reference steady state analysis and discussion. (The initial conditions of the actual accident analysis are then slightly different - see Chap.5.2)

Reference boundary conditions used for stabilization of separated SG model were as follows:

- primary pressure	$P_{PCS} = 12.25 \text{ MPa}$
- loop flowrate	$\dot{M} = 1560 \text{ kg/s}$
- hot leg temperature	$T_{HL} = 295 \text{ }^\circ\text{C}$
- secondary pressure	$P_{SG} = 4.60 \text{ MPa}$
- feedwater temperature	$T_{FW} = 223 \text{ }^\circ\text{C}$

Additional boundary condition (accord.to NPP Dukovany) were:

- nominal narrow range level	$L_{MID} = 2.121 \text{ m}$
- continual drainage flow	$Q_{RY} = 2.33 \text{ m}^3/\text{hr} (\approx 0.5 \text{ kg/s})$

Tab.1 Steady state (300 s) run results:

		R5/M3.1 calc.	Measured values
Steam output	kg/s	125.40	125.5
Recirculation ratio	-	4.92	-
Voidage under level	%	22.28	(23.0)
Secondary coolant mass	ton	32.55	33.0
Collaps.level across TB/DC	m	1.71/1.74	(1.90)
Mix.level in TB/DC region	m	2.22/2.20	-

The basic SG steady state parameters reached after 300 s stabilization are listed and compared in Tab.1. The reference boundary conditions and the measured steady state parameters used for comparison were taken from Ref.5 or from other papers presented at previous seminars. We did not use the secondary inventory mass as a boundary condition, but the FW supply was controlled according to SG narrow range level. More detailed description of SG secondary side status for "final" R5/M3.1 steady-state calculation is presented in Fig.4.

Explanatory notes:

1/ **Recirculation ratio** ... average value.

For more detailed nodalization it is a problem to come to an average recirculation ratio based on DC flows. So we use the mass flows in particular TB volumes and weight them with respect to tubing surface in the volume (or with respect to volume of particular control volumes).

$$REC = \frac{\sum S_i * \dot{M}_{f,i}}{\sum S_i} * \frac{1}{\dot{M}_g} \quad \text{where: } \begin{array}{l} S = \text{surface [m}^2\text{]} \\ i = \text{number of control volume} \\ \dot{M}_f = \text{liquid flow rate [kg/s]} \\ \sum = \text{sum over TB contr.volumes} \\ \dot{M}_g = \text{SG steam outflow [kg/s]} \end{array}$$

If we use usual way of defining of several recirculation ratios relevant to local downcomer flows, we got following values:

Downcomer junction	Downward liq.flow	Local rec.ration
-----	-----	-----
182->172	631.72	5.03
172->171	674.31	5.37
171->170	1062.94	8.47
170->158	418.96	3.34

Simple, non-weighted averaging of these local recirculation ratios leads to average value 5.55 (by weighting of liquid flow in TB volumes - see above - we got the average value 4.92).

2/ **Voidage under level** ... average value (weighted over volumes)

The vapor void fraction in control volumes with mixture level was considered equal to vapor void fraction in the control volume below and for weighting was used only a fraction of the volume occupied by mixture.

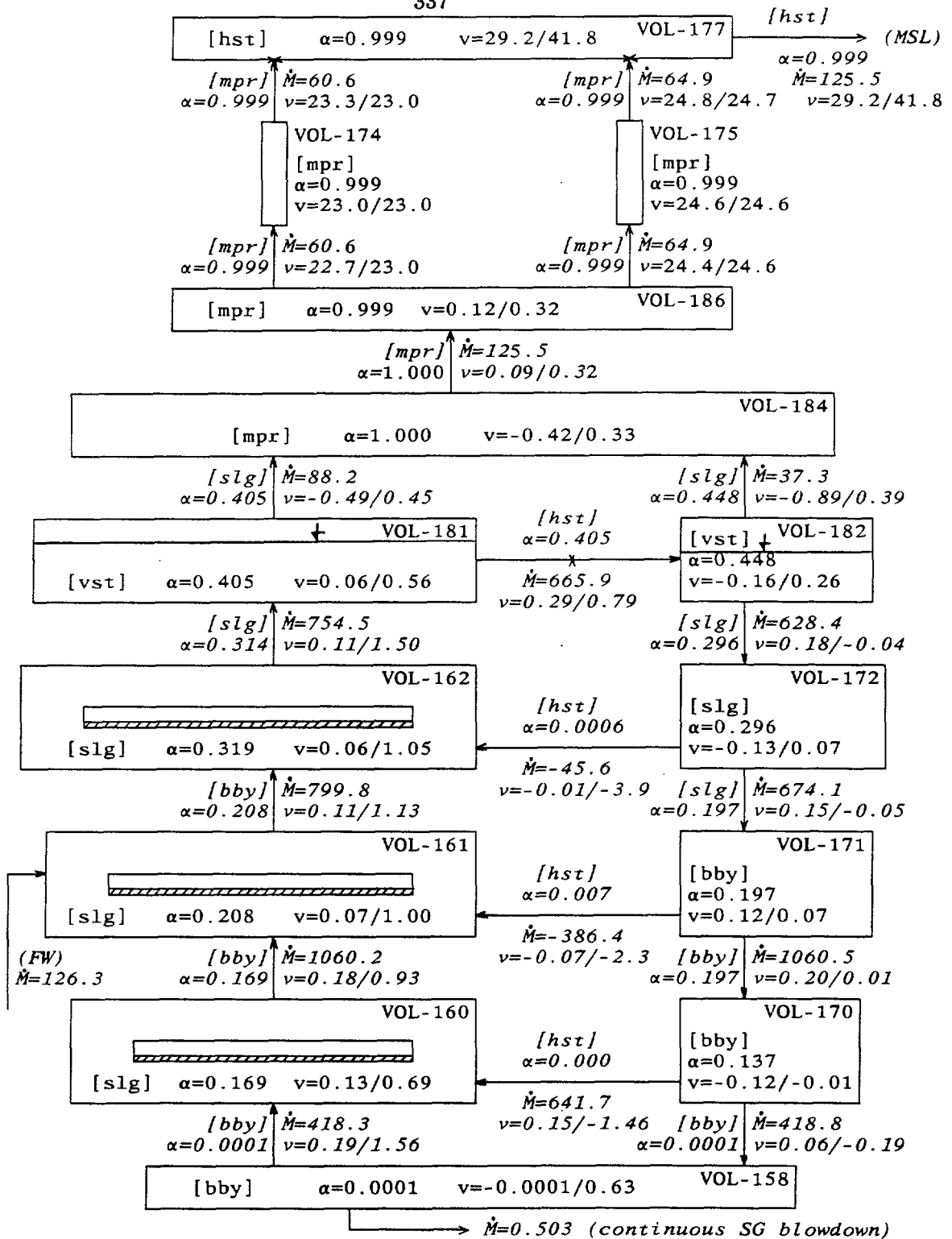


Fig. 4 Main parameters of SG-1 under reference steady-state conditions

### 3/ Mixture level

An auxiliary value computed by help of a set of trips and control variables processing the void fractions in a column of hydrodynamic volumes.

We prepared several types of these modules, differing in:

- criterion for existence of mix.level in partic.volume
- void fraction under level in the volume with mix.level
- protection for cases with two level in the stuck of volumes; smoothing of the final value when the level is crossing boundary of control volumes; etc.

With respect to RELAP5 nature, this value (mixture level) is only of auxiliary character and limited validity, but in many cases it gives a very useful and condensed information about a situation in a vertical parts of the modelled system. Typically, we apply these modules to RV inner regions, PRZ vessel, and to the secondary side of SGs.

### 4/ Orientation of volumes and junctions, etc. (Fig.4)

Vertical volumes (all control volumes except of steam outlet collector horizontal pipe, vol-177) are of upward orientation. Orientation of hydraulic junctions is designate by arrows. Parameters of hydraulic junctions are written by italics. Velocities are presented in "liquid/vapor" velocity form.

### Comments to steady-state results:

#### \* Overall agreement

Although the nodalization applied is relatively simple, the overall agreement of basic parameters (steam output, secondary coolant mass, average voidage under level) with measured data is good. The difference between total collapsed level and measured "dP" level could be partially explained by dynamic pressure difference.

#### \* Problem of horizontal stratification flow regime at junctions between TB and DC volumes.

The switch of junction flow regime map to "HST" is irrelevant for connections between TB and DC, deep under the real interphase level. It results in underestimation of interphase friction. A deactivation option would be very beneficial (similarly like in case of vertical stratification for control volumes).

#### \* Difference between mixture levels above TB and above DC

The mix.levels difference is only about 2 cm, what is probably underestimated (we take into account only approximate character of our mixture level value). This can lead to underestimation of liquid entrainment to steam line in case of "steam line rupture" etc. A more realistic simulation of mixture level profile is expected after application of finer nodalization (not averaging the whole TB region and whole DC region) for a "3-D" code as much as possible verified against measured data.

- \* "Non-VST" flow regimes at junctions adjacent to "VST" volume  
(see the control volumes 181,182 and adjacent junctions in Fig.4)  
There seems to be an undocumented modification in the R5/M3.1 code version against R5/M3.0 (in R5/M3.0: "... a junction is considered vertically stratified if either of its connecting volumes is vertically stratified ..." [Ref.1]).
- \* Oscillations in SG top and outlet collector  
Although the flow regimes are stable, the liquid velocity (and some other parameters) slightly oscillates.

## 4. Longitudinal nodalization of SG tubing

The longitudinal subdivision of SG tubes substantially influence the prediction of heat transfer between primary and secondary side of SG. The decision about number and lengths of inner volumes of modelled SG tubes depends usually on following factors:

- good conditions for primary-to-secondary heat transfer
- Courant limit
- reasonable number of control volumes
- nodalization of secondary side (when used a fine-node nodal.)

### 4.1 Different general modelling attitudes

We started this auxiliary study with 5 inner volumes in each SG tubing layer. Firstly we compare generally different ways of length subdivision - the "constant lengths" nodalization and two nodalizations with extending inner lengths.

Nodaliz. case	Subdivision way	Relative length of inner volumes (from hot to cold collector)				
"A"	... constant lengths	... 20%	+ 20%	+ 20%	+ 20%	+ 20%
"B"	... extending lengths	... 10%	+ 10%	+ 20%	+ 20%	+ 40%
"C"	... logar.subdivision	... 13.5%	+ 15.6%	+ 18.5%	+ 22.8%	+ 29.5%

The calculation were done with RELAP5/MOD3.1 code version under reference boundary condition (same as in Chap.3). The algorithm for preparing of logarithmic subdivision in case "C" was taken from Ref.6 and is based on following two terms:

$$z_i = \ln \left( 1 + \frac{i}{n} * 1.718281828 \right)$$

$$L_i = (z_{n+1-i} - z_{n-i}) * L_T$$

Used variables:  $i$  = number of the inner volume ( $i = 1, \dots, n$ )  
(from hot to cold collector)  
 $L_i$  = length of  $i$ -th inner volume of the pipe  
 $L_T$  = total length of the pipe  
 $n$  = total number of inner volumes  
 $z_i$  = auxiliary variable

The results of steady state calculation (300 s) for these 3 cases are compared in Tab.2 below:

		Nodal. "A"	Nodal. "B"	Nodal. "C"
		constant lengths	expand. 1-1-2-2-4	logar. subdivis.
Steam output	kg/s	120.74	119.01	120.29
Cold leg temperature	°C	267.37	267.73	267.46
Average voidage	%	21.78	21.59	21.73
Recirculation ration	-	5.15	5.24	5.17
Bottom layer outlet temp.	°C	268.39	268.76	268.49
Middle layer outlet temp.	°C	267.32	267.69	267.43
Upper layer outlet temp.	°C	266.87	267.24	266.96
Heat transfer in middle layer:				
1. volume	MW	24.26	14.16	17.89
2. volume	MW	17.29	11.79	15.87
3. volume	MW	12.35	16.81	13.69
4. volume	MW	8.87	12.01	11.70
5. volume	MW	6.43	13.54	9.79
Total	MW	69.20	68.31	68.94

Tab.2 Comparison of 3 different SG tubing longitudinal nodalization

Although the heat transfer in case "A" is the least "homogeneous" (large differences in heat transferred from individual inner volumes), it is the most efficient as for the SG steam output. The total heat transfer is obviously underestimated (required steam output should be about 125 kg/s). In past we solved this problem by artificial increasing of SG tubing material thermal conductivity (usually by 25%).

#### 4.2 Different number of inner volumes

In the next step, we focused on the "constant lengths subdivision" nodalization approach and tested the influence of number of inner volumes on the primary-to-secondary heat transfer efficiency. We tested several cases and finally came to the number of 12 inner volumes as acceptable. For an illustration we compare below the following 3 cases:

Case "D" ... 1 inner volume

Case "A" ... 5 inner volumes (case "A" above)

Case "F" ... 12 inner volumes

The basic results of performed steady-state runs are compared in Tab.3:

		Nodal. "D"	Nodal. "A"	Nodal. "F"
		1 volume	5 volumes	12 volumes
Steam output	kg/s	96.45	120.74	125.40
Cold leg temperature	°C	272.53	267.73	266.35
Average voidage	%	19.53	21.59	22.28
Recirculation ratio	-	6.61	5.24	4.92

**Tab.3 Influence of number of inner volumes on the heat transfer prediction (by constant lengths subdivision)**

The results of "F" case are from the point of view of heat transfer modelling very good (see as well the comparison to measured data in Chap.3) and thus we applied this SG nodalization in the input deck used for the "MSH rupture" analysis (Chap.5).

## 5. Analysis of main steam header rupture accident

In this chapter we describe a best-estimate analysis of double-ended rupture of MSH-1 in VVER-440/213 performed with RELAP5/MOD3.1 code. (The calculation was done with input deck "d63-msh21.i" at 30.October 1994.)

### 5.1 Defining of initiating event

The initiating event of the accident is a full rupture (2x100%) of the MSH-1 (half-collector No.1). The exact break location was between connections of MSLs from SG YB-13 and YB-15. The full opening of the break is considered in 0.1 sec.

The frequency of occurrence of such an event is according to IAEA report [Ref.7] estimated from  $3.9E-2/\text{yr}$  to  $3.8E-8/\text{yr}$ . According to ANSI classification, this accident belongs to the most severe DBA category "Condition IV - Limiting Faults".

We did not consider disablement of the pressure measurement instrumentation installed at MSH-1 (used for processing of time derivation of MSH pressure).

### 5.2 Initial conditions

The pre-transient stabilization is done according to Dukovany NPP 1.unit steady state parameters.

Info about the main controllers and core status:

Operational mode of "ARM-5S" .....	S
Position of the working CR group (No.6) .....	1.75 m
Time in campaign .....	EOL (625 effect.days)
TG-1 controller "TVER" operational mode .....	N
TG-2 controller "TVER" operational mode .....	N
"Pre-optioned" BRU-C .....	BRU-C of TG-2

The main system parameters at the end of stabilization were as follows:

Reactor power .....	1375.00 MW <sub>T</sub>
TG-1 power .....	219.08 MW
TG-2 power .....	220.03 MW
Heat losses in herm.rooms .....	2.43 MW <sub>T</sub>
Reactor flowrate .....	8900.0 kg/s
Coolant temperature in RV lower plenum .....	267.75 °C
Coolant temperature at reactor outlet .....	297.38 °C
Reactor differential temperature .....	29.63 °C
Primary pressure (PRZ vessel top) .....	12.213 MPa
PRZ heaters power .....	180 kW
PRZ level (collaps.from bottom) .....	6.016 m
Continual flow through the PRZ spray system .....	0.12 kg/s
Boric acid concentration .....	0.0 g/kg
SG-1 (single) outlet pressure .....	4.7106 MPa
SG-2 (double) outlet pressure .....	4.7101 MPa
SG-3 (triple) outlet pressure .....	4.7109 MPa
MSH-1 pressure .....	4.4603 MPa
MSH-2 pressure .....	4.4602 MPa
Pressure upstream TG-1 FAV .....	4.312 MPa
Pressure in main FW header .....	6.305 MPa
Difference narrow range level in SG-1 .....	-0.04 cm (≈2.1206m)
Collapsed level across TB/DC of SG-1 .....	1.72/1.74 m
Mixture level above TB/DC of SG-1 .....	2.22/2.20 m
Coolant mass in SG-1 .....	32559.0 kg
SG-1 steam output .....	124.89 kg/s
Continual drainage of SG-1 .....	0.51 kg/s
Working FW pumps .....	FWP-1,2,4,5

### 5.3 Boundary conditions

With respect to the best-estimate character of the analysis, we assumed the operation of all important control and safety system activated during the transient (see also main controllers status in Chap.5.2).

#### Operational systems availability:

- PRZ heaters available
- PRZ spray system available
- RCS make-up/let-down systems available
- 2x2 BRU-C available
- all LPSG signals considered

#### Safety systems availability:

- all SCRAM signals (AZ-1,2,3,4) considered
- all ESFAS signals considered  
(except of high and low hermet.zone pressure)
- all TPSG signals
- other important protections and interlocks
- ECCS availability:
  - 2/3 HPIS
  - 3/4 ACC (2 ACC->DC; 1 ACC->UP)
  - 2/3 LPIS (the trains connected to RV)
- 2/2 PRZ SVs (+ small bypass valve at the pre-heating line)
- 2/2 AFW pumps
- 3/3 SG SVs
- 2/2 BRU-A

We did not assume the loss of off-site power after reactor SCRAM or after turbines trip.

The only conservative assumption was considering the most reactive control rod stuck in its fully withdrawn position and application of conservative power distribution in the core (to compensate the limitations of RELAP5/M3.1 point-kinetics model).

#### 5.4 Timing of main events

Time of occurrence of main events supplemented with explanatory comments are presented below.

<u>Event</u> =====	<u>Time [sec]</u> =====	<u>Comment</u> =====
Start of calculation .....	-500.0	$N_R=100\%$ , EOL
<u>Initiating event</u> .....	0.0	<u>Full double-ended rupture of MSH-1</u>
First LPSG "+75 mm" in SG-1/2/3 ....	2.4/2.2/3.4	Reswitching of main FW control valve (+closing priority)
<u>Closing of TG-1/2 FAV</u> .....	3.6/3.6	From MSH pressure 4.05 and 3.85 MPa (+ 3.5 s delay)
First LPSG "+100 mm" in SG-1/2/3 ...	3.4/3.3/6.0	-> start of closing of FW lines isolat. valves
<u>Reactor SCRAM</u> .....	4.6	From last tripped TG (+1 s delay)
<u>ESFAS signal "MSH Rupture"</u> .....	-	Not actuated
ESFAS signal "Small Break" .....	35.8	PRZ level "-3.2 m" -> <u>HPI initiated</u>
PRZ heaters switch-off (first time) ..	42.0	PRZ level "-3.6 m"
RCP-1/2/3 trip .....	-	
First LPSG "-140 mm" in SG-1/2/3 ...	52./60./-	-> FW lines bypass isol.valve opening -> <u>start of AFV pumps</u>
Start of 2.make-up pump charging ....	80.0	From low PRZ level "-0.4m" + 70 s delay
Make-up pumps switch-off .....	245.0	From "-0.7 m" level in working deaerator
Start of PRZ spraying .....	560.0	From $p_{kO} > 12.64$ MPa
<u>PRZ SV-bypass valve opening</u> .....	1110.0	From $p_{kO} \geq 13.23$ MPa
PRZ vessel fulfilled .....	1375.0	
<u>End of calculation</u> .....	1800.0	

## 5.5 Discussion of system behaviour

At first we will schematically describe the sequence of main processes of the initial phase of the accident:

Rupture of MSH-1:

- > massive steam leak
  - > fast pressure drop in steam line system and SGs
    - > SG level swelling (increase of mixture level and measured narrow range level)
      - > actuation of LPSG signal "+100 mm" at all SGs
        - > start of closing of FW lines isolation valves
    - > closing of TGs FAV from low MSH pressure 4.05/3.85 MPa (at NPP used overpressure 3.95/3.75 MPa)
      - > reactor SCRAM
    - > rapid cool-down of secondary and primary system
      - > PRZ level drop
        - > initiation of ESFAS signal "Small Leak" (start of HPIS)

Full double-ended rupture of MSH-1 leads to massive steam leak (Fig.A-01) and to rapid depressurization of the steam lines system and all SGs (Fig.A-03). The maximum break flow rate is 2330.2 kg/s (at 0.10 s - the 5. time step after transient initiation).

Thanks to the LPSG signal "+100 mm", the FW system does not experience a deeper pressure drop (Fig.A-06) and consequent closing of FW pumps discharge valves (from the low pressure 4.9 (5.0) MPa in the common FW pumps discharge header). That means that for the whole analysed part of the transient we have a high capacity FW source (4 main FW pumps). The FW flow to the SGs (Fig.A-06) is controlled through the FW bypass control valve, the surplus of the main FW pumps capacity is returned back to the FW tanks through the minimal pump bypass trains. If not considering any operator intervention, the main FW pumps would be switched off from the "Low FW Tank Level 0.5 m" signal (after exhausting the initial FW tank, condenser, and demi-water tank inventory). Then, after FW system pressure decrease, the AFW pumps would be able to push through (the AFW pumps shut-off head is 5.46 MPa) and make use of the rest of FW tanks water (in our transient the AFW pumps are started at 60.0 s, but actually they are not able to supply any water to FW header due to high pressure in FW system).

The course of MSH pressure time derivation (separately measured and evaluated in both MSH half-collectors, Fig.A-04) do not fulfill the "requirement" of the ESFAS signal "MSH Rupture" actuation logic (pressure trend:  $dp/dt \leq -0.054$  MPa/s for 5 sec + one must consider as well the time about 5.5 s for resetting of derivator to the required zone). The main reasons for the failure of forming of this ESFAS

signal are the position of steam sink (MSH-1) and steam sources (SGs), big pressure difference at the SG-MSH steam lines (especially at the flow measurement orifices), and the pressure impulses after closing of TG FAVs.

The fast and continuous depressurization of SGs is connected with fast cool-down of secondary and primary system (Fig.A-07). When comparing the reached RCS temperature change trends with the operational limits (RCS cool-down limit is  $30^{\circ}\text{C/hr} = 0.5^{\circ}\text{C/min}$ ), we can see that the limits are at the transient beginning exceeded 135.6x (at 23.s), and after 5 min of the transient the permitted limit is still exceeded 15.9x.

The cool-down of RCS is connected with a "contraction" of primary coolant and decrease of PRZ level and primary pressure. The working make-up system and PRZ heaters are not capable to stop this trend. Thus at 35.8 sec, the PRZ level drops to "-3.2 m" set-point and the ESFAS signal "Small Leak" is formed. The main action of this ESFAS signal is the start of HPIS injection (at 52.0 s) which in some time turns back the negative RCS liquid voluminal balance and PRZ level drop.

Increase of PRZ level starts at 112.0 s (the delay behind the HPIS injection start is a result of temporary domination of cool-down RCS inventory contraction above the HPI volumetric inflow). The increase of PRZ level above "-3.6 m" set-point enable restart of PRZ heaters (at 305.0 s). Make-up system injection is interrupted at 245.0 s, not because of high PRZ level, but due to signal "Low Level -0.7 m" in the working deaerator (source of the make-up water). As the PRZ steam bubble is compressed, the primary pressure increases, which results in PRZ heaters switch off at 540.0 s and opening of the first PRZ spray system valve at 560.0 s. The PRZ spraying is for several hundred seconds able to keep the primary pressure in a quasi-stable course. However, as the increase of PRZ level reduces the steam volume above PRZ level, the spraying becomes less and less effective. As soon as the spray jets are covered by the PRZ level, a sudden pressure increase occurs (at 1090.0 s). This leads in short time to opening of small bypass valve of PRZ SVs (the pre-heating line valve with nominal steam capacity 5 t/hr) at 1110.0 s. At 1375.0 s the PRZ vessel is full of water and the outflow through the "SV-bypass valve" changes from vapor to liquid critical flow.

(The short-time pressure blip-down about the time of PRZ vessel fulfilling is a result of R5/M3.1 problems with vertical stratification in the PRZ top control volumes. Fortunately, at this time of the transient this temporal pressure fall does not activate any safety system signal.)

At the end of the analysed interval (30 min without operator intervention), we can summarize following characteristics of the system:

- reactor deeply subcritical (-19.6 % ; thanks to HPI)
- RCPs still in operation (LP flow = 10919.0 kg/s)
- PRZ vessel full of water
- HPIS injection is in a voluminal balance with PRZ SV-bypass valve outflow
- primary temperature close to the SG sec.side temperature, i.e. slightly above  $100^{\circ}\text{C}$

- PRZ "barbotage" tank will probably soon ventilate primary coolant to the hermetic zone  
(barbotage tank capacity is 2200 kg of steam per hour, maximum pressure 1.41 MPa)
- SGs and steam lines fully depressurized
- SGs narrow range level close to "-50 mm" value  
(according to start-up/shut-down FW controller setting)
- all initially working FW pumps still in operation  
(4 pumps, partially working to the min.bypass lines)
- FW tanks still not empty thanks to demi-water supply
- one AFW pumps operating to the minimal bypass line  
(too high pressure in the FW header)

### 5.6 Steam generator behaviour

The initial SG outflow peak is maximal for the SG-2, where the maximum mass flow at the measurement orifice (in MSL) before the TG trip was 3.6x higher than the nominal steam flow. The maximal flow from SG-1 and SG-3 were 2.4x and 1.9x higher than the nominal steam output, respectively.

The short-time liquid entrainment from SG-2 and consequent phases stratification in MSL are reflected in table below:

<u>Junction</u>	<u>Location</u>	<u>Max.flow</u>	<u>Time</u>
Jun 284->286	(SG dome) .....	2025.9 kg/s	2.20 s
Jun 277->287	(SG horiz.collector outlet) ...	1231.4 kg/s	2.80 s
Jun 289-01	(MSL, measur.orifice) .....	951.9 kg/s	3.60 s

The reasons why just the SG-2 has the maximal increase of steam outflow are as follows:

- double SG-2 does not share its side of break with any other SG (the opposite side of break is shared by single SG-1 and triple SG-3),
- steam lines of SG-2 (YB-11,13) lead directly to TG-1, so before the TG FAV closing the steam from SG-2 goes partly to TG-1, partly to the break.

As for the tracking of the approximate mixture level, the maximal increase of the mixture level (in SG-2 above TB) was about 58 cm. Here one must however consider limitations of our nodalization approach (averaging whole the interphase levels above the TB and the space above the DC), limitations of 1-D code used, and only approximate character of mixture level tracking module.

Maximum liquid void fraction at SG-2 outlet (vol-177) was 6.25 % at 3.0 s of the accident. In Fig.5 we present all main parameters (void fractions, velocities, mass flows, etc.) of SG-2 at the time 2.5 s (the pressure at SG-2 outlet at this time was 4.35 MPa).

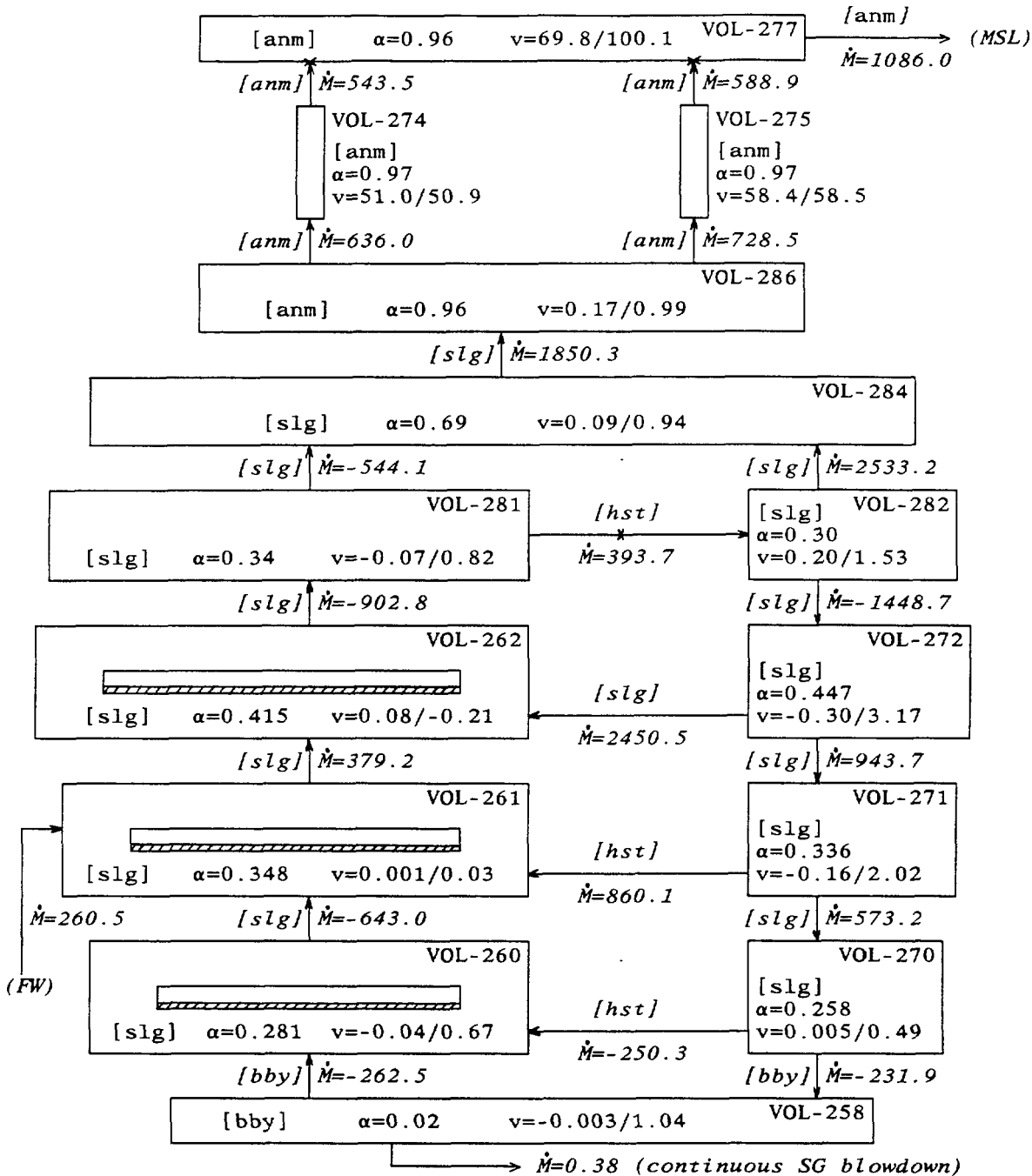


Fig.5 Main parameters of SG-2 at 2.5 sec of the accident  
 (Keep in mind that the SG-2 is a double SG,  
 thus the mass flow rates are 2x higher)

## 6. Conclusions

We will summarize our findings into 3 groups - code oriented findings, the PGV-4 modelling oriented findings, and VVER-440/213 safety oriented conclusions.

### Code (R5/M3.1) oriented findings:

- \* Problem with "horizontal stratification" at SG TB-DC junctions (the junctions between SG tube bundle and downcomer control volumes - deep under real interphase level).  
(same as for R5/M3.0; a deactivation switch in RELAP5 input data would be beneficial)
- \* According to R5/M3 manual the junctions connected to a control volume with vertical stratification (VST) should be also under VST flow regime, but they are not in R5/M3.1 results  
(R5/M2.5 and R5/M3.0 results were O.K.).
- \* Slight flow oscillations in steam lines network in steady-state.  
(same for R5/M3.0 and R5/M2.5; especially by fine-node modelling approach; no evidence of flow regimes oscillation)
- \* Short-time RCS pressure drop at time of PRZ vessel fulfilling.  
(violent transition from vertical stratification to bubbly flow regime in top volume connected with fierce condensation of remaining RCS vapor; pressure course in older R5/M2.5 run was O.K.)
- \* The tracking of approximate mixture level (by help of block of RELAP5 control variables and trips) gives an useful and condensed information about phases distribution in a vertical columns of volumes.
- \* Whereas by usage of R5/M2.5 we did not get any liquid entrainment to the steam lines (in the MSH rupture analysis), the R5/M3.1 shows a short-term entrainment from the most loaded SGs in the beginning of accident.

### SG "PGV-4" modelling issues:

- \* The longitudinal subdivision of SG tubing does not need any sophisticated method, on the other side the number of control volumes strongly influence effectiveness of the heat transfer simulation.
- \* With our relatively simple nodalization of SG secondary side we reached satisfactory agreement with reference data for the steady state operation.
- \* To get a more trustworthy SG secondary interphase level profile - both in steady state and during a transient - one would have to use much more finer nodalization (together with a 3-D code if possible).
- \* For the usual multi-node modelling of SG secondary side we proposed a formula for evaluation of average weighted recirculation ratio.

- \* Often mistake in interpretation of nominal SG pressure 4.61 MPa - this is usually the measured, excessive pressure (the absolute pressure is then  $4.61 + 0.1 = 4.71$  MPa). Similar mistake is sometimes done by interpretation of RCS and MSS pressure set-point, etc.

VVER-440/213 safety issues:

- \* The initiation scheme of ESFAS signal "MSH Rupture" is strongly **unreliable**, what lead in case of MSH rupture accident to following unfavorable phenomena:
  - \* extremely rapid cool-down of both secondary and prim.systems (exceeding by 2 orders of magnitude the permitted operational cool-down trends)
  - \* big loss of secondary coolant (necessary operator intervention)
  - \* potential risk of reaching the secondary criticality (especially in case of failure of HPIS, core at EOL, and incomplete SCRAM - without the most efficient control rod)
  - \* probable evolution to primary LOCA (after fulfilling of PRZ vessel and exceeding of capacity of "barbotage" tank)
- \* As for the initial liquid entrainment from SGs to the steam lines, the results show a short-time entrainment from SG-1 and mainly from SG-2, which are the SGs connected to the broken half of MSH.
- \* The RCS cool-down connected with temporary decrease of PRZ level and pressure do not lead to problems with **heat transfer from core to steam generators**. (the RCPs remain in operation, but there is enough water to remove the core decay heat as well by natural circulation without RCPs)
- \* Thanks to the LPSG intervention the **main FW pumps continue in feed water supply** to the SGs. (if the pressure in common FW pumps discharge header fell under 5.0 MPa, the FW pumps discharge valves would be closed)

## Nomenclature

ACC	accumulator
AFW	auxiliary feedwater
ANSI	American National Standards Institute
ARM	reactor power controller (VVER-440)
ATWS	Anticipated Transient without SCRAM
AZ	reactor trip
BBY	bubbly flow regime (RELAP5)
BRU-A	steam dump to atmosphere
BRU-C	steam dump to condenser
CHF	critical heat flux
CPU	Central Processing Unit
D	dimension; diameter
DBA	Design Basis Accident
DC	downcomer
dP	differential pressure
ECCS	Emergency Core Cooling System
EOL	end of life
ESFAS	Engineered Safety Features Actuation System
FAV	fast acting valve
FW	feedwater
FVP	feedwater pump
HPI	high pressure injection
HPIS	High Pressure Injection System
HST	horizontal stratification flow regime (RELAP5)
IAEA	International Atomic Energy Agency
ISP	International Standard Problem
L	level; length
LP	lower plenum
LPIS	Low Pressure Injection System
LPSG	Local Protection of Steam Generator (VVER-440/213)
$\dot{M}$	mass flowrate
MPR	mist pre-CHF flow regime (RELAP5)
MSH	main steam header
MSL	main steam line
MSS	Main Steam System
NPP	nuclear power plant
NRI	Nuclear Research Institute
NUREG	Nuclear Utility Regulation
p	pressure
PGV	steam generator type (VVER)
PRZ	pressurizer
PSA	Probabilistic Safety Assessment
R5/M2.5	RELAP5/MOD2.5
R5/M3.0	RELAP5/MOD3.0
R5/M3.1	RELAP5/MOD3.1
RCP	reactor coolant pump
RCS	Reactor Coolant System
REC	recirculation
RELAP	Reactor Excursion and Leak Analysis Program
ROM	reactor power limiting control system (VVER-440)
RV	reactor vessel
RY	continual drainage of SGs system
Q	volumetric flow
S	surface; operational regime of ARM controller; valve

SBLOCA	Small Break Loss-of-Coolant Accident
SCRAM	Safety Control Rod Ax Man
SG	steam generator
SLG	slug flow regime (RELAP5)
SV	safety valve
T	temperature
TB	tube bundle
TE	let-down system of RCS
TG	turbine generator
TK	make-up system of RCS
TPSG	Technological Protection of Steam Generator (VVER-440/213)
TVER	turbine controller (VVER-440)
UH	upper head
UP	upper plenum
v	velocity
VOL	control volume
VST	vertical stratification flow regime (RELAP5)
VVER	Water-Cooled Water-Moderated Energetic Reactor
YA	primary loop
YB	steam generator
$\alpha$	vapor void fraction

## References

- [1] Carlson et al: RELAP5/MOD3 Code Manual. Volumes I-V. NUREG/CR-5535. EGG-2596. June 1990.
- [2] Král P.: Proposal on Improvement of VVER-440/213 Dukovany ESFAS/TPSG Signal "MSH Rupture". ÚJV Řež. November 1993.
- [3] Macek J., Krhounková J.: Analysis of ATWS with Feedwater Supply Disturbances. ÚJV Řež. December 1993.
- [4] Idelchik I.E.: Handbook on Hydraulic Losses. Moskva. 1975.
- [5] Titov V.F.: Initial Data for Calculations of Natural Circulation in the Secondary Volumes of PGV-440 and PGV-1000. Gidropress. October 1991.
- [6] Macek J.: PhD Thesis - Mathematical Modelling of Fast Breeder Reactor. Technical University of Prague. 1984.
- [7] Defining Initiating Events for PSA Uses. Draft - Revision 4. IAEA Vienna. January 1992.

## Appendix - A

Results of MSH rupture in VVER-440/213 analysis  
- course of main parameters

Table of figures:

Fig.A-01	Break mass flow
	- immediate total break flow
	- integrated break flow
Fig.A-02	SGs outflow - detail
	- mass flow from SG-1 (YB-15)
	- mass flow from SG-2 (YB-11,13)
	- mass flow from SG-3 (YB-12,14,16)
Fig.A-03	Pressure in MSH and SGs
	- pressure in MSH-1 (broken)
	- pressure in MSH-2 (intact)
	- pressure in SG-1 (YB-15)
	- pressure in SG-3 (YB-12,14,16)
Fig.A-04	Derivations "dp/dt" in MSH
	- dp/dt in MSH-1 (broken)
	- dp/dt in MSH-2 (intact)
Fig.A-05	SG-2 levels
	- narrow range level (shifted middle diff.level)
	- DC collapsed level
	- mixture level above TB (approximate)
Fig.A-06	FW system flows and pressure
	- FW flow to SG-1
	- FW flow to SG-2
	- FW flow to SG-3
	- FW header pressure
Fig.A-07	System cool-down trend
	- SG-1 secondary side bottom dT/dt
	- reactor DC dT/dt
Fig.A-08	Temperature in RCS and MSS
	- maximal cladding temperature
	- average RCS temperature
	- RCS saturation temperature (UP)
	- SG-1 secondary side liquid temperature
Fig.A-09	PRZ pressure and level
	- PRZ pressure
	- PRZ collapsed level (from the PRZ vessel bottom)
Fig.A-10	Mass flowrates at RCS boundary
	- make-up system (TK) flowrate
	- let-down system (TE) flowrate
	- injection from HPIS (2 trains)
	- PRZ SV-bypass valve outflow
Fig.A-11	Reactor power and reactivity
	- total core power
	- reactivity
Fig.A-12	Reactivity contributions
	- control rods contribution
	- boric acid feedback
	- moderator density and moder.and fuel temp.contribution
	- total reactivity

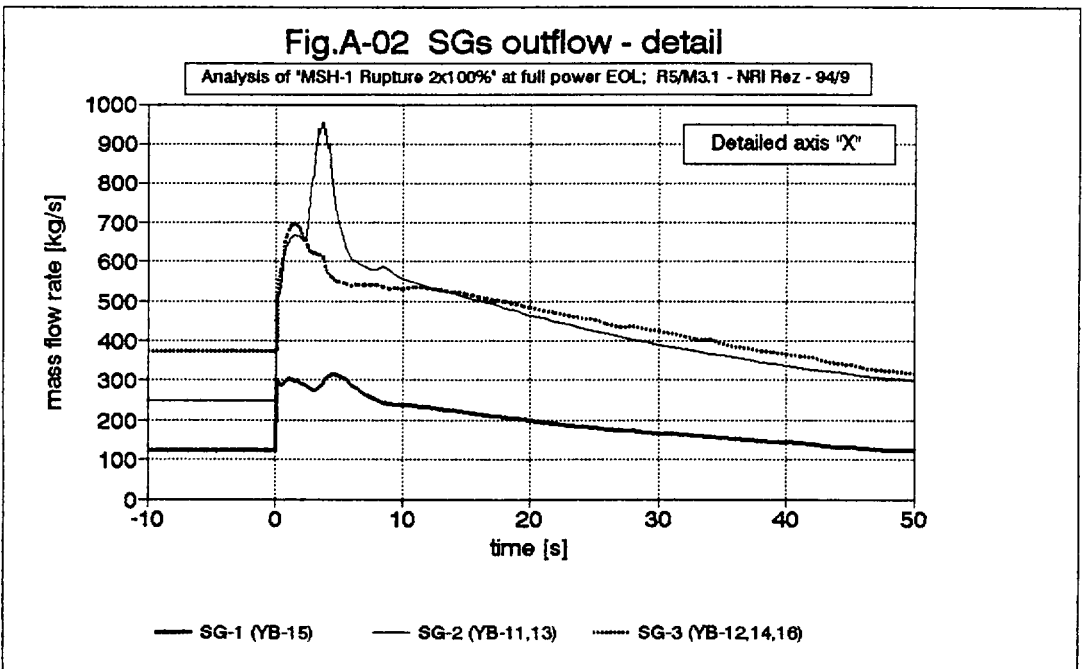
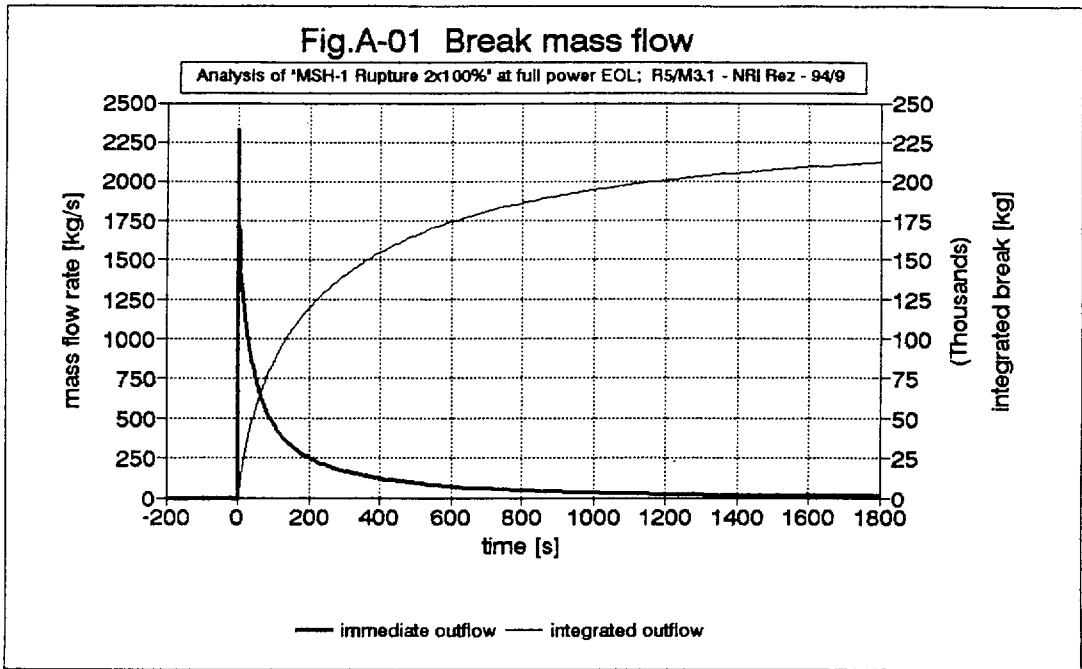


Fig.A-03 Pressure in MSH and SGs

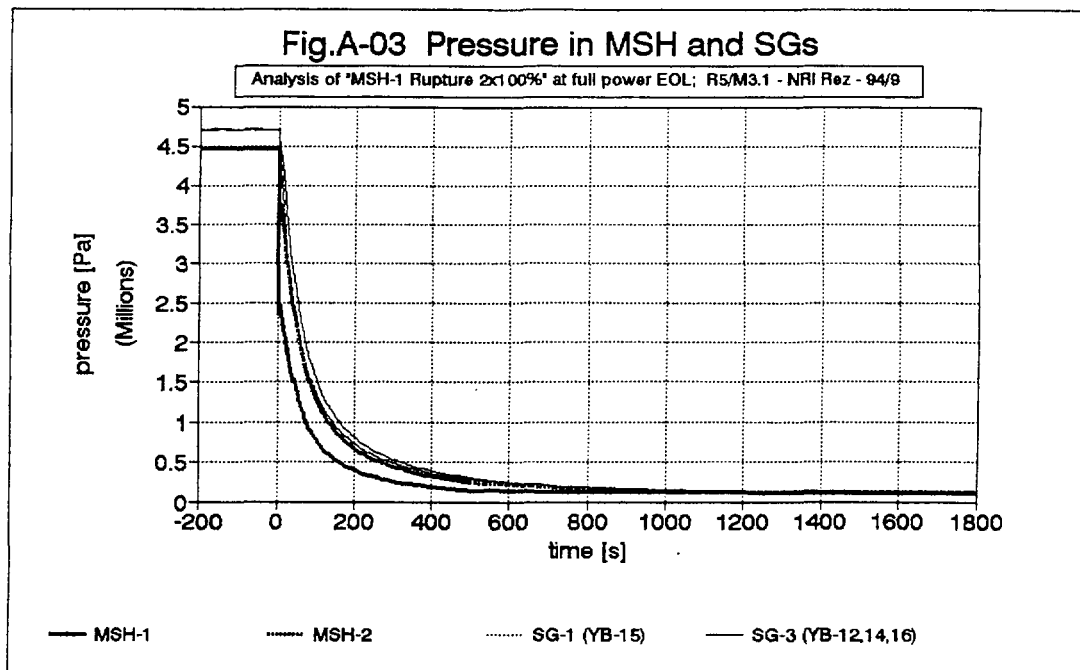


Fig.A-04 Derivations "dp/dt" in MSH

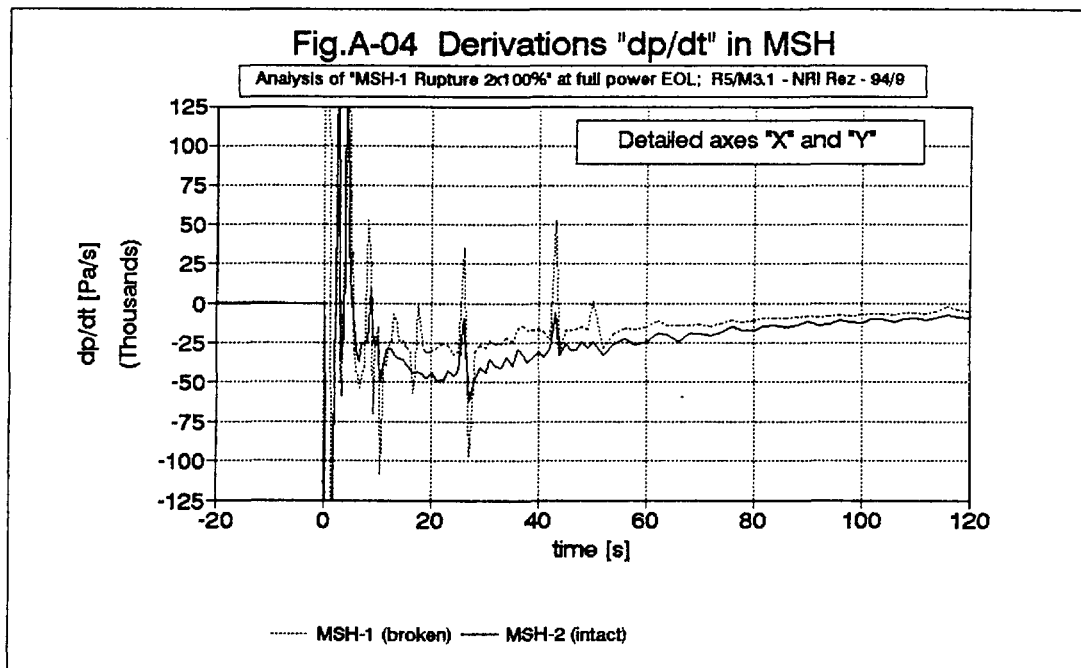


Fig.A-05 SG-2 levels

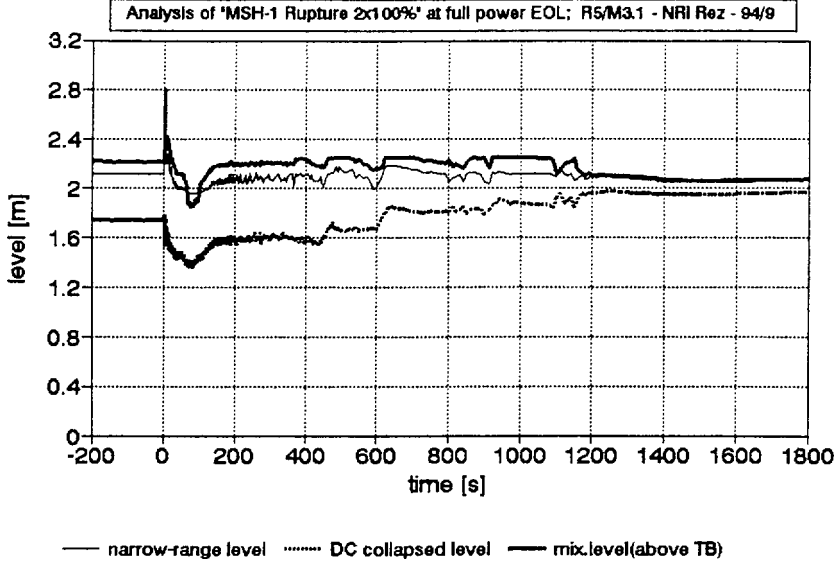
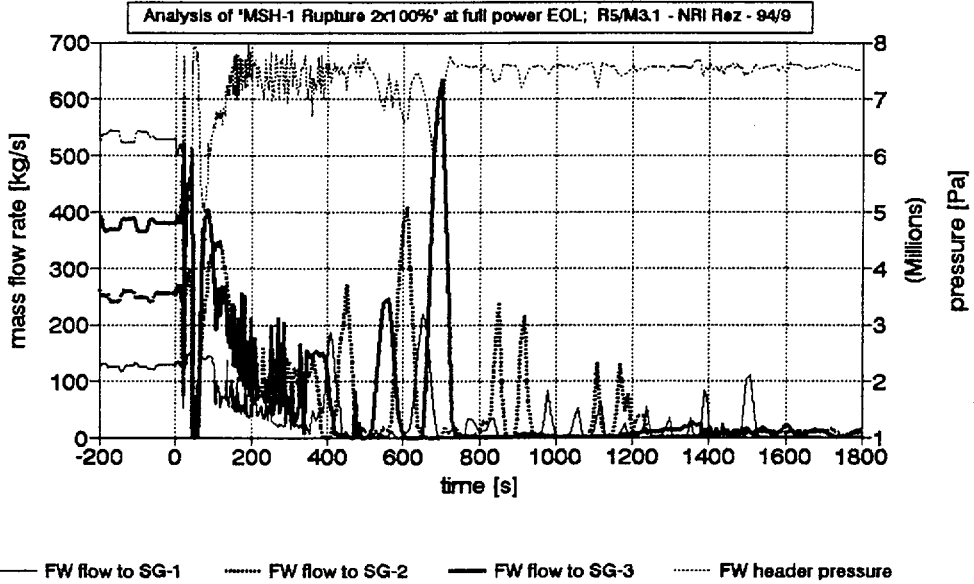
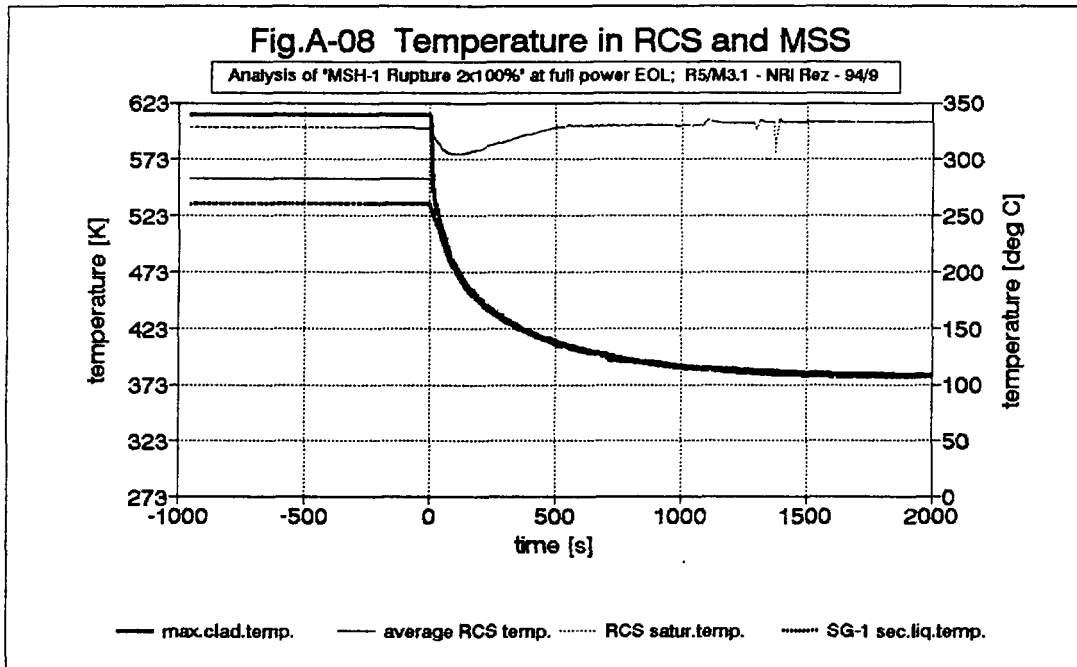
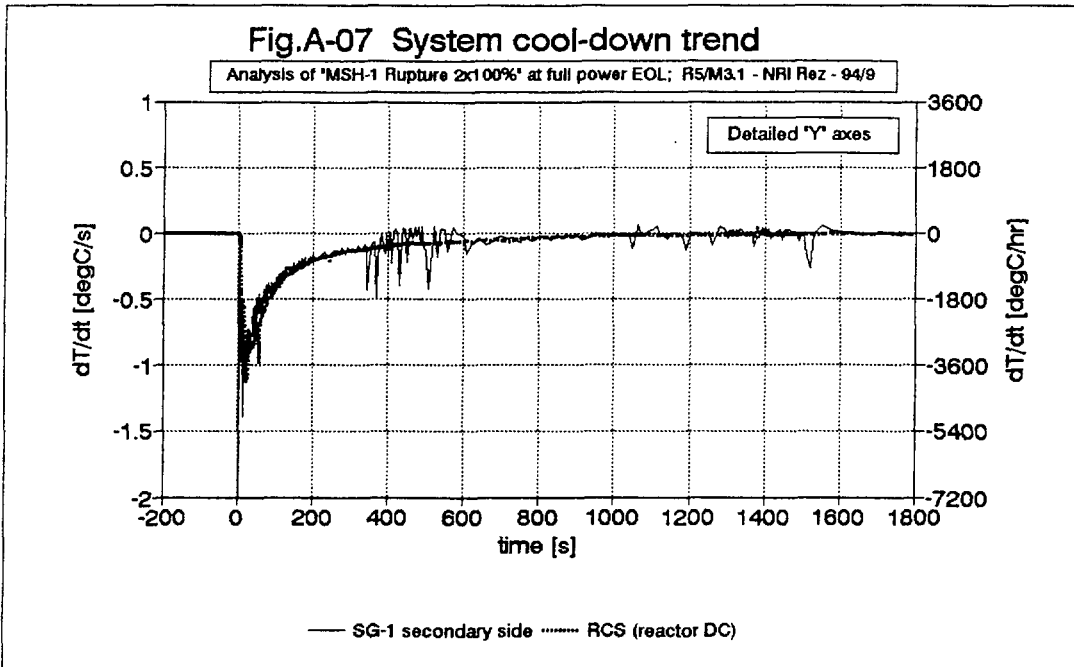
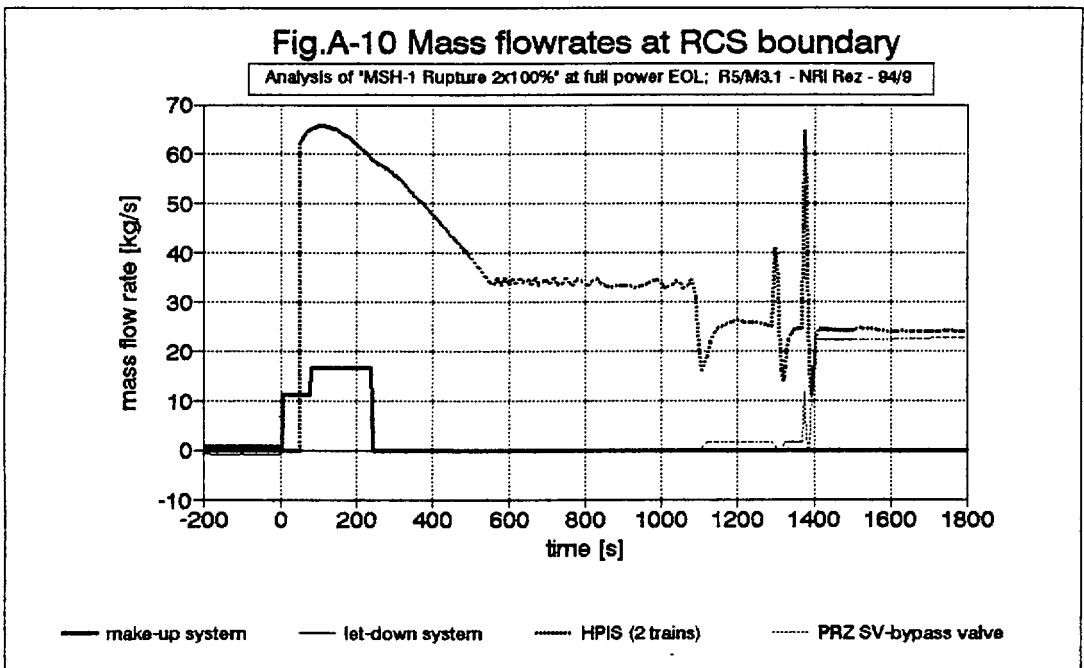
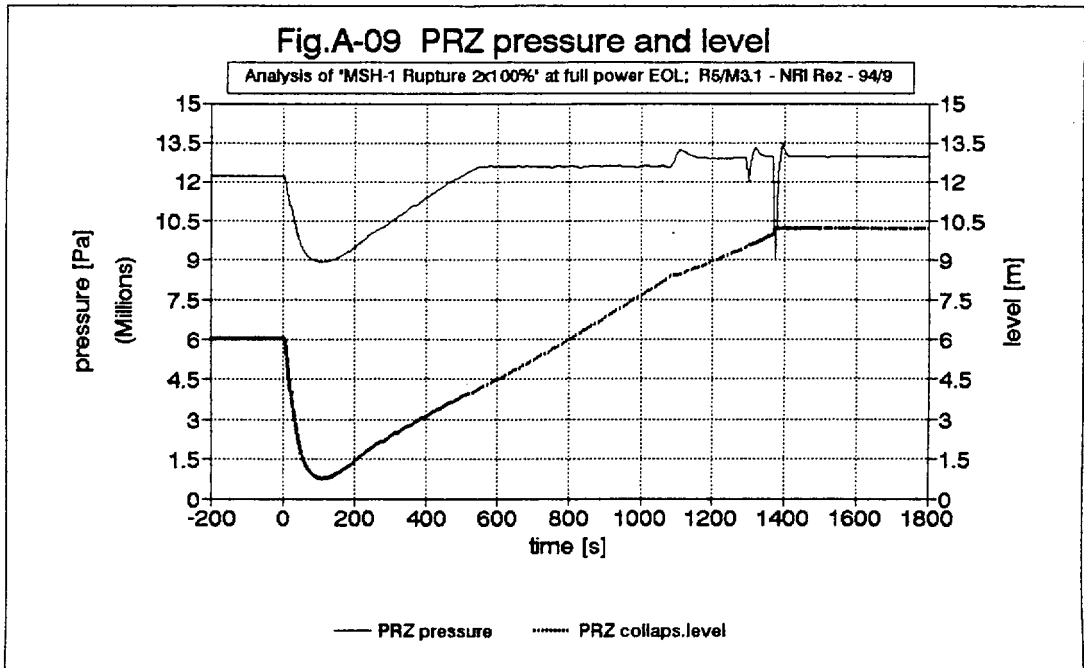


Fig.A-06 FW system flows and pressure







**Fig.A-11 Reactor power and reactivity**

Analysis of 'MSH-1 Rupture 2x100%' at full power EOL; R5/M3.1 - NRI Rez - 94/9

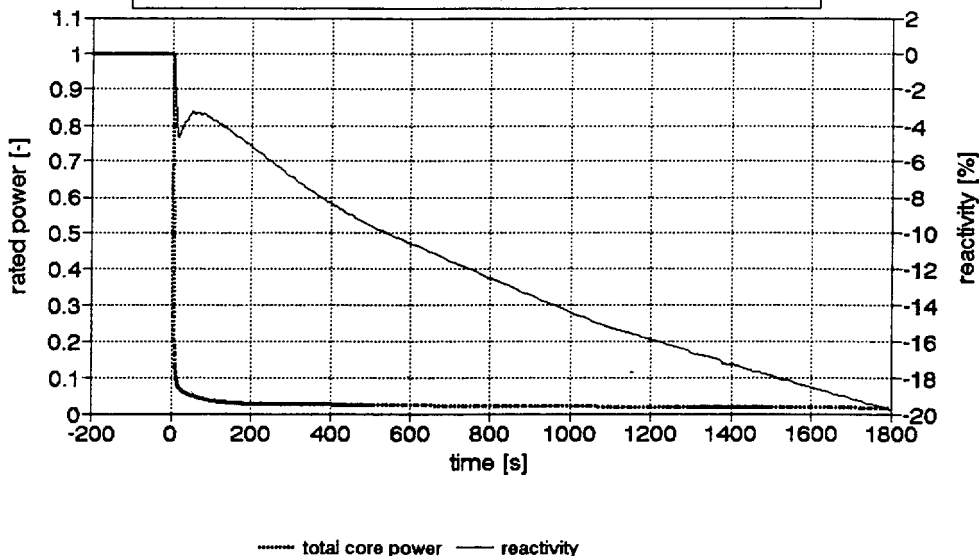
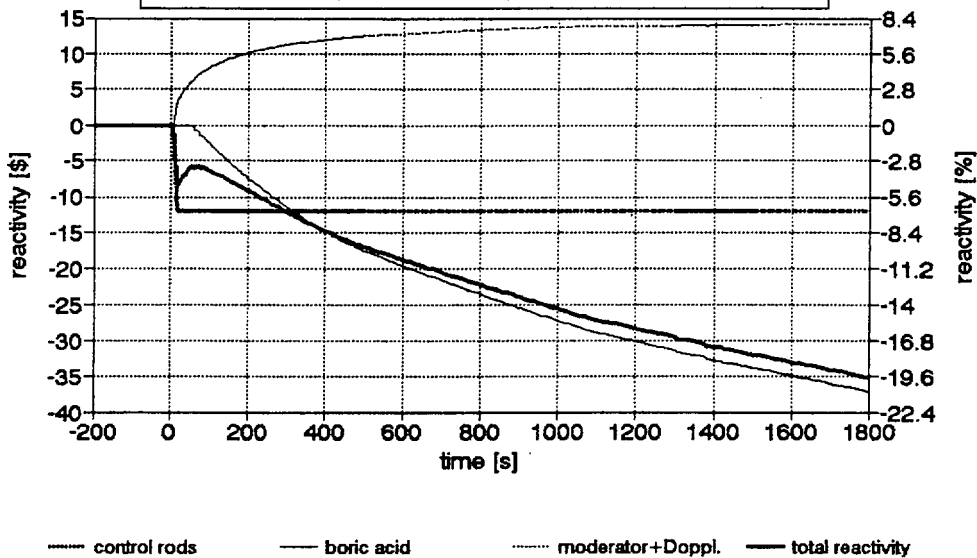


**Fig.A-12 Reactivity contributions**

Analysis of 'MSH-1 Rupture 2x100%' at full power EOL; R5/M3.1 - NRI Rez - 94/9



EDO Hidropress, Rovno NPP, NPP Paks

STUDY OF THERMOHYDRAULIC CHARACTERISTICS OF UPGRADED FEEDWATER  
COLLECTOR IN PGV-440 STEAM GENERATOR

G.A.Tarankov, N.B Trunov., V.F.Titov , V.V.Urbansky,  
I.Lenkei, M.Notarosh

ABSTRACT

Reconstruction of feedwater distribution collector was performed at unit 1 of Rovno NPP. Main results of measurements of temperatures in water volume, separation characteristics and impurities distribution are presented. Analysis of tests results and design criteria is given.

International seminar on horizontal  
steam generators  
Lappeenranta, Finland, 18-20 October  
1994.

## Introduction

At a number of power units with VVER-440 corrosion damages were revealed in feedwater distribution collectors made of carbon steel. Radical solution of the given problem is replacement of the mentioned collectors for the new ones made of stainless steel and placed above SG tube bundle.

The new system of feedwater distribution represents itself pipelines of stainless steel comprising T-piece, bend, laterals, tubes and distributing tubes with nozzles. Design of the feedwater distribution unit is shown in Fig 1.

Distributing tube is placed above the heat exchanging bundle along the corridor of hot side of tube bundle and comprises tube and nozzles for water outlet. On the collector there are more nozzles from the "hot" side of SG, than on "cold" side. All nozzles on "cold" side and part of nozzles on "hot" side are directed to the side of SG vessel (small bank). Number of nozzles on both sides is decreased as reaching the collector end.

All components of feedwater distribution unit are made of stainless steel.

Feedwater collectors replacement was performed at first time at power unit I of Rovno NPP. For substantiation of serviceability SG was equipped with the system of measurements comprises 23 thermocouples, 8 samplers 4 vibroaccelerometers. The given system gives opportunity to measure temperature distribution in water volume near coolant headers and SG vessel, vibration of the collector, steam humidity by salt method and distribution of dissolved impurities. Arrangement of measurement accessories is shown in Fig 1. Tests were performed after planned shutdown in 1994.

#### 1. Features of moisture separation in PGV-4

Structural features of PGV-4 define an ingress of main amount of moisture in steam line through central steam nozzle the most closely located to hot collector that is confirmed by measurement data.

In the region of hot collector there takes place the more highest position of trace from level on the SG wall.

On Fig 2 level trace on SG vessel at Bohunice and Novovoronezh NPP is shown for example. The level trace on the

hot collector (Fig. 3) permits to see that the height of level is significantly higher by the wall above small hot package rather than the large one. This effect may be related with intensive egress of steam through downcomers between packages in the region of hot collector. Water may not be drained into hot channels and is induced to move into the cold side, overcoming steam resistance outflowing from the tubes packages. In this case water issued from small hot package suffers the greatest resistance along its further way. Thus, this vicinity is a critical one from the point of view of level as soon as it is packed due to narrowing of SG vessel from one side and due to intensive outflow of steam-water mixture from the large hot package and channel between packages from other side. Besides, in this region there is a lower edge of louvers which may be subjected to flooding.

Measurements of collapsed level in the end of 4SG-2 of Kola NPP at nominal load have confirmed actual overrating the level above tubes when estimating its height by readings of standard level gauge (with pressure tap on SG bottom). When level gauge indication was 110 mm above the upper row of tubes the sampler of level indicator turned out flooded it was located at 163 mm elevation above tubes.

In relation with leakiness in the region of penetration of collector through plane sheet - the item of separator (annular slot about 1 mm) a significant part of moisture may penetrate through this leakiness together with steam, so in case of level "150 mm above tubes" - by readings of level gauge the moisture in steam line in some SGs already exceeds 0,1% partly penetrating apart from louvers.

## 2. Design principles of the new collector.

During the process of new collector development the aim of copying of the old design was not stated. Design decisions were developed on the basis of experience of similar reconstruction at steam generator PGV-1000. Meanwhile the additional tasks on improvement of SG reliability were specified.

Besides the solution of the problem related to damages of feedwater collectors the given design allows to reduce level swelling in the zone of maximum steam load. Level swelling is reduced due to feedwater supply to the region of small hot bank of tube bundle which, by the data of study of void fraction in

water volume of PGV-440, is critical from the viewpoint of separation. It was important to choose optimal position of feedwater collector upon the SG vessel and coolant headers to overpass the thermocyclic load caused by subcooled feedwater. Although the data obtained during the commercial tests were used.

During replacement of collectors a problem was being solved concerning provision of distribution of salts content in SG in such a way that in the zone of tubing with maximum steam load (hot end) the content of salts will be the least possible. Blowdown bleeding in this case shall take place from the zone with maximum content of salts. The above-mentioned measures allow to improve operational reliability of SG from the viewpoint of corrosion and to extend the inter-washing period.

### 3. Results of measurements of steam moisture

For comparison of separation characteristics of steam space in Fig 3 there is shown an arrangement of samplers in steam volume on the investigated SG as well as on 3SG-1 of Novovoronezh NPP and YB-54 NPP Loviisa. Besides, a position of trace of level swell by the results of measurements of level trace on the vessel and on the SG collector at Bohunice NPP was shown in these Figures also. All the samplers are located practically at the same height, but some of them are differed by arrangement in SG cross-section. The sampler No7 1SG-6 of Rovno NPP is located symmetric about the sampler No6 3SG-1 of Novovoronezh NPP. The sampler No6 of 1SG-6 of Rovno NPP approximately corresponds to the sampler No2 of YB-54 of Loviisa NPP, unit 1.

Comparative separation characteristics of steam volume are presented in Fig. 4. All the data are presented relative to the level above tubes.

It is seen from the graph that characteristics of the reference samplers No7 of 1SG-6 of Rovno NPP and No6 of 3SG-1 of Novovoronezh NPP are almost equal. Characteristics of the reference samplers of No6 of 1SG-6 of Rovno NPP and No2 of YB-54 of Loviisa NPP, unit 1 are differed markedly. Increase of moisture in the sampler No6 begins at the level of about by 70 mm higher than in the sampler No2. And this fact apparently testifies to improvement of the profile of swell level subsequent to replacement of feedwater collector. That is to

say supply of significant amount of feed water into the region of hot package permitted to equalize the swell level near by the hot collector that decreases a probability of underflooding the lower edge of louvers. In fact the samplers No6,7 of 1SG-6 of Rovno NPP give practically similar values of moisture. At the same time the sampler No8 gives moisture significantly smaller that corresponds to estimation about the profile of swell level.

Dependence of steam moisture on a number of different SG on water level above tubes at nominal load are presented in Fig.5. It follows from the comparison that there no reasons to consider that reconstruction of feedwater collector markedly affected the value of steam moisture in steam line. The value of limiting level (which is determined by steam moisture 0,25%) for the majority of these SGs is approximately the same except for 2SG-6 of Kola NPP where it is significantly lower. Possibility of such impaired characteristics can not be excluded and for other SGs. It is to be noted that during tests of six SGs at Loviisa NPP the characteristic of YB-54 was approximately average.

#### 4. Results of study of distribution of impurities in water volume of SG.

Results of measurement of  $\text{Na}^+$  concentration are shown on the graph of Fig.6. Sodium concentrations are presented in relative values, i.e. in relation to concentration in water of continuous blowdown.

It is seen from the presented data that distribution of  $\text{Na}^+$  ions corresponds to design backgrounds, i.e.  $\text{Na}^+$  concentration in the continuous blowdown water significantly exceeds the concentration in other points of water volume. Proceedings from experience of studies on PGV-1000 the  $\text{Na}^+$  concentration is more significant from the point of view of assessment of distribution of the dissolved impurities. Let us note that  $\text{Na}^+$  concentrations at points 2,3 located near the point of sampling of continuous blowdown, but by 1200 mm above, don't exceed concentration in blowdown that testifies about inexpediency of blowdown sampling over height of water volume.

On the basis of data on distribution of  $\text{Na}^+$  one can assess the efficiency of SG blowdown, i.e. relation of impurity concentration in blowdown to average concentration of

impurities in SG. Average concentration of impurities in SG may be obtained by integrating the curve on the graph that gives efficiency of blowdown about 1,6-1,7. Unfortunately, the data on distribution of impurities in water volume before SC reconstruction are too limited that doesn't permit to perform a comparison.

Significant variation in distribution of other water chemistry parameters was not discovered.

## 5. Results of temperature measurements

Temperature measurements in water volume were performed under static and transient conditions.

Analysis of data obtained at different power levels corroborates that heating up of feedwater is finished approximately in the area of tubes of the small hot bank at SG vessel. Under static conditions pulsations are recorded by thermocouples mounted on the tubes being close to nozzles (T6,T9,T12) and on the tubes being in the middle of the tube bundle (T5,T8,T11). If we consider nominal power conditions with HPH disconnected, average values of temperatures for thermocouples T5,T8,T11 amounted to 255,7;253,3;254,6°C, respectively, that is heating up in this area has not been finished yet. We shall note that close values of these temperatures indirectly corroborate optimality of feedwater distribution (proportionally to local steam load). At the same time pulsations are weak for thermocouples T4,T7,T10 and average temperature practically is equal to  $T_s$ . The same pattern is typical for all static conditions with partial and nominal power. Maximum amplitude of pulsation was recorded by thermocouple T6 at 55% power and was equal to 37°C. At 100% power with HPH connected on the tubes near the vessel the following maximum amplitudes of pulsations were recorded: T4=5,1°C, T7=5,5°C, T10=3,1°C.

The obtained data may be compared with the results of temperature measurements of water volume obtained at Novovoronezh NPP and Kola NPP where thermocouples were mounted opposite the distribution nozzles over the width of intertube corridor in different cross-sections. It is expedient to perform comparison by the value of relative subcooling.

$$T_{rel} = (T_s - T_i) / (T_s - T_{fw})$$

where  $T_s$  - saturation temperature;

$T_i$  - thermocouple reading at this point;

$T_{fw}$  - feedwater temperature.

As per data obtained at Novovoronezh NPP average subcooling in the middle of the corridor in the different cross-sections amounted to 0 - 0,3, at the end of the corridor from 0 to 0,2. As per data of Kola NPP this value in the middle of the corridor was equal to 0-0,5 and at the end of the corridor - from 0 to 0,4. We can see that maximum values of subcooling (peak) obtained at 1SG-6 of Rovno NPP are considerably lower: up to 0,2 in the middle of the corridor and up to 0,13 at the end of the corridor. So we may consider that for the new design of collector the feedwater heating up occurs with the rate which is not less than for the collector of the old design. Under transient conditions no sufficient increase of pulsations amplitude was noticed. Temperature around coolant headers was stable under all studied conditions.

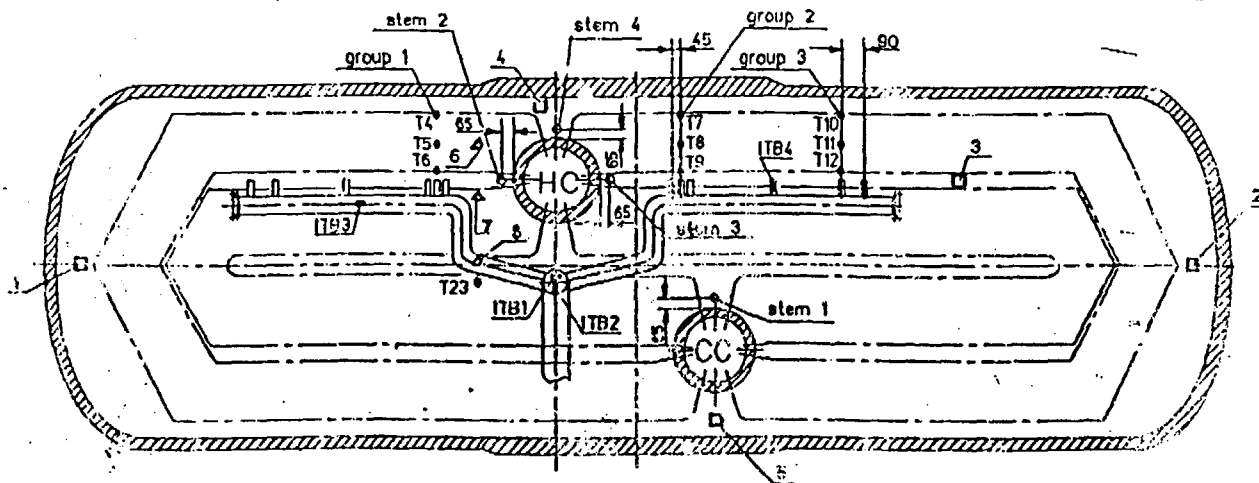
#### 6. Results of measurements of vibrations

Measurements shows low level of vibrations of feedwater collector under static and transient conditions and doesn't depend upon the power level. Resonance behavior was not noticed. The given results showed weak dependance of vibration upon the hydrodynamic processes in SG.

#### Conclusion

Analyses of measurement results showed absence of phenomena in SG not considered in design. Obtained values of the temperature pulsations not exceed values recorded in steam generators WWER-440 in operation and level of vibroacceleration not exceed the check value. Design value of generated steam moisture is provided. The place of continuous blowdown tap selected in SG design is an optimal one for the SG with the reconstructed feedwater collector.

Diagram of arrangement of measuring accessories on ISG-6 Rovno NPP



group 1 - T4, T5, T6  
 group 2 - T7, T8, T9  
 group 3 - T10, T11, T12

stem 1 T1 0 mm  
 T2 -500 mm  
 T3 -1000 mm  
 T22 (bottom)

stem 3 T16 0 mm  
 T17 -500 mm  
 T18 -1000 mm

□ - sampler water (-800 mm)  
 Δ - sampler steam (+720 mm)  
 • - thermocouple  
 ■ - accelerometer  
 ○ - stem

T23 4000 mm

stem 2 T13 0 mm  
 T14 -500 mm  
 T15 -1000 mm

stem 4 T19 0 mm  
 T20 -500 mm  
 T21 -1000 mm

Elevations of level trace on the developed view of steam generator vessel

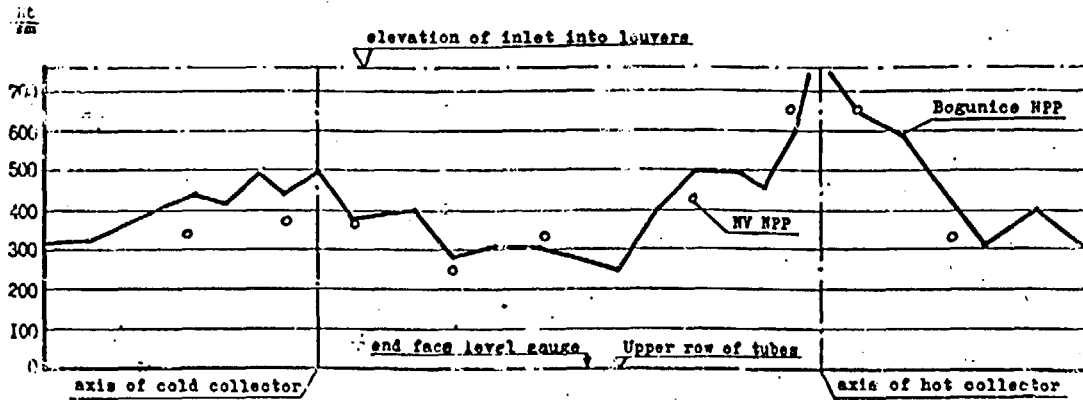


Fig. 2

Arrangement of steam samplers in SG steam space. Location of level trace in SG at Bohunice NPP

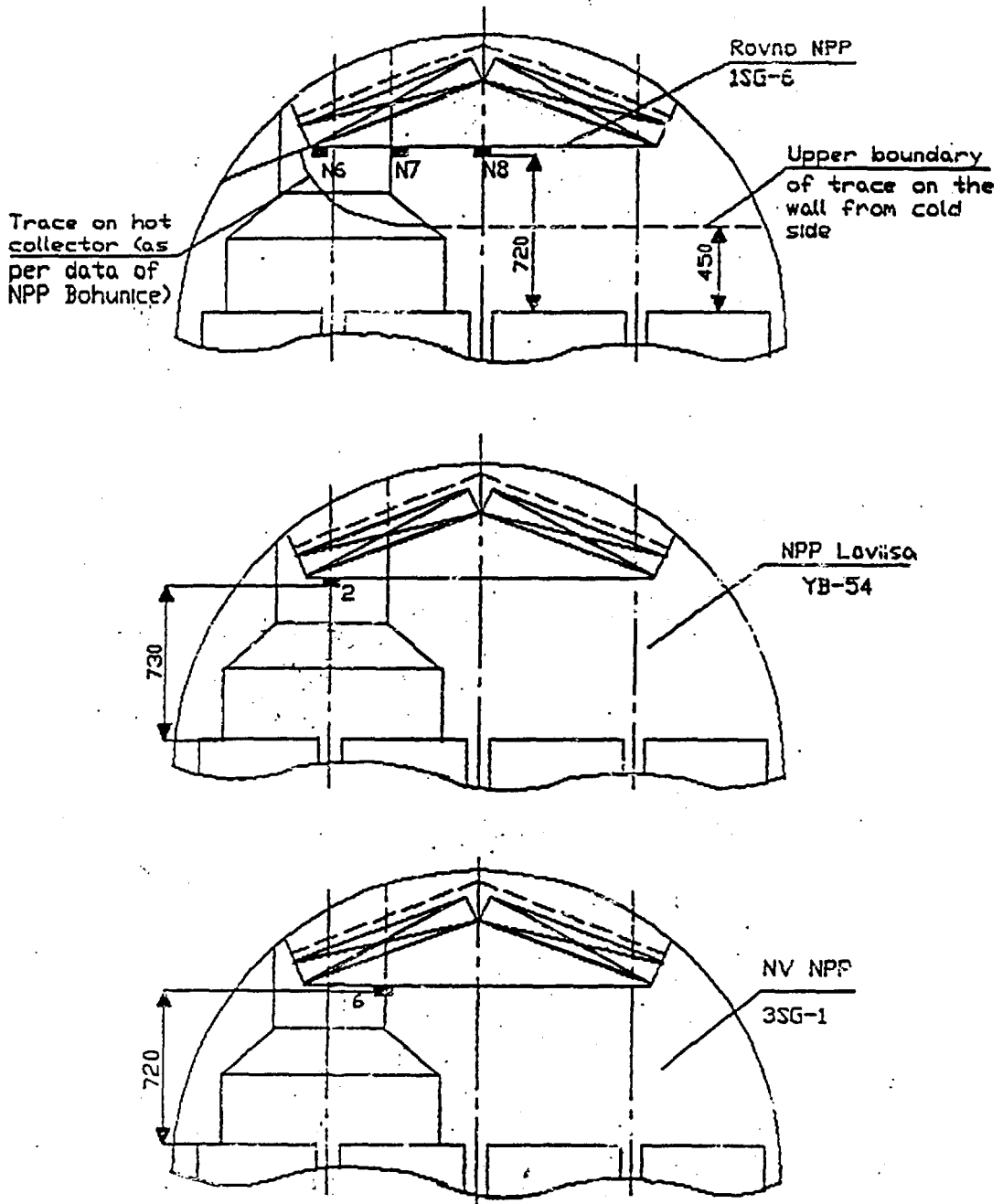


Fig.3



## Comparison of separation characteristics in PGV-4

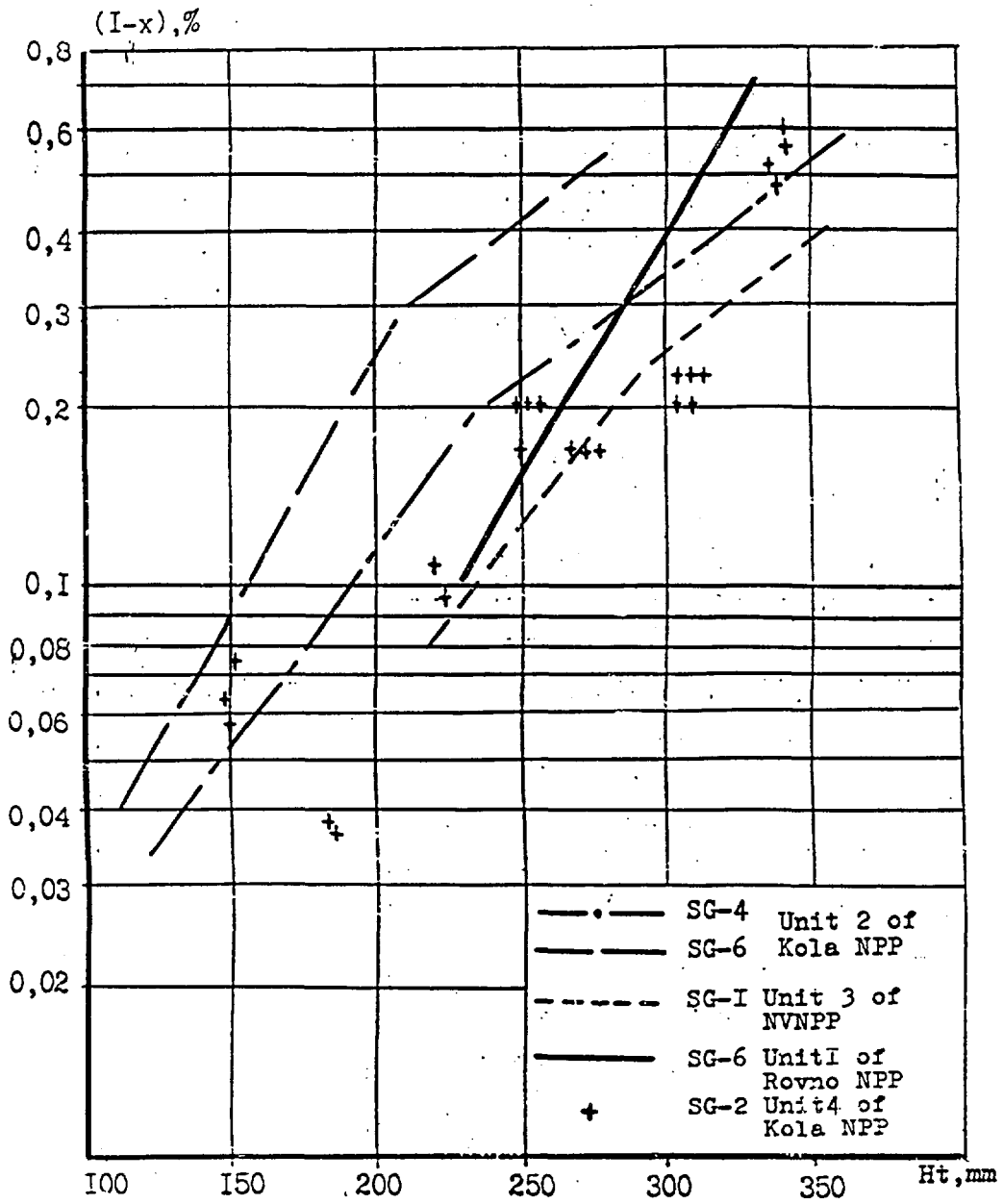


Fig.5

Relative Na<sup>+</sup> content in SG volume

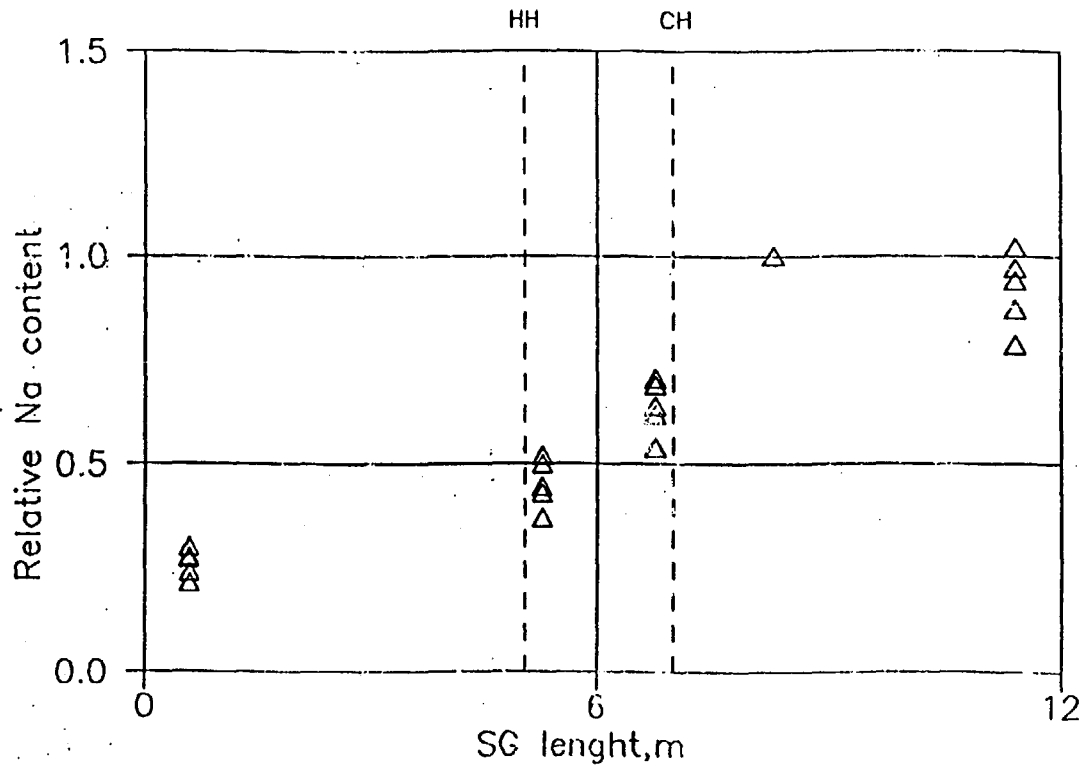


Fig.6

# ADVANCED FEED WATER DISTRIBUTING SYSTEM FOR WWER 440 STEAM GENERATORS

---

Oldřich MATAL <sup>a</sup>, Karel GRATZL <sup>b</sup>, Jozef KLINGA <sup>a</sup>, Jozef TISCHLER <sup>c</sup>, Milan MIHÁLIK <sup>c</sup>

a - Energovýzkum Ltd., Brno, Czech Republic

b - Vítkovice s.c., Ostrava, Czech Republic

c - SEP Atomové elektrárne Bohunice, Jaslovské Bohunice, Slovak Republic

Prepared for "Third International Seminar on Horizontal Steam Generators, 18 - 20 October 1994, Lappeenranta, Finland

## Abstract:

The original designed feed water distributing system was replaced by an advanced one. The characteristics of both feed water distributing systems have been measured and evaluated.

The paper deals with a program of measurement and evaluation of both feed water distributing system characteristics and comparison of selected data obtained.

## 1. INTRODUCTION

Through wall defects in the feed water distributing system (FWDS) inside steam generators have been reported at many WWER 440 units. In all cases the defects have occurred at the original designed FWDS. This FWDS consists of one feed water pipe connected to a T - piece and horizontal feed water distributing pipe of 159 mm O.D. with total 180 horizontal oriented nozzles, Fig. 1.

The repair of damaged FWDSs can be performed by:

- bushing using special tools, or,
- reconstruction of the FWDS connected with installation of an advanced FWDS.

For the advanced FWDS are typical three structural members:

- two legs of feed water pipe inside the SG,
- connecting pipes,
- mixing chambers.

To demonstrate positive characteristics of the advanced FWDS and compare them with those typical for the original FWDS design an extensive program of measurements have been prepared and applied on steam generators (SG) in SEP - EBO Jaslovské Bohunice.

## PROGRAM OF MEASUREMENTS [ 1 ]

To obtain data for FWDS characteristic comparison and evaluation following groups of parameters have been on-line measured and stored:

- 2.1. Local surface temperatures at SG pressure vessel, nozzles and feed water pipeline outside the SG.
- 2.2. Local temperature of water inside the SG.
- 2.3. Vibrations of SG and FWDS structure.
- 2.4. Emitted wave motion at high frequencies.
- 2.5. Pressure losses in the feed water systems
- 2.6. Dynamic characteristics of the feed water systems.
- 2.7. Sodium and chlorides concentrations in water along the tube bundle (sampling).
- 2.8. Sodium and chlorides concentrations in the blowdown water (sampling).

The schematic hardware diagram of measurements is in Fig. 2.

### 3. SELECTED RESULTS

RMS values of vibrations versus time measured at the steam generator with the Russian original FWDS and at the steam generator with the advanced FWDS are in Fig 3a and Fig 4a, respectively. The corresponding feed water flow rates are shown in Fig 3b and Fig 4b, respectively.

No significant differences in RMS values can be observed at nominal SGs power level for both FWDS solutions.

Selected results on WWER 440 SG vibration were also reported earlier, Ref [2] and [3].

RMS values of acoustic emission signals versus time of both FWDS studied are in Fig 5a and Fig 5b, respectively.

RMS values are of the similar magnitudes at the nominal SG power level for both FWDS solutions.

A positive contribution of connecting pipes design of the advanced FWDS is illustrated in Fig 6b at the local feed water nozzle temperature  $t_2$ , especially in the time feed water is batched in to the SG. The temperature of the SG pressure vessel is  $t_1$ .

### 4. CONCLUSION

The program of measurement and evaluation of the original and advanced feed water distributing system has been carried out since August 1994 in Jaslovské Bohunice.

The installation of the on-line measurement system as well as of the advanced feed water distribution system was performed during the planned outage of the WWER 440 unit.

## REFERENCES

[1] Matal,O., Klinga,J., Šimo,T., Pavlik,I., Holý,F.

Design documentation of measurements at SGs with original and advanced feed water distributing system, Report QR-EM-57-94, Energovýzkum Ltd, Brno, August 1994 (in Czech)

[2] IŠadilek, J., Matal,O.

Some causes of vibrations monitored on steam generators by operational diagnostic system at the 1st and 2nd units of the Dukovany NPP, (in Russian), *Jaderná energie* 35(1989), No3, p.101

[3] Matal,O., et al.:

Characteristics of the WWER 440 steam generator feed water system derived from temperature and vibration measurements, (in Czech), *Jaderná energie* 37(1991), No6, p.208

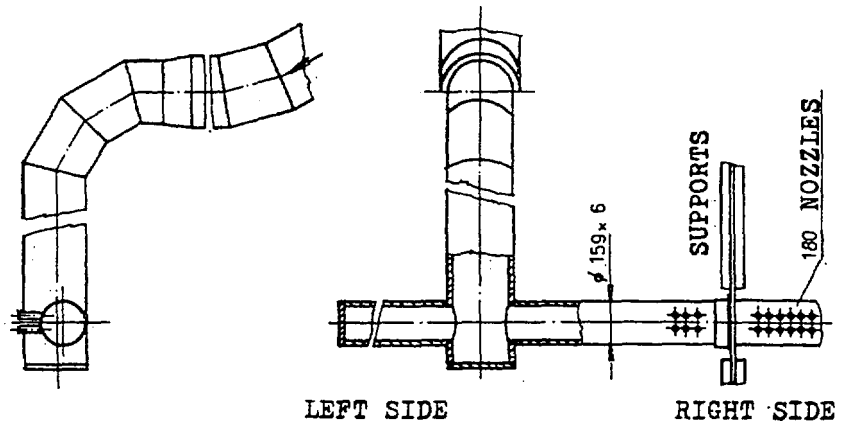


Fig 1: SCHEMATIC DIAGRAM OF THE ORIGINAL FEED WATER DISTRIBUTING SYSTEM

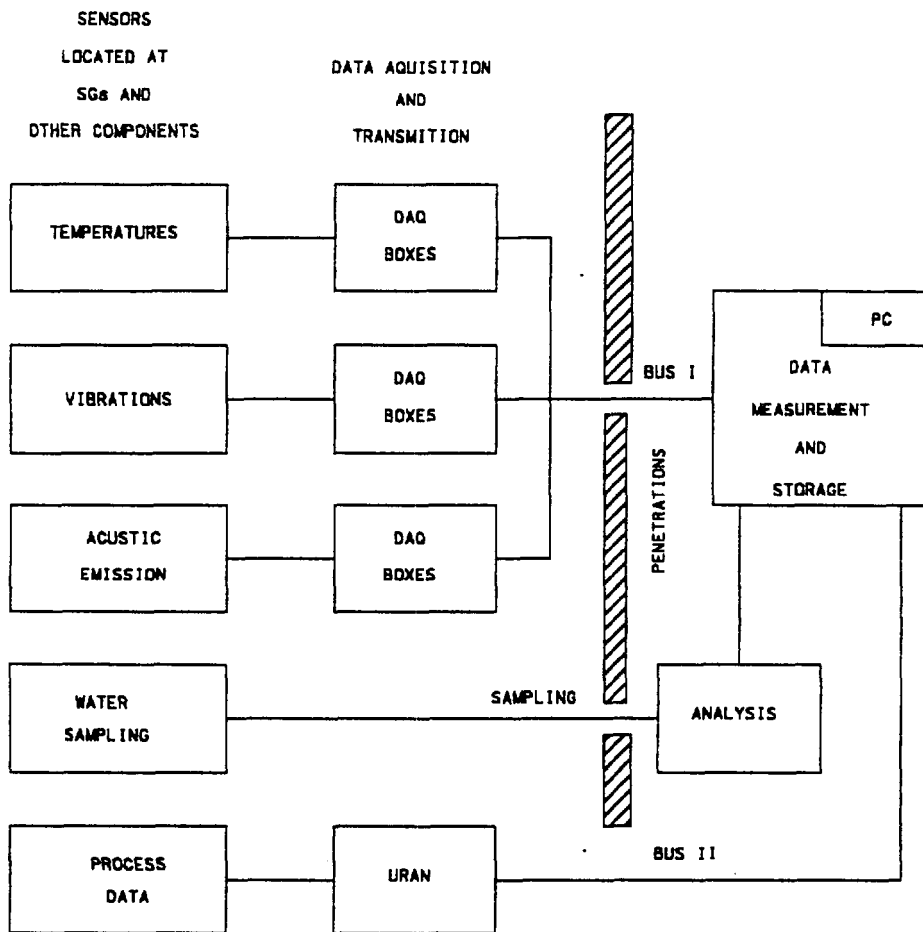


Fig.2: Schematic diagram of on-line measurements to demonstrate FWDS characteristics

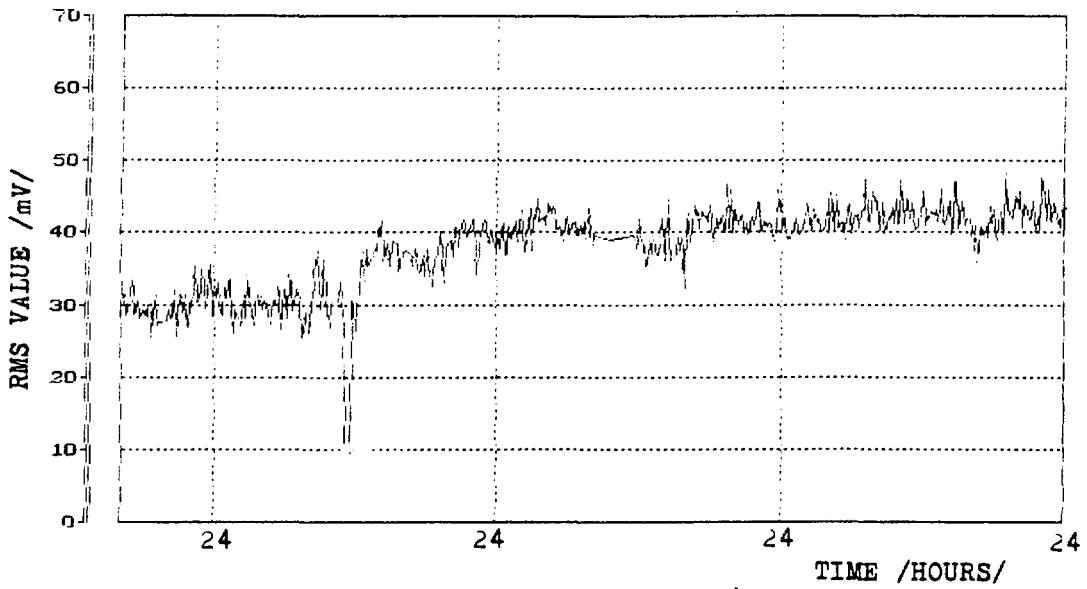


Fig 3a: RMS vibration levels measured at the SG with original feed water distributing system

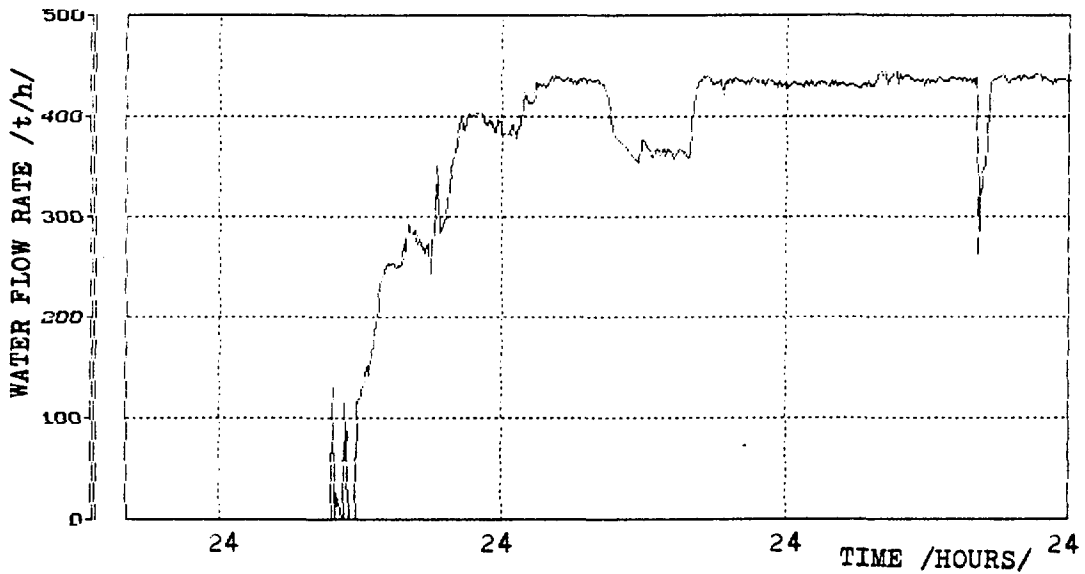


Fig 3b: Feed water flow rate versus time at the SG with original FWDS

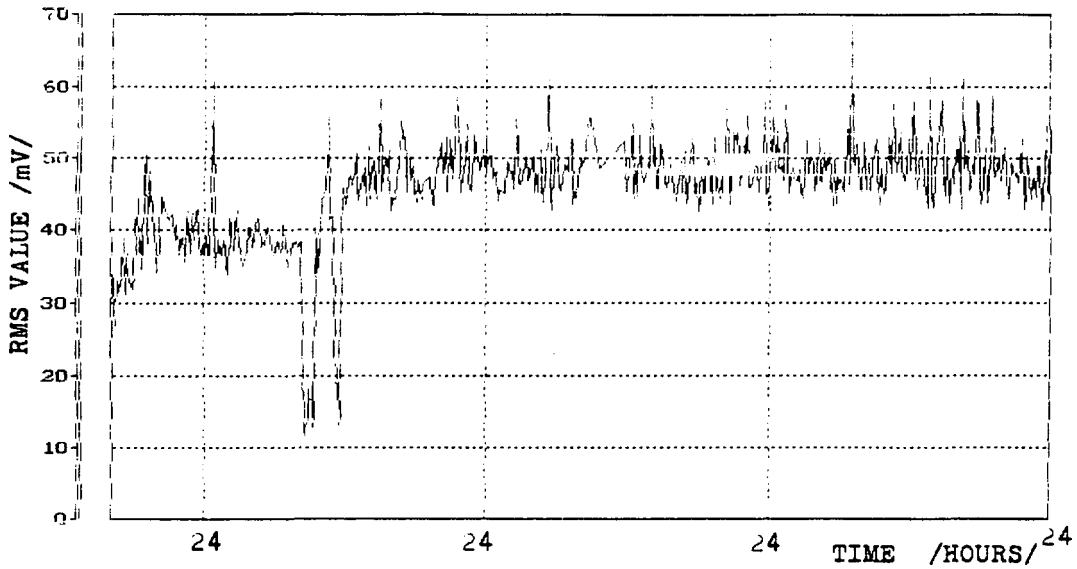


Fig 4a: RMS vibration levels measured at the SG with advanced feed water distributing system

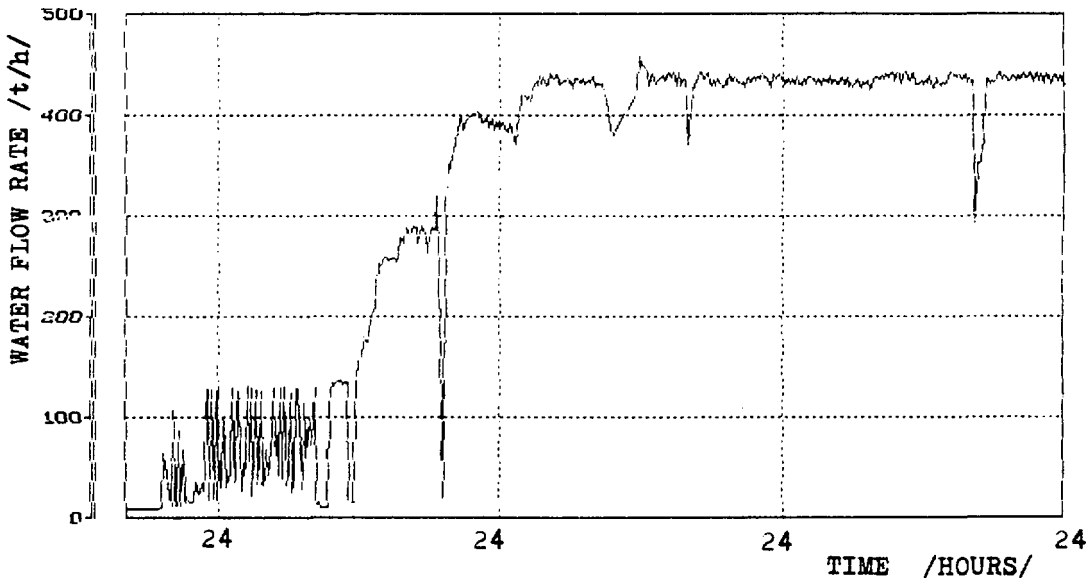


Fig 4b: Feed water flow rate versus time at the SG with advanced FWDS

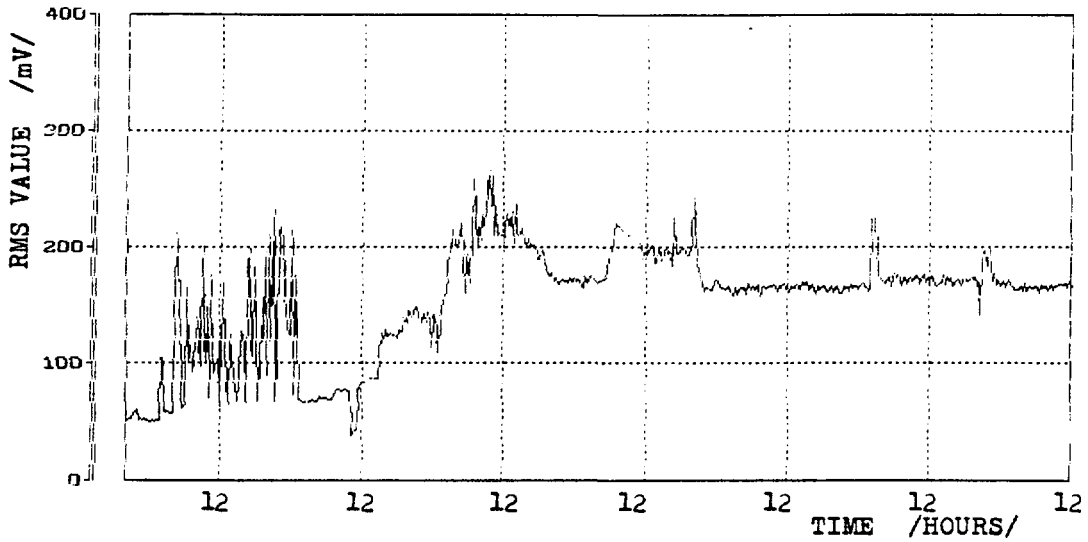


Fig 5a: Acoustic emission signal RMS values versus time measured at the SG with original FWDS

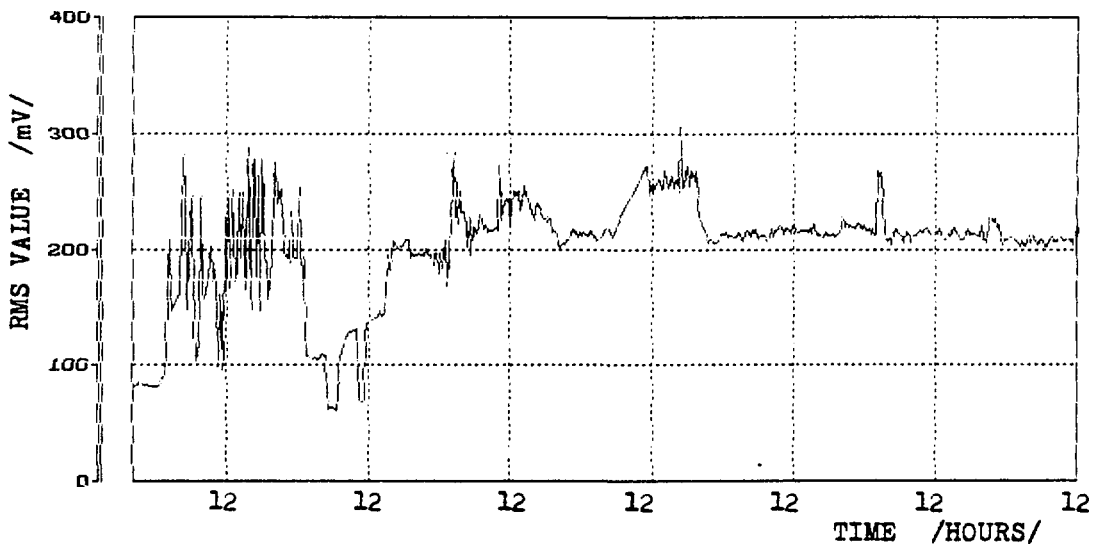


Fig 5b: Acoustic emission signal RMS values versus time measured at the SG with advanced FWDS

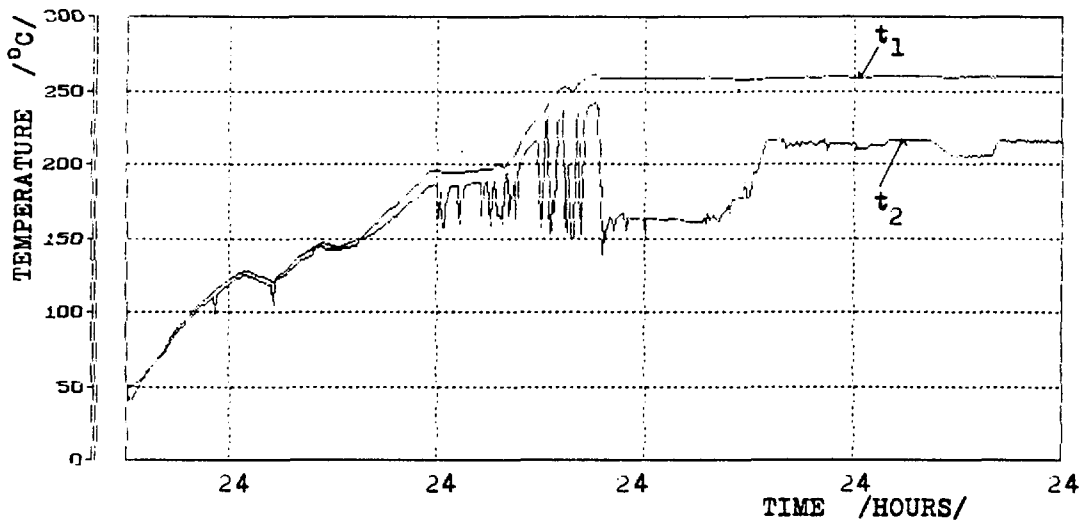


Fig 6a: SG pressure vessel temperature ( $t_1$ ) and feed water nozzle local temperature ( $t_2$ ) versus time observed at the SG with the original FWDS

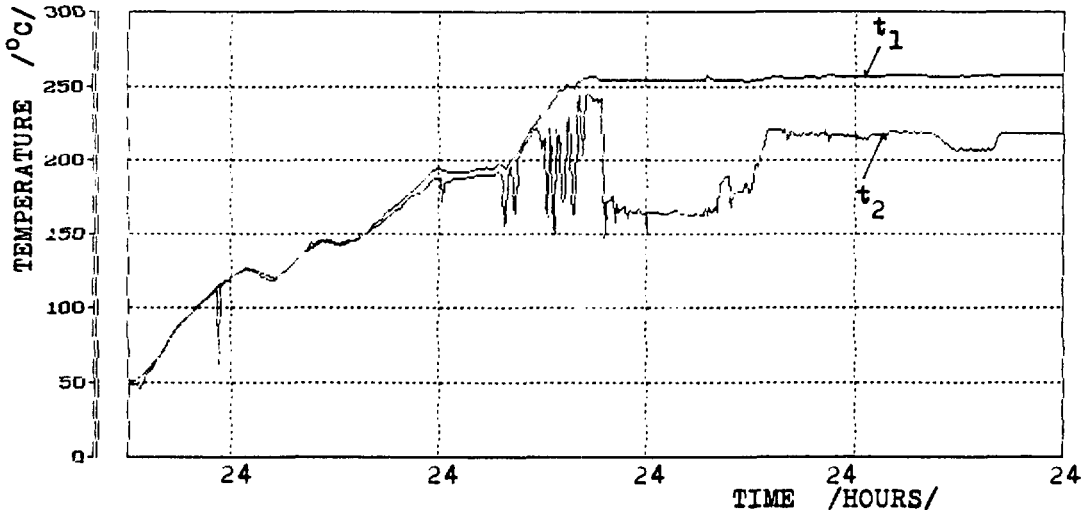


Fig 6b: SG pressure vessel temperature ( $t_1$ ) and feed water nozzle local temperature ( $t_2$ ) versus time observed at the SG with the advanced FWDS

THIRD INTERNATIONAL SEMINAR  
ON  
HORIZONTAL STEAM GENERATORS

18-20 OCTOBER 1994, LAPPEENRANTA, FINLAND

FEED WATER DISTRIBUTION PIPE REPLACEMENT AT LOVIISA NPP

S.Savolainen, B.Elsing  
Imatran Voima Oy, Loviisa NPP

ABSTRACT

Imatran Voima Oy operates two VVER-440 reactors. Unit 1 and has been operating since 1977 and unit 2 since 1981. First damages of feed water distribution (FWD) pipe were observed in 1989. The FWD-pipe T-connection had suffered from severe erosion corrosion damages. Similar damages have been found also in other VVER-440 type NPPs. In 1989 the nozzles of the steam generator YB11 were inspected. No signs of the damages or signs of erosion were detected. The first damaged nozzles were found in 1992 in steam generators of both units.

In 1992 it was started studying different possibilities to either repair or replace the damaged FWD-pipes. Due to the difficult conditions for repairing the damaged nozzles it was decided to study different FWD-pipe constructions.

In 1991 two new feedwater distributors had been implemented at Dukovany NPP designed by Vitkovice company. Additionally OKB Gidropress had presented their design for new collector. In spring 1994 all the six steam generators of Rovno NPP unit 1 were replaced with FWD-pipes designed by OKB Gidropress. After the implementation an experimental program with the new systems was carried out. Due to the successful experiments at Rovno NPP Unit 1 it was decided to implement 'Gidropress solution' during 1994 refueling outage into the steam generator YB52 at Loviisa 2.

The object of this paper is to discuss the new FWD-pipe and its effects on the plant safety during normal and accident conditions.

## 1. INTRODUCTION

Imatran Voima Oy is operating two VVER 440 type reactors at the Loviisa site. Unit one was taken into commercial operation in 1977 and unit 2 in 1981. The operation performances since have been very good.

In the operation history of the steam generators have been at the starting time a repair of the primary collector welds. Since this repair no faults were detected until 1989 when the first inspection of the T-connection of the FWD-pipe was performed. The FWD-pipe T-connection had suffered from severe erosion corrosion damages. Similar damages have been found also in other VVER-440 type NPPs. The inspections were carried out after the information from other VVER-440 operators.

In 1989 a TV-inspection of the steam generator YB11 nozzles was performed. No signs of damages were observed. In 1992 additional inspections of the nozzles were carried out based on the information from other VVER-440 operators. Visual inspections were performed on two steam generators at each unit. Some damages were detected at the FWD-nozzles.

In 1992 it was started studying different possibilities to either repair the damaged FWD-nozzles or replace the complete FWD-pipe. Due to the difficult conditions for repairing the damaged nozzles it was decided to study different FWD-pipe constructions.

In 1991 two new feed water distribution pipes had been implemented at Dukovany NPP designed by Vitkovice company. Additionally OKB Gidropress had presented their design for new collector. In spring 1994 all the six steam generators of Rovno NPP unit 1 were replaced with feed water distribution pipes designed by OKB Gidropress. After the implementation, experiments with the new feed water distribution construction were carried out. Due to the successful experiments at Rovno NPP Unit 1 it was decided to implement 'Gidropress solution' into the steam generator YB52 at Loviisa Unit 2. The Loviisa specific distribution pipe was designed by OKB Gidropress together with Loviisa NPP. Additional strength and thermal hydraulic calculations were carried out by IVO International.

The new FWD-pipe differs radically from the old design. In the old design the feed water is injected *into tube bundle*. The new FWD-pipe is *implemented* above the tube bundle. Feed water is distributed in the hot part of the heat transfer tubes.

## 2. REPAIR OF THE T-CONNECTION OF FEED WATER DISTRIBUTION PIPE

According to the information from other VVER-440 operators the inspections of the T-connection were performed. A manually operating manipulator for the wall thickness measurement of the horizontal pipe near the T-connection was designed and manufactured by a Dutch company Röntgen Technische Dienst b.v. together with Loviisa NPP in short time.

The wall thickness measurements were performed for all 12 steam generators during outages in 1989 and 1990. According to these measurements the schedule of the T-connection repair was decided.

During a visual inspection in 1989 a hole near the T-connection was detected in YB11 at Loviisa 1. The pipe was repaired primarily by installing a sleeve in the horizontal pipe. The work was carried out in short preparation time by Siemens AG, Germany. According the visual inspections and the wall thickness measurement results in 1989 repairing of other steam generators was needed. The final repair work at T-connection was performed during outages 1990 –1992 by replacing the vertical pipe including an elbow and parts of the horizontal pipe with a pipe made of austenite steel. The repair was carried out for six and four steam generators at unit 1 and 2, respectively. The work was designed and carried out by Siemens AG, Germany.

### 3. INSPECTION OF FEED WATER DISTRIBUTION NOZZLES

The first visual TV-inspection of the FWD-nozzles from the inside of the FWD-pipe were performed in 1989 during the repair of the T-connection of the YB11 at Loviisa 1. No damages or signs of erosion defects were detected at the region of the nozzles. Additional inspections of the FWD-nozzles were performed after the information from the other VVER-440 operators. The FWD-nozzles were visually inspected from outside. The results of the inspection were the following:

- some nozzles were half eroded (most of them near the T-connection)
- variation of erosion rate
- some of the nozzles were plugged by sludge
- no nozzles were lost

In the 1994 annual outage an extensive inspection of the nozzles was performed for eight steam generators. The analysis of the results is still undergoing. As preliminary results it can be seen that erosion damages at the nozzles have been detected in each inspected steam generator. Additionally 5 and 7 nozzles have been removed by cutting at unit 1 and unit 2, respectively.

Due to damages of the FWD-nozzles it was started studying different options to either repair the FWD-nozzles or replace the FWD-pipe. The following repair possibilities were discussed:

- slewing of the nozzles from the inside
- slewing of the nozzles from the outside
- replacement of the FWD-pipe including nozzles at the same place
- replacement of the FWD-pipe with a new designed distribution unit for feeding water at the same level but into a different part of the tube bundle (VITKOVICE design)
- replacement of the FWD-pipe with a new designed FWD-pipe for feeding water over the tube bundle (OKB GIDROPRESS design)

For more detailed evaluation two concepts were chosen:

- the Vitcovice design  
and
- the Gidropress design.

Both designs had advantages. After long and thorough discussions Loviisa NPP made their choice for the Gidropress design.

#### 4. REPLACEMENT OF FEED WATER DISTRIBUTION PIPE

During spring 1994 six feed water distribution pipes were implemented to the steam generators of Rovno plant unit 1. One steam generator was implemented with thermometers to measure temperature differences during start up and full power conditions. Additionally the steam moisture and impurities of secondary water were measured. A representative from Loviisa NPP, Paks NPP and Finnish regulatory body (STUK) followed the implementation work and experimental program.

After successful experiments the final decision was made to replace the first distribution pipe in steam generator YB52 at Loviisa 2 during the 1994 annual refuelling outage. A special design for Loviisa NPP was needed according to following details:

- the lay out of the steam generator room is different from other VVER-440 plants. That means that the FWD-pipe may only be installed in parts no longer than one meter.
- installing of the different parts by flange connections to reduce the time spent inside the steam generator → less radiation

At the same time extensive stress and thermal hydraulic calculations were performed by IVO International. The important calculation was performed in the area of feeding cold emergency cooling water through the feed water pipe into the steam generator at the tube bundle. This calculation had a direct influence on the construction of the pipe supports. Necessary changes were made also during the assembly.

The new FWD-pipe, manufactured by OKB Gidropress was installed during the annual refuelling outage in Loviisa NPP unit 2. Before the maintenance work the whole primary circuit was decontaminated. The working conditions were preferable due to low radiation level inside and outside the steam generator. Specially radiation protection actions were not required, only protection for lousing parts and protection of the header tubes against damages caused by working tools.

The assembly was carried out by two welders and one foremen. The assembly group was supported by the Gidropress project leader and a design engineer from Loviisa NPP.

At first the old feed water pipe elbow was removed. After locking the old vertical pipe to the tube supports the installation of new FWD-pipe was started. Because of the Loviisa design, only one pipe to pipe weld and the welding of the pipe supports had to be performed inside the steam generator. The welding work of the other pipe to pipe welds were performed in front of the man-hole. A few problems came up during the assembly. These problems were caused by missing exact dimension dates of the steam generator. Most of the problems were solved by a few changings of construction parts like supports a.s.o.

#### 4.1 Full scale experiments in Rovno NPP and Loviisa 2 NPP

Due to complicated thermal-hydraulic conditions in the secondary side it was decided that the acceptance of collector is based on the thermal hydraulic experiments at Rovno NPP. The most important full scale transients were:

- PCP-trip/start-up
- disconnection of high pressure heaters
- steam generator water level increase/decrease
- 10 % step-wise power decrease/increase
- turbine trip

The main plant parameters as temperatures, pressures and mass flow rates were recorded during the experiments. Additionally temperature distribution inside the steam generator and the vibration of the collector was recorded. Furthermore, distribution of impurities in the secondary water and the steam moisture content was recorded.

The object of these experiments was to ensure that the new collector does not have any additional effects during typical plant transients or normal and start up conditions.

For Loviisa NPP some additional thermal stress calculations were carried out by IVO International. The steam generators of the Loviisa NPP differs from the other VVER-440 steam generators because both normal and emergency feed water is injected through the same feed water distribution pipe. In other VVER-440 steam generators there is an additional feed water distribution pipe close to the steam separators. Additionally studies of water hammer conditions were performed.

The thermal-hydraulic behavior of the steam generator can be divided in different fields:

- operation during normal conditions including shut down conditions
- operation during transients
- operation during accident conditions

The most important parameters during normal operation are:

- steam moisture
- distribution of impurities
- heat transfer coefficient

For the two first items two parallel steam generators YB52 and YB54 at Loviisa 2 have been implemented with additional instrumentation. In both steam generators the content of the impurities are measured. Furthermore, experiments for determining the steam moisture content with different water levels will be carried out. During the start-up procedures some experiments concerning water hammer phenomena was performed. After the plant had reached full power the full scale plant experiences were carried out. The experimental program at Loviisa 2 is presented in the table 1. The analysis of the results are undergoing, so far. As a preliminary result it can be concluded that the operation of the steam generator has not been changed.

#### 4.2 Effect of the new distribution pipe on the plant safety

While the different feed water distribution constructions were studied the safety of the plant was one of the key factors. Major attention was paid to the following questions:

- secondary mass inventory
- heat transfer tube life time
- probability of water hammer conditions

It was assumed that the secondary side water inventory will be decreased after the collector replacement. When the water is injected above the tube bundle and if the heat transfer coefficient is constant the void fraction in the tube bundle will be higher. According to rough hand calculations the secondary water mass inventory decreases about 400 kg. The hand calculations are presented in appendix 1.

During the LOss off Feed Water accidents (LOFW) or LOss of Off site Power (LOOP) accidents the upmost tubes may be uncovered within minutes. If the feed water is injected above tube bundle the thermal oscillation of the tube surface seems to be evident. The heat transfer coefficient fluctuates between water-phase convection, two-phase boiling and dry-out conditions. Roughly the surface temperature may oscillate between feed water temperature and primary loop hot leg temperature.

In Loviisa NPP both normal and emergency feed water is taken from the normal feed water tank. During transient and accident conditions the initial feed water temperature is approximately 165 °C. If the high pressure preheaters are working properly the temperature is about 220–225 °C. In case of low level in the feed water tank, low pressure in the feed water line or low feed water mass flow rate cold feed water is automatically (minimum temperature 5 °C) injected into the steam generators.

According to preliminary calculations with extremely conservative boundary conditions the minimum lifetime of the tube might be as short as two hours !! The lifetime is strongly dependent on the tube surface temperature behavior that is determined by the next variables:

- primary temperature
- feed water temperature
- local heat transfer mode at tube surface

The primary temperature is typically less than 290 °C. Typical value during LOOP or LOFW accident is about 260 °C. The temperature of the feed water stream seems to be rather complicated to determine. If the water level drops below tube bundle and the emergency feed water pumps are actuated the typical mass flow rate fluctuates between 5–20 kg/s into one steam generator. In these conditions the feed water is preheated in the collector due to steam condensation. The effect of the condensation has been assumed to be between 20–150 °C depending on the feed water mass flow rate and condensing heat transfer mode. If the temperature of the feed water would be say 100 °C the lifetime would increase up to 8 hours. One should keep in mind that the problems are the same with the old construction if the water level decreases below the distribution pipe (1.2 m). The only difference is that the time delay causing the tube damage is about 1–2 hours depending on accident. At Loviisa 2 some modifications have been made to emergency procedures to isolate emergency feed water injection to the steam generator YB52 if cold feed water is injected. Additional studies of the heat transfer tube life time will be carried out during 1994–1995.

Due to the limited capacity of computer codes to predict so called water hammer phenomenon the water hammer studies were based on rough hand calculations. The studies were divided into two parts:

- required preconditions for water hammer
- consequences of water hammer.

During conditions when the FWD-pipe is fully or partially filled with steam and the feed water flow rate is recovered, cold water may condense the steam causing sufficient forces possibly damaging the FWD-pipe or even the tube bundle. Due to lower feed water temperature (5–164 °C) the pressure in the distributor tends to decrease and steam flows into the pipe.

If the condensing rate is high enough the stratified flow pattern will be changed in to a slug flow pattern. If the condensing is effective the steam bubbles may be collapsed causing sufficient force to the distribution pipe.

According to Deitel-Dukler criteria the onset of slugging will be avoided even with 5°C feed water temperature. According to the calculations mass flow rates may be between 10 – 60 kg/s with water temperatures 164°C are in the region of slug flow and the conditions then are preferable for water hammer conditions.

Due to the FWD-pipe design the consequences of water hammer may not be very dangerous. In the top of the water seal there is a small pipe for equalizing pressures inside the descending part of the pipe. Additionally the volume of the collector is rather small so the maximum volume of steam is small, too.

During 1994 –1995 additional water hammer studies and tube thermal stress studies may be carried out. It seems evident that experiments are needed for determining the condensing heat transfer coefficient as a function of feed water mass flow rate. Additionally, an experimental program is needed to determine the lifetime of the heat transferring tubes when cold feed water is injected to uncovered tubes. The extent of the experiments will be decided in the near future. Parallel to these studies the schedule of replacement work will be decided. As preliminary schedule it has been decided to implement all distribution pipes till 1996.

## CONCLUSIONS

During the refuelling outage at Loviisa NPP unit 2 one FWD-pipe was replaced by the new Gidropress designed FWD-pipe. An extensive research and test program was performed to fulfill the requirements for operation and safety. For further replacements more studies and tests have to be performed. The operating experience under normal operating conditions is good.

## INITIAL CONDITIONS

Experiment	$P_{YB}$ $T_{YB}$	$T_{FW}$	$m_{fw}$	$l_{YB}$	$\Phi_{YC}$
water hammer	44 256	165	3	-0.12	0
water hammer	44 256	165	5	-0.12	0
water hammer	44 256	165	7	-0.12	0
PCP-trip	44 256	225	120	nominal	100
HPH-disconnection	44 256	225	120	nominal	100
steam line moisture	44 256	225	120	*	100 **
distribution of impurities (Continuous measurement)	44 bar 256	225	120	+0.0	100

$P_{YB}$  = pressure in the steam generator [bar]

$T_{YB}$  = saturated temperature in the steam generator [°C]

$T_{FW}$  = feed water temperature [°C]

$m_{fw}$  = feed water mass flow rate [kg/s]

$l_{YB}$  = water level in the steam generator [m]

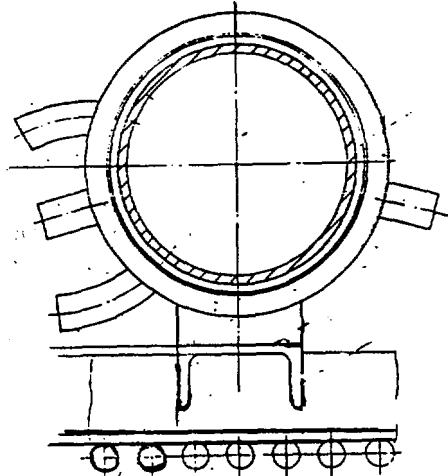
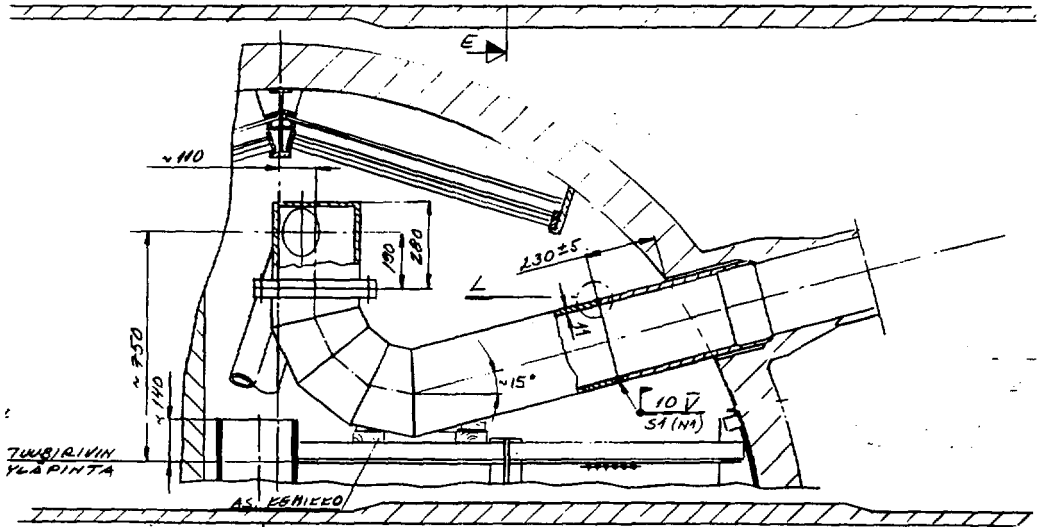
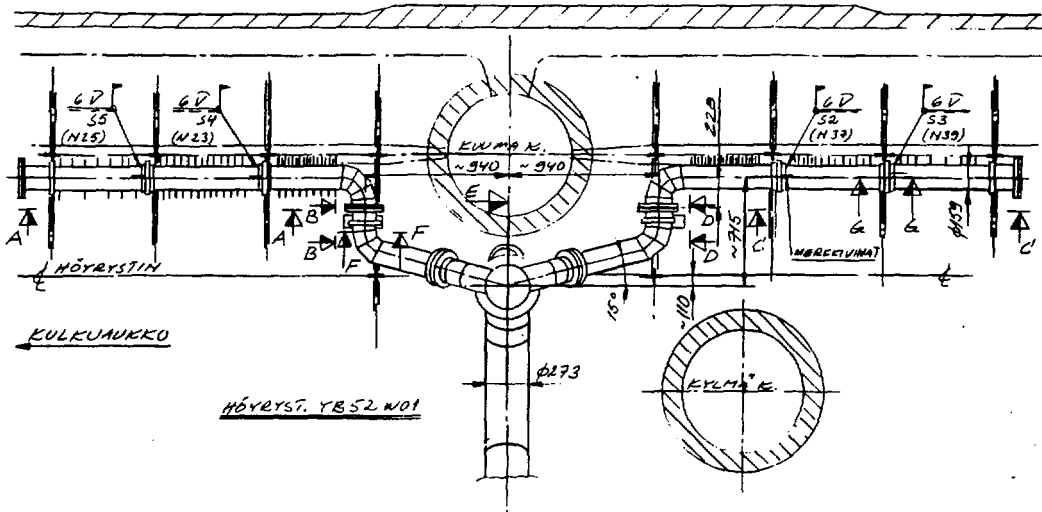
$\Phi_{YC}$  = reactor thermal power [%]

Moisture experiments will be carried out also with steam generator YB54.  
Additional water samples are taken from YB54, too.

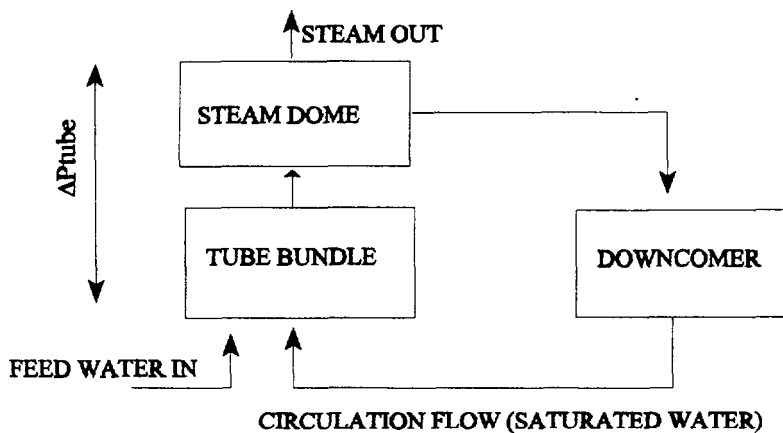
\* Water levels will be changed from -0.1 up to +0.2 with 0.05 m steps.

\*\* Experiments will be repeated with lower thermal power levels 90 % and 95 %. Water level will be fixed during experiments. Level will be chosen after full power moisture experiments.

Table 1. Full scale experiments in Loviisa 2.



## THE EFFECT OF THE FEED WATER INJECTION TO THE SECONDARY SIDE WATER MASS INVENTORY



Simplified figure of the old construction

### Assumptions:

$$P = 4.5 \text{ MPa}; \rho' = 788 \text{ kg/m}^3; \rho'' = 22.7 \text{ kg/m}^3; T_{\text{feedwater}} = 222 \text{ } ^\circ\text{C}$$

$$\Delta P_{\text{tube}} = 2.05 \cdot 9.81 \cdot 788 = 15848 \text{ Pa} \quad *$$

\* it has been assumed that wide scale water level measurement represents the  $\Delta P$  over the tube bundle

1. Calculation of the friction coefficient over the tube bundle (homogenous flow)

$$\Delta P = 15848 = \bar{\rho} g \Delta h + k \bar{\rho} \bar{\omega}^2 \quad (1)$$

$$\bar{\rho} = \text{mixture density} = (1 - \alpha) \rho' + \alpha \rho''$$

$$g = 9.81 \text{ m/s}^2$$

$$\Delta h = 2.0 \text{ m} = \text{height of the tube bundle}$$

$$\bar{\omega} = \text{homogenous reference mixture velocity}$$

$$\alpha = \text{tube bundle void fraction} = 0.25$$

$$k = \text{non-dimensional friction factor}$$

$T_{FW}$  = feed water temperature = 225 °C

$\dot{m}''$  = steam mass flow rate

$\Phi$  = reactor thermal power = 1375 MW

$$\dot{m}'' = \frac{\Phi}{6 \cdot (h'' - h')} = \frac{1375 \cdot 10^3 \text{ kW}}{6 \cdot (2798 - 997) \text{ kJ/kg}} = 12.7 \text{ kg/s}$$

Homogenous flow

$$\Rightarrow \bar{\omega} = \frac{\dot{m}''}{\rho'' \alpha A}$$

$\alpha$  = average void fraction

$A$  = reference area

$\bar{\omega}$  = reference velocity of steam

$$\Rightarrow \Delta P = \bar{\rho} g \Delta h + k \bar{\rho} \left( \frac{\dot{m}''}{\rho'' \alpha A} \right)^2$$

**Note:** The area and steam density are constant values  $\Rightarrow$  they can be included in the friction factor

$$\Delta P = \bar{\rho} g \Delta h + k \bar{\rho} \left( \frac{\dot{m}''}{\alpha} \right)^2$$

$\Rightarrow \Rightarrow$

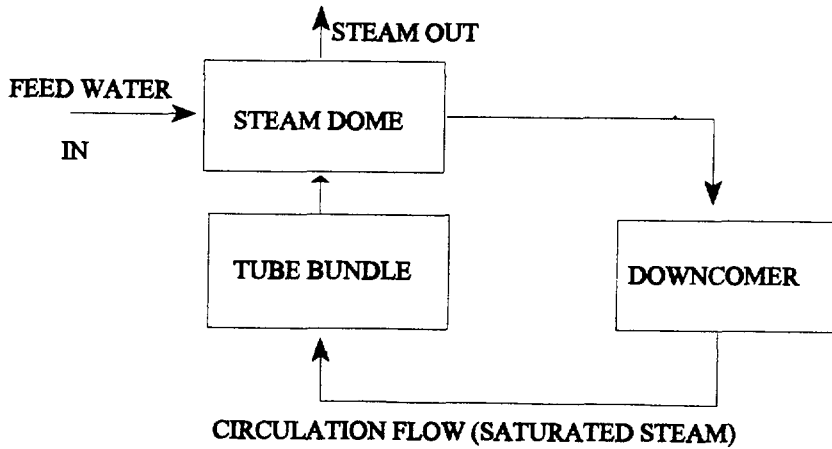
$$K = \frac{\Delta P - \bar{\rho} g \Delta h}{\bar{\rho} \left( \frac{\dot{m}''}{\alpha} \right)^2} = \frac{15848 - [(1 - \alpha) \cdot 788 + \alpha \cdot 22] \cdot 2.0 \cdot 9.81}{(1 - \alpha) \cdot 788 + \alpha \cdot 22} \left( \frac{127}{\alpha} \right)^2 \quad (2)$$

$$\Rightarrow \quad K = 2.69 \cdot 10^{-5}$$

With new construction it is assumed that friction factor is independent of the place of feed water injection.

According to the operation at Rovno NPP and Loviisa NPP the values of Wide scale level measurements are similar as before replacement =>  $\Delta P$  over the tube bundle is constant

$$\Rightarrow \Delta P = \bar{\rho} g \Delta h + k \bar{\rho} \omega^2 = \bar{\rho} g \Delta h + k \bar{\rho} \left( \frac{\dot{m}''}{\alpha} \right)^2$$



Simplified figure of the new construction

$$\Delta P = 15848 = [(1-\alpha)\rho' + \alpha\rho''] g \Delta h + k [(1-\alpha)\rho' + \alpha\rho''] \left( \frac{\dot{m}''}{\alpha} \right)^2 \quad (3)$$

**Note:** Steam mass flow rate will be higher because water is now preheated at the steam dome.

$$\Rightarrow \dot{m}'' = 137 \text{ kg/s}$$

By rearranging the equation (3) we get:

$$\alpha = \dot{m}'' \sqrt{\frac{k[(1-\alpha)\rho' + \alpha\rho'']}{\Delta P - [(1-\alpha)\rho' + \alpha\rho''] g \Delta h}}$$

After substituting steam mass flow rate = 137 kg/s and iterations

$M_{SG}$  = water mass inventory in steam generator

$M_{SG} = \beta (1-\alpha)$ ,  $\beta = \text{constant}$ ,  $\alpha = 0.25$ ,  $M_{SG} = 33 \cdot 10^3$

$M_{SG} = 33 \cdot 10^3 / 0.75 (1-0.25) = 32.6 \cdot 10^3 \text{ kg}$

=> water mass inventory decreases  $\Delta M = 400 \text{ kg}$

## FEED WATER PIPING IN SG 440 MW

Prepared: Ivo Kusák  
Frant. Cikryt

International Seminar on Horizontal SG  
Lappeenranta, Finland  
18-20 october 1995

VÍTCOVICE a.s. POWER SYSTEMS ENGINEERING - 603.3

### UPPER FEED WATER PIPING SYSTEM

#### 1. Current State

Feed water piping system in VVER 440 SG under operation consists of feed water nozzle connected to a central f.w. distribution system of OD 273 x 16 mm. The system is situated next to the wall of inlet primary collector and goes below the secondary water level. Two horizontal distributing pipes of OD 156 x 6 then connect into two rows of outlet tubes of OD 25 x 2.5 mm which are fed from central feeding system situated in the bottom one third of SG. Small outlet tubes are arranged within the intermediate spaces between the heat exchange tube bundle. Such configuration has disadvantages and leads to pipe defects in joints between central piping and branches of distributing piping. This is because of large mass of continuously fed water whose flow direction and rate are continually changing so that pipe leakage may occur due to cavitation erosion and water suppression of movement of tubes in brackets and other effects. Such defects result in unexpected leakage of secondary water in the vicinity of inlet primary collector and may cause subsequent collector defects due to stresses from non uniform heat loads. Another disadvantage is demanding technological repair work which requires relatively long SG shutdown and which may lead to a complete block shutdown. Location of the pipes between tube bundles also prevents easy dismantling and repair. Piping is made from GOST Steel 20, feedwater temperature is 223°C, secondary water temperature is 260°C in normal operation, secondary circuit pressure is 4.6 MPa.

#### 2. Modified State

##### 2.1 Design

Modified feed water inlet piping (see sketches 1 to 3) is based on new configuration and position of inlet pipe (1) connected to distribution piece (4) followed by distribution piping (5) and branches which are placed above heat exchange tube bundle (8). From distributing pipe (5) runs a system of outlet tubes (9) into mixing box (10) reaching intertube space below water level of SG. In order to prevent local cooling of SG shell from feed water a flow rectifying plate (12) is situated there and fixed to post of tube bundle supporting system.

Inlet pipe is made from OD 273 x 16, distributing piece is sized to comply with OD of inlet and two outlet pipes of OD 159 x 6 mm.

Distributing piping is made from two tubes of OD 159 x 6 mm and their left and right hand branches are situated above hot side of tube bundle. Feed water runs out through the system of bent end tubes of OD 35 x 2.5 mm. End tubes are fitted with orifice gauges and piped to mixing boxes. The lengths of left and right hand branches are not the same and are according to configuration of SG.

From left branch run two sets of 12 bent tubes from right branch there are four sets of 12 tubes. For assembly and system toughness reasons the systems are of 35 x 2.5 end tubes connected by flat bar sections to which mixing boxes are welded. Bases of boxes are fixed to the tube bundle support posts. Box sizes are 600 x 57 mm and 450 mm in height. Boxes side plates are made from perforated plates with perforations of OD 10 mm and configured in two columns with pitch distances of 19 mm horizontally and vertically. The box side plate next to the hot collector is not perforated.

In order to rectify the feed water flow running from boxes there are single water stream rectifiers mounted at level of original feed water piping. These rectifiers are made of bent plate fixed by two clamps to tube bundle post supports.

Feeding system is mounted on tube bundle wake system by means of clamps which enable axial and cross sectional movement of distribution pipes

All elements of a modified distribution system are made from CSN Class 17 alloyed stainless steel. This steel grade is approved by SG head designer for use on atmospheric pressure parts.

## 2.2 Operation

Feed water is supplied through nozzle and pipe (1) see sketch Nos. 1 - 37 into distributing pipe (4) and runs into left and right hand branches. In order to ensure end tube water flow rate in specified amounts each tube is fitted with individual orifice gauge 50 that increased flow rate is concentrated into collector hot area where maximum heat flows occur.

In box miners initial hot water and steam water mix are blended with feed water. Box miner side walls rectify and control water flow so that no local whirlpools arise which could withdraw water from upper heat exchange tube rows. Since feedwater piping is situated above water level steam mix is washed through feed water streams. Due to configuration of end tubes projected into box mixers there is also a suction effect and steam mix is partially ejected. Combination of the suction effect and increased feed rate into hot collector area result in equalizing of water mass level in SG. Water flow from bases is then rectified to the venter of SG body. This rectification should prevent local cooling of SG shell.

## 2.3 Advantages Over Current System

A substantial advantage is that an unambiguous and instant visual inspection of feed water system can be provided in SG thanks to positioning the whole system above heat exchange tube bundles. In this way we can specify the scope of possible defects of the piping and prevent hot primary collector from being exposed to cold water flow. In the same way we can examine specified allowance between sleeve and distributing pipe and prevent undesirable stresses in case of no expansion. For current design an expansion fit limitation with no opportunity to examine it in the actual configuration of feed water piping may significantly contribute to the occurrence of defects.

Another advantage is discharging of feed water in upper part of SG so that boiler water circulation is improved. Feed water enters tube bundle interspace already blended with steam/water mix and boiler water and in this way decreases tube bundle heat load when compared with current configuration.

## 2.4 Fabrication and Assembly Work

Fabrication of the whole system is designed so that subassemblies are shipped from the Workshop in their transportable and with SG manhole compatible maximum sizes. After fabrication of the whole system is completed in the shop a total assembly inspection follows in order to minimize exposure to radiation of fitters at site.

Fitting the modified piping system into SG shall follow technology procedure prepared by the manufacturer.

## **2.5 Documentation and Examinations**

Detailed workshop drawings are prepared and accepted by Institute of Technical Inspection Praha branch office Ostrava. Basic and welding filler materials are subject to examinations according to specification PKJ 567/84.

The whole system is designed in accordance with Soviet rules PK 1517-79 OP 1513-72 and "Rules for Safety Operation"

Strength and lifetime calculations were provided under retention No. 4-001600-20.

The whole piping assembly (nod) is subject to Individual Quality Assurance Programme control

## **2.6 Acceptance of the System by Independent Organization**

The whole system of upper feed water distribution system was assessed at VUT BRNO FS - Technical University of Brno, Department for Thermodynamics. Project assessment was prepared by Professor Frantisek Dubšek at the request of Dukovany NPP.

Examination/Examiners proceedings held on April 15 1992 at Technical University Brno were attended by examiner Dukovany NPP and Vitkovice specialists.

Examiner's comments were implemented into documentation and after its completion examiner recommended acceptance of modified feedwater piping system.

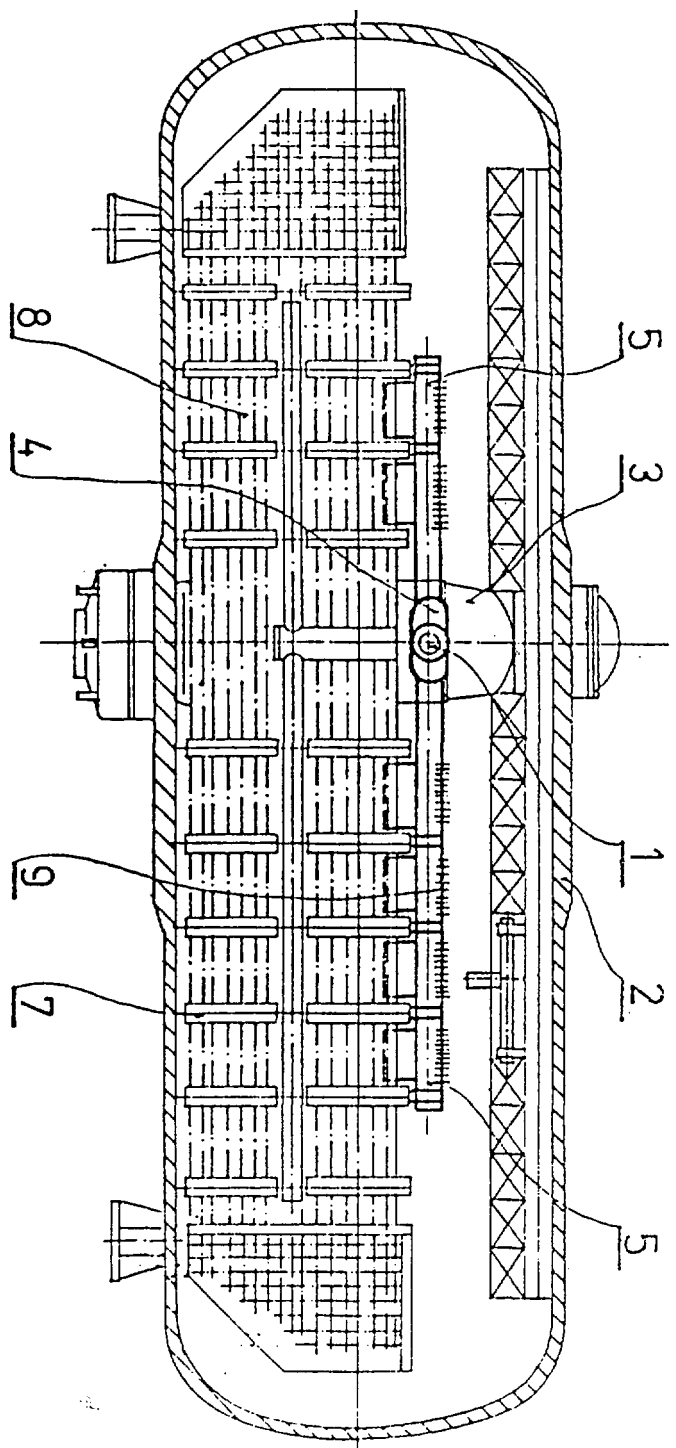


Fig. 1

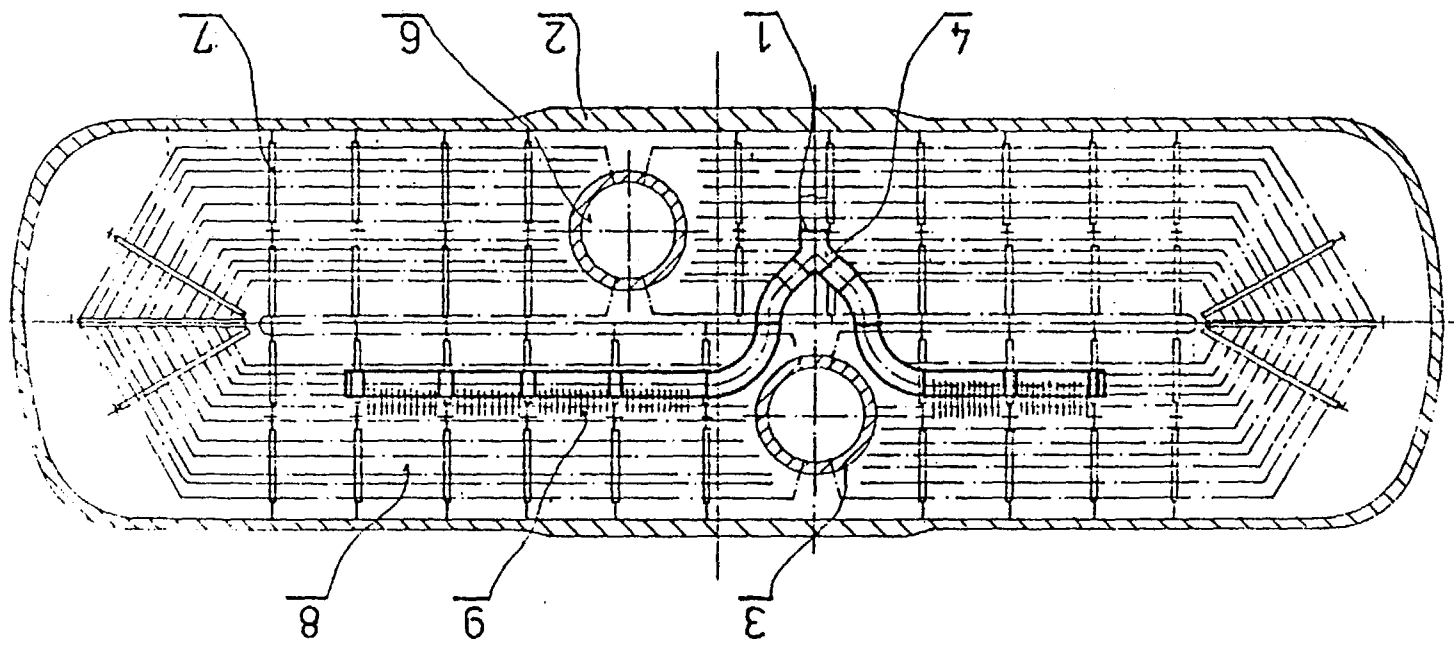
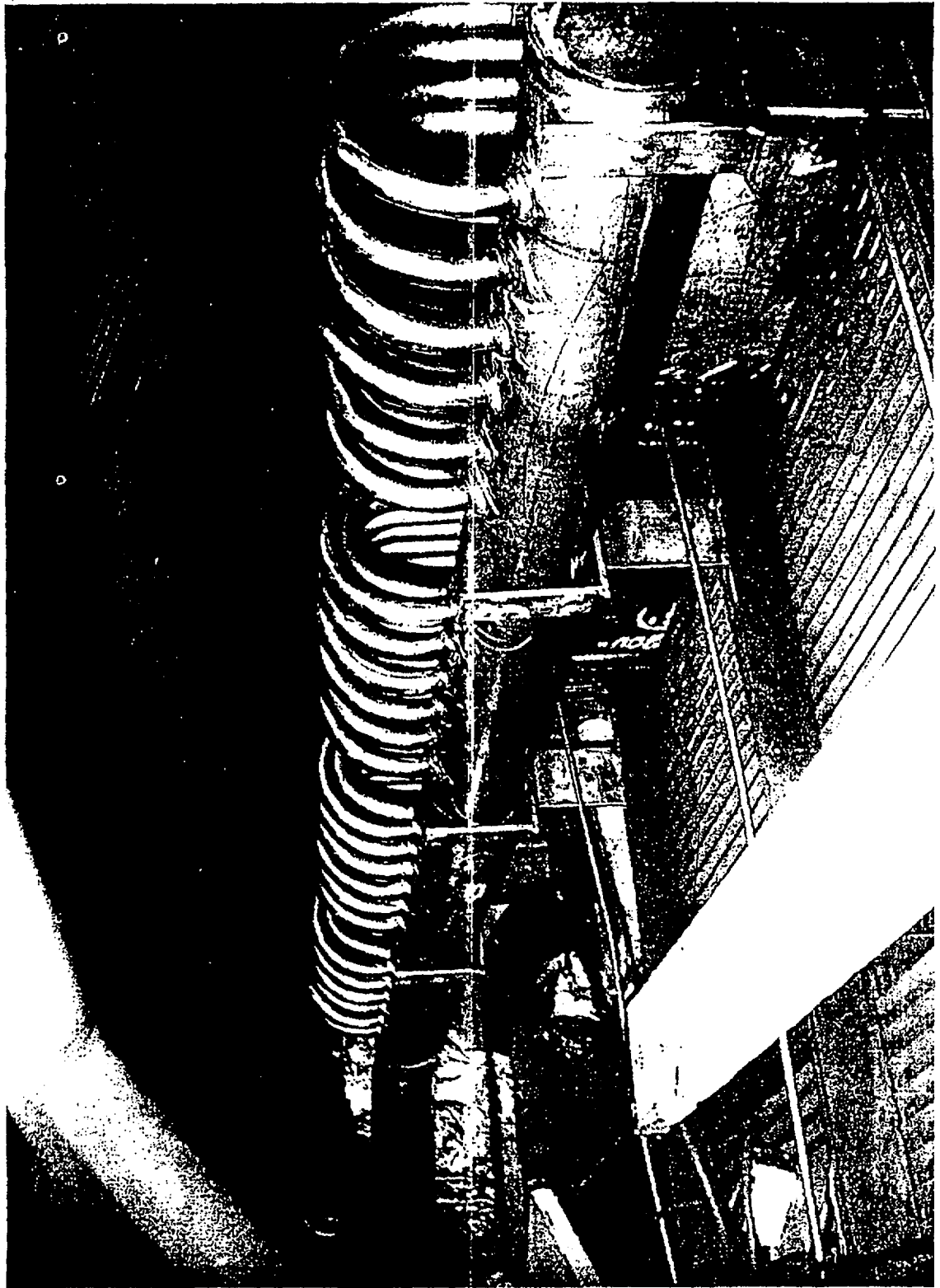


Fig. 2



VÍTKOVICE Service of NPPs

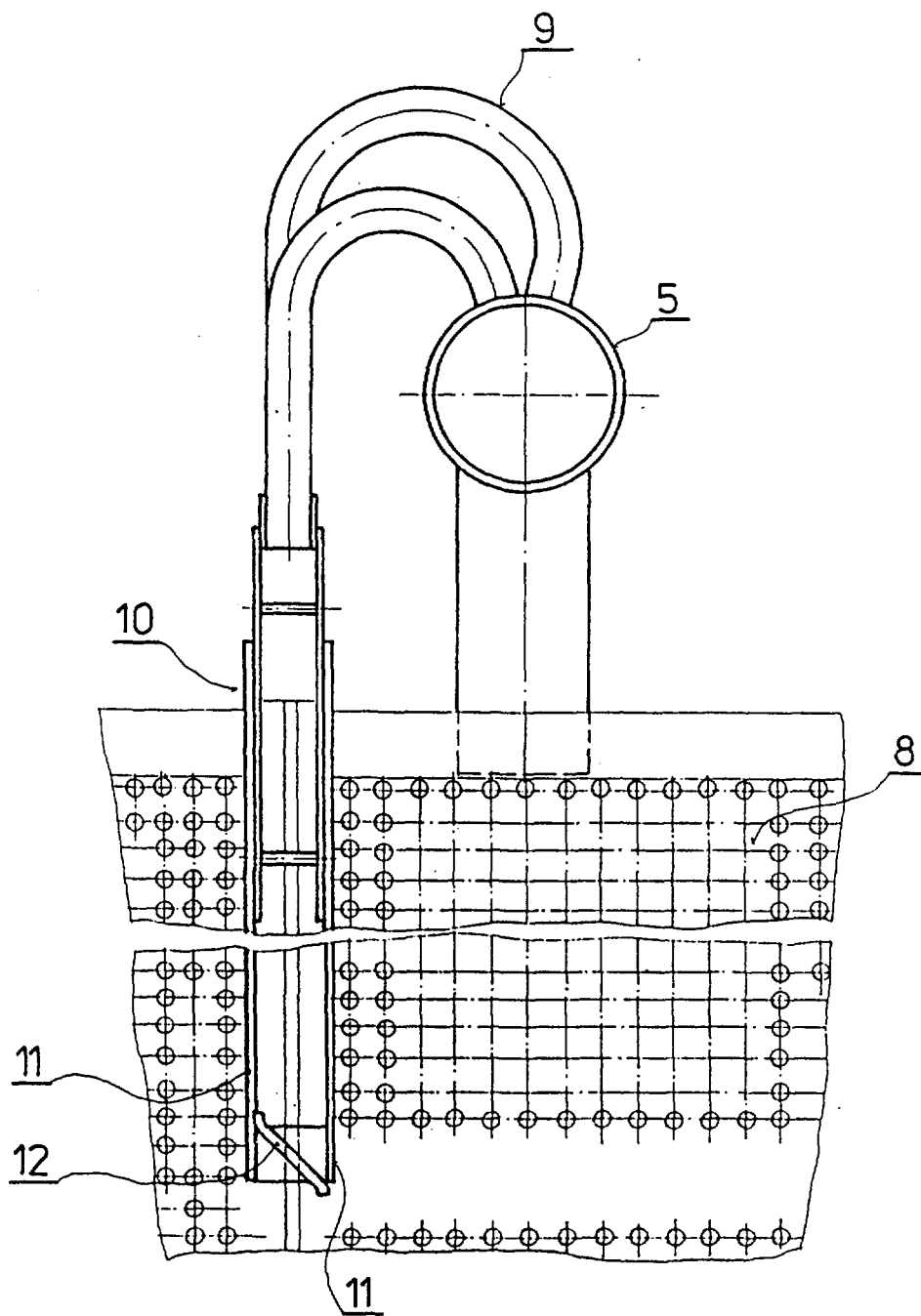


Fig. 3

## References

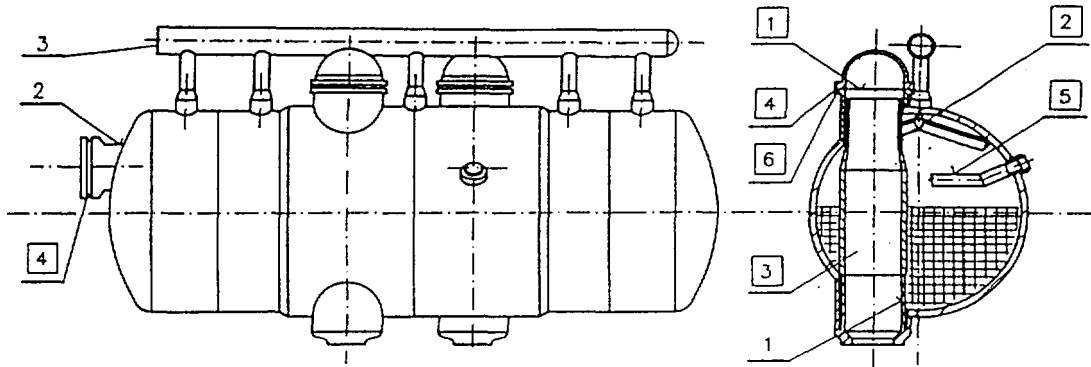
References of Vítkovice a.s.

Components for nuclear power plants

Year	PC	Type	Destination
1978	1	PR 440	Rovenska (Ukraine)
1979	3	PR 440	Paks (Hungary) Rovenska (Ukraine) Kolska (Russia)
1980	2	PR 440	Paks (Hungary) Kolska (Russia)
1981	2	PR 440	Bohunice (Slovakia) Dukovany (Czech Republic)
	5	SG 440	Bohunice (Slovakia)
1982	9	SG 440	Dukovany (Czech Republic)
1983	2	PR 440	Paks (Hungary)
	7	SG 440	Bohunice( Slovakia) Bohunice( Slovakia) Dukovany (Czech Republic)
1984	2	PR 440	Paks (Hungary) Dukovany (Czech Republic)
	9	SG 440	Dukovany (Czech Republic) Bohunice( Slovakia)
1985	2	PR 440	Greifswald (Germany) Dukovany (Czech Republic)
	6	SG 440	Dukovany (Czech Republic) Greifswald (Germany)
1986	6	SG 440	Mochovce (Slovakia)
1987	1	PR 440	Mochovce (Slovakia)
	7	SG 440	Mochovce (Slovakia)
1988	1	PR 440	Mochovce (Slovakia)
	7	SG 440	Mochovce (Slovakia) Greifswald (Germany)
1989	1	PR 440	Mochovce (Slovakia)
	6	SG 440	Mochovce (Slovakia) Greifswald (Germany) Zarnowlec (Poland)
1990	1	PR 1000	Belene (Bulgaria)
	4	SG 440	Mochovce (Slovakia) Zarnowiec (Poland)
	2	SG 1000	Temelin (Czech Republic)
1991	1	PR 440	Mochovce (Slovakia)
	1	PR 1000	Temelin (Czech Republic)
	2	SG 1000	Temelin (Czech Republic)
1992	2	SG 1000	Temelin (Czech Republic)
1993	1	SG 1000	Temelin (Czech Republic)
1994	1	SG 1000	Temelin (Czech Republic)



Steam Generator of type 213 C for VVER 440 MWe Nuclear Power Plant



Steam Generators produced in VITKOVICE (Ostrava, the Czech Republic) are of horizontal type. They are produced in 2 types and 5 versions, which differ from each other in location of collectors of primary circuit (1) manhole of bottom (2) steam collector discharge (3) which result from requirements of all power plant project.

During production several technical and technological improvements took place:

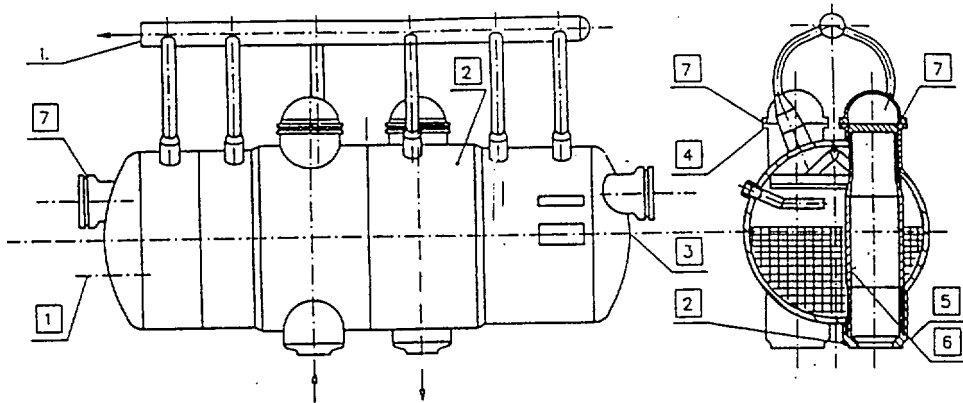
1. Replacement of ribbled cover of primary circuit by a flat one which has more positive impact on additional stress of bolted joints.
2. Protection of outside surface of Collector in steam space by high-nickel weld deposit (cladding)
3. Hydraulic sealing of heat transferring tubes (HTT)
4. Production of sealing weld deposits of secondary circuit by flux welding
5. New distribution of feed water
6. Production of threads of manhole flange joints by milling operation (Ingersol)

Modification of chemical composition and structure of steel at base material of pressure parts with the aim to improve its safety against failure and reliability (reducing degradation speed) at high mechanic and corrosive stress in the frame of operation.

We also arrange for steam generator produced in such a manner:

- author s supervision and consultation during operation
- check of all HTT by eddy current including plugging of weak tubes
- all repair activity
- assembling diagnostic systems
- evaluation of service life exhaustion in relation to achieved operation regimes

Steam Generator of type 1000M for VVER 1000 MWe Nuclear Power Plant



Steam generators produced in VITKOVICE (Ostrava the Czech Republic) are of horizontal type. Steam generators are produced in 2 versions on the basis of power plant project.

These versions differ from each other in steam collector discharge (1.).

There are several improvements in comparison to the russian project in VITKOVICE by means of which a reliability and utility value of steam generator is increased:

1. Modification of location of surface blowdown removal
2. Modification for application of diagnostic system
3. One-part bottom of steam generator (without any weld)
4. Production of threads of manhole flange joints secondary covers and primary collectors by milling operation (Ingersol)
5. Drilling of openings in collectors with minimum deformation and minimum surface stress
6. Hydraulic sealing of heat transferring tubes (HTT)
7. Welding on of sealing afield deposits at manholes secondary covers and primary collectors by flux welding

Use of controlled electric heating at warming welding and postheating of pressure parts of steam generator.

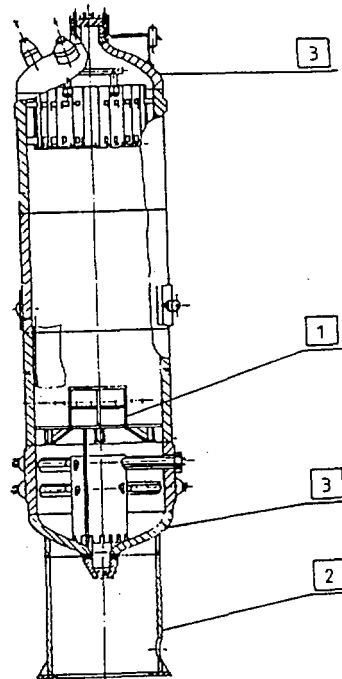
Modification of chemical composition and structure of steel at base material of pressure parts with the aim to improve its safety against failure and reliability (reducing degradation speed) at high mechanic and corrosive stress in the frame of operation.

We also arrange for steam generator produced in such a manner:

- author's supervision and consultation during operation
- check of all HTT by eddy current including plugging of weak tubes
- all repair activity
- assembling diagnostic systems
- evaluation of service life exhaustion in relation to achieved operation regimes



Volume Compensator for VVER 1000 MWe Nuclear Power Plant



There are several improvements in comparison to the russian project in VITKOVICE, by means of which a reliability and utility value of steam generator is increased:

1. Cancellation of built-in - surfaces, replacement with air bag
2. Pedestal modification
3. Bottom are produced from one part (without any weld)

Use of controlled electric heating at warming, welding and postheating of pressure parts of steam generator.

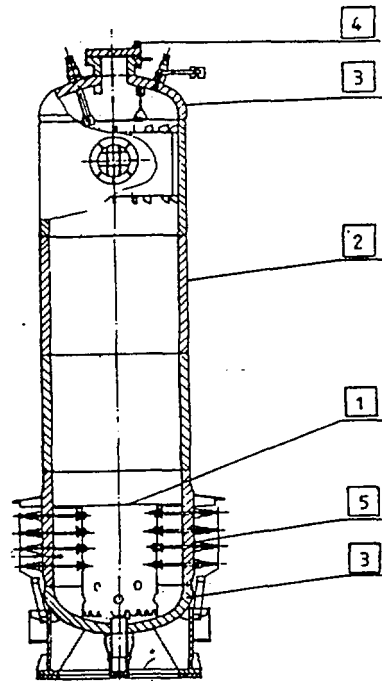
Modification of chemical composition and structure of steel at base material of pressure parts with the aim to improve its safety against failure and reliability (reducing degradation speed) at high mechanic and corrosive stress in the frame of operation.

We also arrange for steam generator produced in such a manner:

- author's supervision and consultation during operation
- all repair activity
- assembling diagnostic systems
- evaluation of service life exhaustion in relation to achieved operation regimes



Volume Compensator for VVER 440 MWe



During production several technical and technological improvements took place:

1. Cancellation of built-in system - replacement with air back
2. Replacement of welded shells from plate with forged shells
3. Bottoms are produced from one part without longitudinal weld
4. All screws are drilled with measuring rod - originally only 4
5. Nozzles for electrical heating produced by electroslag instead of welding

Use of controlled electrical heating welding and postheating of pressure parts.

Modification of chemical composition and structure of steel at base material of pressure parts with the aim to improve its safety against failure and reliability (reducing degradation speed) at high mechanic and corrosive stress in the frame of operation.

We also arrange for steam generator produced in such a manner:

- author's supervision and consultation during operation
- all repair activity
- assembling diagnostic systems
- evaluation of service life exhaustion in relation to achieved operation regimes

## PANEL DISCUSSION

### SAFETY ISSUES CONNECTED WITH HORIZONTAL STEAM GENERATORS IN WWER NUCLEAR POWER PLANTS

*Chair: Dr A. Strupczewski, IAEA, Vienna*

*Co-Chair: Mr J. Mišák, Nuclear Regulatory Authority, Slovak Republic*

Panel Members: Mr S. Savolainen, IVO, Loviisa, Finland, Dr N. Trunov, Hidropress, Russia, Dr V.F. Titov, Hidropress, Russia, Dr O. Matal, Energovýzkum, Czech Republic, and Mr J. Hyvärinen, STUK, Finland

**Dr. Strupczewski** clarified the objectives of the panel discussion, described examples of safety issues evaluated under the IAEA Extrabudgetary Programme on the Safety of WWER NPPs, discussed the structure of safety issues and illustrated it with data collected on "Primary collector integrity" as provided in the IAEA documents. He asked the panelists to express their views of ranking the safety issues of the WWER steam generators.

**Mr. Savolainen** characterized the papers presented at the meeting as related to two main fields, namely normal operation and accident analyses. This was also reflected in the analysis session, where half of the papers dealt with the design calculation methods and half of the papers dealt with the accident analysis models. The developmental stage of 3-D codes seems to be satisfactory. These codes are needed mostly by the designers of the steam generators, who naturally want to use the best estimate codes and to model so exactly as possible the designed geometry and the parameters of the steam generator. On the other hand, although accident analyses constituted a large part of the papers, the models which have been used are all models developed for the nominal conditions. There is a need of models with conservative, simplified assumptions, which will be quite sufficient for accident analyses.

For example, the problem of recirculation rate, which is important for nominal conditions, has no effect whatsoever on the results of accident analyses. Similarly, cross-flow connections bring no changes in the results of accidents. Generally, it can be stated that while steady state models are often made more and more detailed in order to fit the results of calculations to the available data, in many cases the complication of the model does not bring any improvements in the analyses of the transient and accident processes. What is more, the increasing complexity of the models involves a danger of losing the physical sense of thermal hydraulic processes. In order to be able to perceive the influence of changes of various parameters, we should try to construct simpler models, assuming certain parameters such as the behaviour of the secondary side of the steam generator as the boundary conditions for analyses of the primary side. Simplification is needed for better understanding.

Problems of ageing should be discussed in the future. As of today, we can see the problems of primary collector integrity, and feedwater collector corrosion and erosion damage mechanisms as the safety issues. Other problems are not apparent today, they will undoubtedly appear as the time goes by.

**Dr. Matal** stressed the need for collecting specific data for evaluation of ageing effects. First of all the data should be provided by the manufacturer, then the operational data

should be collected (impurities, interaction of components with medium). We need methodology determining how to utilize the gathered data. Up to now only very limited information is available. Data collection is necessary for extension of the lifetime. Operating procedures are not sufficiently detailed from the viewpoint of sensitive parts of the steam generator.

**Mr. Hyvärinen** remarked that the ranking of issues depends on specific plant conditions, so he would not be ready to attach rank to the issues in general, without relation to the plant.

Concerning the analyses he stated that reasonable safety measures can be taken without modelling steam generators by means of 3-D models. It is more important to understand the physics of the process. An example of such a successful approach can be the design of WWER 440/213 plants, which is quite satisfactory although no detailed modelling was involved in the design process.

There are new safety aspects of horizontal steam generator processes, which have not been modelled yet, such as reactivity effects, influence of steam generators on severe accidents, importance of primary-secondary boundary for containing radioactivity during severe accidents (deposits on tubes, heating of steam generator tubes with the potential for damages etc).

**Dr. Trunov** took up the question of steam generator modelling. He agreed that very often a simple approach can be very effective, but for complicated questions analyzed e.g. with ATHLET code different models are needed in relationship to the purposes of analyses. 3-D codes should be further developed.

Data collection in the past had been conducted for specific purposes, so usually the data accumulated are not sufficient for code validation. That is why today new experiments are proposed and new measurement methods should be implemented. The Russian delegation expresses support for the organization of an international group which would deal with those questions.

An important safety aspect is the prevention of the break of the primary collector in the steam generator. The importance of the secondary level location should be stressed. The oscillations of this level, which in some cases in the past would reach even the level of the bolts connecting the cover flange of the collector, have very detrimental effect on the lifetime of the collector. Therefore more accurate measurements of the secondary water level are needed, as e.g. in Loviisa. Other measures can be also used to stabilize the water level, e.g. perforated submerged sheets can be utilized.

**Prof. Titov** observed that the requirements for safety have been increasing and this trend will be continued in the future. Horizontal steam generators have two important functions: they provide leak-tight boundary of the reactor coolant system and they assure effective heat removal from the RCS.

In order to solve the problem of leakages from the primary to secondary cooling system, which involves threats to the core cooling and results in releases of radioactive steam to the environment, there should be a well coordinated activity including:

- classification of leakages and emergency operating procedures for each type of leakages,
- calculations and analyses of scenarios after leakages (behaviour of steam generator components, operator actions),

- measures to prevent leakages, to detect damages to primary collectors, to decrease frequency of damages.

In the case of steam generator tube ruptures the methods for leakage identification should be developed, more attention should be paid to chemical conditions, and emergency operating procedures should be developed to provide clear guidance to the operator in the case of such an accident. In view of the damages observed in feedwater systems new investigations are needed. The damages of feedwater collectors can lead to the impact of cold water on steam generator tubes or collectors, or broken pieces of the feedwater collectors can remain stuck among tubing, increasing chances of its damages. Investigation of mechanisms of deterioration of collector cover fastening bolts should be continued in order to finally establish the reasons of failures.

The main safety issues connected with primary collector breaks are:

- determination of the mechanism of collector damages,
- calculation of the remaining lifetime of the collectors.

The extension of the subject of the seminar has turned out to be successful, as shown by the increasing number of participants and the improved quality of the presentations. The sponsorship provided by the IAEA has been an important factor which made participation of several specialists from eastern Europe possible.

**Mr. Mišák** presented plant-specific problems connected with horizontal steam generators. He discussed the problems of manufacturing, maintenance and operational regimes giving examples from the operation of Bohunice V-1 and V-2 units. He stressed the necessity to consider and analyze the consequences of feedwater collector replacements, which are under way in most WWER 44/213 plants.

**Mr. Česla** from Vítkovice in Czech Republic presented the problem of feedwater collector replacement. He compared various approaches to the problem taken in various factories and NPPs. He recommended to organize a meeting on the methods of feedwater collector repair and replacement, with presentation of measurements and comparisons of results.

**Dr. Papp** from Vítkovice in Czech Republic confirmed the need for long-term operational studies of steam generator components, which should give the data needed to evaluate the influence of ageing processes on components' lifetime. He mentioned deficiencies still persisting in evaluation methods. Systematic data collection is needed, including basic material properties. The Institute in Vítkovice is evaluating ageing properties of materials, which maybe later implemented in the design of steam generator components.

**Mr. Melikhov** from EREC, Russia, commented the problem of code development. He stressed that 3-D processes need 3-D models. The code developers from EREC hope to be on the right path. Simplified models can be acceptable for specific purposes. He agreed that 3-D codes are needed in the first range for the designers of the steam generators.

**Dr. Strupczewski** summarized the discussion and suggested that specific proposals for activities should be sent to the IAEA as proposals from member countries.

**Dr. Tuomisto** closed the seminar informing the participants that the next seminar will be tentatively scheduled to be held in Lappeenranta in summer 1996.

1. OLKKONEN, TAUNO. Tuotteen tuotantoteknisen suunnittelun ohjaaminen. 1973. 148 s. Väitösk.
2. SUVIOLAHTI, MATTI. Yksinkertaisesti tuetun ympyrälierökuorikaton Hooken kimmolaikiin perustuva lujuusopillinen ratkaisu käyttämällä Fourierin sarjakehitelmiä. 1975. 67 s.
3. SUVIOLAHTI, MATTI. Jatkuvan ympyrälierökuorikaton Hooken kimmolaikiin perustuva ja reunaehdot tarkasti toteuttava lujuusopillinen matemaattinen ratkaisu käyttämällä Fourier'n sarjakehitelmiä. 1975. 187 s. Väitösk.
4. SÄÄKSJÄRVI, MARKKU. Eräs puunhankinnan yhteistyömalli: hyödyn jakaminen peliteoreettisena ongelmana. 1976. 115 s. Väitösk.
5. RUOTTU, SEPPO. Aineen, impulssin ja energian siirtyminen turbulentissa hiukkas-kaasu-suspensiossa. 1976. 46 s. Väitösk.
6. KOSKELAINEN, LASSE. Analysis of pipe networks using linear theories. 1977. 36 s.
7. PENTTINEN, SEPPO. Experimental studies of electromagnetic transitions in the selfconjugated  $^{30}\text{P}$ ,  $^{32}\text{S}$  and  $^{34}\text{Cl}$  nuclei through the  $(p,\beta)$  reaction. 1977. U.s. Diss.
8. KOSKELAINEN, LASSE. A model for optimal design of district heating networks. 1978. 88 s. Diss.
9. LAITINEN, HEIKKI. Determining risk potential through accidents and near-accidents: an empirical study in a steel factory. 1984. 125 s. Diss.
10. LAINE, JOUKO. Calculation of process response with matrices. 1985. 75 s.
11. LUKKA, ANITA. On method and system design for a problem in vehicle routing and scheduling. 1987. 169 s. Diss.
12. HOLSTIUS, KARIN. Project business as a strategic choice: a theoretical and empirical study of project marketing. 1989. 105 s.
13. YLI-HARJA, OLLI. Median filters: extensions, analysis and design. 1989. 173 s. Diss.
14. ZAMANKHAN, PIROOZ. The temperature distribution of viscous fluid flowing in constricted or widened tubes far downstream from the beginning of the heated-section. 1989. 37 s. Diss.
15. HYPÄNEN, TIMO. An experimental and theoretical study of multiphase flow in a circulating fluidized bed. 1989. 207 s. Diss.
16. MARTIKAINEN, JUKKA. On the effects of welding parameters on weld quality of plasma arc keyhole welding of structural steels. 1989. 132 s. Diss.
17. Proceedings of the 4th Finnish Mechanics Days, June 5-6, 1991, Lappeenranta, Finland / ed. by Erkki Niemi. 1991. 388 s.
18. International Seminar of Horizontal Steam Generator Modelling March 11-13, 1991, Lappeenranta, Finland. 1991. 181 s.
19. Proceedings of the 3rd Conference on Laser Materials Processing in the Nordic Countries: NOLAMP-3 August 21-22, 1991 Lappeenranta, Finland / ed. by Tapani Moisio. 1991. 228 s.
20. SIERILÄ, PENTTI. Corporate planning, strategies, and critical factors in forest industries: methodology and contents. 1991. U.s. Diss.
21. LAATIKAINEN, MARKKU. Stability of aqueous emulsions of synthetic and extracted wood pitches. 1992. 28 s.
22. SUN, ZHENG. Laser beam welding of austenitic-ferritic dissimilar steel joints. 1992. 87 s. Diss.
23. KOIKKALAINEN, PASI. Neurocomputing systems: formal modeling and software implementation. 1992. 142 s. Diss.

24. PIRTTILÄ, TIMO. Empirical analyses of inventory intensity in the Finnish engineering industry. 1992. 118 s. Diss.
25. KOVANEN, M.A. Monte Carlo study of charged particle behaviour in Tokamak plasmas. 1992. U.s. Diss.
26. KALLAS, JUHA et al. Treatment technology of wastewater containing phenols and phenolic compounds. 1992. 40 s.
27. VAKKILAINEN, ESA K. Offdesign operation of kraft recovery boiler. 1992. 83 s. Diss.
28. LAMPINEN, JOUKO. Neural pattern recognition: distortion tolerance by self-organizing maps. 1992. U.s. Diss.
29. PUUMALAINEN, PERTTI. Paperin laadun ja siihen valmistusprosessissa vaikuttavien tekijöiden on-line mittaukset. 1993. 279 s. Väitösk.
30. Second International Seminar of Horizontal Steam Generator Modelling September 29 - 30, 1992, Lappeenranta, Finland. 1993. 195 s.
31. NYKÄNEN, TIMO.  $M_k$ -factor equations and crack growth simulations for fatigue of fillet-welded T-joints. 1993. 198 s. Diss.
32. KOSKINEN, JUKKA TAPIO. Use of population balances and particle size distribution analysis to study particulate processes affected by simultaneous mass and heat transfer and nonuniform flow conditions. 1993. U.s. Diss.
33. TUUNANEN, JARI. Thermal-hydraulic studies on the safety of VVER-440 type nuclear power plants. 1994. U.s. Diss.
34. ZHANG, ZHILIANG. A practical micro-mechanical model-based local approach methodology for the analysis of ductile fracture of welded T-joints. 1994. 151 s. Diss.
35. KÄLVIÄINEN, HEIKKI. Randomized Hough Transform: new extensions. 1994. U.s. Diss.
36. HEIKKONEN, JUKKA. Subsymbolic Representations, Self-Organizing Maps, and Object Motion Learning. 1994. 119 s. Diss.
37. KOSKINEN, JUKKA ANTERO. Knapsack sets for cryptography. 1994. 81 s. Diss.
38. TURUNEN, ESKO. A mathematical study of fuzzy logic; an algebraic approach. 1994. U.s. Diss.
39. JANHUNEN, ANTERO. Toimitustäsmällisyyden suunnittelumenetelmä. 1994. 161 s. Väitösk.
40. LARES-MANKKI, LAURA. Strategy implementation bottlenecks: identification, analysis and removal. 1994. 150 s. Diss.
41. French-Finnish Colloquium on Safety of French and Russian Type Nuclear Power Plants. 1994. 275 s.
42. KORPELA, JUKKA. An analytic approach to distribution logistics strategic management. 1994. U.s. Diss.

ISBN 951-763-942-2  
ISSN 0356-8210